

AD-A064 169

CALIFORNIA UNIV BERKELEY GEOTECHNICAL ENGINEERING
EARTH PRESSURES ON CONDUITS AND RETAINING WALLS. (U)
SEP 78 D W QUIGLEY, J M DUNCAN

F/G 13/2

UNCLASSIFIED

UCB/GT/78-06

DACW39-76-C-0035

NL

1 OF 4
AD
A064169

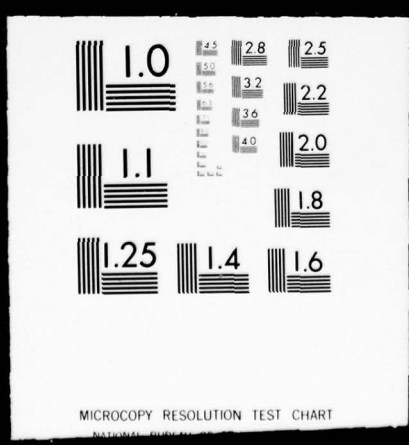


CLASSIFIED

1 OF 4

AD

A064169



ADA064169

DDC FILE COPY.

(13)
(10.5)
411056

GEOTECHNICAL ENGINEERING

EARTH PRESSURES ON CONDUITS AND RETAINING WALLS

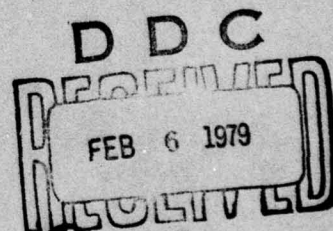
by
DONALD W. QUIGLEY
and
J. M. DUNCAN

REPORT NO. UCB/GT/78-06

A REPORT ON RESEARCH SPONSORED BY THE
U.S. ARMY ENGINEER WATERWAYS EXPERIMENT STATION
UNDER RESEARCH CONTRACT NO. DACW39-76-C-0035

SEPTEMBER 1978

1105
✓ DEPARTMENT OF CIVIL ENGINEERING



DISTRIBUTION STATEMENT A

Approved for public release;
Distribution Unlimited

UNIVERSITY OF CALIFORNIA • BERKELEY

79 01 22 041



13

GEOTECHNICAL ENGINEERING

9 Doctoral thesis

6 EARTH PRESSURES ON CONDUITS AND RETAINING WALLS.

by

10 Donald W. Quigley and J. M. Duncan

12 348 p.

14

Report No. UCB/GT/78-06

A Report on Research Sponsored by
The U. S. Army Engineer Waterways Experiment Station
under Research Contract No. DACW39-76-C-0035

15

11

September 1978

DISTRIBUTION STATEMENT A

Approved for public release;
Distribution Unlimited

College of Engineering
University of California
Berkeley, California

441 056

DISTRIBUTION STATEMENT A		
Approved for public release; Distribution Unlimited		
College of Engineering University of California Berkeley, California		
441 056		
A		

TABLE OF CONTENTS

	<u>Page</u>
LIST OF SYMBOLS	iii
FOREWORD	1
SUMMARY	2
CHAPTER I	3
INTRODUCTION	
<u>PART A--CONDUITS</u>	5
CHAPTER II	5
CURRENT DESIGN METHODS FOR PREDICTING EARTH PRESSURES ON CONDUITS	
A. Marston-Spangler Theory	5
B. Other Design Methods	8
C. Corps of Engineers Design Methods	12
CHAPTER III	14
REVIEW OF CASE HISTORIES IN LITERATURE--CONDUITS	
A. Measured Earth Pressures	14
B. Conduit Failures	22
CHAPTER IV	26
FINITE ELEMENT STUDIES OF EARTH PRESSURES ON CONDUITS	
A. Scope of Finite-Element Analyses	26
B. Conduit Stiffness	27
C. Soil Type	31
D. Conduit Size	36
E. Depth of Soil Foundation	36
F. Height of Fill Cover	52
G. Conduit Shape	56
H. Rock Foundation	83
I. Shallow Trench Placement	116
CHAPTER V	133
OTHER DESIGN CONSIDERATIONS--CONDUITS	
A. Embankment Stress Distribution	133
B. Conduit Settlement	141
C. Embankment Cracking and Hydraulic Fracturing	148
CHAPTER VI	152
PROPOSED DESIGN PROCEDURES--CONDUITS	
A. Design Earth Pressures	152
B. Simplified Procedures for Circular and Oblong Conduits	165
C. Finite-Element Analyses	165
CHAPTER VII	176
ANALYSIS OF CORPS OF ENGINEERS CASE HISTORIES--CONDUITS	
A. Cochiti Dam	176

79 01 22 041

	B. DeQueen Lake Dam	182
	C. Dierks Lake Dam	187
	D. Lake Kemp Dam	198
CHAPTER VIII	CONCLUSIONS AND RECOMMENDATIONS-- CONDUITS	202
	<u>PART B--RETAINING WALLS</u>	204
CHAPTER IX	CURRENT DESIGN METHODS FOR PREDICTING EARTH PRESSURES ON RETAINING WALLS	204
	A. Classical Earth-Pressure Theories	204
	B. Empirical Methods	206
	C. Elastic-Continuum Methods	208
	D. Corps of Engineers Design Methods	209
CHAPTER X	REVIEW OF CASE HISTORIES IN LITERATURE--RETAINING WALLS	210
	A. Measured Earth Pressures	210
	B. Retaining Wall Failures	228
CHAPTER XI	ANALYTICAL AND EXPERIMENTAL STUDIES OF EARTH PRESSURES ON RETAINING WALLS	232
	A. Active Earth Pressures	232
	B. Passive Earth Pressures	241
	C. At-Rest Earth Pressures	248
CHAPTER XII	RECOMMENDED DESIGN PROCEDURES-- RETAINING WALLS	258
	A. Active Earth Pressures	258
	B. At-Rest Pressures	259
	C. Passive Earth Pressures	259
CHAPTER XIII	ANALYSIS OF CORPS OF ENGINEERS CASE HISTORIES--RETAINING WALLS	261
	A. Bankhead Lock and Dam	261
	B. West Point Dam	267
	C. Thompson Creek Channel	272
	D. San Jose Creek Channel	279
CHAPTER XIV	CONCLUSIONS AND RECOMMENDATIONS-- RETAINING WALLS	287
BIBLIOGRAPHY		289
APPENDIX A	FINITE-ELEMENT ANALYSES	A-1
APPENDIX B	CALCULATIONS OF EARTH PRESSURES ON CONDUITS	B-1

LIST OF SYMBOLS

<u>Symbol</u>		<u>Units</u>
B	width of trench or conduit	L
B _c	width of conduit	L
B _d	width of ditch at top of a conduit	L
C	load coefficient	-
C _I	crown pressure correction factor	-
C _M	coefficient of proportionality (moment)	-
C _n	correction factor for crown pressure on oblong conduits	-
C _T	coefficient of proportionality (thrust)	-
C _V	coefficient of proportionality (shear)	-
D _C	diameter of conduit	L
E	modulus of elasticity	F/L ²
EF _P	equivalent fluid pressure	F/L ² /L
EI	flexural stiffness	FL ² /L
H	height of fill or height of retaining wall	L
H _c	height of conduit	L
H _f	depth of soil foundation	L
I	moment of inertia	L ⁴ /L
K	pressure coefficient	-
K _a , K _A	active pressure coefficient	-
K _h	horizontal component of active pressure coefficient	-
K _o	at-rest pressure coefficient	-
K _{or}	at-rest pressure coefficient (rebound)	-
K _p	passive pressure coefficient	-

List of Symbols (Continued)

<u>Symbol</u>		<u>Units</u>
ΔM	change in moment in conduit	FL
ΔM_C	change in moment at crown of conduit	FL
N	crown pressure factor	-
OCR	overconsolidation ratio	-
P	resultant pressure force	F
P_a	total active force	F
P_h	horizontal component of active pressure	F/L^2
P_p	total passive force	F
PI	plasticity index	percent
R	rise (projection) of a conduit above its foundation	L
RC	relative compaction	percent
R/S	rise/span ratio	-
S	span (width) of a conduit	L
ΔT	change in thrust in conduit	F
ΔT_S	change in thrust at the springline of a conduit	F
V	vertical pressure on a horizontal plane	F/L^2
ΔV	change in shear in conduit	F
ΔV_{QP}	change in shear at the quarter-point of a conduit	F
W	width of trench; width of dam core	L
\overline{W}	bottom width of sloping trench	L
W_c	vertical load on top of conduit	F/L
Z_c	critical depth for compaction machines	L

<u>Symbol</u>		<u>Unit</u>
Z_o	depth of influence of compaction machines	L
C	cohesion	F/L^2
d_c	shortening of vertical height of conduit	L
dh	infinitesimal distance	L
h	distance from ground surface to a horizontal plane	L
i	slope of backfill surface	degrees
m	edge pressure factor	-
n	foundation reaction factor (soil foundation)	-
n^i	foundation reaction factor (rock foundation)	-
p	projection ratio; pressure	$; F/L^2$
p	change in pressure	F/L^2
p_c	normal pressure at crown of conduit	F/L^2
p_s	normal pressure at side of conduit	F/L^2
r	progressivity index	-
r_{sd}	settlement ratio	-
s_f	settlement of conduit into its foundation	L
s_g	settlement of ground surface adjacent to conduit	L
s_m	compression strain of soil columns adjacent to conduit	L
γ	unit weight of fill	F/L^3
$\Delta\sigma_c$	change in normal pressure at crown of conduit	F/L^2
θ	angle	degrees
τ	shear stress	F/L^2
σ	normal stress	F/L^2
ϕ	soil friction angle	degrees
β	slope of trench; slope of retaining wall	degrees

<u>Symbol</u>		<u>Units</u>
δ	wall friction angle	degree
ϕ', ϕ	drained soil friction angle	degrees
ϕ_{ps}	peak friction angle (plane strain)	degrees
ϕ_{mass}	average value of friction angle in soil	degrees
ϕ_{cv}	critical-state value of friction angle	degrees
ϵ	axial strain in triaxial compression test	-
ν	Poisson's ratio	-
λ	empirical coefficient (Alpan)	-
μ'	coefficient of friction between fill material and sides of a ditch	-
$\Delta\sigma$	change in normal pressure on conduit	F/L^2
$\Delta\tau$	change in side-shear stress on conduit	F/L^2
$\Delta\sigma_v$	change in vertical pressure on conduit	F/L^2
$\Delta\sigma_h$	change in horizontal pressure on conduit	F/L^2
$\Delta\tau_{QP}$	change in side-shear stress at the quarter point of a conduit	F/L^2
ϵ_h	horizontal strain	-
ϵ_v	vertical strain	-
σ_1	major principal stress	F/L^2
σ_3	minor principal stress	F/L^2
Δ	wall deflection	L

FOREWORD

The work described in this report was performed under Contract No. DACW39-76-C-0035 (Neg), "Earth Pressures on Conduits and Retaining Walls," between the U. S. Army Engineer Waterways Experiment Station (WES) and The University of California at Berkeley. This report is the doctoral dissertation of Donald W. Quigley performed under the supervision of Dr. J. M. Duncan, Professor of Civil Engineering.

The objective of this research, which began in September 1975, was to develop a better understanding of the earth pressures that act upon rigid (concrete) conduits and retaining walls and to review presently accepted methods, particularly the methods given in Corps guidelines, for predicting earth pressures in light of recent research and to compare earth pressures calculated by present methods and advanced numerical techniques (the finite element method) with extensive field and experimental earth pressure cell measurements.

The research was sponsored by the Office, Chief of Engineers, under the Civil Works Research and Development Program: Materials, Soils; CWIS No. 31173, "Special Studies for Civil Works Soils Problems, Task 10, Analysis of Earth Pressure Cell Data." The contract was monitored by Mr. C. L. McAnear, Chief, Soil Mechanics Division, under the general direction of Mr. J. P. Sale, Chief, Geotechnical Laboratory.

Commanders and Directors of WES during the preparation and publication of this report were COL G. H. Hilt, CE, and COL J. L. Cannon, CE. Technical Director was Mr. F. R. Brown.

SUMMARY

✓ The objective of this investigation was to improve current design procedures for predicting earth pressures on rigid (concrete) conduits and retaining walls of the type frequently built by the U. S. Army Corps of Engineers. The present design methods of the Corps are based upon simplified theories which have been reviewed in the light of recent advancements in numerical techniques (the Finite-Element Method) for the solution of earth-pressure problems and also compared with extensive field and experimental data.

→ A comprehensive literature review was made to determine the generally accepted design methods (in addition to those of the Corps of Engineers) for predicting earth pressures on rigid conduits and retaining walls and to accumulate case-history data of earth pressures measured in laboratory model tests or in field installations. Instructive examples from the literature of conduit and retaining wall failures were also reviewed.

→ Finite-element computer studies were performed to investigate the nature of earth pressures on buried conduits. The results of the analyses were simplified into earth pressure diagrams suitable for structural analyses of cast-in-place concrete conduits by hand or computer methods. Simplified moment, thrust and shear diagrams were also presented for various common conduit shapes (circular and oblong), which can be used directly in structural design.

→ Analytical comparisons were made of the many theories available for predicting earth pressures on retaining walls. The analyses and the case history data found in the literature were studied and conclusions were drawn regarding the most appropriate methods by which earth pressures on rigid retaining walls should be predicted for design purposes.

→ Several suggested improvements to present Corps of Engineers design methods resulted from this study. The recommended procedures were compared with earth pressure data from several Corps of Engineer projects. In general, the suggested changes resulted in more accurate predictions of earth pressures on rigid conduits and retaining walls than are calculated by the present methods.

This investigation has indicated several areas of inadequate present knowledge that could warrant further field and/or analytical study. ↗

CHAPTER 1

INTRODUCTION

Each year the U. S. Army Corps of Engineers designs and constructs literally hundreds of conduits and retaining walls in connection with flood control and river navigation projects for which it is responsible. A typical use for a conduit or pipe is for the outlet works of an embankment dam beneath or through which the conduit must pass. Retaining walls are often used at the sides of concrete-lined, flood-control channels. Very large walls, similar in scale to concrete dams, have been used to retain high embankments.

General guidelines for the design of conduits and retaining walls are given in the following Corps of Engineers manuals:

1. EM 1110-2-2902 (3 Mar 1969)
Conduits, Culverts and Pipes
2. EM 1110-2-2502 (29 May 1961)
Retaining Walls

The design procedures are based upon (1) empirical rules, developed by observing the performance of previous structures, and/or (2) theoretical analyses based on simplifying assumptions concerning the behavior of conduits and backfills. The resulting uncertainty concerning the performance of structures designed by these methods must be accounted for by an appropriate choice of factor of safety. The judicious selection of a factor of safety is not always a simple matter. It must be high enough to account for inaccuracies of design theories as well as variations in field conditions from design assumptions. However, the factor of safety must not be so high as to result in an uneconomical structure.

For these reasons, as well as to confirm the intended behavior of conduit and retaining wall structures, the Corps of Engineers frequently instruments and monitors the performance of structures it builds. Field data from four conduit and four retaining wall installations, recently constructed by various districts of the Corps of Engineers, formed the impetus for these studies. It was felt that a critical review of the data might lead to an improved understanding of earth pressures on conduits and retaining walls, and might provide a basis for safer or more economical design procedures.

The scope of these studies, as it finally evolved, has been to review the design procedures recommended in the previously cited Corps of Engineers manuals in light of:

1. A thorough review of presently available analytical theories and design methods.
2. Analytical studies including use of the finite-element method.

3. Analyses of case history data provided by the Corps of Engineers or available in the literature.

The approaches taken for the conduit and the retaining wall studies have differed. Because analytical techniques for the determination of earth pressures on conduits are few and involve many simplifying assumptions and because model test and field measurements of earth pressures are relatively scarce, extensive finite-element analyses have been performed to develop a better understanding of conduit problems. In contrast, theories for predicting earth pressures on retaining walls are numerous as are data from model tests and actual wall installations. Consequently the thrust of the retaining wall study has been aimed at determining the applicability and limitations of current earth pressure theories to actual design practice.

The results of these studies have been used to develop:

1. A summary of the important factors related to the prediction of earth pressures for design purposes,
2. Recommendations for modifications and/or additions to the Corps of Engineers manuals,
3. An indication of areas of inadequate knowledge that appear to be in need of further research.

To improve the effectiveness of these studies, their extent has been limited to an investigation of the common types of structures considered in the Corps of Engineers manuals, primarily cast-in-place, reinforced-concrete conduits and retaining walls (of the gravity or cantilever type) backfilled with compacted soil or rock fill. In particular, the emphasis has been on relatively stiff structures as opposed to flexible ones such as corrugated metal pipes and sheetpile retaining walls. Consequently, the terms "conduit" and "retaining wall," as used in this text, exclude structures that deform significantly under load so as to greatly affect the earth pressures acting upon them. The terms "rigid conduits" and "rigid retaining walls" are frequently found in the literature to describe the type of structures that are the main consideration of these studies.

The studies have also given emphasis to structures placed beneath or adjacent to relatively high fills such as those representative of embankment dams on the order of tens or hundreds of feet high.

PART A - CONDUITS

CHAPTER II

CURRENT DESIGN METHODS FOR PREDICTING

EARTH PRESSURES ON CONDUITS

A. Marston-Spangler Theory

By far the most commonly used design method for determining earth loads on buried culverts and conduits is that developed, starting about 1920, at Iowa State University by Marston, Schlick and Spangler. The method is described in numerous references (Spangler, 1951 and 1962; Tschebotarioff, 1973; Watkins, 1975*). It is recommended by many organizations in the United States, including the following:

1. American Concrete Pipe Association (1974)
2. New York State Highway Department (Butler, 1972)
3. Portland Cement Association (1958)
4. U. S. Bureau of Public Roads (Townsend, 1963)
5. U. S. Bureau of Reclamation (1960)
6. U. S. Navy Facilities Engineering Command (1971)

According to Clarke (1963, 1967) and Karado (1969) the Marston-Spangler method of design is in general use throughout Great Britain, the European continent and Japan.

The Marston-Spangler theory considers four basic classes of conduit installations as shown in Fig. II-1. The theory is considered to be applicable to both flexible and rigid conduits. For each class of installation, the prism of fill over the conduit is assumed to be supported by the conduit and by friction between the adjacent soil prisms on either side of the conduit. Equations of equilibrium are established for an element of back-fill such as the ones shown in Fig. II-2. Solution of the equations result in formulae which can be used to compute the total vertical load on the conduit. The formulae are of the form:

$$W_c = CYB^2 \quad (II-1)$$

where,

W_c = vertical load on top of conduit, plf

*References are listed in the Bibliography.

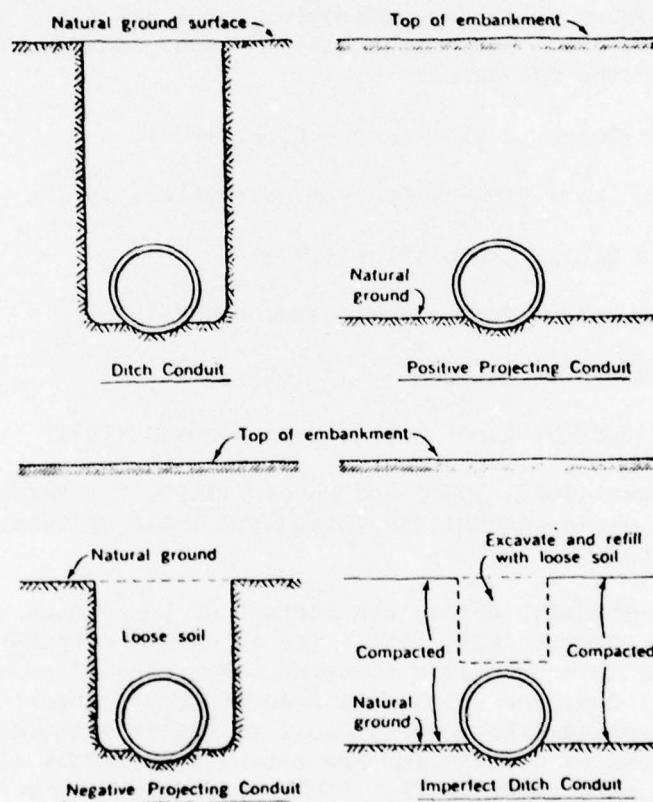
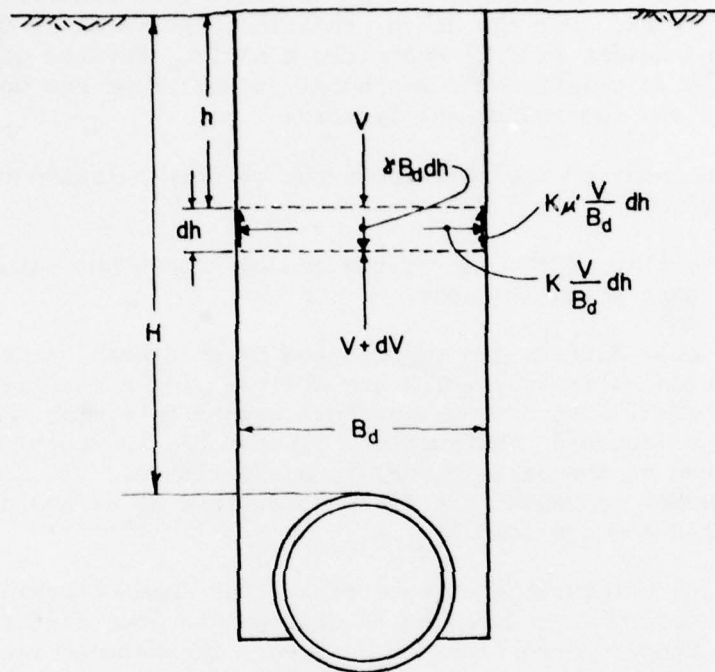


FIG. II-1 CLASSES OF CONDUIT INSTALLATION CONSIDERED BY MARSTON-SPANGLER THEORY

(After Spangler, 1962)



- γ = unit weight of fill material, pcf
 V = vertical pressure on any horizontal plane, plf
 B_d = width of ditch at top of conduit, ft
 H = height of fill above top of conduit, ft
 h = distance from natural ground surface to horizontal plane, ft
 $\mu' = \tan \phi'$ = coefficient of friction between fill material and sides of ditch
 K = ratio of active lateral pressure to vertical pressure

FIG. II-2 FREE-BODY DIAGRAM (DITCH CONDITION) ASSUMED IN MARSTON-SPANGLER THEORY
 (After Spangler, 1962)

γ = unit weight of fill, pcf

B = width of trench or conduit, ft, depending upon class of installation

C = load coefficient

Values of C, the load coefficient, can be obtained from figures given in the appropriate references. For the ditch condition, the value of C depends upon soil type and height of fill above the conduit. For the other classes of installation, C is relatively independent of soil type but does depend on height of fill and two additional factors:

1. The settlement of the soil above the conduit relative to the adjacent soil.
2. The projection of the top of the conduit above the natural ground surface upon which it rests.

These additional factors are represented by the terms "settlement ratio," r_{sd} , and "projection ratio," p, which are defined, for a positive projecting conduit, in Fig. II-3. There is no rational way to determine the settlement ratio in advance of conduit construction. Therefore, in practice, design values are selected on the basis of previous experience. The settlement ratio must reasonably represent the field conditions as it has a large effect upon the calculated conduit load.

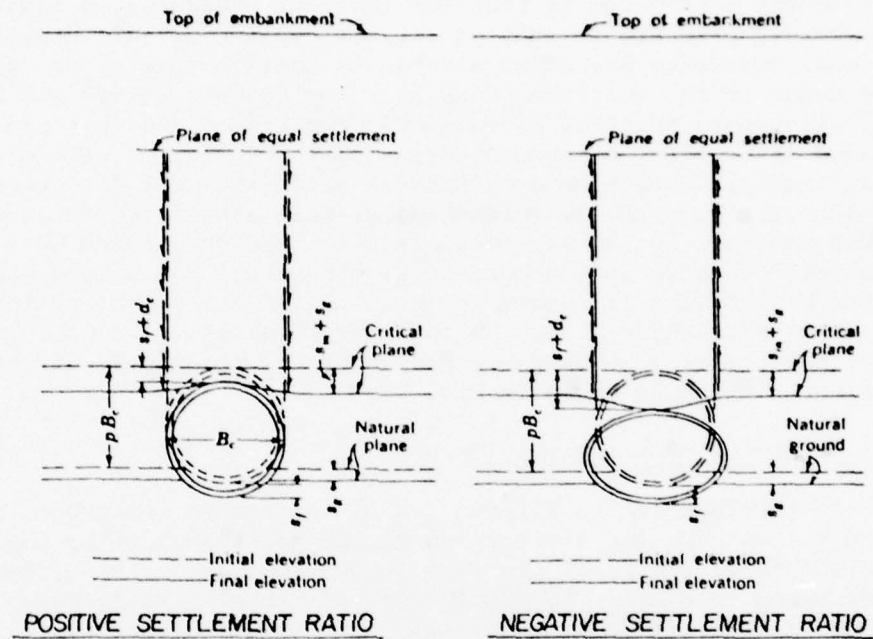
For the design of precast-concrete pipes, the load determined by the Marston-Spangler theory is reduced by an appropriate load factor which is dependent on the bedding conditions to be used. The reduced load is then compared to tabulate values of three-edge bearing strength, which have been determined experimentally for various standard classes of pipe. The suitable class for the required pipe diameter is thus chosen. The bedding load factors which have been determined empirically relate the field supporting strength of a pipe to its laboratory, three-edge bearing strength (with some additional margin of safety). Thus the design method must be considered semi-empirical because any inadequacies in calculation of earth load by the theoretical formulae are overcome by use of appropriately chosen load factors.

The Marston-Spangler theory is not well suited for use in designing conduits by structural analysis techniques. The theory does not predict how the vertical load is distributed over the top of the pipe, nor how the upwards reaction occurs at the bottom of the pipe. Horizontal soil loads are not considered at all by the theory and their magnitude and distribution must be assumed on some other basis. Since conduits that must be designed by structural analysis are not of standard shape, no extensive body of field data is available to relate "field" strength to "design" strength by way of a load factor as for standard-sized, precast-concrete pipes.

B. Other Design Methods

1. Empirical Procedures

Many designers simply assume the magnitude and distribution of the



$$\text{SETTLEMENT RATIO, } r_{sd} = \frac{(S_m + S_g) - (S_f + d_c)}{S_m}$$

where,

- S_m = compression strain of side columns of soil of height pB_c
- S_g = settlement of natural ground surface adjacent to conduit
- S_f = settlement of conduit into its foundation
- d_c = shortening of vertical height of conduit
- B_c = outside diameter or width of conduit, ft
- p = projection ratio

FIG. II-3 SETTLEMENT & PROJECTION RATIOS (POSITIVE PROJECTING CONDUIT)
ACCORDING TO MARSTON-SPANGLER THEORY (After Spangler, 1962)

vertical and horizontal soil pressures that will act upon a buried conduit and calculate the corresponding moments, shears and axial forces for design. The assumptions regarding the earth pressures are usually based on judgment and past experience, particularly on previous measurements of earth pressures on conduits.

A frequent assumption is that the vertical pressures is equal to the soil overburden pressure (height of fill multiplied by soil density). Lateral soil pressures are often assumed to equal active or at-rest values, or to be equal to the vertical pressure. For example, Davis and Bacher (1972, 1974) report that the recommended practice of the California Division of Highways is to consider two criteria for the design of reinforced-concrete culverts; namely, vertical and horizontal effective soil densities equal to 140 and 42 pcf, respectively (essentially, this amounts to the use of the overburden pressure in the vertical direction and 30 percent of overburden of overburden pressure in the horizontal direction) and both vertical and horizontal effective soil densities equal to 140 pcf (both vertical and lateral soil pressures equal to the overburden pressure). Gould (1970) described the criteria assumed for design of the box subway structures for the Washington Metro as shown in Fig. II-4.

2. Theory of Elasticity Solutions

Within the last ten to fifteen years, various investigators have attempted to overcome the limitations of the Marston-Spangler theory and the uncertainty of empirical pressure assumptions by deriving theoretical solutions based on elastic theory (Burns and Richard, 1964; Malishev, 1965; Hoeg, 1968; Krizek, et. al., 1961; Allgood, 1971; Abel and Kay, 1976). The objective has been to develop solutions which describe completely the stresses and deformations that occur in buried conduits. Of necessity the solutions developed have been restricted to simple cases of circular conduits, composed of elastic materials, buried deeply in weightless, homogeneous, isotropic, linearly-elastic soil. Loads are simulated by the application of a surface overpressure. The solutions indicate that the pressures acting upon a circular conduit, and the resulting deflections, moments, thrusts and shears depend upon the applied surface pressure, the radius of the conduit, and most importantly, the stiffness of the conduit relative to the surrounding soil. However, in the usual ranges of sizes of concrete structures, it is found that the relative stiffness of the conduit and the surrounding soil does not vary substantially.

3. Finite-Element Methods

The elastic-continuum approach has been extended by numerical methods and the use of computers to study many types of conduit problems which because of their complexity do not lend themselves to closed-form solutions based on elastic theory (Brown, 1967; Brown, et. al., 1968; Pawsey and Brown, 1968; Allgood and Takahashi, 1972; Duncan, 1975, 1976a, 1976b, 1977). The finite-element method has been used to study conduits of various shapes and flexibilities for various placement and backfill conditions. The non-linear stress-strain behavior of the soil surrounding the conduit can be included in the analysis so as to simulate real field conditions as closely as possible (Krizek and Kay, 1972; Wong and Duncan, 1974). The many

THIS PAGE IS BEST QUALITY PRACTICABLE
FROM COPY FURNISHED TO DDG

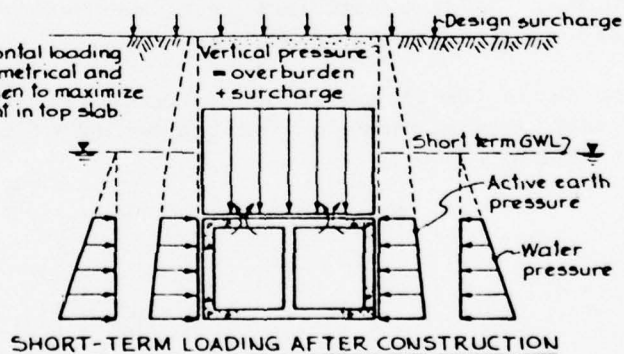
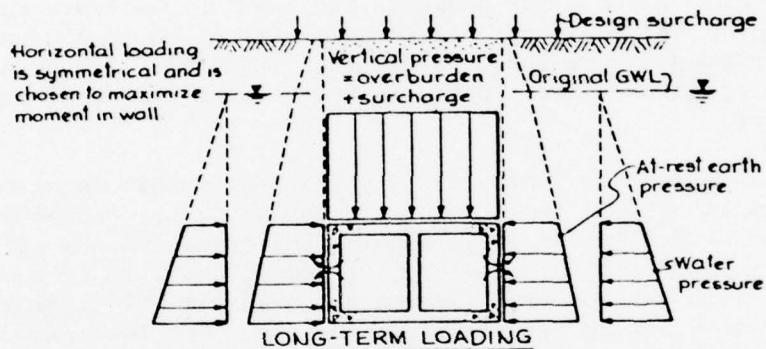
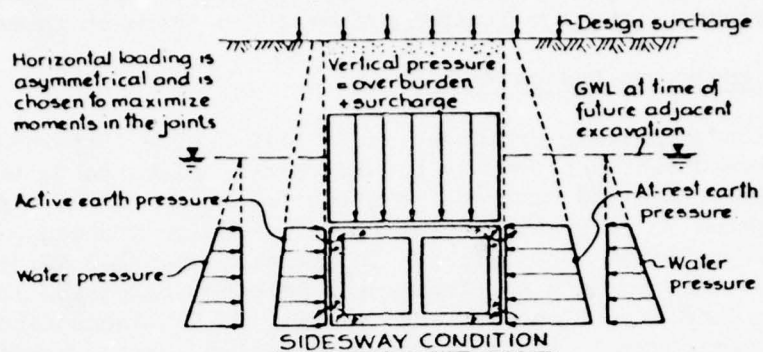


FIG. II - 4 DESIGN CRITERIA FOR LOADS ON CONCRETE BOX SUBWAY STRUCTURE FOR WASHINGTON METRO (After Gould, 1970)

advantages of the finite-element method are offset somewhat by the expense of performing the analyses. For this reason, with regard to buried conduits, the method has been thus far limited primarily to research investigations.

C. Corps of Engineers Design Methods

The design guidelines presented in EM 1110-2-2902 (Department of the Army, 1969) are directed primarily toward cast-in-place conduits through embankment dams. Limited coverage is given to the design of pipes; instead reference is made to relevant literature. The design procedures recommended in the manual are largely empirical. The Marston-Spangler theory is recommended for determining vertical loads on conduits placed in ditches, i.e., loading Condition I as described in Fig. II-5. The horizontal pressure is assumed to be equal to the Rankine active value. For conduits beneath embankments (Condition III) uniformly distributed vertical and horizontal soil pressures are assumed for design. Two loading cases are considered: Case 1, where the vertical and horizontal pressures equal 150 and 50 percent of the overburden soil pressure, respectively; and Case 2, where the vertical and horizontal pressures are assumed to be the same and equal to the overburden pressure.

For the intermediate Condition II where the conduit is placed in a shallow trench beneath an embankment, the design manual recommends that the soil pressures be determined by interpolation between values calculated by the Conditions I and III methods. For all conditions, it is recommended that conduits with vertical walls which are cast directly against rock should be designed for no lateral soil pressure. For the structural design of circular and oblong conduits, tabulated values of moment, thrust and shear coefficients at various sections of the conduits are given for different loading assumptions. Bedding load factors to be used in the selection of standard, precast concrete pipe are also given.

Flathau and Sager (1964) report that procedures similar to those in EM 1110-2-2902 have been recommended for the design of buried, reinforced-concrete arches (USAWES, 1962).

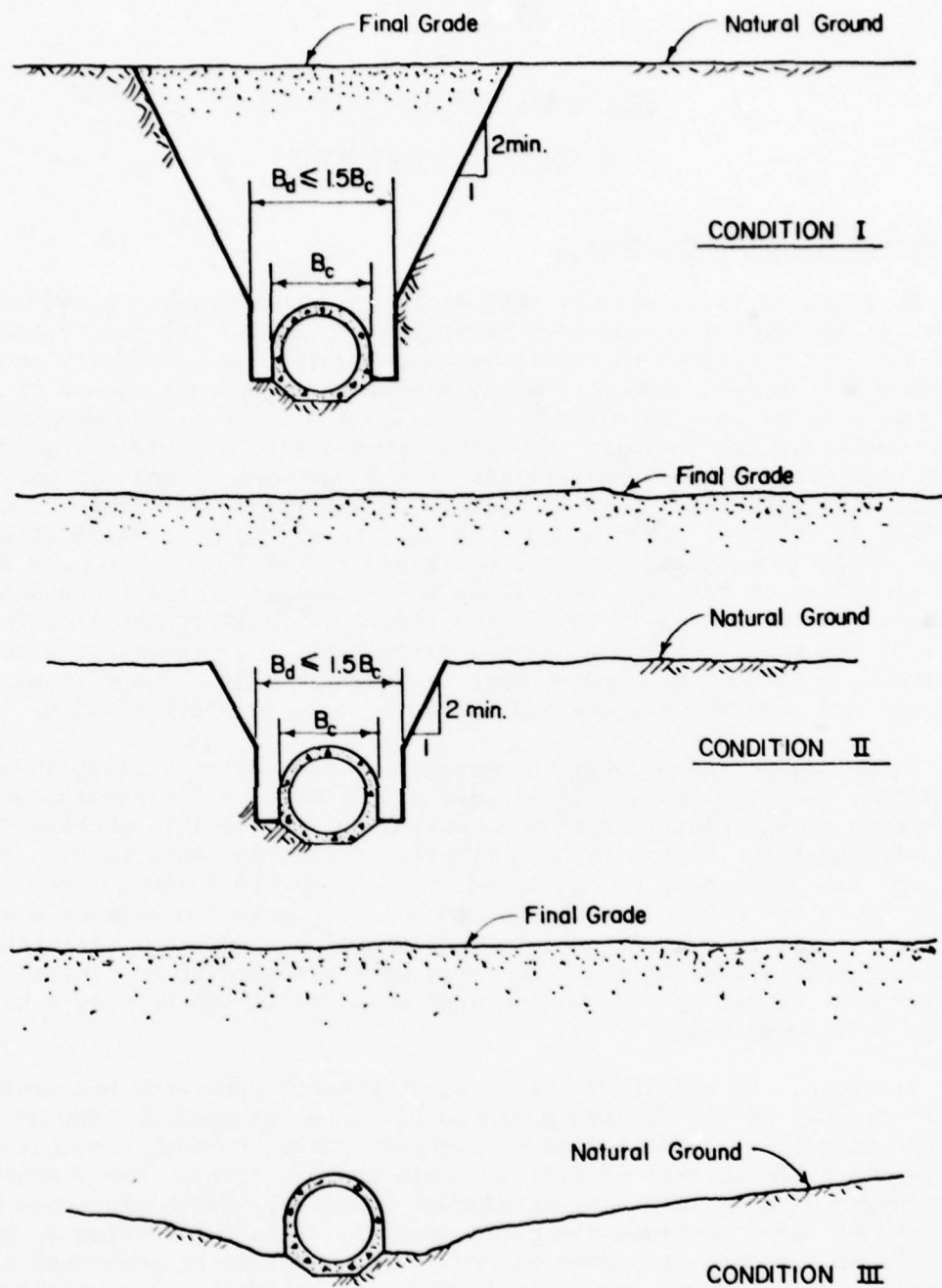


FIG. II-5 CONDUIT LOADING CONDITIONS CONSIDERED BY CORPS OF ENGINEERS DESIGN MANUAL (After Dept. of the Army, 1969)

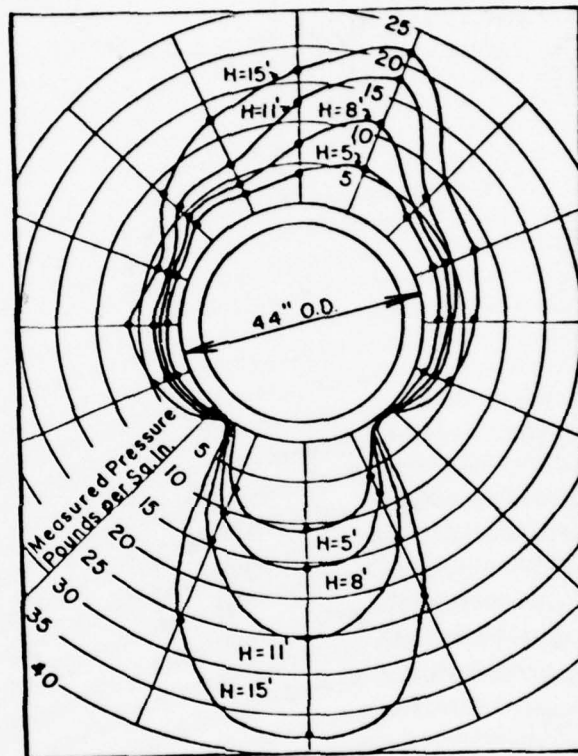
CHAPTER IIIREVIEW OF CASE HISTORIES INLITERATURE - CONDUITSA. Measured Earth Pressures

To evaluate the available methods for predicting earth pressures on conduits, it is helpful to consider several experimental and full-scale installations for which the earth pressures acting upon conduits have been measured. Prominent among the early measurements of earth loads on buried pipes were those made by Marston and his colleagues while developing their design method. The conduits they investigated were typically of modest size (less than six feet in diameter) and were covered by relatively low heights of fill (typically less than 25 feet). In accordance with construction practice at the time (1920's and 1930's), the backfill received little or no formal compaction, particularly above pipes placed in ditches. As a result, soil pressures on the pipe were found to be highest at the top and bottom of the pipe and relatively low at its sides. This is illustrated in Fig. III-1 by the pressures measured on a 44-inch-outside-diameter concrete pipe covered by a 15 foot high embankment (Spangler, 1974). The fill was placed by teams and wheeled scrapers and compacted only by their traffic.

A comparable field test, representative of current fill-construction practices, was reported by Krizek, et. al. (1974). A 60-inch-inside-diameter pipe was placed beneath an embankment at the Ohio Highway Transportation Research Center in East Liberty, Ohio. As shown in Fig. III-2, the pipe was surrounded by compacted granular backfill and covered to a height of 25 feet by compacted silty clay. The measured pressures are fairly uniform, except at the invert of the pipe, and generally exceed the weight of the overlying fill. The very high pressure at the invert is likely to have been caused by placing the pipe on a local high spot or a hard spot in the bedding material.

Trollope, et. al. (1963) have reported earth pressures measured on the outlet conduit of the Tullaroop Dam in Victoria, Australia. The horseshoe-shaped conduit, of 15-foot inside diameter, passes through the left abutment of the dam under 75 feet of fill as shown in Fig. III-3. The conduit was constructed of cast-in-place, reinforced concrete. Earth pressures were measured at three sections along the conduit. Data for Section T, beneath the axis of the dam, are shown in Fig. III-3. It can be seen that the measured side pressures are approximately one-third of the vertical pressure at the crown of the conduit. The crown pressure is more than 50 percent greater than the weight of the overlying fill. The high pressures were attributed by Trollope to cross-valley arching of the embankment as its thicker portion in the stream valley settled. However, similar observations on other conduits indicate that high vertical pressures can be expected when there is no cross-valley arching.

Pettibone and Howard (1967) report the results of a laboratory research investigation by the U. S. Bureau of Reclamation, to measure the loads on



(H=height of fill over pipe, feet)

FIG. III-1 PRESSURE DISTRIBUTION ON A 44-IN O.D. CONCRETE PIPE

(After Sangler, 1974)

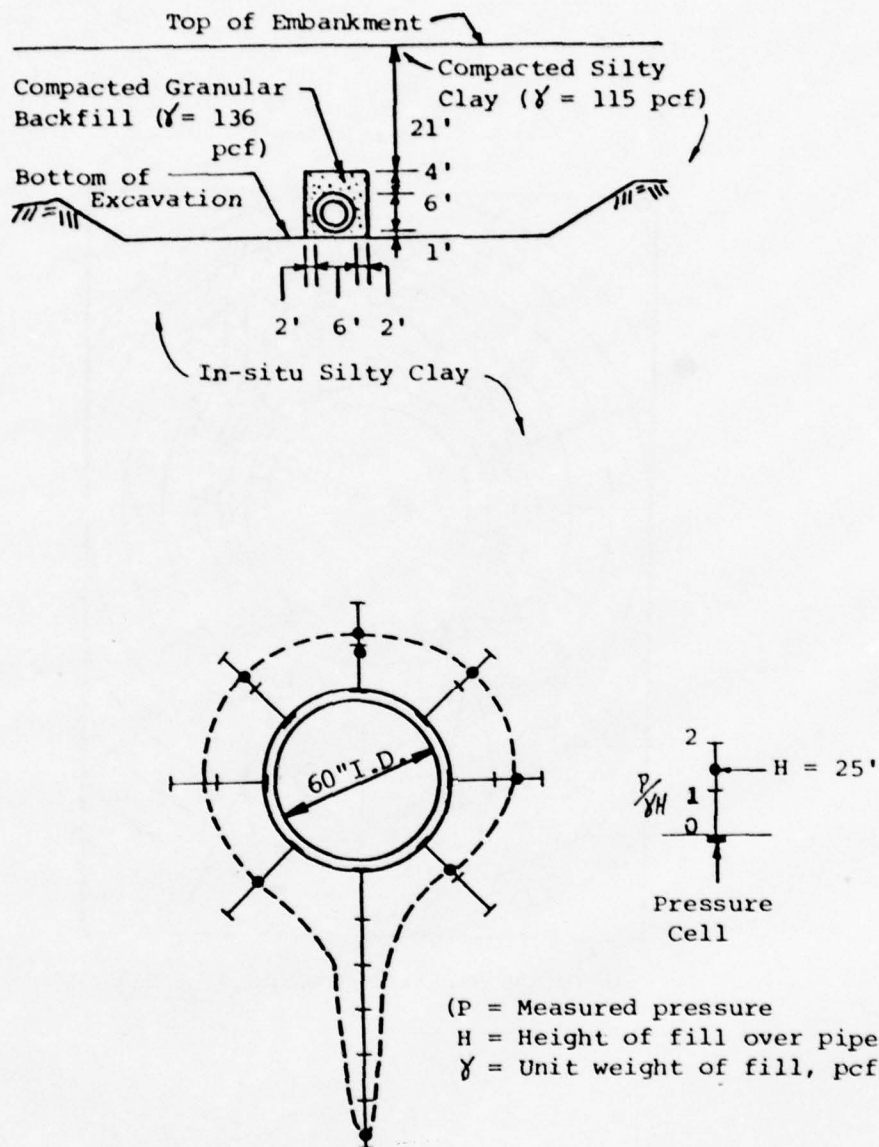


FIG. III-2 PRESSURE DISTRIBUTION ON 60" I.D. CONCRETE PIPE,

OHIO TEST INSTALLATION

(After Krizek, et. al., 1974)

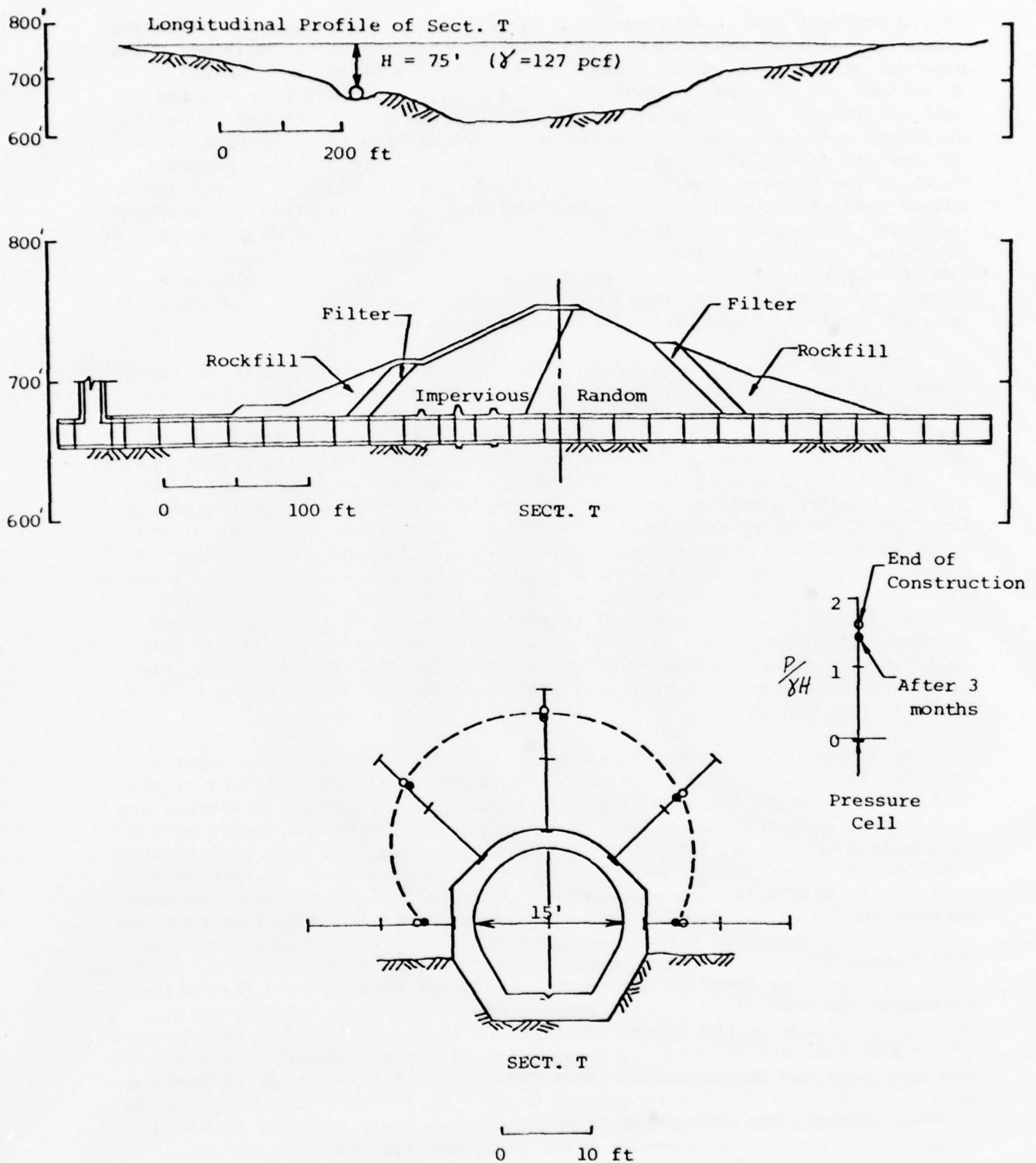


FIG. III-3 PRESSURE DISTRIBUTION ON 15-FT. I.D. CONCRETE CONDUIT,
TULLAROOP DAM
(After Trollope, et. al., 1963)

buried concrete pipe. They tested a 24-inch O.D. pipe buried in soil within a six-foot-wide by seven-foot-long by seven-foot-deep steel container. The pipe was separated from the container by a minimum of two feet in all directions. A variety of placement and bedding conditions were studied using different foundation and backfill materials and degrees of compaction. Surcharge loads were applied to the soil surface by a large testing machine. The results of two of the test series are shown in Fig. III-4. Series A, in which the pipe was surrounded by soil of moderate density, showed approximately similar crown and invert pressures equal to the applied (overburden) pressure. Side pressures were about 40 percent of the applied pressure. By contrast, the Series C results in which a hard foundation material lay immediately below the pipe indicated more than a 100 percent difference between crown and invert pressures. Soil pressures below the pipe springline were as little as 30 percent of the crown pressure.

Davis and Bacher (1968, 1972, 1974) described the results of an extensive research program by the California Division of Highways to determine the structural behavior of buried conduits. One prototype culvert selected for testing was an eight foot, reinforced-concrete arch beneath Interstate 5 where it crosses Posey Canyon, south of Bakersfield, California. The culvert is covered by as much as 240 feet of fill. Measured earth pressures for three instrument sections are shown in Fig. III-5. The pressures generally equalled or slightly exceeded the overburden pressure at the crown of the arch, whereas side pressures were much smaller. Some of the pressures at points other than the crown increased by as much as 100 percent over a period of two years following construction. Pawsey and Brown (1968) performed finite-element analyses to calculate earth pressures on the Posey Canyon culvert. Considering the approximate nature of the analyses (linear-elastic soil) and the unusual geometry of the culvert installation, the calculated pressures compare surprisingly well with the measured values at Sect. 7 as shown in Fig. III-5.

Pertinent data from the case histories described above are compared in Fig. III-6. In the upper portion of the figure, measured pressures at the crown of the conduits (normalized by dividing the overburden pressures) are compared with theoretical values determined by the Marston-Spangler method (assuming a uniform distribution of load). The data from each case history are plotted as horizontal bands on the figure where a range of theoretical values result from various reasonable choices of the assumptions that must be made in the calculations. Data plotted as a vertical band represent the range of pressures that were measured on the conduits. The data indicate some rather wide variations in both measured and theoretical values. Although there is a general trend of agreement between the measured and theoretical pressures, in some cases the differences are on the order of 50 percent. The lower portion of the figure compares the measured side and crown pressure. Except for the data reported by Krizek, et. al., the measured side pressures are less than the corresponding crown pressures. The two Corps of Engineers design assumptions for the embankment conditions (II) are also shown on the figure. Clearly the assumption of both vertical and horizontal pressures equal to the overburden pressure (Case 2) is not supported by the data. The Case 1 assumption appears to be more reasonable and, compared to the data, generally conservative.

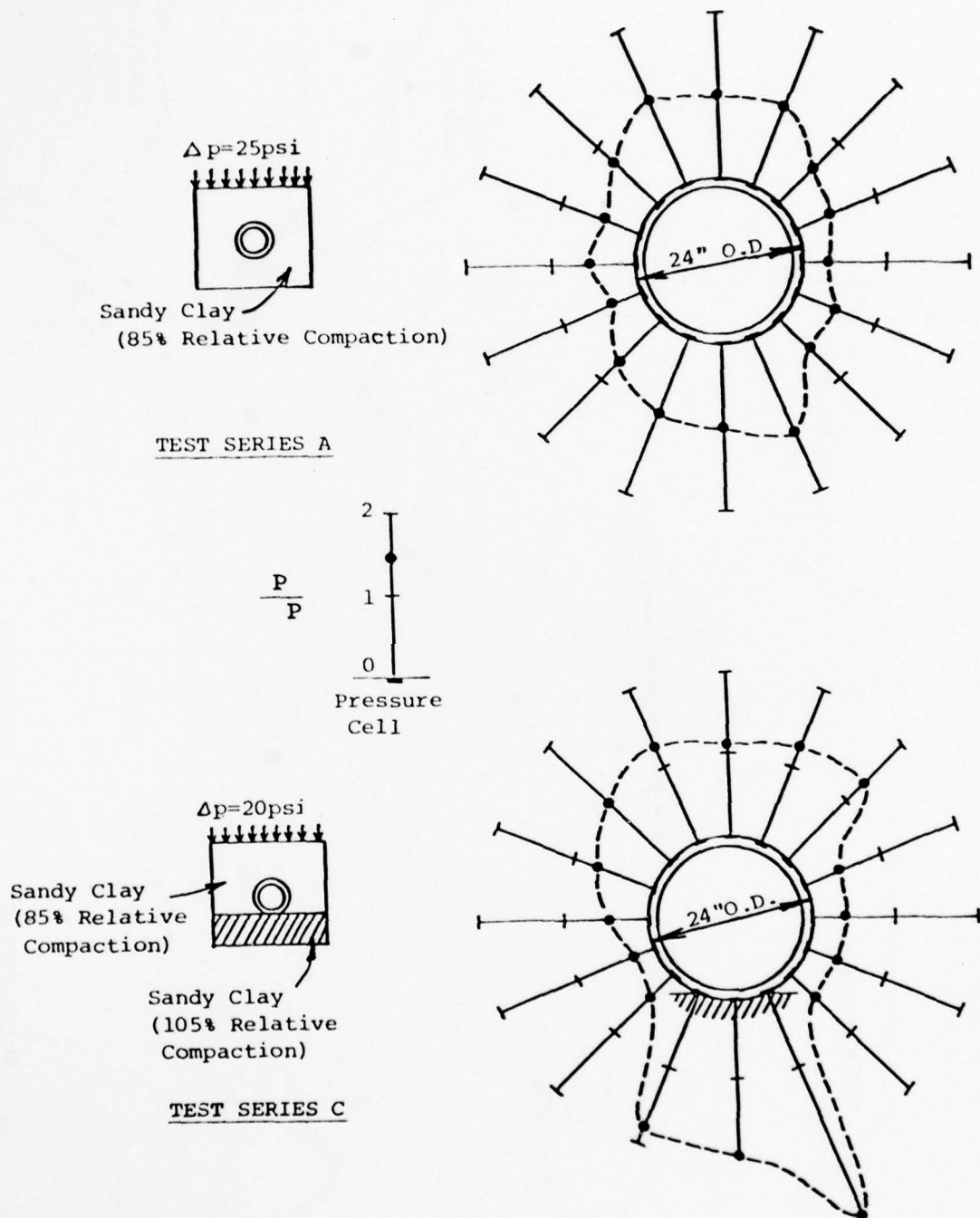


FIG. III-4 PRESSURE DISTRIBUTION ON 24" O.D. CONCRETE PIPE,
USBR LABORATORY TESTS

(After Pettibone and Howard, 1967)

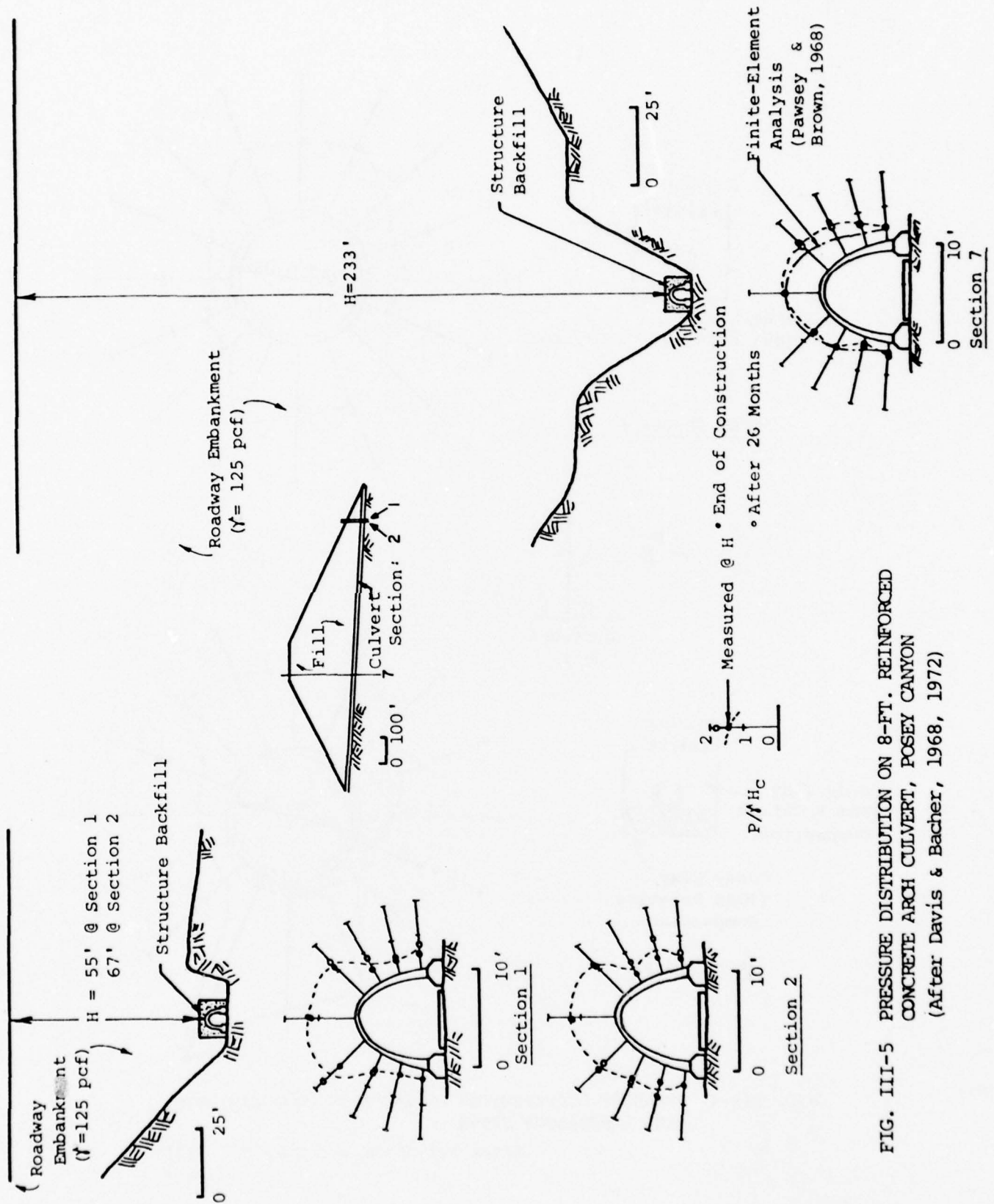


FIG. III-5 PRESSURE DISTRIBUTION ON 8-FT. REINFORCED CONCRETE ARCH CULVERT, POSEY CANYON (After Davis & Bacher, 1968, 1972)

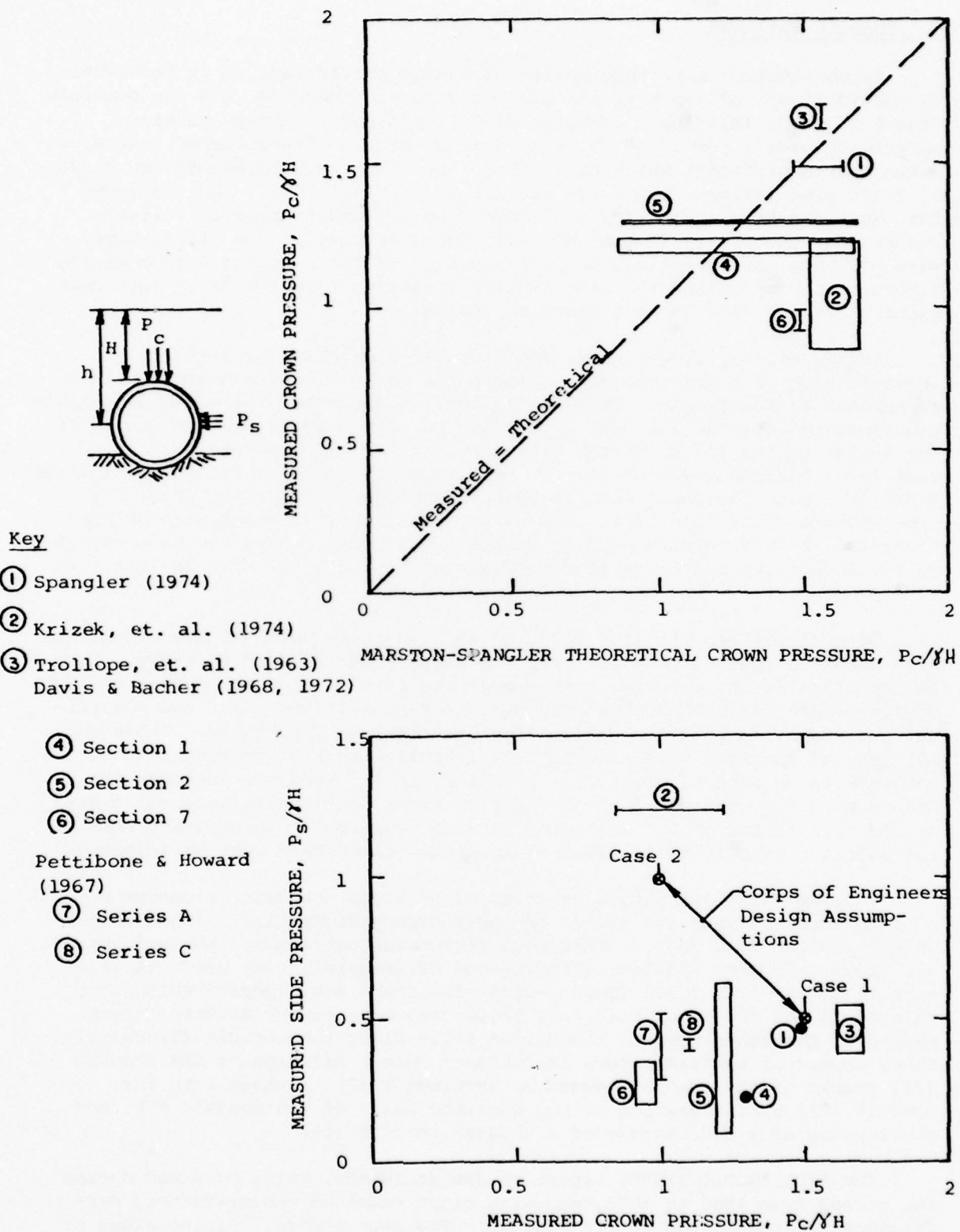


FIG. III-6 COMPARISON OF MEASURED PRESSURES - CASE HISTORIES

B. Conduit Failures

In conjunction with this review of design procedures, it is interesting to consider various types of failures of concrete culverts, and the possible causes of these failures. Spangler (1974) reported a summary of his experience over a period of 20 years during which he investigated several dozen buried pipelines which had failed. He cited ten representative cases of rigid pipe failure; these are summarized in Table III-1. He concluded that most structural difficulties arose from failure to provide suitable bedding for the pipe. Though the earth loads on most of the failed pipes were probably not excessive, the distribution of the reaction forces at the bottom of the pipes and the side support pressures were likely to have been quite different from those assumed in design.

Davis, et. al. (1974) confirmed Spangler's conclusions with their investigation of a concrete pipe culvert placed as a test beneath a highway embankment in California. The 90-inch-outside-diameter pipe was considerably underdesigned for the 136 feet of fill to be placed above it. According to the design tables in use at the time (about 1970) the pipe was considered safe for a maximum cover of only 16 feet. Yet for certain bedding conditions (shallow trench placement with an effective projection ratio of 0.5) the pipe withstood the load of as much as 40 feet of fill without perceptible distress. Less favorable bedding conditions such as laying the pipe directly on the foundation soils resulted in cracking of the pipe under as little as 19 feet of fill.

Deen (1969) reported the cracking of a 48-inch-inside-diameter concrete pipe under 36 feet of rock fill for a highway embankment in Kentucky. During construction of the culvert, cracks began to form in the pipe before the full design weight of fill had been reached. A review of the plans and specifications indicated that the design pipe strength was inadequate. Subsequent portions of the pipe were successfully installed by the imperfect ditch method with no sign of distress. Spangler, in a discussion accompanying Deen's paper, points out that the initial section of the culvert was overloaded by a factor of 2.3 according to Marston-Spangler theory, and thus the observed cracks, up to 1/4-inch in width, could have been anticipated.

The remaining literature on failures of rigid conduits is concerned with failures of conduits (or of the surrounding backfills or embankments) which resulted from causes other than structural overloads. Sherard, et. al. (1963), present Middlebrook's listing of unsatisfactory performance of earth dams prior to 1953. Twenty-eight incidents are reported which were related to the outlet conduit. Of these, the most common occurrence was piping of the embankment or foundation soils along the conduit (19 cases). Other causes of unsatisfactory performance were: breakage of the conduit (3), cracks of the conduit caused by settlement (2), leakage into the conduit (2), disintegration of the concrete walls of the conduit (1), and overtopping of a dam because of a clogged conduit (1).

The ASCE/USCOLD (1975) report on dam incidents, which occurred during the period from 1966 to 1972, contains eight cases of unsatisfactory performance related to the outlet conduit. The causes were: piping along or into the conduit (3 cases), opening of pipe joints as a result of foundation

TABLE III-1

Examples of Conduit Failures (Spangler, 1974)

<u>Description of Conduit</u>	<u>Observed Damage</u>	<u>Installation Details</u>	<u>Conclusions</u>
Six, RCP highway culverts, 60-to 84-in. diameter, under 25 - 30 ft. of fill	Spalling of concrete at invert and cracks at crown	Pipes placed one-inch above stiff glacial till; loose sand backfill up to springline	High reaction at invert led to large bending moments
66-in. RCP culvert under 13-21 feet of fill	Cracks and spalling at invert	Backfill not compacted beneath haunches of pipe	High reaction and large bending moments at invert
Four, RCP culverts, 42-72 in. dia., under 23-65 feet of fill	Wide longitudinal cracks, spalling, gross deflections	Shallow rock underlying the pipe (as close as 4 in.)	Soil bedding over rock was too thin and of less quality than assumed in design. Design factor of safety (1.25) was too low.
84-in. and 96-in. RCP culvert under 9-17 ft. of fill	Longitudinal cracks in invert and crown; spalling of concrete	Pipes lain on flat surface (compact gravelly sand); Backfill pushed over pipes with no compaction below haunches. Some pipes had only 50 percent of steel specified. Temporary soil stockpiles placed over completed backfills at some locations.	Pipes were of inferior quality. Bedding was poor and reactions high at invert. Lateral support was poor. Pipes were overloaded in some locations by stockpiles
27-in. and 36-in. dia., RCP sewer in 10-ft. (?) deep ditch	Numerous longitudinal cracks, some greater than .01-in. wide. Transverse cracks wider than 5/8 - 3/4 in. at center of 10 ft. long pipe sections	4-12 in. of fine-grained bedding material over coarse gravel and cobbles; bedding not shaped to fit pipe	Bedding probably thin at center of pipe which caused a concentration of reaction to soil load

TABLE III-1
(Continued)

Examples of Conduit Failures (Spangler, 1974)

<u>Description of Conduit</u>	<u>Observed Damage</u>	<u>Installation Details</u>	<u>Conclusions</u>
42-in., RCP sewer	Pipe moved 33 in. laterally and 18 in. vertically after completion; No structural damage	Pipe installed in former swamp	Subsequent placement of crushed rock over site, and heavy compaction by vibration, caused liquefaction of swamp soils. Partially buoyant pipe drifted laterally and upwards in semi-fluid soil
60-in., RCP sewer under 27 ft. of fill	General collapse	Pipe and heavy junction box founded on loose, saturated sand. Backfill placed wet and without compaction	Settlement of junction box led to cracks in adjacent pipe sections; saturated sands and water flowed through cracks into pipe; erosion of sand eliminated support for pipe and led to destructive collapse of backfill.
18-in. VCP sewer bell-and-spigot	Longitudinal cracks and breaks in pipe wall and broken bells	Ledge rock present close to invert of pipe (few inches)	Bells probably rested on rock and pipe was therefore supported only at ends
24-in., unreinforced bell-and-spigot	Extensive failures; had to be replaced	Installed in trench that was 20 to 33% wider than specified. Haphazard excavation of bell holes	Wider trench resulted in overload on pipe; high reactions at bells
120-in. RCP storm sewer under 10-27 ft. of fill	Cracks in crown and spalling of invert	Bedding was 4-6 in. of crushed slag over hard, stiff clay; bedding was not shaped; trench was narrow (9-in. to each side of pipe); temporary stockpiles placed over completed backfill.	High reactions caused by poor bedding and loose backfill beneath haunches of pipe. Failure only occurred where temporary stockpile exceeded 10 ft.

movements (2), erosion of the concrete walls of the conduit (1), breakage of a cast iron pipe (1), and collapse of a discharge pipe as a result of a control-valve malfunction (1).

Petzer (1967) describes the foundation spreading and settlement during construction of the West Branch Dam in Ohio. The movement caused some of the joints of the triple-cell, concrete-box outlet conduit to open by as much as 8.5 inches. Cappleman (1967) reports that in the late 1950's, several Soil Conservation Service dams were also adversely affected by longitudinal spreading of their outlet conduits. In some conduits the joints between pipe sections had been pulled completely open. In others, the pipes had failed in longitudinal tension between joints.

Hale and Dyer (1963) report the collapse of a brick-lined sewer in England. They attributed the failure to ground-water flow along and into the sewer and resulting erosion of the surrounding soil. The failure caused the gross subsidence of the residential street below which the sewer had been lain.

From the above discussion it appears that:

1. Present methods of structural design of conduits are generally safe but are likely to be overconservative because there are so few reported cases of conduit failures resulting from soil overloads. The reported structural failures have been related primarily to improper bedding conditions.
2. Piping along the outlet conduit is a significant cause of unsatisfactory performance of earth dams.
3. Settlement and lateral spreading of conduits on compressible foundations beneath embankments can be of sufficient magnitude to open joints excessively or cause the conduit to fail in longitudinal tension if adequate expansion joints are not provided.

CHAPTER IV

FINITE-ELEMENT STUDIES OF EARTH

PRESSURES ON CONDUITS

A. Scope of Finite-Element Analyses

Finite-element analyses were performed to supplement the available field data in an effort to achieve a better understanding of the factors which affect the magnitude and the distribution of earth pressures on buried rigid conduits. The analyses were limited to conduit installations believed to be typical of Corps of Engineer practice. In general these limitations were:

1. Reinforced-concrete conduits
2. Circular, oblong and rectangular conduit shapes
3. Embankment or shallow trench installations
4. Relatively stiff soil or rock foundations
5. Compacted backfills
6. 30-ft maximum diameter or width of conduit
7. 600-ft maximum thickness of fill over conduit

The analyses were primarily expected to provide improved design guidance for the structural analysis of cast-in-place concrete conduits placed through or beneath embankment dams. However, it was hoped that the result of the analysis would give some insight into the more general problem of earth pressures on buried conduits, culverts, and pipes.

The finite-element analyses were performed using procedures developed at the University of California, Berkeley. The procedures of each analysis are described in detail in Appendix A. (Only the results of the analyses will be discussed in the main body of this report.) In general, the finite-element analyses proceeded as follows:

1. Each analysis was performed in a series of steps, which simulate the placement of the structure or a layer of backfill.
2. Values of Young's modulus and Poisson's ratio are assigned to each soil element during successive steps in the analysis and are adjusted in accordance with the calculated stresses in the element.
3. The parameters used to relate soil moduli to stresses are determined from triaxial compression and/or consolidation tests on the fill materials.

4. Linear elastic behavior was assumed for the conduit structure.
5. The analyses provide stresses and strains in each soil element and moments, thrusts, shears and deflections of each structural element for each step of the backfilling process.

The facilities of the University of California Computer Center (CDC 6400 Computer) were used to perform the finite-element computations.

B. Conduit Stiffness

Analytical studies, based on the theory of elasticity (such as by Burns and Richards, 1964), indicate that for the usual range of conduit sizes, the response of reinforced concrete conduits should essentially be independent of the flexural stiffness, EI (modulus of elasticity, E , multiplied by cross-sectional moment of inertia, I), of their walls. To confirm that this conclusion applies to conduits placed beneath deep soil backfills, exhibiting non-linear stress-strain behavior, preliminary finite-element analyses were performed.

1. Circular Conduits. Circular conduits of three diameters and various flexural stiffnesses were analyzed. As shown in Fig. IV-1, it was assumed that each conduit was supported by a depth of soil H_c , equal to the conduit diameter, D_c . Both the foundation soil and the backfill were assumed to be silty/clayey sand (Unified Soil Classification: SM-SC) at a relative compaction, RC , of 90 percent (based on the Standard Proctor compaction test). The maximum height of fill above the conduits, H , was limited to 600 feet. Calculated moments at the invert of each conduit, for various heights of fill and flexural stiffnesses, are shown in Fig. IV-2. The calculated moments have been normalized by dividing by the term, $\gamma H D_c^2$, where γ = total soil unit weight. The data indicates that for any of the conduit diameters and heights of fill, the invert moment varies by no more than 15 percent over a large range of flexural stiffnesses. In fact the range of corresponding wall thicknesses, t , shown in the figure (assuming an unreinforced concrete section, for which $I = t^3/12$) would be much larger than encountered in practice.

The results of the analyses have been summarized in a different manner in Fig. IV-3. The figure shows the maximum height of fill that could be placed over a conduit of any particular stiffness and diameter without exceeding an allowable compressive stress in the concrete equal to 2225 psi (assuming no compression steel reinforcement). The allowable stress would be typical of concrete with an ultimate strength of 5000 psi. Though approximate in nature because only one soil type and foundation condition were considered, Fig. IV-3 was used in subsequent analyses for selecting a suitable value of EI for the particular diameter of conduit being considered. The EI was conservatively selected as the value corresponding to an "allowable" height of fill equal to 600 feet.

2. Rectangular Conduits. Later studies of rectangular conduits provided additional data in support of the conclusion that the flexural stiffness of typical conduit sizes does not significantly affect the calculated earth pressures or moments. A 10-foot-square conduit was represented in an analysis by two methods. In the first, the conduit was

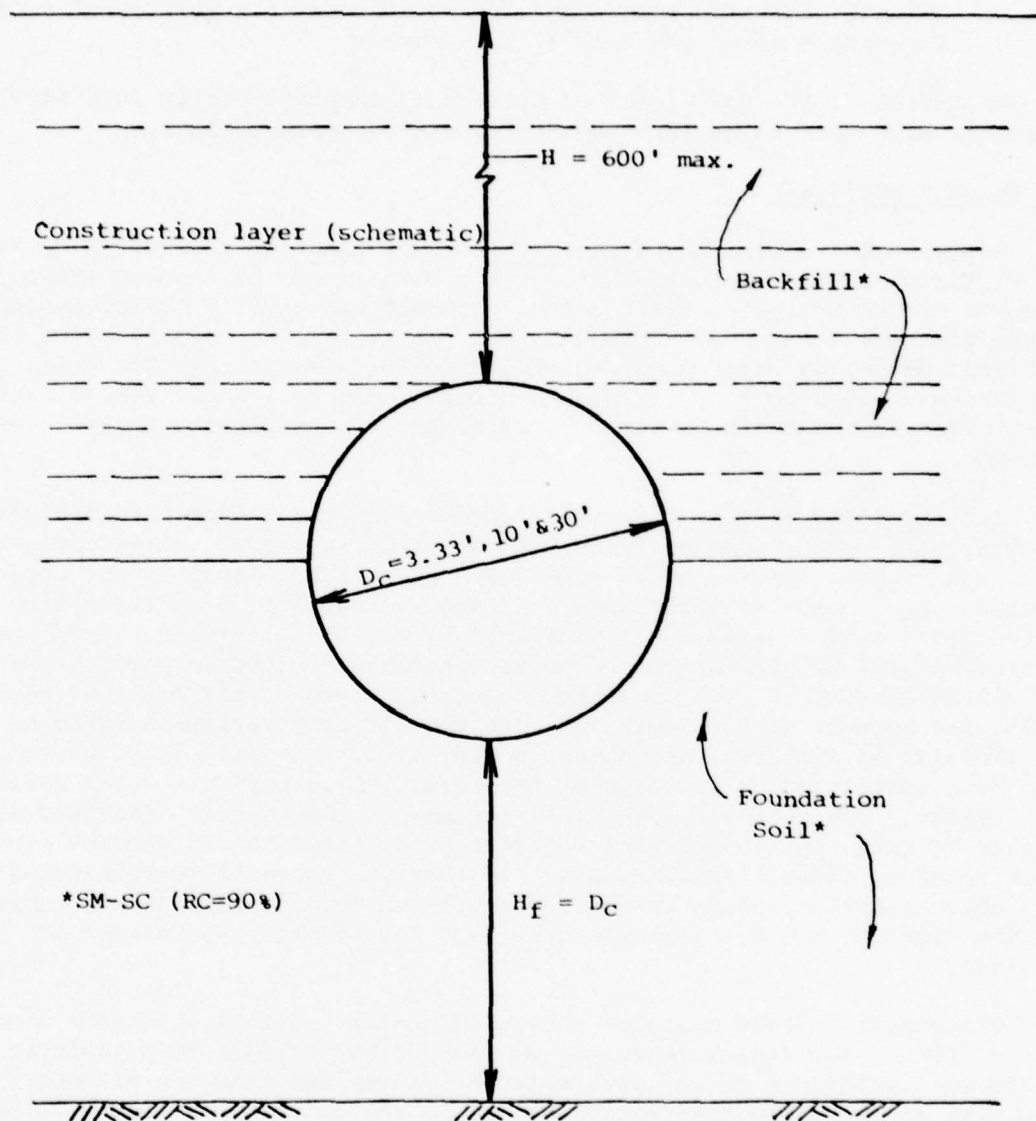


FIG. IV-1 CIRCULAR CONDUIT ANALYZED TO DETERMINE THE EFFECTS OF FLEXURAL STIFFNESS

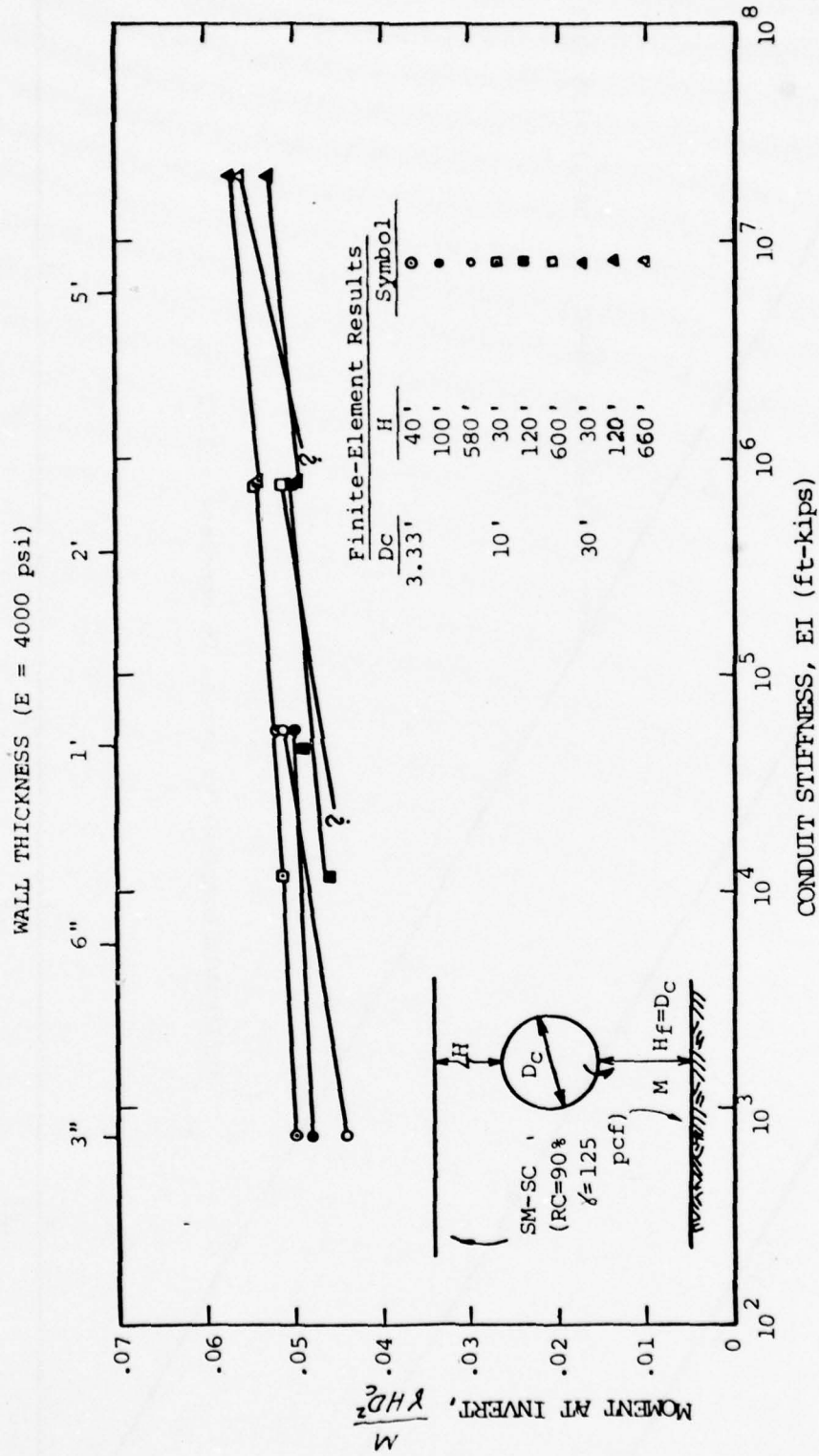


FIG. IV- 2 MOMENT AT INVERT OF CIRCULAR CONDUIT FOR VARIOUS CONDUIT STIFFNESS

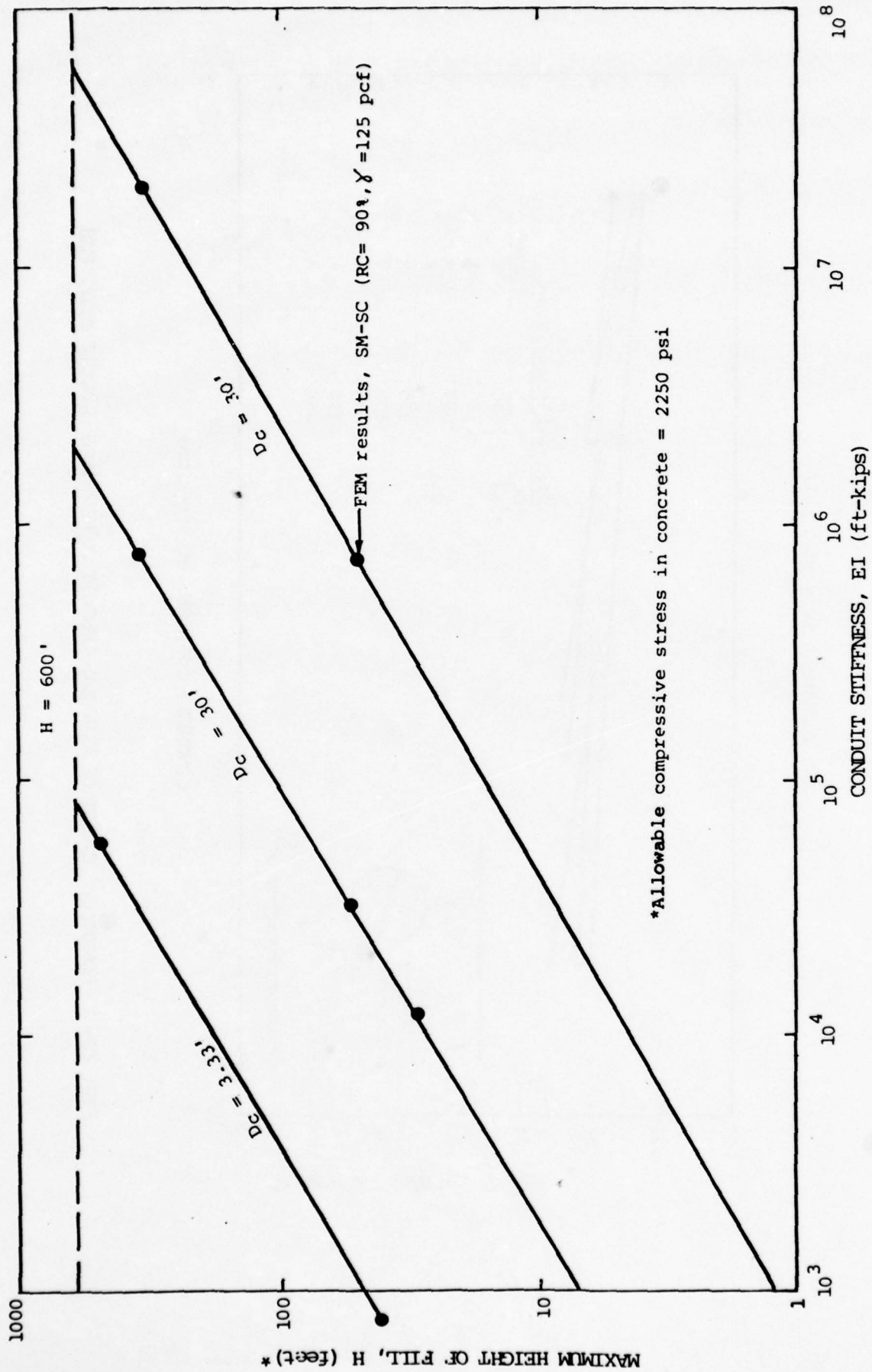


FIG. IV-3 MAXIMUM HEIGHT OF FILL VS. CONDUIT STIFFNESS, CIRCULAR CONDUIT

considered to be a solid plug and in the second it was given a conventional wall thickness and flexural stiffness. The resulting earth pressures under 600 feet of fill were essentially the same in both cases.

C. Soil Type

According to Marston-Spangler theory and elastic theory, the effect of soil type should not be great for rigid conduits in an embankment (projection) condition. However, since it is known that soil type and degree of compaction are quite important for flexible conduits, it was decided to investigate these factors with regard to concrete conduits by finite-element analyses.

1. Circular Conduits. The case of a 10-foot-diameter circular conduit with a shallow soil foundation ($H_f = 0.1D_c$) was chosen to study the effect of soil type. Soil parameters, representative of four soils, ranging from clays to gravels, at two densities each, were selected for study (see Appendix A). The foundation and backfill soils were assumed to be the same in each analysis. Fig. IV-4 shows how the moment at the crown of the conduit varies with height of the backfill for the various soil types. Fig. IV-5 shows how the normal pressure at the crown of the conduit varies with height of fill. Note that the data have been normalized in terms of γ , H , and D_c . Also, the data given are for changes in moment and normal pressure that occur after the backfill reaches the crown of the conduit. (The effects of backfilling to the top of a rigid conduit are small, they will be discussed later in this chapter.) It can be seen that the differences that exist for the various soil types are greatest at low heights of fill. As the backfill thickness approaches ten conduit diameters, the differences between soil types becomes relatively insignificant; for example, the crown moments vary by less than 15 percent. The results for two soil types, namely, the silty/clayey sand (SM-SC) at a relative compaction of 100 percent and the silty clay (CL) at 90 percent relative compaction can be seen to be approximate upper and lower bounds, respectively, to the majority of the calculated moments over the entire range of fill heights. The CL (RC = 90%) soil provides a softer cushion beneath the invert and thus results in slightly smaller (normalized) moments in the culvert. The two soil types are also representative of the calculated crown pressures for the various soils studied.

The distribution of moments and normal pressures around the conduit are shown in Fig. IV-6 and IV-7 for the SM-SC (RC = 100%) and CL (RC = 90%) soils at two heights of fill. Note that the calculated values at any particular point on the conduit have been normalized by dividing by the magnitude of the corresponding value at the crown. It can be seen that the differences in the results for the different soil types are small, particularly at the larger fill heights.

Other analyses not presented herein have shown that the effects of soil type, in terms of both magnitude and distribution of pressures, moments, and forces on a conduit are even less for greater soil foundation depths.

2. Rectangular Conduits. The effect of backfill-soil type was also investigated for the case of a 10-foot-square conduit underlain by a shallow

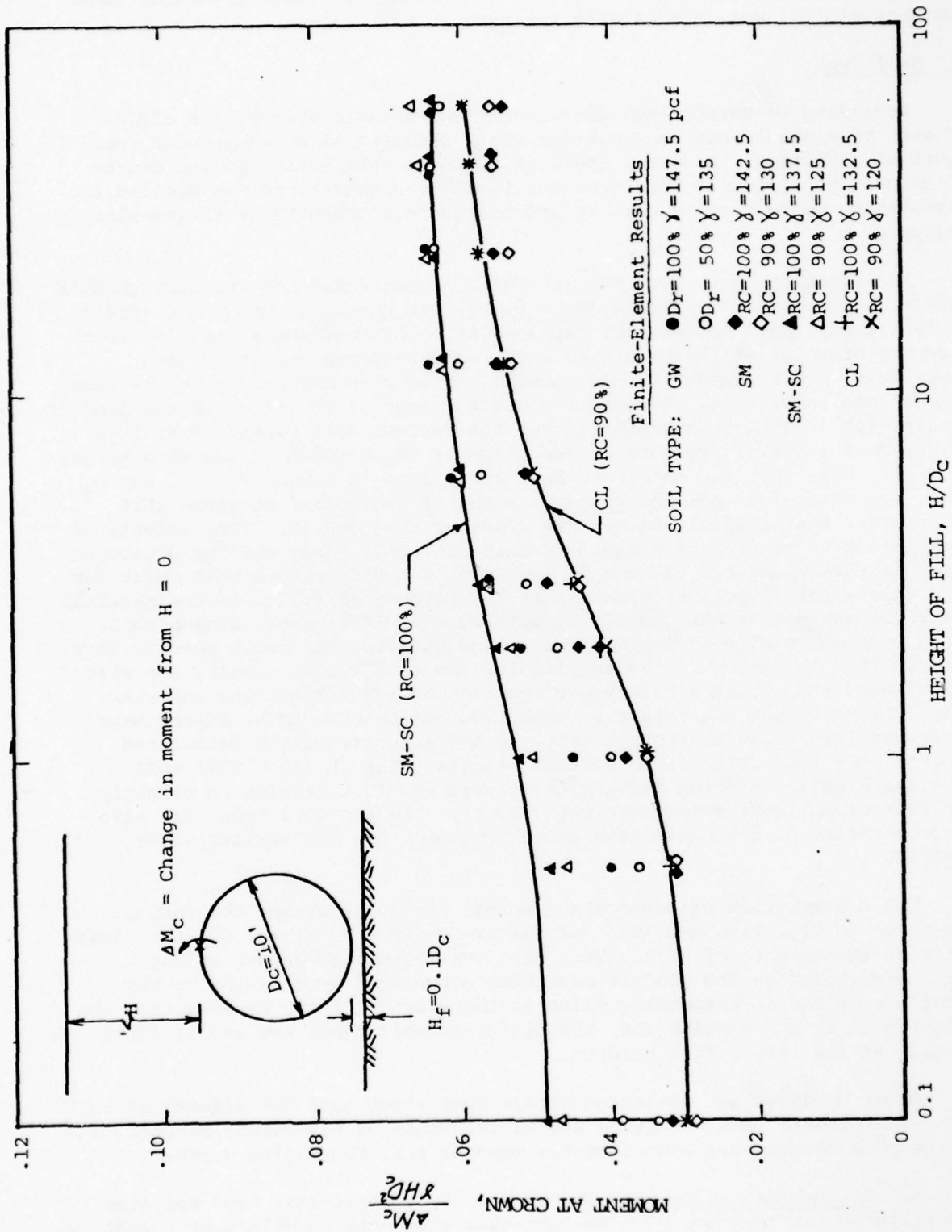


FIG. IV-4 MOMENT AT CROWN OF CIRCULAR CONDUIT FOR VARIOUS SOIL TYPES

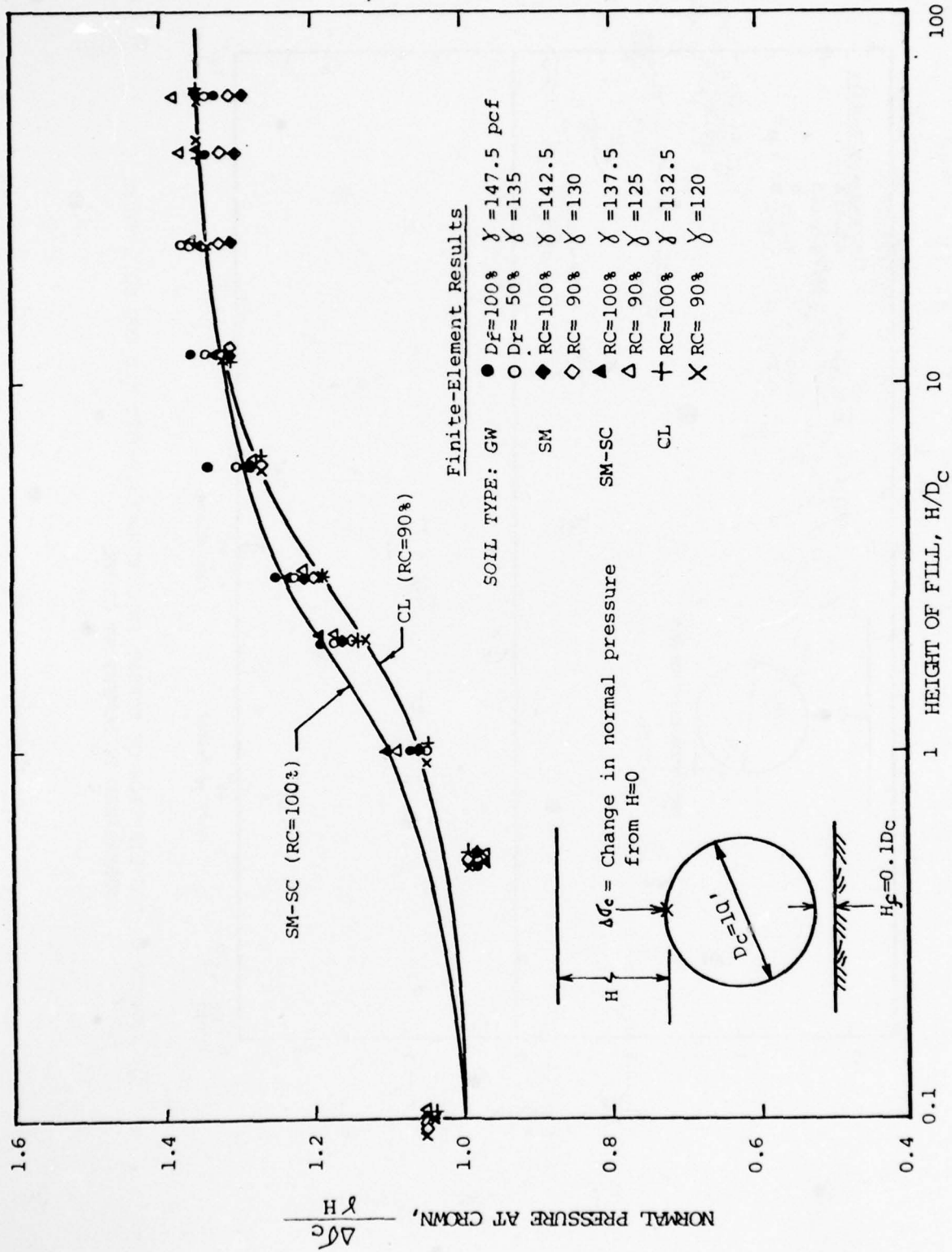


FIG. IV-5 NORMAL PRESSURE AT CROWN OF CIRCULAR CONDUIT FOR VARIOUS SOIL TYPES

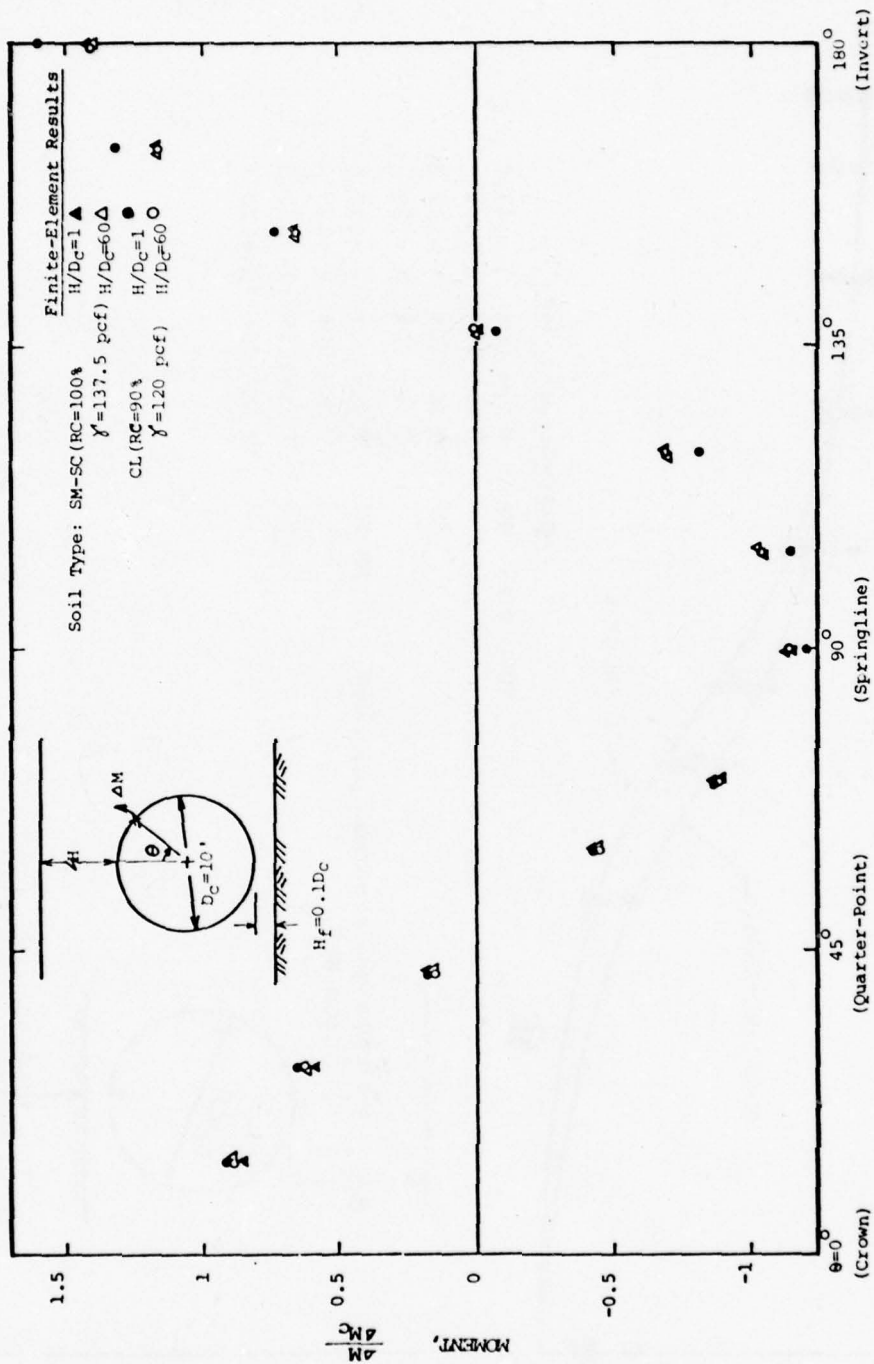


FIG. IV-6 DISTRIBUTION OF MOMENT IN CIRCULAR CONDUIT FOR TWO SOIL TYPES
(NORMALIZED TO MOMENT AT CROWN)

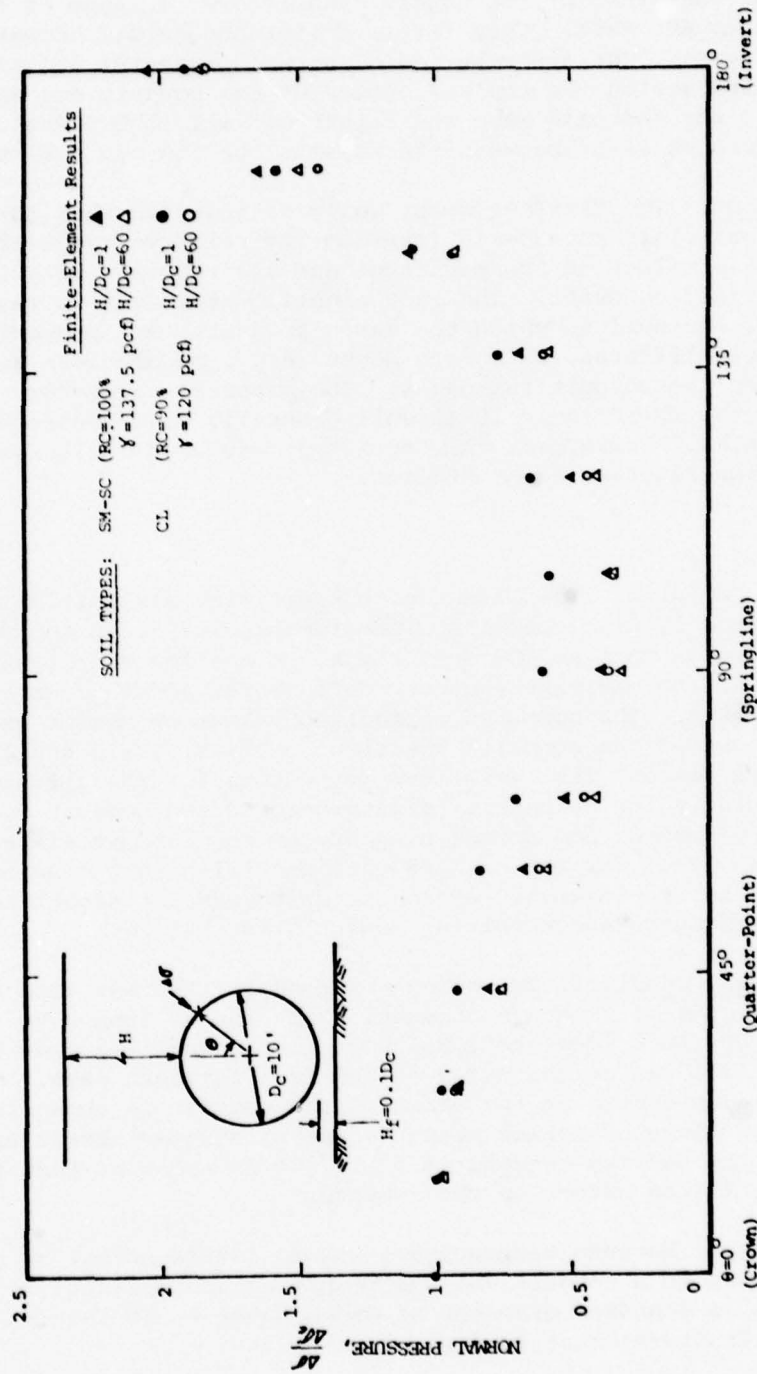


FIG. IV-7 DISTRIBUTION OF NORMAL PRESSURE ON CIRCULAR CONDUIT FOR TWO SOIL TYPES
 (NORMALIZED TO NORMAL PRESSURE AT CROWN)

soil foundation (H_f equals one foot). The SM-SC (RC = 100%) and CL (RC = 90%) soils were used in the analyses since they had generally given extreme results in the circular conduit studies. Fig. IV-8 shows the variation in normal pressure at the crown of the square conduit over a range of fill height to as much as 600 feet. Very little difference exists between results for the two soil types. The distribution of normal pressures and side-shear stresses (shear stresses on the top and bottom of the conduit are small) are shown in Fig. IV-9 for the case when the height of fill is 600 feet. No significant differences exist between the results for the two soil types.

3. Conclusions. The finite-element analyses indicate that for the type of backfill materials considered (minimum 90% relative compaction), soil type has little effect on the magnitude and distribution of soil pressures on buried, rigid conduits. The only significant effect is caused by the unit weight of the soil to which the earth pressures are proportional. The effects of soil stiffness, which are never large, become less as the height of fill over the conduit increases. The material parameters representative of the SM-SC (RC = 100%) soil generally give conservative (upper bound) results. Therefore, this soil type was used exclusively in the remainder of the finite-element studies.

D. Conduit Size

1. Circular Conduits. The effect of conduit size was initially studied by analyzing circular conduits with diameters of 3, 10 and 30 feet, and covered by fills as much as 600 feet thick. A shallow soil foundation ($H_f = 0.1D_c$) was used to maximize whatever differences might occur as a result of conduit size. The computed normalized values of moment and normal pressure at the crown of the conduits are shown in Figs. IV-10 and IV-11 for the various conduit sizes. The variations in results for the different sizes are small, particularly for heights of fill exceeding ten conduit diameters. The distributions of moment and normal pressure on the conduit are shown in Figs. IV-12 through IV-13 for the case of maximum fill height (600 feet). The data indicate that the diameter of the conduit does not significantly affect the earth pressures and resulting moment distributions.

2. Rectangular Conduits. The effect of conduit size was also studied by considering the case of a square conduit, which ranged from 3 to 30 feet in width. The SM-SC (RC = 100%) soil was used in the analyses and the maximum height of fill was on the order of 600 feet for each case. The variations in normal pressure at the crown of the conduit is shown in Fig. IV-14. The distributions of normal pressure and side-shear stress are shown on Fig. IV-15 for the maximum heights of fill. It is apparent that the size of the conduit has little effect on the results.

3. Conclusions. Because the analyses showed little effect of conduit size on the pressures on a conduit and the resulting (normalized) values of moments and forces, a standard diameter or width equal to 10 feet was used in the subsequent finite-element studies.

E. Depth of Soil Foundation

1. Circular Conduits. The influence of the thickness of the soil foundation beneath a circular conduit (i.e., the depth to rock or other

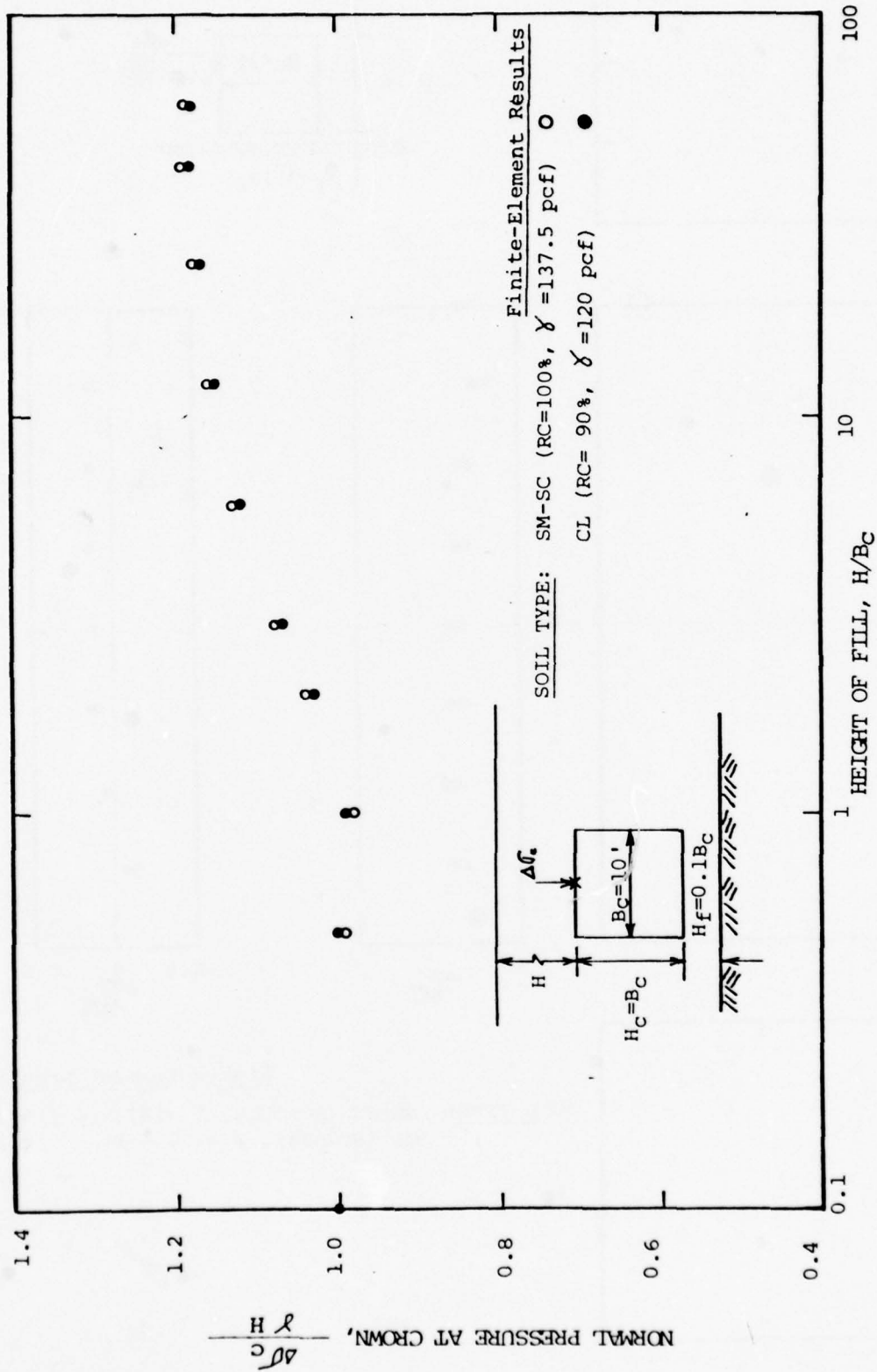


FIG. IV-8 NORMAL PRESSURE AT CROWN OF SQUARE CONDUIT FOR TWO SOIL TYPES

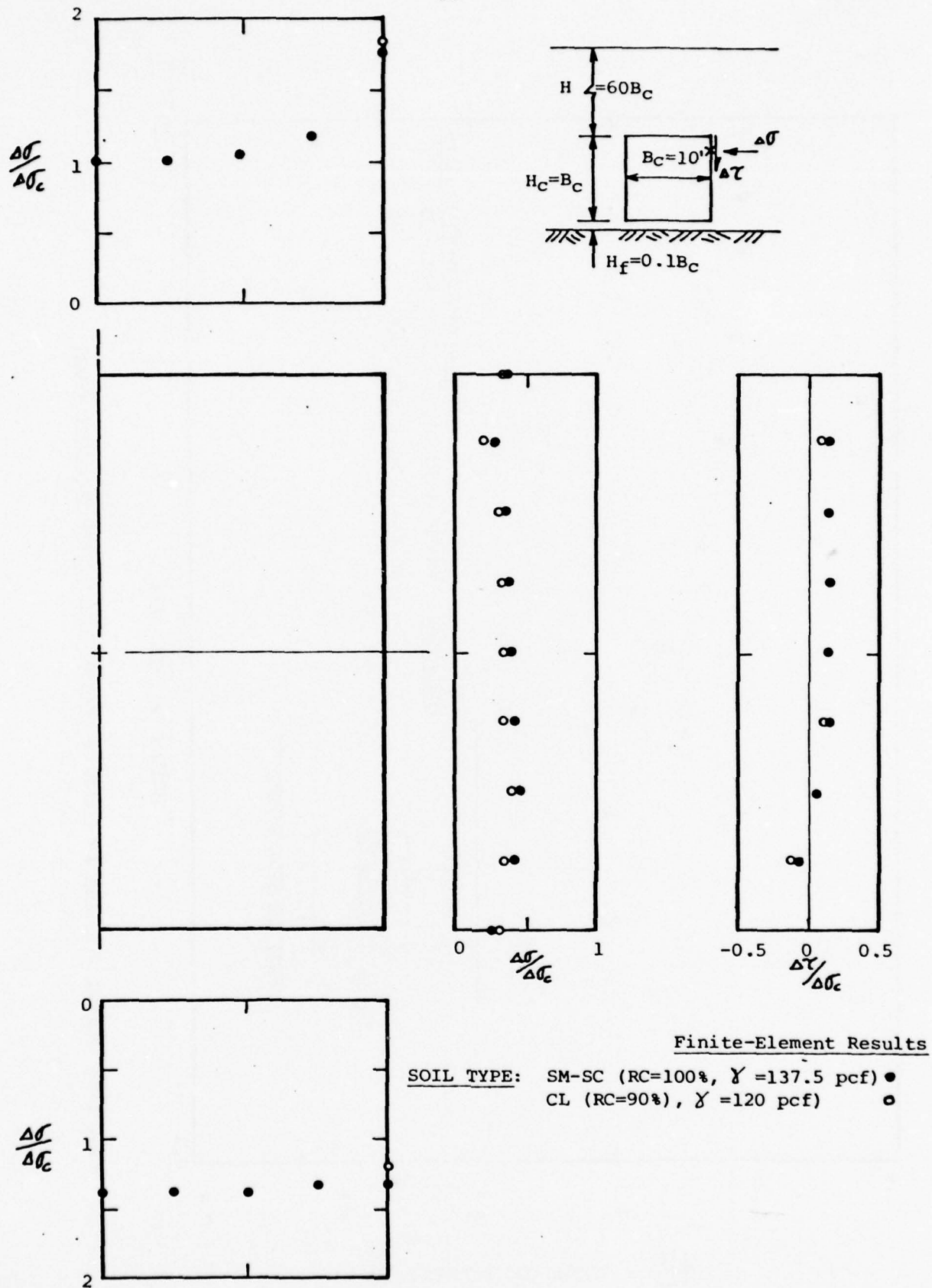


FIG. IV-9 DISTRIBUTION OF NORMAL PRESSURE, $\Delta\sigma$, AND SIDE-SHEAR STRESS, $\Delta\tau$, ON SQUARE CONDUIT FOR TWO SOIL TYPES (NORMALIZED TO NORMAL PRESSURE AT CROWN)

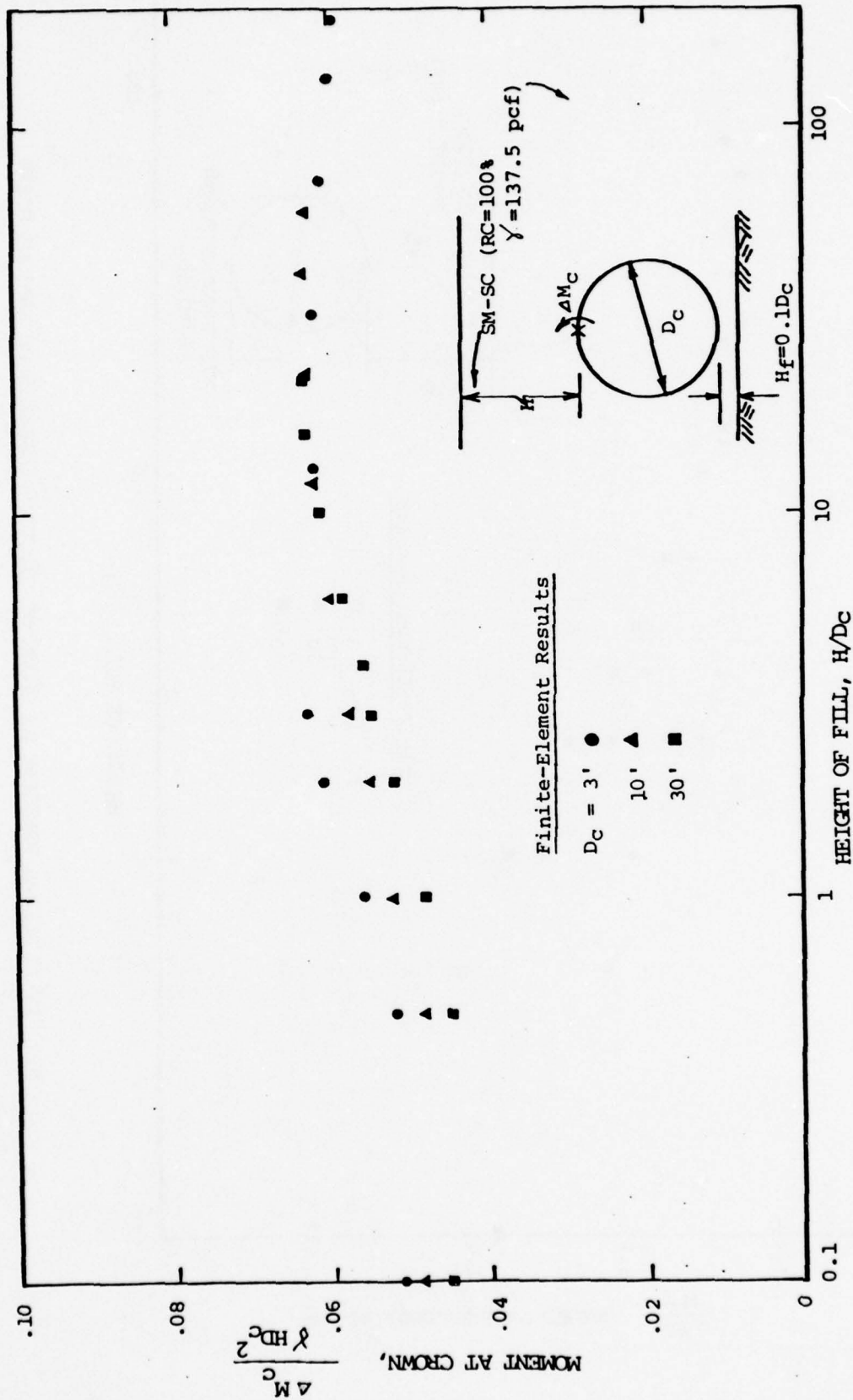


FIG. IV-10 MOMENT AT CROWN OF CIRCULAR CONDUITS OF VARIOUS SIZES

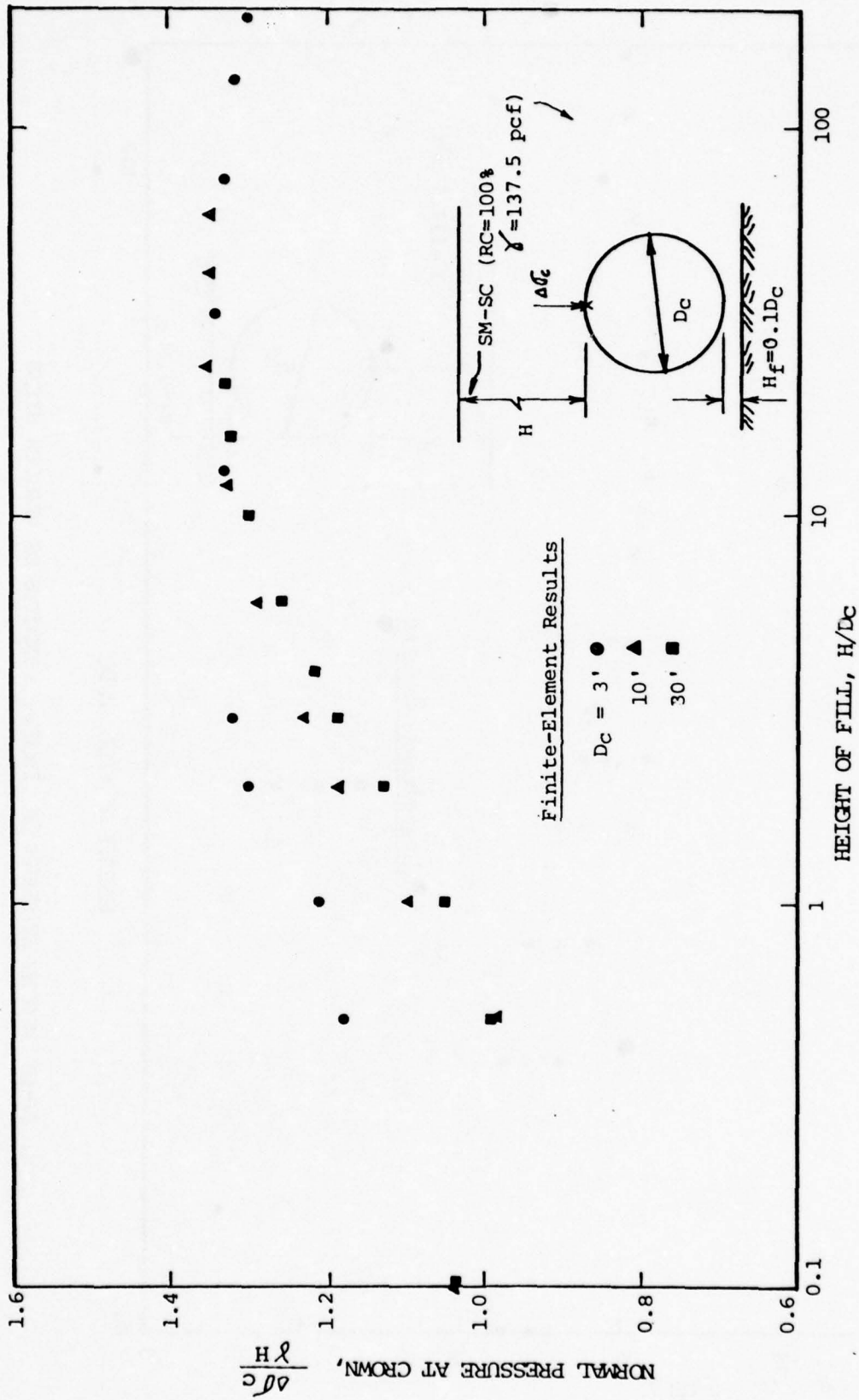


FIG. IV-11 NORMAL PRESSURE AT CROWN OF CIRCULAR CONDUITS OF VARIOUS SIZES

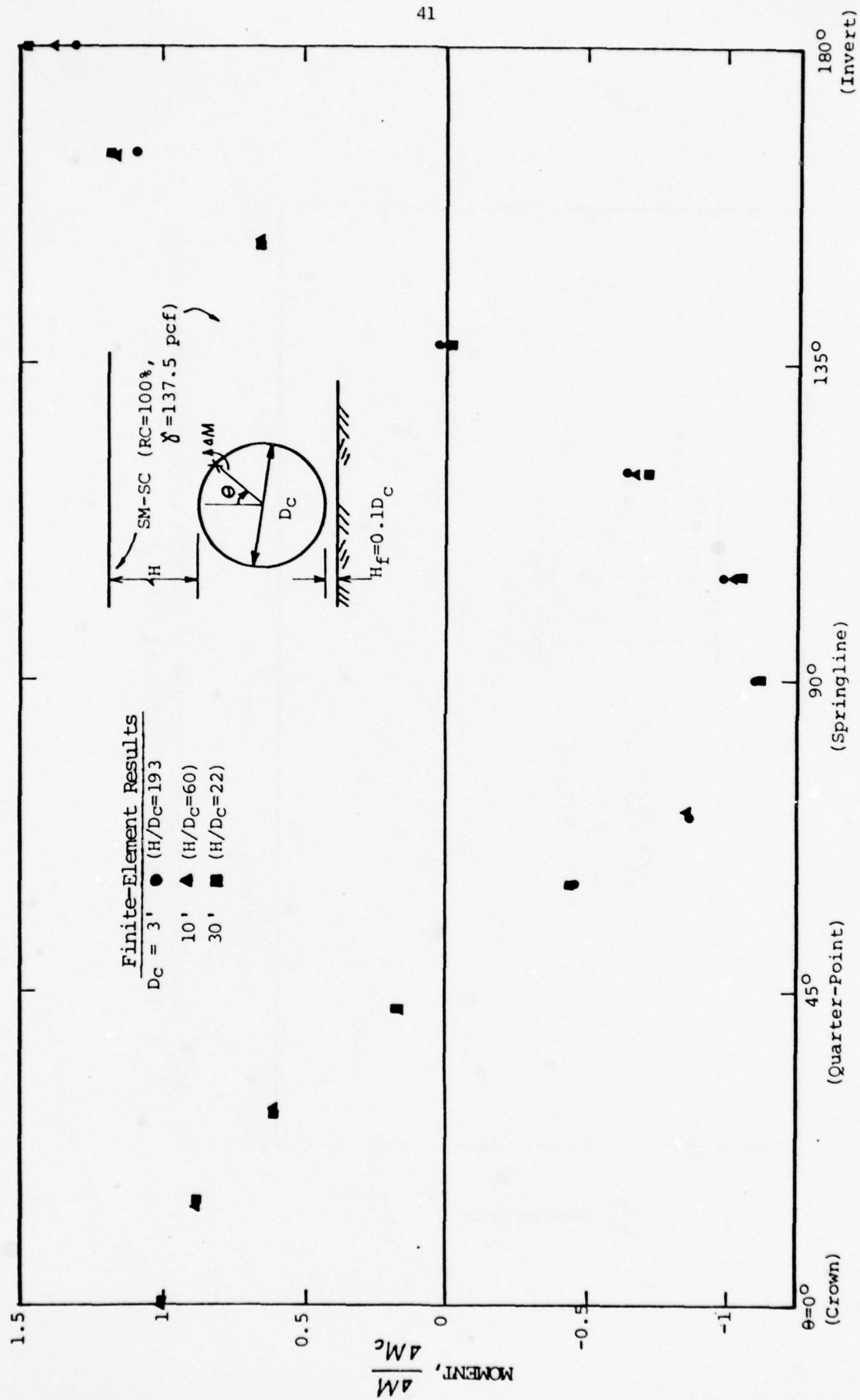


FIG. IV-12 DISTRIBUTION OF MOMENT IN CIRCULAR CONDUITS OF VARIOUS SIZES (NORMALIZED TO MOMENT AT CROWN)

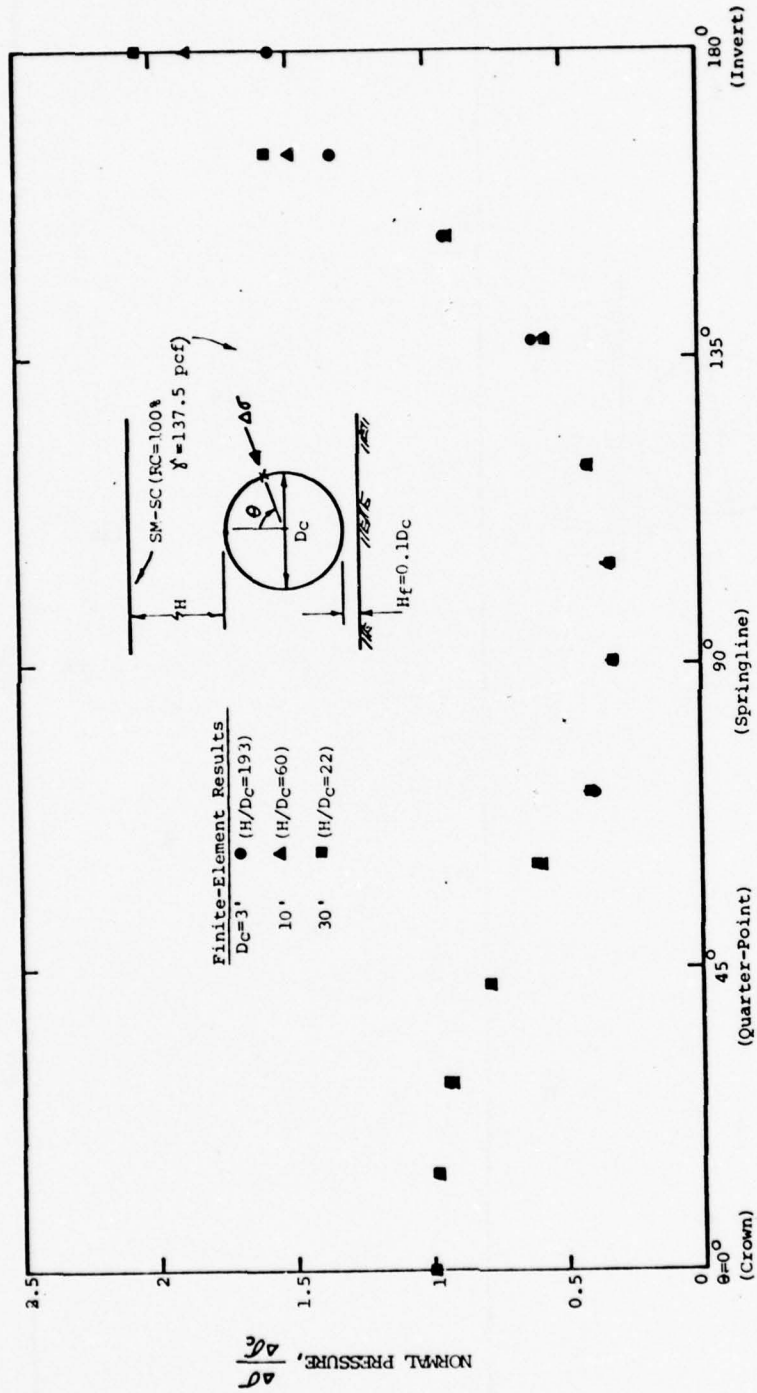


FIG. IV-13 DISTRIBUTION OF NORMAL PRESSURE ON CIRCULAR CONDUITS OF VARIOUS SIZES
(NORMALIZED TO NORMAL PRESSURE AT CROWN)

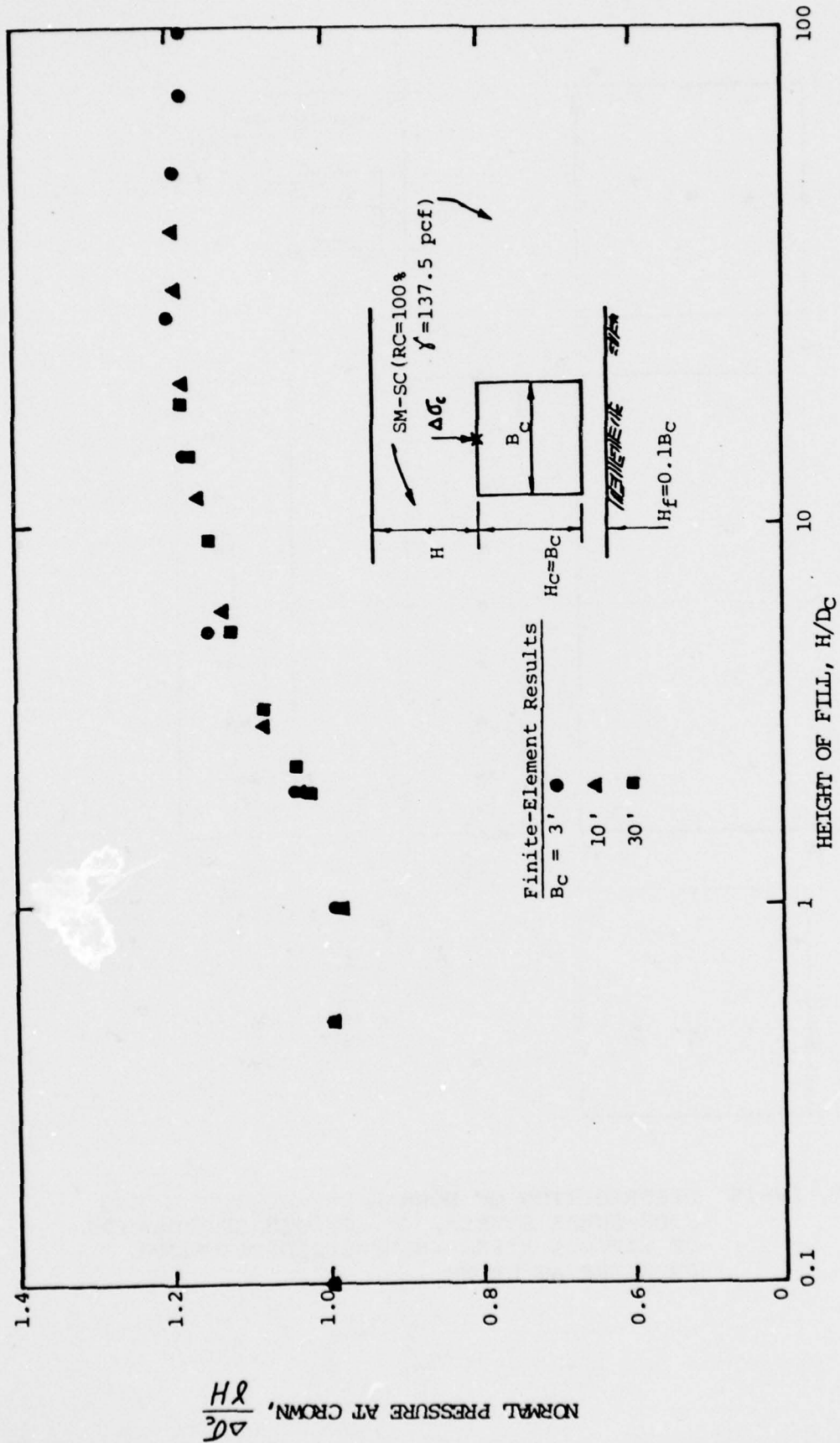


FIG. IV-14 NORMAL PRESSURE AT CROWN OF SQUARE CONDUITS OF VARIOUS SIZES

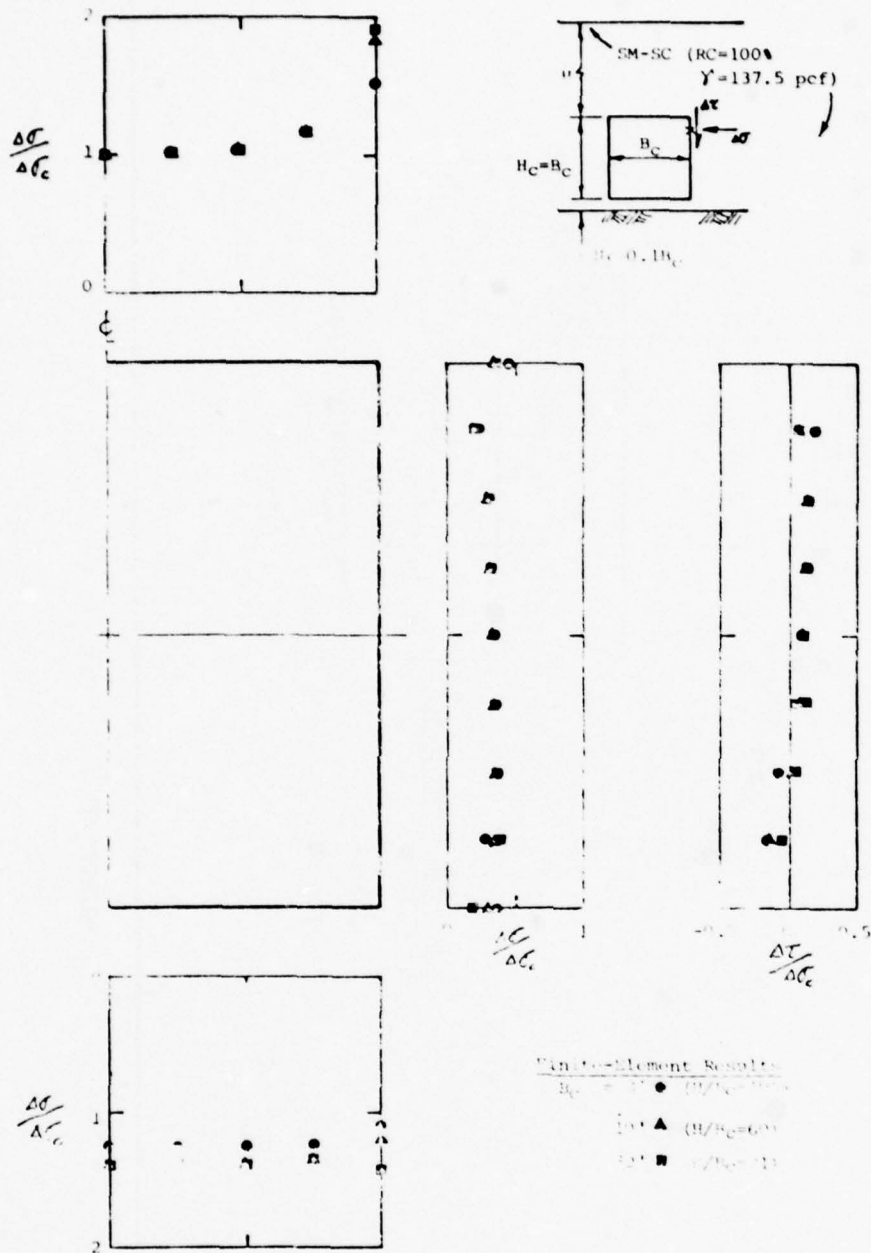


FIG. IV-15 DISTRIBUTION OF NORMAL PRESSURE, $\Delta\sigma$, AND SIDE-SHEAR STRESS, $\Delta\tau$, ON SQUARE CONDUITS OF VARIOUS SIZES (NORMALIZED TO NORMAL PRESSURE AT CROWN)

incompressible material) can be illustrated by the results of an analysis of a 10-foot-diameter conduit covered by a maximum of 600 feet of SM-SC (RC = 100%) backfill. Soil foundation depths of one foot and 30 feet were studied. The results, in terms of magnitude and distribution of earth pressures and the resulting moments on the conduits, are presented in Figs. IV-16 through IV-19. Clearly the shallow soil foundation results in much more severe moments and forces in the conduit, particularly near the invert. The adverse effects of the shallow soil foundation are caused by two factors. First, the earth load on the conduit is greater than for the deep soil foundation, as evidenced by the magnitude of the normal pressure at the crown of the conduit (Fig. IV-16). The larger pressure undoubtedly results from increased differential settlement between the conduit and the adjacent soil. Because the soil above the conduit settles less than the soil to either side, shearing forces develop and additional loads are transmitted to the top of the conduit. The second and more important factor related to shallow soil foundations is the increased reaction at the invert which causes very large moments and shears in the conduit. The thickness of soil immediately below the invert is small and the soil is restrained from lateral movement by the underlying base. Thus the soil acts as a semi-rigid material with a much higher modulus of deformation than the adjacent (thicker) soil beneath the sides of the conduit. The conduit reacts in a manner analogous to a beam on an elastic foundation which is composed of two materials of different stiffness. The foundation pressures on the beam (conduit) are greatest where the foundation is stiffest (invert). Fig. IV-18 shows that the soil pressure at the invert of the conduit on the shallow foundation is nearly twice that of the conduit on deep soil. As a result the moment at the invert and the shear near the lower quarter-points are increased by almost 60 percent.

2. Rectangular Conduits. The influence of foundation depth is also significant for rectangular conduits. Results of the analysis of a 10-foot-square conduit are shown in Figs. IV-20 and IV-21. In Fig. IV-20, it can be seen that the normal pressure at the crown of the conduit is greater for the shallow foundation case. The distributions of normal pressure and side-shear stress are less favorable for the shallow foundation as shown in Fig. IV-21. Because the normal pressures on the sides of the conduit are less for the shallow foundation, there would be a smaller resisting moment available for offsetting the moment caused by the vertical loads on the top and bottom of the conduit. The shear stresses on the sides of the conduit act essentially downward for the shallow foundation case and an increase of the reaction at the base would be expected. The distribution of the base reaction is also changed and the largest pressures occur at the centerline of the conduit on a shallow soil foundation. As a result, the invert moment would be increased over that for a conduit on a deep soil foundation. However, the increase in invert moment would not be as pronounced as it is for circular conduits because there is no similar large concentration of soil reaction at the invert.

3. Conclusions. The analyses indicate that the depth of the soil foundation is an important factor which can significantly affect the earth pressures on a buried conduit. The analyses confirm the numerous field observations of pipe failures caused by the presence of rock or other hard material at a shallow depth below the invert of pipe.

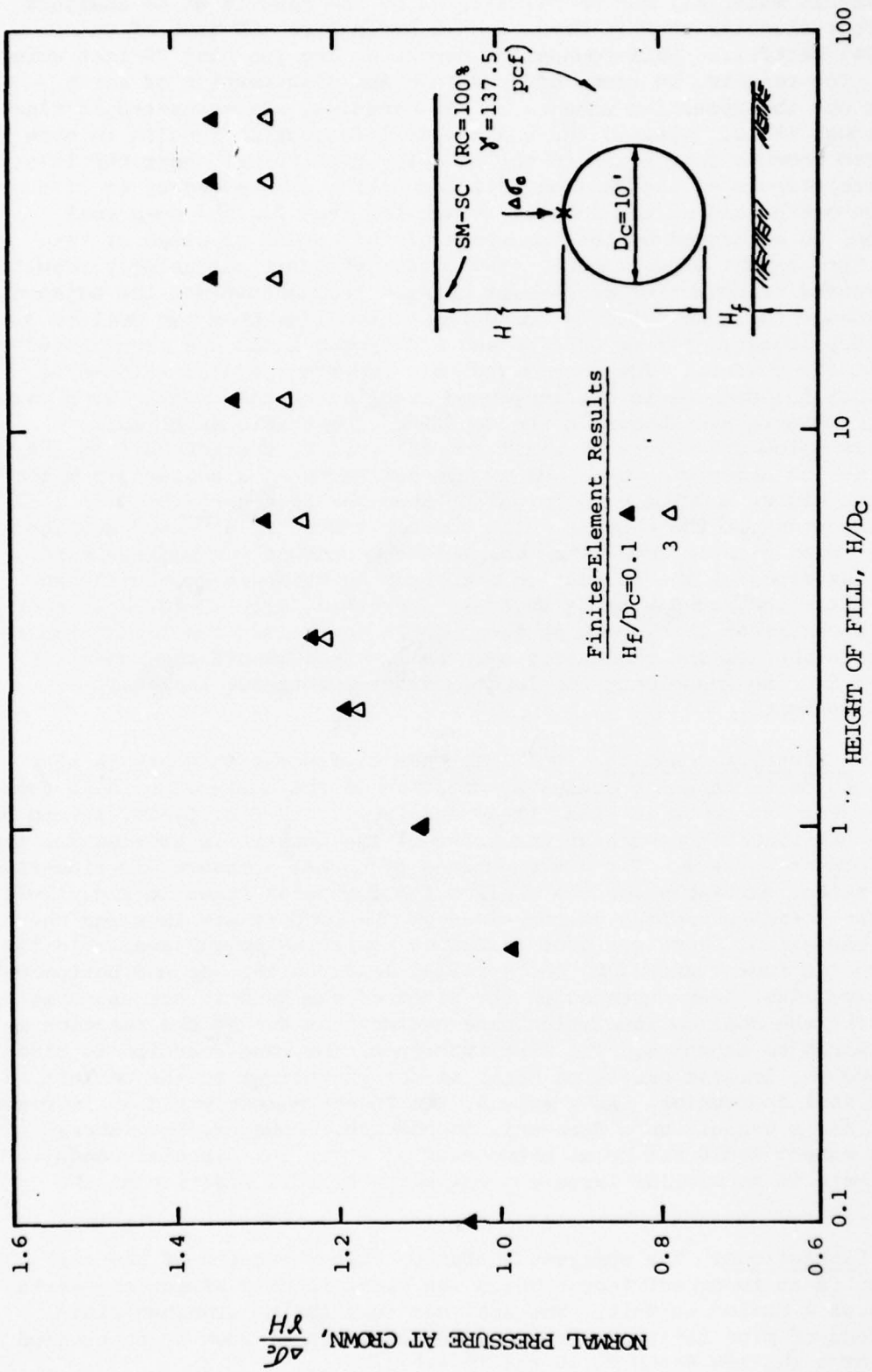


FIG. IV-16 NORMAL PRESSURE AT CROWN OF CIRCULAR CONDUIT FOR DIFFERENT SOIL FOUNDATION DEPTHS

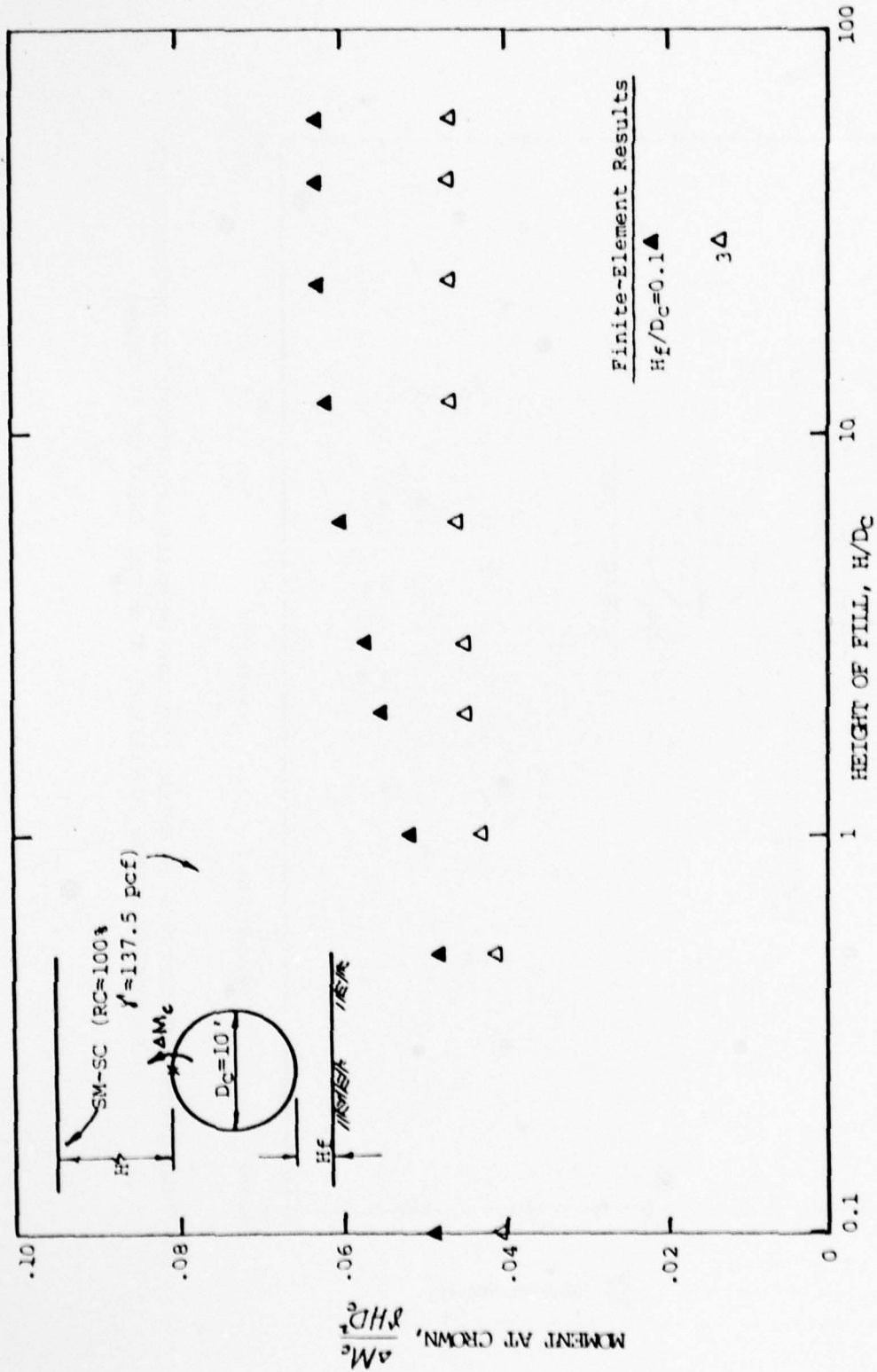


FIG. IV-17 MOMENT AT CROWN OF CIRCULAR CONDUIT FOR DIFFERENT SOIL FOUNDATION DEPTHS

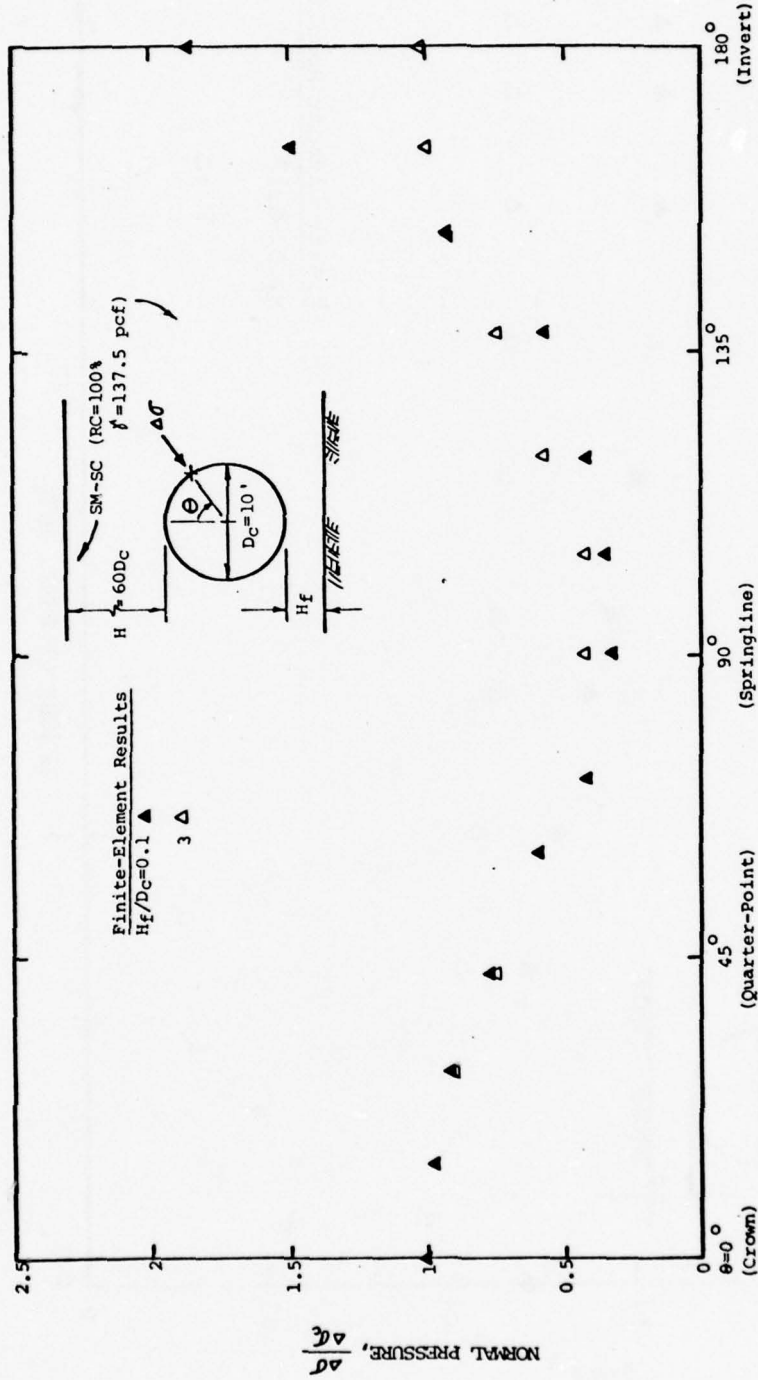


FIG. IV-18 DISTRIBUTION OF NORMAL PRESSURE ON CIRCULAR CONDUIT FOR DIFFERENT SOIL FOUNDATION DEPTHS (NORMALIZED TO NORMAL PRESSURE AT CROWN)

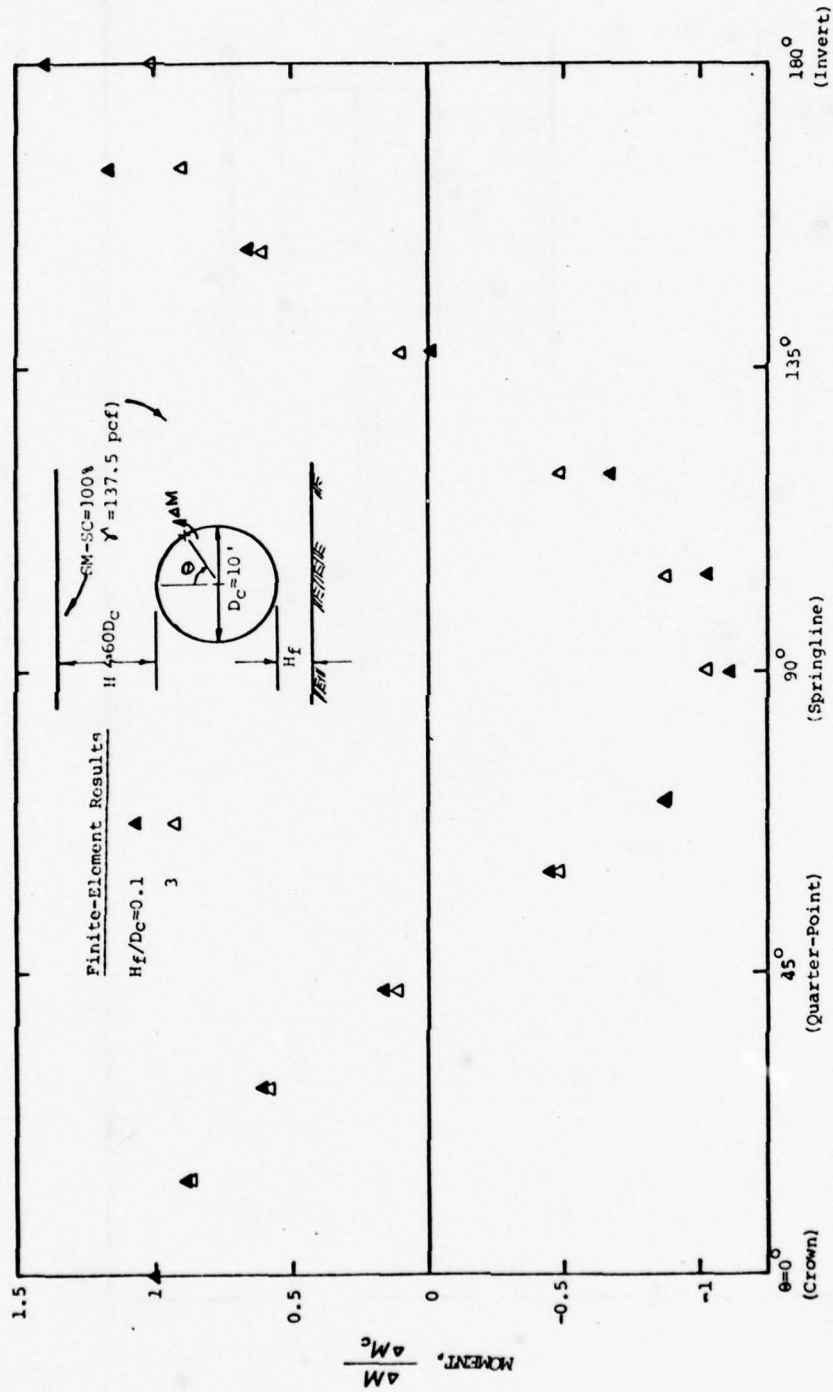


FIG. IV-19 DISTRIBUTION OF MOMENT IN CIRCULAR CONDUIT FOR DIFFERENT SOIL FOUNDATION DEPTHS (NORMALIZED TO MOMENT AT CROWN)

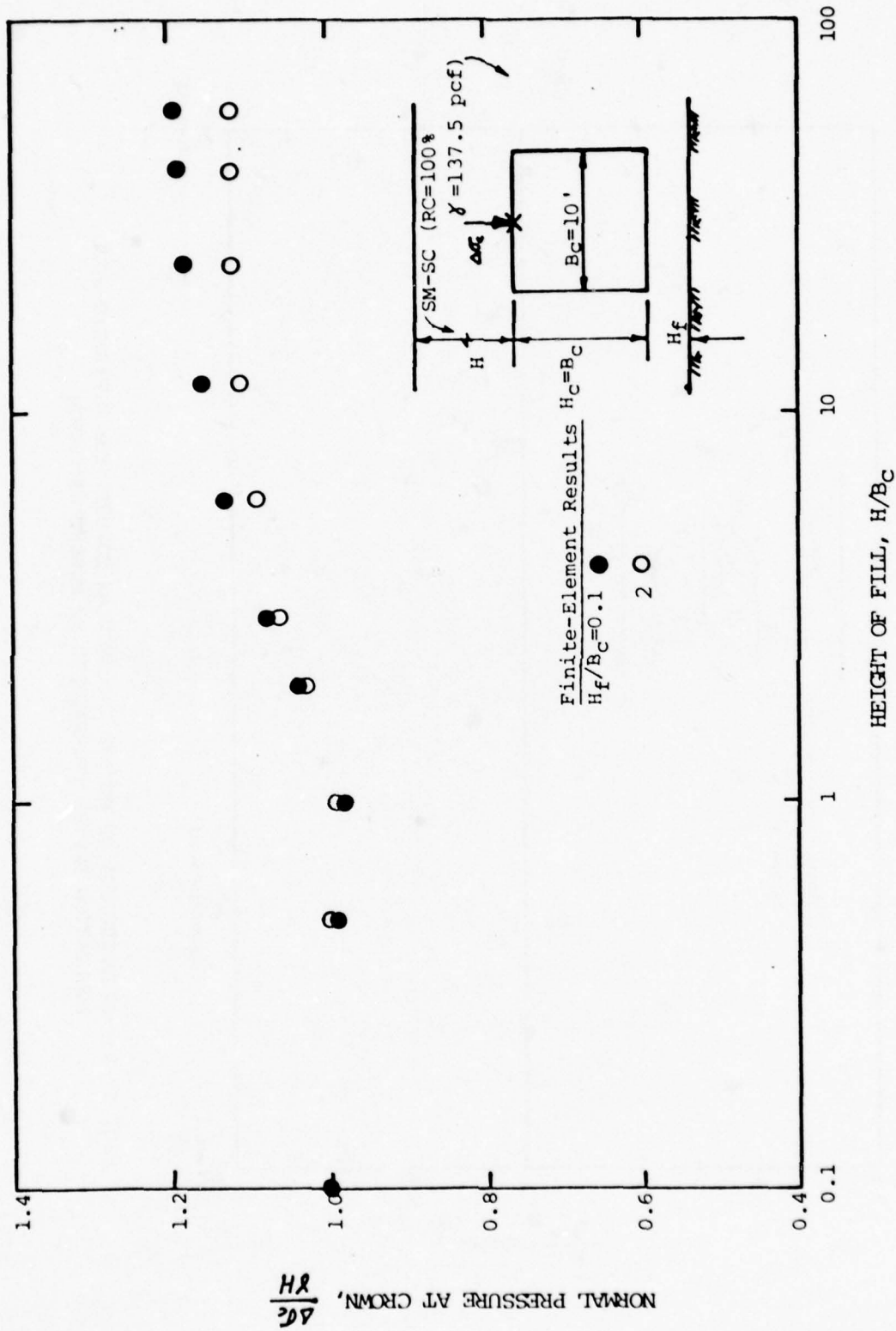


FIG. IV-20 NORMAL PRESSURE AT CROWN OF SQUARE CONDUIT FOR DIFFERENT SOIL FOUNDATION DEPTHS

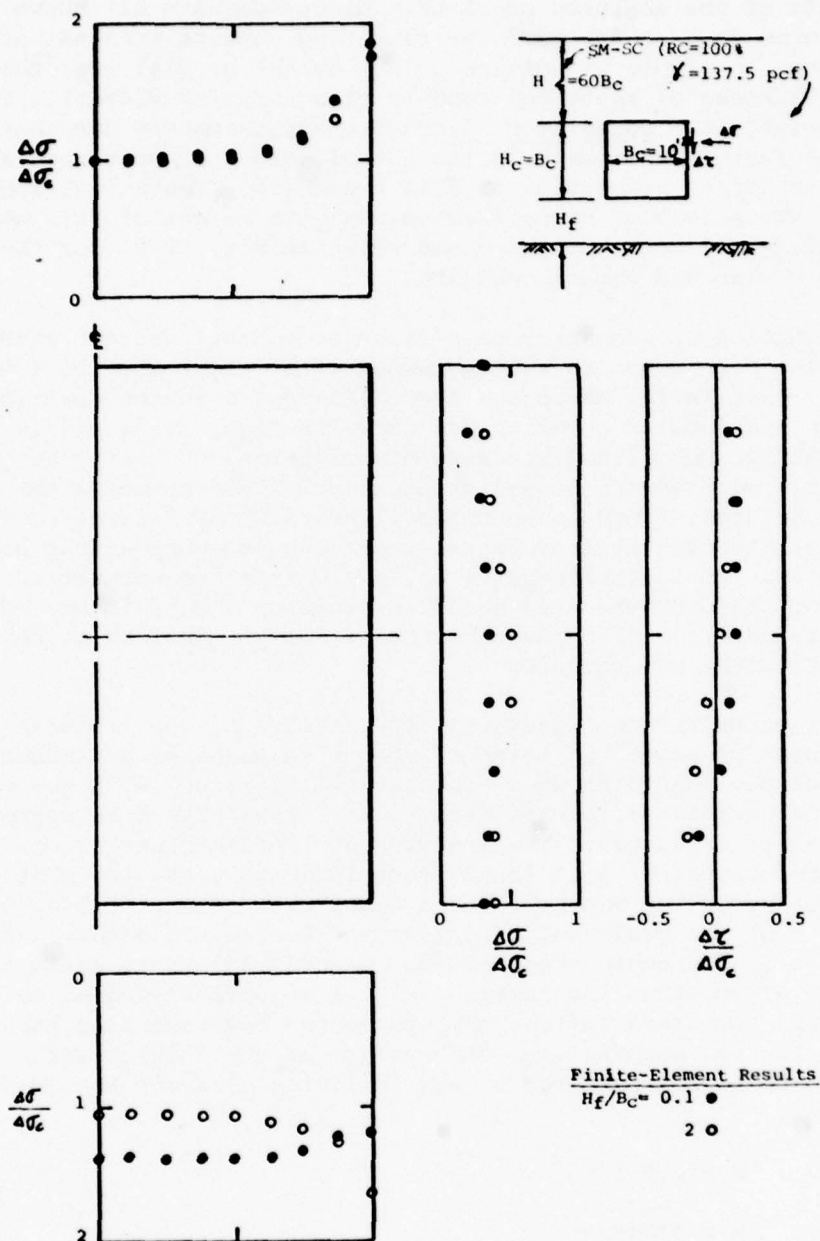


FIG. IV-21 DISTRIBUTION OF NORMAL PRESSURE, $\Delta\sigma$, AND SIDE STRESS, $\Delta\tau$, ON SQUARE CONDUIT FOR DIFFERENT SOIL FOUNDATION DEPTHS (NORMALIZED TO NORMAL PRESSURE AT CROWN)

F. Height of Fill Cover

The results of the analyses previously discussed have all shown that the soil pressures on a conduit and the resulting moments increase at a greater rate than in simple proportion to the height of fill over the conduit until a fill thickness of about ten conduit diameters (or widths). For greater fill heights the normalized values are approximately constant, thus indicating that further increases in the actual values of pressures and moments occur in direct proportion to fill thickness. Convenient approximations to the variations of normalized values with height of fill can be achieved by straight lines, such as those shown in Fig. IV-22 for the crown pressures on circular and square conduits.

The distribution of pressures on a circular conduit and the resulting moments have also been shown to vary somewhat with height of fill (see Figs. IV-6 and IV-7). Similarly, there are some differences in the distributions of pressures on rectangular conduits, as shown in Figs. IV-23 and IV-24. It is apparent that the normalized pressure distributions for large heights of fill are slightly more severe (cause greater normalized moments) than those for small fill heights. This is so because the ratio of lateral pressures on the conduit to the vertical pressures decreases somewhat as the height of fill increases. It is conservative to assume that the normalized distributions of normal pressures and shear stresses on a conduit are equal to the values representative of a large height of fill regardless of the actual thickness of fill over the conduit.

Until this point in the discussion, the results of the finite-element analyses have been presented in terms of change in pressure and moment in the conduit from the condition where the backfill is level with the top of the conduit. The effects of backfilling to the crown have been neglected for the reasons now discussed. The analyses of 10-foot-diameter conduits on shallow (one-foot-thick) soil foundations indicate that, for most of the soil types considered, the moments at the completion of backfilling to the crown level ($H = 0$) are small and of opposite sense to those that later occur as fill is placed above the conduit. Clearly for these soils it is conservative to assume that the initial ($H = 0$) moments are equal to zero. For the few soils that have initial moments of the same sense as those resulting from further backfilling, the neglect of the initial value is not of any consequence as demonstrated by the following data for the SM-SC (RC = 100%) soil:

$$\text{At } H = 0, \quad M = 0.0012YD_c^3 \quad (\text{IV-1})$$

$$\text{At } H > 0, \quad \Delta M \geq 0.05YHD_c^2 \quad (\text{IV-2})$$

Therefore,

$$\text{at } H > 0, \quad M \geq 0.0012YD_c^3 + 0.05YHD_c^2 \quad (\text{IV-3})$$

$$\text{and,} \quad M \geq 0.0012YD_c^3 + 0.05YD_c^3 \cdot \left(\frac{H}{D_c}\right) \quad (\text{IV-4})$$

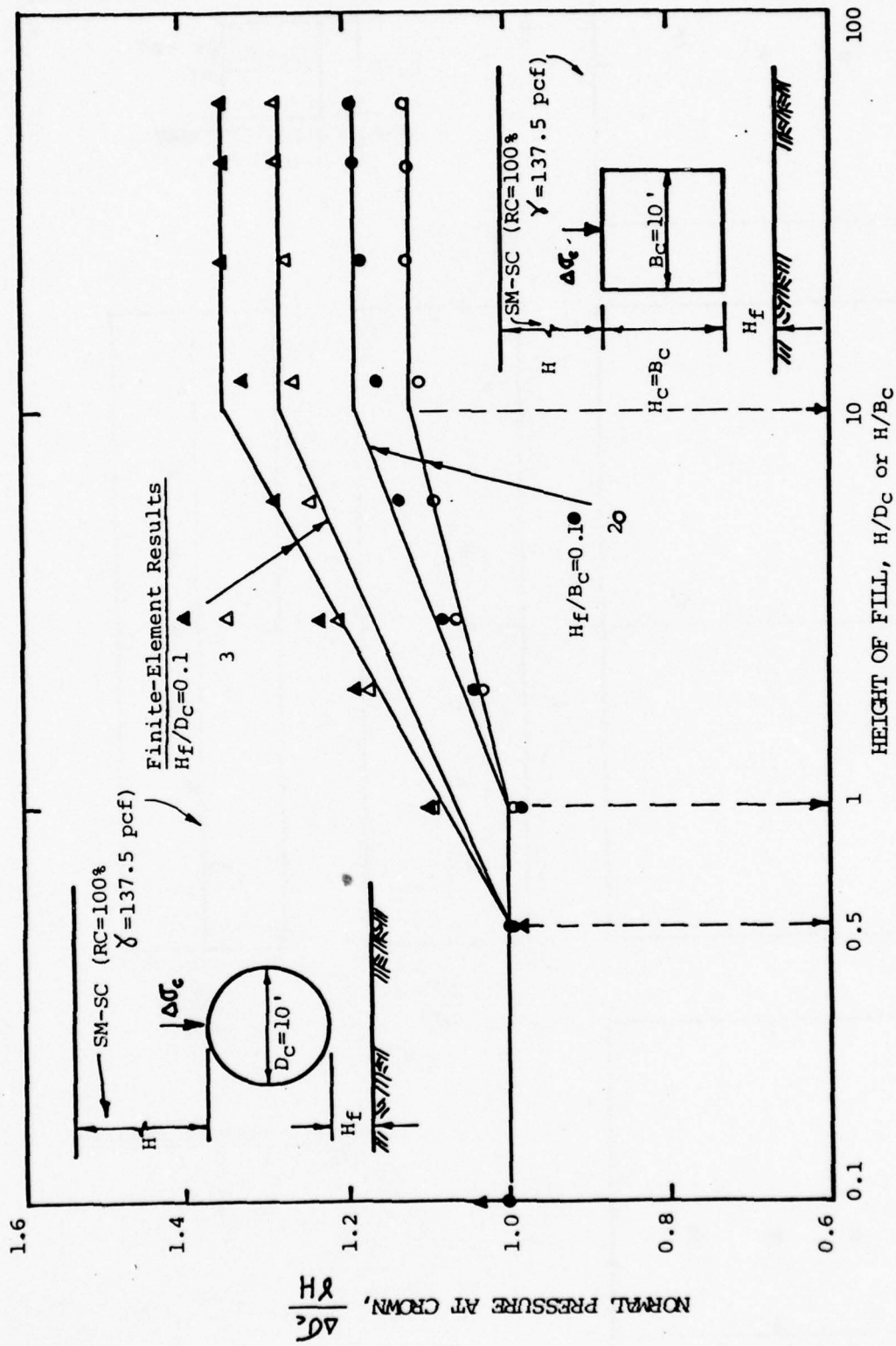


FIG. IV-22 STRAIGHT-LINE APPROXIMATIONS OF THE VARIATION OF NORMAL PRESSURE AT THE CROWN OF CIRCULAR AND SQUARE CONDUITS FOR DIFFERENT HEIGHTS OF FILL

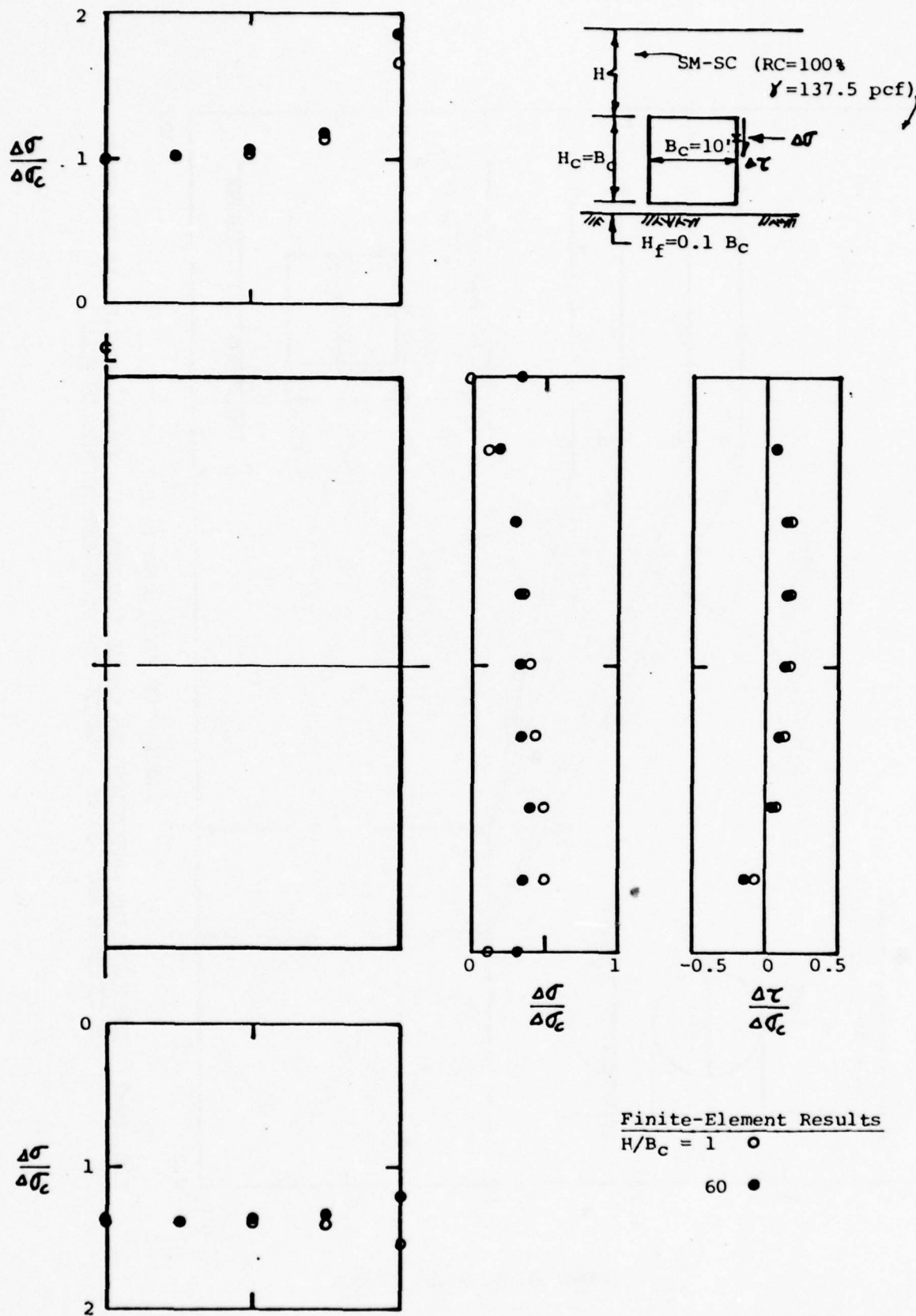


FIG. IV-23 DISTRIBUTION OF NORMAL PRESSURE, $\Delta\sigma$, AND SIDE SHEAR STRESS, $\Delta\tau$, ON SQUARE CONDUIT FOR DIFFERENT HEIGHTS OF FILL, SHALLOW SOIL FOUNDATION (NORMALIZED TO NORMAL PRESSURE AT CROWN)

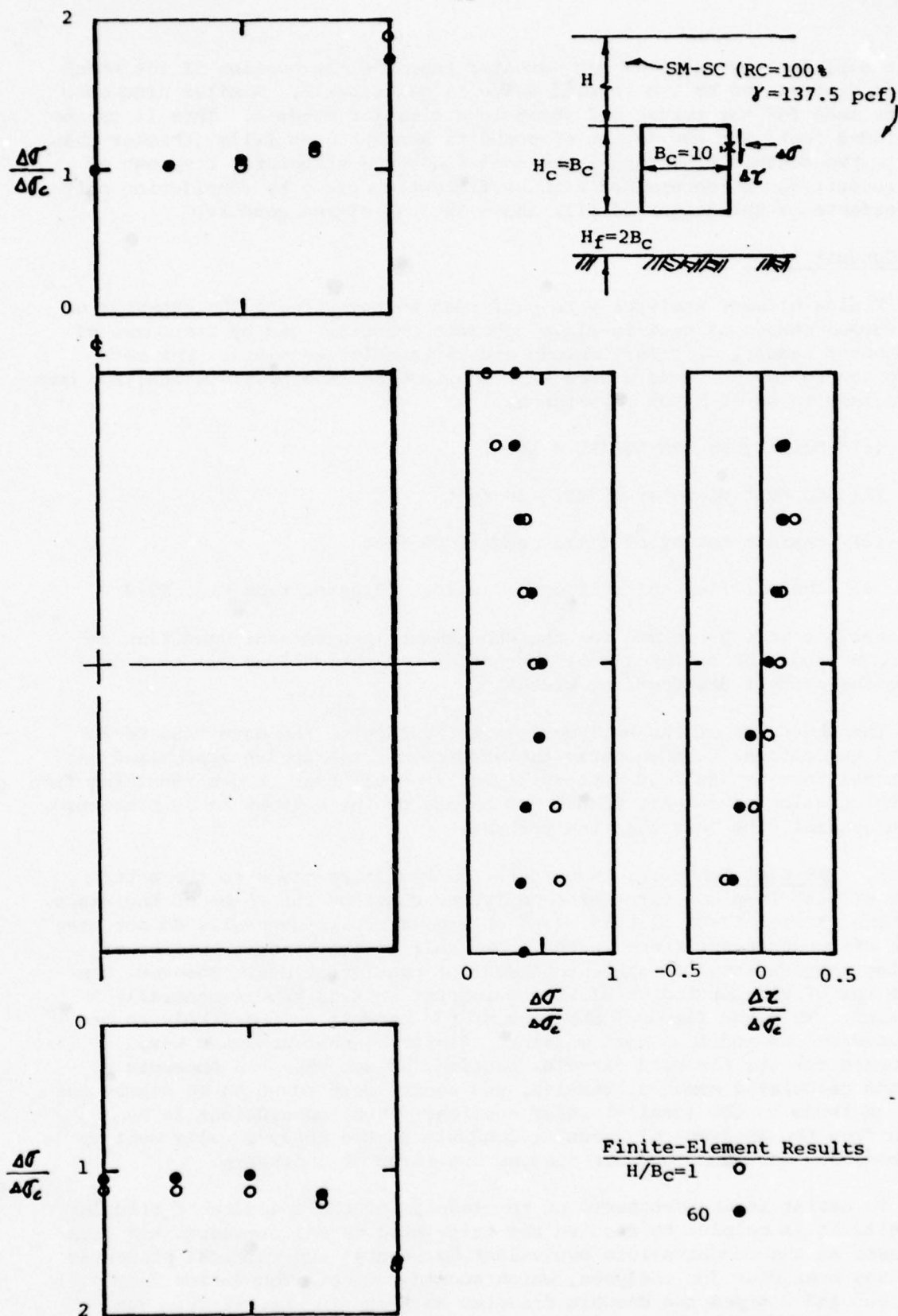


FIG. IV-24 DISTRIBUTION OF NORMAL PRESSURE, $\Delta\sigma$, AND SIDE SHEAR STRESS, $\Delta\tau$, ON SQUARE CONDUIT FOR DIFFERENT HEIGHTS OF FILL, DEEP SOIL FOUNDATION (NORMALIZED TO NORMAL PRESSURE AT CROWN)

Obviously, for any value of H/D_c greater than one the portion of the total moment represented by the initial value is quite small. Similar arguments can be made for the thrust and shear in a circular conduit. Thus it can be concluded that, for the design of conduits beneath deep fills (thicker than one to two conduit diameters), the soil loads and structural response of the conduit can be determined with sufficient accuracy by considering only the effects of the height of fill above the top of the conduit.

G. Conduit Shape

Finite-element analyses were performed to investigate the behavior of the common shapes of cast-in-place concrete conduits used by the Corps of Engineers; namely, circular, oblong and rectangular sections. For each study the following factors were kept constant because previous analyses had shown them to be of minor importance:

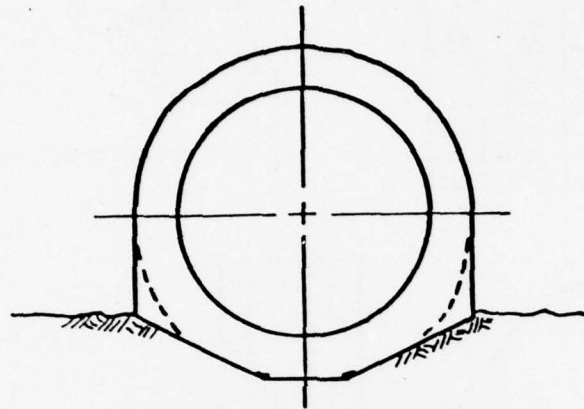
- (1) Soil type: SM-SC (RC = 100%)
- (2) Conduit diameter width: 10 feet
- (3) Maximum height of fill: about 600 feet
- (4) Conduit flexural stiffness: values selected from Fig. IV-3

The analyses were performed for the embankment (projection) condition and for each study the depth of soil foundation was varied from 0.1 to 2 or 3 times the conduit diameter (or width).

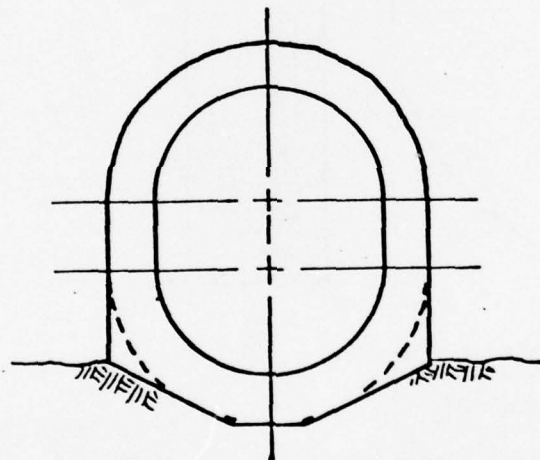
The objective of the analyses was to synthesize the data into useful design guidelines. Consequently the accuracy of the chosen approximations to actual results has been kept sufficiently small that errors resulting from the calculation of moment, thrust and shear, by the methods to be presented, would generally be less than ten percent.

1. Circular Conduits. Consideration was first given to the actual shape of cast-in-place circular conduits as built by the Corps of Engineers. As shown in Fig. IV-25 circular (and oblong) conduits generally do not have walls of constant thickness in the lower half of the conduit because of forming requirements and other construction considerations. However, the outer row of reinforcing steel in the conduit wall is kept essentially circular. Thus the flexural behavior of the conduit is not likely to be affected by the modified bottom shape. Finite-element analyses were performed for the modified circular section, as described in Appendix A, and the calculated moments, thrusts, and shears were found to be nearly the same as those in the ideal circular section. Thus, conclusions to be drawn from the analyses of circular conduits should apply equally well to the modified sections that are used by the Corps of Engineers.

To assist in the synthesis of the results of the analyses of circular conduits it is helpful to resolve the calculated normal pressures and shear stresses on the conduits into equivalent horizontal and vertical pressures. This has been done for analyses, which considered soil foundation depths of 0.1, 0.5 and 3 times the conduit diameter as shown in Fig. IV-26. The pressures have been normalized by dividing by the magnitude of the respective



MODIFIED CIRCULAR SECTION



MODIFIED OBLONG SECTION

FIG. IV-25 TYPICAL CIRCULAR AND OBLONG CONDUITS AS BUILT
BY THE CORPS OF ENGINEERS
(After Dept. of Army, 1969)

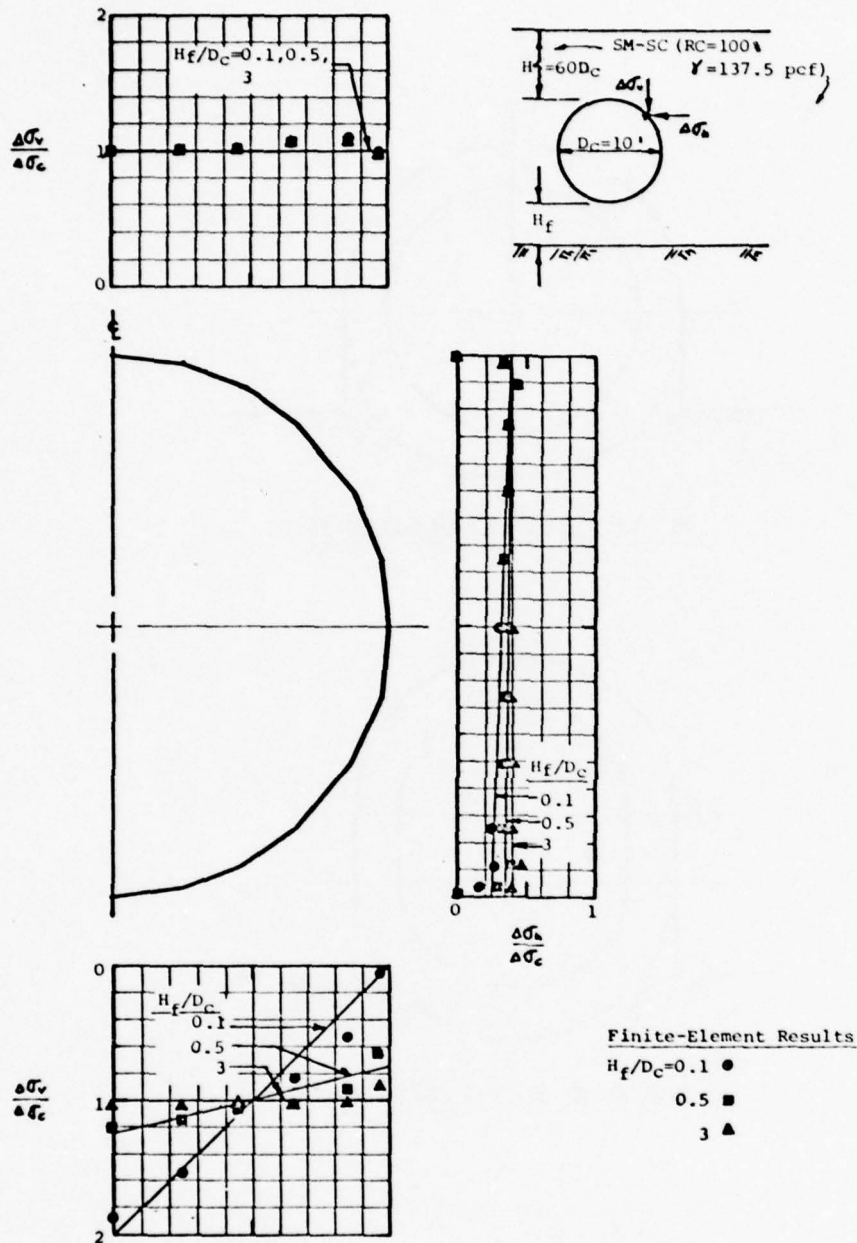


FIG. IV-26 STRAIGHT LINE APPROXIMATIONS OF THE DISTRIBUTION OF VERTICAL PRESSURE, $\Delta\sigma_v$, AND HORIZONTAL PRESSURE, $\Delta\sigma_h$, ON CIRCULAR CONDUITS FOR VARIOUS SOIL FOUNDATION DEPTHS (NORMALIZED TO NORMAL PRESSURE AT CROWN)

crown pressure in each case. The straight-line approximations shown in the figure are reasonable representations of the analytical results.

These data show that earth pressures on circular conduits are of the form given in Fig. IV-27. Two factors are defined in the figure. The Crown Pressure Factor, N , is simply the normal pressure at the crown of the conduit, divided by the overburden pressure. The value of N at a fill height, $H = 60 D_c$, varies with foundation depth as shown in Fig. IV-28. (Note that additional results for a foundation of one conduit diameter are included in the figure). The value of N also varies with height of fill, as was previously shown in Fig. IV-22. The dashed lines in Fig. IV-28 represents the probable values of crown pressure factor, at different fill heights, that can be estimated from the available data. The Foundation Reaction Factor, n , which is shown in Fig. IV-27, represents the change in pressures on the conduit that occur as a result of shallow foundation depths. The value of n , for a height of fill, $H = 60 D_c$, varies as shown in Fig. IV-28. It has been previously shown that the distributions of earth pressure on a conduit are slightly more severe for large heights of fill. Thus the values of n given in Fig. IV-28 could be used, conservatively, for all fill heights.

The appropriateness of the pressure diagrams in Fig. IV-27 was verified by comparing the finite-element results with structural analysis calculations (see Appendix A) made assuming external loads on a circular conduit in accordance with the approximate pressure distributions. The comparisons for a 10-foot-diameter conduit and a height of fill equal to 600 feet are shown in Figs. IV-29 through IV-33. The calculated values of moment, thrust and shear in the conduit and the normal pressures and shear stresses on the conduit are very close to the results of the finite-element analyses.

2. Oblong Conduits. As was previously shown in Fig. IV-25, the bottom portion of an oblong conduit, as built by the Corps of Engineers, deviates from a circular ring. However the structural behavior is not likely to differ significantly from an ideal section, as explained previously for circular conduits. Consequently oblong sections of circular bottom shape were considered in the finite-element analyses performed for this investigation. Two oblong sections, with height-to-width (H/B_c) ratios of 1.25 and 1.50, were selected for study. These shapes were understood to cover the usual range considered in practice by the Corps of Engineers (Department of the Army, 1969).

The variation of calculated pressures at the crown of the oblong conduit, with a value of H_c/B_c of 1.25 is shown in Fig. IV-34 for both shallow and deep soil foundations.^c The straight line approximations of the data are similar to those for circular conduits (Fig. IV-22). The largest discrepancies between the approximations and the actual data are at small heights of fill. The distribution of calculated horizontal and vertical pressures on the oblong conduit and the shear stresses along the tangent section at its side are shown in Fig. IV-35. The data are normalized in terms of the normal pressure at the crown. The pressure distributions are similar to those for circular conduits (Fig. IV-26) with the exception of the addition of side-shear stresses. For the shallow foundation case ($H_f/B_c = 0.1$) all side shear stresses act in a downward sense and increase

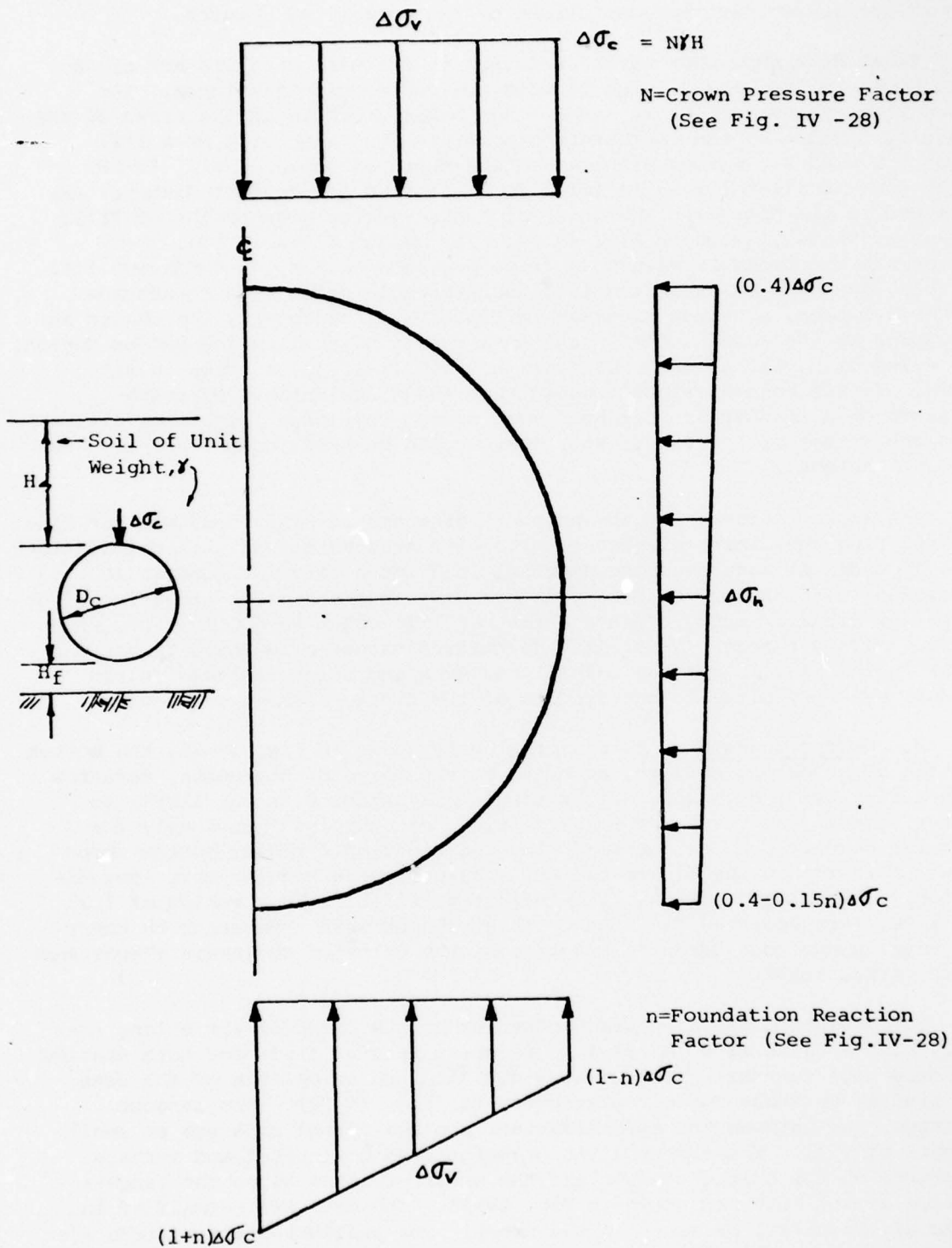


FIG. IV-27 APPROXIMATIONS OF VERTICAL PRESSURE, $\Delta\sigma_v$, AND HORIZONTAL PRESSURE, $\Delta\sigma_h$, FOR CIRCULAR CONDUITS (SOIL FOUNDATION)

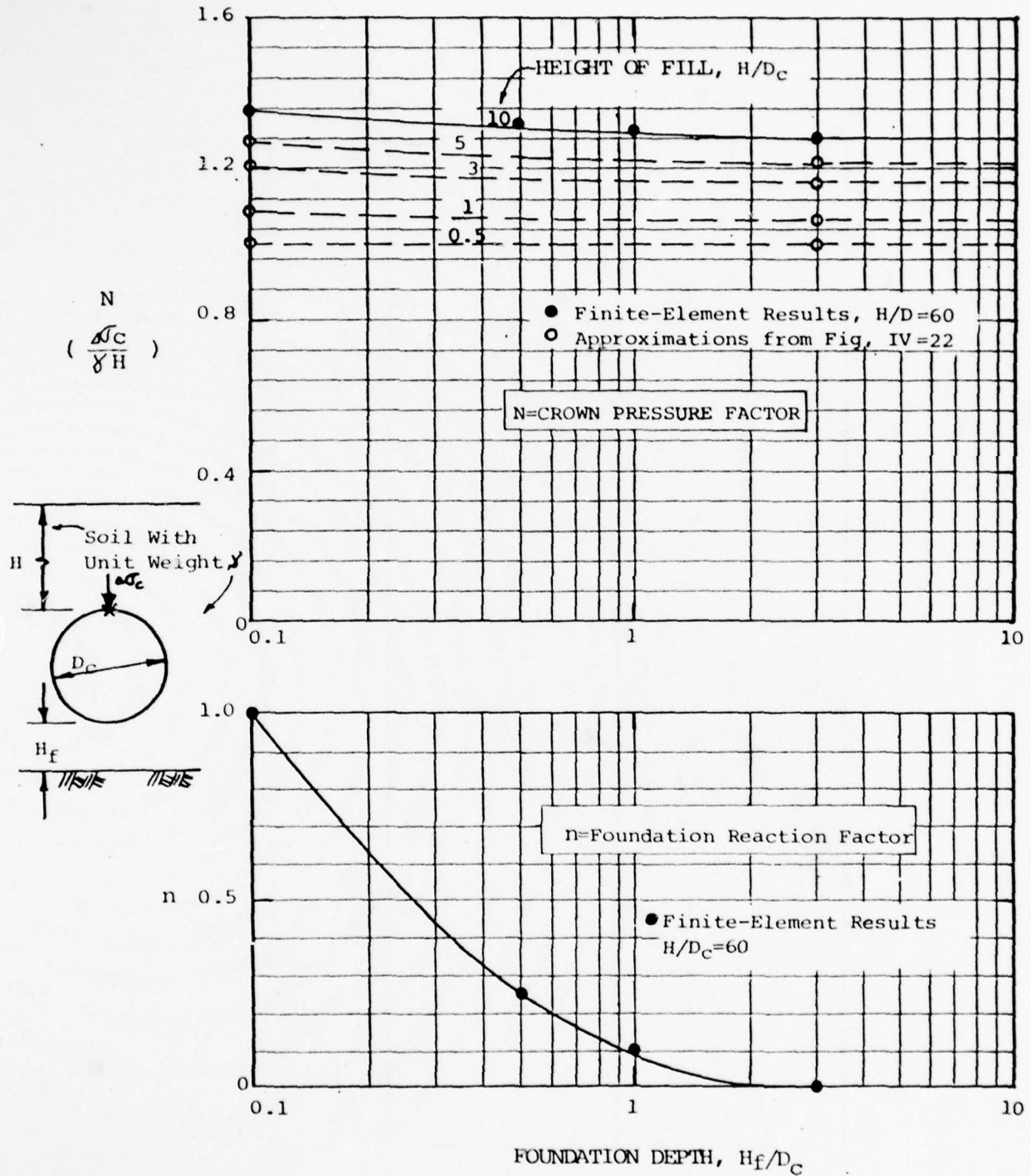


FIG. IV-28 CROWN-PRESSURE FACTOR AND FOUNDATION-REACTION FACTOR FOR CIRCULAR CONDUITS ON SOIL FOUNDATIONS

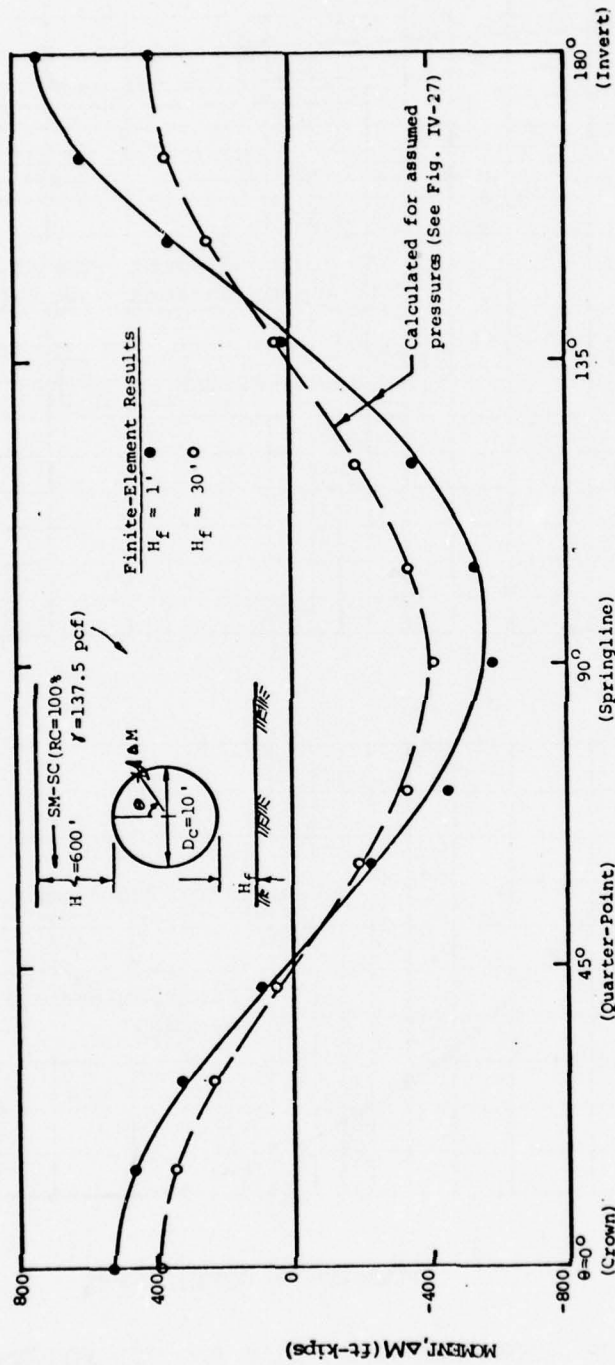


FIG. IV-29 MOMENT IN CIRCULAR CONDUIT, COMPARISON OF FINITE-ELEMENT RESULTS WITH VALUES CALCULATED FOR ASSUMED PRESSURES (SOIL FOUNDATION)

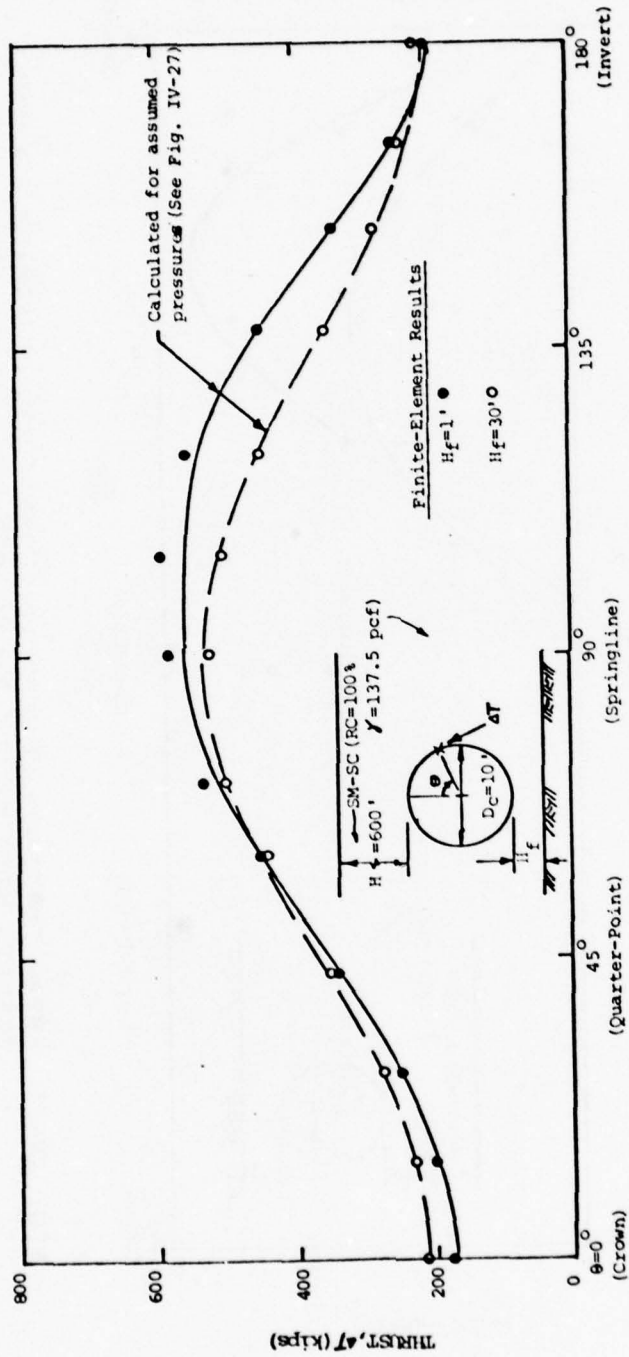


FIG. IV-30 THRUST IN CIRCULAR CONDUIT, COMPARISON OF FINITE-ELEMENT RESULTS WITH VALUES CALCULATED FOR ASSUMED PRESSURES (SOIL FOUNDATION)

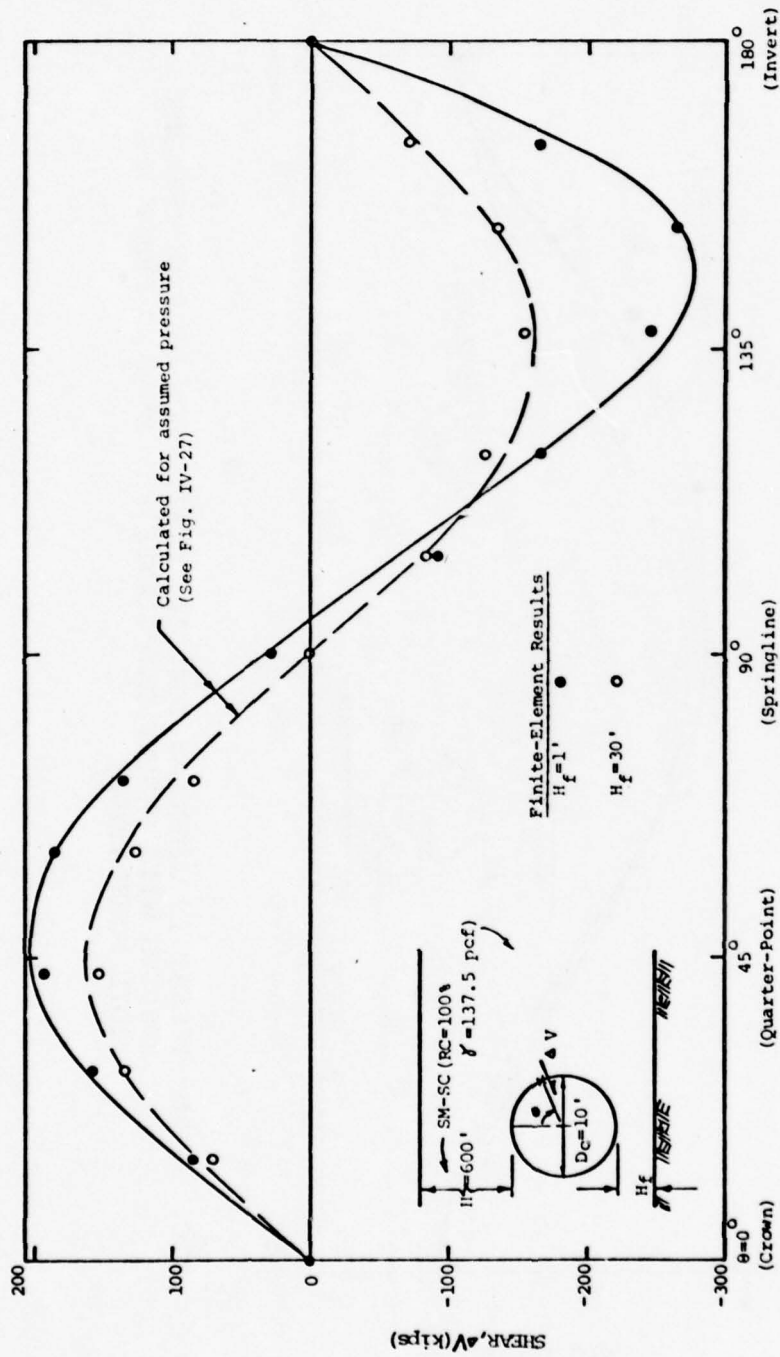


FIG. IV-31 SHEAR IN CIRCULAR CONDUIT, COMPARISON OF FINITE ELEMENT RESULTS WITH VALUES CALCULATED FOR ASSUMED PRESSURES (SOIL FOUNDATION)

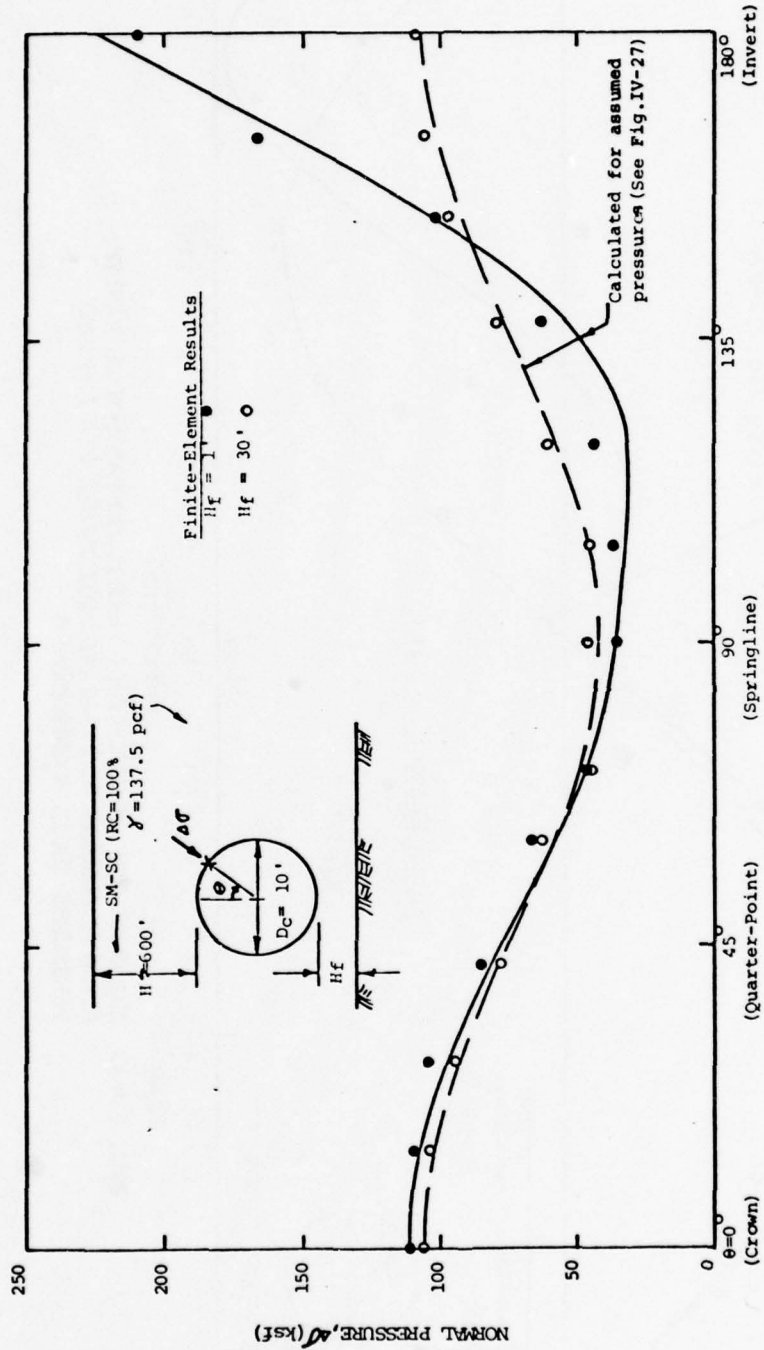


FIG. IV-32 NORMAL PRESSURES ON CIRCULAR CONDUIT, COMPARISON OF FINITE-ELEMENT WITH VALUES CALCULATED FOR ASSUMED PRESSURES (SOIL FOUNDATION)

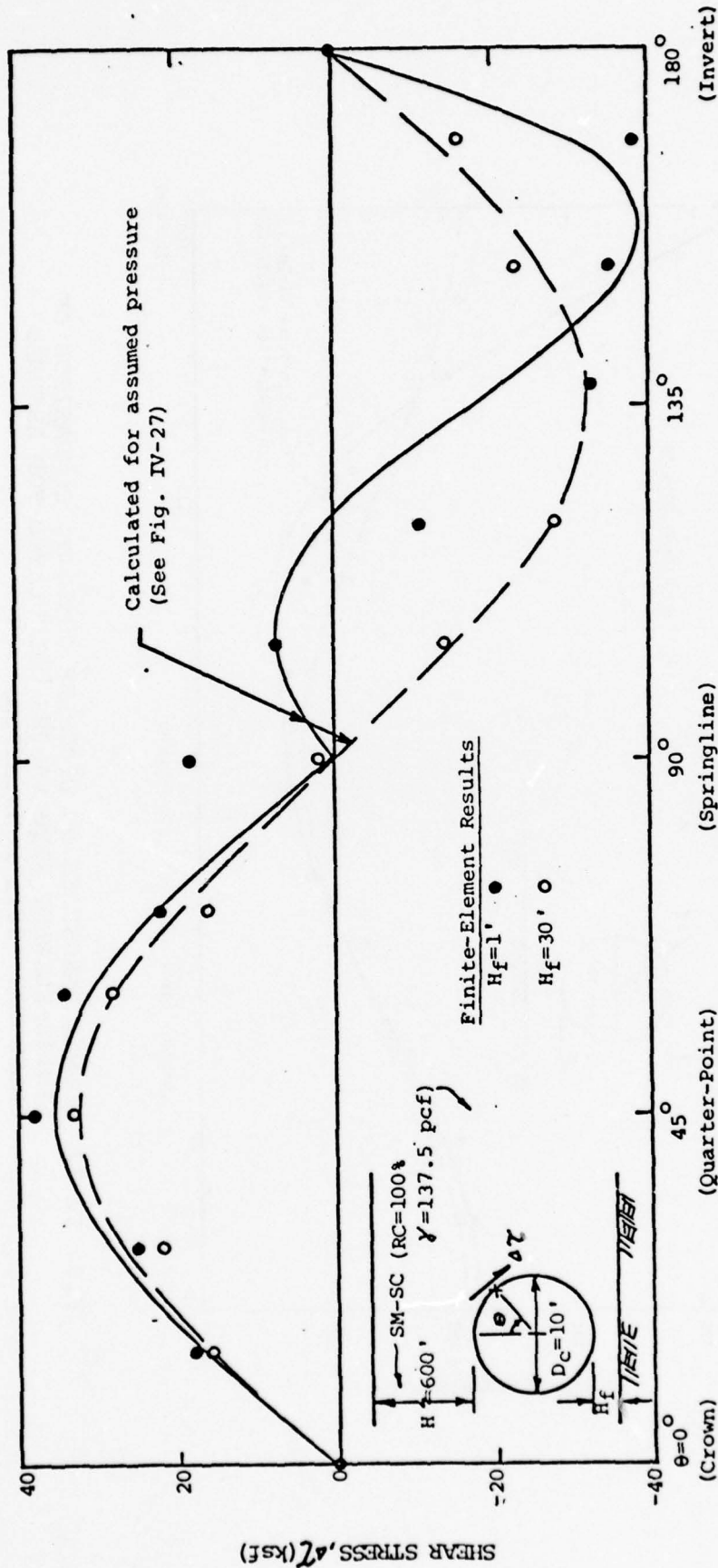


FIG. IV-33 SHEAR STRESS ON CIRCULAR CONDUIT, COMPARISON OF FINITE-ELEMENT RESULTS WITH VALUES CALCULATED FOR ASSUMED PRESSURES (SOIL FOUNDATION)

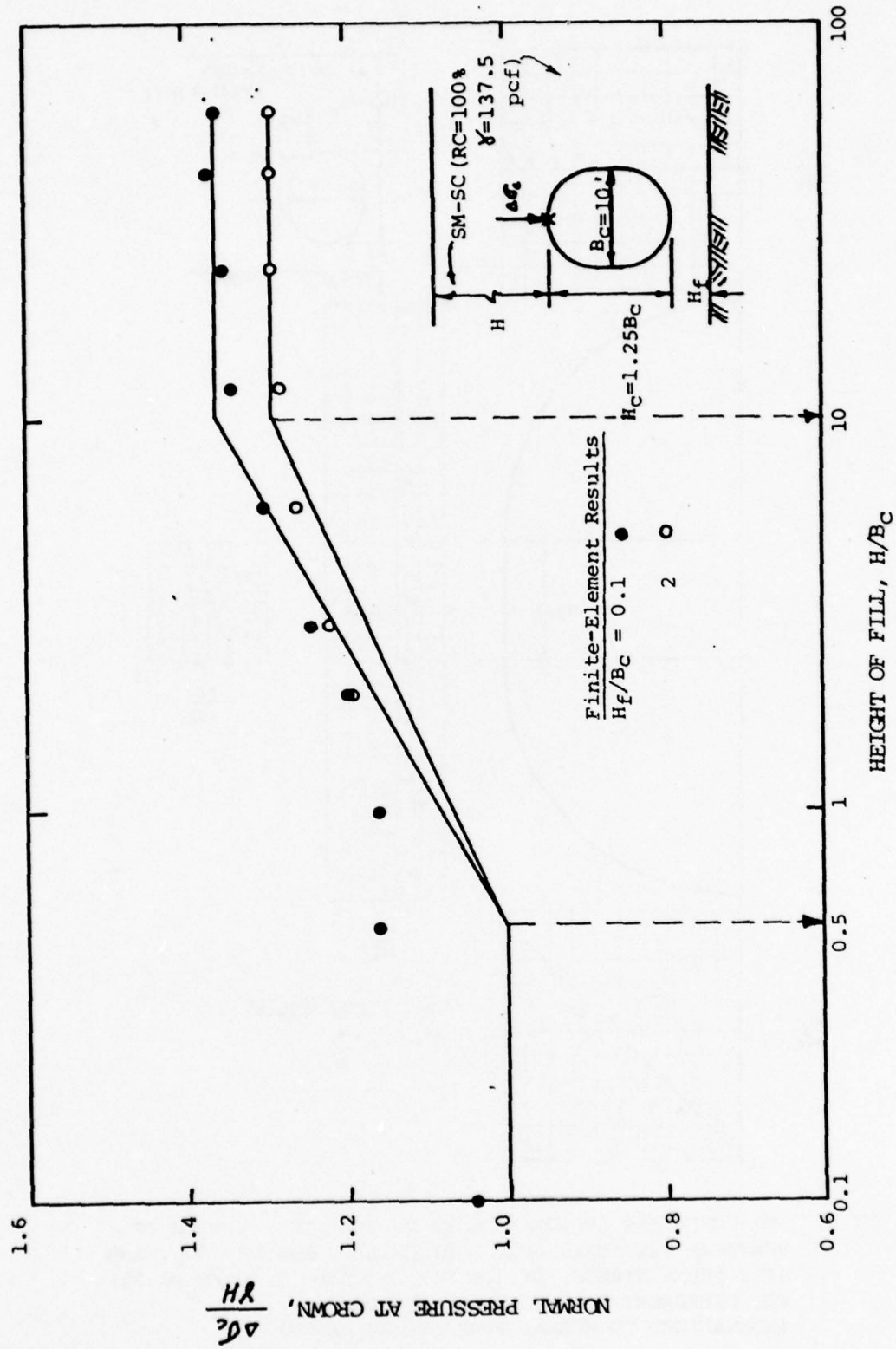


FIG. IV-34 NORMAL PRESSURE AT CROWN OF OBLONG CONDUIT
 ($H_c/B_c=1.25$) FOR DIFFERENT SOIL FOUNDATION
 DEPTHS

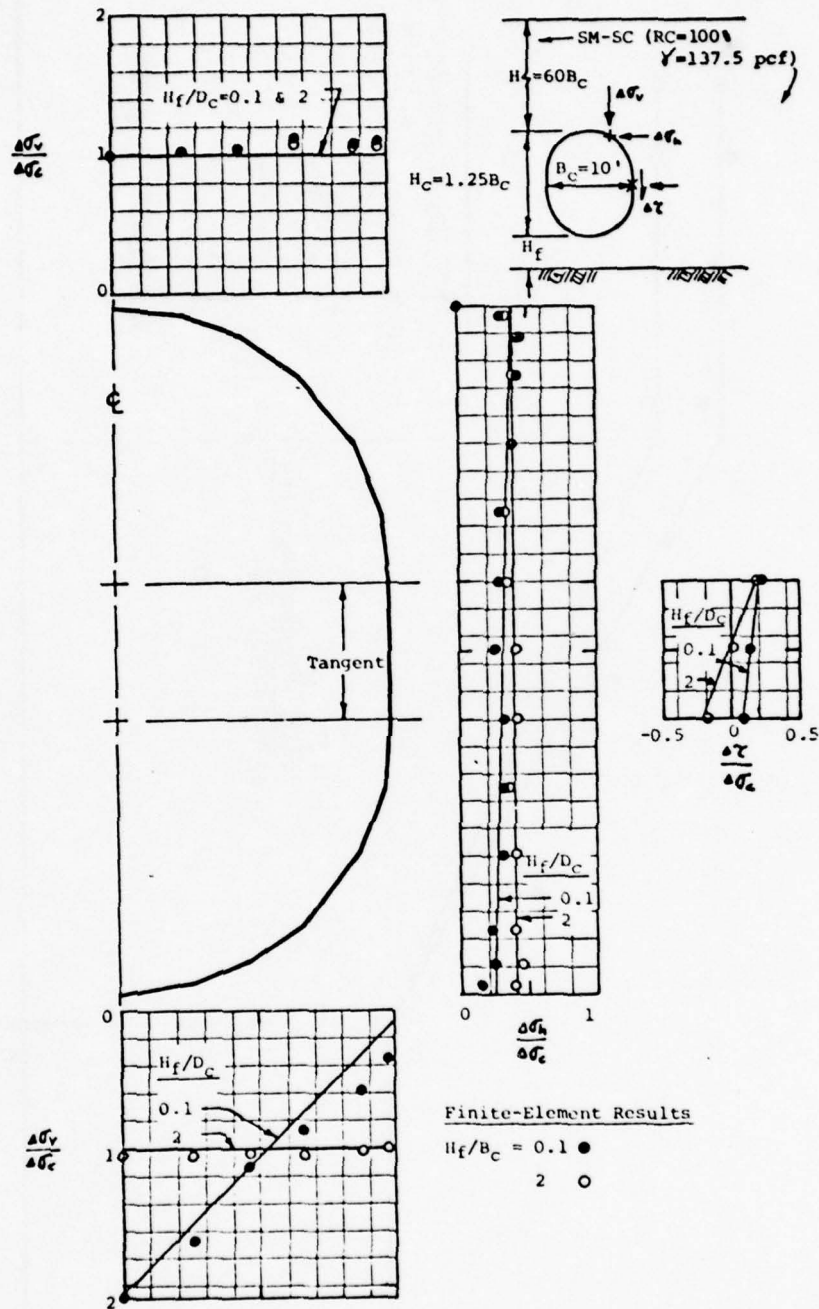


FIG. IV-35 STRAIGHT-LINE APPROXIMATIONS OF THE DISTRIBUTION OF VERTICAL PRESSURE, $\Delta\sigma_v$, HORIZONTAL PRESSURE, $\Delta\sigma_h$, AND SIDE SHEAR STRESS, $\Delta\tau$, ON OBLONG CONDUIT ($H_c/B_c = 1.25$) FOR DIFFERENT SOIL FOUNDATION DEPTHS (NORMALIZED TO NORMAL PRESSURE AT CROWN)

the vertical reactions at the base of the conduit. The straight lines drawn in the figure can be seen to be reasonable approximations of the data. The results of the analysis for the oblong conduit, of $H_f/B_c = 1.5$, are presented in Figs. IV-36 and IV-37. The pressure diagrams C_c given in Fig. IV-38 summarize the results of the analyses of oblong conduits. The vertical pressure at the base of the conduit includes a uniformly-distributed reaction to the vertical shear along the tangent section of the conduit. Values of N , the Crown Pressure Factor can be determined from Fig. IV-34 for foundation depths equal to 0.1 and 2 times the conduit width. For immediate depths of soil foundations the factor N would be expected to vary as it does for circular conduits (Fig. IV-28). Values of n , the Foundation Reaction Factor, are equal to those for circular conduits at the extreme conditions of soil foundation depth (i.e., n equals 0 at H_f/B_c greater than about 2 and n equals 1 at H_f/B_c equals to 0.1). At intermediate foundation depths it seems reasonable that the values of n for oblong conduits would be approximately equal to those for circular conduits (Fig. IV-28).

The pressure diagrams in Fig. IV-38 have been used to calculate the structural response of oblong conduits with values of H_f/B_c equal to 1.25 and 1.5. The calculated values of moment, thrust, shear C_c , normal pressure and shear stress are compared with the results of the finite-element analyses in Figs. IV-39 through IV-48. Data are presented for shallow and deep soil foundations for the case where the height of fill equals 600 feet. In each figure the data have been normalized by dividing by the magnitudes at selected points on the conduits. Thus separate evaluations can be made of (1) the appropriateness of the calculated distributions and (2) the accuracy of the magnitude of the calculated values, in comparison with the finite-element results. In general, it can be said that the normalized distributions that result from the assumed pressures given in Fig. IV-38 do reasonably represent the finite-element results. On the other hand the magnitudes of the calculated values at the selected points are generally less than the finite-element results. (The exceptions to this statement are the crown pressures which must be equal because the crown-pressure factors were determined from the finite-element results.) Therefore, if the assumed pressures in Fig. IV-38 are to be used for design, the crown-pressure factors must be made greater than the actual finite-element results to achieve more accurate predictions of moments, thrusts and shears in a conduit. Appropriate correction factors are given in Table IV-1. The values were selected giving emphasis to the results for moments in the oblong conduits (Figs. IV-39 and IV-44).

TABLE IV-1

Correction Factors to Apply to Crown Pressure
Factors* for Oblong Conduits

Ratio of Height to Width H_f/B_c	Correction Factor C_n
1.25	1.05
1.5	1.20

*Fig. IV-36

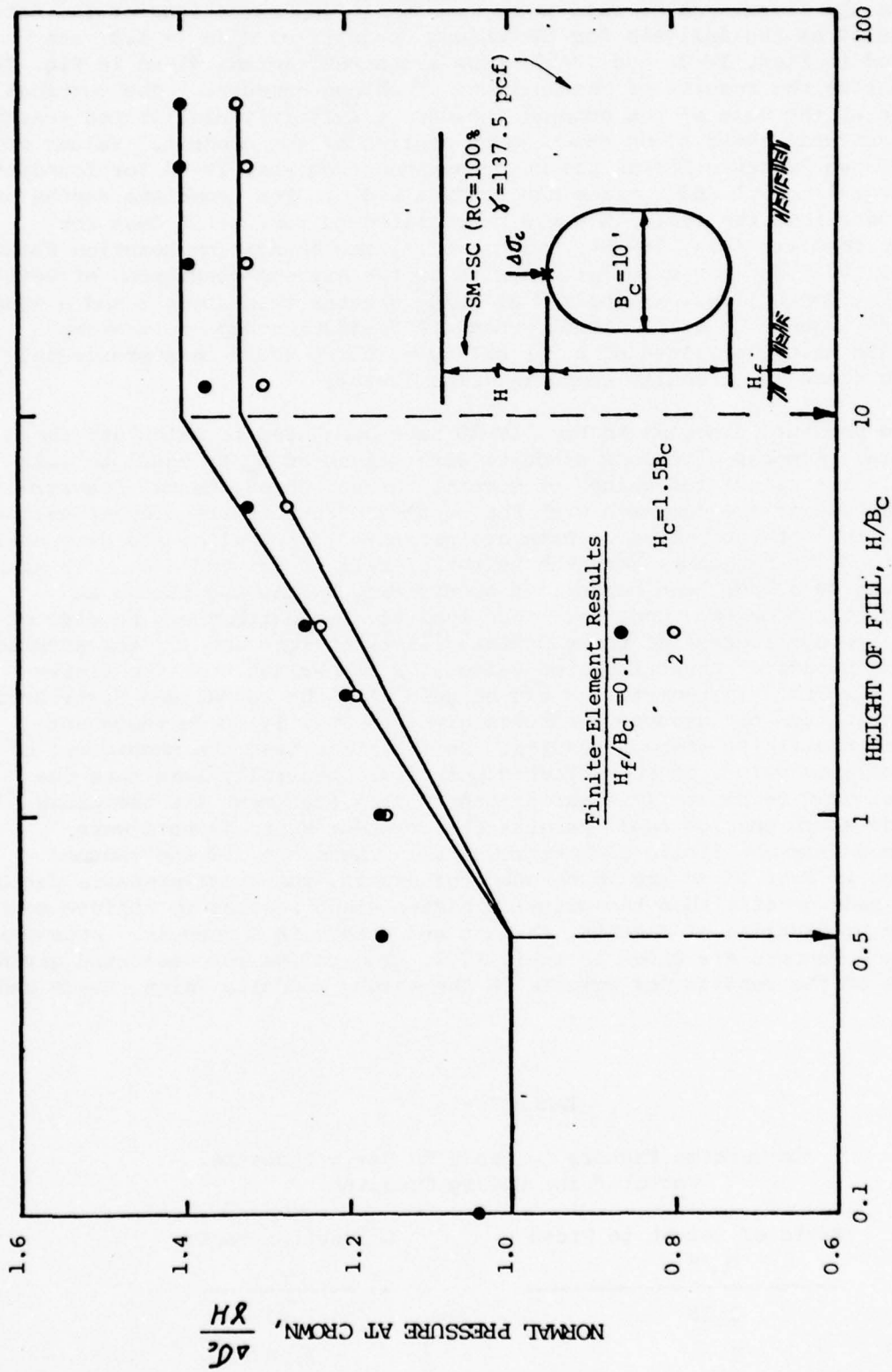


FIG. IV-36 NORMAL PRESSURE AT CROWN OF OBLONG CONDUIT ($H_f/B_c=1.5$) FOR DIFFERENT SOIL FOUNDATION DEPTHS

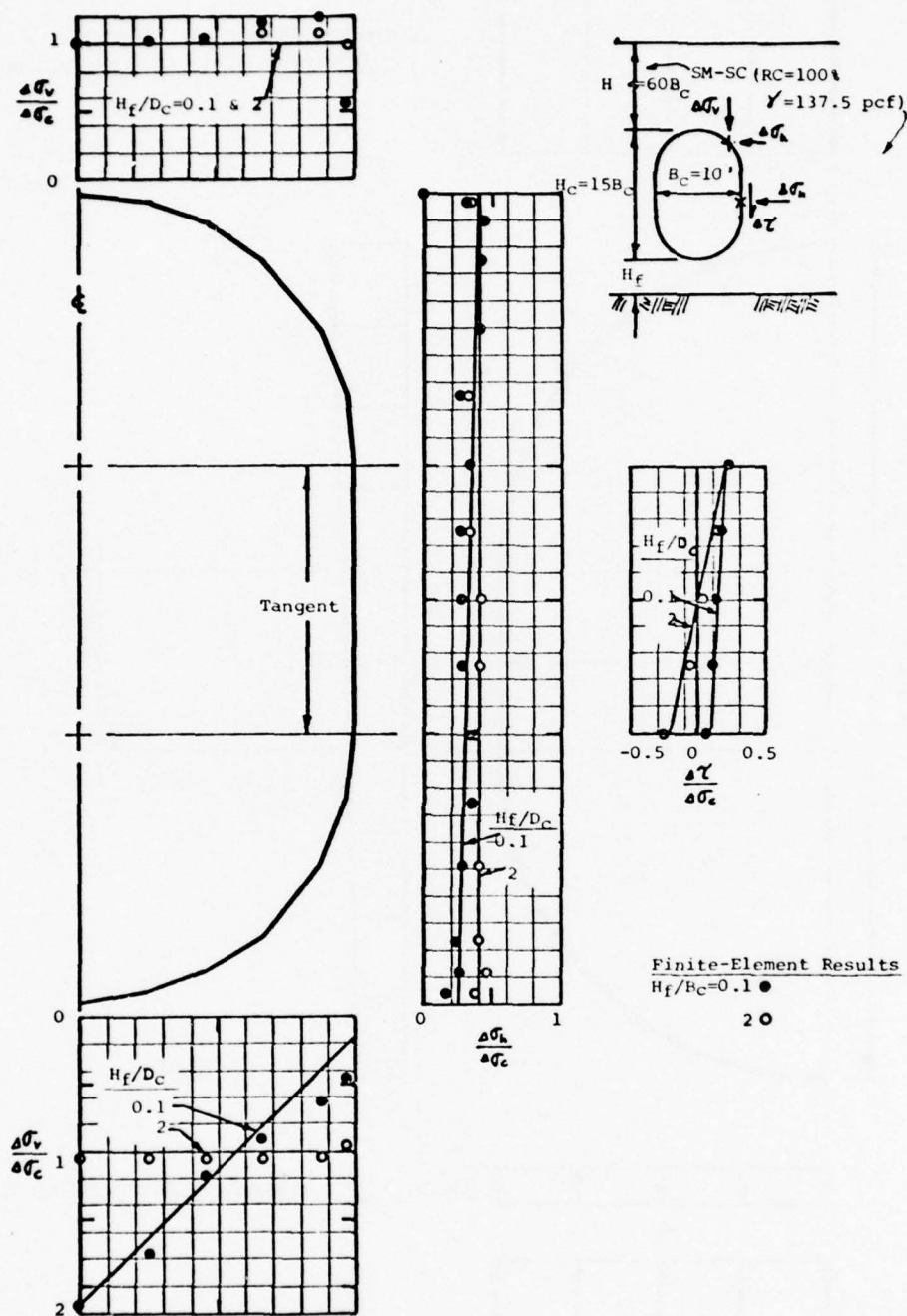


FIG. IV-37 DISTRIBUTION OF VERTICAL PRESSURE $\Delta\sigma_v$, HORIZONTAL PRESSURE, $\Delta\sigma_h$, AND SIDE SHEAR STRESS, $\Delta\tau$, ON OBLONG CONDUIT ($H_C/B_C = 1.5$) FOR DIFFERENT SOIL FOUNDATION DEPTHS (NORMALIZED TO NORMAL PRESSURE AT CROWN)

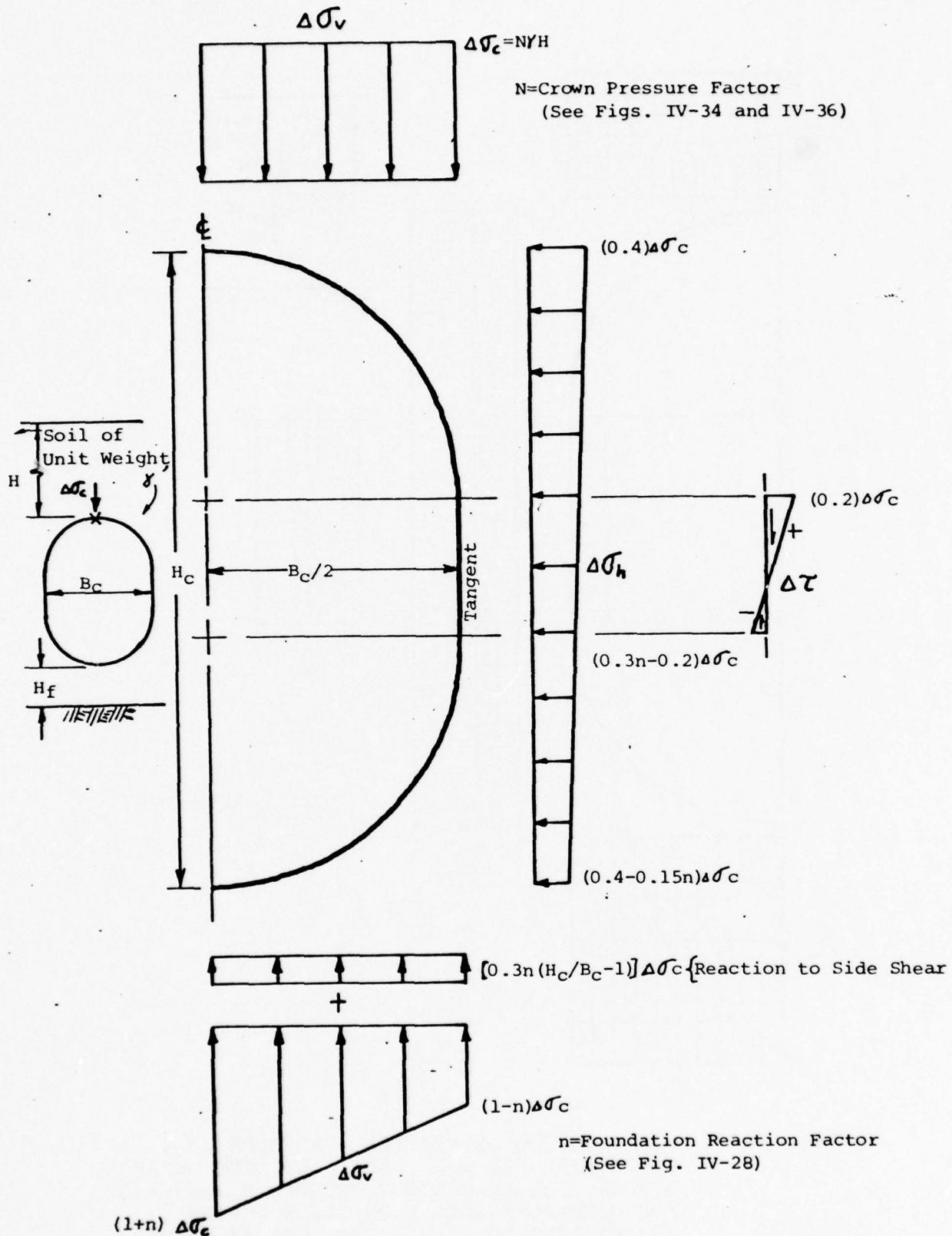


FIG. IV-38 APPROXIMATIONS OF VERTICAL PRESSURE, $\Delta\sigma_v$, HORIZONTAL PRESSURE, $\Delta\sigma_h$, AND SIDE SHEAR STRESS, $\Delta\tau$, FOR OBLONG CONDUITS, SOIL FOUNDATION (NORMALIZED TO NORMAL PRESSURE AT CROWN)

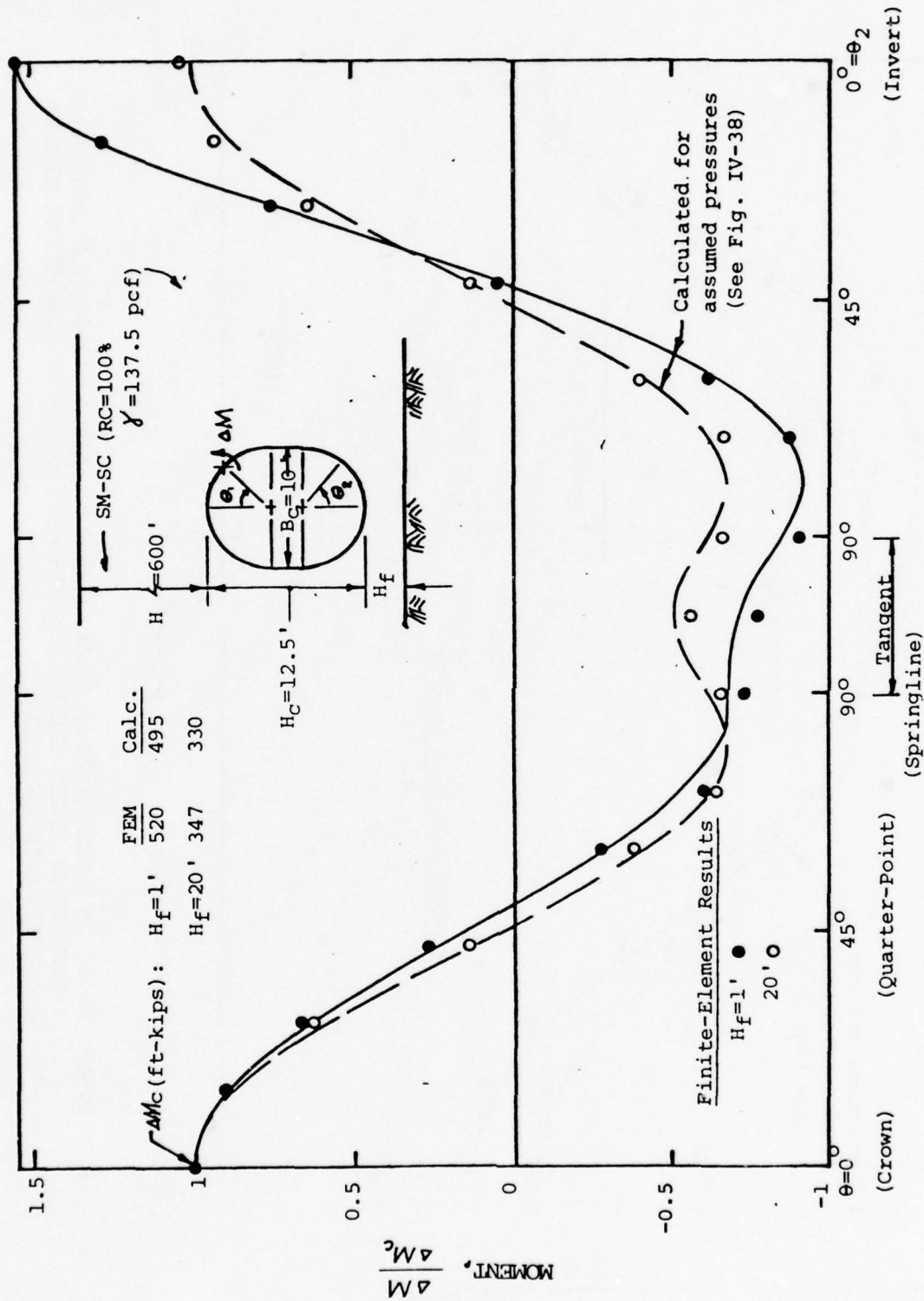


FIG. IV-39 MOMENT IN OBLONG CONDUIT, $H_c/B_c = 1.25$ (NORMALIZED TO MOMENT AT CROWN):
 COMPARISON OF FINITE-ELEMENT RESULTS WITH VALUES CALCULATED FOR
 ASSUMED PRESSURES, SOIL FOUNDATION

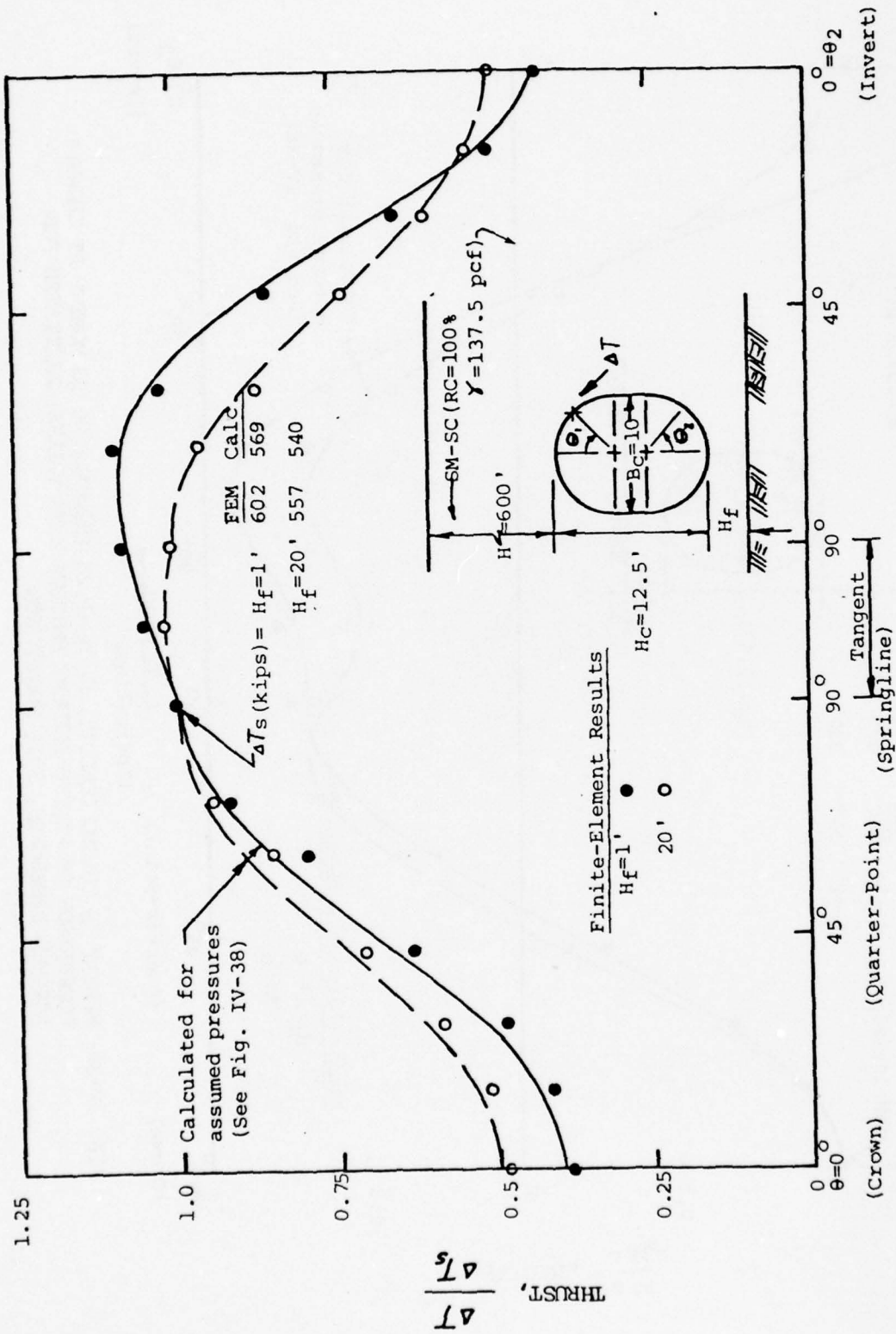


FIG. IV-40 THRUST IN OBLONG CONDUIT, $H_C/B_C = 1.25$ (NORMALIZED TO THRUST AT SPRINGLINE):
COMPARISON OF FINITE-ELEMENT RESULTS WITH VALUES CALCULATED FOR ASSUMED PRESSURES, SOIL FOUNDATION

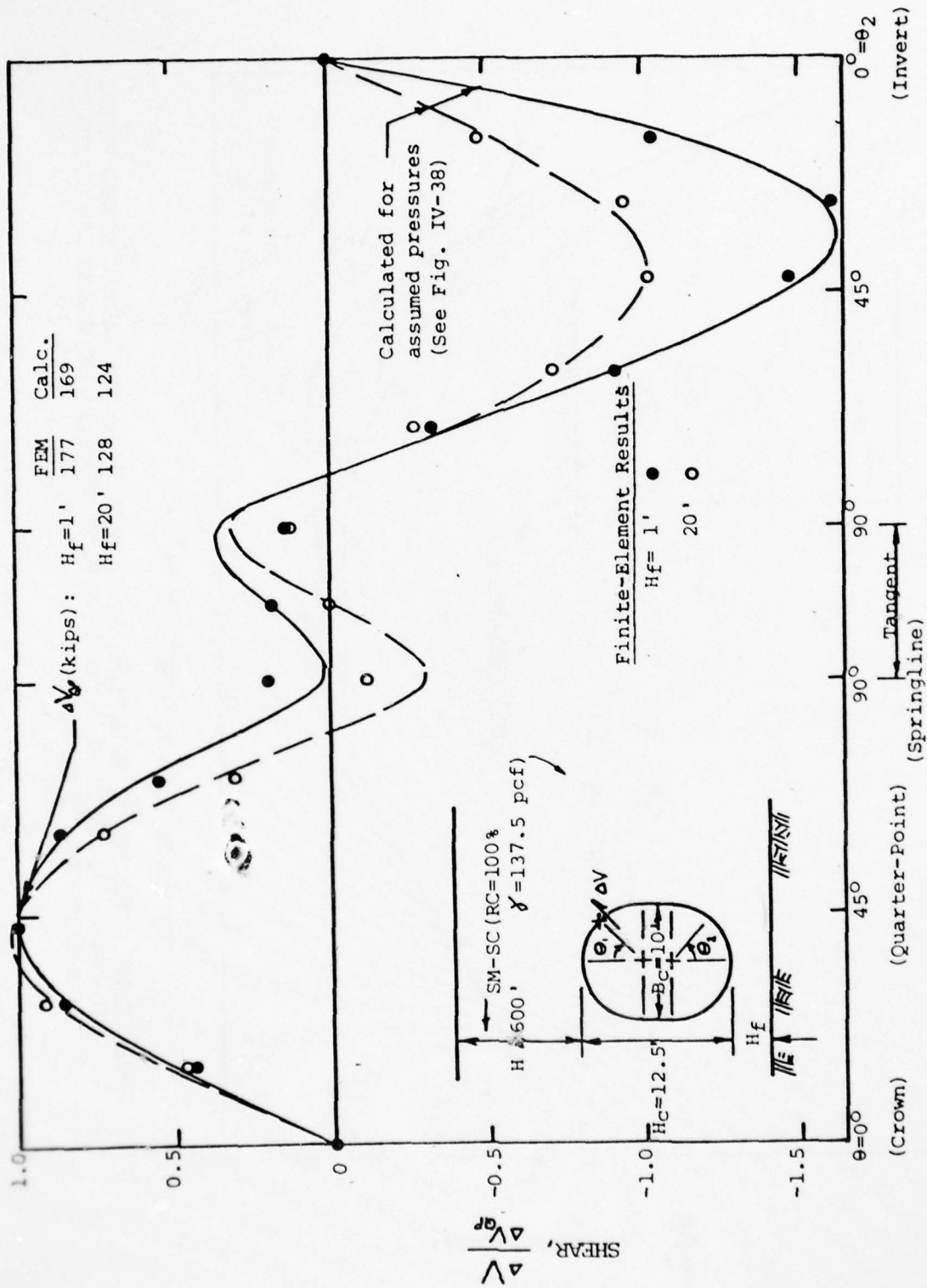


FIG. IV-41 SHEAR IN OBLONG CONDUIT, $H_c/B_c = 1.25$ (NORMALIZED TO SHEAR AT QUARTER-POINT):
 COMPARISON OF FINITE-ELEMENT RESULTS WITH VALUES CALCULATED FOR ASSUMED
 PRESSURES, SOIL FOUNDATION

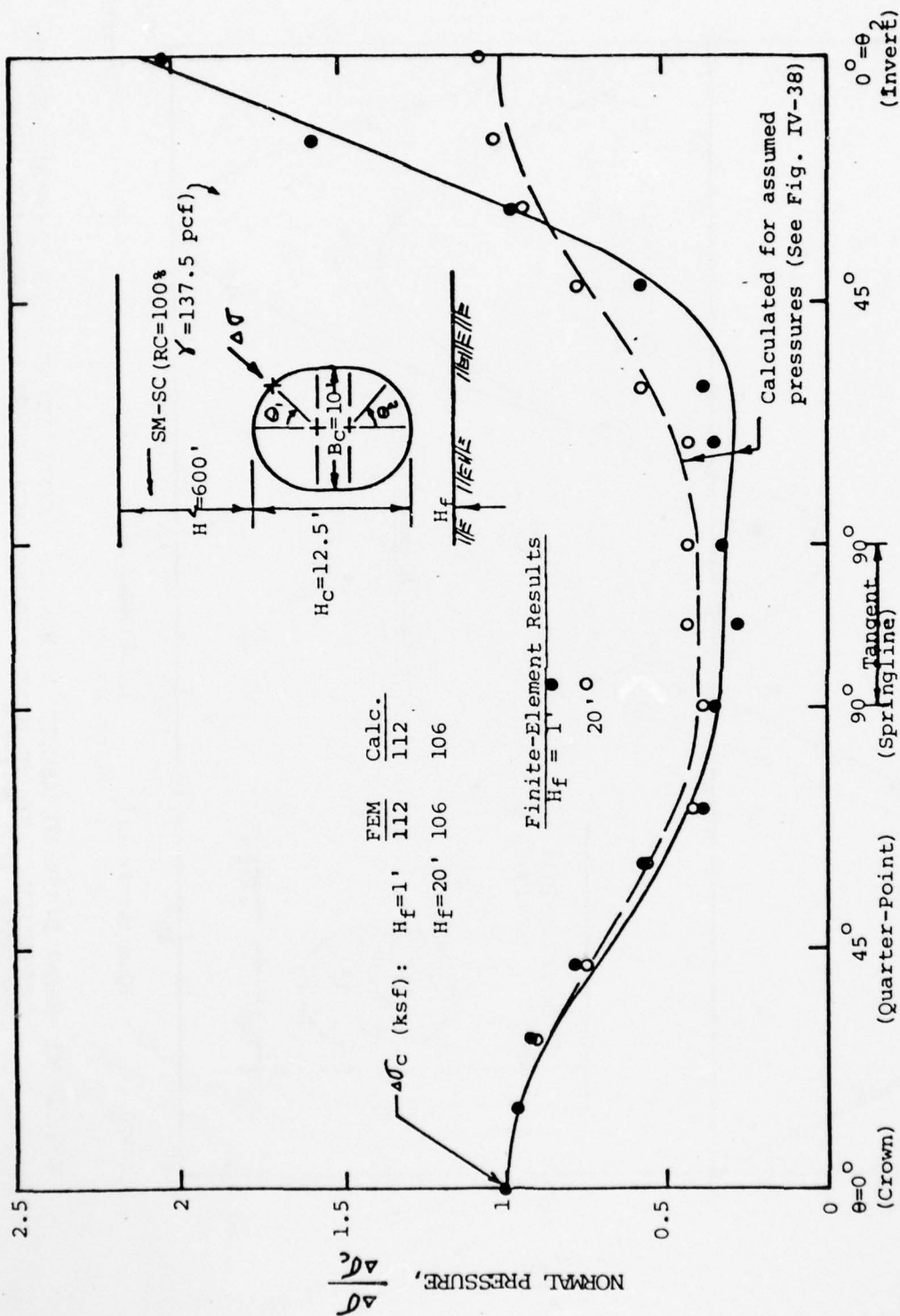


FIG. IV-42 NORMAL PRESSURE ON OBLONG CONDUIT, $H_c/B_c = 1.25$ (NORMALIZED TO NORMAL PRESSURE AT CROWN): COMPARISON OF FINITE-ELEMENT RESULTS WITH VALUES CALCULATED FOR ASSUMED PRESSURES, SOIL FOUNDATION

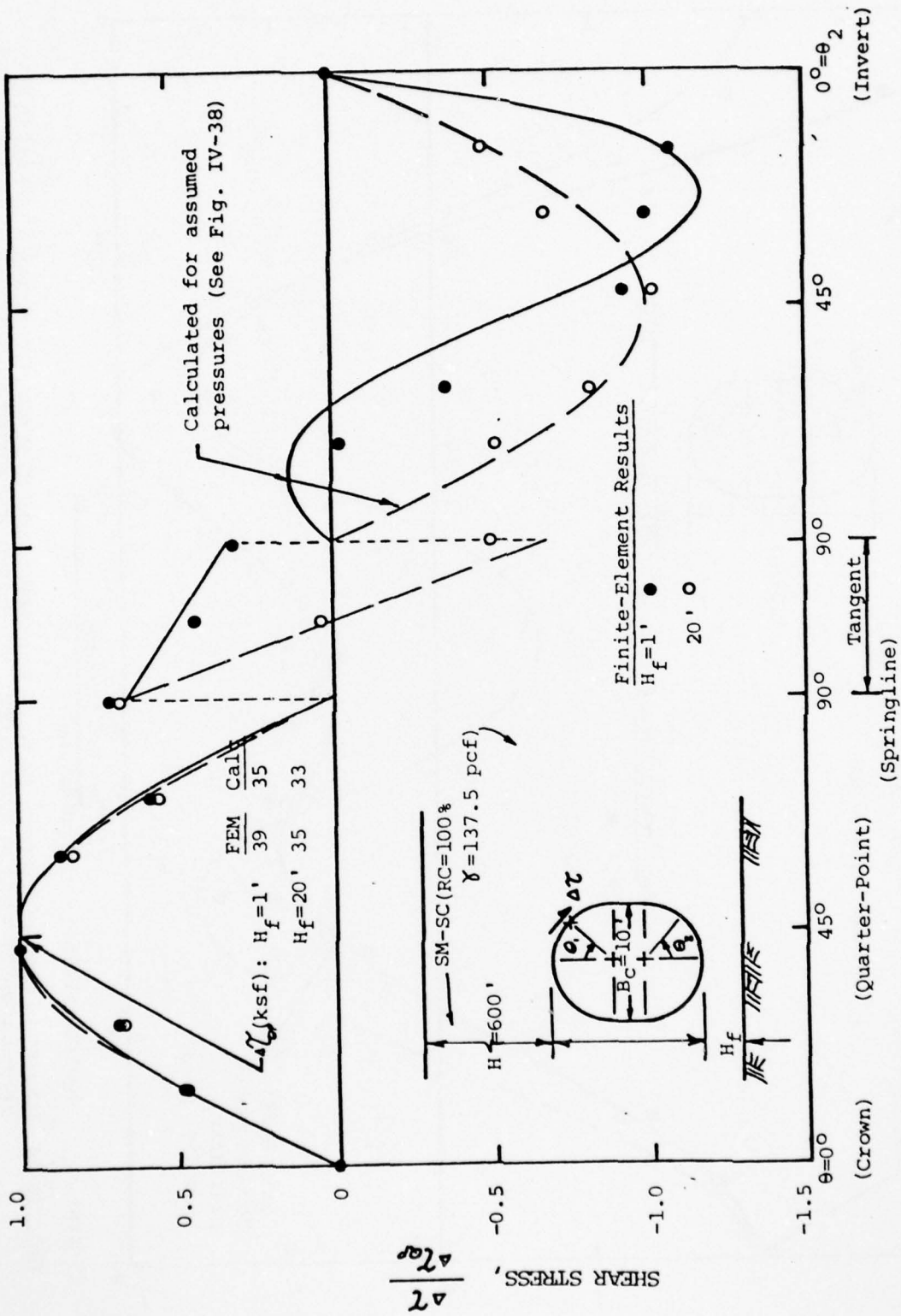


FIG. IV-43 SHEAR STRESS ON OBLONG CONDUIT, $H_o/B_c=1.25$ (NORMALIZED TO-SHEAR STRESS AT QUARTER-POINT): COMPARISON OF FEM RESULTS WITH VALUES CALCULATED FOR ASSUMED PRESSURES, SOIL FOUNDATION

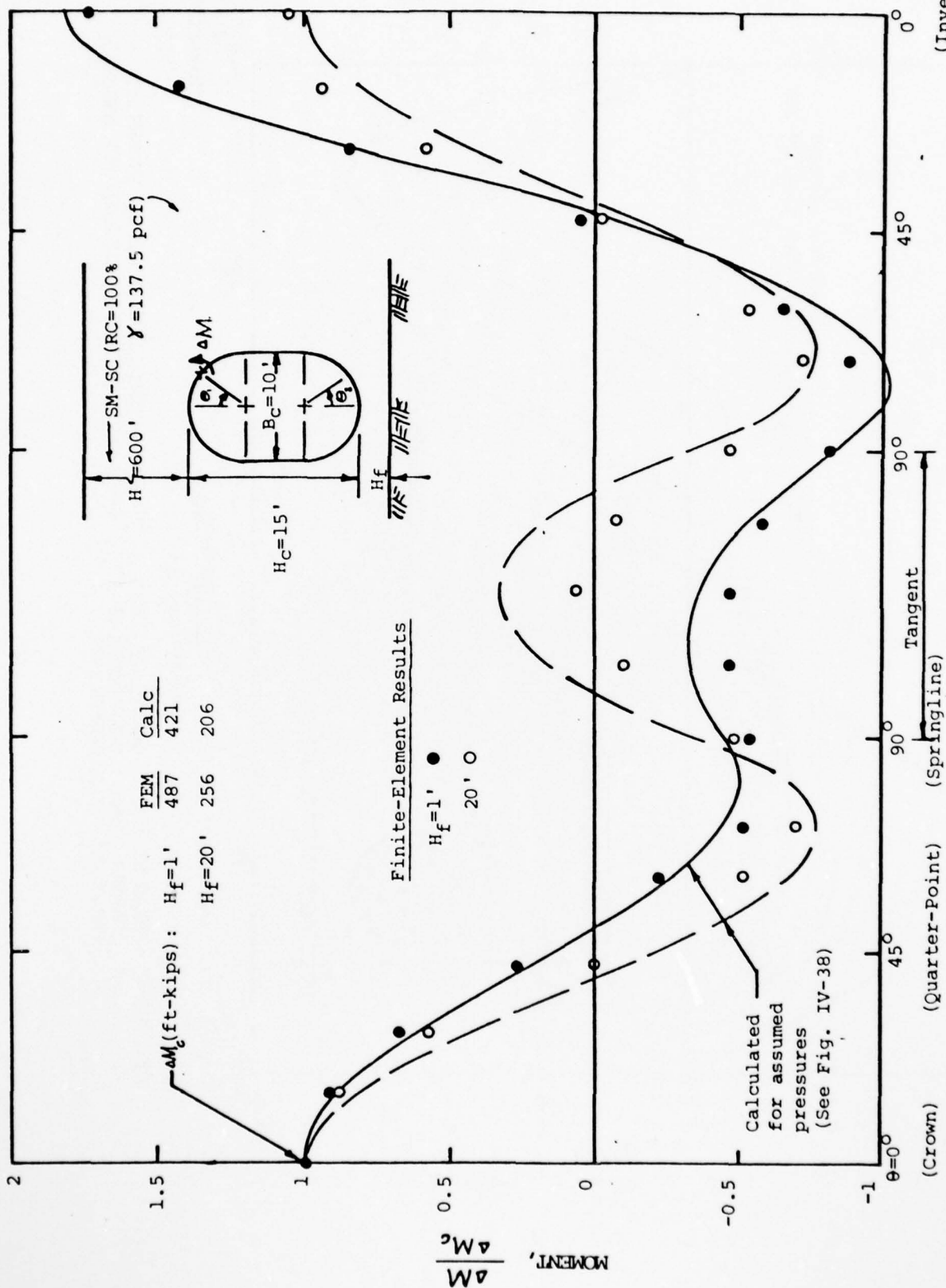


FIG. IV-44 MOMENT IN OBLONG CONDUIT, $H_c/B_c = 1.5$ (NORMALIZED TO MOMENT AT CROWN): COMPARISON OF FINITE-ELEMENT RESULTS WITH VALUES CALCULATED FOR ASSUMED PRESSURES, SOIL FOUNDATION

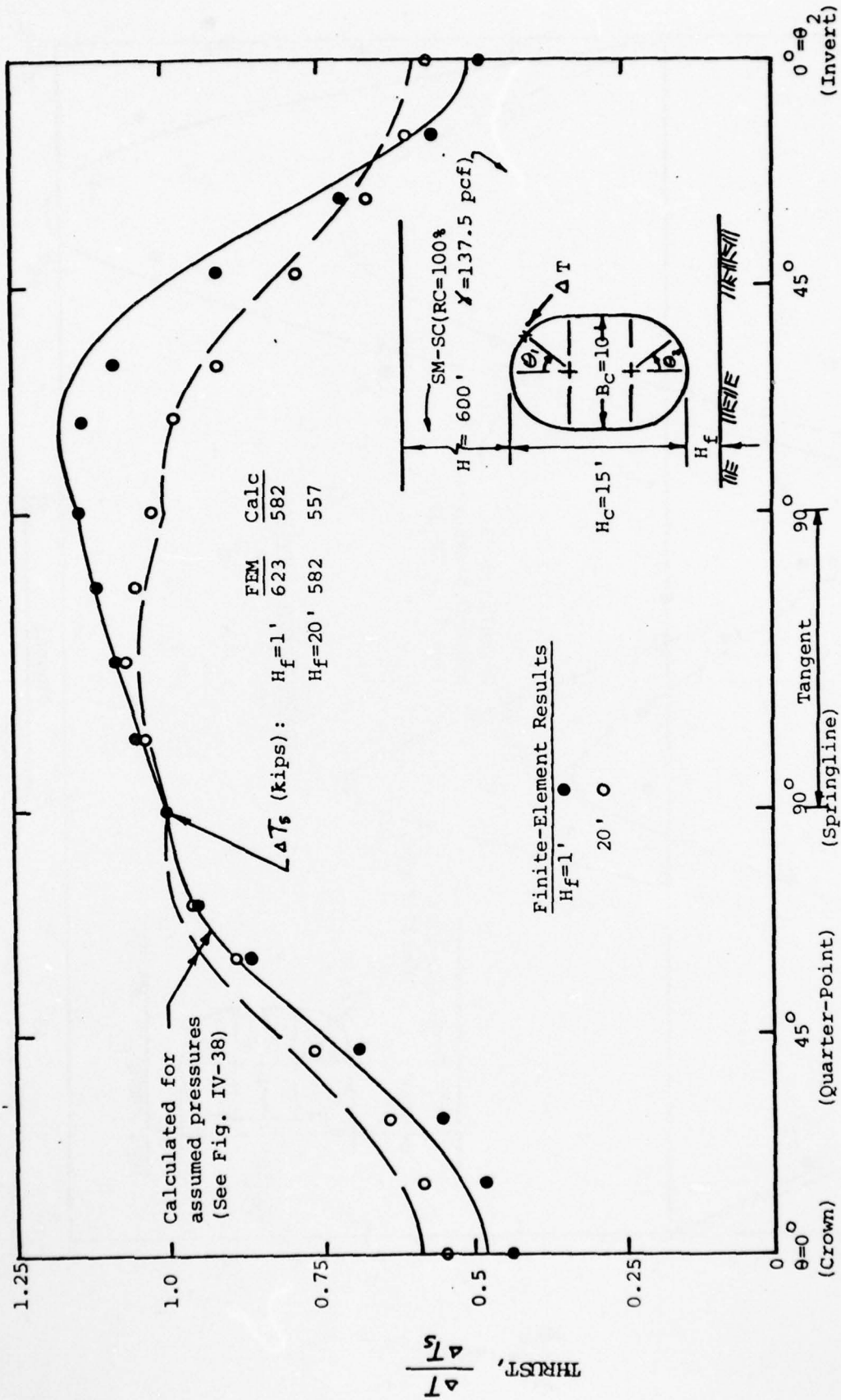


FIG. IV-45 THRUST ON OBLONG CONDUIT, $H_c/B_c=1.5$ (NORMALIZED TO THRUST AT SPRINGLINE): COMPARISON OF FINITE-ELEMENT RESULTS WITH VALUES CALCULATED FOR ASSUMED PRESSURES, SOIL FOUNDATION

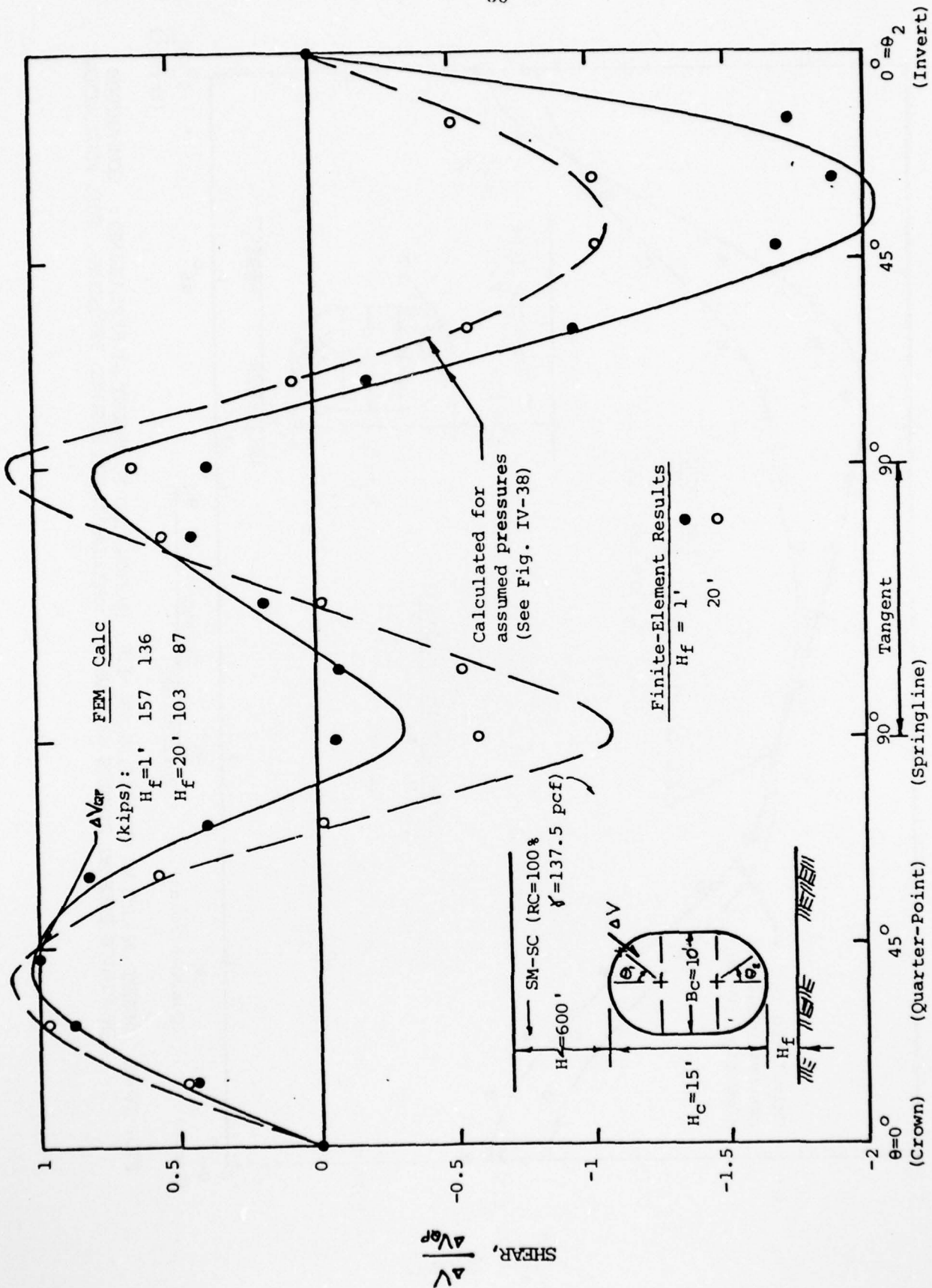


FIG. IV-46 SHEAR ON OBLONG CONDUIT, $H_c/B_c=1.5$ (NORMALIZED TO SHEAR AT QUARTER-POINT): COMPARISON OF FINITE-ELEMENT RESULTS WITH VALUES CALCULATED FOR ASSUMED PRESSURES, SOIL FOUNDATION

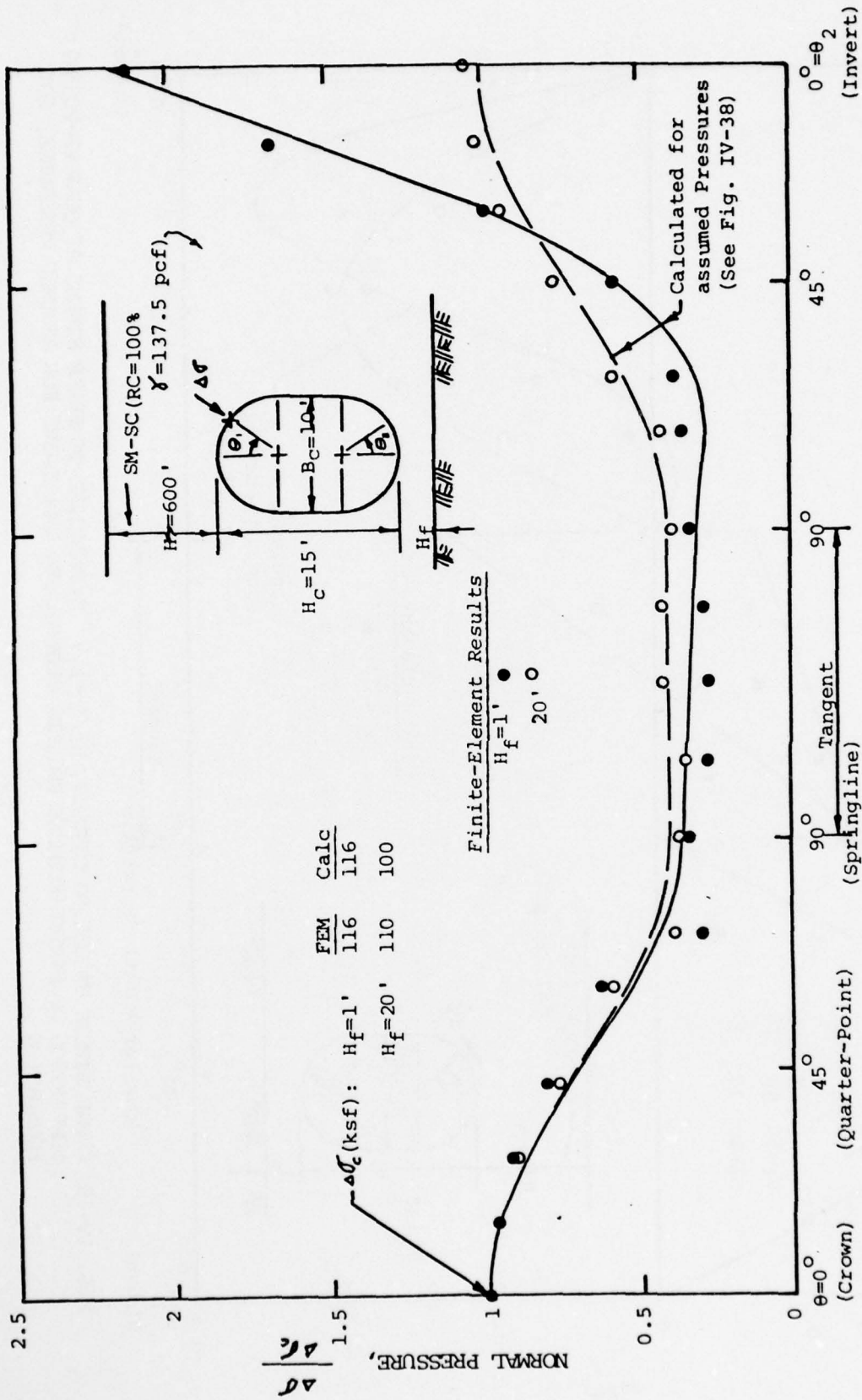


FIG. IV-47 NORMAL PRESSURE ON OBLONG CONDUIT, $H_c/B_c = 1.5$ (NORMALIZED TO NORMAL PRESSURE AT CROWN): COMPARISON OF FINITE-ELEMENT RESULTS WITH VALUES CALCULATED FOR ASSUMED PRESSURES, SOIL FOUNDATION

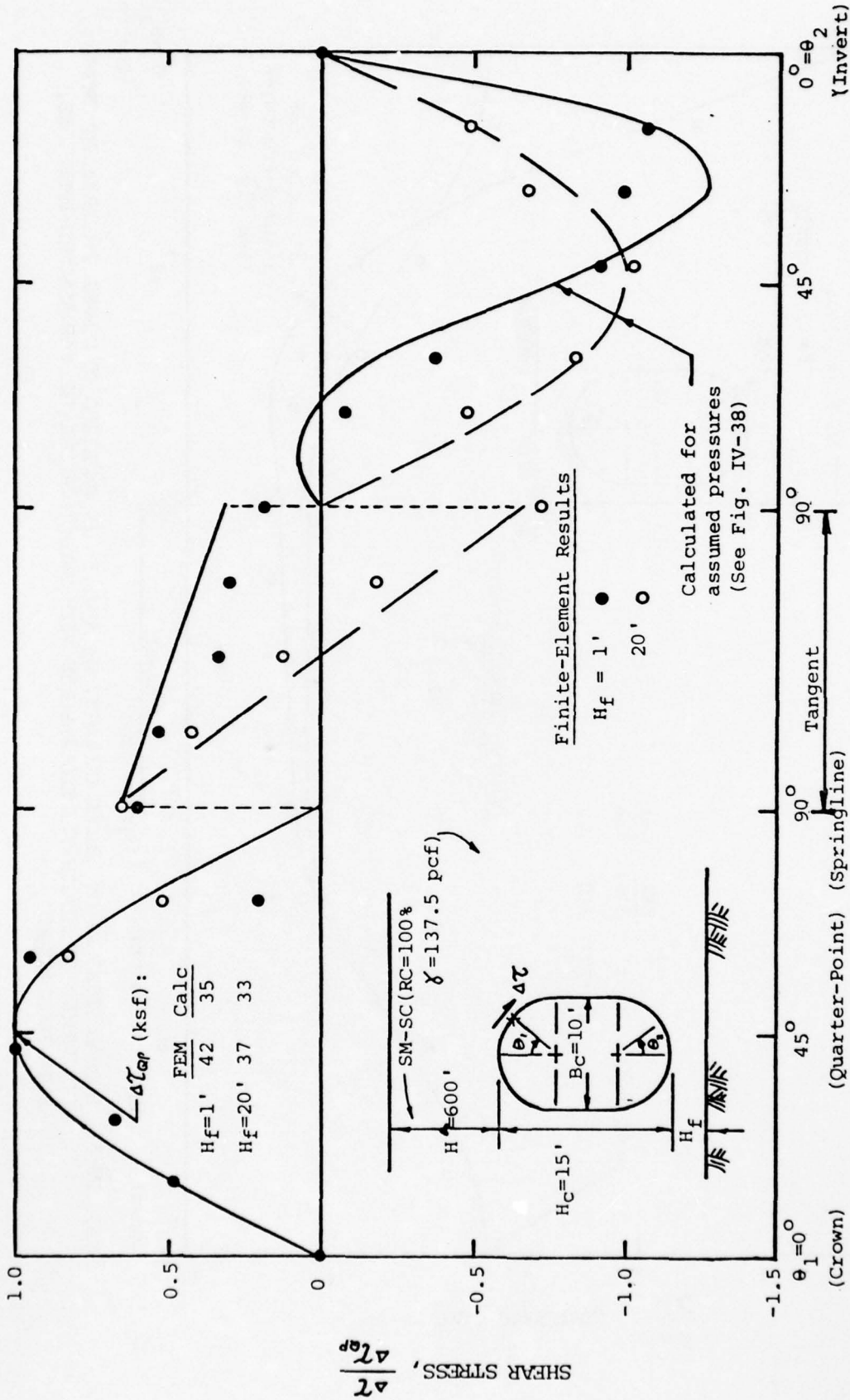


FIG. IV-48 SHEAR STRESS ON OBLONG CONDUIT, $H_c/B_c = 1.5$ (NORMALIZED TO SHEAR STRESS AT QUARTER-POINT): COMPARISON OF FINITE-ELEMENT RESULTS WITH VALUES CALCULATED FOR ASSUMED PRESSURES, SOIL FOUNDATION

3. Rectangular Conduits. In addition to the square conduit which has been previously discussed in some detail, finite-element analysis were performed for rectangular conduits with height-to-width ratios of 0.25 and 1.5.

Finite-element values of crown pressure on a square conduit for various fill heights and soil foundation depths have already been presented (Fig. IV-22). Similar results for the other two rectangular sections studied are presented in Figs. IV-49 and IV-50.

The distribution of calculated normal pressures and side-shear stresses on the three rectangular sections that have been studied are shown in Figs. IV-51 and IV-52. The straight-line approximations given in the figures can be summarized by the pressure diagrams in Fig. IV-53. The pressure diagrams differ from those previously described for circular and oblong conduits (Figs. IV-27 and IV-38, respectively) in the following ways:

- a. The vertical pressures at the top of the rectangular conduits are largest at the edge.
- b. The vertical pressures at the base are uniform for a shallow soil foundation, for a deep foundation the pressures are largest at the edge of the conduit.
- c. The horizontal pressures are greatest near the midheight of the conduit and decrease towards the top and base.

The increased vertical pressures near the edge of the rectangular conduits have been represented by an Edge Pressure Factor, m . Values of m , as determined from the finite-element results are presented in Fig. IV-54. The values of m were determined for the data at a height of fill equal to 600 feet and should be conservative for smaller heights of fill (see for example, the data in Figs. IV-23 and IV-24).

Values of N , the Crown Pressure Factor, can be determined from Figs. IV-22, IV-49, and IV-50, for the different rectangular conduit shapes. The figures are for soil foundations depth of 0.1 and 2 times the conduit width. For intermediate foundation depths, the factor N probably varies in a manner similar to that for circular conduits (Fig. IV-28). Values of n , the Foundation Reaction Factor, are also likely to be similar to those determined for circular conduits (Fig. IV-28).

The pressure diagrams in Fig. IV-53 were used to calculate the structural response of a 10-foot-square conduit for the case of a shallow soil foundation and a height of fill above the conduit equal to 600 feet. Calculated values of moment, thrust and shear are compared with finite-element results in Figs. IV-55 through IV-57. The agreement is quite good.

H. Rock Foundation

The finite-element analyses discussed thus far were performed for conduits underlain by soil. In this section consideration is given to the earth pressures on conduits founded directly on rock.

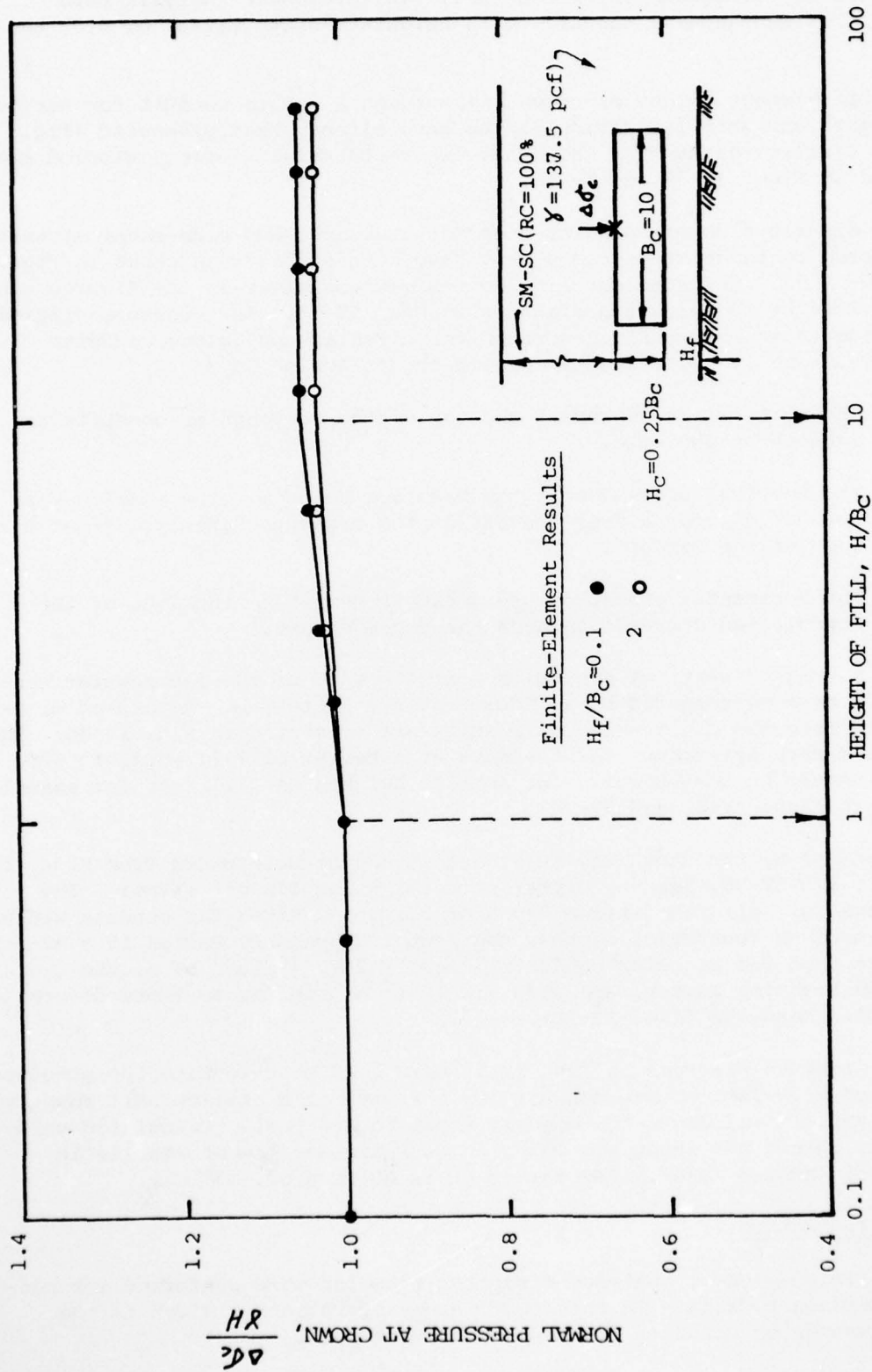


FIG. IV-49 NORMAL PRESSURE AT CROWN OF RECTANGULAR CONDUIT ($H_c/B_c=0.25$) FOR DIFFERENT SOIL FOUNDATION DEPTHS

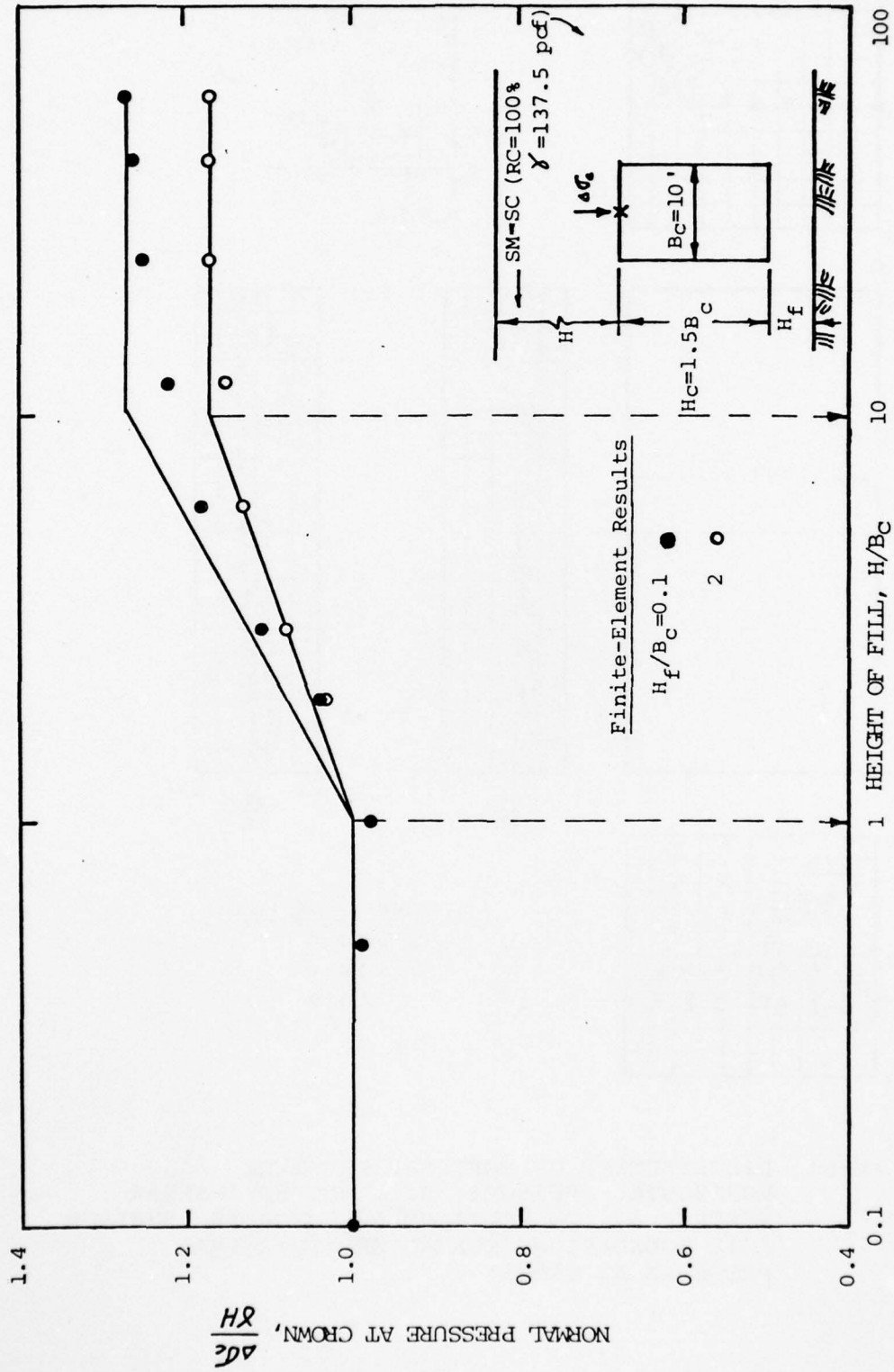


FIG. IV-50 NORMAL PRESSURE AT CROWN OF RECTANGULAR CONDUIT ($H_C/B_C=1.5$) FOR DIFFERENT SOIL FOUNDATION DEPTHS

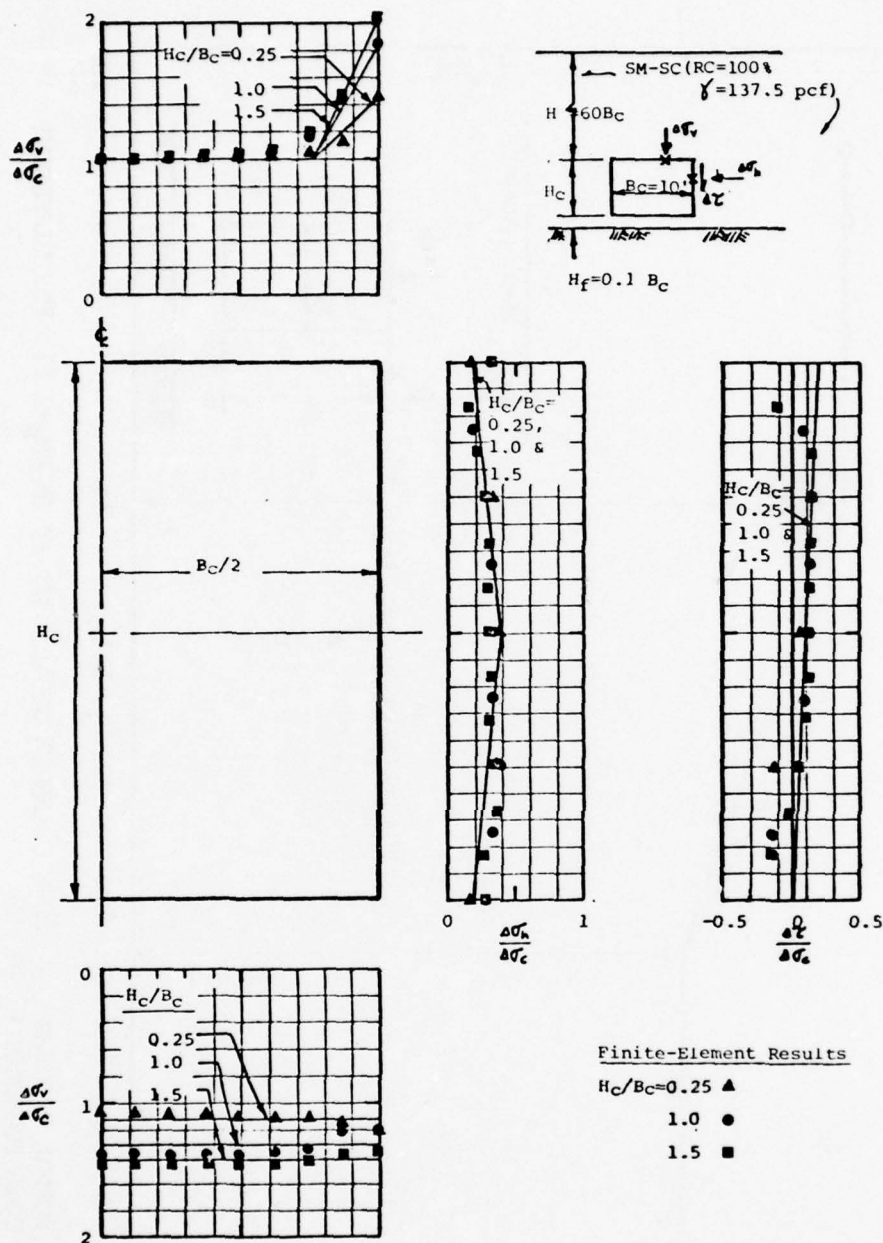


FIG. IV-51 DISTRIBUTION OF VERTICAL PRESSURE, $\Delta\sigma_v$, HORIZONTAL PRESSURE, $\Delta\sigma_h$, AND SIDE-SHEAR STRESS, $\Delta\tau$, ON RECTANGULAR CONDUITS, SHALLOW SOIL FOUNDATION (NORMALIZED TO NORMAL PRESSURE AT CROWN)

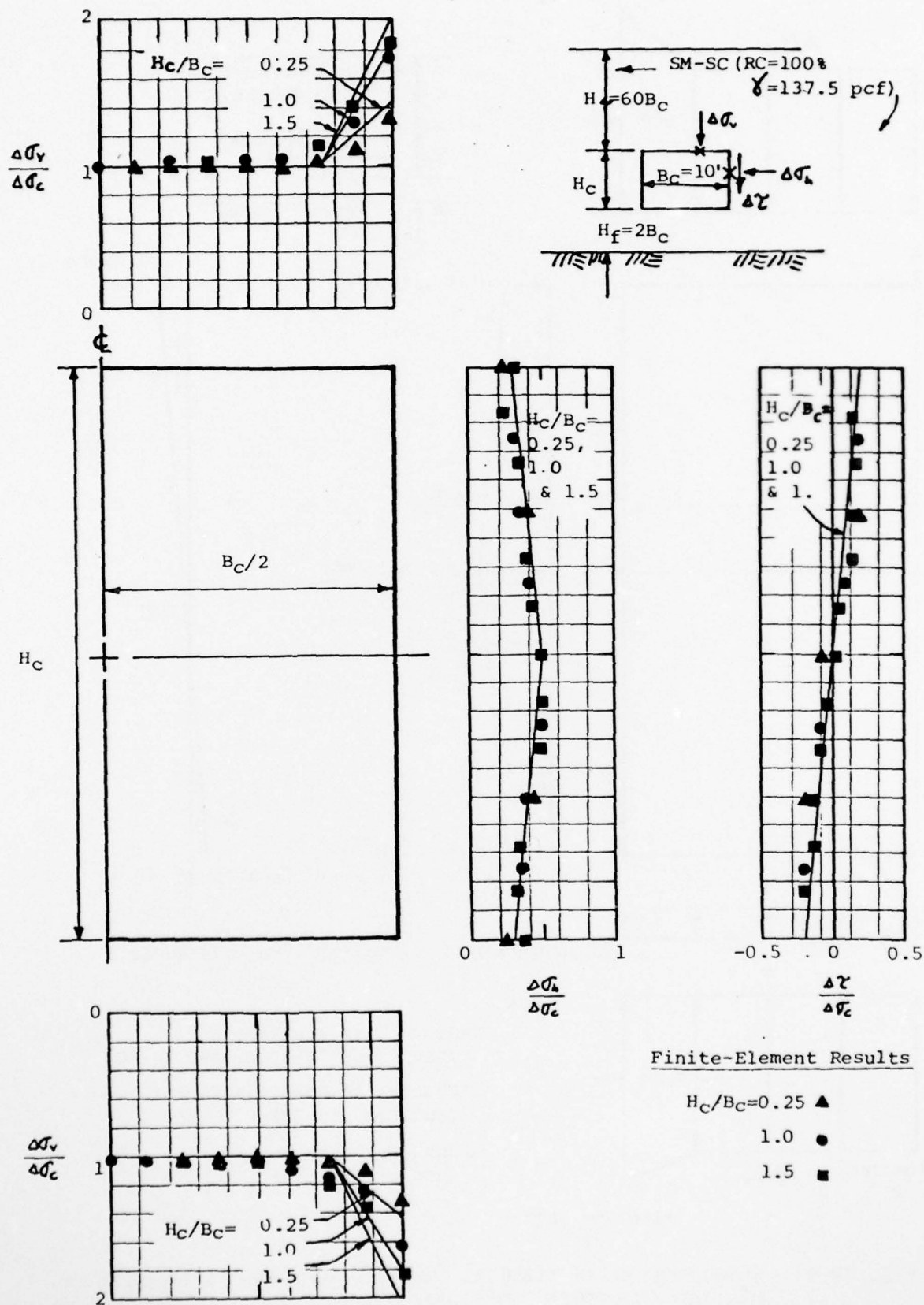


FIG. IV-52 DISTRIBUTION OF VERTICAL PRESSURE, $\Delta\sigma_v$, HORIZONTAL PRESSURE, $\Delta\sigma_h$, AND SIDE-SHEAR, $\Delta\tau$, ON RECTANGULAR CONDUITS, DEEP SOIL FOUNDATION (NORMALIZED TO NORMAL PRESSURE AT CROWN)

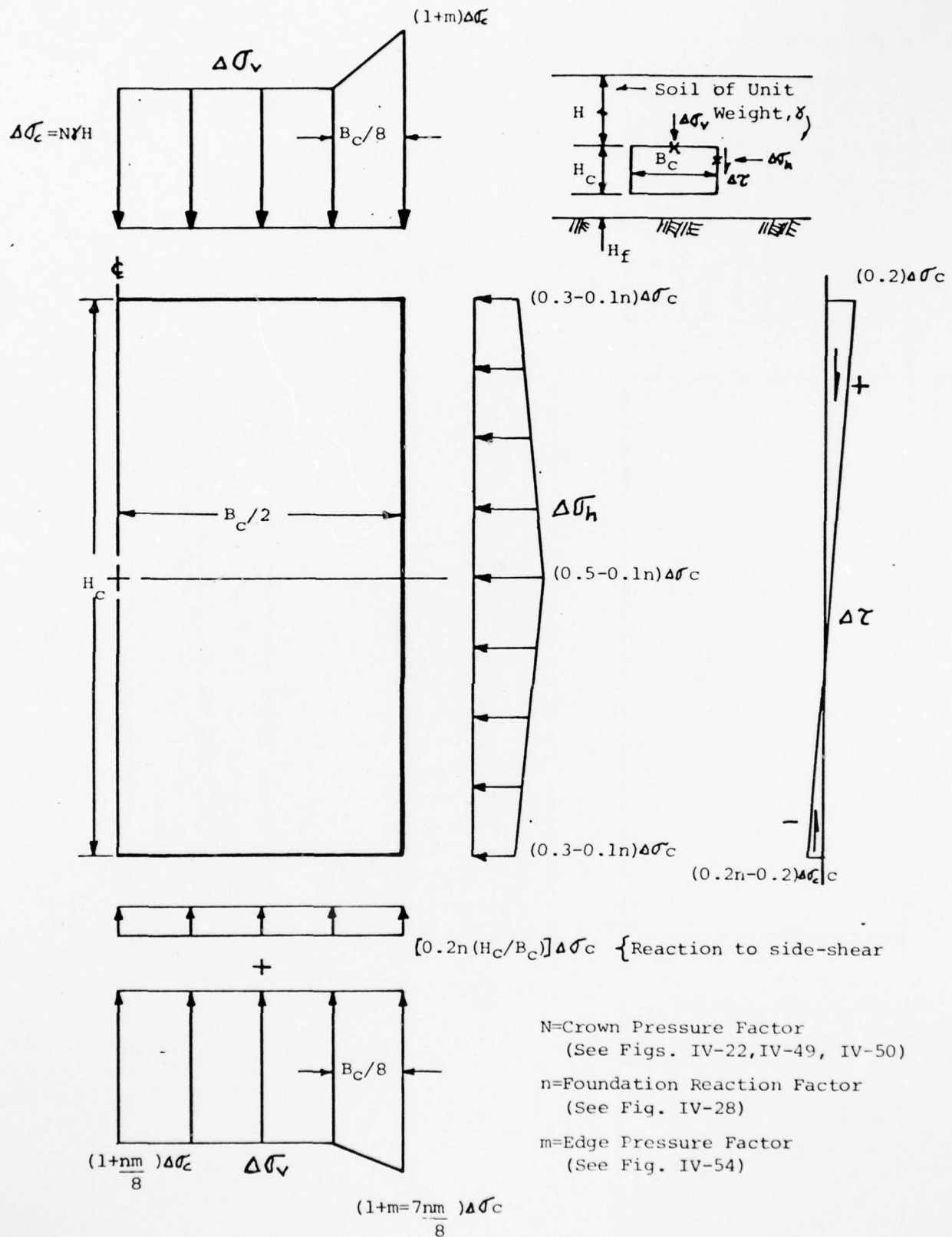


FIG. IV-53 APPROXIMATIONS OF VERTICAL PRESSURE, $\Delta\sigma_v$, HORIZONTAL PRESSURE, $\Delta\sigma_h$, AND SIDE-SHEAR STRESS, $\Delta\tau$, FOR RECTANGULAR CONDUITS, SOIL FOUNDATION (NORMALIZED TO NORMAL PRESSURE AT CROWN)

AD-A064 169

CALIFORNIA UNIV BERKELEY GEOTECHNICAL ENGINEERING
EARTH PRESSURES ON CONDUITS AND RETAINING WALLS. (U)
SEP 78 D W QUIGLEY, J M DUNCAN

F/G 13/2

UNCLASSIFIED

UCB/6T/78-06

DACW39-76-C-0035

NL

2 OF 4
AD
A064169

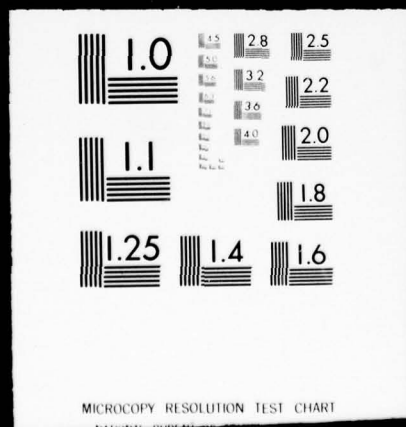


ASS IF I

2 OF

AD

A064169



MICROCOPY RESOLUTION TEST CHART

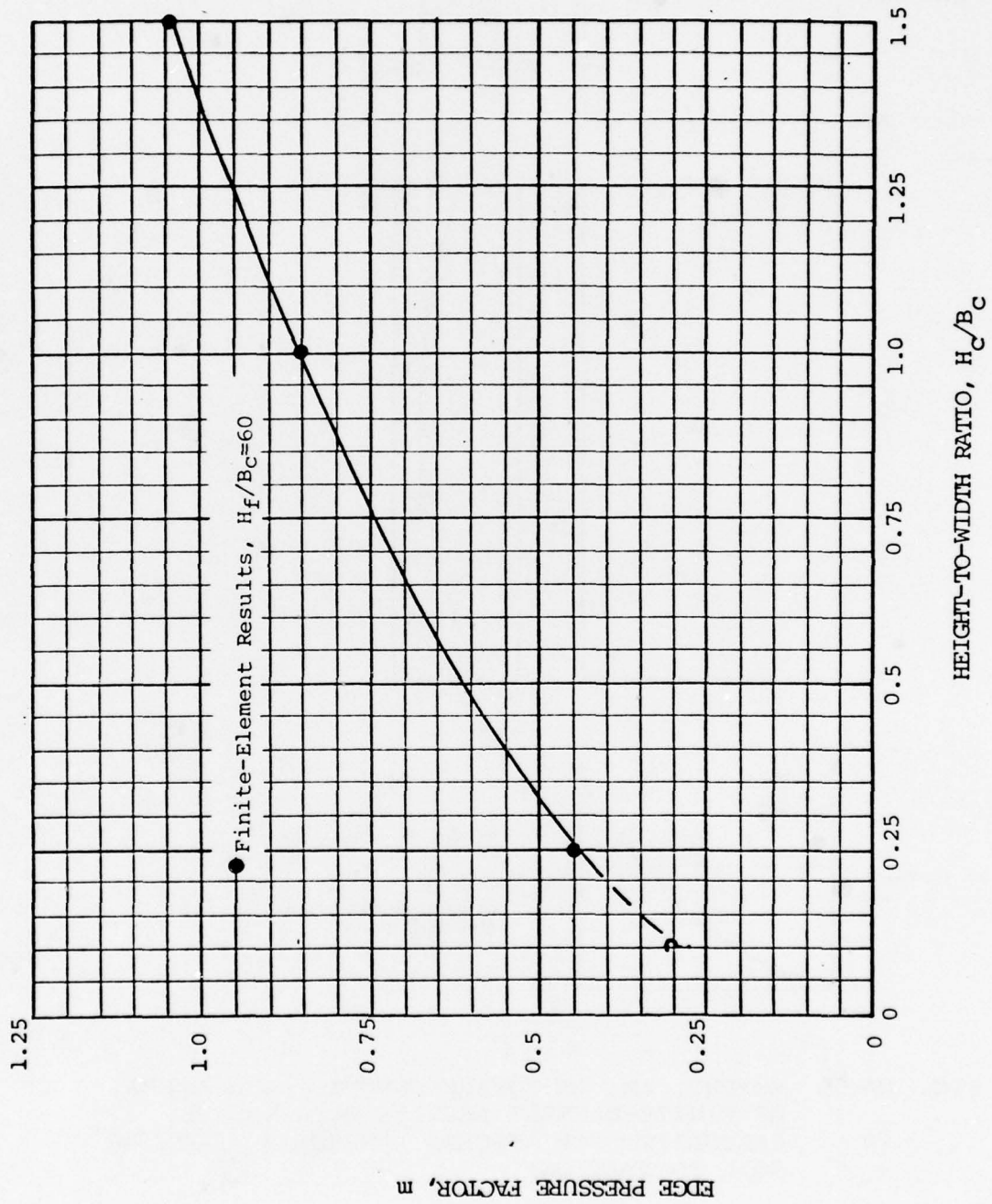


FIG. IV-54 EDGE-PRESSURE FACTOR FOR RECTANGULAR CONDUITS ON SOIL FOUNDATIONS.

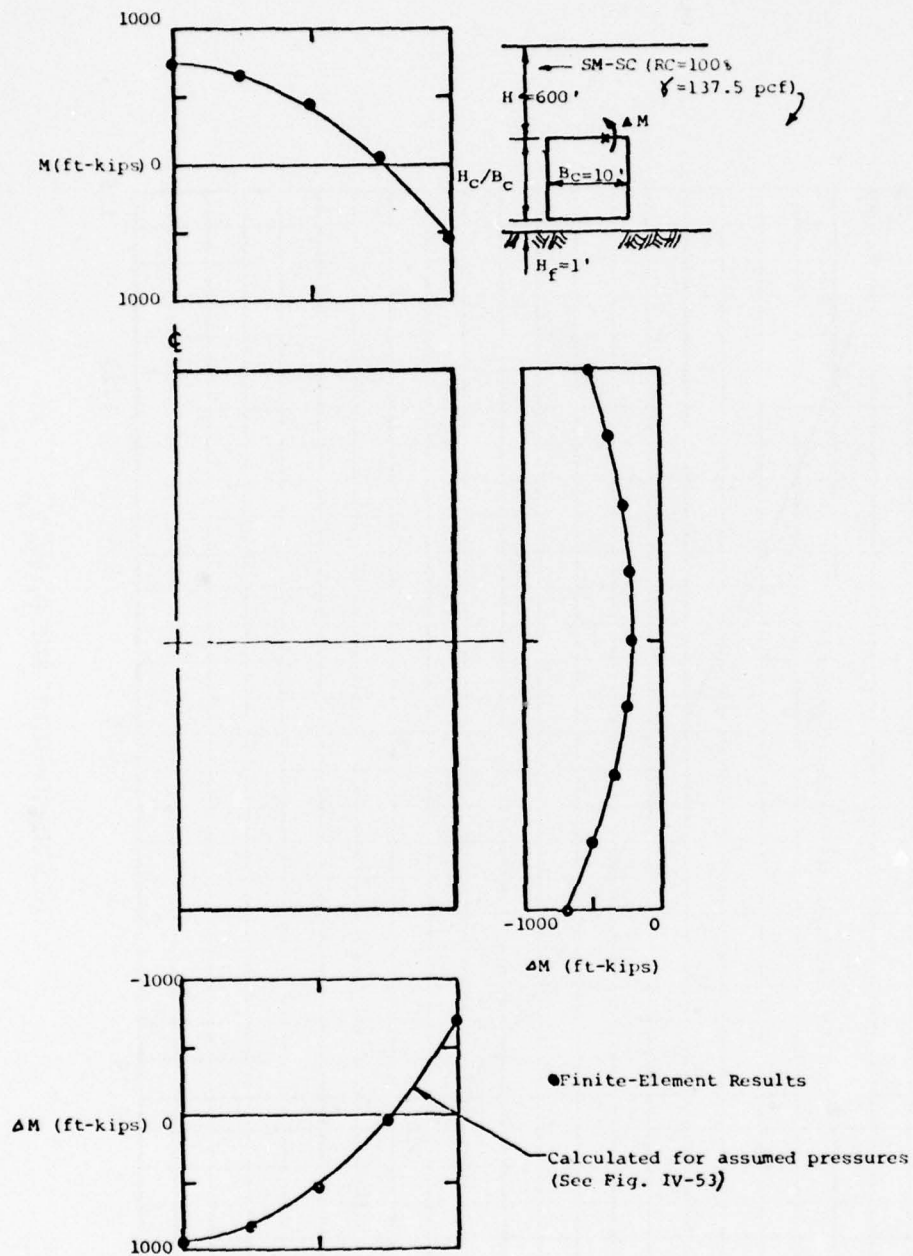


FIG. IV-55 MOMENT, ΔM , IN SQUARE CONDUIT, COMPARISON OF FINITE-ELEMENT RESULTS WITH VALUES CALCULATED FOR ASSUMED PRESSURES (SHALLOW SOIL FOUNDATION)

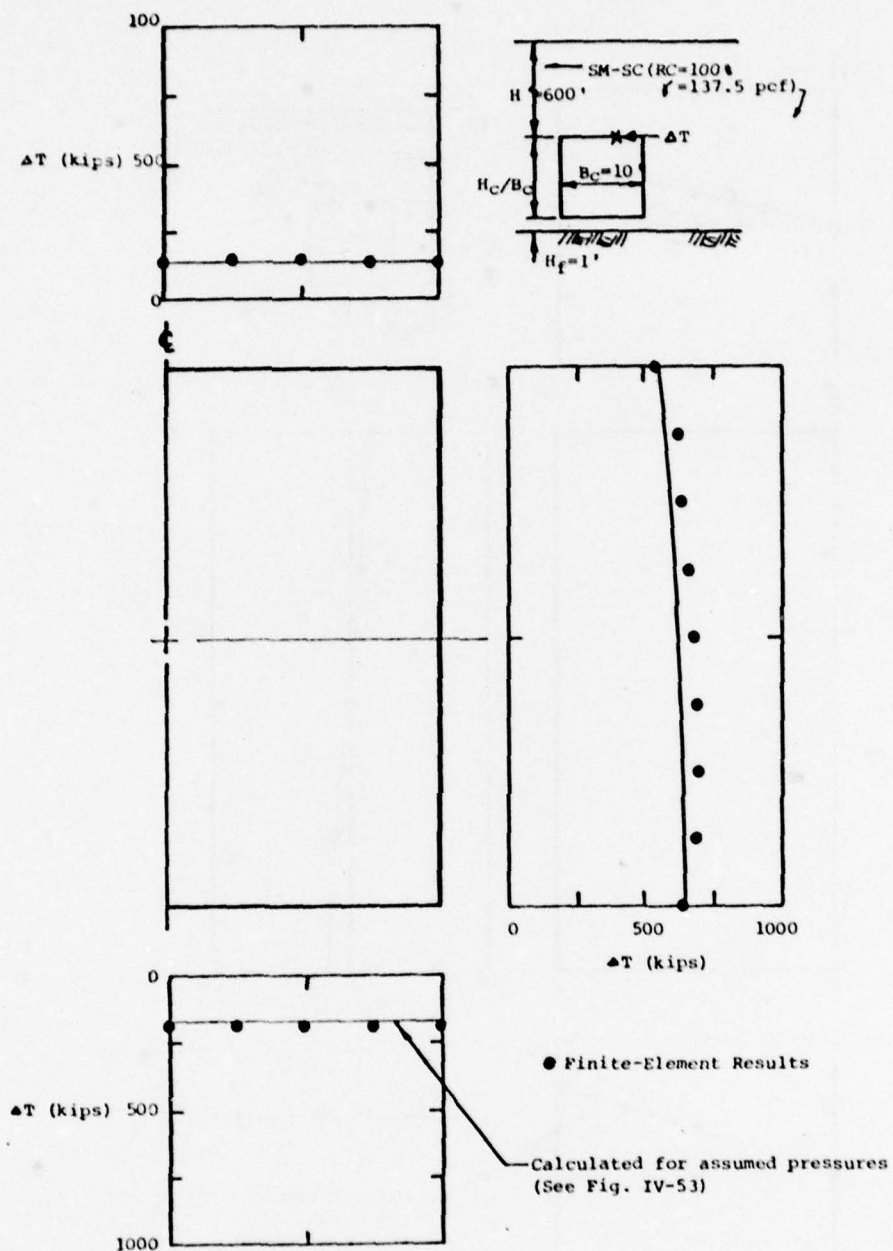


FIG. IV-56 THRUST, ΔT , IN SQUARE CONDUIT, COMPARISON OF FINITE-ELEMENT RESULTS WITH VALUES CALCULATED FOR ASSUMED PRESSURES (SHALLOW SOIL FOUNDATION)

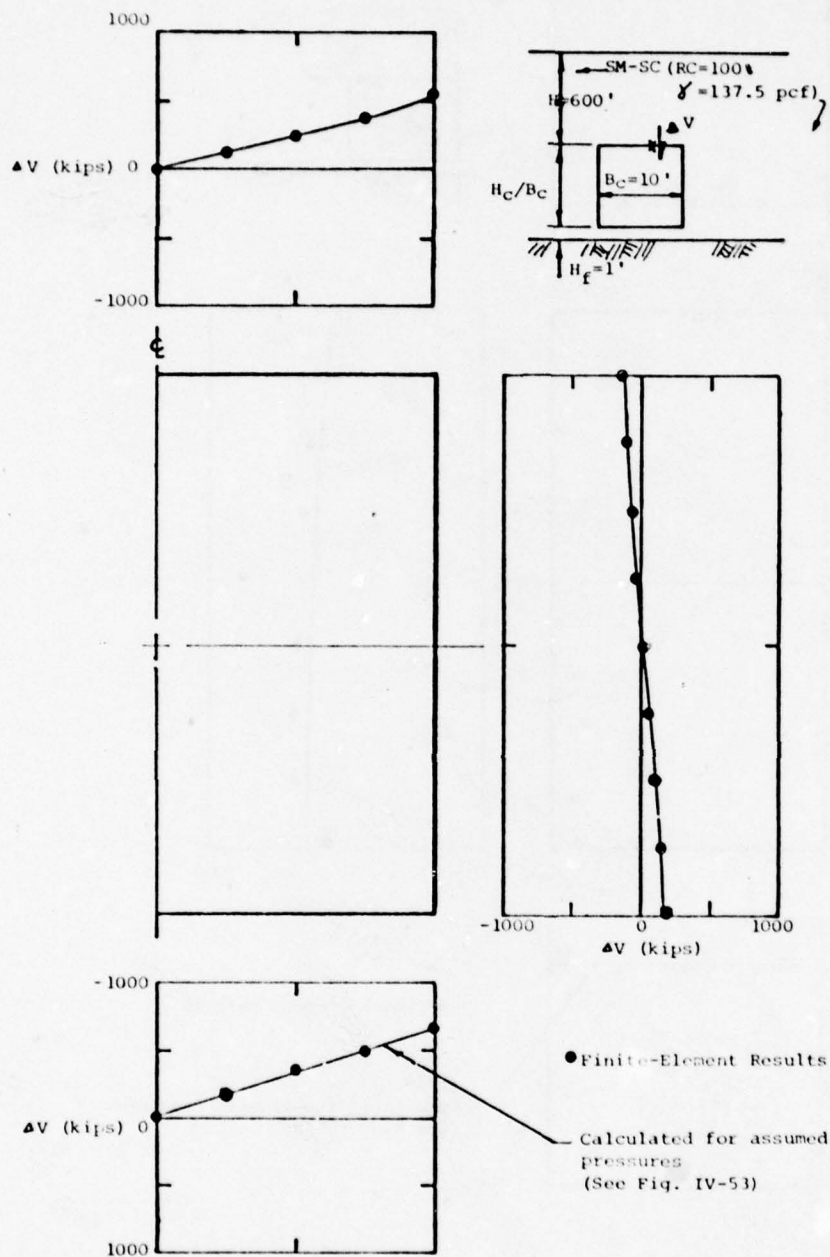


FIG. IV-57 SHEAR, ΔV , IN SQUARE CONDUIT, COMPARISON OF FINITE-ELEMENT RESULTS WITH VALUES CALCULATED FOR ASSUMED PRESSURES (SHALLOW SOIL FOUNDATION)

1. Rectangular Conduits. It is useful to consider first the results of finite-element analyses of a square conduit whose base lies on the surface of a rock foundation. The rock was assumed to have a modulus of elasticity equal to that of the concrete in the conduit, a reasonable assumption judging from values of rock moduli reported in the literature.

At a height of fill equal to 600 feet, the normal pressure at the crown of the conduit was essentially the same as that for a square conduit on a shallow soil foundation (of H_c/B_c equal to 0.1). The distribution of vertical and horizontal pressures and side-shear stresses on the conduit are shown in Fig. IV-58. The data are similar to the pressure distributions for a square conduit on a shallow soil foundation (Figs. IV-51 and IV-53) with the exception of a slight edge pressure on the base of the conduit.

Next consider the case of a square conduit embedded below the surface of the rock foundation such that it has a projection ratio of 0.5 as shown in Fig. IV-59. The calculated pressure at the crown of such a conduit (10 foot width) was found to be approximately equal to the value that would be expected for a rectangular conduit on a shallow soil foundation that has a height-to-width ratio of 0.5, as shown in Fig. IV-60. Thus it is apparent that the rise-to-span ratio (R/S), as defined in the figure, is the controlling parameter which determines the crown-pressure factor for a rectangular conduit on either a rock or shallow soil foundation. Fig. IV-61 indicates the distribution of horizontal and vertical pressures and shear stresses on the partially embedded conduit. Note that results are given for analyses performed with and without friction at the interface between the conduit and the rock. It is felt that the results for no side friction are more likely to represent actual field conditions for the following reasons:

- a. The face of a vertical rock cut could be relatively loose and weak compared to the intact rock mass.
- b. The horizontal pressures at the conduit-rock interface are relatively small. Because, in reality, the frictional force that could be developed at the interface would be proportional to the horizontal pressure, it would also be small.

The approximations to the data for no side friction, which are shown in Fig. IV-61, are similar to those given previously for rectangular conduits on shallow soil foundations but account for the fact that the equivalent height-to-width (or rise-to-span) ratio of the conduit is only 0.5 (i.e., the portion above the rock surface). It has also been conservatively assumed that the horizontal pressures below the rock surface are zero.

Approximate pressure distributions for rectangular conduits on rock foundations based on the finite-element analyses are given in Fig. IV-62. Appropriate values of N , the Crown Pressure Factor, and m , the Edge Pressure Factor, can be assumed to equal those for rectangular conduits on shallow soil foundations (Figs. IV-22, IV-49, IV-50, IV-60 and IV-54, respectively).

2. Circular and Oblong Conduits. Finite-element analyses were performed for two circular conduits embedded in rock as shown in Fig. IV-63.

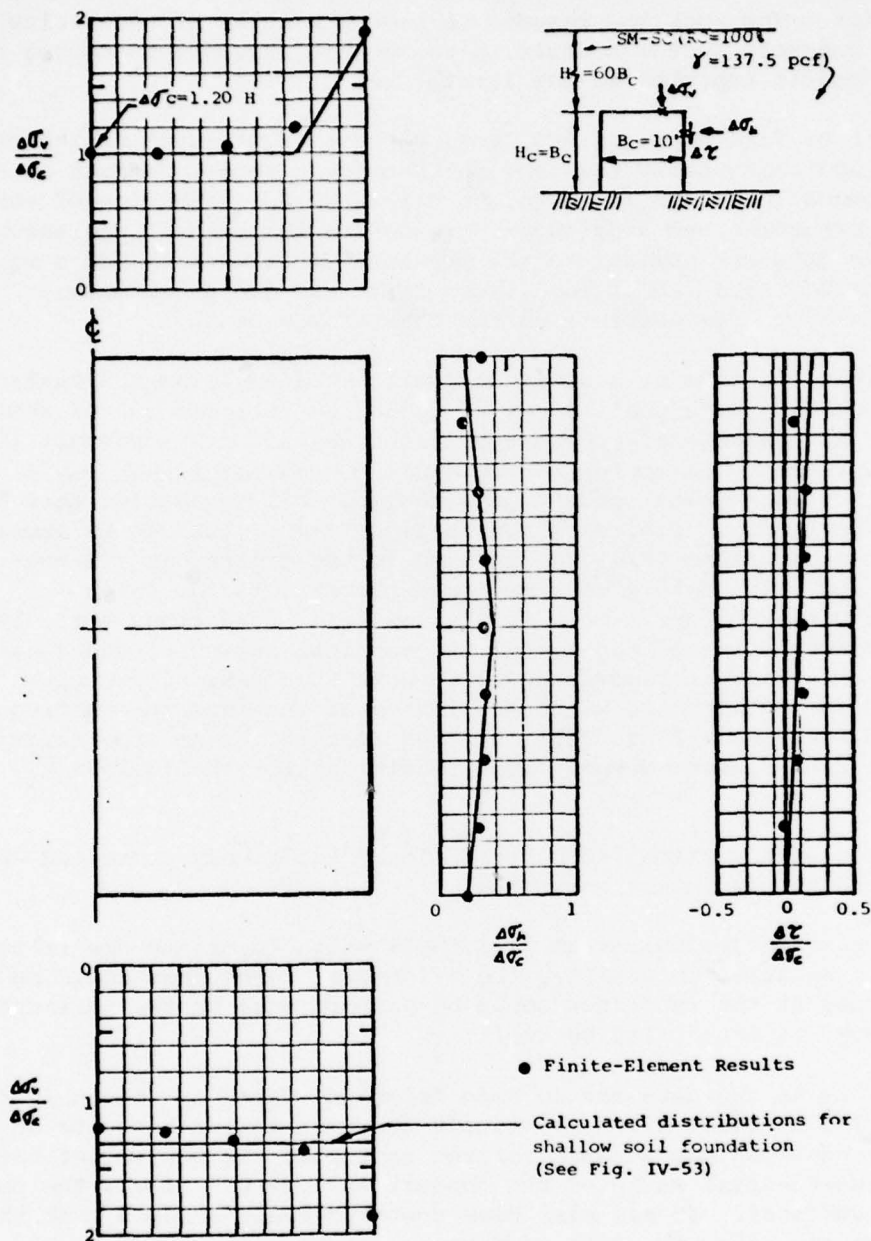


FIG. IV-58 DISTRIBUTION OF VERTICAL PRESSURE, $\Delta\sigma_v$, HORIZONTAL PRESSURE, $\Delta\sigma_h$, AND SIDE-SHEAR STRESS, $\Delta\tau$, ON A SQUARE CONDUIT ON A ROCK FOUNDATION (NORMALIZED TO NORMAL PRESSURE AT CROWN)

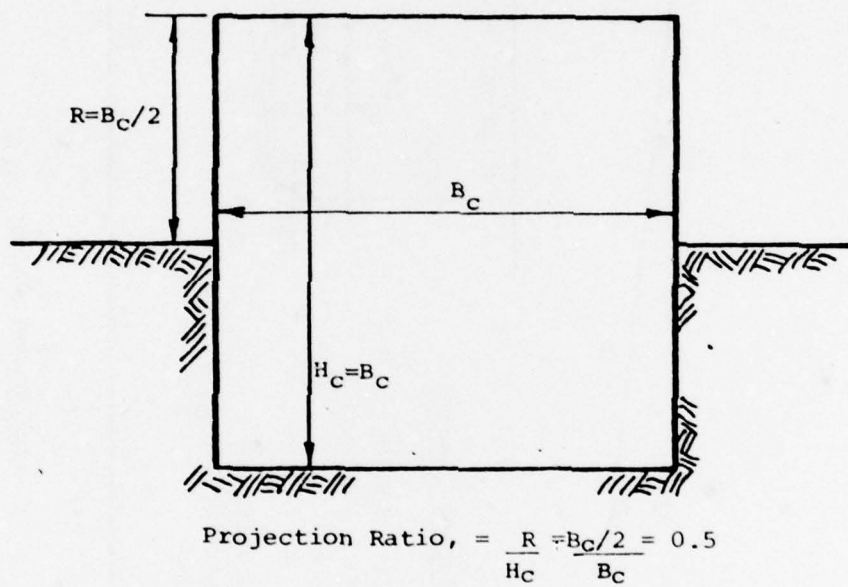


FIG. IV-59 SQUARE CONDUIT PARTIALLY EMBEDDED IN
ROCK FOUNDATION (Projection Ratio=0.5)

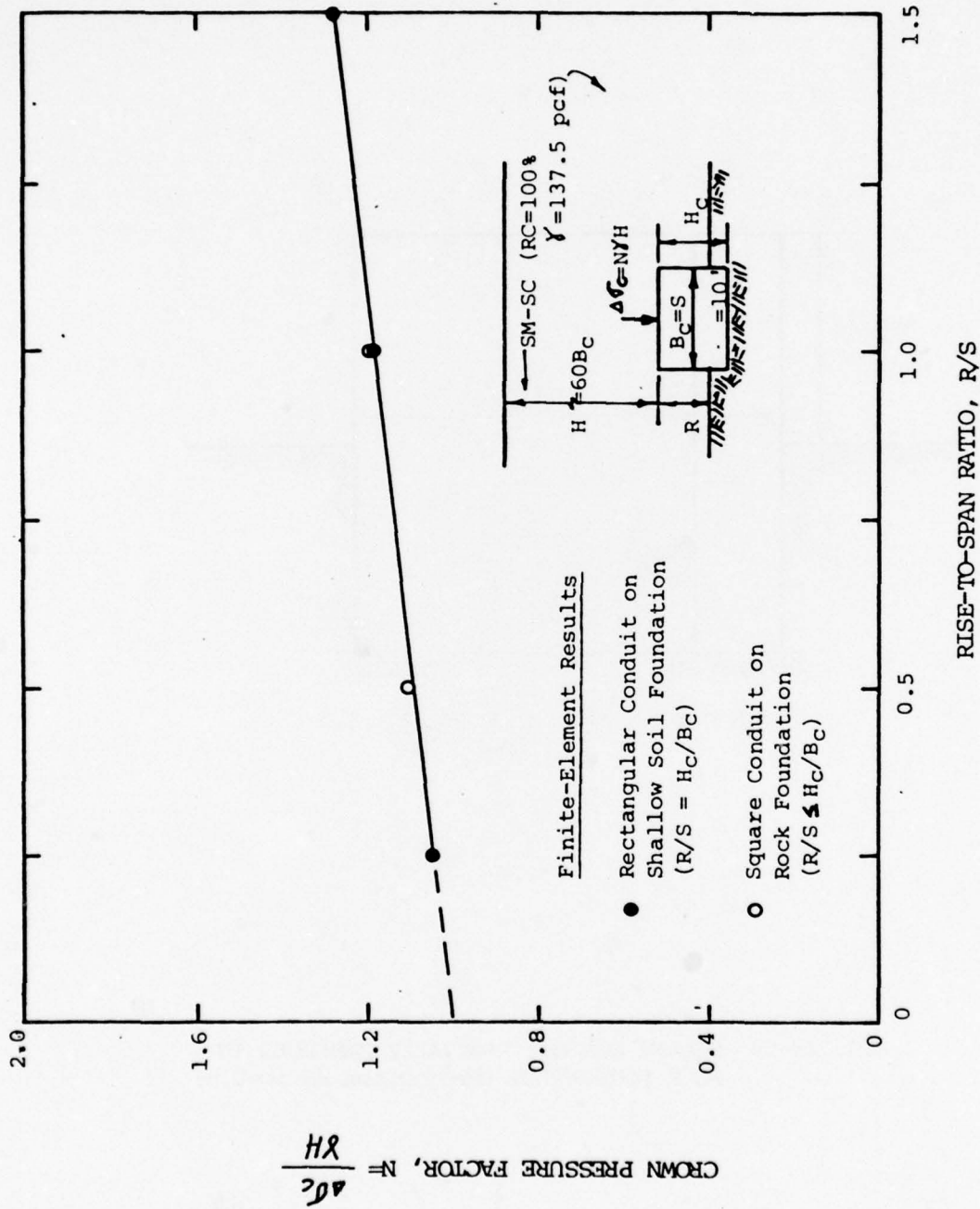


FIG. IV-60 CROWN PRESSURE FACTOR VS. RISE-TO-SPAN RATIO FOR RECTANGULAR CONDUITS (SHALLOW SOIL OR ROCK FOUNDATION)

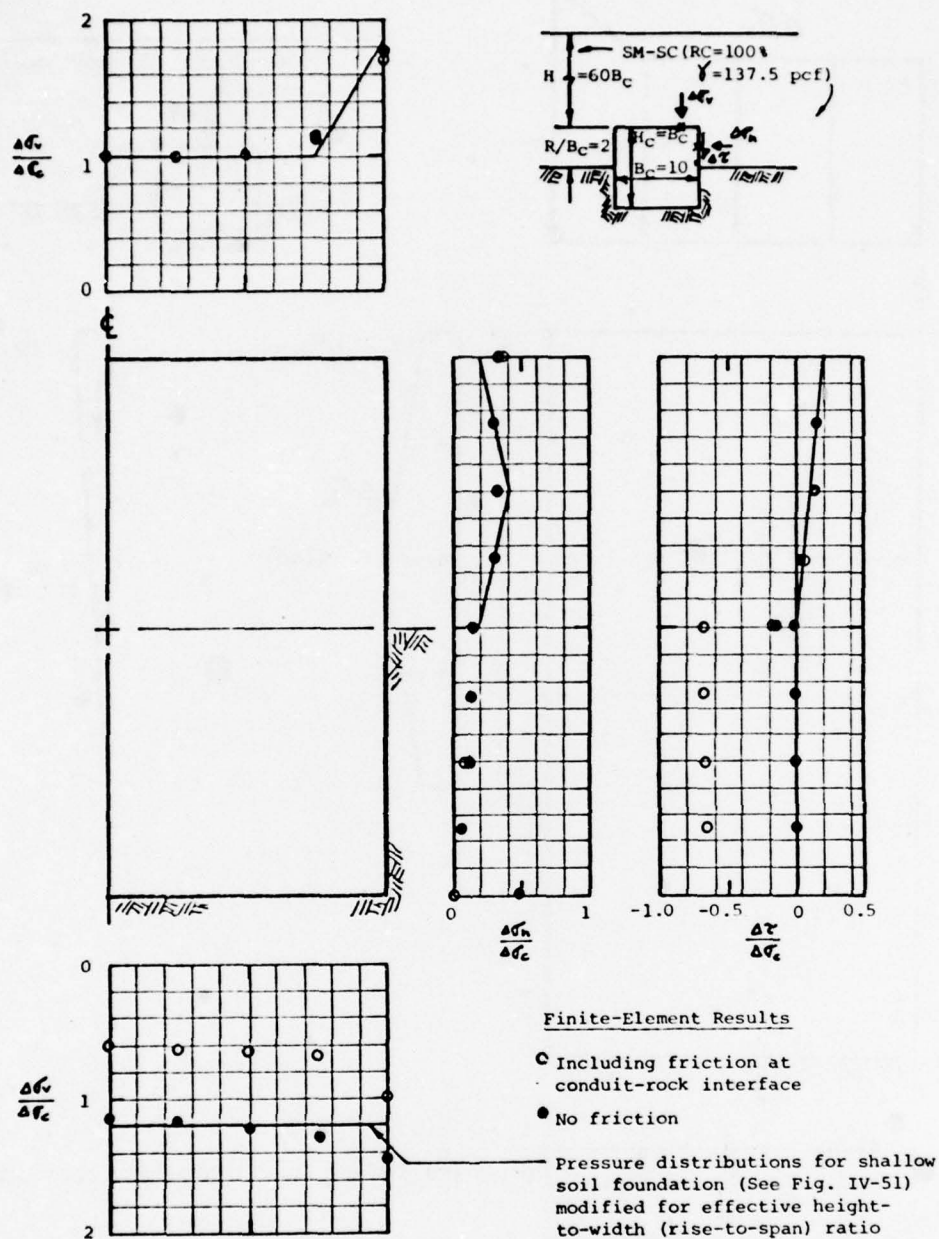


FIG. IV-61 DISTRIBUTION OF VERTICAL PRESSURE, $\Delta\sigma_v$, HORIZONTAL PRESSURE, $\Delta\sigma_h$, AND SIDE-SHEAR STRESS, $\Delta\tau$, ON SQUARE CONDUIT EMBEDDED IN A ROCK FOUNDATION (NORMALIZED TO NORMAL PRESSURE AT CROWN)

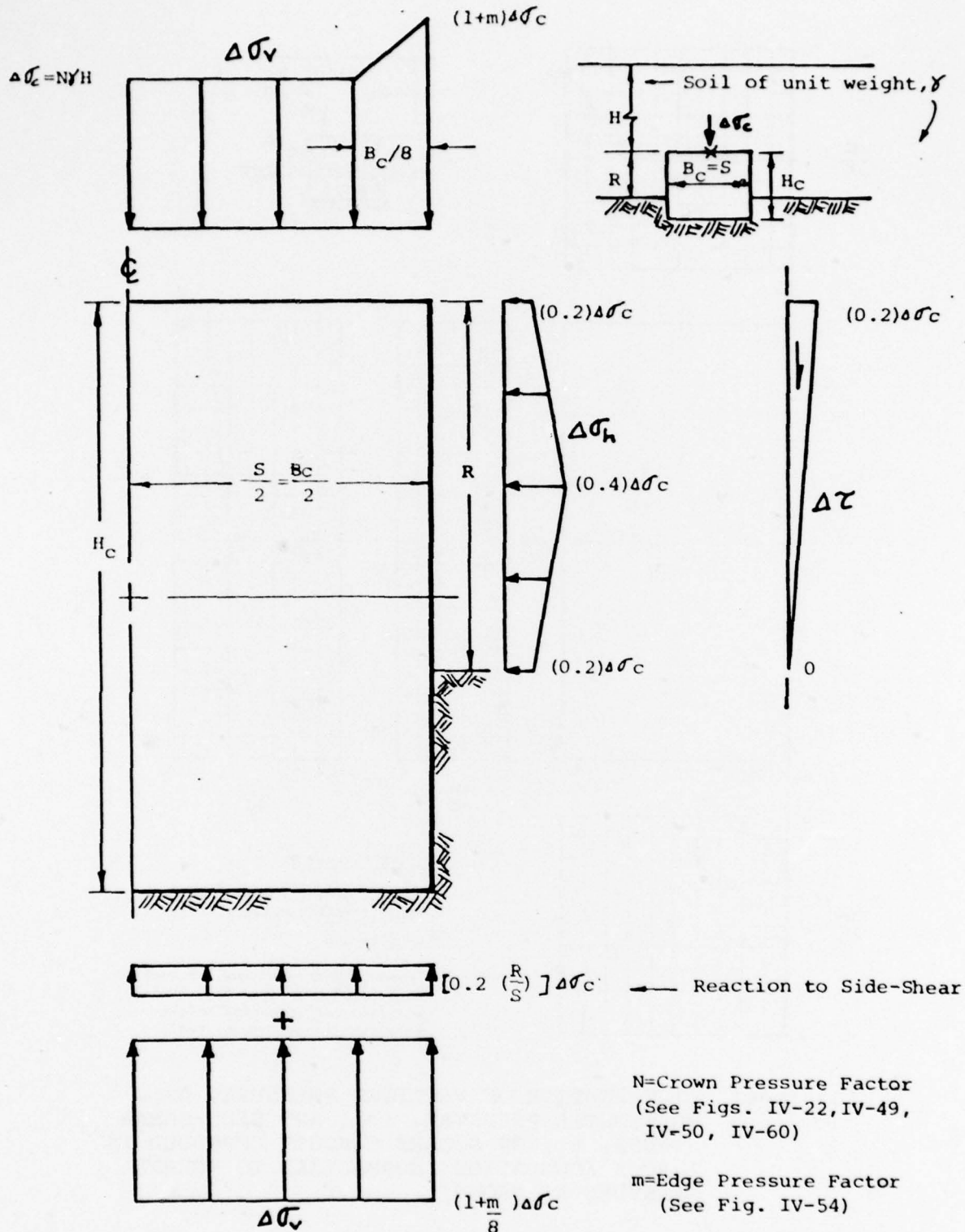
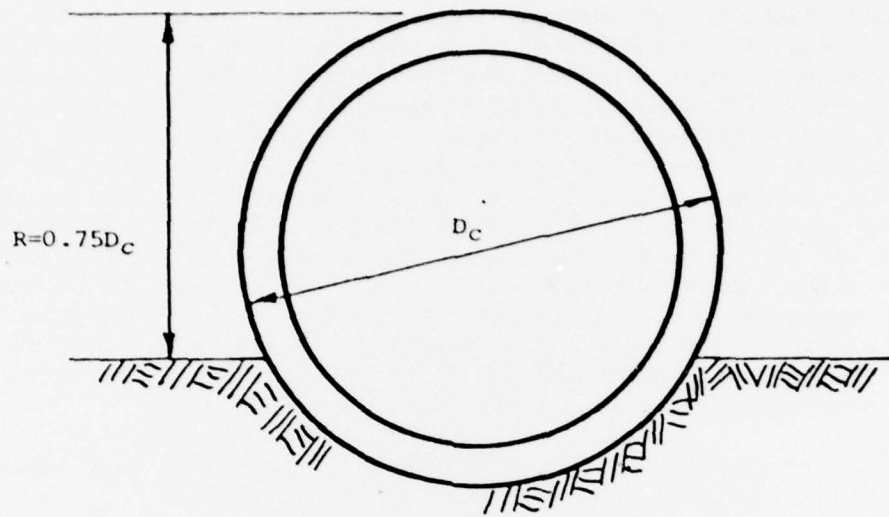
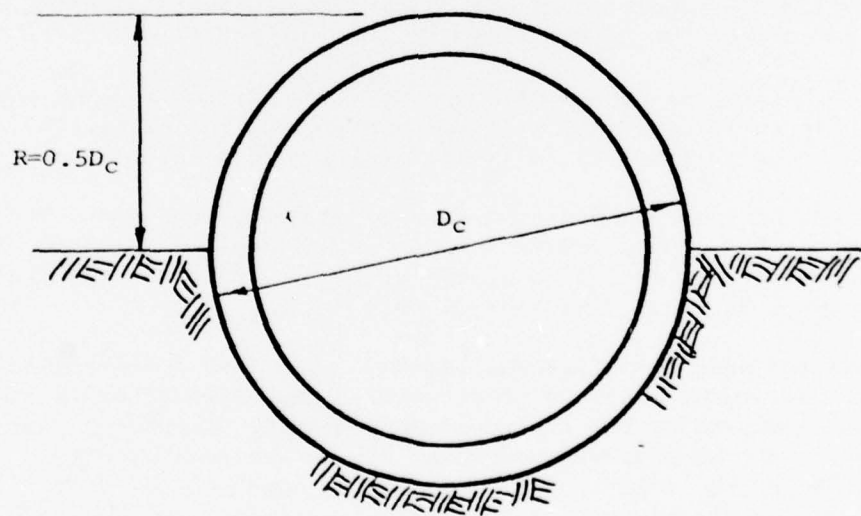


FIG. IV-62 APPROXIMATIONS OF VERTICAL PRESSURE, $\Delta\sigma_v$, HORIZONTAL PRESSURE, $\Delta\sigma_h$, AND SIDE-SHEAR STRESS, $\Delta\tau$, FOR RECTANGULAR CONDUITS (ROCK FOUNDATION)



Projection Ratio, $p=0.75$



Projection Ratio, $p=0.5$

FIG. IV-63 CIRCULAR CONDUITS PARTIALLY EMBEDDED
IN ROCK FOUNDATIONS

The normal pressures at the crown of each 10-foot-diameter conduit, for a height of fill equal to 600 feet are consistent with the previous data for circular and oblong conduits on shallow soil foundations as shown in Fig. IV-64. The distribution of horizontal and vertical pressures on the conduits are shown in Figs. IV-65 and IV-66. Data are presented for analyses made with and without friction along the conduit-rock interface. It can be seen that the effect of friction along the interface is quite pronounced. When it is included, horizontal pressures below the rock surface are small and the vertical reaction is greatest at the rock surface. When friction is not included, the horizontal pressures are quite large and the vertical reaction is a minimum at the rock surface. In neither case is there a large vertical reaction at the invert of the conduit as for a shallow soil foundation. The behavior of actual conduits under field conditions is likely to be somewhere between the extremes of full or no friction at the conduit-rock interface. However, it is intuitively clear that where the interface is close to vertical, friction is likely to be small, as for rectangular conduits, and horizontal pressures should also be small.

As an approximation of the real behavior of circular conduits partially embedded in rock, the following assumptions can be made:

- a. The vertical pressures on top of the conduit will be similar to those on circular and oblong conduits on shallow soil foundations, taking into account the smaller rise-to-span ratio (Fig. IV-64).
- b. The vertical reaction at the base of the conduit will be uniformly distributed over the area of the conduit that is in contact with rock. The magnitude of the reaction must equal the total vertical pressure on top of the conduit.
- c. The horizontal pressures above the rock surface will be equal to those for a comparable shallow soil foundation condition. Below the rock surface the horizontal pressure are assumed to be zero.

Pressure distributions based on the above assumptions are described in Fig. IV-67. Values of Foundation Reaction Factor, n , are given in Fig. IV-68. The pressure distributions are compared with the results of the finite-element analyses in Figs. IV-65 and IV-66.

The assumed pressure distributions have been used to calculate the theoretical structural response of circular conduits embedded in rock similar to the cases analysed by the finite-element method. Comparisons of moment, thrust, shear, normal pressure and shear stress are given in Figs. IV-69 through IV-78 for the condition of fill height equal to 600 feet. The figures show that the assumed pressure distributions give generally conservative results for the conduits analyzed (moments at the crown overestimated by 10-20 percent). The conservatism probably results from the complete neglect of lateral pressures on the portion of the conduit below the rock surface.

No analyses were performed for oblong conduit sections because it was felt that the results would be similar to those for circular sections. However, it would be necessary to include side-shear forces on the portion

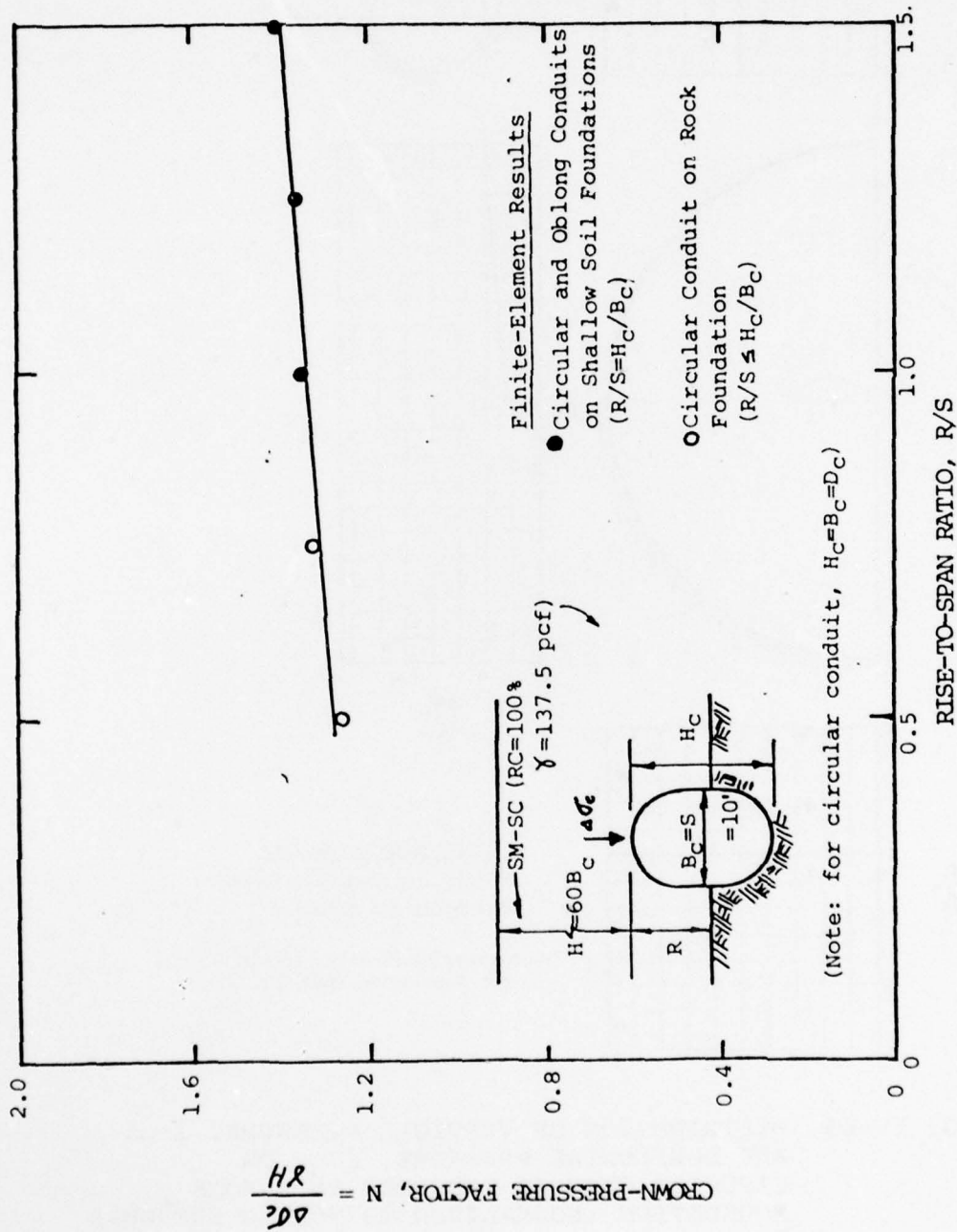


FIG. IV-64 CROWN-PRESSURE FACTOR VS. RISE-TO-SPAN RATIO FOR CIRCULAR AND OBLONG CONDUITS (SHALLOW SOIL OR ROCK FOUNDATION)

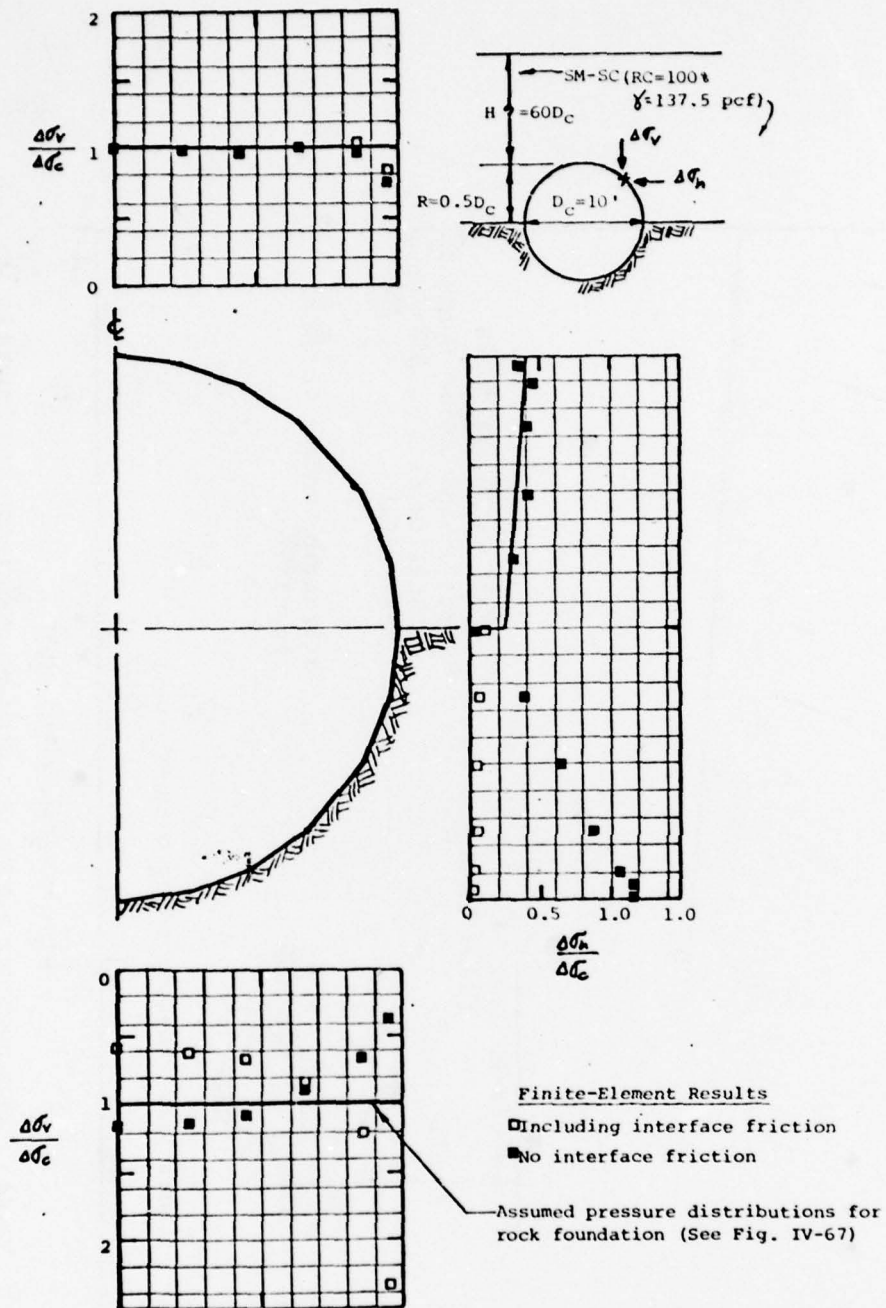


FIG. IV-65 DISTRIBUTION OF VERTICAL PRESSURE, $\Delta\sigma_v$, AND HORIZONTAL PRESSURE, $\Delta\sigma_h$, ON CIRCULAR CONDUIT EMBEDDED IN A ROCK FOUNDATION (NORMALIZED TO NORMAL PRESSURE AT CROWN)

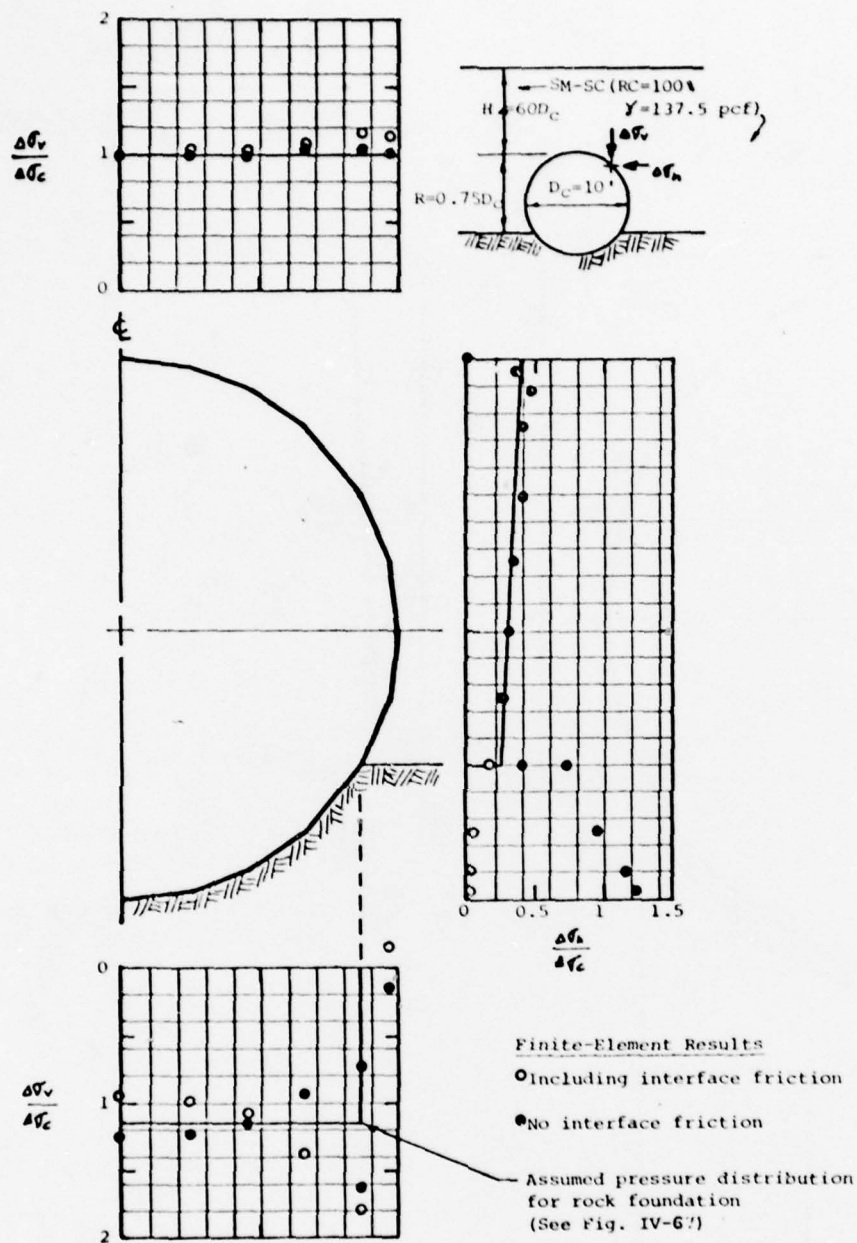


FIG. IV-66 DISTRIBUTION OF VERTICAL PRESSURE, $\Delta\sigma_v$, AND HORIZONTAL PRESSURE, $\Delta\sigma_h$, ON CIRCULAR CONDUIT EMBEDDED IN ROCK FOUNDATION (NORMALIZED TO NORMAL PRESSURE AT CROWN)

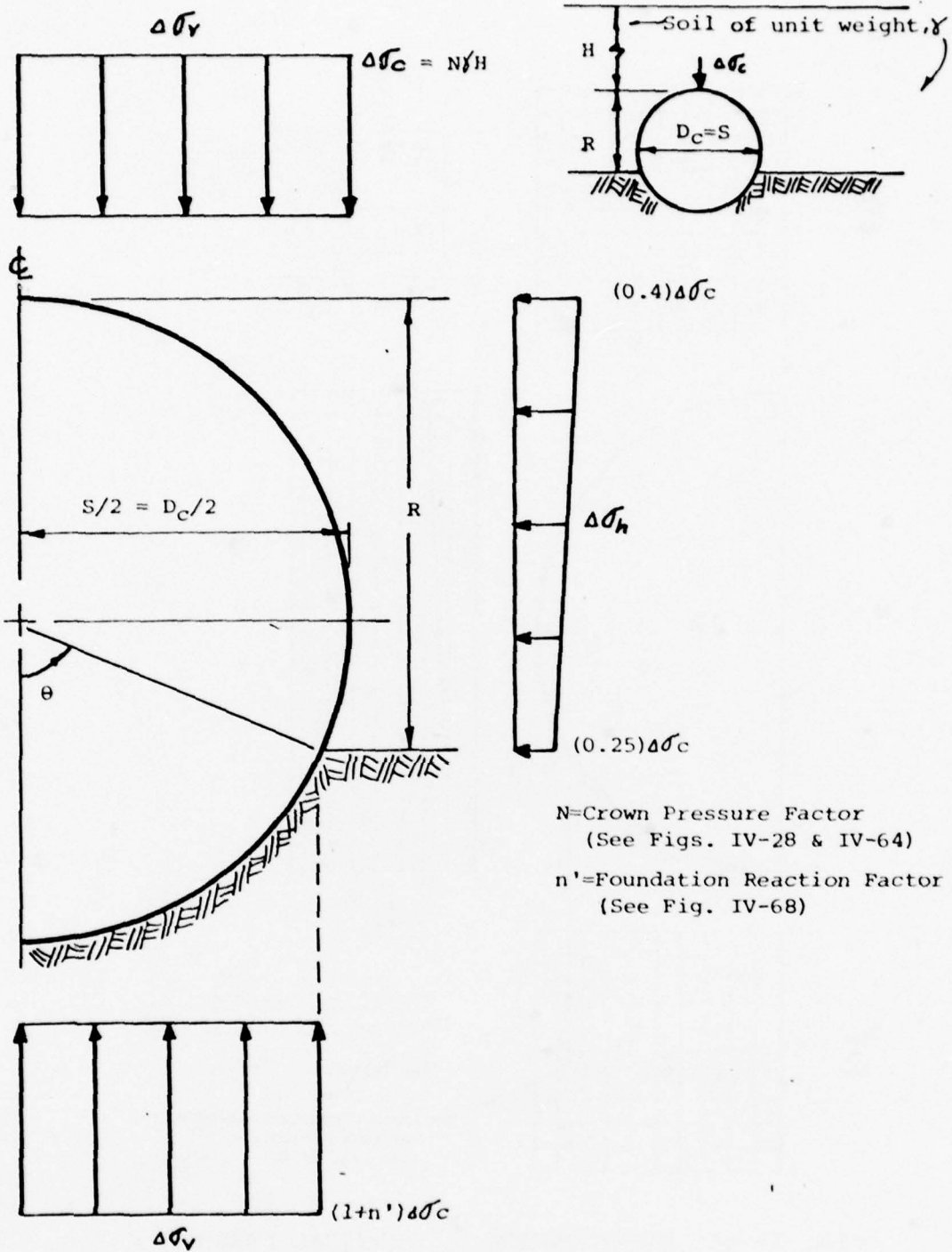


FIG. IV-67 APPROXIMATIONS OF VERTICAL PRESSURE, $\Delta\sigma_v$, AND HORIZONTAL PRESSURE, $\Delta\sigma_h$, FOR CIRCULAR CONDUITS (ROCK FOUNDATION)

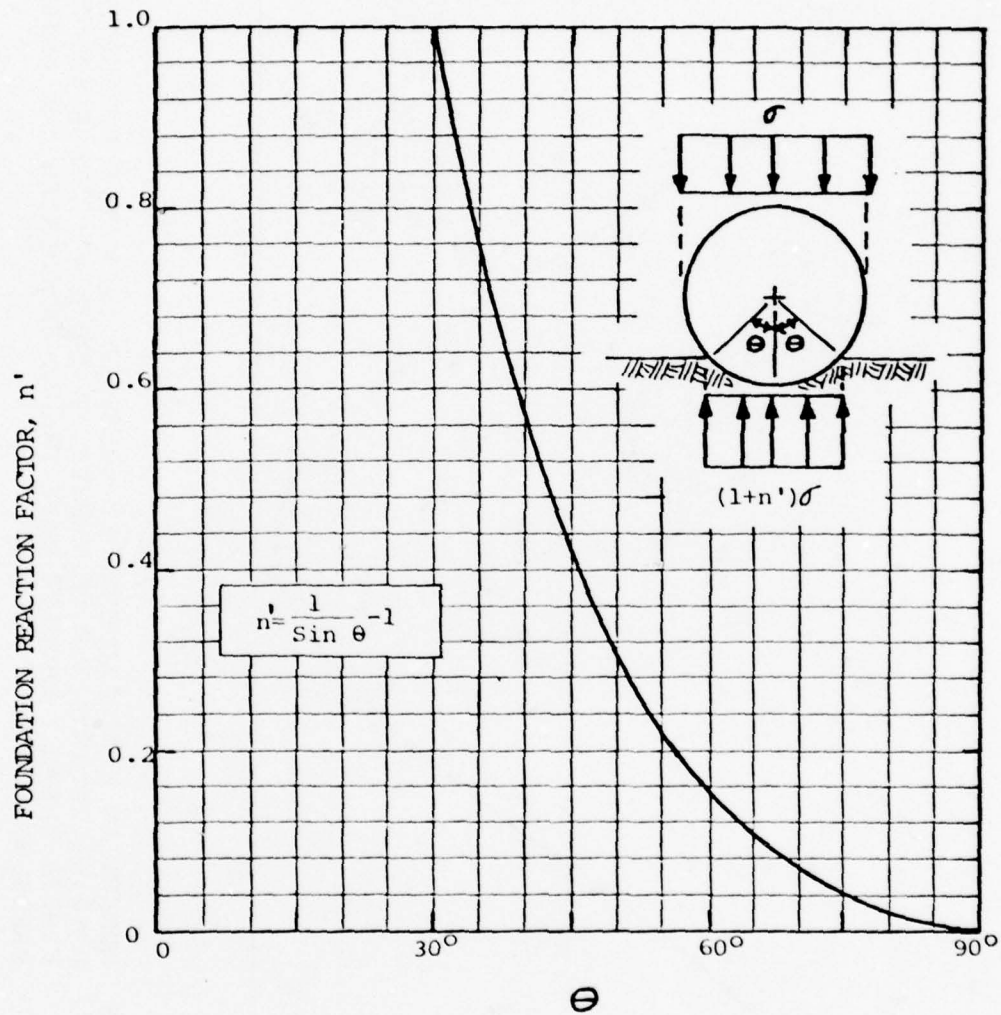


FIG. IV-68 FOUNDATION REACTION FACTOR FOR CIRCULAR CONDUITS ON ROCK FOUNDATIONS

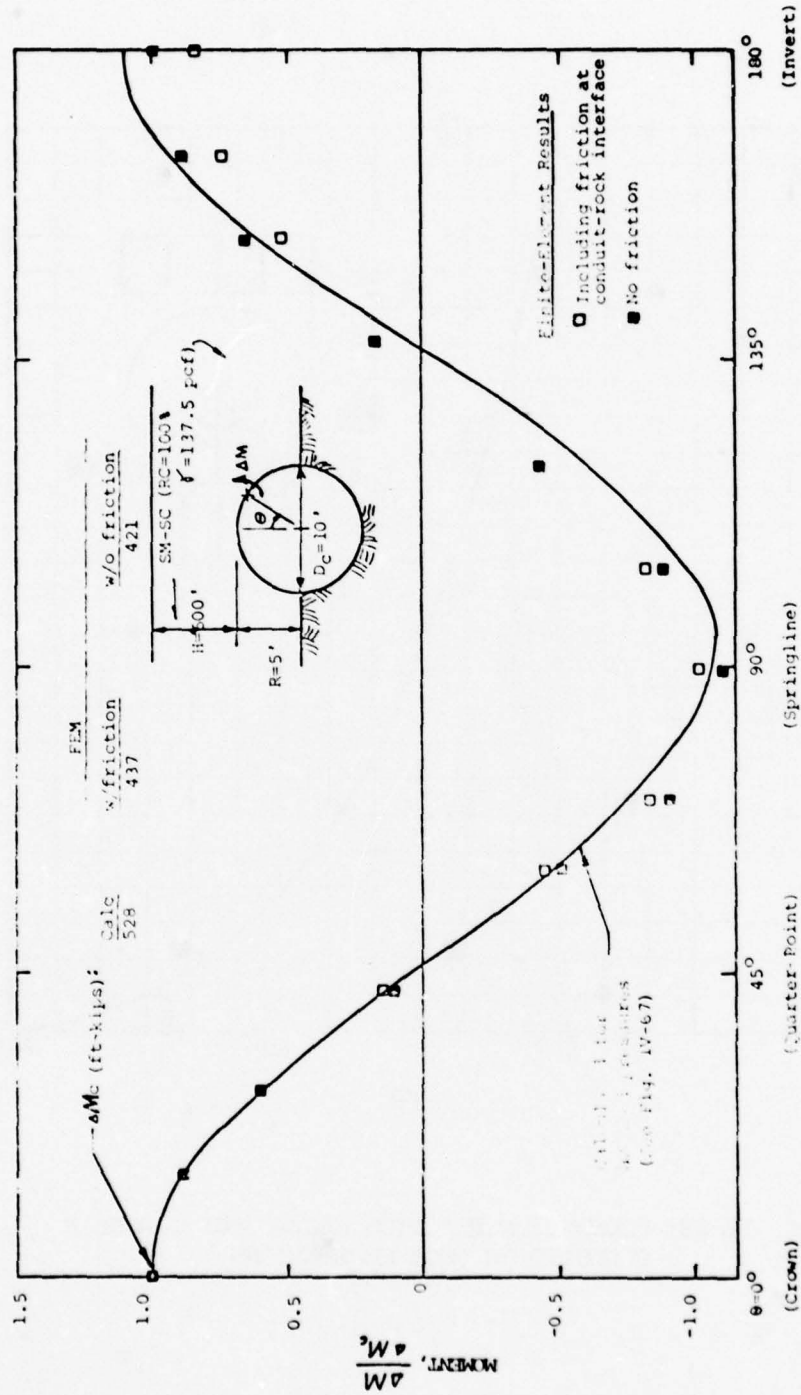


FIG. IV-69 MOMENT IN CIRCULAR CONDUIT EMBEDDED IN A ROCK FOUNDATION, $p = 0.5$, (NORMALIZED TO MOMENT AT CROWN): COMPARISON OF FINITE-ELEMENT RESULTS WITH VALUES CALCULATED FOR ASSUMED PRESSURES

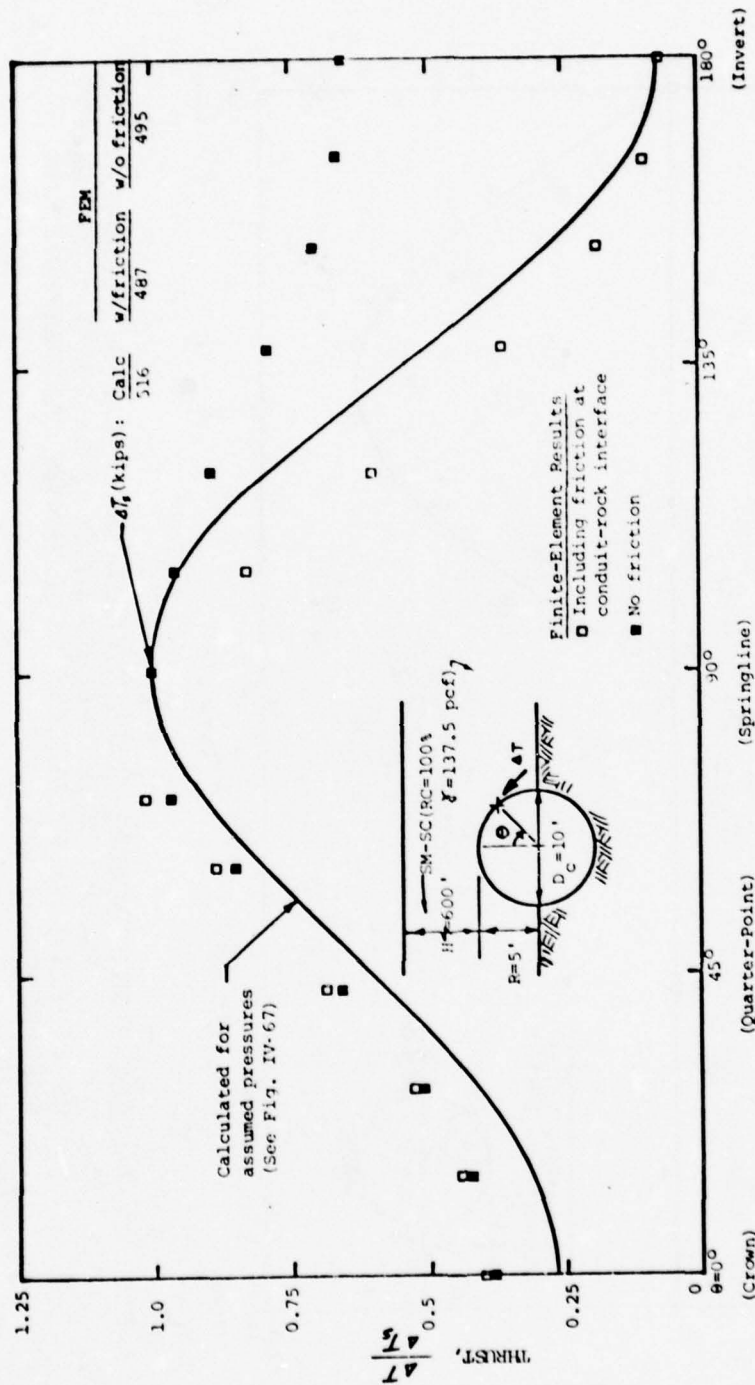


FIG. IV-70 THRUST IN CIRCULAR CONDUIT EMBEDDED IN A ROCK FOUNDATION, $p = 0.5$, (NORMALIZED TO THRUST AT SPRINGLINE): COMPARISON OF FINITE-ELEMENT RESULTS WITH VALUES CALCULATED FOR ASSUMED PRESSURES

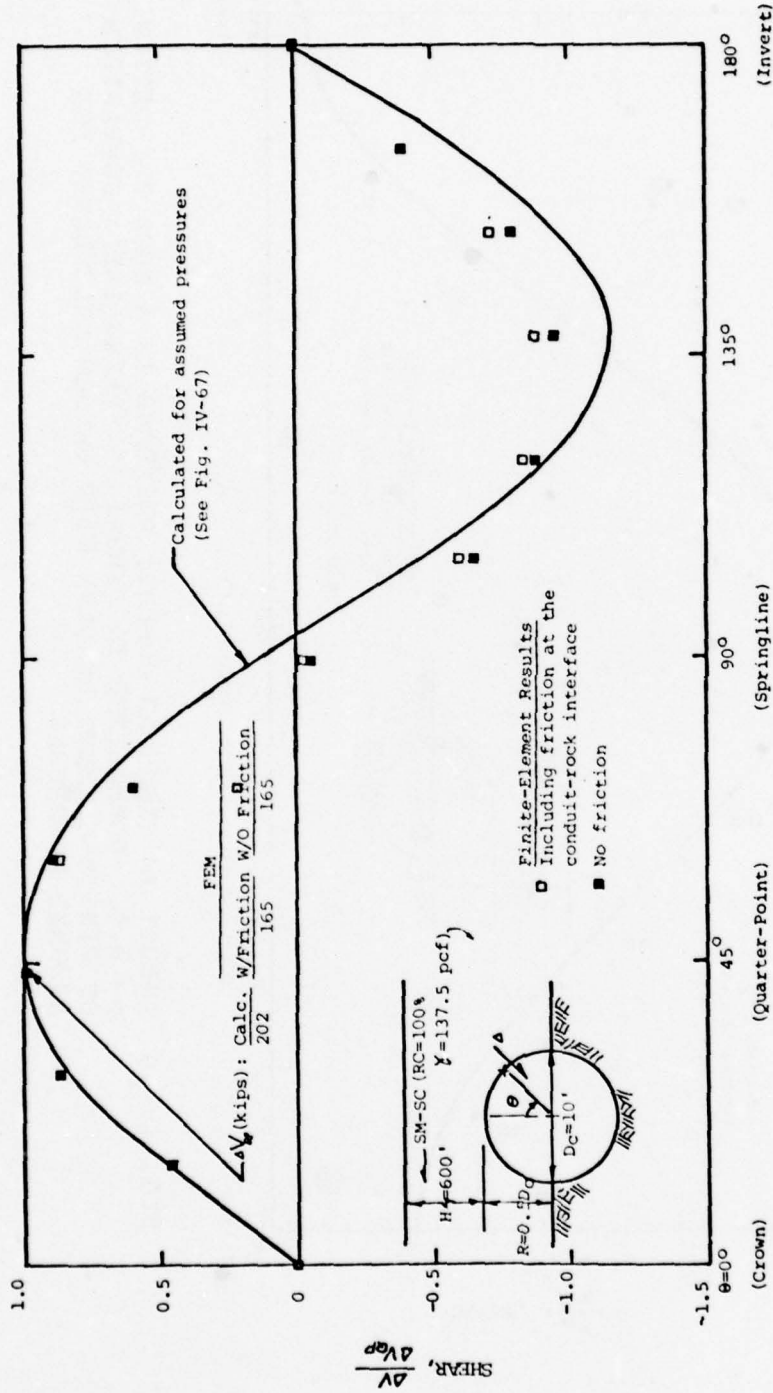


FIG. IV-71 SHEAR IN CIRCULAR CONDUIT EMBEDDED IN A ROCK FOUNDATION, $p = 0.5$, (NORMALIZED TO SHEAR AT QUARTER-POINT): COMPARISON OF FINITE-ELEMENT RESULTS WITH VALUES CALCULATED FOR ASSUMED PRESSURES

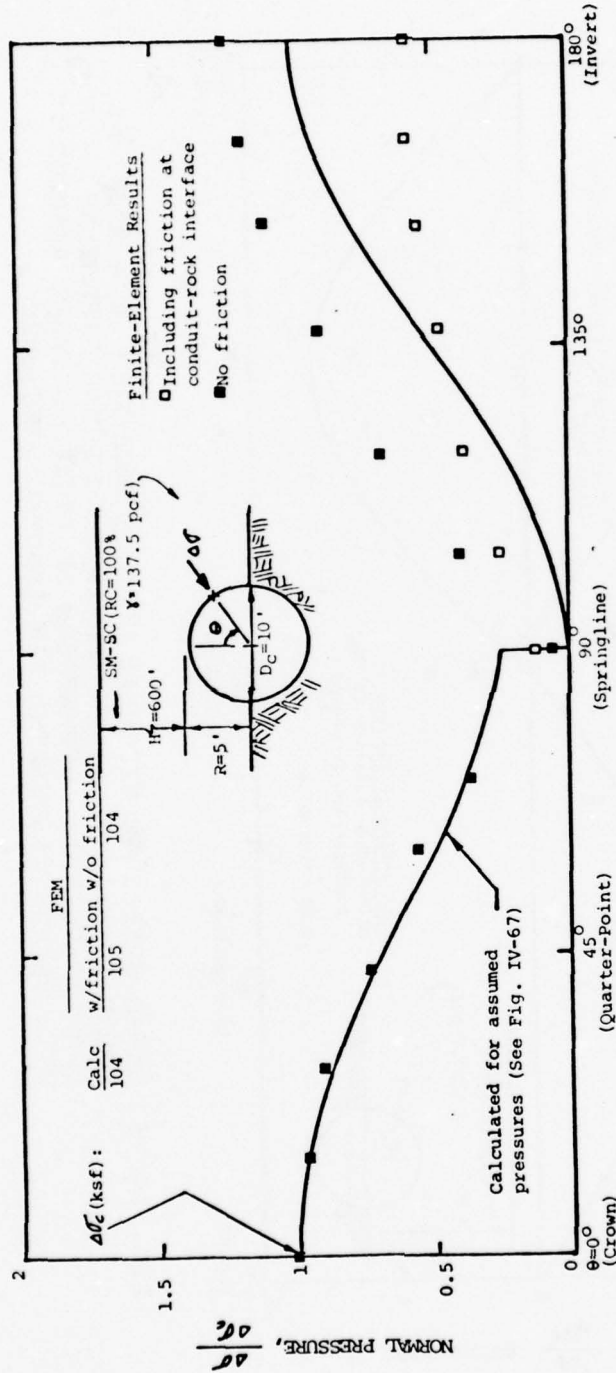


FIG. IV-72 NORMAL PRESSURE ON CIRCULAR CONDUIT EMBEDDED IN A ROCK FOUNDATION, $p = 0.5$, (NORMALIZED TO NORMAL PRESSURE AT CROWN): COMPARISON OF FINITE-ELEMENT RESULTS WITH VALUES CALCULATED FOR ASSUMED PRESSURES

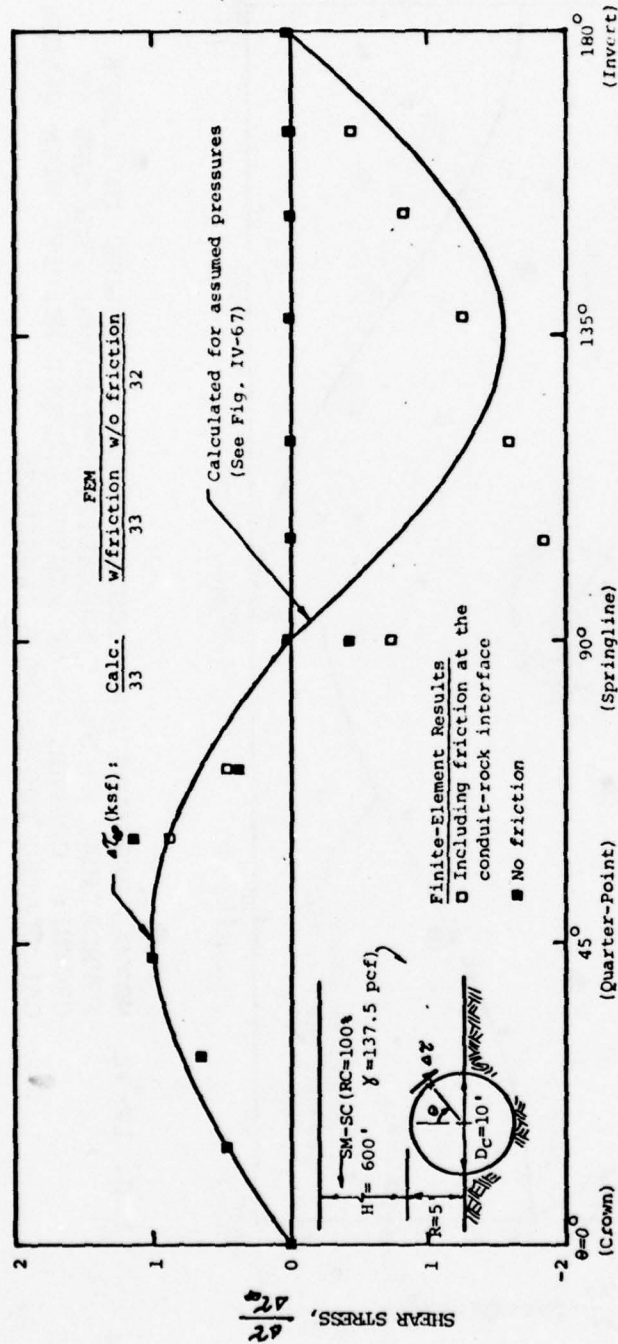


FIG. IV-73 SHEAR STRESS ON CIRCULAR CONDUIT EMBEDDED IN A ROCK FOUNDATION, $p = 0.5$, (NORMALIZED TO SHEAR STRESS AT QUARTER-POINT): COMPARISON OF FINITE-ELEMENT RESULTS WITH VALUES CALCULATED FOR ASSUMED PRESSURES

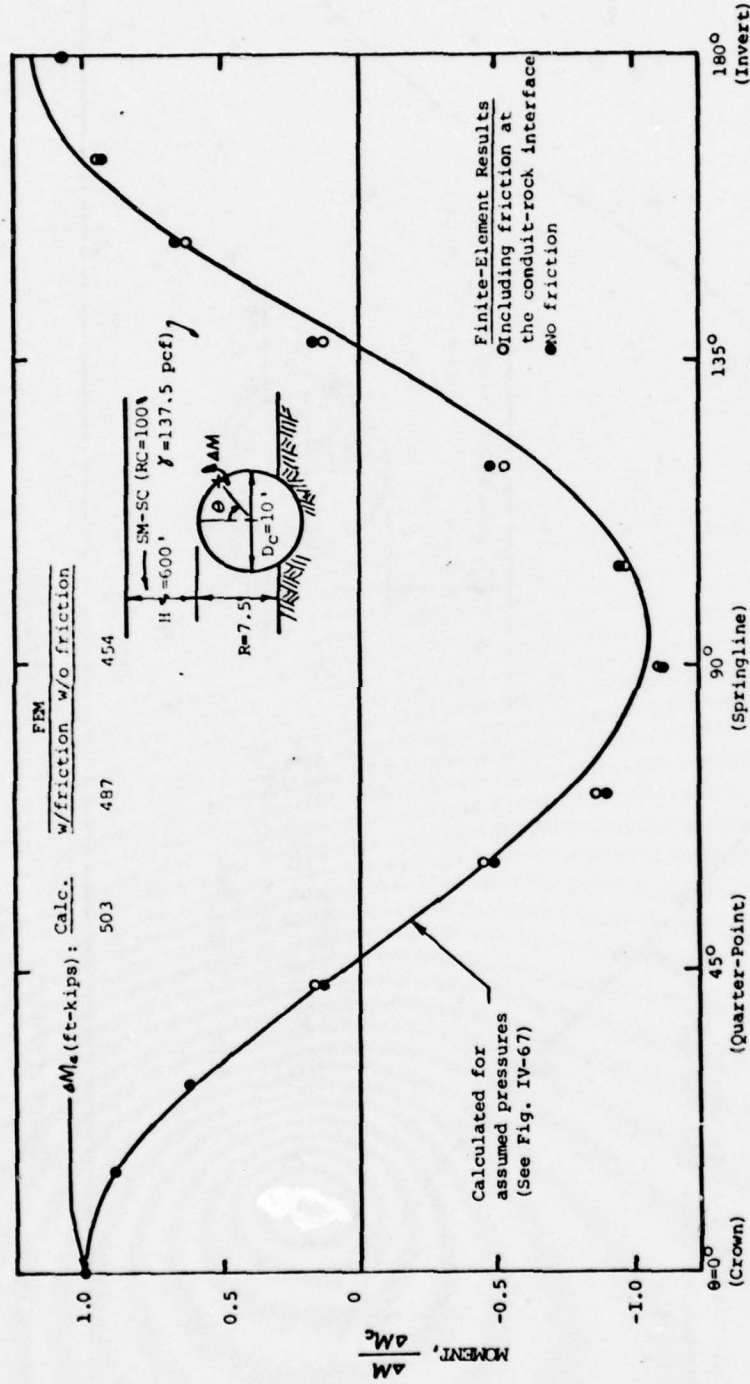


FIG. IV-74 MOMENT IN CIRCULAR CONDUIT EMBEDDED IN A ROCK FOUNDATION, $p = 0.75$, (NORMALIZED TO MOMENT AT CROWN): COMPARISON OF FINITE-ELEMENT RESULTS WITH VALUES CALCULATED FOR ASSUMED PRESSURES

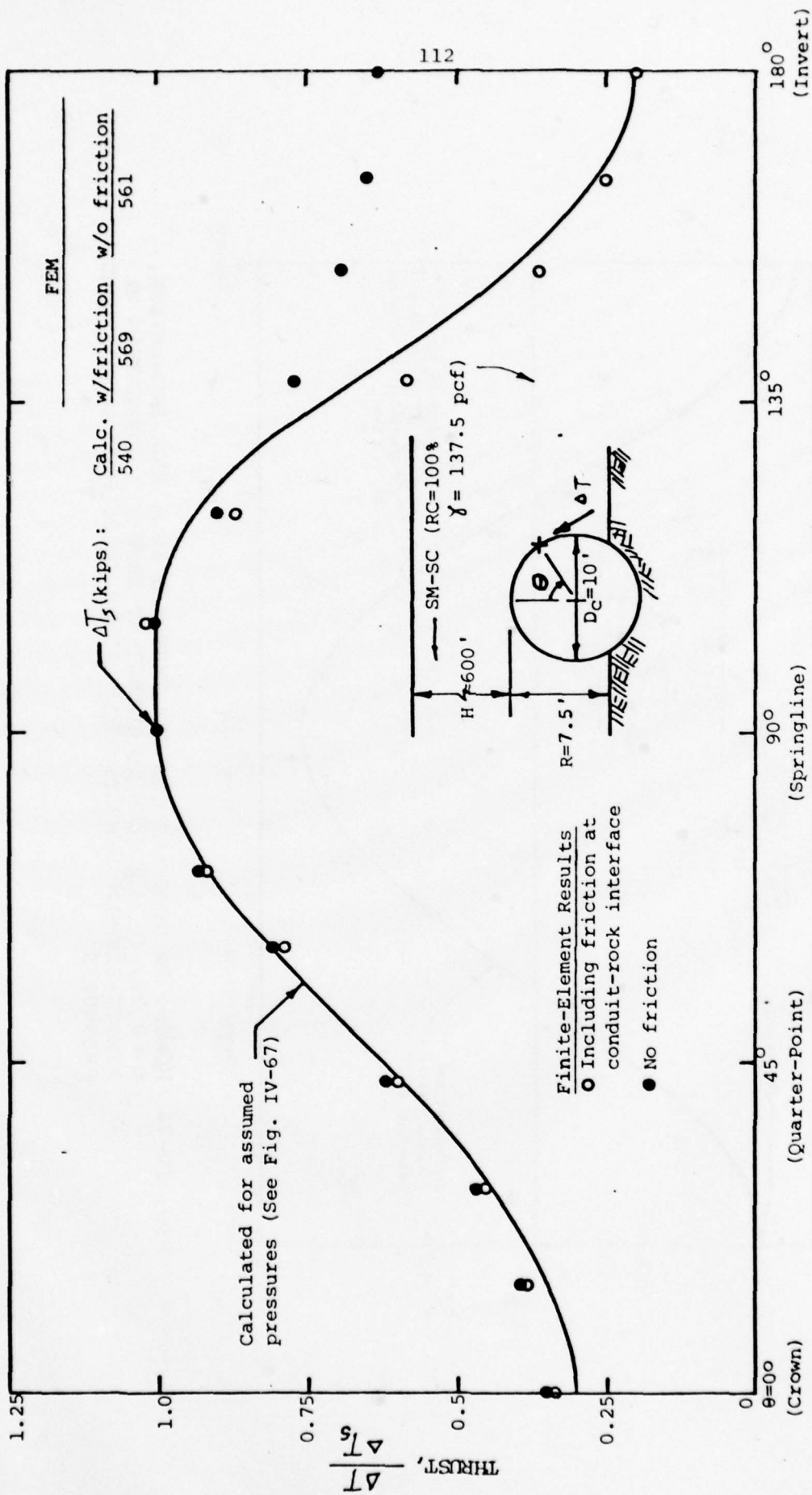


FIG. IV-75 THRUST IN CIRCULAR CONDUIT EMBEDDED IN ROCK FOUNDATION, $p=0.75$, (NORMALIZED TO THRUST AT SPRINGLINE):
 COMPARISON OF FINITE-ELEMENT RESULTS WITH VALUES CALCULATED FOR ASSUMED PRESSURES

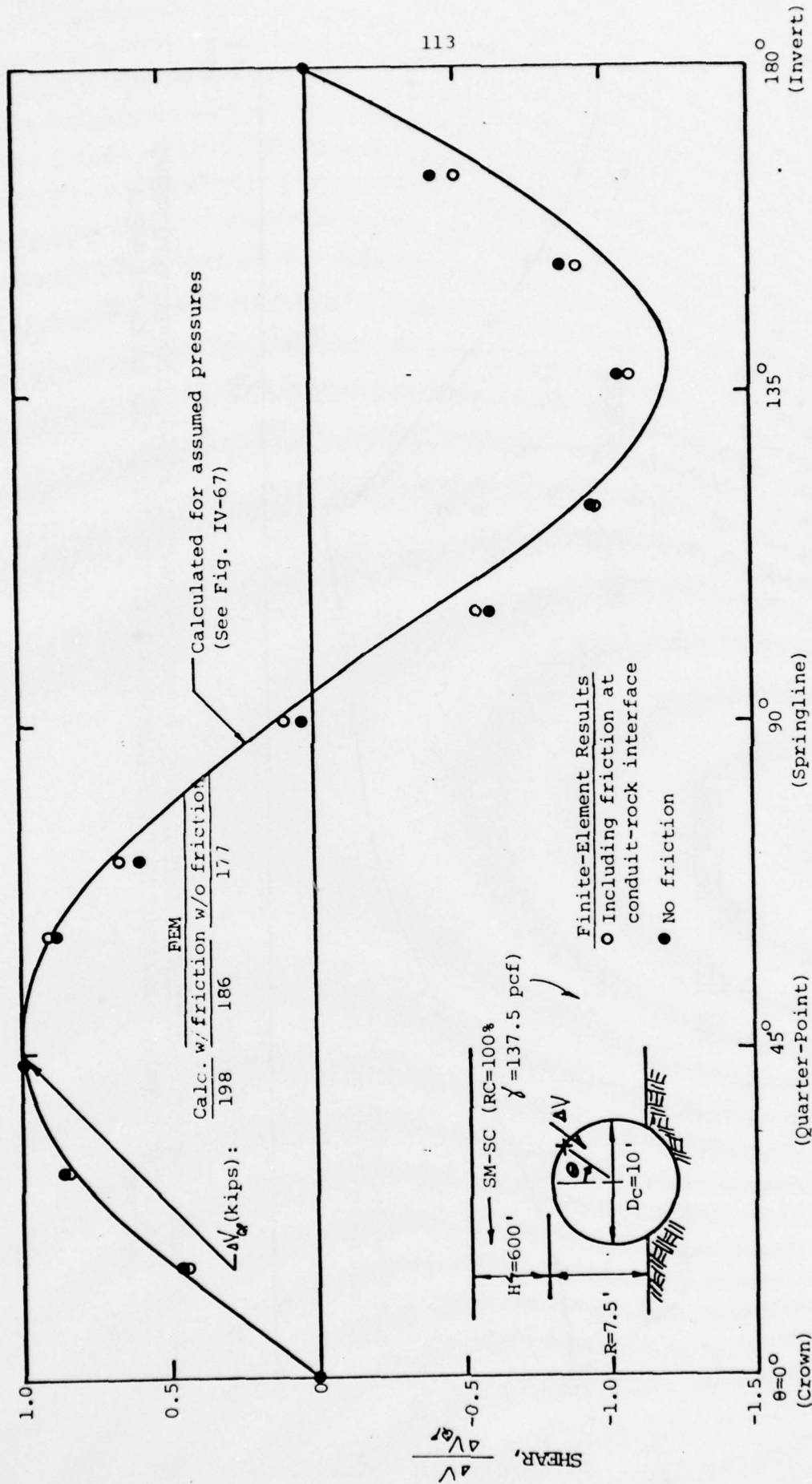


FIG. IV-76 SHEAR IN CIRCULAR CONDUIT EMBEDDED IN A ROCK FOUNDATION, $p=0.75$, (NORMALIZED TO SHEAR AT QUARTER-POINT): COMPARISON OF FINITE-ELEMENT RESULTS WITH VALUES CALCULATED FOR ASSUMED PRESSURES.

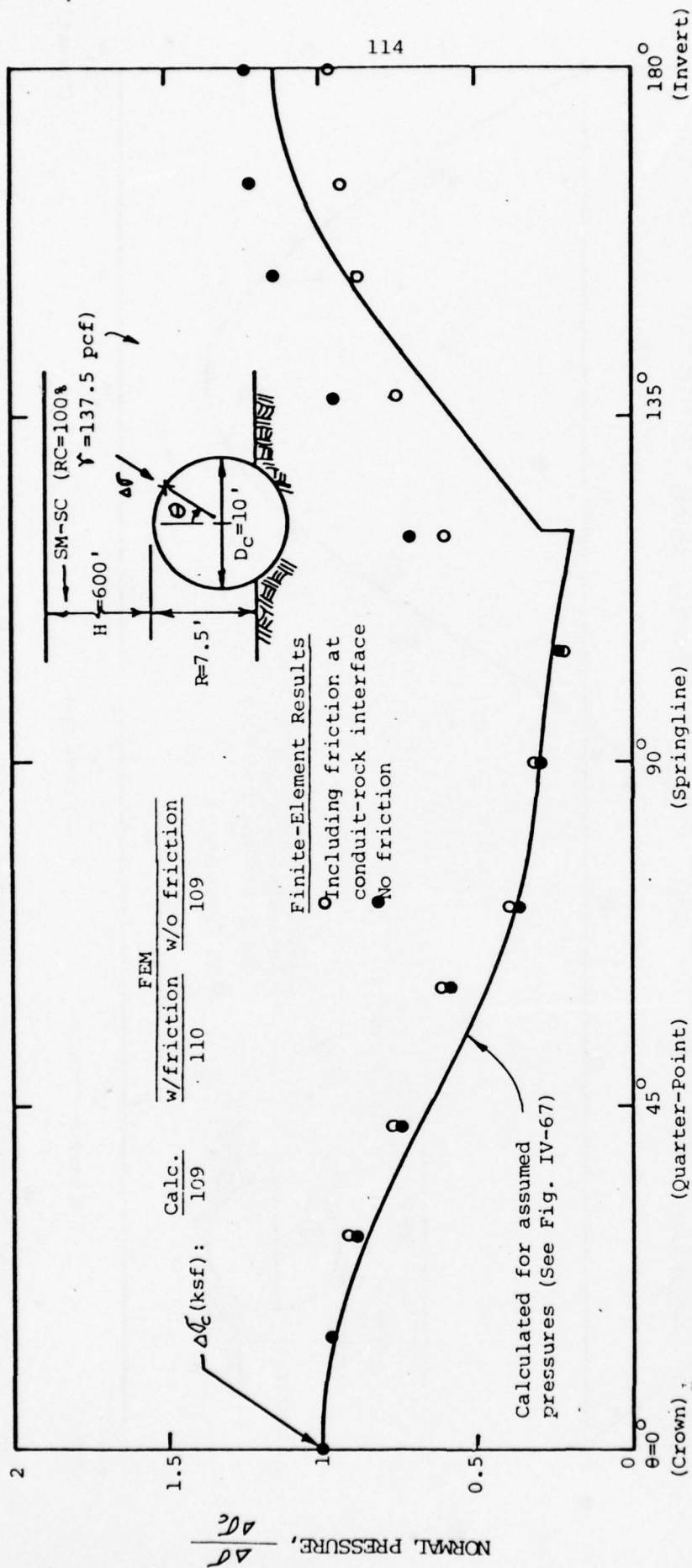


FIG. IV-77 NORMAL PRESSURE ON CIRCULAR CONDUIT EMBEDDED IN ROCK FOUNDATION, $p=0.75$, (NORMALIZED TO NORMAL PRESSURE AT CROWN): COMPARISON OF FINITE-ELEMENT RESULTS WITH VALUES CALCULATED FOR ASSUMED PRESSURES

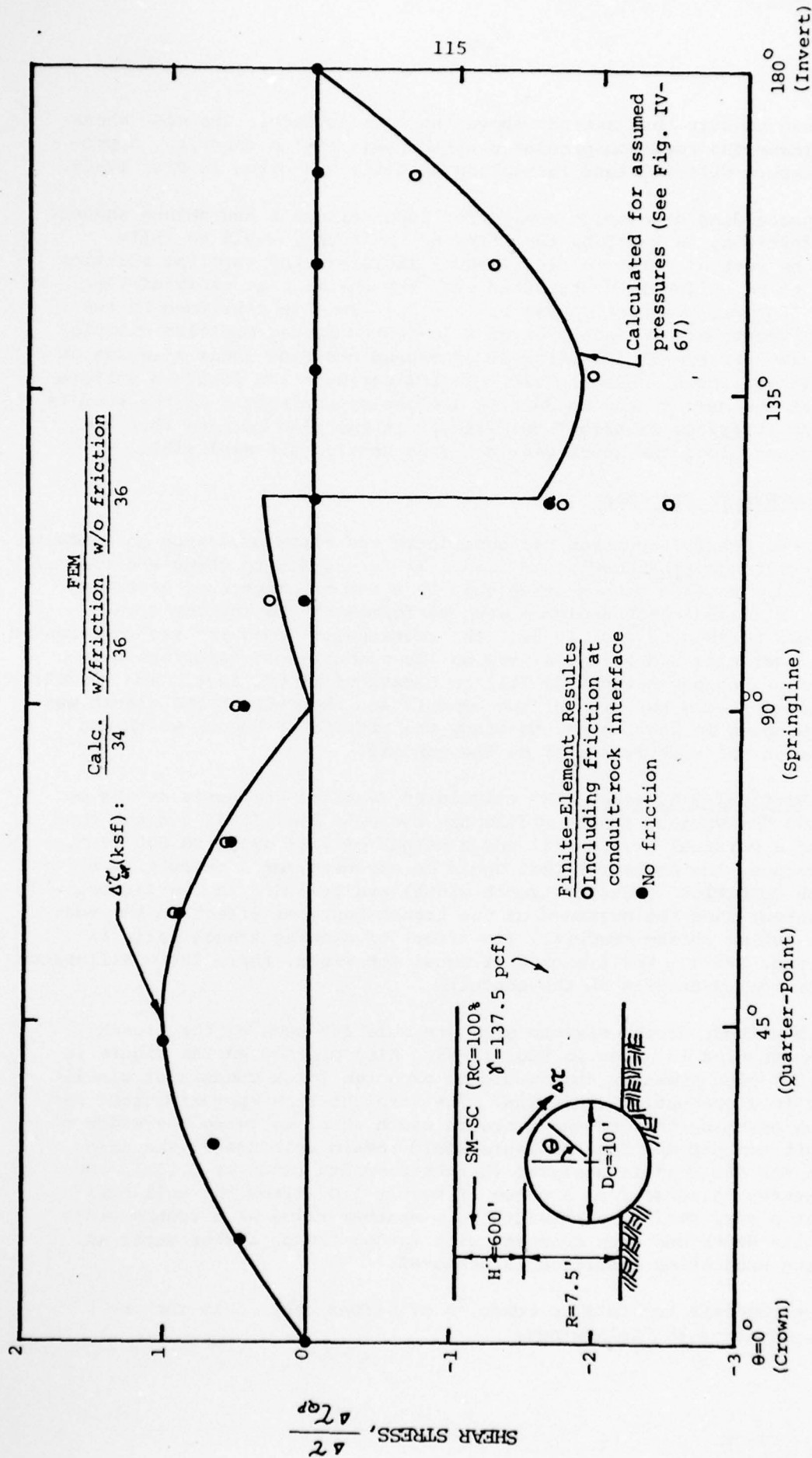


FIG. IV-78 SHEAR STRESS ON CIRCULAR CONDUIT EMBEDDED IN ROCK FOUNDATION, $p=0.75$, (NORMALIZED TO SHEAR STRESS AT QUARTER-POINT): COMPARISON OF FINITE-ELEMENT RESULTS WITH VALUES CALCULATED FOR ASSUMED PRESSURES

of an oblong conduit that extends above the rock surface. The side shear would increase the reaction pressures at the base of the conduit. Appropriate pressure distributions for oblong conduits are given in Fig. IV-79.

The preceeding discussion considered ideal circular and oblong shapes. Modified sections, as built by the Corps of Engineers, would be fully supported by rock as shown in Fig. IV-80. Therefore the vertical reaction is likely to be uniformly distributed over the entire base width of the conduit. (Foundation Reaction Factor, $n = 0$.) This is confirmed by the results of finite-element analyses of a 10-foot-diameter modified circular section. The horizontal and vertical pressures and side shear stresses on the conduit are shown in Fig. IV-81. As indicated in the figure a uniform reaction at the base of the conduit is a close approximation of the results for the "no interface friction" condition. It can also be seen that the shear stresses along the short vertical side section are negligible.

I. Shallow Trench Placement

The preceeding discussion has considered the earth pressures on conduits in a projection or embankment condition. It is helpful to study the case of a conduit in a shallow trench since this is a common occurrence in actual practice. Finite-element analyses were performed of the shallow trench conditions described in Fig. IV-82. The rectangular "conduit" was represented by a rigid material and the pressures on the conduit-soil interface were determined at various heights of fill to a maximum of 600 feet. The geometry of the space between the side of the conduit and the wall of the trench was varied, as shown in the figure, to study the effects of trench width and wall slope on the soil pressures on the conduit.

1. Vertical Pressures. The calculated vertical pressures acting on the conduit for various trench widths are shown in Fig. IV-83 for the conditions of a vertical trench wall and a height of fill equal to 600 feet. For comparison, the pressures that would be expected for a conduit in a projection condition (infinite trench width) are included in the figure. It is apparent that the presence of the trench has some effect in the edge pressures acting on the conduit. The effect of sloping trench walls is shown in Fig. IV-84. For trenches of equal top width, there is no difference in the vertical pressures on the conduit.

The magnitude of the maximum edge pressure for each of the trench conditions studied is given in Fig. IV-85. Also plotted on the figure is the value of edge pressure that would be expected for a conduit of similar shape but in a projection condition. The straight-line approximations have been drawn assuming that beyond a trench width equal to twice the width of the conduit the maximum edge pressure would remain unchanged. The data show that for the conduit analyzed (height-to-width ratio of 0.125), the edge pressures increase from a value of nearly 1.0 (times the soil overburden) at a very small trench width to a maximum value at a trench width equal to its depth and then decrease with larger trench widths until an approximate projection condition is achieved.

To extrapolate the data to conduits of widths other than the one analyzed, consider the following:

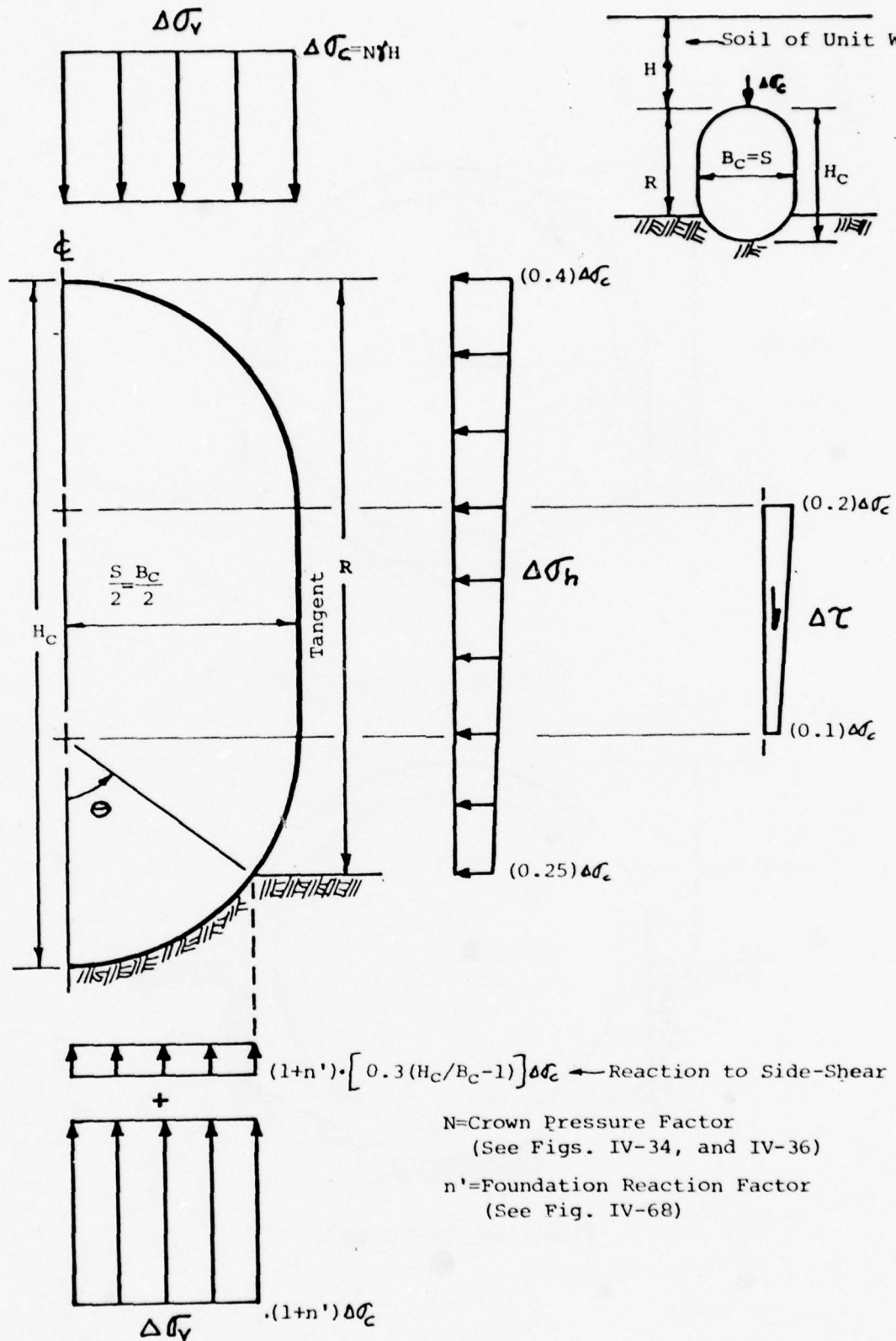
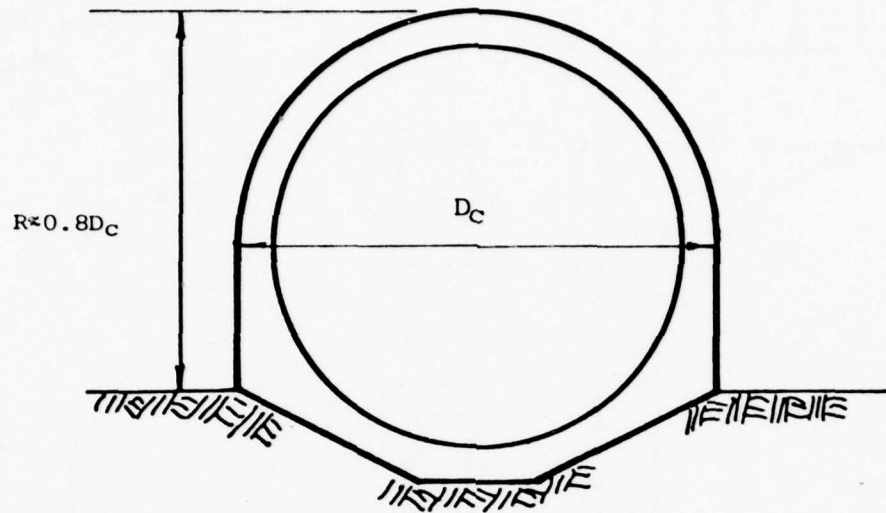
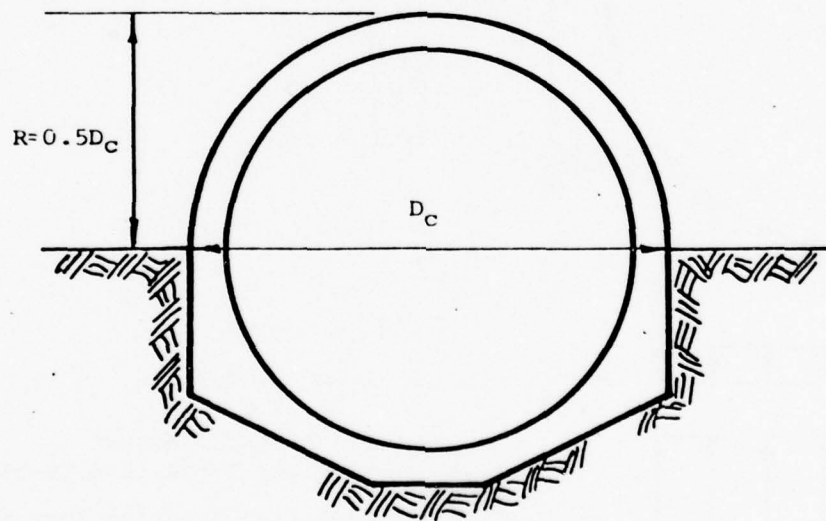


FIG. IV-79 APPROXIMATIONS OF VERTICAL PRESSURE, $\Delta\sigma_v$, HORIZONTAL PRESSURE, $\Delta\sigma_h$, AND SIDE-SHEAR STRESS, $\Delta\tau$, FOR OBLONG CONDUITS (ROCK FOUNDATION)



Projection Ratio, $p \approx 0.8$



Projection Ratio, $p = 0.5$

FIG. IV-80 MODIFIED CIRCULAR CONDUITS PARTIALLY EMBEDDED IN ROCK FOUNDATIONS

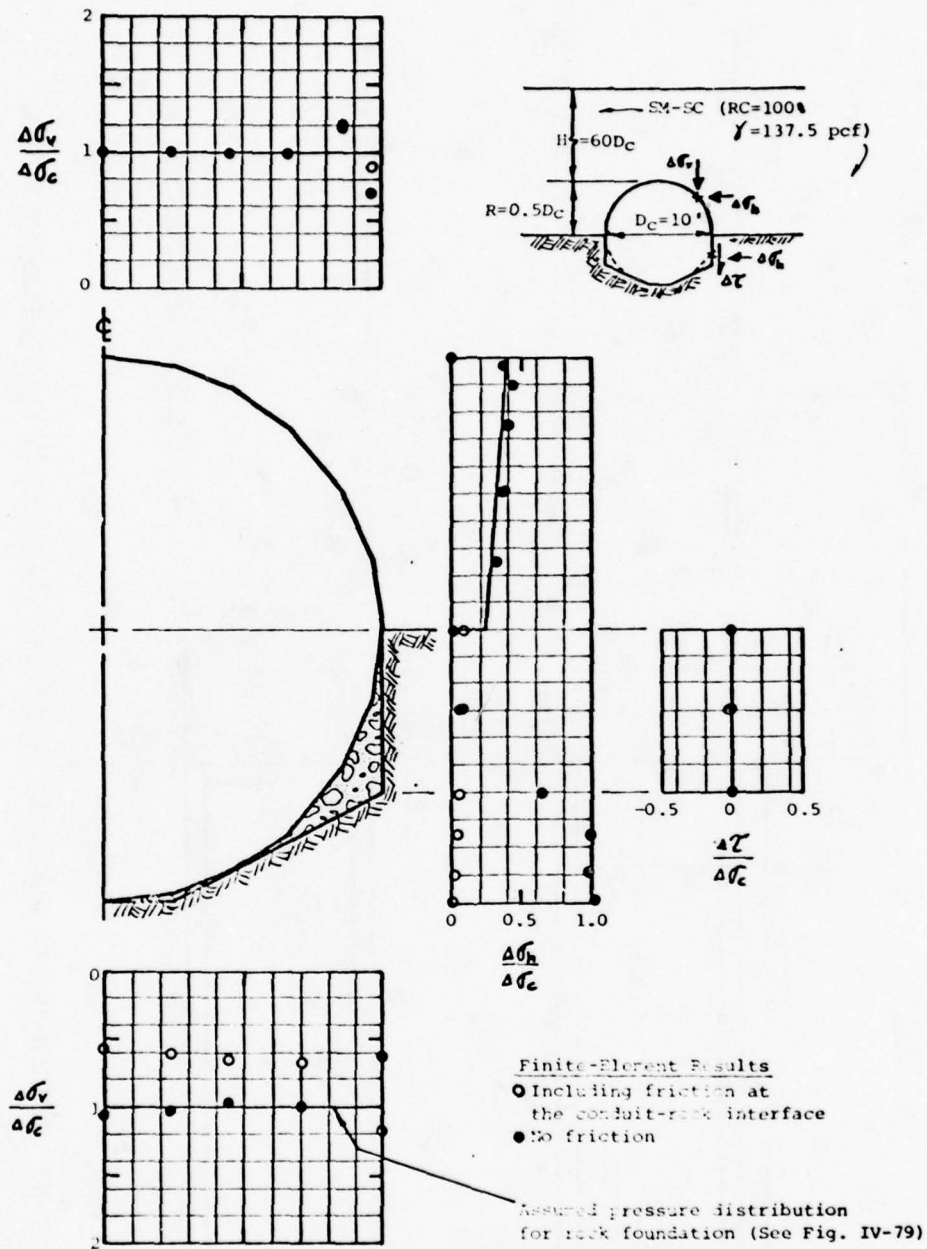


FIG. IV-81 DISTRIBUTION OF VERTICAL PRESSURE, $\Delta\sigma_v$, HORIZONTAL PRESSURE, $\Delta\sigma_h$, AND SIDE-SHEAR, $\Delta\tau$, ON MODIFIED CIRCULAR CONDUIT EMBEDDED IN ROCK FOUNDATION

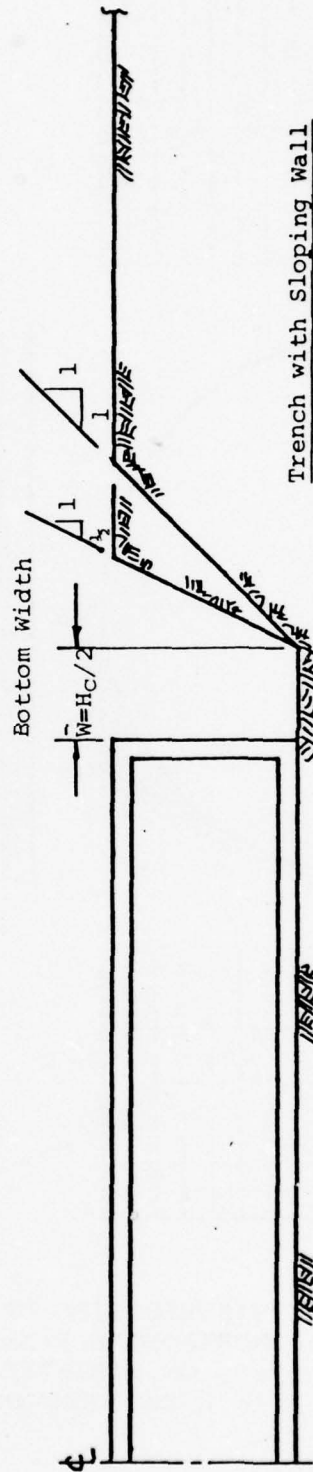
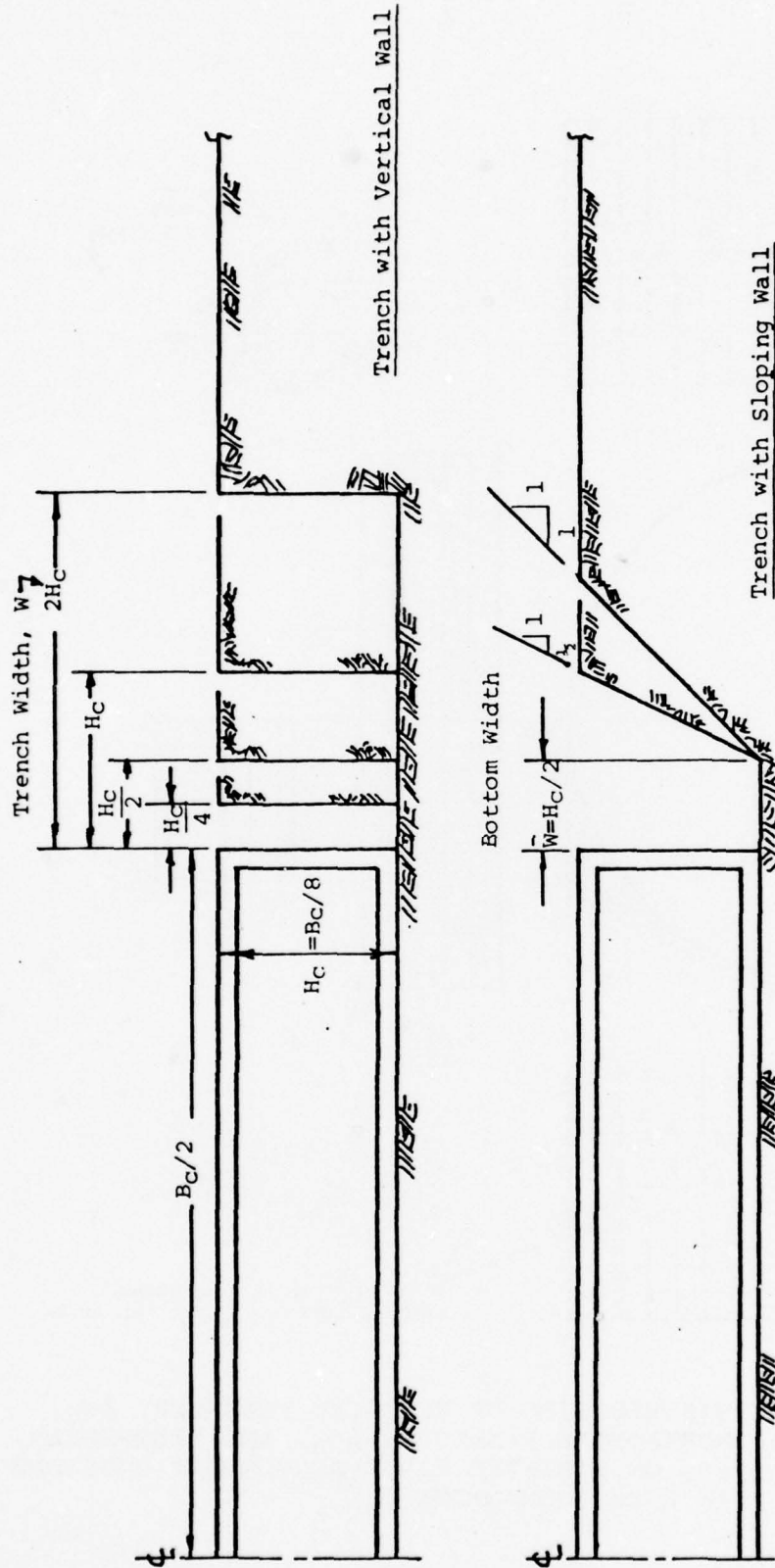


FIG. IV-82 SHALLOW TRENCH PLACEMENT CONDITIONS ANALYZED BY FINITE-ELEMENT METHOD

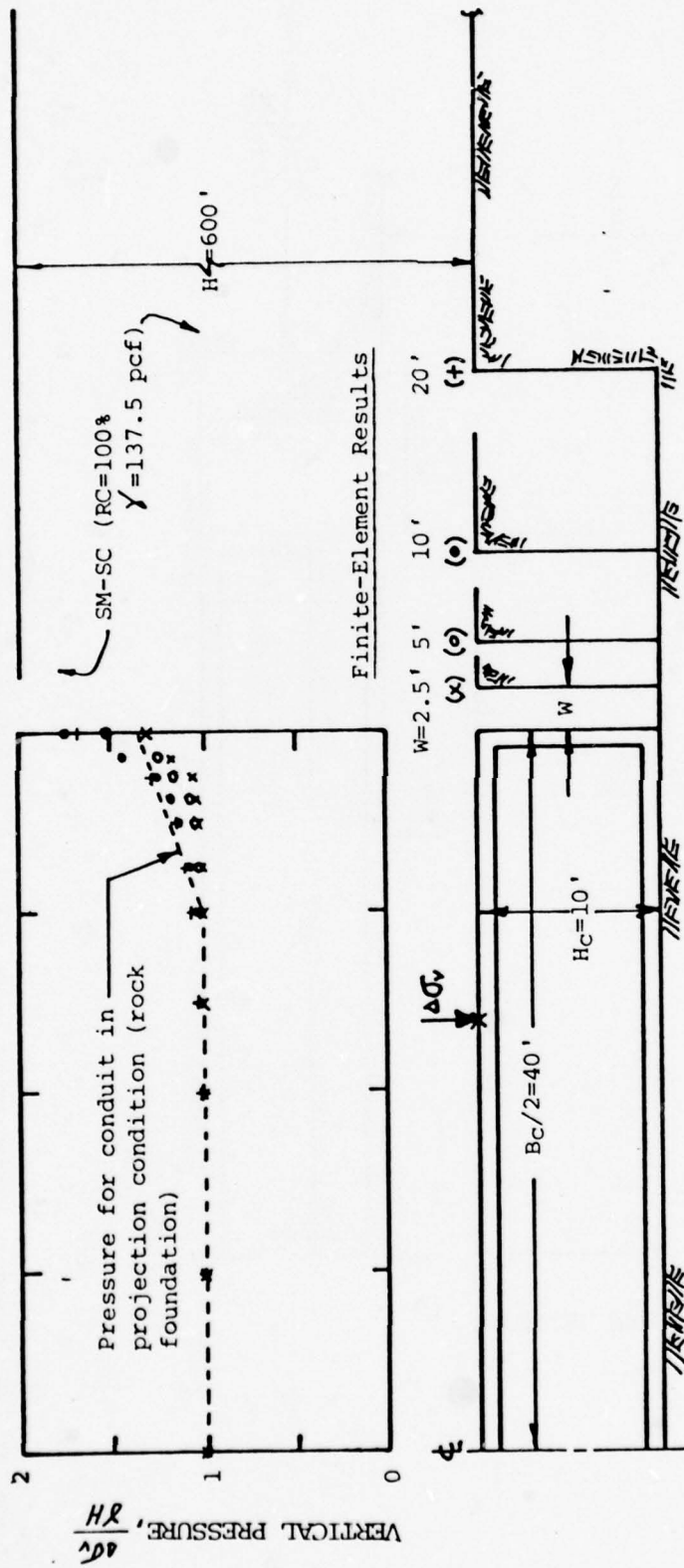


FIG. IV-83 VERTICAL PRESSURE ON RECTANGULAR CONDUIT IN SHALLOW TRENCH WITH VERTICAL WALL

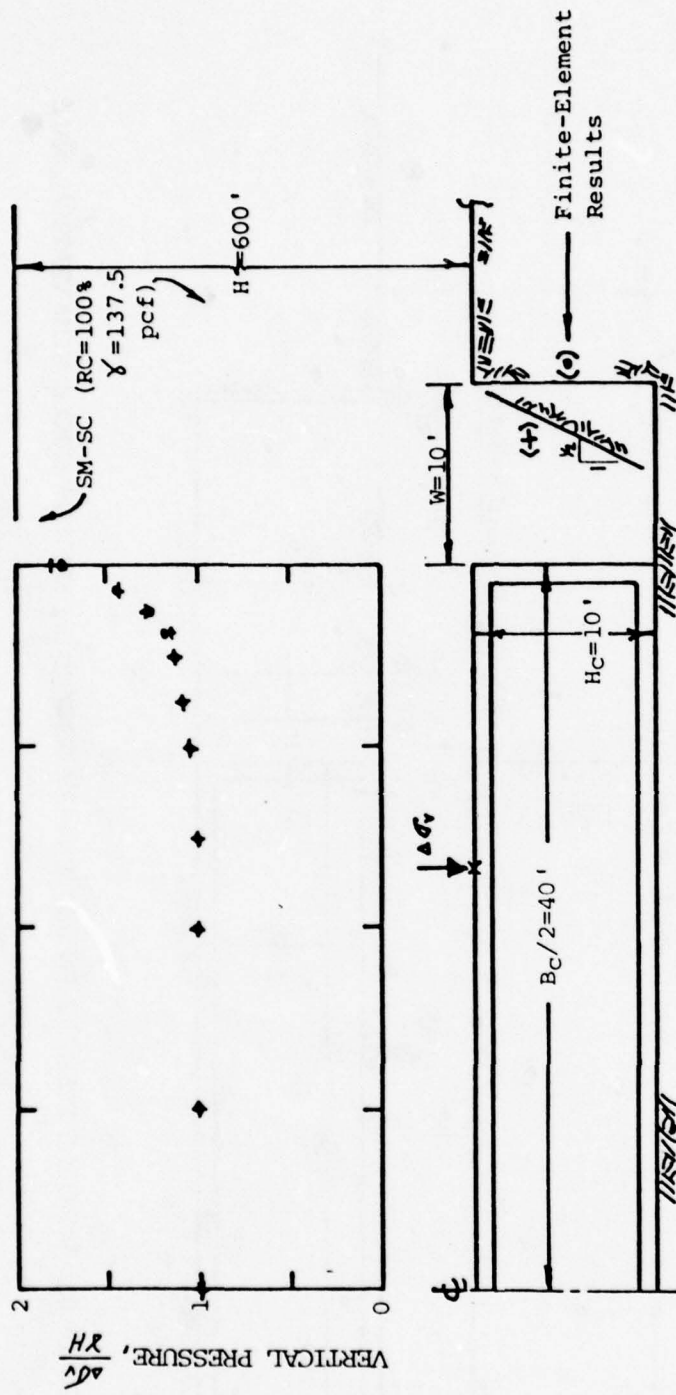


FIG. IV.-84 VERTICAL PRESSURE ON RECTANGULAR CONDUIT IN SHALLOW TRENCH WITH VERTICAL AND SLOPING WALLS

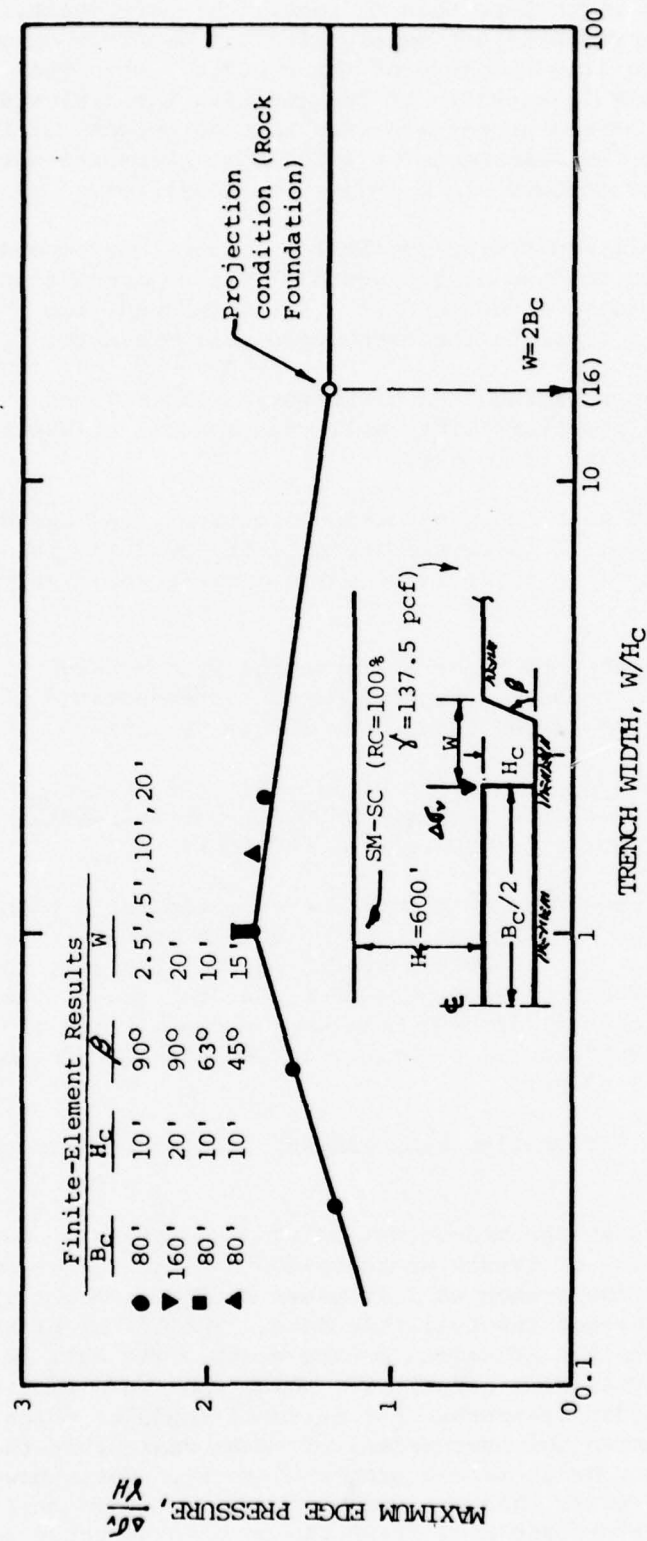


FIG. IV-85 MAXIMUM EDGE PRESSURE FOR RECTANGULAR CONDUITS IN SHALLOW TRENCH

- a. Data from Fig. IV-83 have been replotted in Fig. IV-86 to show that for trenches of width less than or equal to their depth, the increased edge pressures act mainly within a distance of one-half the trench width from the side of the conduit. Note that because of the relatively large width of the conduit, the distances over which the edge pressures act are less than one-eighth of the conduit width, which is the distance over which edge pressures have been found to act for conduits in a projection condition.
- b. Thus, any conduit would have vertical pressures corresponding to the one analyzed so long as the width of the adjacent trench is no more than the width of the conduit. For this condition the crown pressure will be equal to the overburden soil pressure.
- c. For greater trench widths, the distribution of vertical pressure on a conduit of arbitrary width will change until an approximate projection condition is reached.
- d. If it is assumed that the projection condition is achieved at a trench width equal to twice the width of the conduit, then the vertical pressures on conduits of various sizes would vary as shown in Fig. IV-87.
- e. The figure indicates that for all conduits with a height-to-width ratio greater than about 0.5, edge pressures associated with adjacent trenches cannot be larger than those of the projection condition.

2. Horizontal Pressures. Data for horizontal pressures on the side of the conduit studied are presented in Fig. IV-88 for various widths of trenches with a vertical wall and for a fill height of 600 feet.

For comparison the pressures that would be expected for a conduit in a projection condition are included in the figure. In general, the horizontal pressures are less for the trench condition, particularly when the trench is very narrow. The increased pressures near the top of the conduit are probably the result of soil arching between the conduit and the wall of the trench. In Fig. IV-89 data are plotted for trenches of constant bottom width but of various wall slopes.

It is apparent that the smaller slope angles lead to greater horizontal pressures on the conduit.

Horizontal pressures at the mid-height of the conduits have been plotted in Fig. IV-90 as a function of trench width-to-depth ratio. The approximate effect of slope angle of the trench wall is given by the straight lines that have been interpolated through the available data. The effect of trench wall slope is greatest for trenches of narrow bottom width. The data in the figure apply to a relatively wide conduit for which the crown pressure is equal to the soil overburden pressure. For narrower conduits which have crown pressures greater than the overburden, it seems reasonable that the horizontal pressures would be increased proportionately. Note, however, that if the trench is no wider than the conduit then the crown pressure will equal the overburden pressure and Fig. IV-90 can be used directly for rectangular conduits of any size.

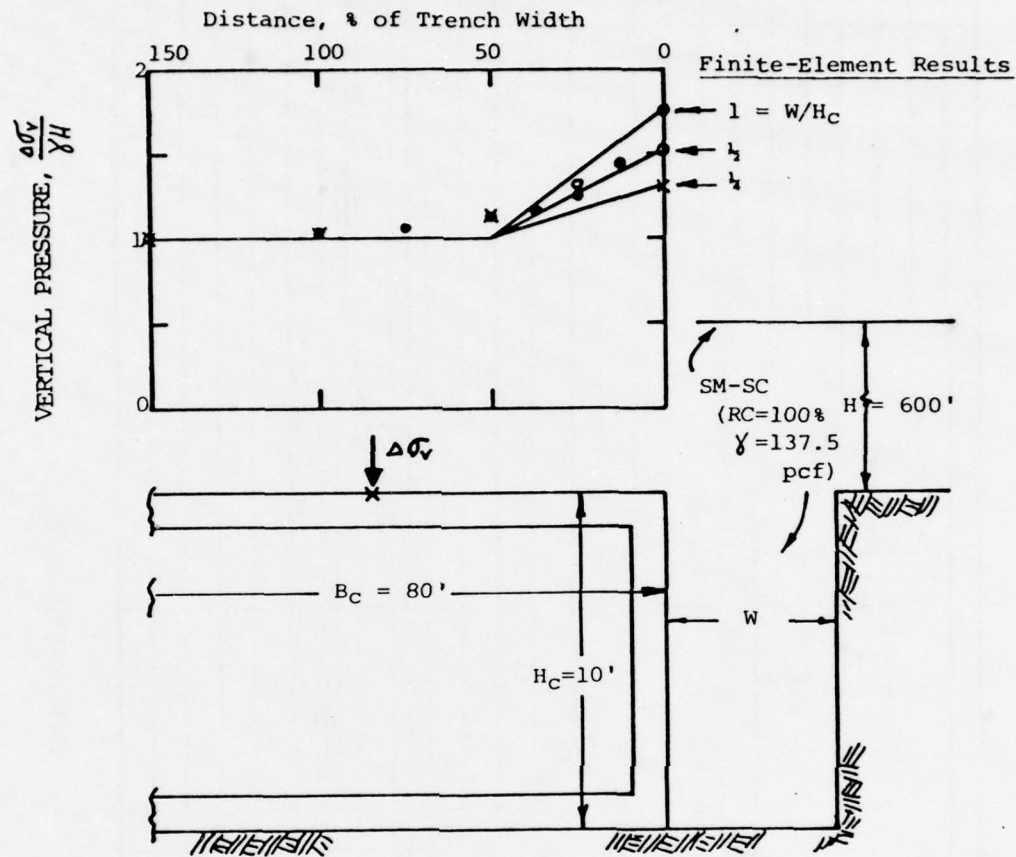


FIG. IV-86 VERTICAL PRESSURE NEAR EDGE OF RECTANGULAR CONDUIT IN SHALLOW TRENCH WITH VERTICAL WALL ($W/H_C \leq 1$)

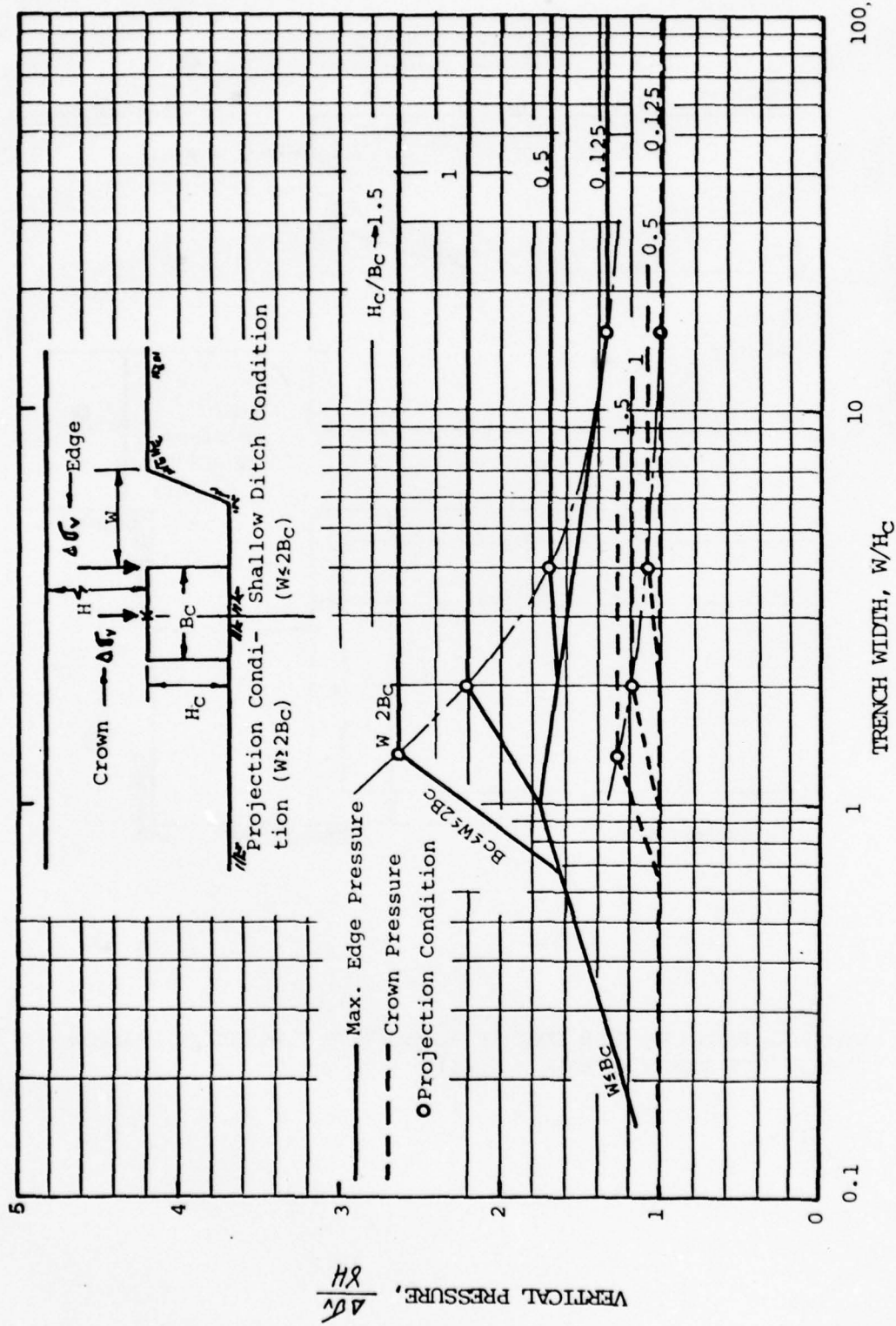


FIG. IV-87 VERTICAL PRESSURES ON RECTANGULAR CONDUIT IN SHALLOW TRENCH

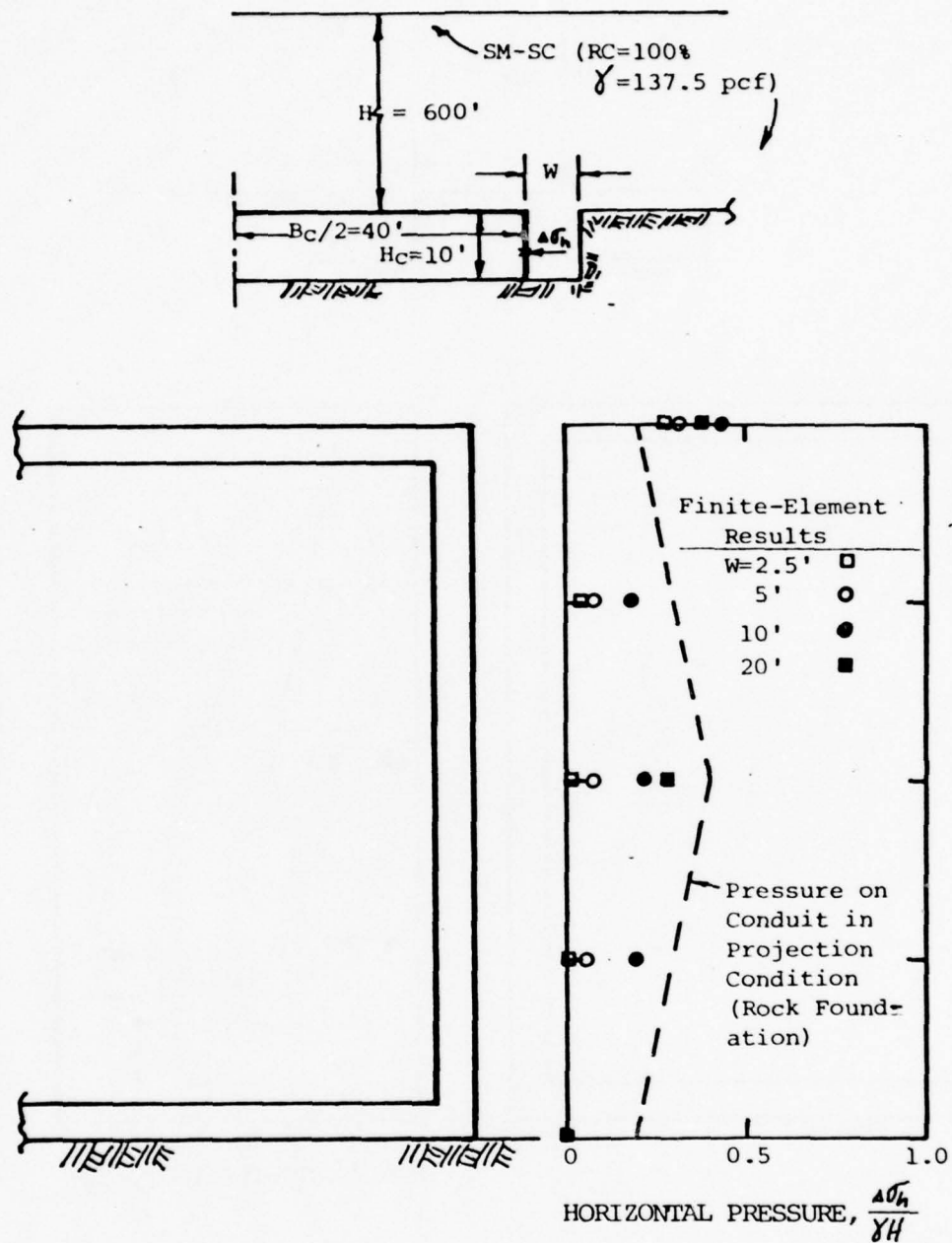


FIG. IV-88 HORIZONTAL PRESSURE ON CONDUIT IN SHALLOW TRENCH WITH VERTICAL WALLS

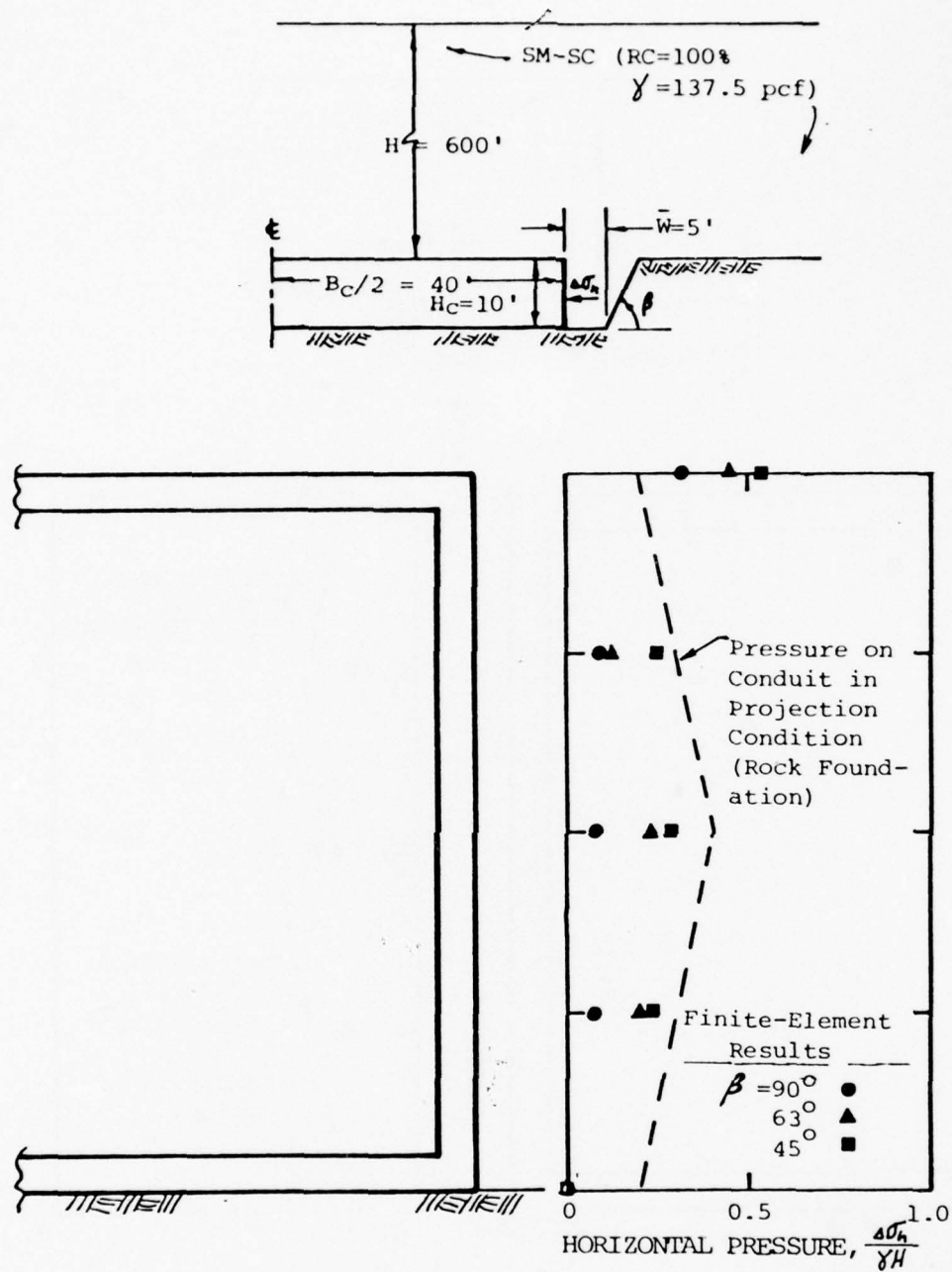


FIG. IV-89 HORIZONTAL PRESSURES ON RECTANGULAR CONDUIT IN A SHALLOW TRENCH WITH SLOPING WALL

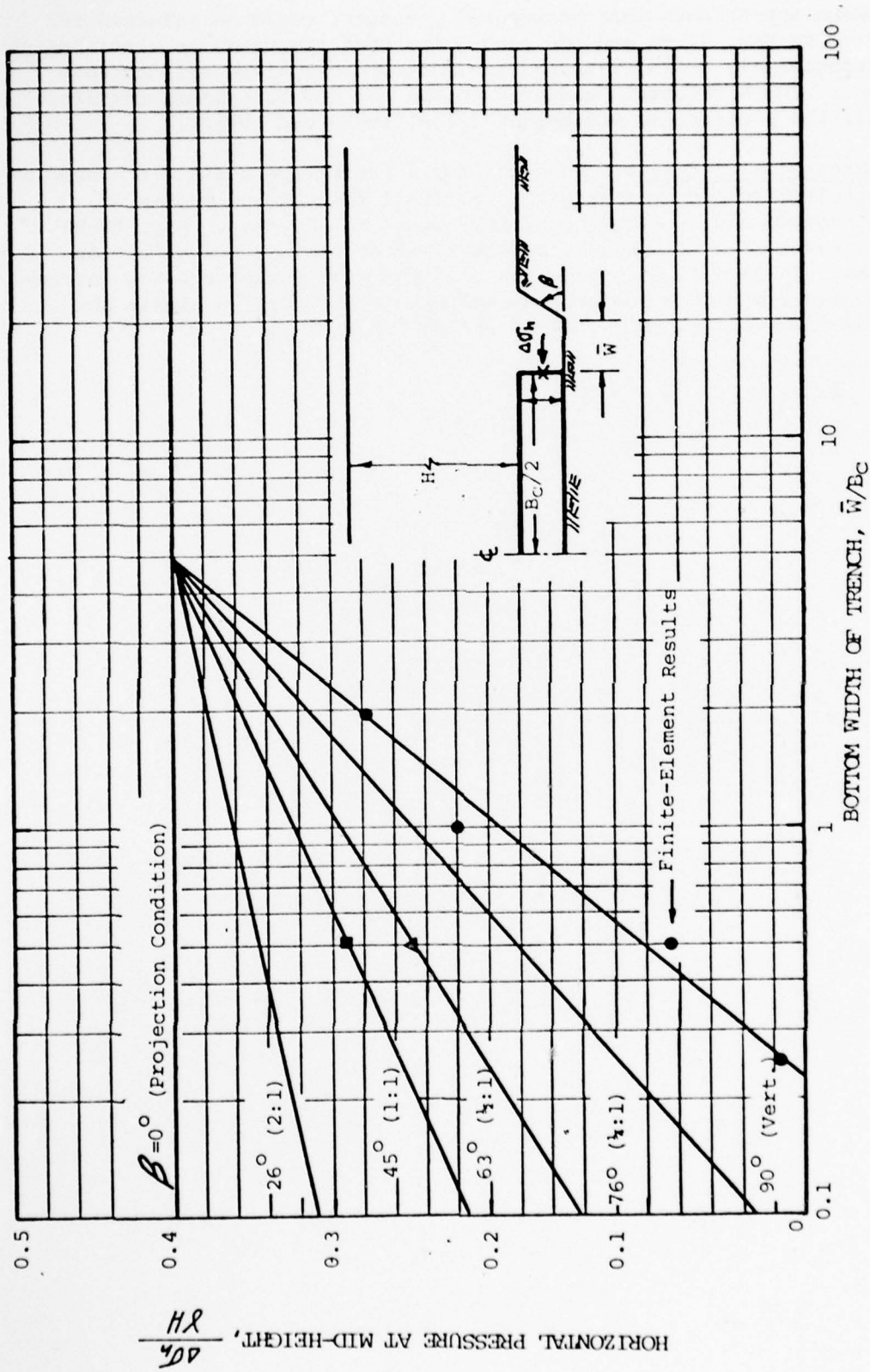


FIG. IV-90 HORIZONTAL PRESSURE AT MID-HEIGHT OF RECTANGULAR CONDUIT IN SHALLOW TRENCH ($H_c/B_c = 0.125$)

It seems appropriate that horizontal pressures could be selected for design based on Fig. IV-90 and the assumption that the pressure distribution will be trapezoidal, as for rectangular conduits on shallow soil or rock foundations. The horizontal pressures at the top and base would therefore be one-half the pressure at mid-height (Figs. IV-53 and IV-62).

3. Side Shear Stresses. The data for shear stresses along the side of the conduit studied are presented in Fig. IV-91 for various widths of vertical trenches and at a height of fill equal to 600 feet. Fig. IV-92 shows the results for trenches of constant bottom width but with various wall slopes. In each figure it can be seen that the shear stresses corresponding to a conduit in a projection condition are generally higher and could be used for design (Figs. IV-53 and IV-62).

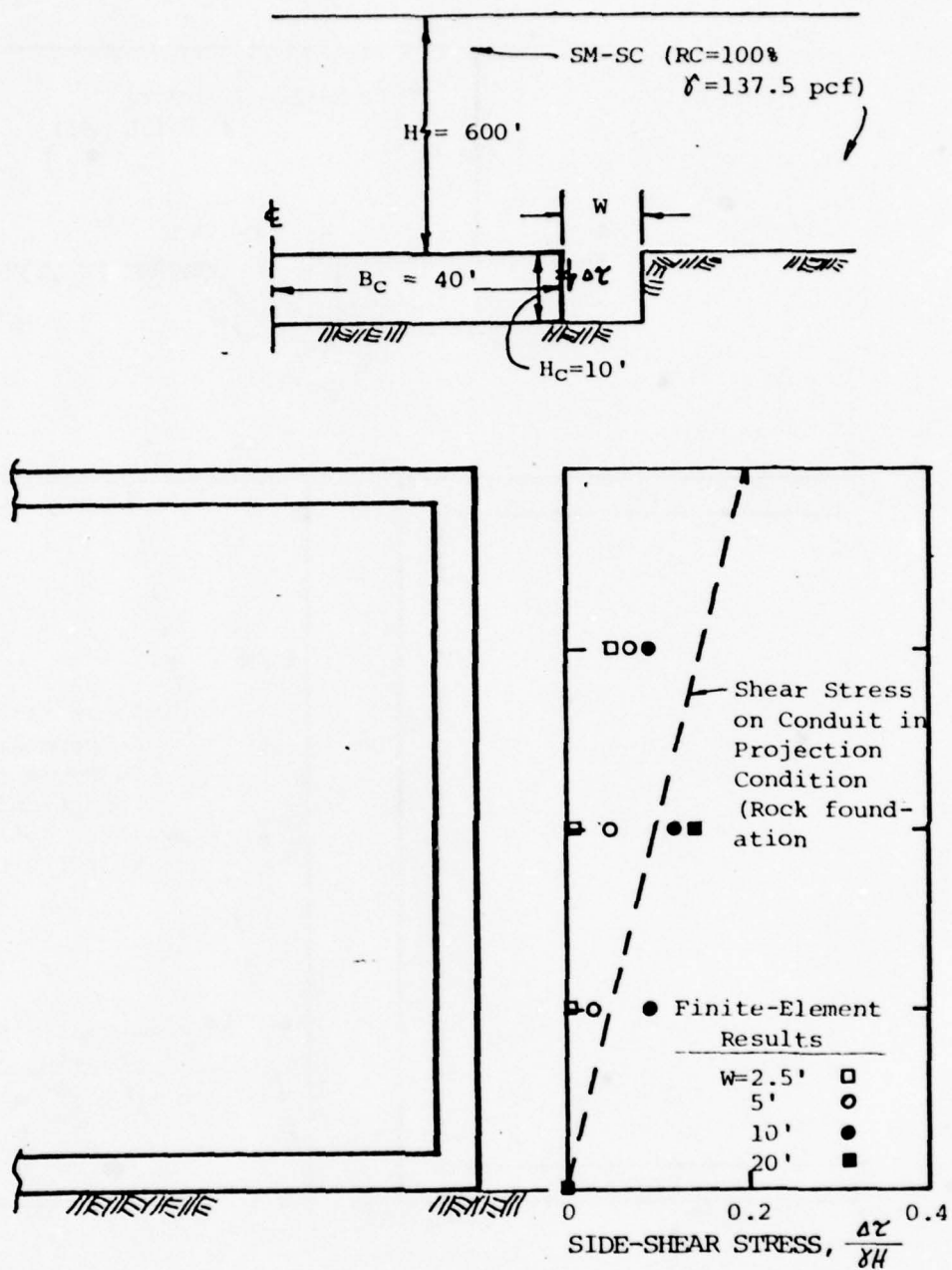


FIG. IV-91 SIDE-SHEAR STRESS ON RECTANGULAR CONDUIT IN SHALLOW TRENCH WITH VERTICAL WALLS

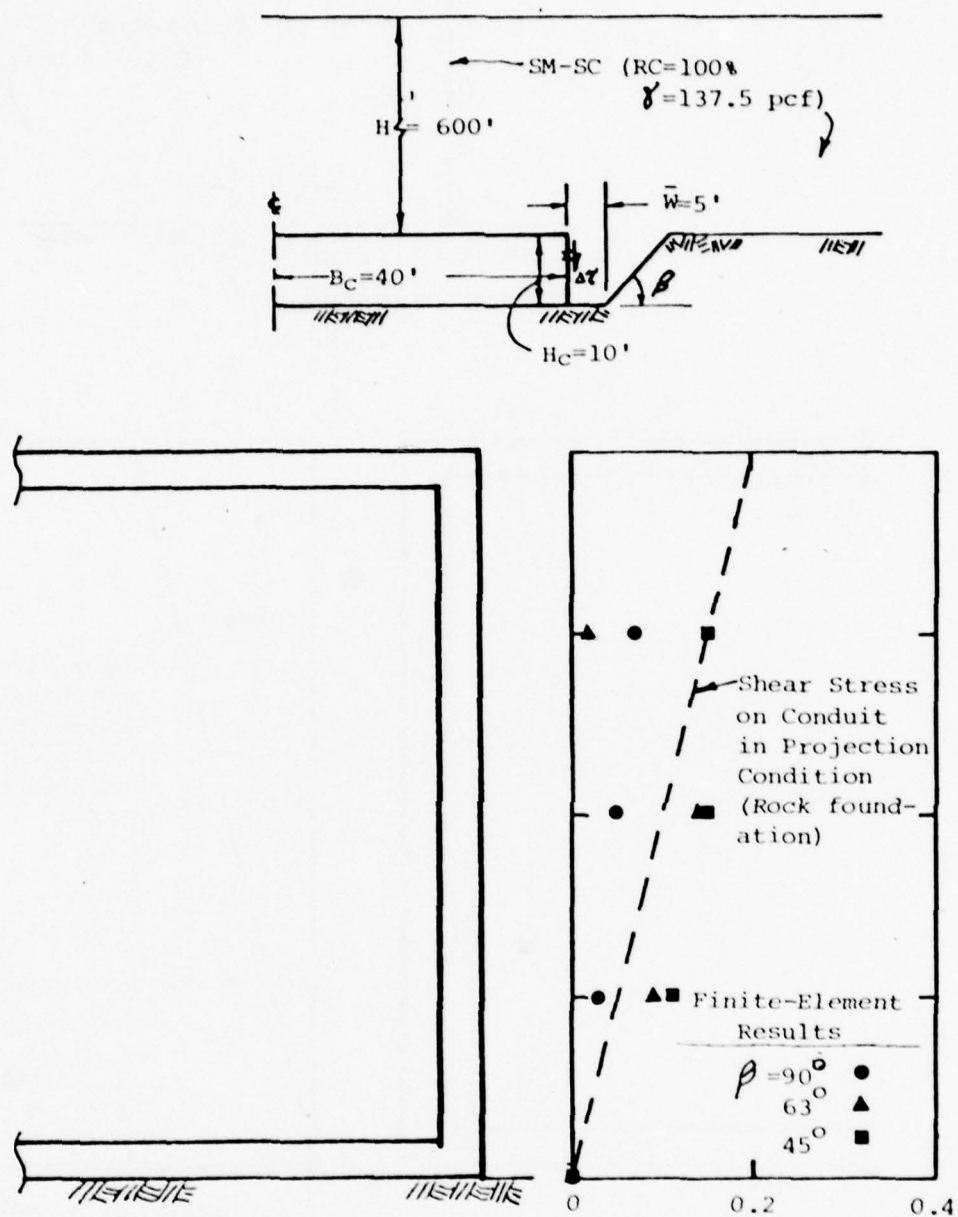


FIG. IV-92 SIDE-SHEAR STRESS ON RECTANGULAR CONDUIT IN SHALLOW TRENCH WITH SLOPING WALL

CHAPTER V

OTHER DESIGN CONSIDERATIONS - CONDUITS

Before presenting proposed design procedures for buried conduits (Chapter VI) it is useful to discuss several additional factors that should be considered during design namely: embankment stress distribution, conduit settlement, embankment cracking and hydraulic fracturing.

A. Embankment Stress Distribution

The finite-element analyses, which were presented in Chapter IV, assumed plane-strain conditions. In other words, the backfill or embankment over the conduit was assumed to be of infinite extent along the length of the conduit (perpendicular to the sections analyzed). The analyses were also made for embankments extended laterally (in the plane of the section) for a sufficiently large distance that side boundary effects could be ignored. Thus, the conditions analyzed were representative of wide, area fills, which would cause earth pressures to be uniform along the length of the conduit.

In actual practice, many conduits are placed through or beneath embankment dams that are approximately triangular in cross-section (along the longitudinal profile of the conduit). A common design procedure for these conditions is to independently analyze several sections along the length of the conduit, considering the earth loads to be directly proportional to the height of fill above the conduit at each section. For a homogeneous dam, composed of a single earth material, this procedure is usually conservative. For example, Lefebvre, et al. (1963) performed three-dimensional, finite element analyses of hypothetical embankment dams in valleys of various geometries (1:1, 3:1 and 6:1 valley slopes). As shown in Fig. V-1, the calculated major principal stresses at the base of the dams (along the bottom of the valleys) were generally less than the overburden pressure. However, the low stresses that occur for the valley with steep (1:1) slopes must have been accompanied by increased stresses at the abutments on the valley walls.

In zoned embankments, the different stress-strain properties of the various dam materials will often cause stress redistributions which concentrate earth loads in the zones of stiffer material, with an accompanying decrease in stress in adjacent zones of softer material. Kulhawy, et. al. (1969) were among the first to analytically study the stresses that occur within zoned dams. By using the finite-element method (two-dimensional analyses) they considered the stresses that would occur in a central-core dam about 800 feet high, as shown in Fig. V-2. The soil properties used in the analyses were comparable to those of the materials in Oroville Dam in northern California. Analyses were performed for "soft" and "stiff" core materials, which differed in stiffness by a factor of ten. As shown in the figure, the calculated principal stresses at the base of the dam were not equal to the overburden pressure near the central core. The same would

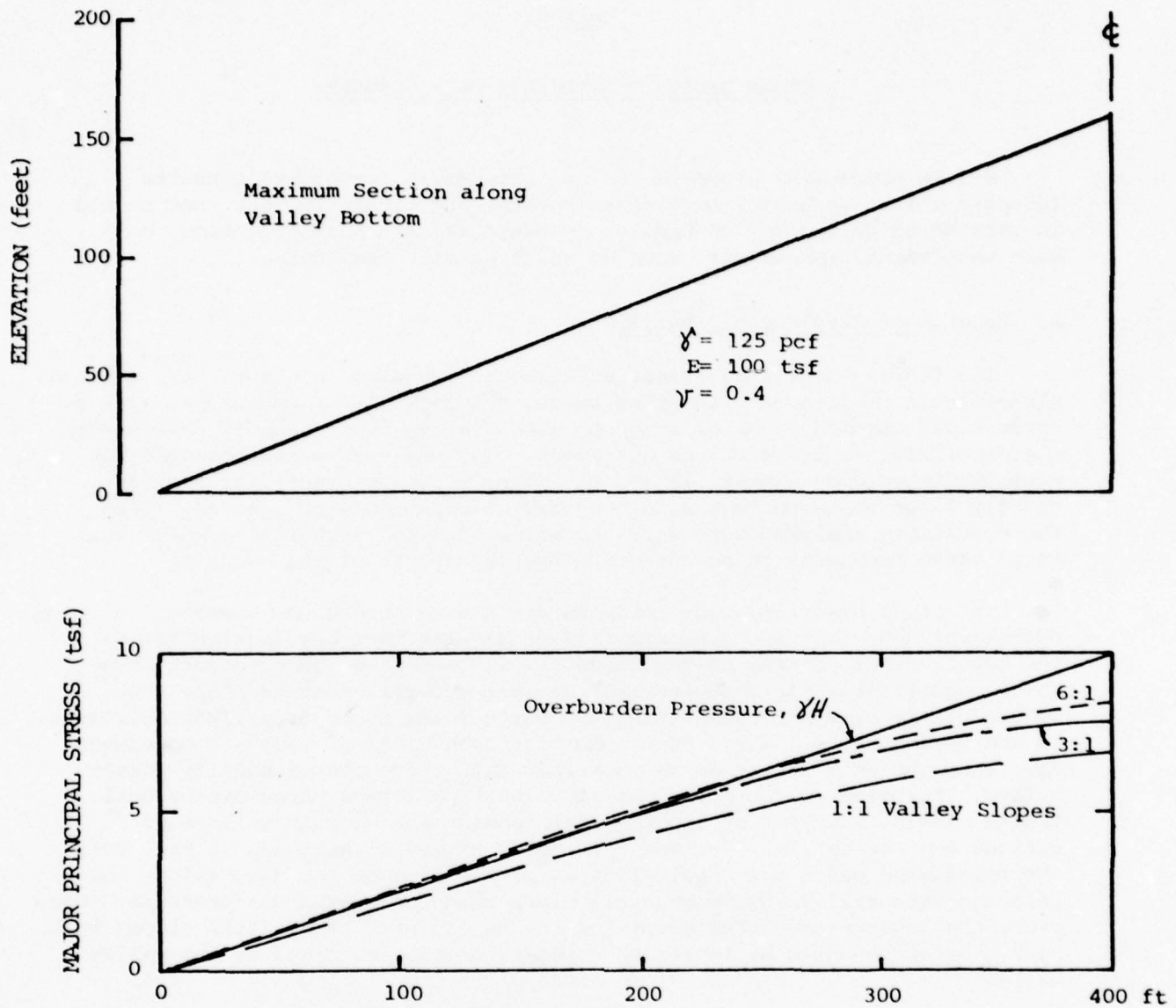


FIG. V-1 CALCULATED MAJOR PRINCIPAL STRESS AT BASE OF THREE-DIMENSIONAL DAM
(Lefebvre, et.al., 1973)

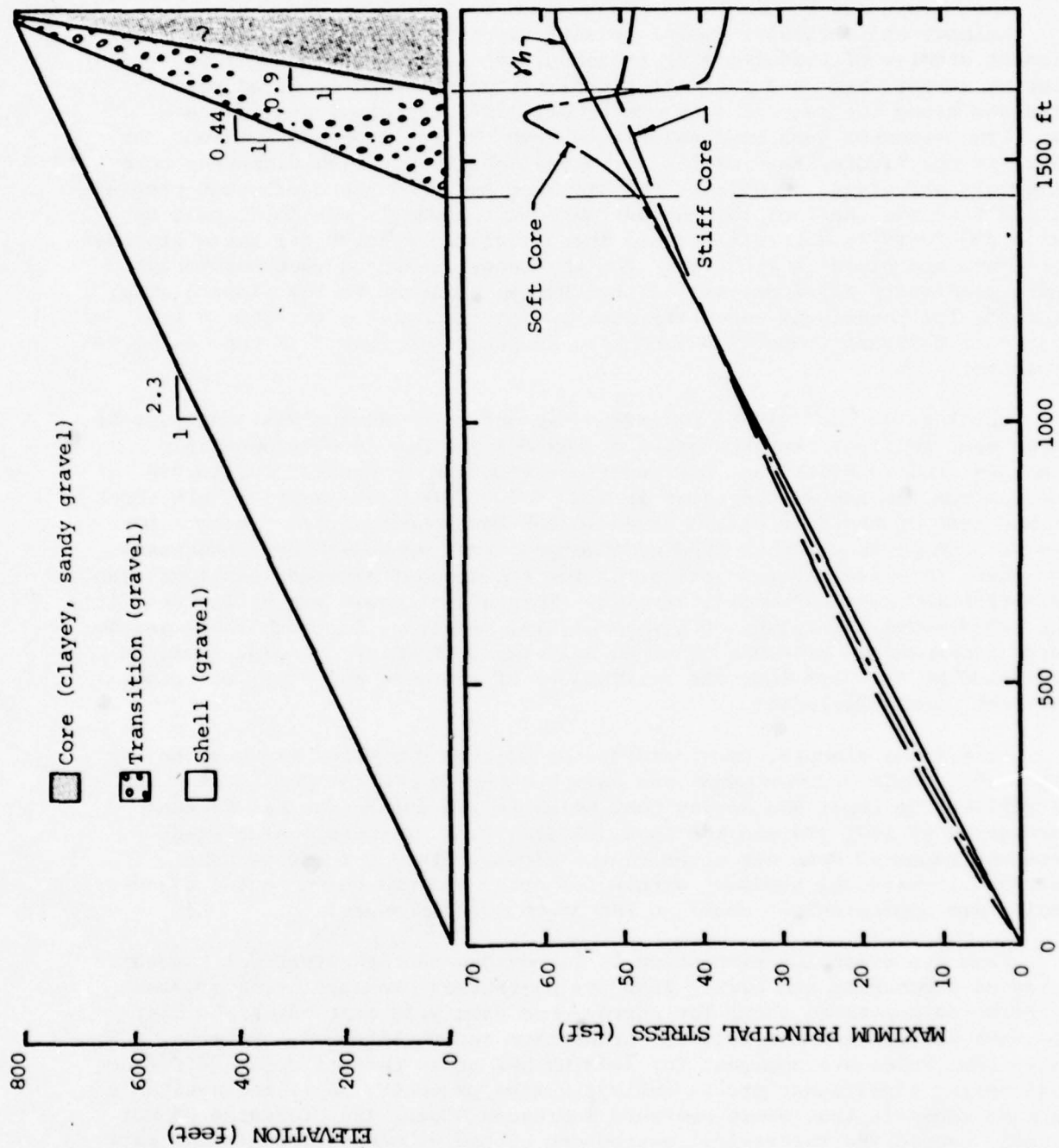


FIG. V-2 CALCULATED MAXIMUM PRINCIPAL STRESS AT BASE OF CENTRAL-CORE DAM (Kulhawy, et.al., 1969)

have been true for the vertical stresses, which are usually approximately equal to the maximum principal stresses in the central portion of an embankment. The figure shows that the redistribution of stresses depends upon the relative stiffness of the core and transition/shell materials. The maximum stress increase was about 20 percent above the overburden pressure in the transition zone adjacent to the "soft" core material.

Kulhawy and Gurtowski (1976) recently reported the results of finite-element studies of load transfer in zoned dams with either central or sloping cores. Fig. V-3 presents the distribution of major principal stresses along the base of a hypothetical, 122-meter-high, central-core dam. The stresses have been calculated from the reported information. As shown in the figure, the results for three embankments with different core materials are given. Generally the stresses exceeded the overburden pressure slightly in the shell of the dam but were much lower in the core, particularly the "wet" (i.e., soft) core. The calculated results for three sloping-core dams are given in Fig. V-4. For the cases presented (wet core only) there were quite large stress redistributions adjacent to the sloping core. In fact, for the widest core, the stresses at the base of the dam in the adjacent, upstream transition zone were 50 percent larger than the overburden pressure.

Quigley, et. al. (1976) performed two-and-three-dimensional analyses of embankment sections representative of New Melones Dam, a 600-foot-high, central-core, rockfill dam, now under construction in central California. The maximum dam section is shown in Fig. V-5. Calculated vertical pressures at the base of the section are given in the lower half of the figure. Note the difference in computed pressures between the two-and-three-dimensional analyses. The reduction in pressures for the three-dimensional analysis can be attributed to cross-valley arching. This effect could not be included in the two-dimensional (plane strain) analysis. However, for both analyses, no large increases in pressure occurred near the core(s) of the dam. This is explained by the fact that the stiffnesses of the core and shell materials were not vastly different.

As a final example, consider the Los Angeles Dam which is shown in Fig. V-6. Finite-element analyses have been performed for design of a dam to replace the Lower Van Norman Dam, which failed during the San Fernando earthquake of 1971 (Valera and Chen, 1974). Base pressures calculated from the reported data are given in the figure. Though there is some decrease in vertical pressure within the core, the pressures in the adjacent shells are approximately equal to the overburden pressure.

From the preceding discussion it is obvious that the vertical pressures below an embankment can differ from the overburden pressure. The greatest differences appear to occur for narrow-core dams with core materials that are much softer than the adjacent transition and shell zones. However, no convenient rules are apparent for judging how great the stiffness difference must be for significant stress redistribution to occur. But, the available data do indicate that where pressure increases occur, the pressures do not usually exceed the theoretical overburden pressure beneath the highest part of the dam (see Fig. V-2, V-3 and V-4). The distance over which the increased pressures occur is about equal to one-half the core width at the level of

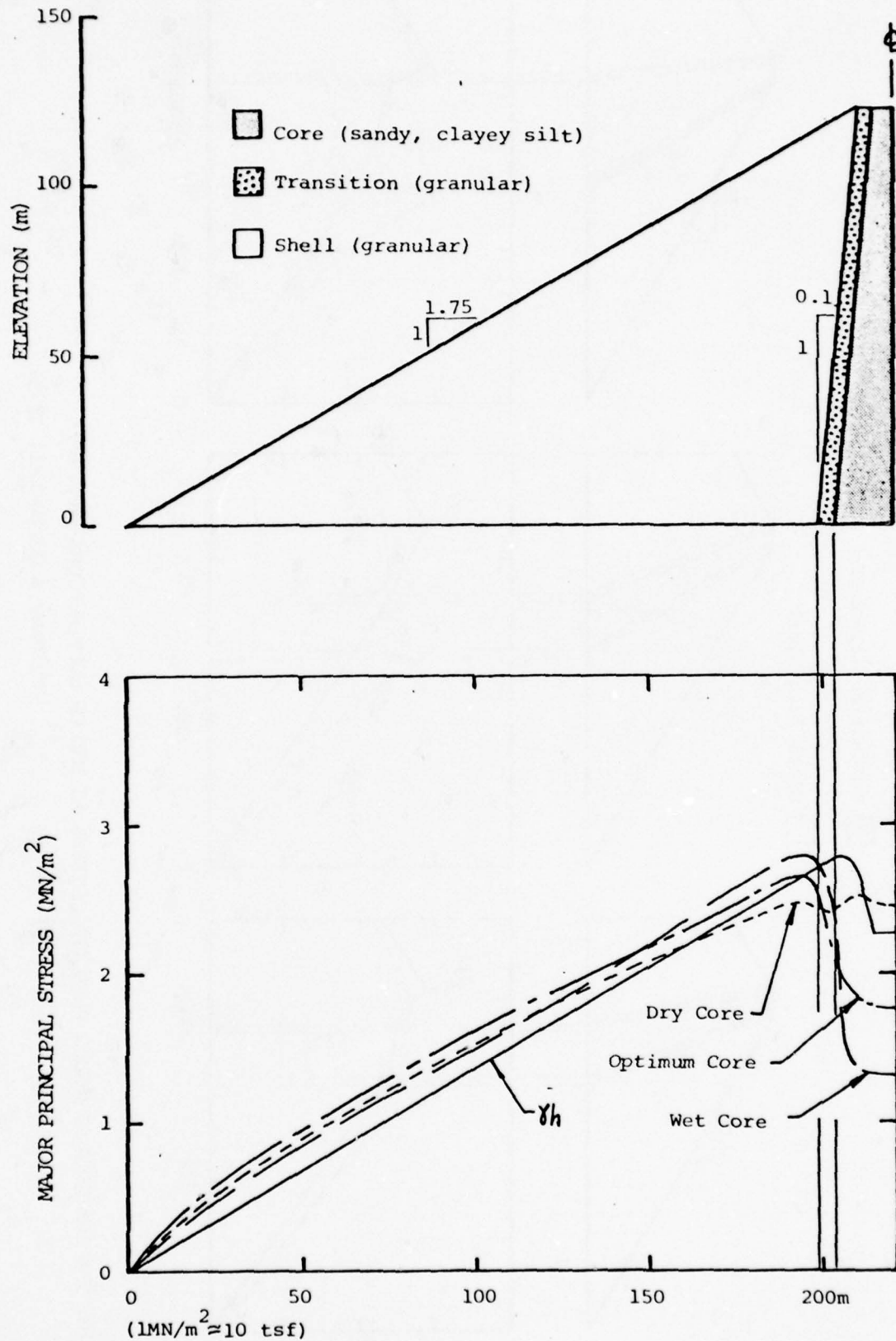


FIG. V-3 CALCULATED MAJOR PRINCIPAL STRESS AT BASE OF CENTRAL-CORE DAM
(Kulhawy & Gurtowski, 1976)

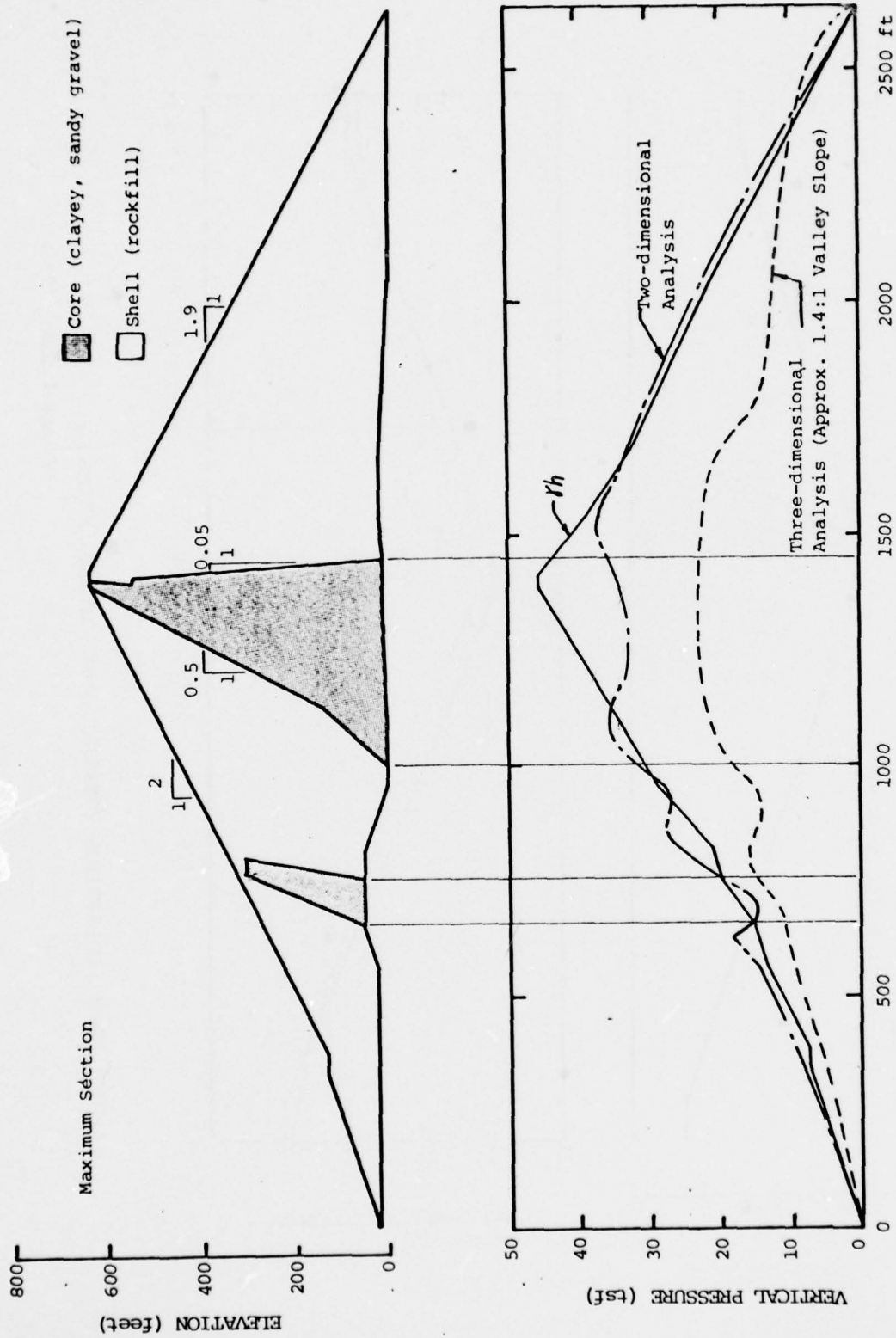


FIG. V-5 CALCULATED VERTICAL PRESSURE AT BASE OF NEW MELONES DAM
(Quigley, et. al., 1976)

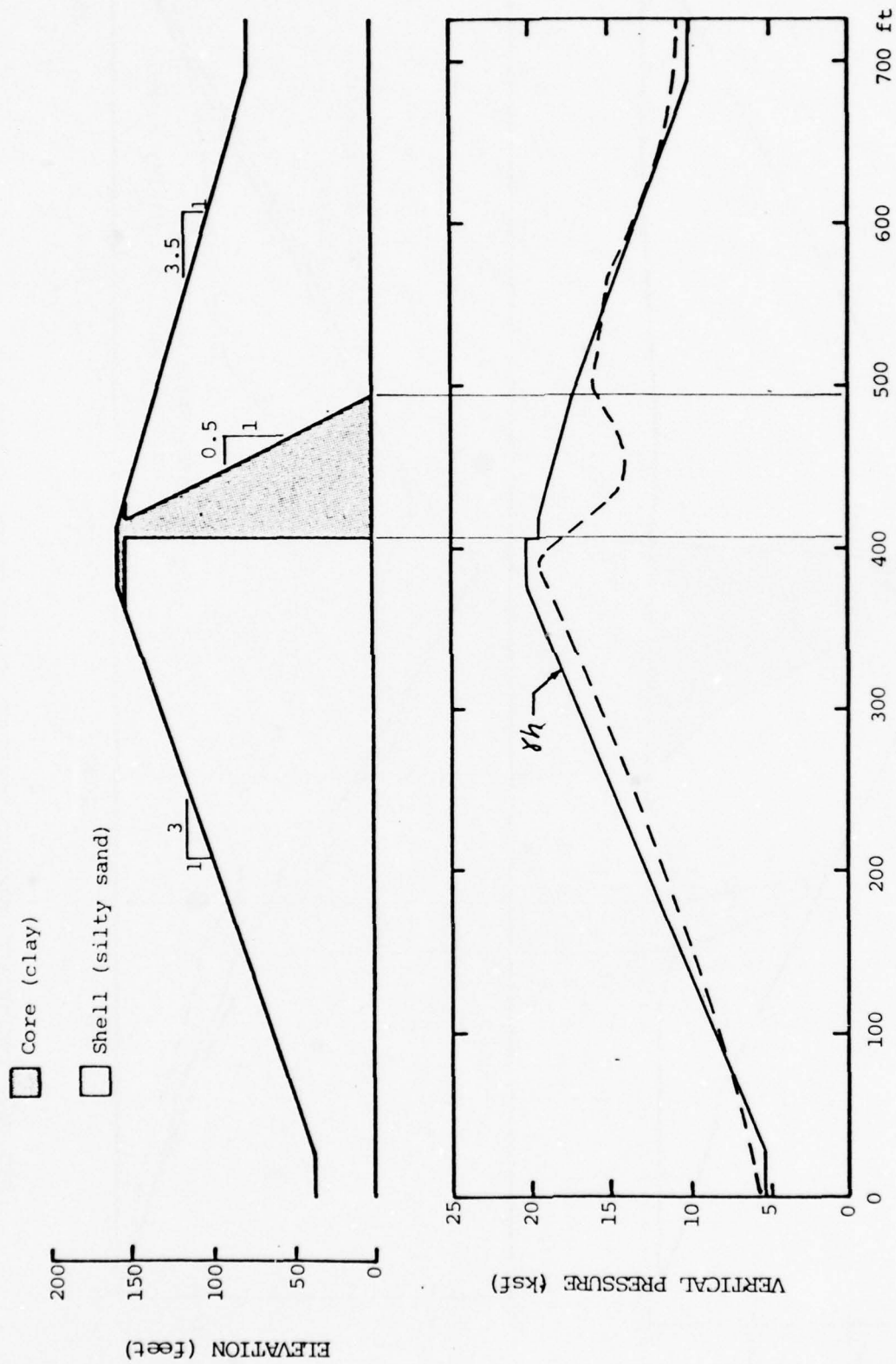


FIG. V-6 CALCULATED VERTICAL PRESSURE AT BASE OF LOS ANGELES DAM

(Valera & Chen, 1974)

interest. Pressure increases are accompanied by similar pressure decreases within the core. To determine earth loads for design, finite-element analysis could be performed using the properties and geometry appropriate for the particular dam in question. In lieu of finite-element analyses, the approximations given in Fig. V-7 could be used to estimate the possible magnitude of vertical pressure redistribution. To be conservative, a pressure equal to the maximum overburden, γH , could be assumed within the limits shown in the figure. In reality, the total pressure on the base could not exceed the weight of the dam.

Accordingly, conduits located below zoned embankments should be designed for equivalent heights of fill corresponding to anticipated pressure increases as a result of stress redistribution. Pressure reduction in the core should be ignored for structural design of the conduit, unless finite-element analyses are performed to determine the magnitude of this effect.

B. Conduit Settlement

Conduits are normally designed to resist earth pressures that act in a plane transverse to their longitudinal axis. However, a conduit that passes through or beneath an embankment supported by a compressible foundation will settle along with the embankment. In general, elastic, plastic (shear) and consolidation settlements can occur, and with each there will be associated horizontal movements. As a result, the conduit, unless it is provided with adequate expansion/contraction joints, could experience significant tensile and/or compressive stresses in the longitudinal direction. Concrete conduits (either precast or cast-in-place) are usually built in jointed segments to avoid the occurrence of large longitudinal stresses. The purpose of this section is to review available methods for determining the magnitude of longitudinal strains at the base of an earth dam so that adequate joints can be provided.

Rutledge and Gould (1973) reported the results of extensive studies, performed by their firm for the Soil Conservation Service, U. S. Department of Agriculture (Mueser, et. al., 1968), of the movements of articulated conduits under earth dams on compressible foundations. They developed design procedures for estimating conduit extension by applying the theory of elasticity to the problem of a triangular dam built on a compressible soil deposit of limited thickness (see Fig. V-8). Both vertical loads caused by the weight of the dam and shear stresses along the dam base were included in the analysis. The vertical and horizontal strains that result from the applied loads were found to be functions of the height and width of the dam and the thickness, modulus and Poisson's ratio of the foundation soil. Design charts were prepared from which the ratio of maximum horizontal strain to maximum vertical strain could be determined for any dam/foundation geometry. In practice, the maximum vertical strain was calculated by normal methods of settlement analysis and the charts were used to estimate the corresponding horizontal strains. The design procedures were subsequently confirmed by finite-element parameter studies and by comparison with field measurements of the movements beneath 20 selected earth dams of the Soil Conservation Service.

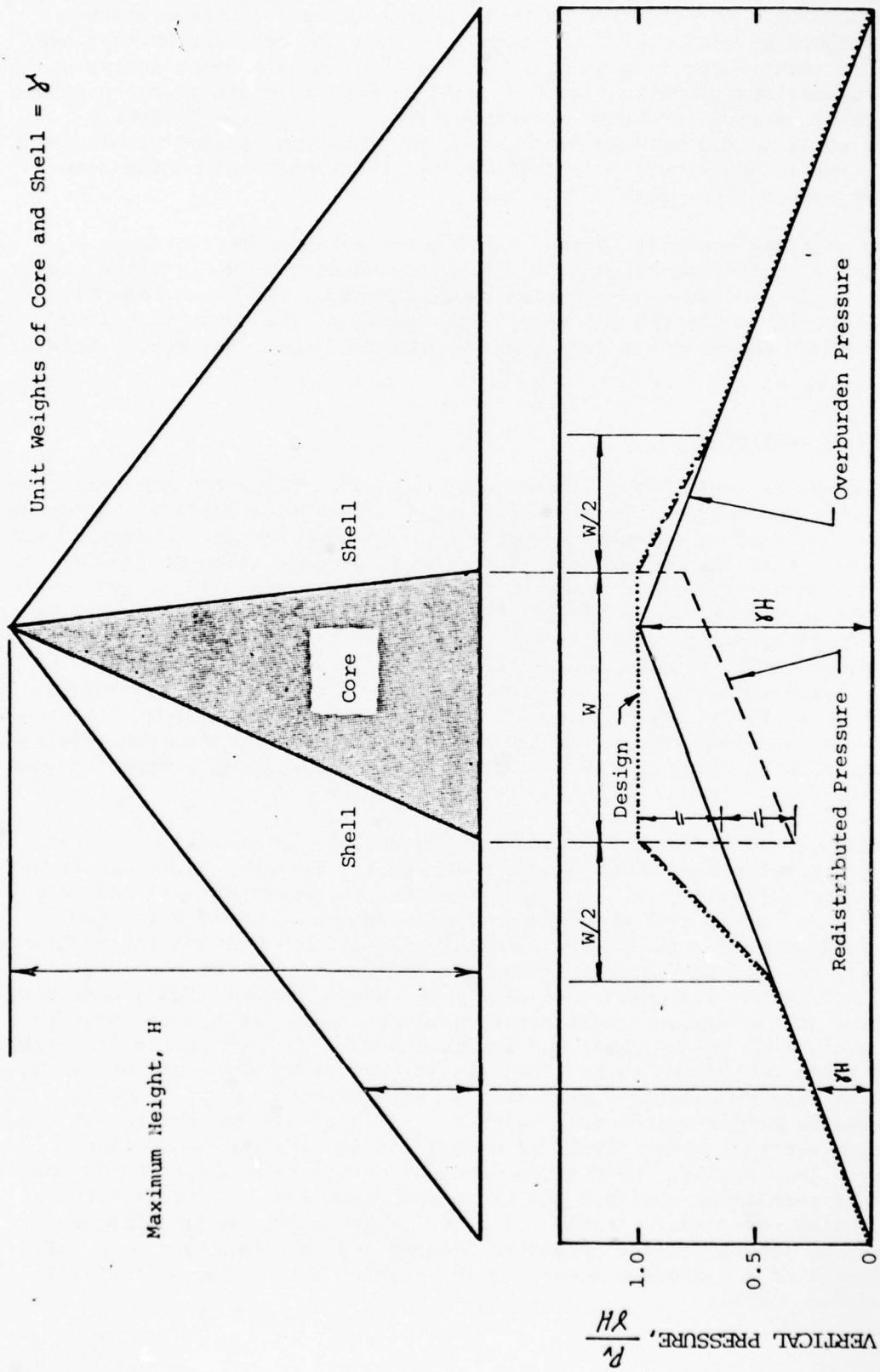


FIG. V-7 APPROXIMATE REDISTRIBUTION OF VERTICAL PRESSURES AT THE BASE OF A ZONED EMBANKMENT DAM

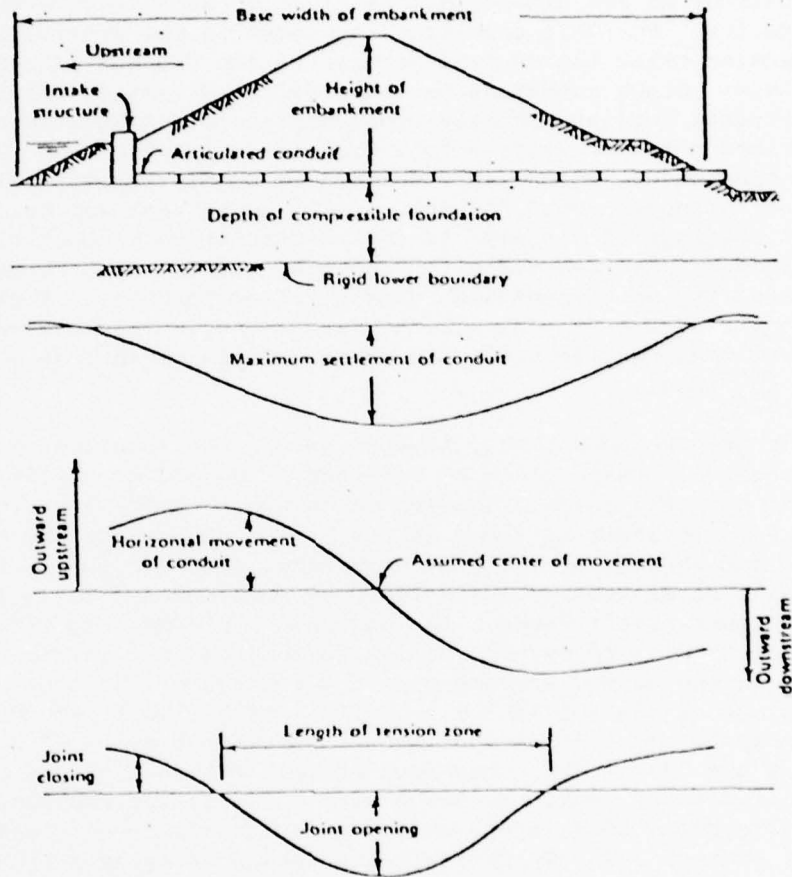


FIG. V-8 CONDUIT MOVEMENTS BENEATH AN EMBANKMENT ON A COMPRESSIBLE FOUNDATION
(Rutledge and Gould, 1973)

It is interesting to consider the field data reported by Rutledge and Gould. Fig. V-9 compares the predicted and observed strain ratios for the 20 dams. It is clear that their design procedure is a conservative, upper-bound solution.

It should be understood that the SCS design procedure is only applicable to the conditions shown in Fig. V-8, where the conduit lies at the base of an embankment that is directly supported by the compressible foundation. For this condition, as shown in the figure, the conduit is in tension below the central portion of the dam and in compression beneath the toes. Other investigators have reported similar observations for embankments resting directly upon compressible foundations. Hughes (1969) described a 224 ft long, 8-foot-diameter culvert beneath a 55-foot-high sand embankment, which was underlain by highly-plastic, silty clay. The culvert extended about 5.3 feet as the embankment was built. Maximum joint openings of the pipe (8-foot sections) were about 0.6 feet and occurred beneath the center of the embankment. Bozozuk and Leonards (1972) reported the settlement and lateral spreading of a 12-foot-high granular test fill over a deep deposit of marine clay. The measured horizontal strains were tensile below the center of the embankment and compressive near the toes.

There are conditions, however, where the location of the tensile and compressive strains could be reversed. Lee and Shen (1969) considered the subsidence of a surface loading on an upper, stiff layer overlying a deep, compressible layer as shown in Fig. V-10. The resulting horizontal movements and strains at the ground surface, as shown in the figure, are in opposite directions to those found by Rutledge and Gould for the condition of no upper, stiff layer. Lee and Shen performed experimental and finite-element studies to develop design guidelines that relate horizontal movements of the ground surface to the thickness of the upper, stiff layer and the slope of the subsidence profile. Ortiz (1967) provides field data from the Zumpango Test Embankment that confirms the types of movements predicted by Lee and Shen. The embankment was 6.5 meters high and consisted of compacted silty sand. As shown in Fig. V-11, the embankment was built upon a stiff, silty sand layer, which was underlain by very soft clay (natural water content over 300 percent) and subsequently by another layer of stiff, silty sand. The movements of the embankment and the foundation soils are given in the figure. The base of the embankment was compressed laterally as the fill settled. Note, however, that the bottom of the upper, stiff, silty sand layer underwent extension. It is clear that the longitudinal deformations of a conduit beneath the embankment would have been largely dependent upon the depth at which the conduit was founded.

Finite-element methods could be used to predict the horizontal movements and strains that would occur in conduits beneath embankments on compressible foundations. However, care should be taken in applying the analytical results to design because predictions of horizontal movements are among the least accurate results of such analyses at the present time. As Poulos (1972) pointed out, a number of comparisons between measured horizontal movements of embankments and values predicted by finite-element analyses have been shown considerable lack of agreement, despite the fact

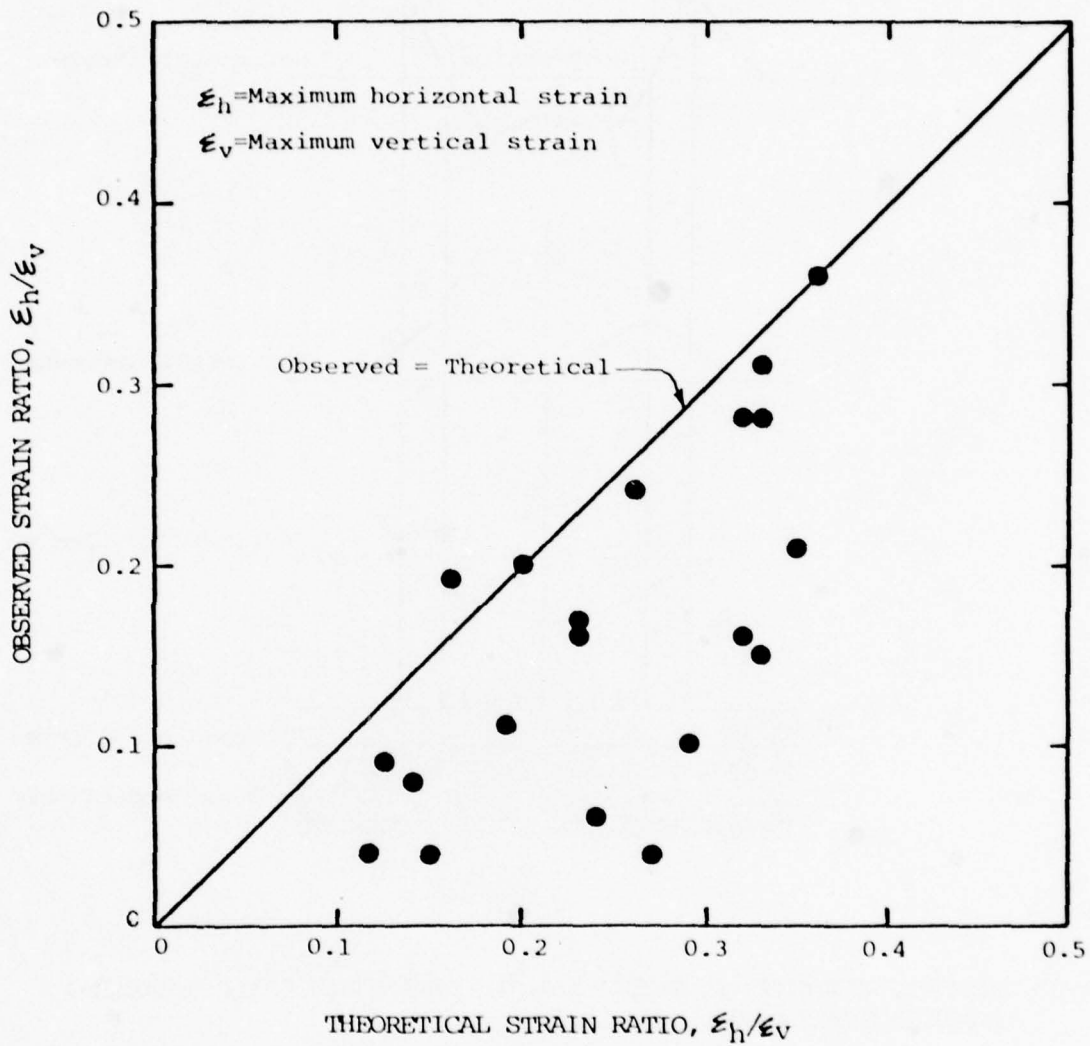


FIG. V-9 COMPARISON OF OBSERVED AND THEORETICAL STRAIN RATIOS FOR CONDUITS BENEATH TWENTY SCS DAMS

(Rutledge and Gould, 1973)

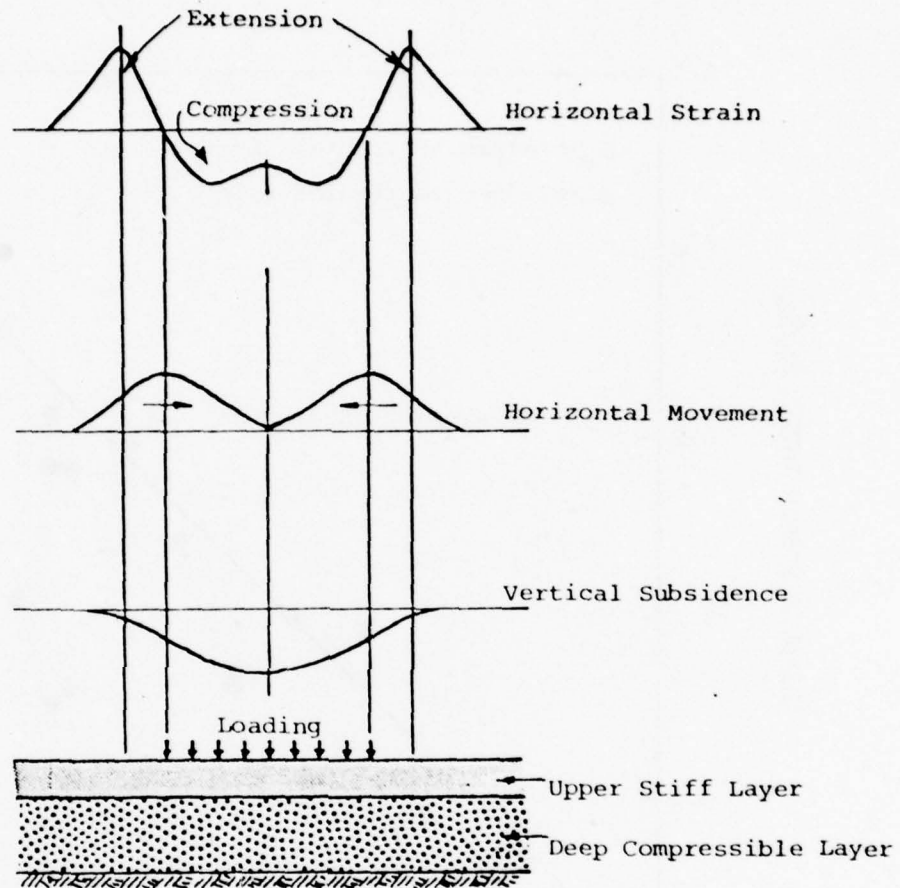
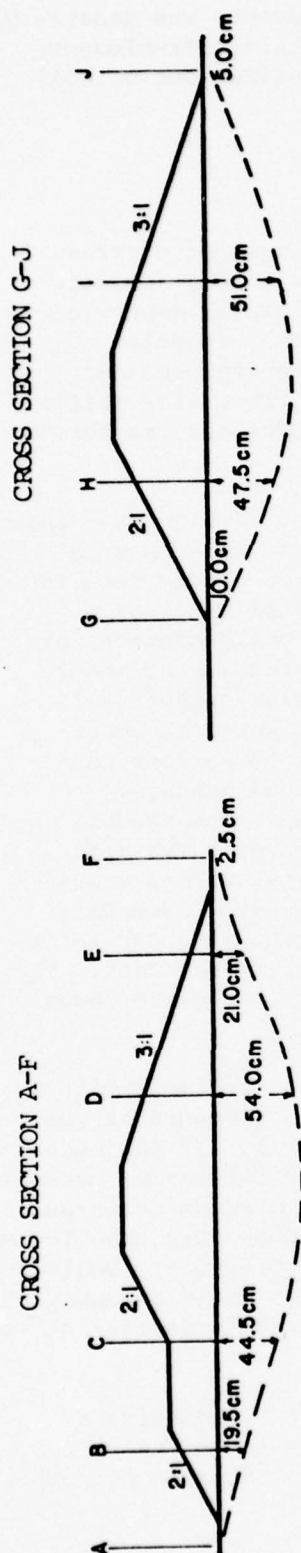
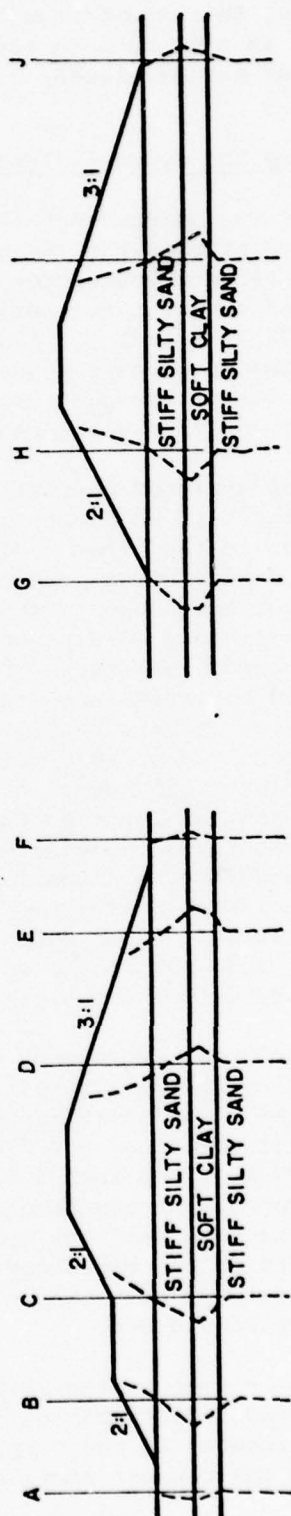


FIG. V-10 SURFACE MOVEMENTS BENEATH A LOADING ON A STIFF LAYER OVERLYING A COMPRESSIBLE LAYER

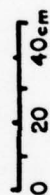
(Lee and Shen, 1969)



SETTLEMENT



HORIZONTAL MOVEMENT SCALE



HORIZONTAL MOVEMENT

FIG. V-11 MOVEMENTS AT ZUMPANGO TEST EMBANKMENT (Ortiz, 1967)

that the agreement between measured and predicted settlements was generally quite good. Hopefully, this limitation of the use of the finite-element method will disappear in time as more realistic characterizations of soil stress-strain behaviour are developed.

C. Embankment Cracking and Hydraulic Fracturing

In Chapter III it was pointed out that a frequent cause of distress in embankment dams is piping of the embankment along the outlet conduit. Often the piping has been attributed to poor compaction of the impervious backfill immediately adjacent to the outlet conduit. More recently (Sherard, et. al., 1972; Sherard, 1973) attention has been focused on embankment piping caused by excessive leakage through differential settlement cracks near conduits or through cracks caused by hydraulic fracturing in zones of low embankment stress adjacent to conduits.

The finite-element analyses performed for this investigation have shown that the stresses in the soil adjacent to a conduit can in fact be much lower than the stresses in the "free field" at some distance away from the conduit. For example, the minimum pressure on the vertical sides of a rectangular conduit that rests upon a shallow soil on rock foundation have been shown to be approximately 20 percent of the crown pressure or about 20 percent of the overburden pressure for a relatively wide conduit. In contrast the free-field horizontal pressures in the soil would be about 45 percent of overburden. Thus a reduction of more than 50 percent can occur as result of stress redistribution in the soil around conduit. Furthermore, the calculated minimum principal stresses near the conduit were only about two-thirds as large as the minimum stresses on vertical planes. Typical distributions of major and minor principal stress around square and circular conduits are shown in Figs. V-12 and V-13. The data are results of finite-element analyses of 10-foot-wide conduits, partially embedded in rock foundations, under heights of fill equal to 600 feet. The lowest pressures occur adjacent to the vertical sides of the square conduit and are less than 20 percent of the overburden pressure.

Consider a 600-foot-high embankment dam impounding a reservoir with a water level 50 feet below the dam crest. The hydrostatic pressure at the base of the dam would be about 34 ksf (550 ft. \times 0.062 kcf). If the embankment material has a unit weight of 0.130 kcf, the (total) overburden pressure at the base would be 78 ksf (600 feet \times 0.130 kcf). The minimum principal stress adjacent to a conduit at the base of the dam would be less than 16 ksf (0.20 \times 78 ksf), or less than half the hydrostatic water pressure. Neglecting the tensile strength of the embankment material, which would probably not exceed 0.5 ksf, it is evident that the potential for hydraulic fracturing is great for the condition considered.

The condition can be even more critical if the dam is zoned with a narrow soft core. Stress redistribution could further decrease the effective overburden pressure in the core (and thereby the minimum principle stress in the plane of the conduit section).

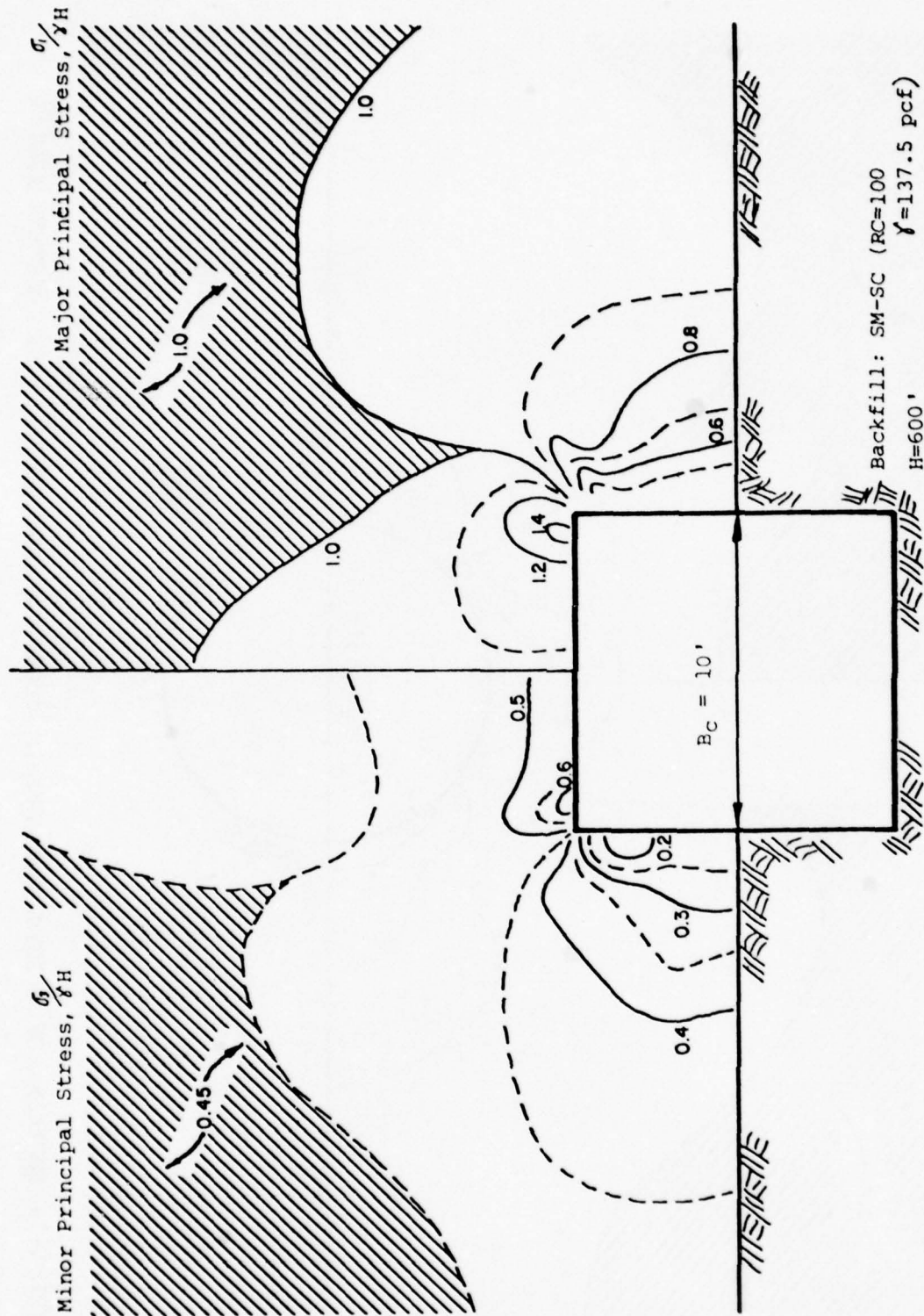


FIG. V-12 DISTRIBUTION OF PRINCIPAL STRESSES AROUND SQUARE CONDUIT, FINITE-ELEMENT RESULTS

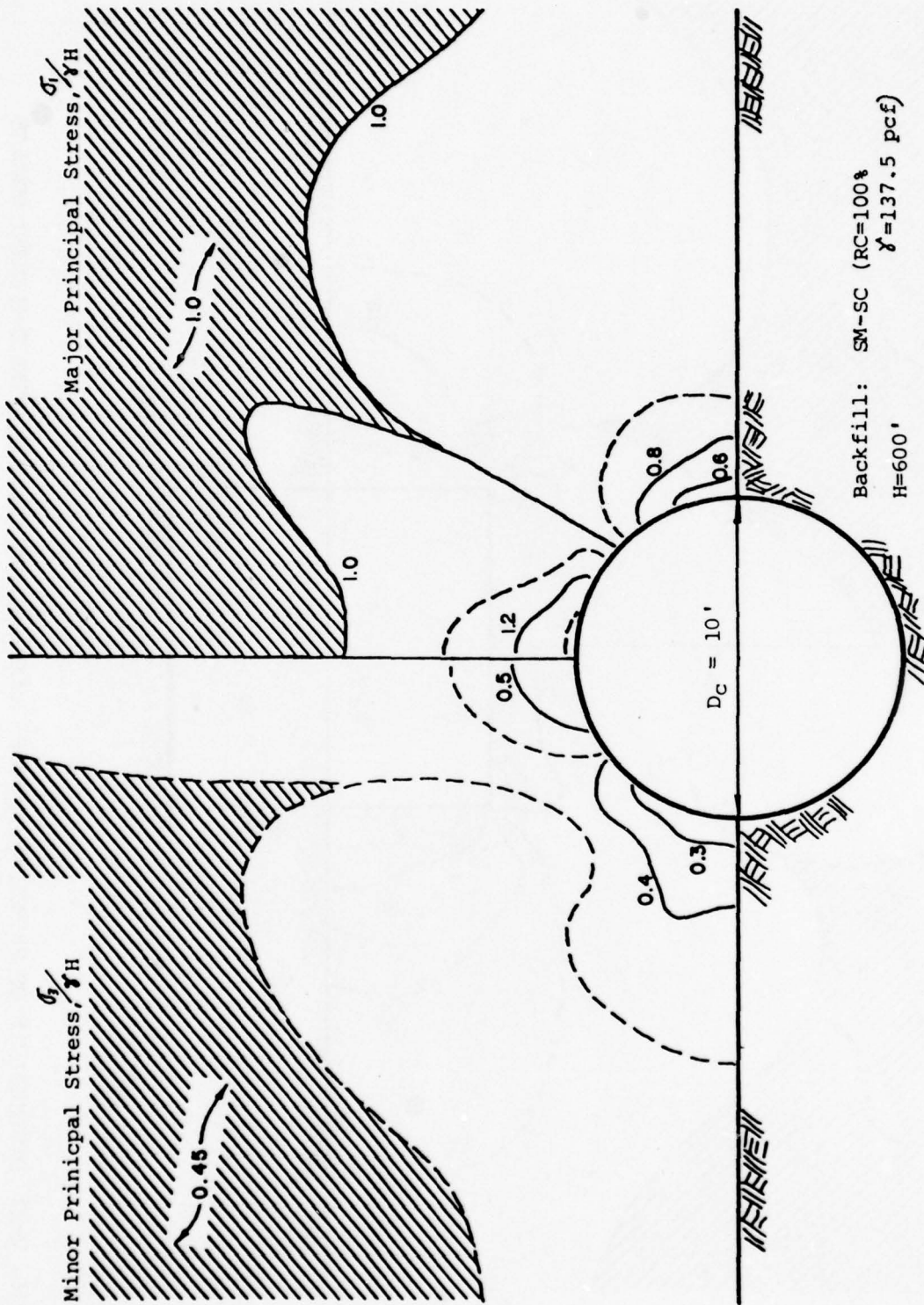


FIG. V-13 DISTRIBUTION OF PRINCIPAL STRESSES AROUND CIRCULAR CONDUIT, FINITE-ELEMENT RESULTS

The preceding discussion indicates that proper design of conduits that pass through or beneath earth dams must include consideration of the effects of the conduit upon the surrounding backfill and not just the calculation of earth pressures that the conduit must resist.

CHAPTER VI

PROPOSED DESIGN PROCEDURES - CONDUITS

In this chapter, the result of analytical studies of earth pressures on buried conduits are summarized and three different design procedures are suggested which can be applied to the design of cast-in-place, reinforced-concrete conduits beneath high embankments. These procedures which are described in subsequent sections of this chapter are:

1. Design based on structural analysis of the conduit using simplified design earth pressure distributions,
2. Design based on moment, shear and thrust coefficients (no structural analyses needed),
3. Design based on finite-element analyses of the interaction between the culvert and the surrounding embankment.

A. Design Earth Pressures

Recommended pressure diagrams for the structural design of circular, oblong, and rectangular conduits founded on soil or rock foundations are presented in Figs. VI-1 and VI-2. To establish the magnitude of the normal pressures and side-shear stresses for a particular conduit, the following steps should be followed:

1. The Crown-Pressure Factor, N , can be determined directly from Fig. V-3 for the following conditions:
 - a. Height of fill, H , greater than ten conduit width, and
 - b. Conduit rests on rock (or other incompressible material), or
 - c. Conduit rests on a shallow soil foundation (H_f/B_c greater than 2).
2. For immediate soil foundation depths, calculate the ratio of N -values (from Fig. VI-4 with the calculated N -ratio to determine the corrected N corresponding to the foundation depth of interest.
3. For heights of fill less than ten conduit widths, use Fig. VI-5 to determine the appropriate Crown-Pressure Factor.
4. As indicated in Figs. VI-1 and VI-2, the design normal pressure of at crown of the conduit will be:

$$\Delta\sigma_c = NYH$$

(VI-1)

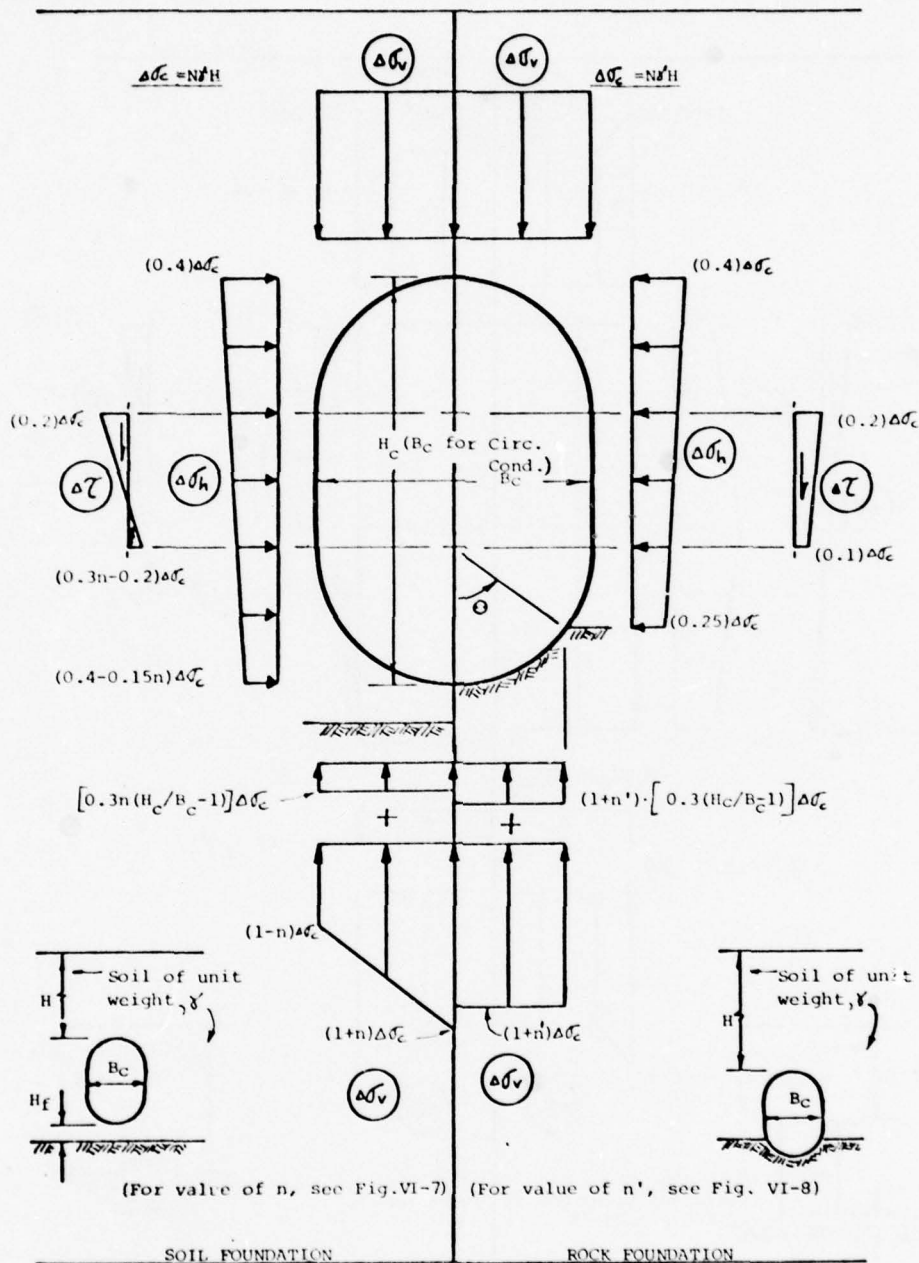


FIG. VI-1 DESIGN EARTH PRESSURES FOR CIRCULAR AND OBLONG CONDUITS, EMBANKMENT CONDITION

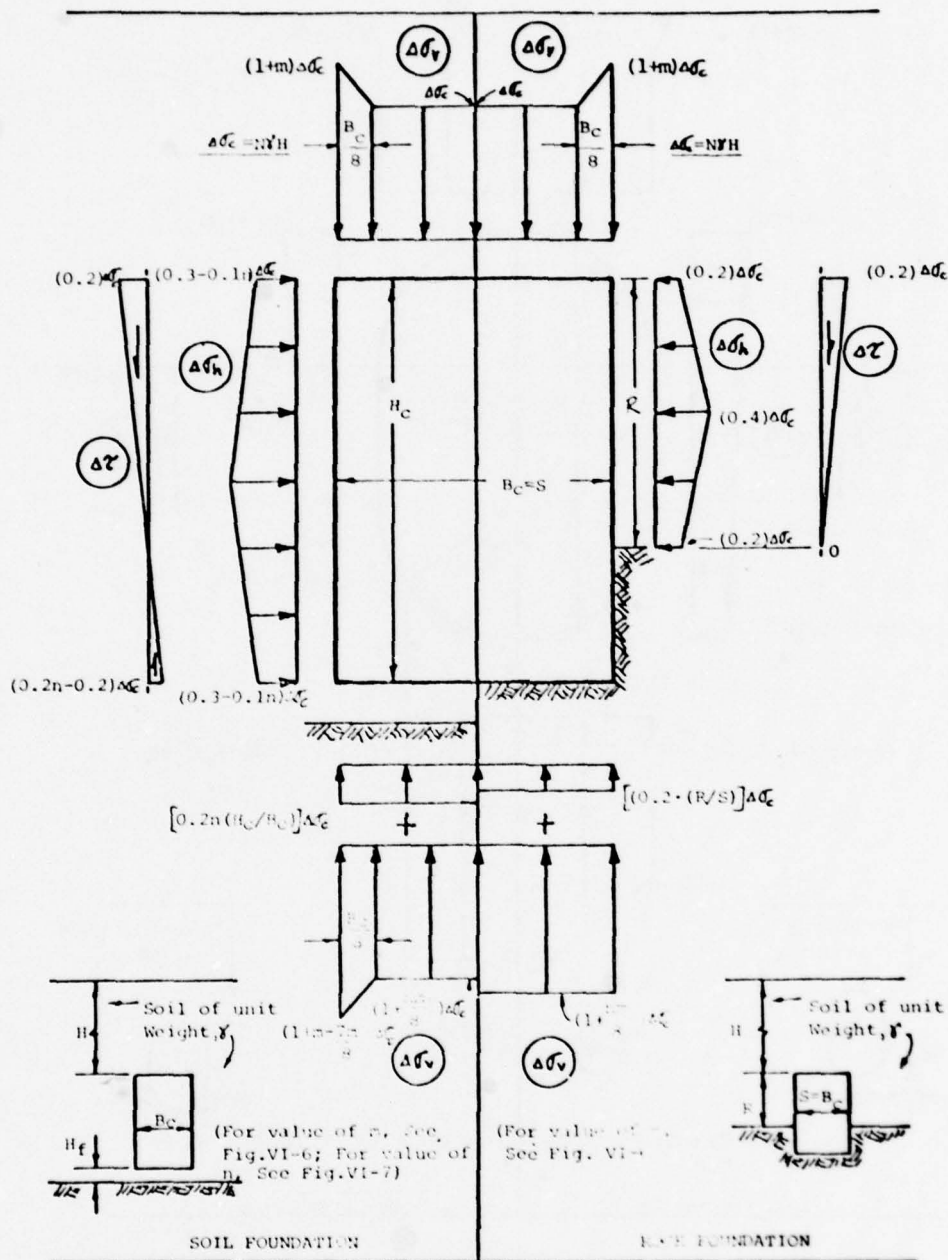


FIG. VI-2 DESIGN EARTH PRESSURES FOR RECTANGULAR CONDUITS, EMBANKMENT CONDITION

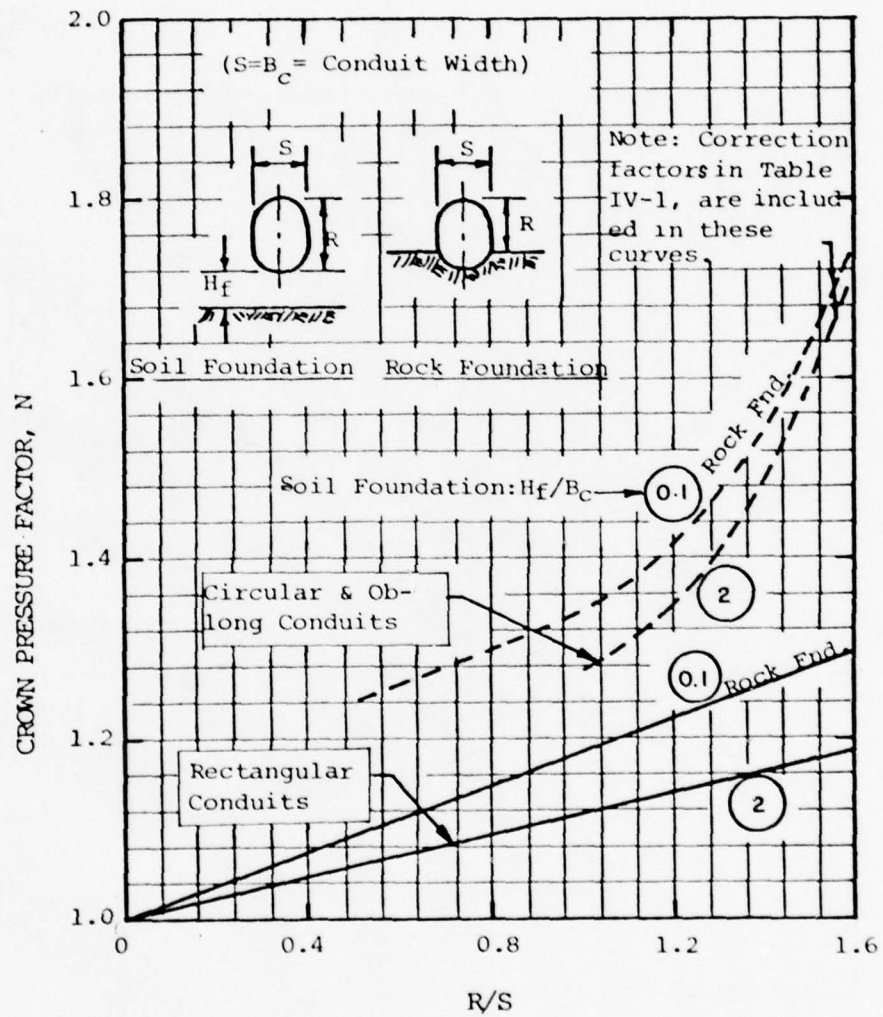


FIG. VI-3 CROWN PRESSURE FACTOR FOR LARGE HEIGHTS OF FILL ($H/B_c \geq 10$), EMBANKMENT CONDITION

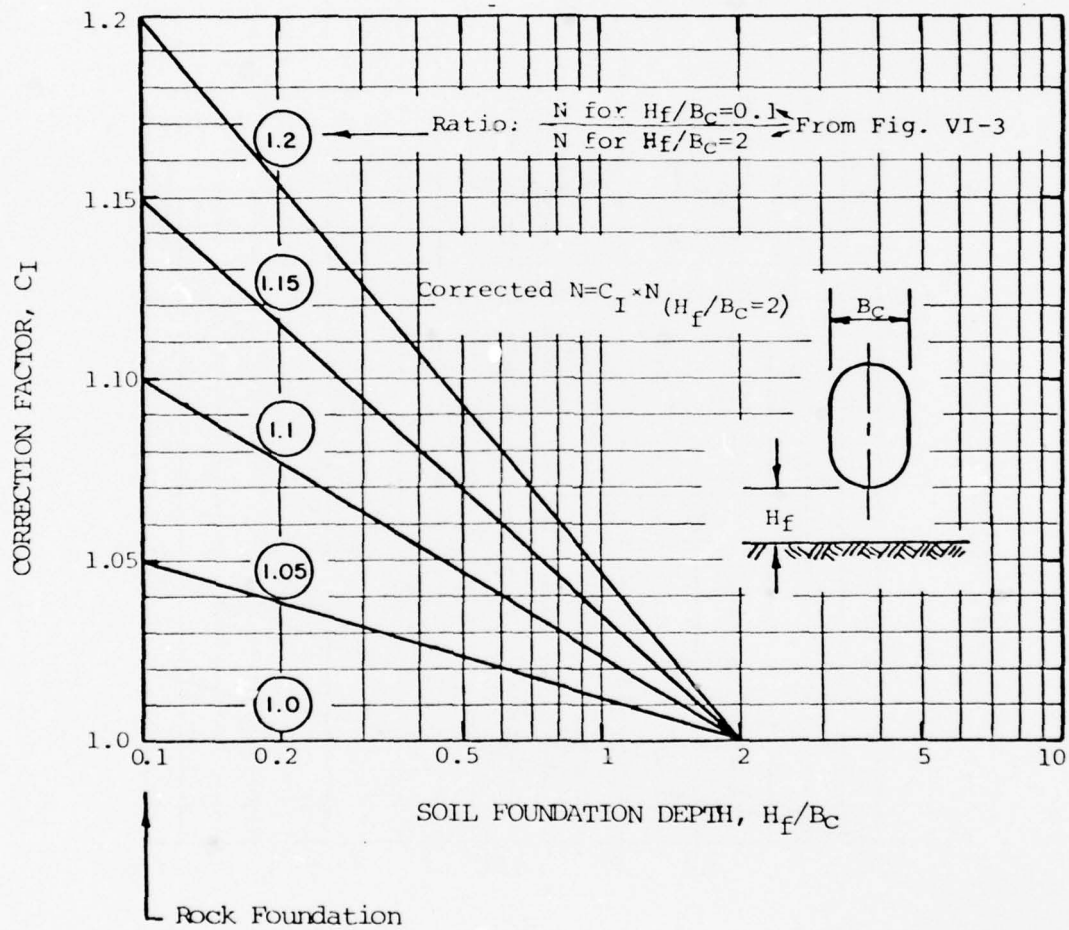


FIG. VI-4 CROWN PRESSURE CORRECTION FACTOR FOR INTERMEDIATE SOIL FOUNDATION DEPTHS AND LARGE HEIGHTS OF FILL ($H/B_C > 10$), EMBANKMENT CONDITION

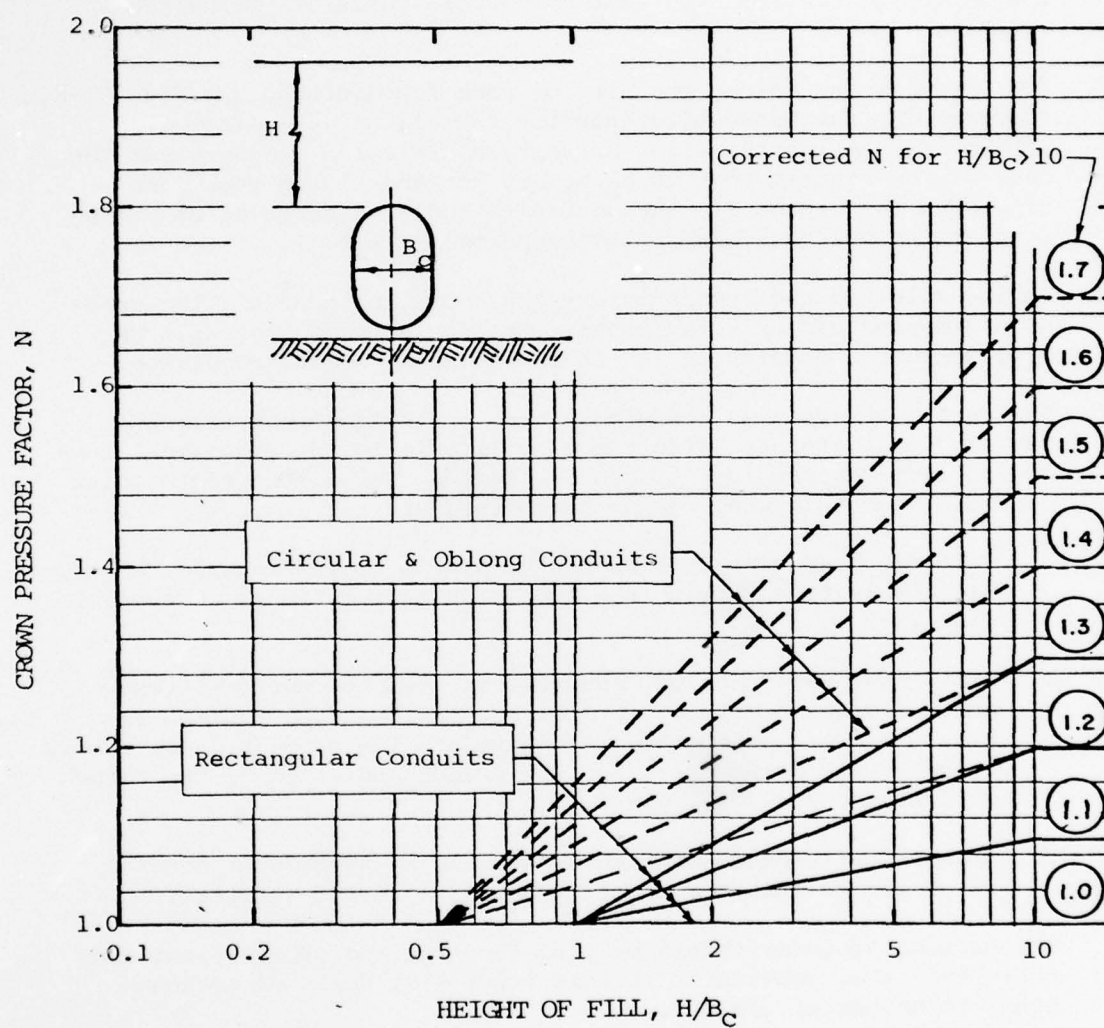


FIG. VI-5 CROWN PRESSURE FACTOR FOR HEIGHTS OF FILL LESS THAN TEN CONDUIT WIDTHS, EMBANKMENT CONDITIONS

The γH term should be the effective overburden pressure, considering possible embankment stress redistribution (see Chapter V).

5. For rectangular conduits, use Fig. IV-6 to determine the Edge-Pressure Factor, m . The factor represents the increases in vertical pressures that can occur near the sides of a conduit.
6. For conduits on soil foundations, determine the Foundation Reaction Factor, n , from Fig. VI-7. The factor reflects the influence of the depth to rock (or other incompressible material) below the conduit.
7. For circular and oblong conduits on rock foundations, use Fig. VI-8 to determine the Foundation Reaction Factor, n' . The factor represents the concentration of vertical reaction pressures at the base of the conduit that is caused by the underlying rock. As discussed in Chapter IV, the base of a modified circular or oblong conduit can be considered fully supported ($\theta = 90^\circ$).
8. Having selected the appropriate values of m and n or n' , the pressure diagrams can be established. The design pressures will be applicable to conduits in an embankment (projection) condition.
9. The earth pressures on conduits placed in shallow rock trenches can vary significantly from those applicable to the embankment condition (see Chapter IV). Based on limited analyses of rectangular conduits, the following design guidelines are suggested:
 - a. Vertical pressures as represented by the Crown-Pressure Factor, are likely to vary with the top width of the trench as shown in Fig. VI-9.
 - b. Horizontal pressures on conduits, in trenches narrower than about five conduit widths, will be less than the horizontal pressures for an embankment condition. The pressures are likely to vary with bottom width of the trench and slope of the trench wall as shown in Fig. VI-10.
 - c. Side shear stresses can conservatively be assumed to equal those for an embankment condition and a rock foundation.

Engineering judgment should be used for trenches of different geometry than that considered in this study lie, depth of trench equal to height of conduit.

Examples of earth pressure diagrams are given in Fig. VI-11 for a square conduit placed on deep soil and on the surface of a rock foundation. As noted in the figure, the pressure diagrams for the rock foundation are also appropriate for a square conduit on a shallow soil foundation ($H_f/B_c = 0.1$).

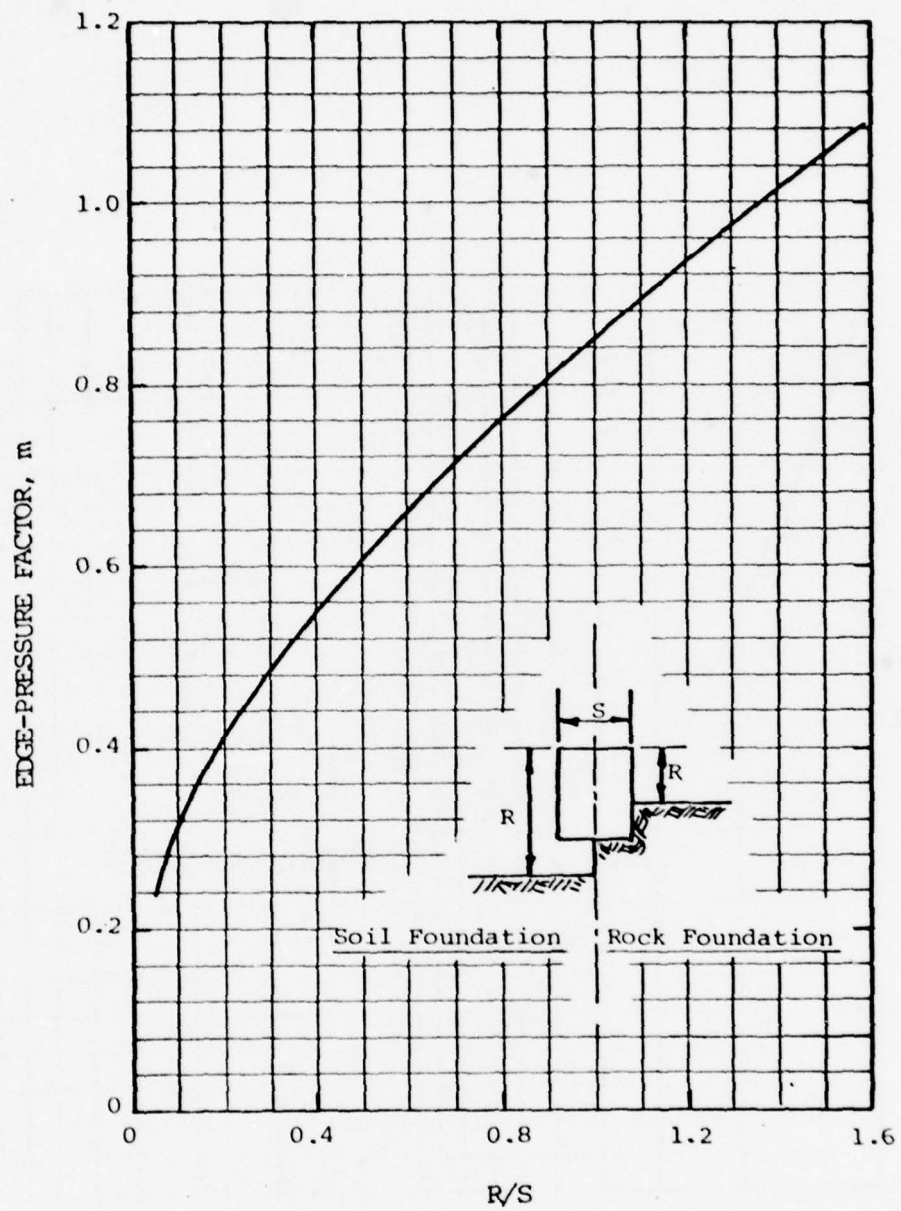


FIG. VI-6 EDGE-PRESSURE FACTOR FOR RECTANGULAR CONDUITS

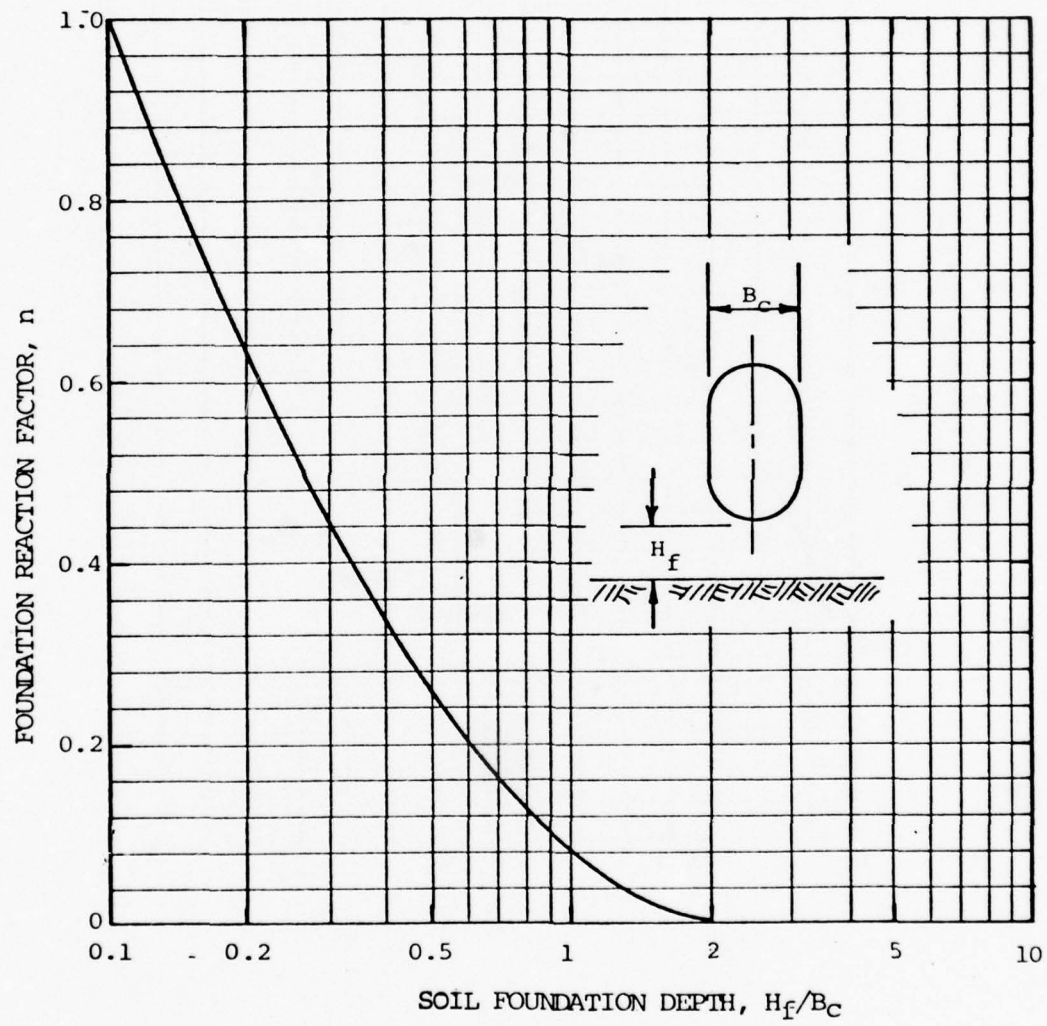


FIG. VI-7 FOUNDATION REACTION FACTOR FOR CONDUITS ON SOIL FOUNDATION

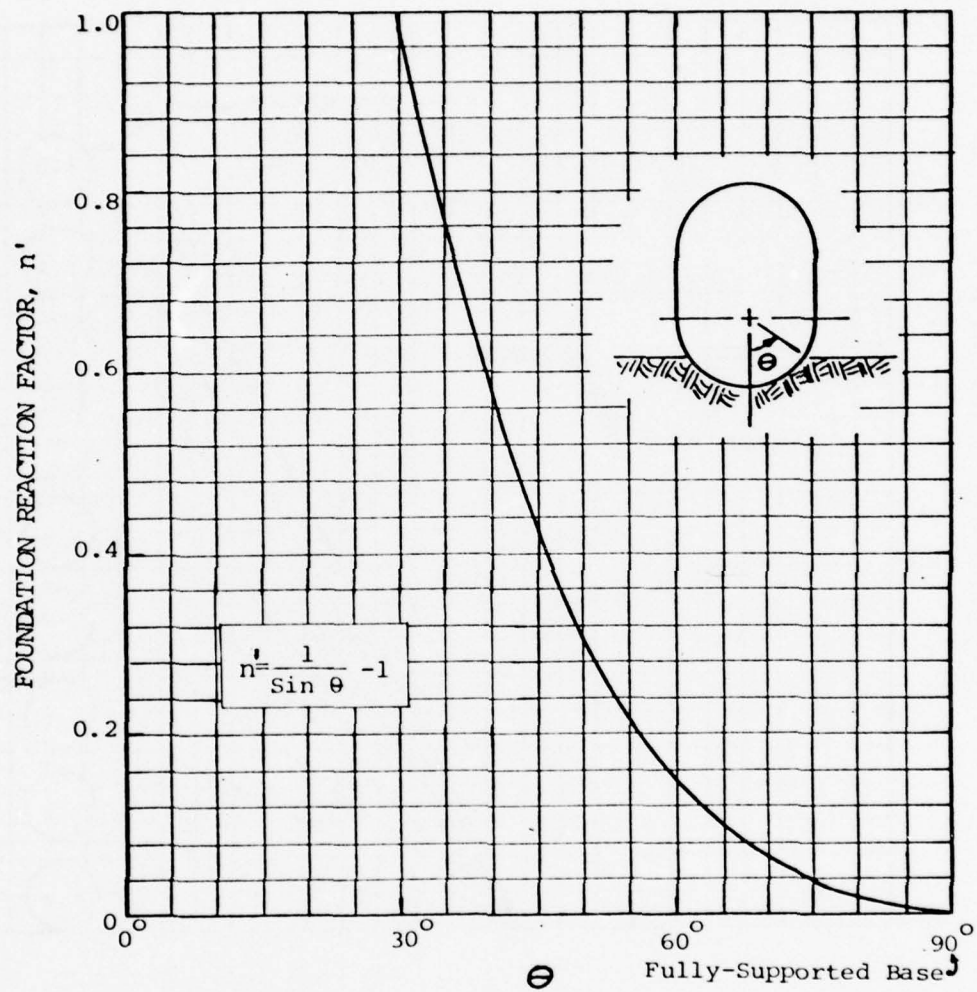


FIG. VI-8 FOUNDATION REACTION FACTOR FOR CIRCULAR AND OBLONG CONDUITS ON ROCK FOUNDATIONS

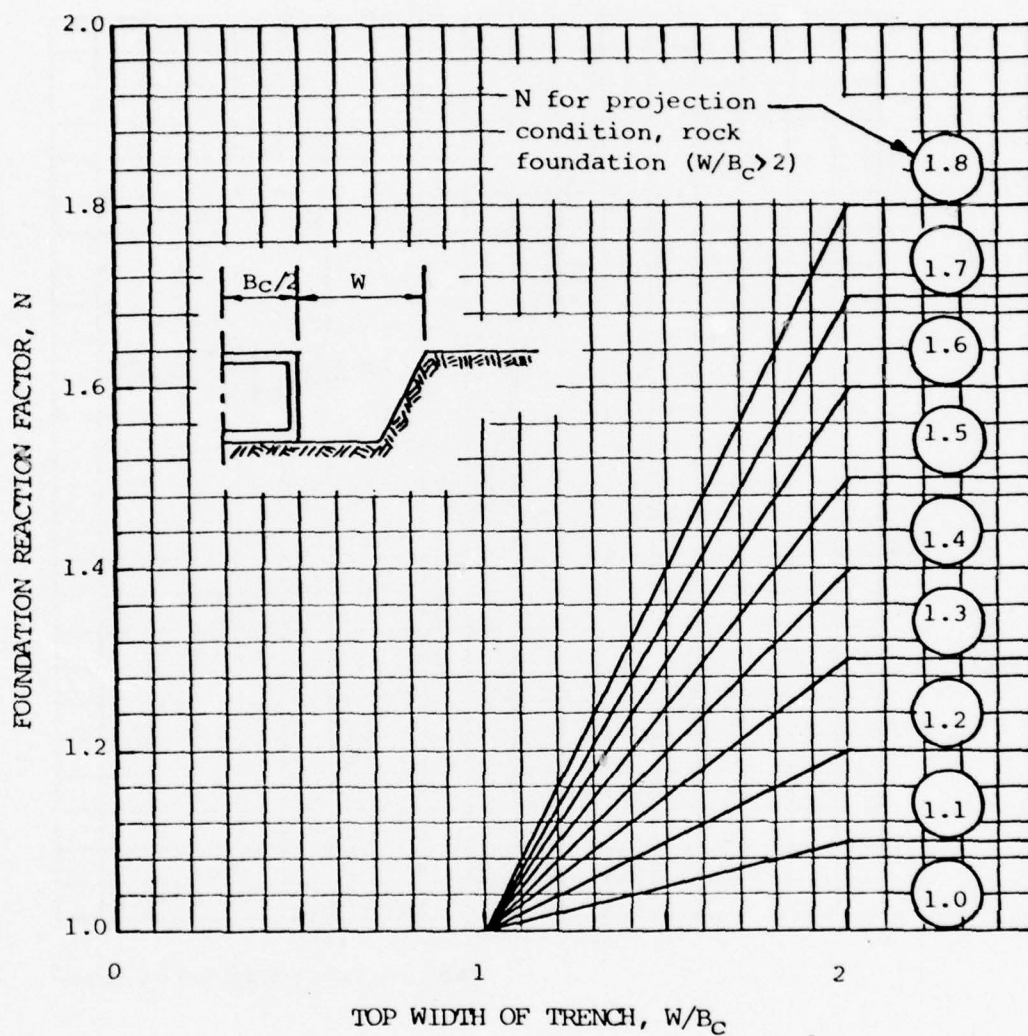


FIG. IV-9 CROWN-PRESSURE FACTOR FOR CONDUIT IN SHALLOW, ROCK TRENCH

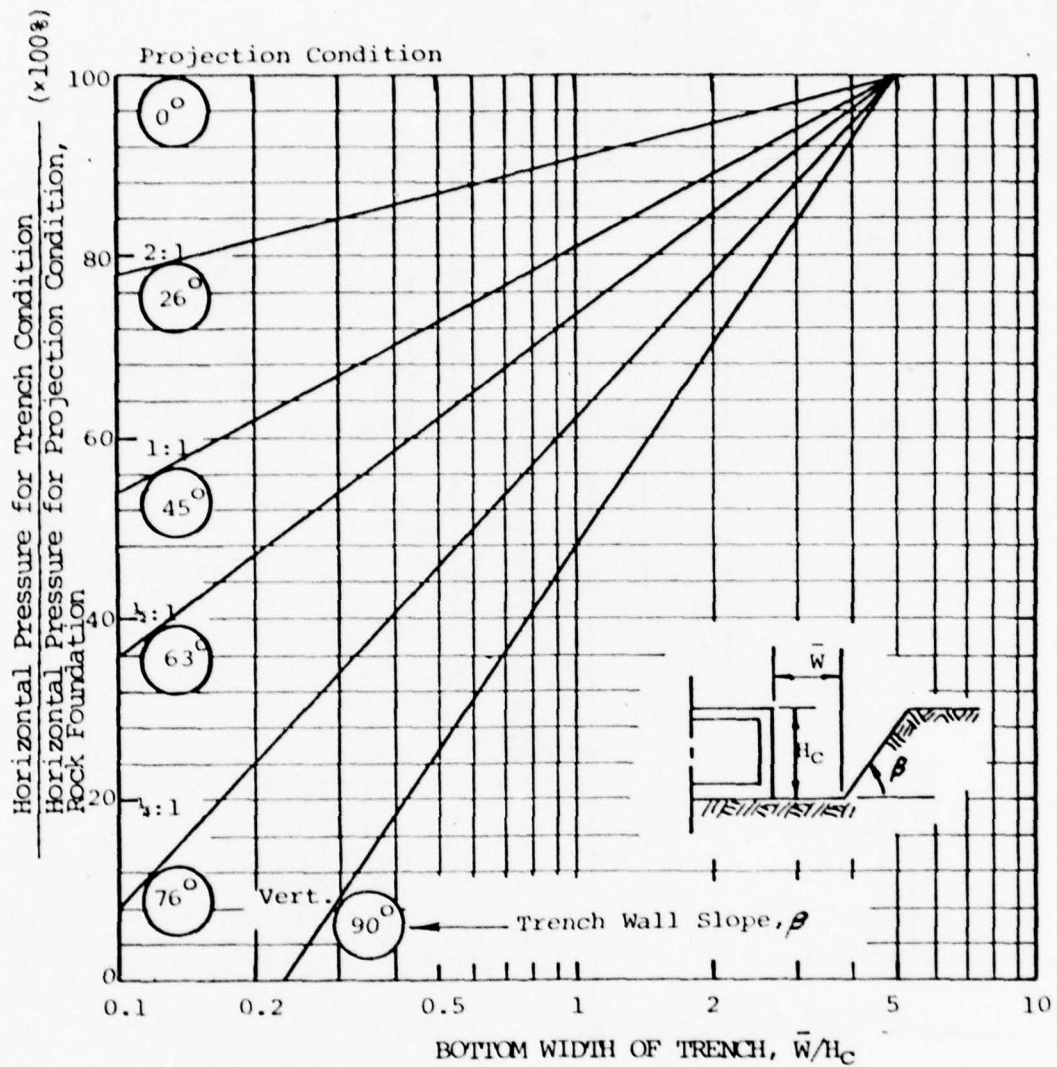


FIG. VI-10 HORIZONTAL PRESSURE FOR CONDUIT IN SHALLOW ROCK TRENCH

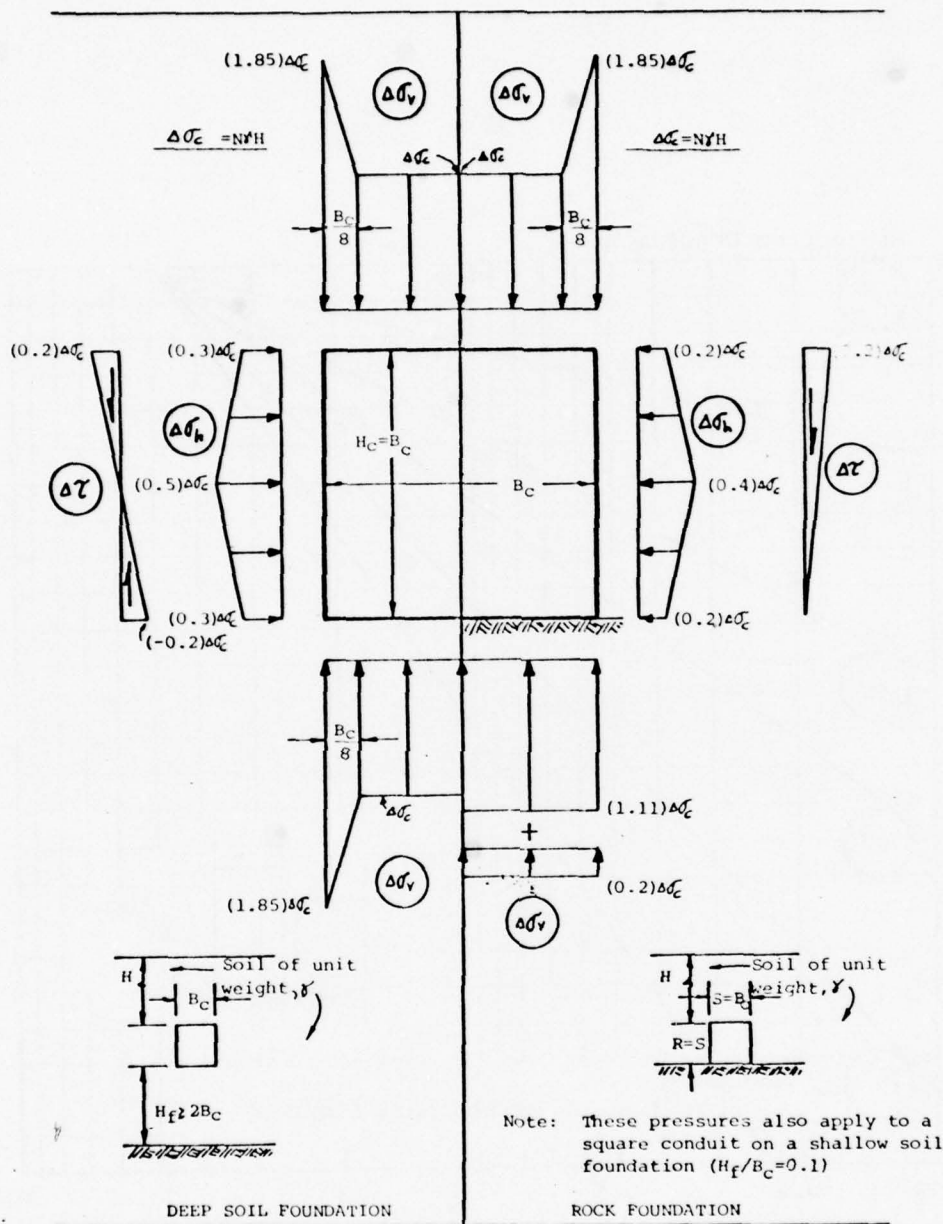


FIG. VI-11 EARTH PRESSURE DIAGRAMS FOR A SQUARE CONDUIT ON DEEP SOIL AND ROCK FOUNDATIONS

B. Simplified Procedures for Circular and Oblong Conduits

Structural analysis of rectangular conduits using the recommended earth pressure diagrams can be accomplished using conventional rigid frame analysis procedures by means of hand calculations or computer analyses. Because analyses of circular and oblong shapes are relatively complicated, even for simple rectangular and triangular load distributions, it is likely that the use of a computer would be necessary to limit the time required for design.

As an alternative to detailed analysis of each conduit, normalized moment, thrust and shear diagrams can be prepared for typical conduit shapes and placement conditions. These diagrams can be used to calculate moment, thrust and shear without performing structural analyses. A similar procedure is used in the present Corps of Engineers design manual.

To illustrate this procedure, moment, shear and thrust diagrams have been prepared for circular and oblong conduits (of H_c/B_c equal to 1.0, 1.25, and 1.5) founded on shallow and deep soil foundations (H_f/B_c equal to 0.1 and 2). The design earth pressure diagrams for the conduit shapes are given in Figs. VI-12 through VI-14. Corresponding moment, thrust and shear diagrams for the shallow foundation case are presented in Figs. VI-15 through VI-17; and for the deep foundation case in Figs. VI-18 through VI-20. In each of the diagrams, the moment, thrust or shear at each location on the conduit has been normalized in terms of the value at one of three particular points (crown, springline or quarterpoint). The values at the particular points are given in general terms as functions of Crown-Pressure Factor, N , conduit width, B_c , fill height, H , unit weight of fill material, γ , and coefficients of proportionality (C_M , C_T and C_V , respectively), as indicated by the formulas in each figure.

For the conduit shapes and foundation conditions encompassed by these figures, design can be accomplished by first determining the appropriate Crown-Pressure Factor from Figs. VI-3 through VI-5 as previously discussed. Design values of moment, thrust and shear can then be obtained from the normalized diagrams. Values for intermediate height-to-width ratios could be determined by interpolation.

The design figures were prepared by analyzing idealized conduit shapes with a simple structural analysis computer program (see Appendix A). In the computations the conduits were represented by beam elements having zero wall thickness and the earth pressures acted directly upon the centroidal axis of the conduit. The walls of actual reinforced-concrete conduits have appreciable thickness. Therefore, in applying the design figures, the conduit width used in the calculations should be taken as the outside width. This should be a slightly conservative approach.

C. Finite-Element Analysis

The far-ranging capabilities of the finite-element method should be considered when designing conduits which are unusual with regard to shape, placement conditions, foundation support or backfill materials.

A typical application would be in the design of a conduit beneath a high

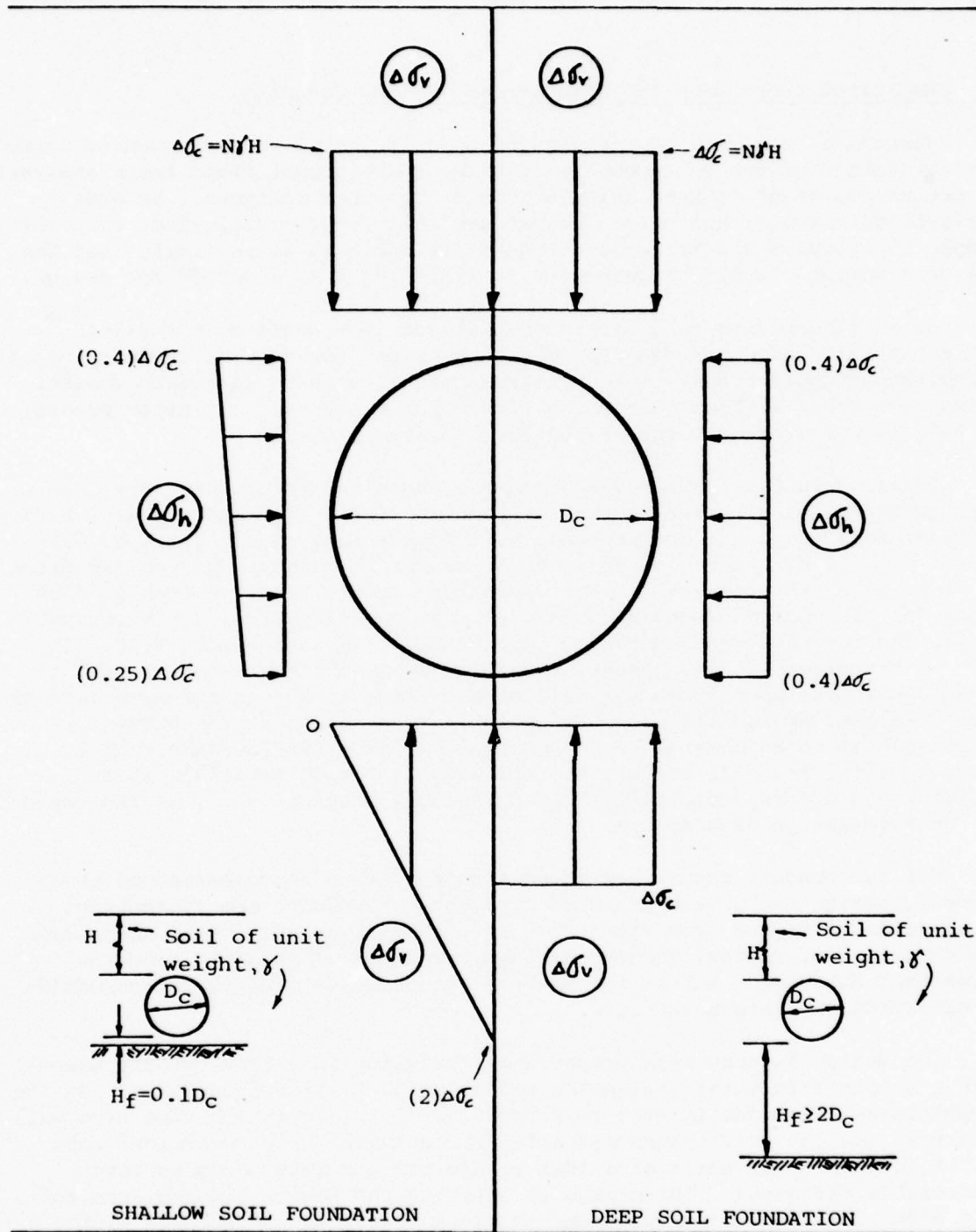


FIG. VI-12 EARTH PRESSURE DIAGRAMS FOR A CIRCULAR CONDUIT ON SHALLOW AND DEEP SOIL FOUNDATIONS

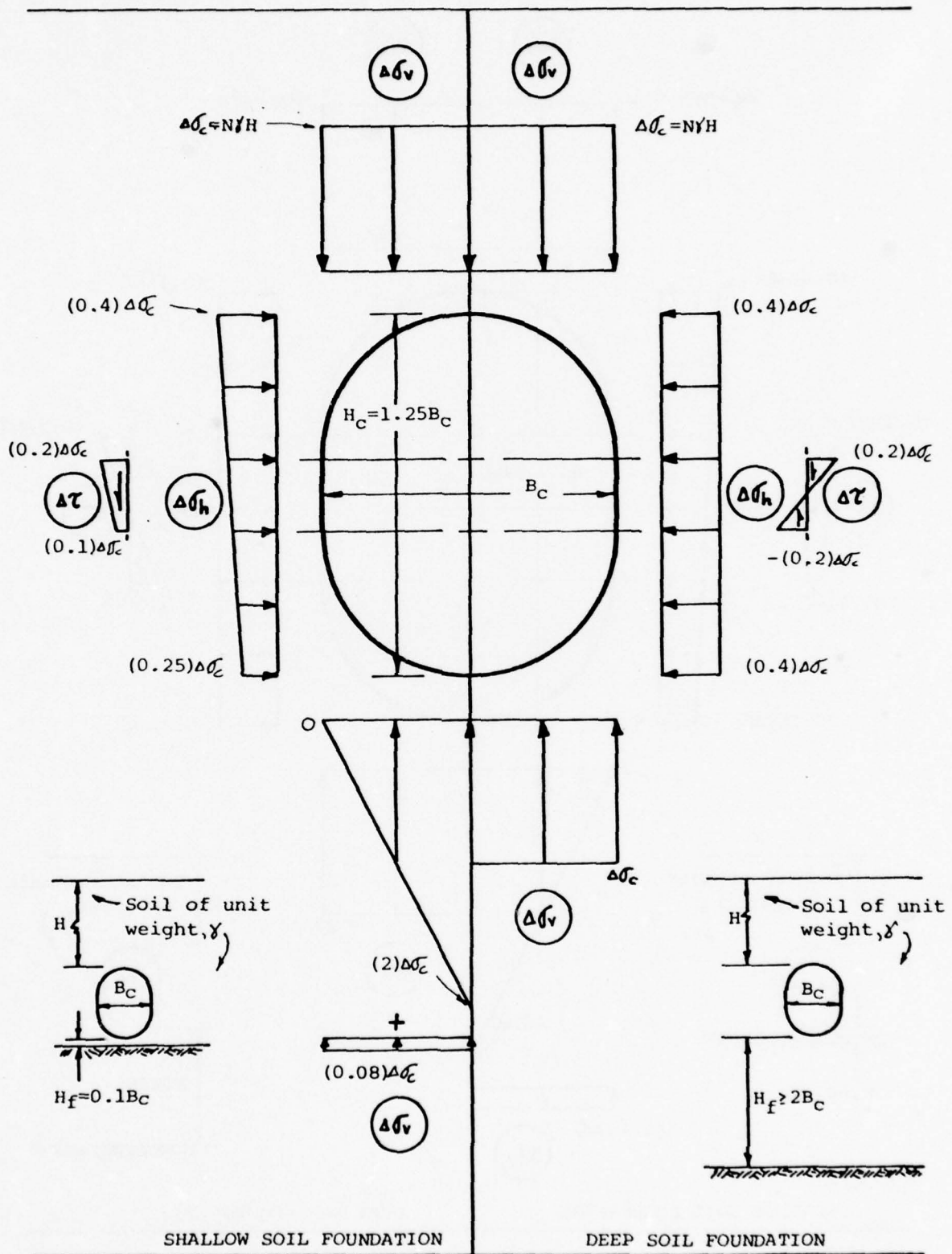


FIG. VI-13 EARTH-PRESSURE DIAGRAMS FOR OBLONG CONDUIT ($H_C/B_C=1.25$) ON SHALLOW AND DEEP SOIL FOUNDATIONS

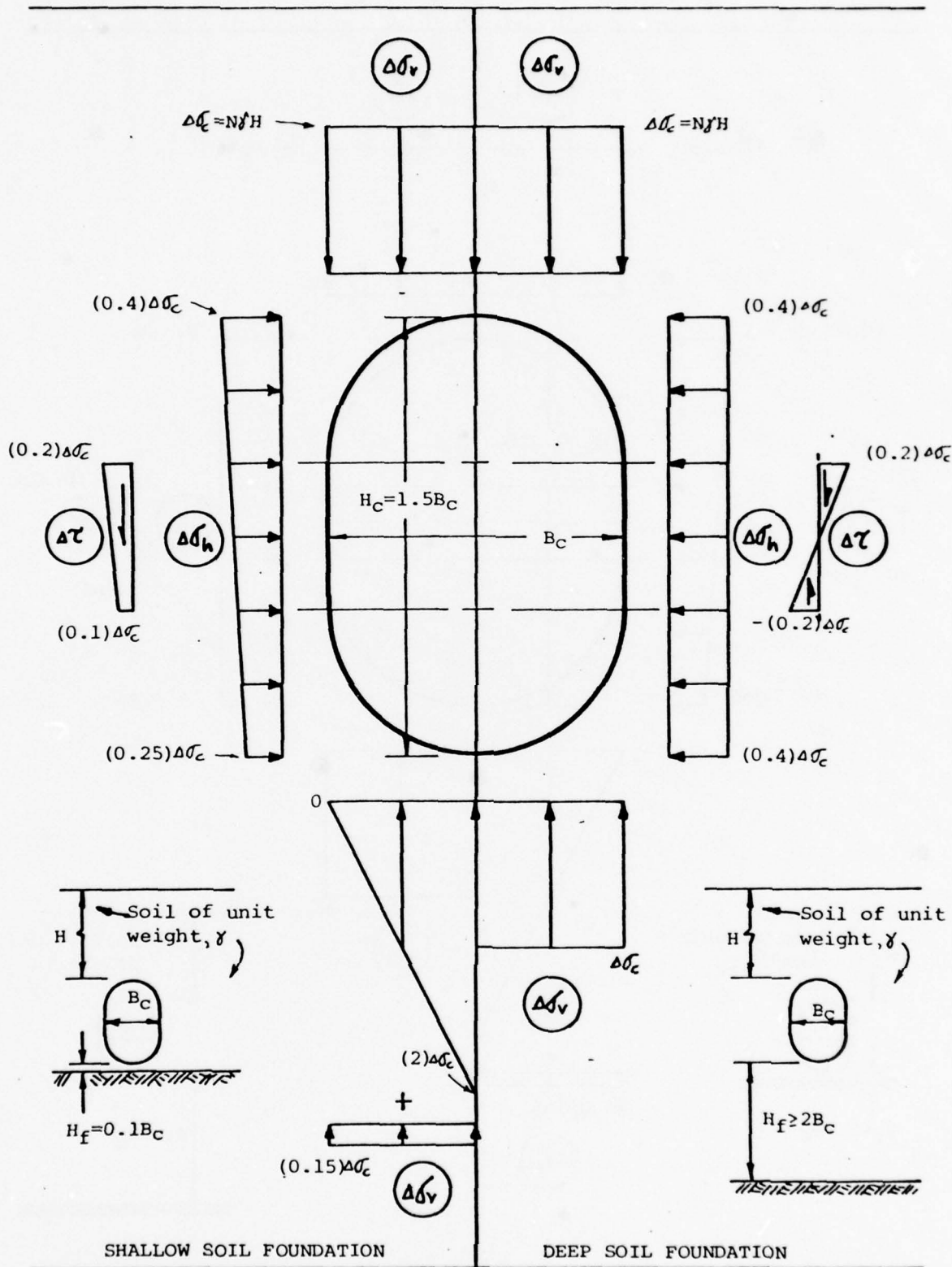


FIG. VI-14 EARTH-PRESSURE DIAGRAMS FOR OBLONG CONDUIT ($H_C/B_C = 1.5$) ON SHALLOW AND DEEP SOIL FOUNDATIONS

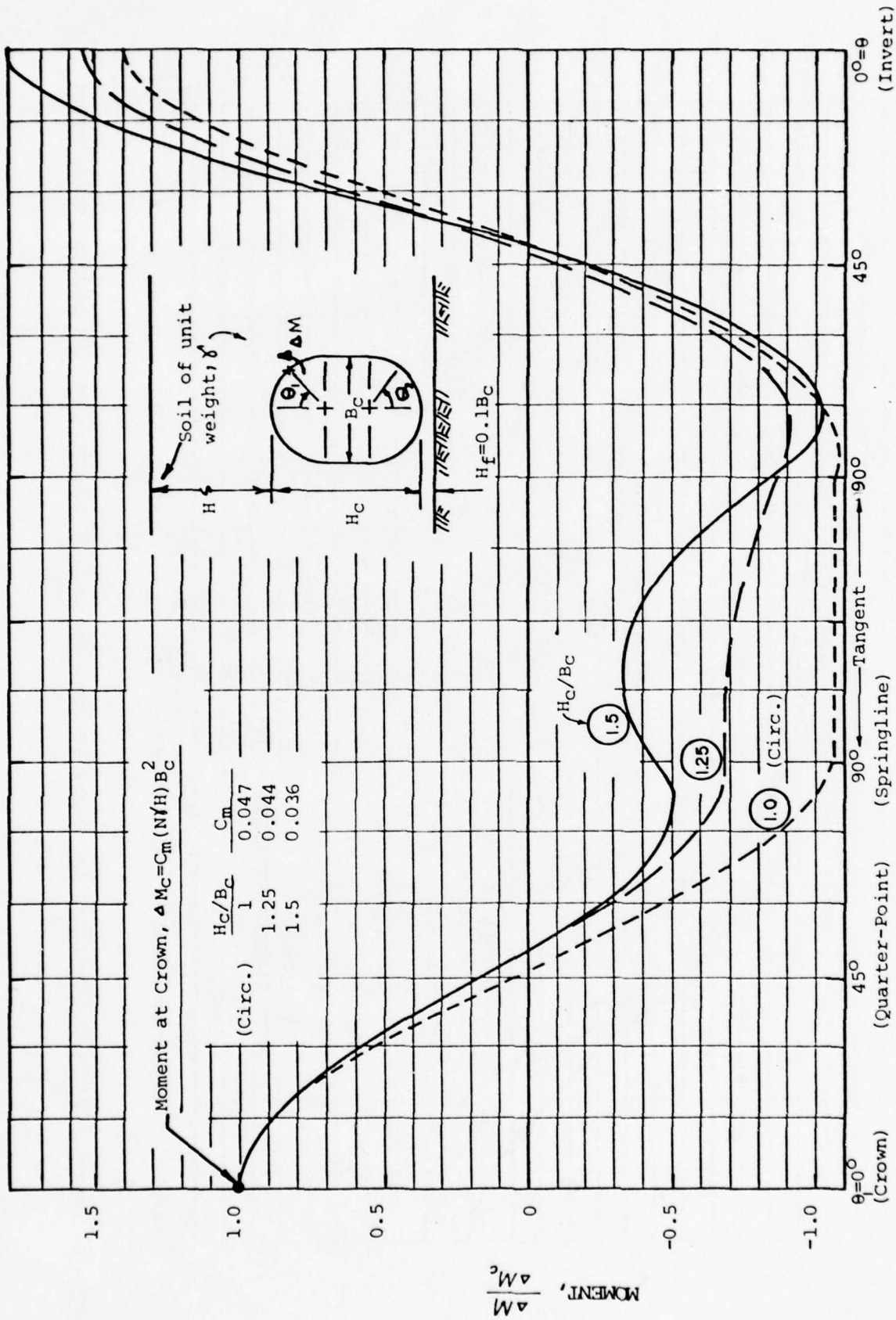


FIG. VI-15 MOMENT DIAGRAMS FOR CIRCULAR AND OBLONG CONDUITS ON SHALLOW SOIL FOUNDATION, EMBANKMENT CONDITION

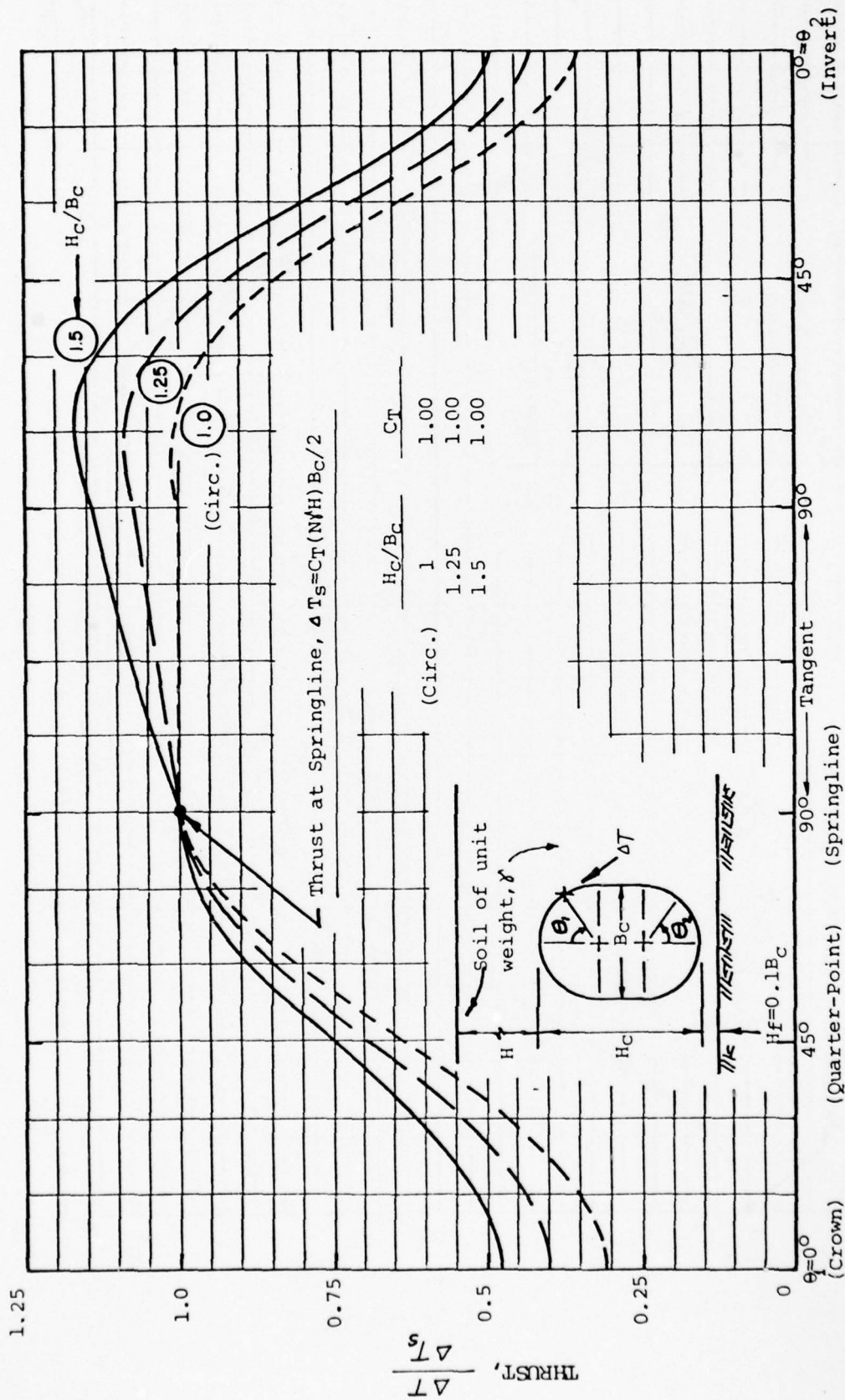


FIG. VI-16 THRUST DIAGRAMS FOR CIRCULAR AND OBLONG CONDUITS ON SHALLOW SOIL FOUNDATION, EMBANKMENT CONDITION

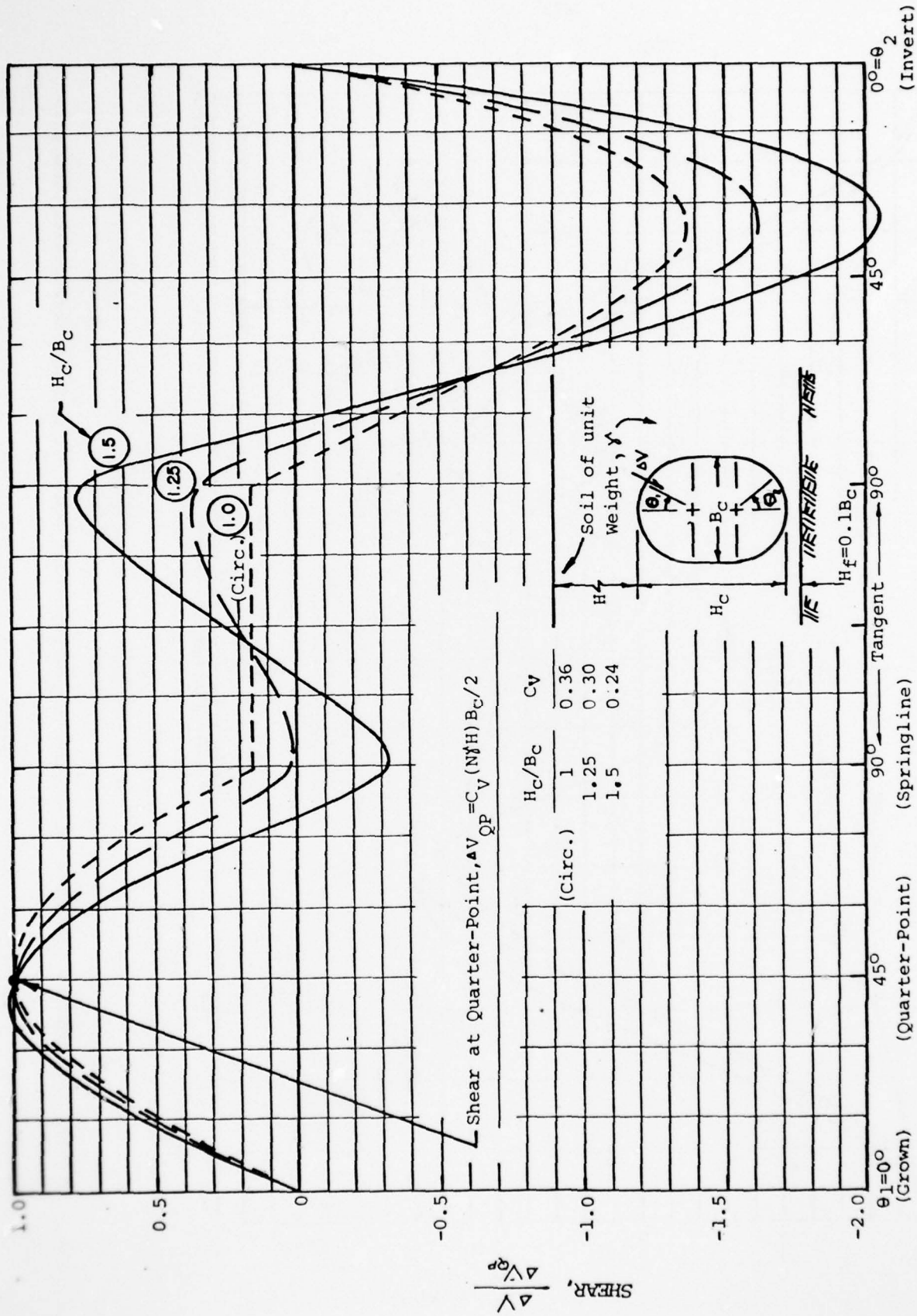


FIG. VI-17 SHEAR DIAGRAMS FOR CIRCULAR AND OBLONG CONDUITS ON SHALLOW SOIL FOUNDATION, EMBANKMENT CONDITION

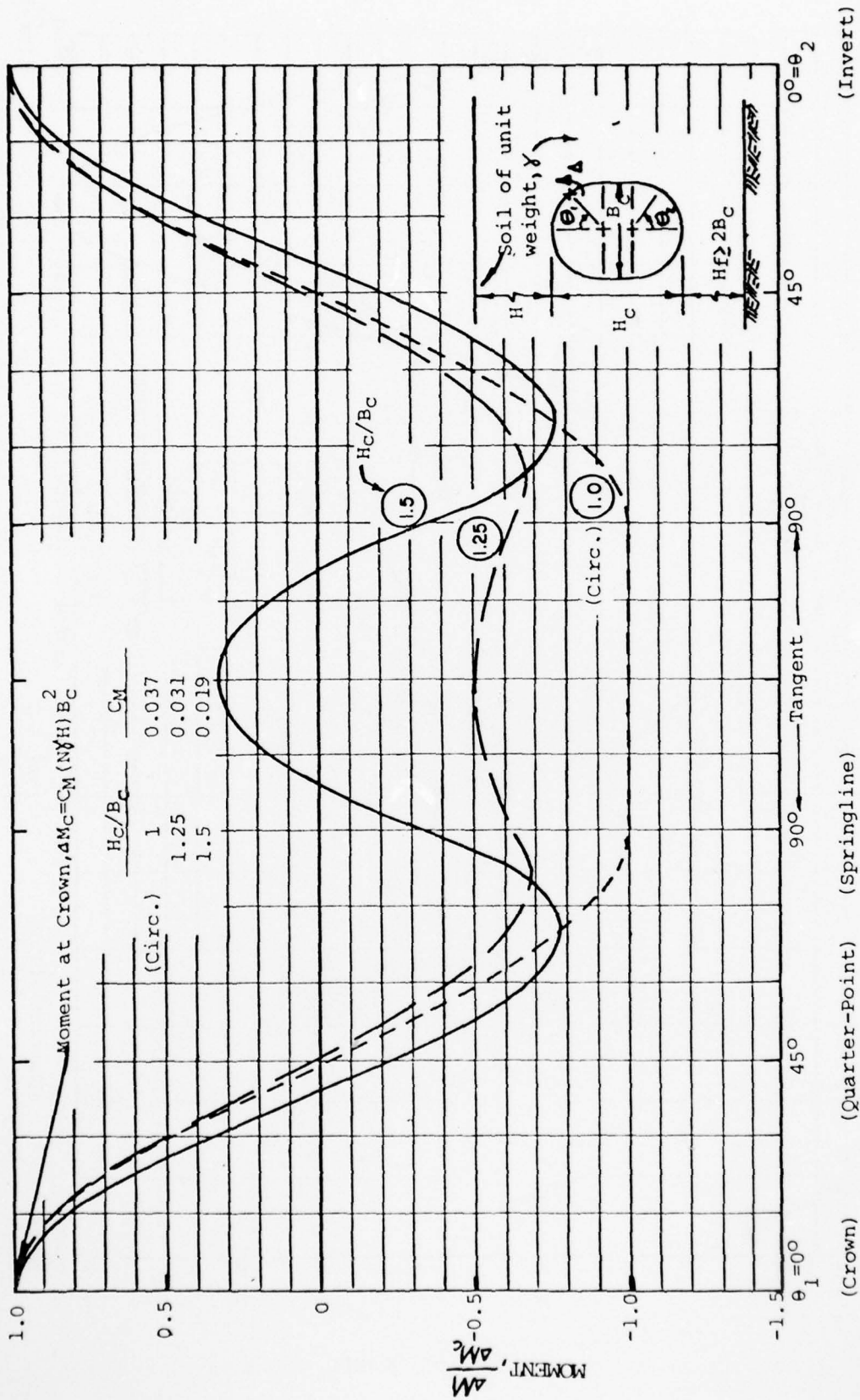


FIG. VI-18 MOMENT DIAGRAMS FOR CIRCULAR AND OBLONG CONDUITS ON DEEP SOIL FOUNDATION, EMBANKMENT CONDITION

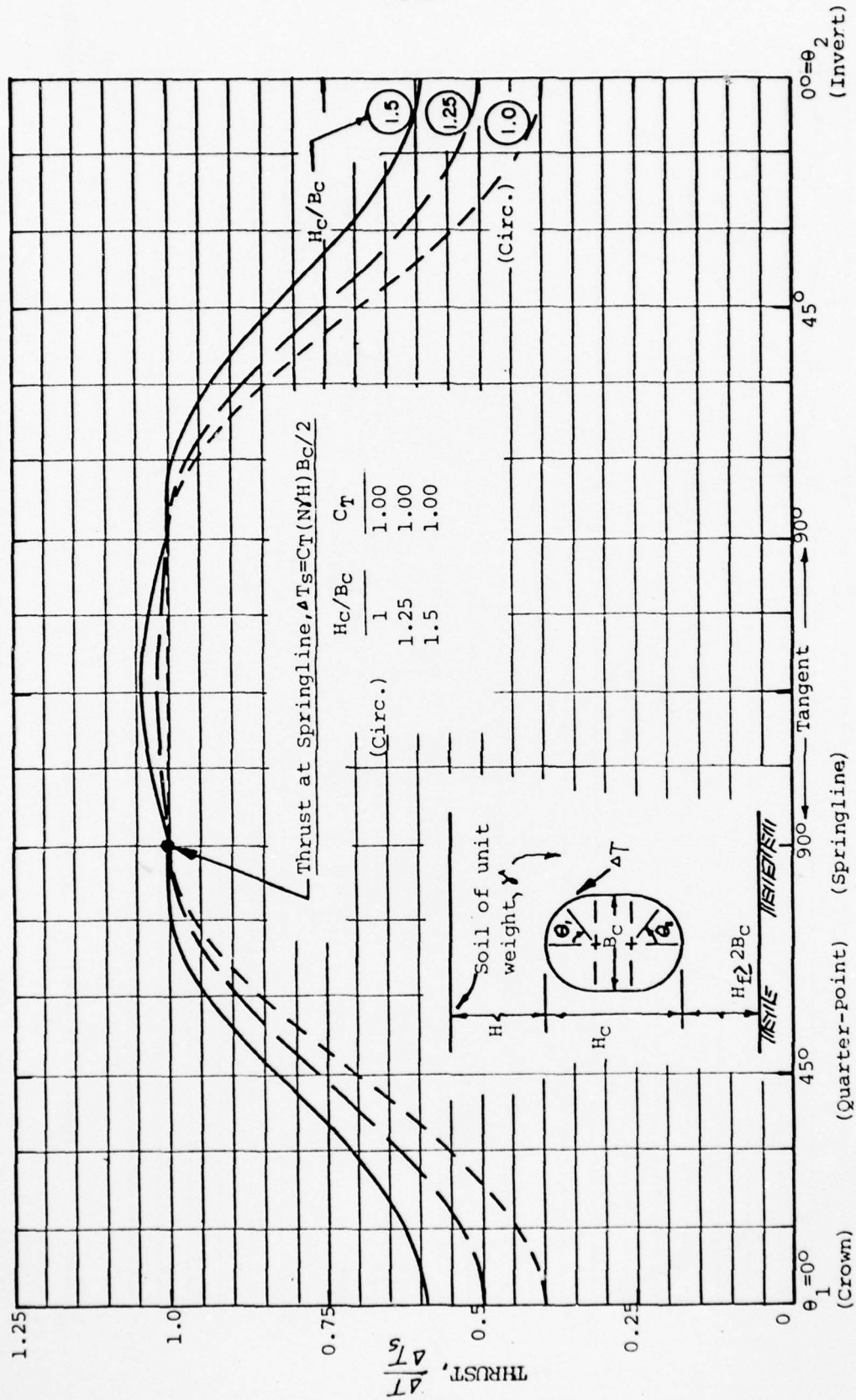


FIG. VI-19 THRUST DIAGRAMS FOR CIRCULAR AND OBLONG CONDUITS ON DEEP SOIL FOUNDATION, EMBANKMENT CONDITION

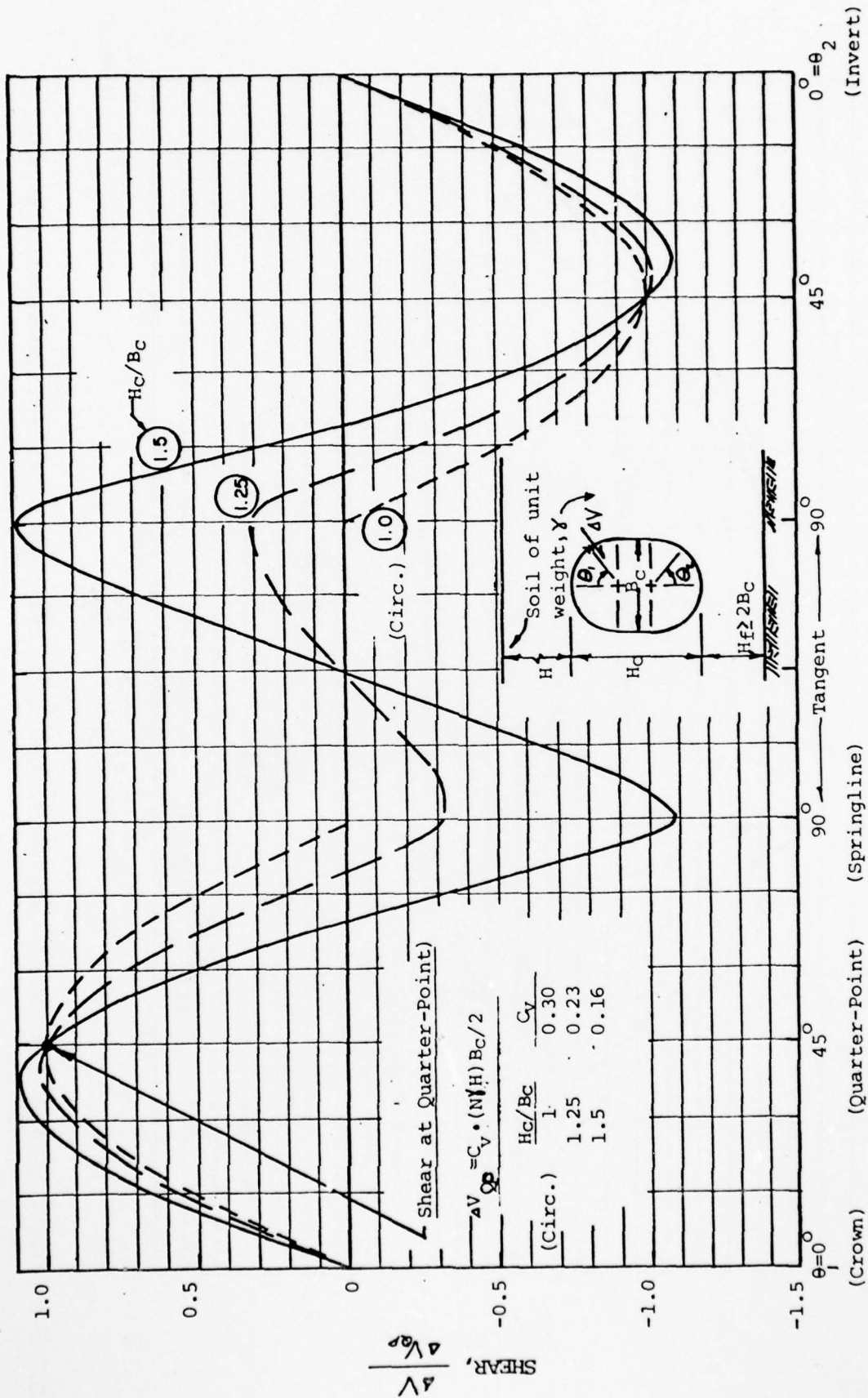


FIG. VI- 20 SHEAR DIAGRAMS FOR CIRCULAR AND OBLONG ON DEEP SOIL FOUNDATIONS, EMBANKMENT CONDITION

zoned embankment-dam. The redistribution of stresses in and near the core of the dam could be analyzed to determine the effective overburden pressures along the length of the conduit. Because finite-element analyses of high, embankment sections can be useful for studying other aspects of dam behavior as well, the information applicable to conduit design can be obtained from the results of studies performed for other purposes.

Finite-element analyses of transverse sections of a conduit can provide detailed information about the magnitude and distribution of earth pressures that will act upon the conduit as well as the stress redistribution that will occur in the adjacent embankment. The latter information can be used to evaluate the potential for hydraulic fracturing around the conduit.

Finite-element analyses can also be of value in predicting the vertical and horizontal displacements of a conduit beneath an embankment on a compressible foundation (see Chapter V).

CHAPTER VIIANALYSIS OF CORPS OF ENGINEERSCASE HISTORIES-CONDUITS

In this chapter, earth pressures measured on conduits beneath four embankment dams are compared with values predicted using the proposed procedures described in Chapter VI. The purpose of the comparisons is to evaluate the suitability of the proposed design methods, considering the variations from ideal conditions which always accompany real design problems.

The data from the four projects were supplied by the responsible districts of the Corps of Engineers. Pertinent source documents are listed in the bibliography.

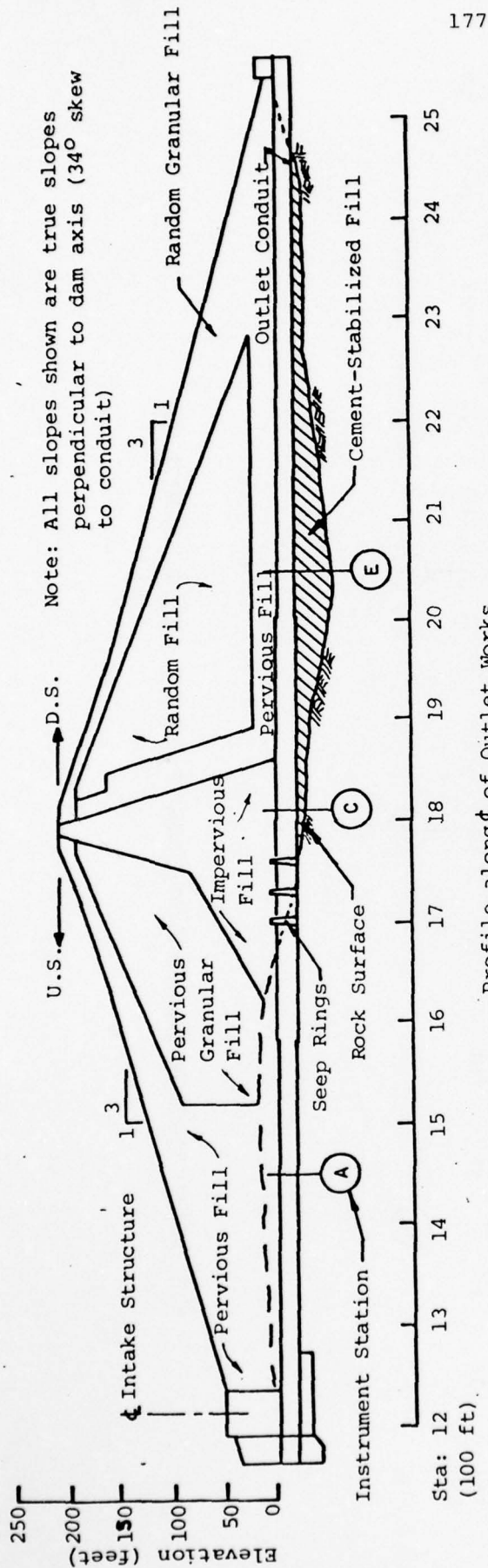
A. Cochiti Dam

Cochiti Dam is located in north-central New Mexico on the Rio Grande River. The 200-foot-high zoned embankment was completed in 1975 by the Albuquerque District of the Corps of Engineers. The outlet works for the project includes a triple-cell, reinforced-concrete conduit which varies in width from 32 to 38 feet and in height from 18 to 21 feet as shown in Fig. VII-1. A profile of the dam along the centerline of the outlet works is also given in the figure. Note that the conduit orientation is at a skew of about 34° to the axis of the dam. Instrument stations at which earth pressures and pore water pressures were measured are indicated on the profile.

A finite-element analysis of the dam section along the outlet works centerline was performed for this study to evaluate the possible stress redistributions which could have occurred adjacent to the core of the dam. Details of the analysis are given in Appendix A. Because of the skew of the section to the dam axis, the finite-element results, which assumed plane-strain conditions, must be considered approximate. The computed vertical pressures at the end of construction along the level of the top of the conduit are shown in Fig. VII-2. At the instrument stations within the upstream and downstream shells, there are no significant differences between the calculated vertical pressures and the overburden pressure; but at the instrument station in the core, the calculated pressures are only about three-fourths of the overburden pressure.

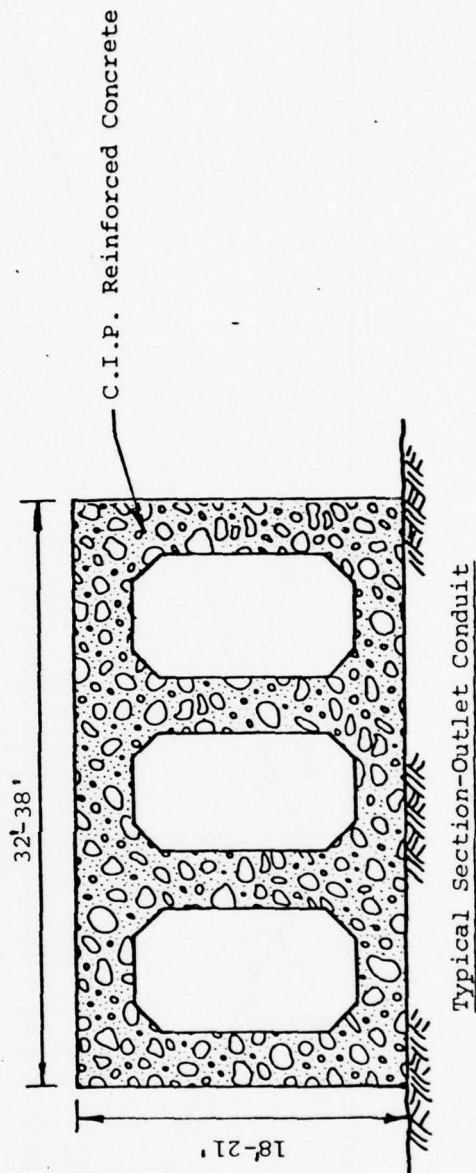
Earth pressures measured on the conduit at each of the instrument stations are summarized in Figs. VII-3 through VII-5. Note that pressures are plotted as a function of the height of fill over the conduit until the maximum cover is achieved. Thereafter, the data are plotted as a function of time. In general the pressures increased in approximate proportion to the height of fill. For comparison, the theoretical overburden pressures are included in the figures. For the period covered by the data (about two years), there have been few significant changes in earth pressures since construction was completed.

Several of the pressure data are noted with a question mark on the



177

Profile along 1/4 of Outlet Works



Typical Section-Outlet Conduit

FIG. VII-1 OUTLET WORKS, COCHITI DAM

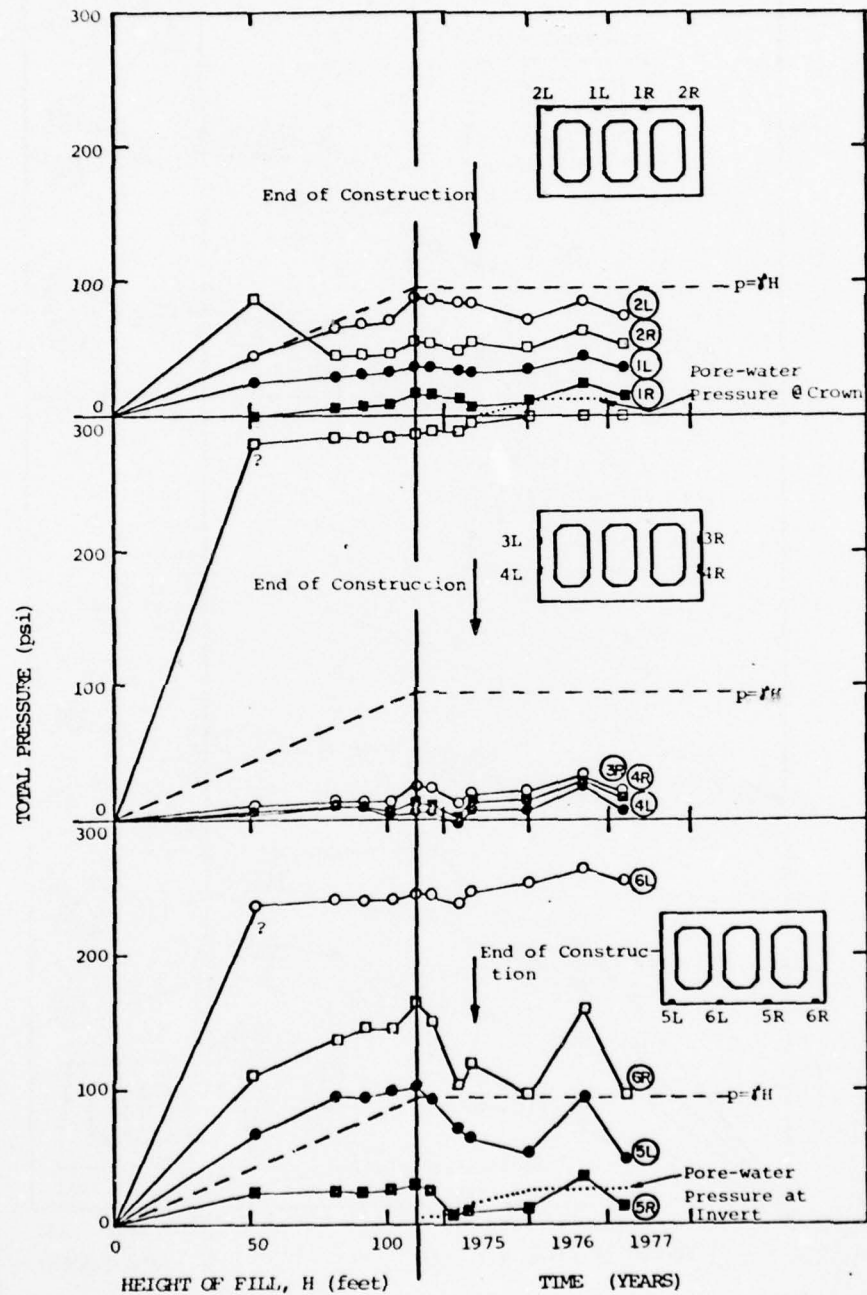


FIG. VII-3 MEASURED PRESSURES AT INSTRUMENT STATION A, COCHITI DAM

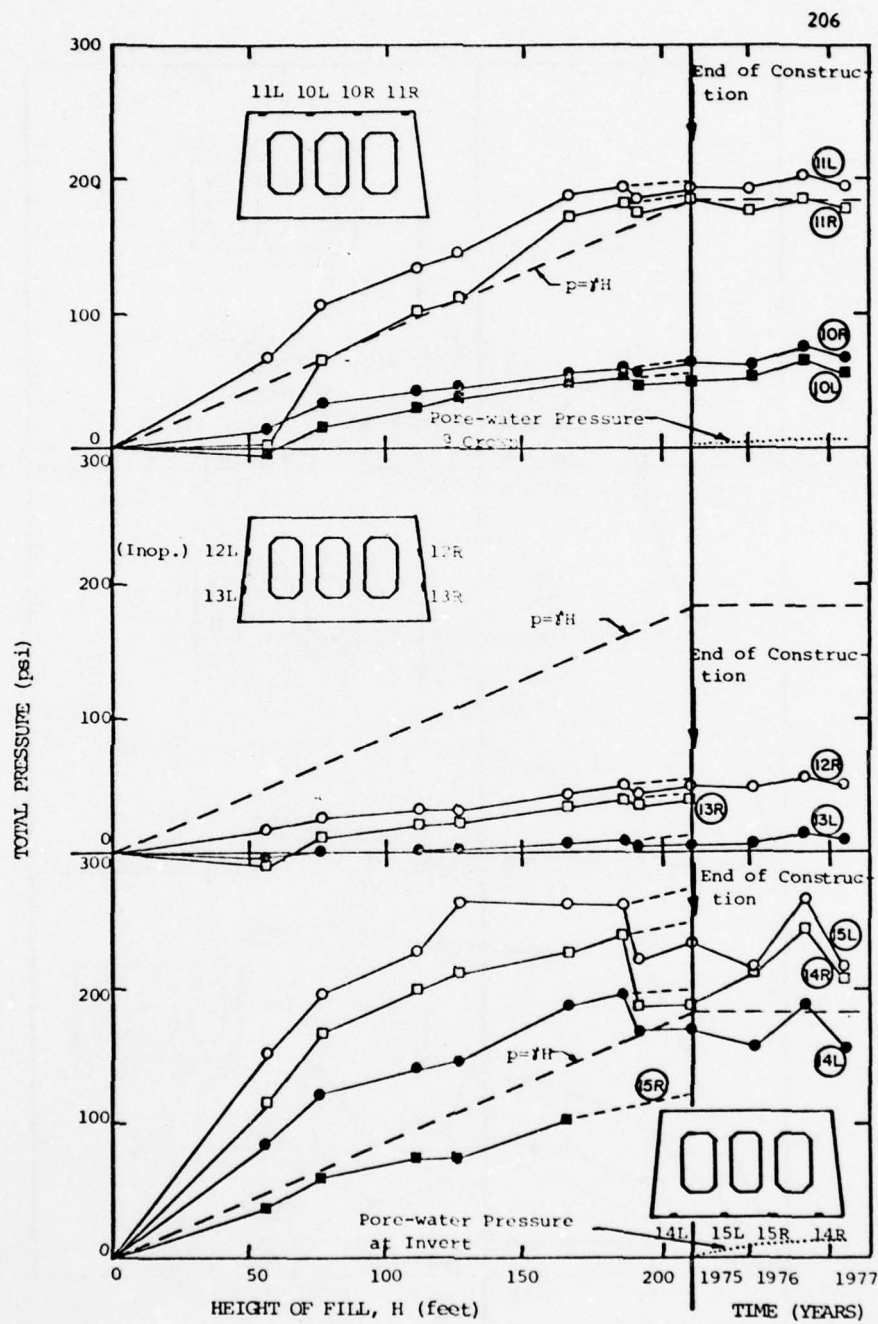


FIG. VII-4 MEASURED PRESSURES AT INSTRUMENT STATION C, COCHITI DAM

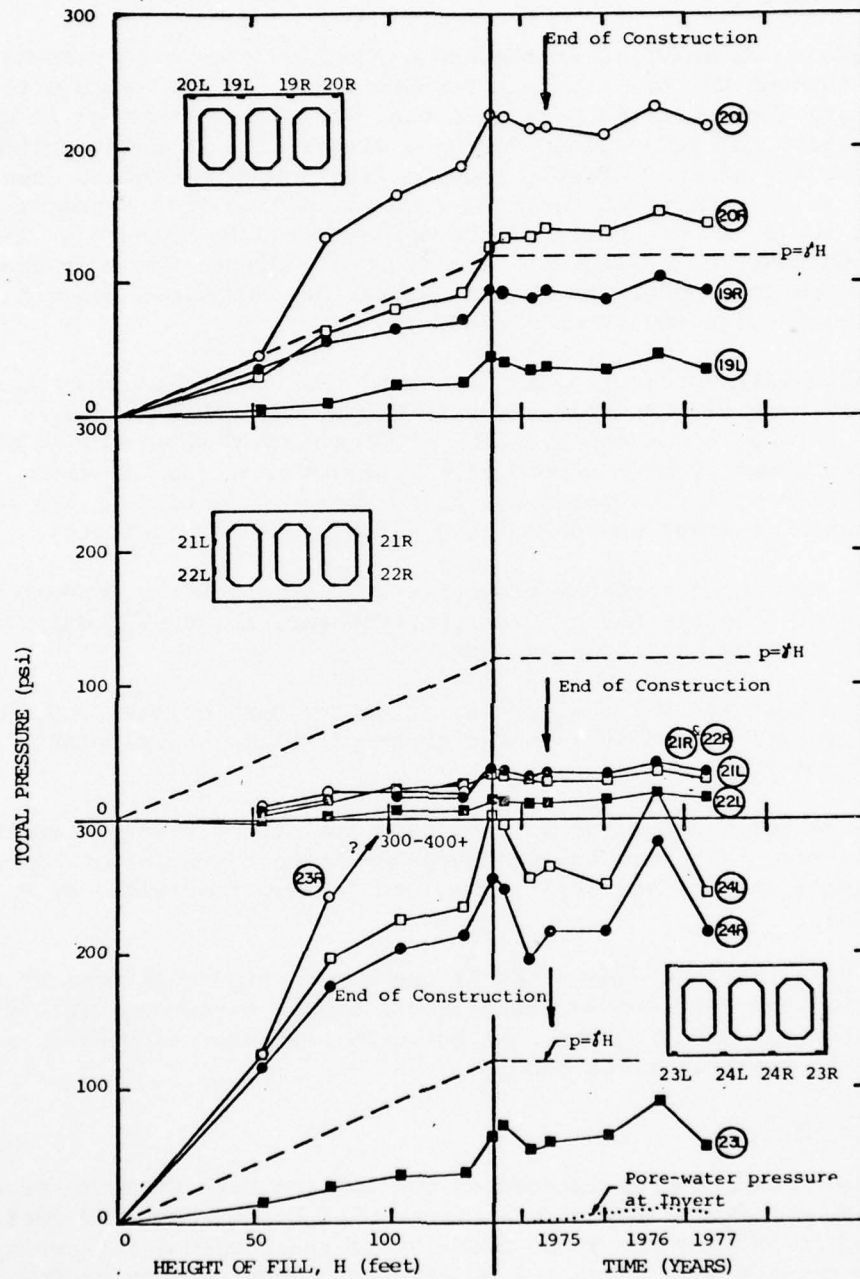


FIG. VII-5 MEASURED PRESSURES AT INSTRUMENT STATION E, COCHITI DAM

figures to indicate that the measurements are suspect for various reasons. For instance, at Station A pressure cells 3L and 6L indicated very high pressures at the first readings (height of fill equal to 50 feet) but little change thereafter.

Earth pressures measured at the end of construction are presented in Figs. VII-6 through VII-8. The data for Station C, located within the core of the dam, are the estimated pressures that would have occurred if no stress relaxation had taken place during a winter lull in construction when the embankment was about 25 feet below its final crest elevation (see Fig. VII-4). The relaxation which could have resulted from load transfer between the core and the adjacent shells of the dam amounted to as much as 15 percent of the measured pressures. The figures indicate the pressures that were measured on the conduit as well as at various locations beneath the embankment in the vicinity of the conduit.

Calculated earth pressures, as determined by the design procedures proposed in Chapter VI, are also shown in Figs. VII-6 through VII-8. The calculations were based on the probable effective overburden pressures (Fig. VII-2) and the geometry of the conduit installation at each instrument station. Details of the calculations are given in Appendix B. The comparisons between measured and calculated earth pressures indicate:

1. The calculated vertical pressures at the top of the conduit are greater than the measured values; however, increased edge pressures are shown by both sets of data.
2. The calculated vertical pressures on the base of the conduit are in general agreement with the measured values, particularly for Section C.
3. The calculated horizontal pressures are slightly more than those measured. The very low pressures measured on the sides of the conduit in a trench (Station A) are in agreement with the calculated values.

Considering that the geometries of the conduit installations at the instrument stations vary considerably from a simple embankment (projection) condition, it is encouraging that the agreement between calculated and measured earth pressures is so good.

B. DeQueen Lake Dam

The DeQueen Lake Dam is located on the Rolling Fork River in Arkansas. It is a zoned, embankment-dam with a maximum height of about 160 feet. It was completed in 1976 by the Tulsa District of the Corps of Engineers. The outlet works consist of a 12-foot I.D. circular conduit, constructed of cast-in-place, reinforced concrete. A 42-inch I.D. pipe was encased in concrete adjacent to the conduit as shown in Fig. VII-9. The figure also shows a profile through the dam along the centerline of the outlet works. The location of three instrument stations at which earth pressures were measured are shown on the profile.

The pressures measured on the conduit at each of the instrument stations

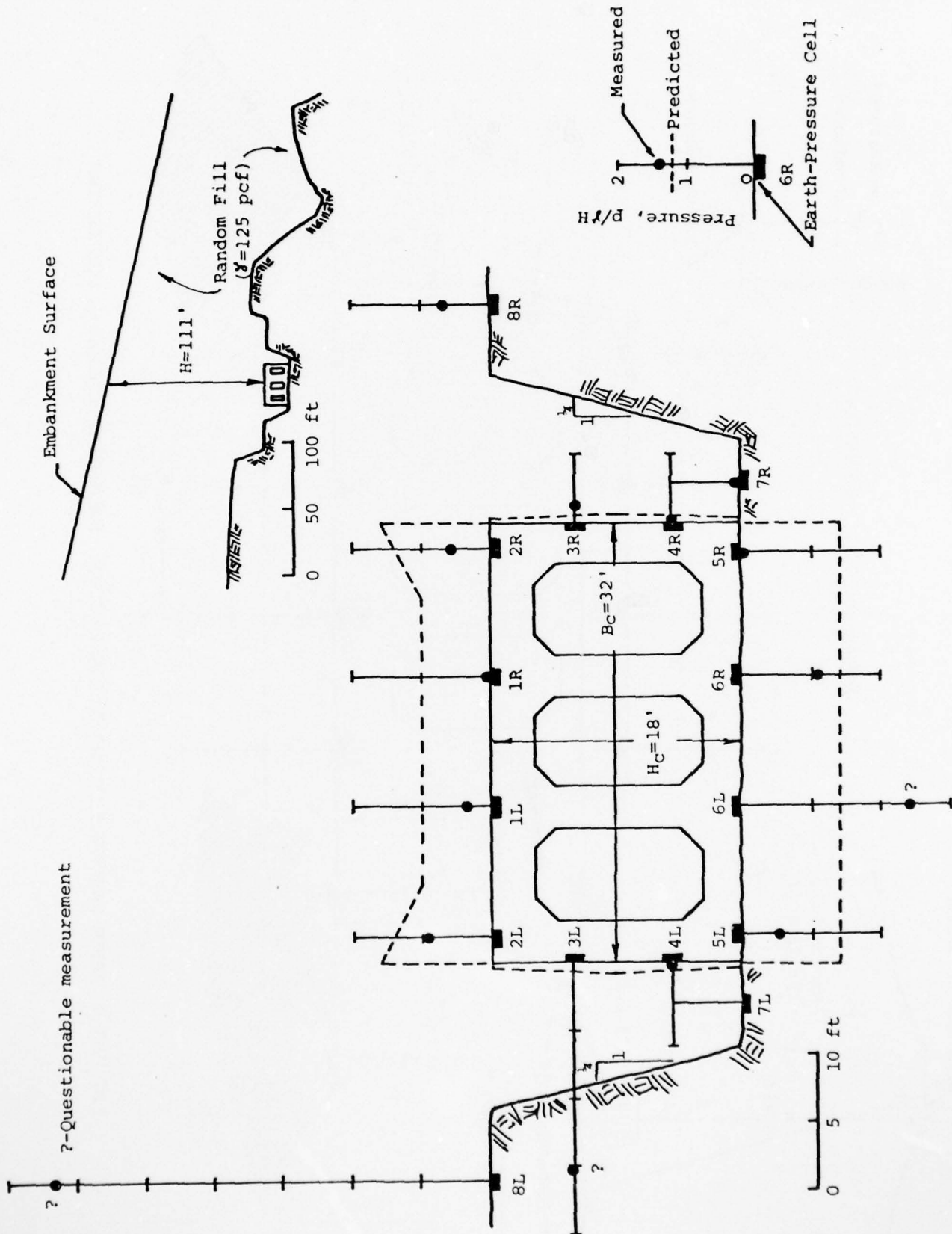


FIG. VII-6 EARTH PRESSURES AT END OF CONSTRUCTION, INSTRUMENT STATION A, COCHITI DAM

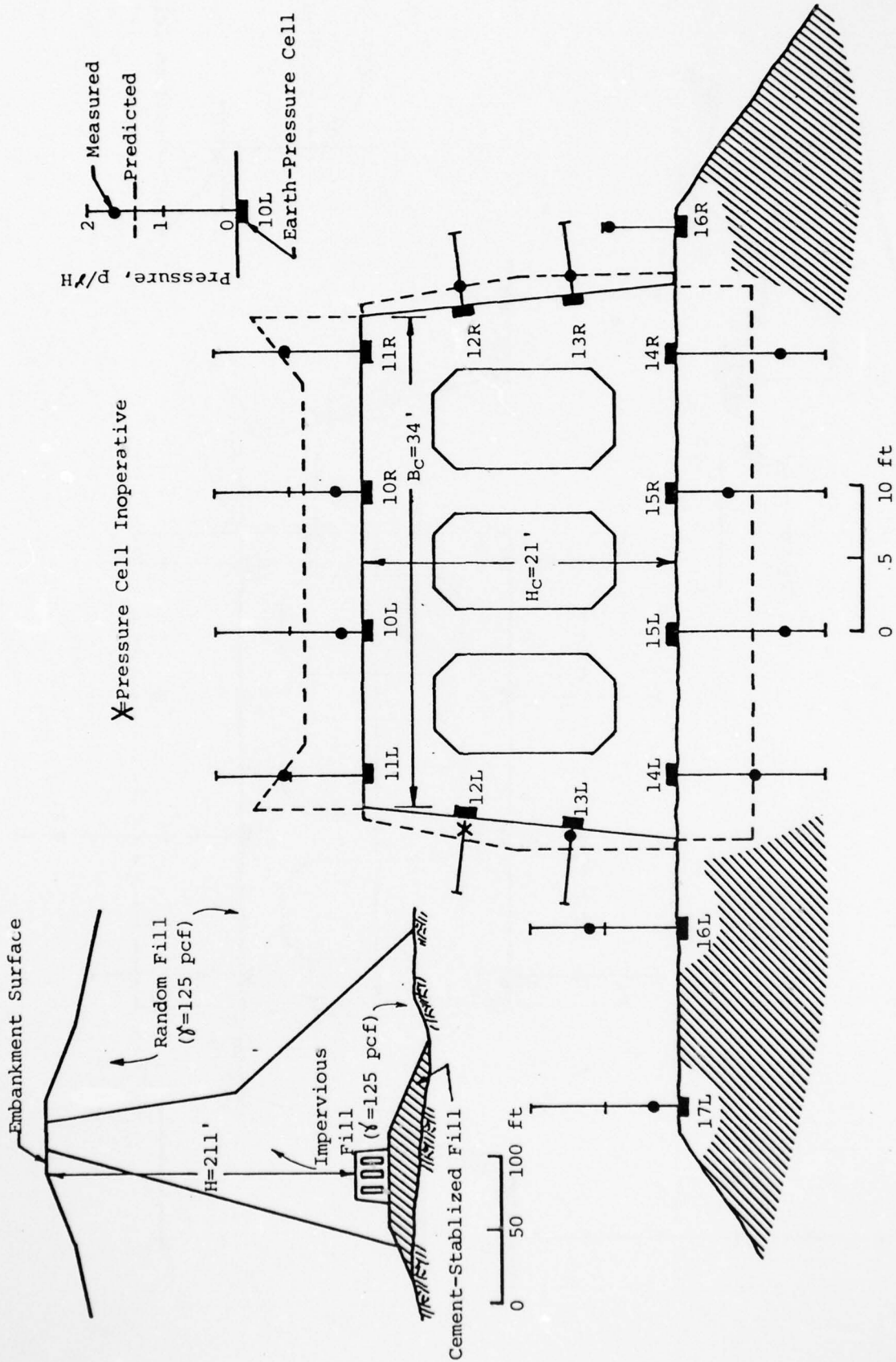


FIG. VII-7 EARTH PRESSURES AT END OF CONSTRUCTION, INSTRUMENT STATION C, COCHITI DAM

AD-A064 169

CALIFORNIA UNIV BERKELEY GEOTECHNICAL ENGINEERING
EARTH PRESSURES ON CONDUITS AND RETAINING WALLS. (U)
SEP 78 D W QUIGLEY, J M DUNCAN

F/G 13/2

DACW39-76-C-0035

NL

UNCLASSIFIED

UCB/GT/78-06

3 OF 4
AD
A064169





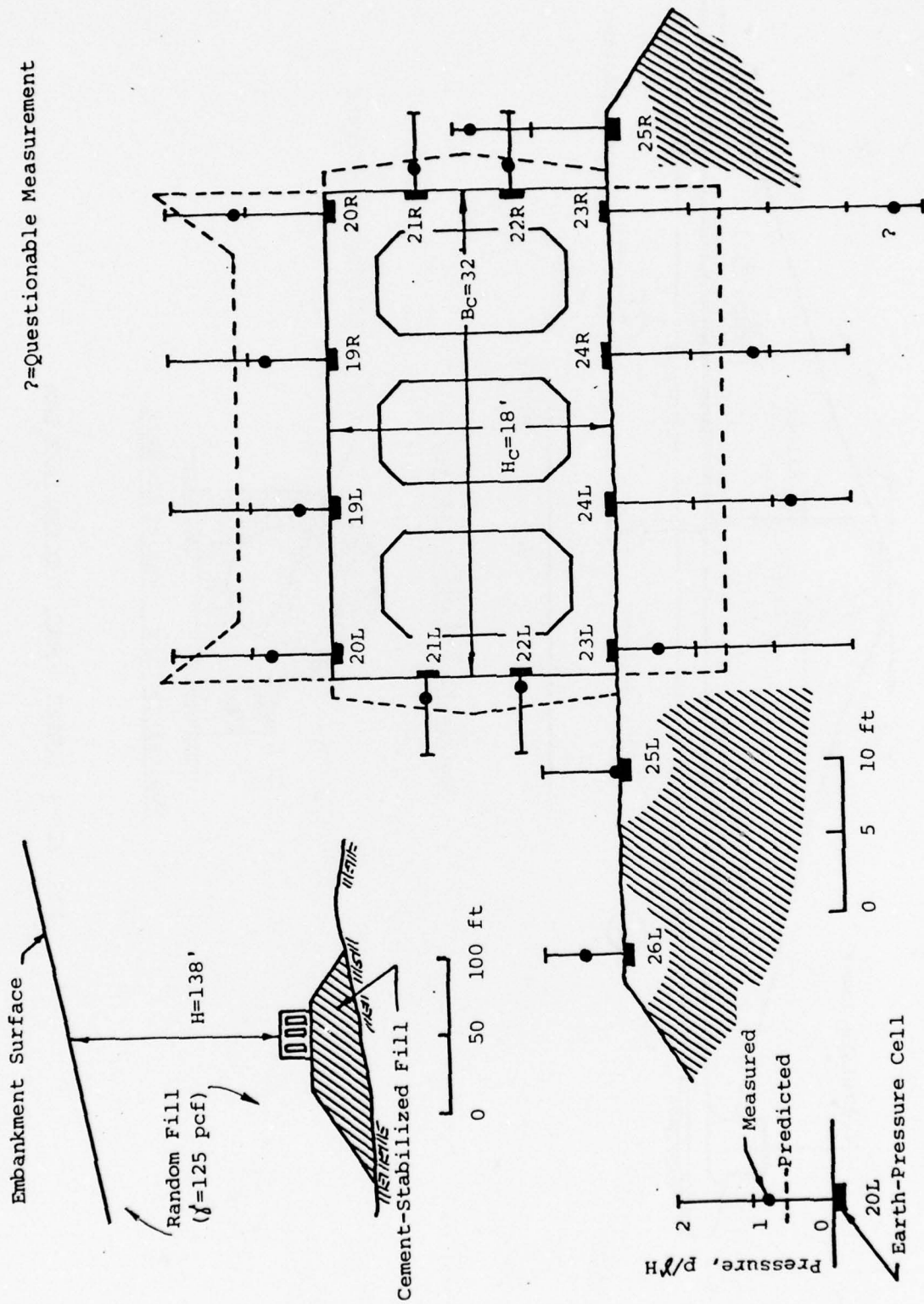
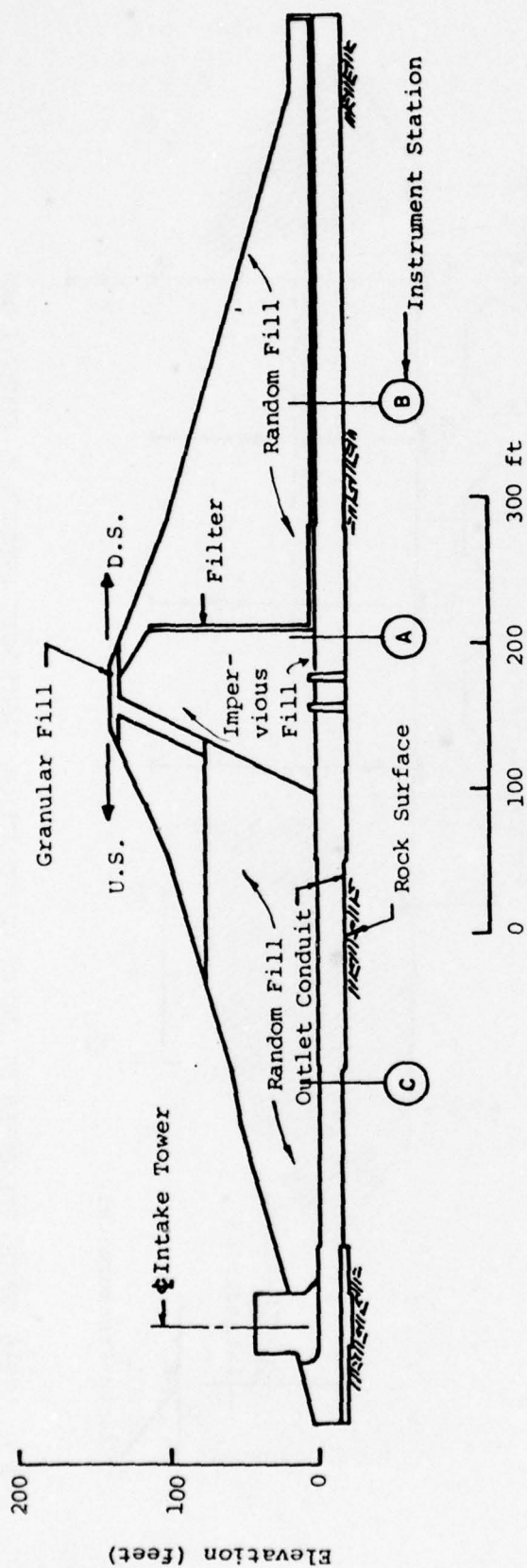


FIG. VII-8 EARTH PRESSURES AT END OF CONSTRUCTION, INSTRUMENT STATION E, COCHITI DAM



Profile Along Centerline of Outlet Works

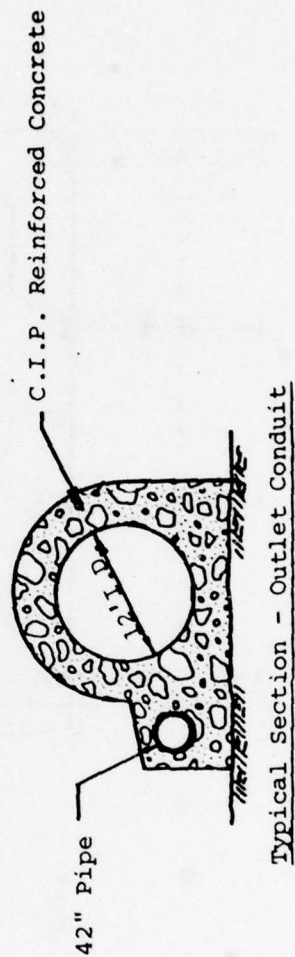


FIG. VII-9 OUTLET WORKS, DEQUEEN LAKE DAM

are given in Fig. VII-10. The data for several of the pressure cells is peculiar and therefore their validity is questionable. For instance, at Station A, cells 2-1 and 2-2 indicated reductions in pressures during periods when the fill height was increasing.

The earth pressures measured at each instrument station at the end of construction are presented in Figs. VII-11 through VII-13. Also shown in the figures are calculated pressures based on the procedures of Chapter VI. The effective overburden pressures for the two instrument stations in the shells of the dam were assumed to equal the value of YH at each location. At Station A which is very near the downstream edge of the core, the effective overburden was assumed to be equal to the theoretical value for maximum dam height (see Chapter V). The geometry of the rock foundation at each conduit section was also considered, in an approximate manner, when the pressures shown by the dotted lines were calculated (see Appendix B).

The calculated pressures are generally greater than the measured values. Only at Station C did apparently valid pressures exceed those calculated (cells 1-3 and 1-5). Conclusions are difficult to draw from the comparisons because of the number of pressure cells that either did not function or gave questionable results. It is interesting, however, that the vertical pressures measured at the base of the trenches adjacent to the conduit were quite low. This is in agreement with the finite-element studies of shallow trenches performed for this investigation.

C. Dierks Lake Dam

Dierks Lake Dam was built on the Sabine River in Arkansas by the Tulsa District of the Corps of Engineers. The zoned embankment-dam has a maximum height of about 130 feet and was completed in 1974. The outlet works include a cast-in-place, reinforced-concrete conduit of oblong shape as shown in Fig. VII-14. The outside width of the conduit is about 8 feet and the height is about 11 feet. A profile through the dam along the center-line of the outlet conduit is also shown in the figure. As indicated, six instrument stations were included to measure earth pressures on and near the conduit and on top of one of the seep rings in the core of the dam.

The pressures measured on the conduit during construction, and for more than a year thereafter, are shown in Figs. VII-15 and VII-16. All the data appear valid except Cell 24 at Station D-D. In general, the pressures increased to maximum values at the end of construction and then remained approximately constant. The earth pressures measured at the end of embankment construction are shown in Figs. VII-17 through VII-19. Pressures calculated by the methods proposed in Chapter VI are also shown in the figures. The effective overburden pressures at the instrument stations in the dam core (A-A through C-C) were assumed to be equal to the theoretical overburden pressure beneath the crest of the dam. For the downstream stations (D-D through F-F) it was assumed that the overburden corresponded directly to the height of fill over the conduit.

Comparing the results of the calculated and measured earth pressures, the following can be noted:

1. At the two instrument stations that have pressure cells at the

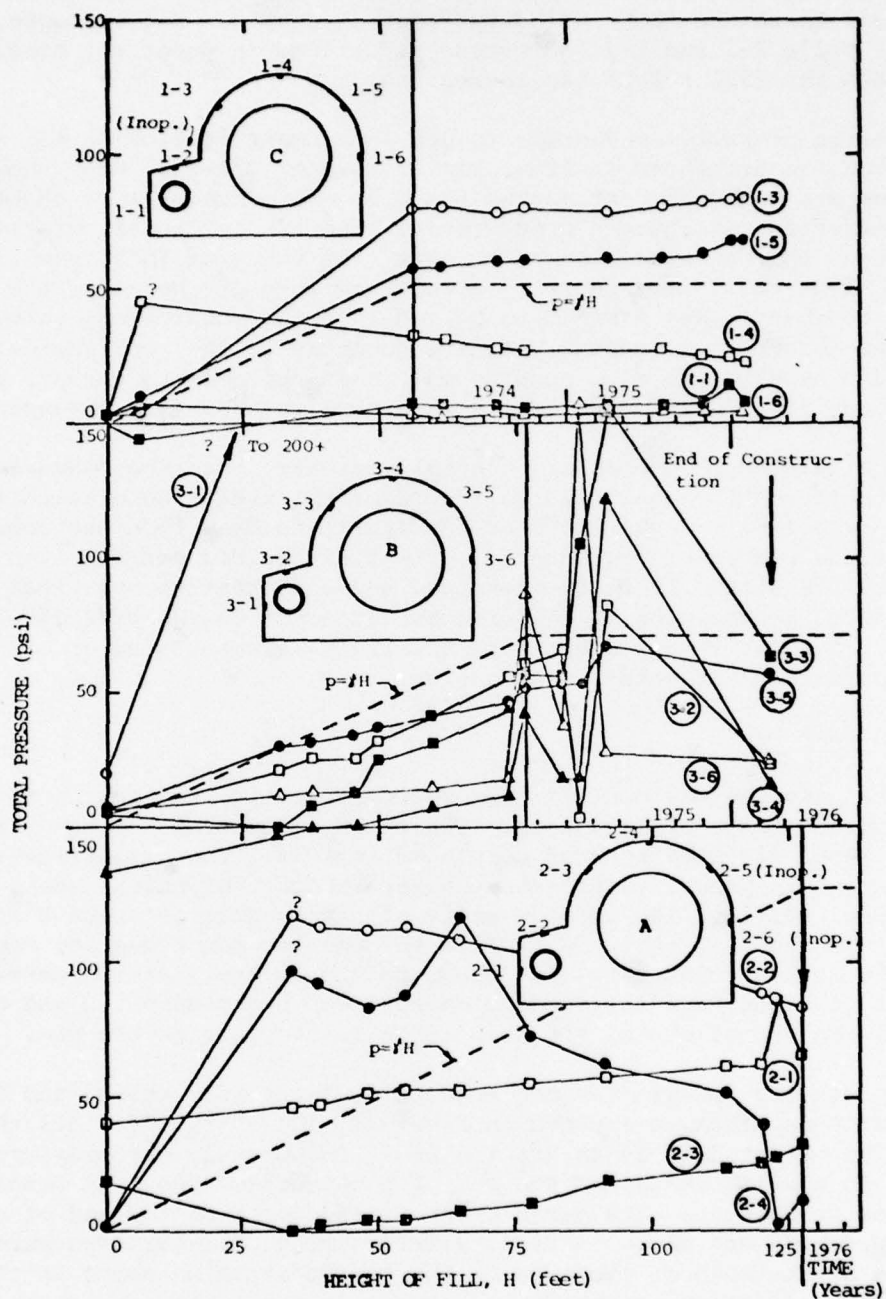


FIG. VII-10 MEASURED PRESSURES AT INSTRUMENT STATIONS A, B AND C, DEQUEEN LAKE DAM

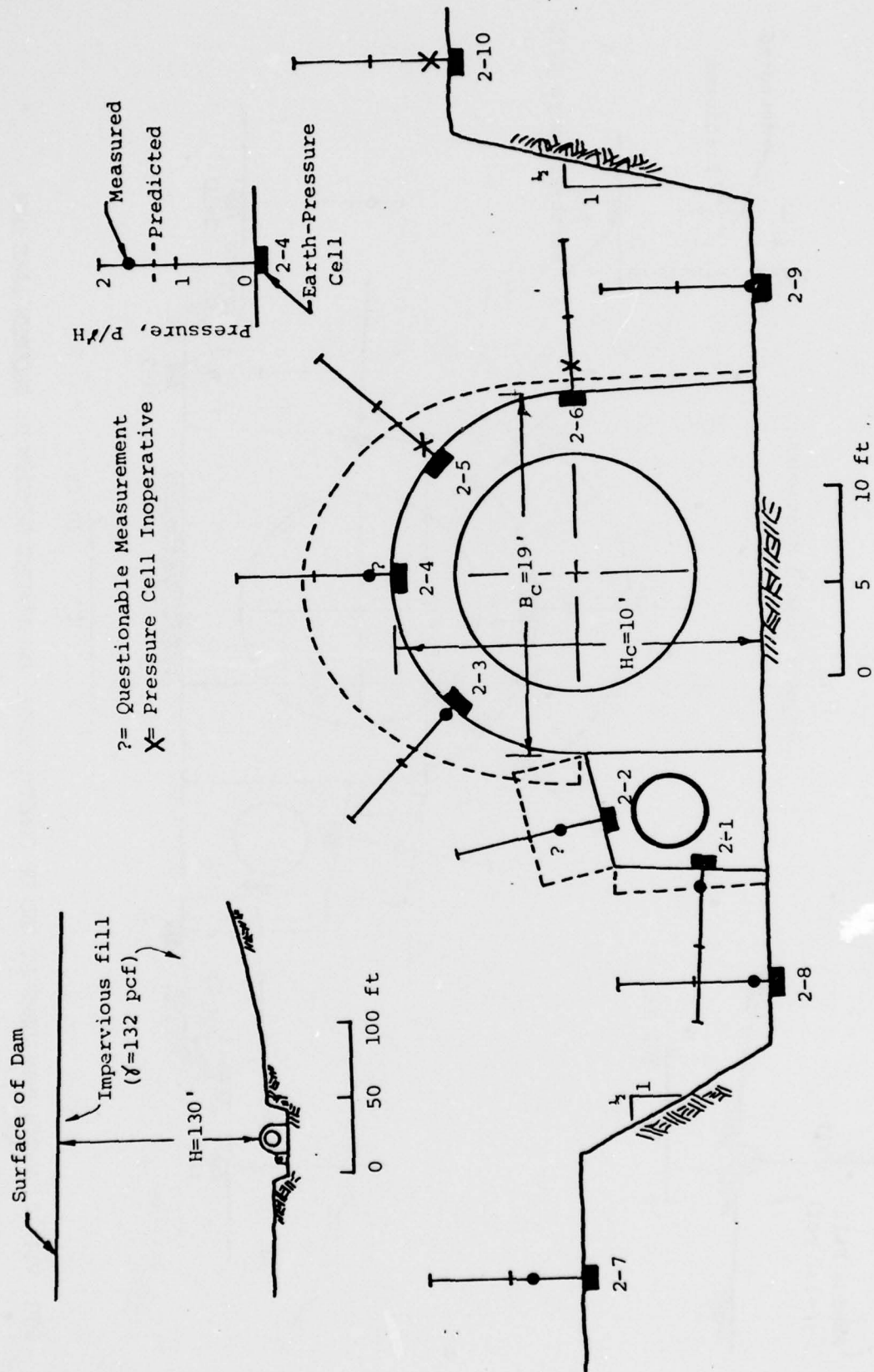


FIG. VII-11 EARTH PRESSURES AT END OF CONSTRUCTION, INSTRUMENT STATION A, DEQUEEN LAKE DAM

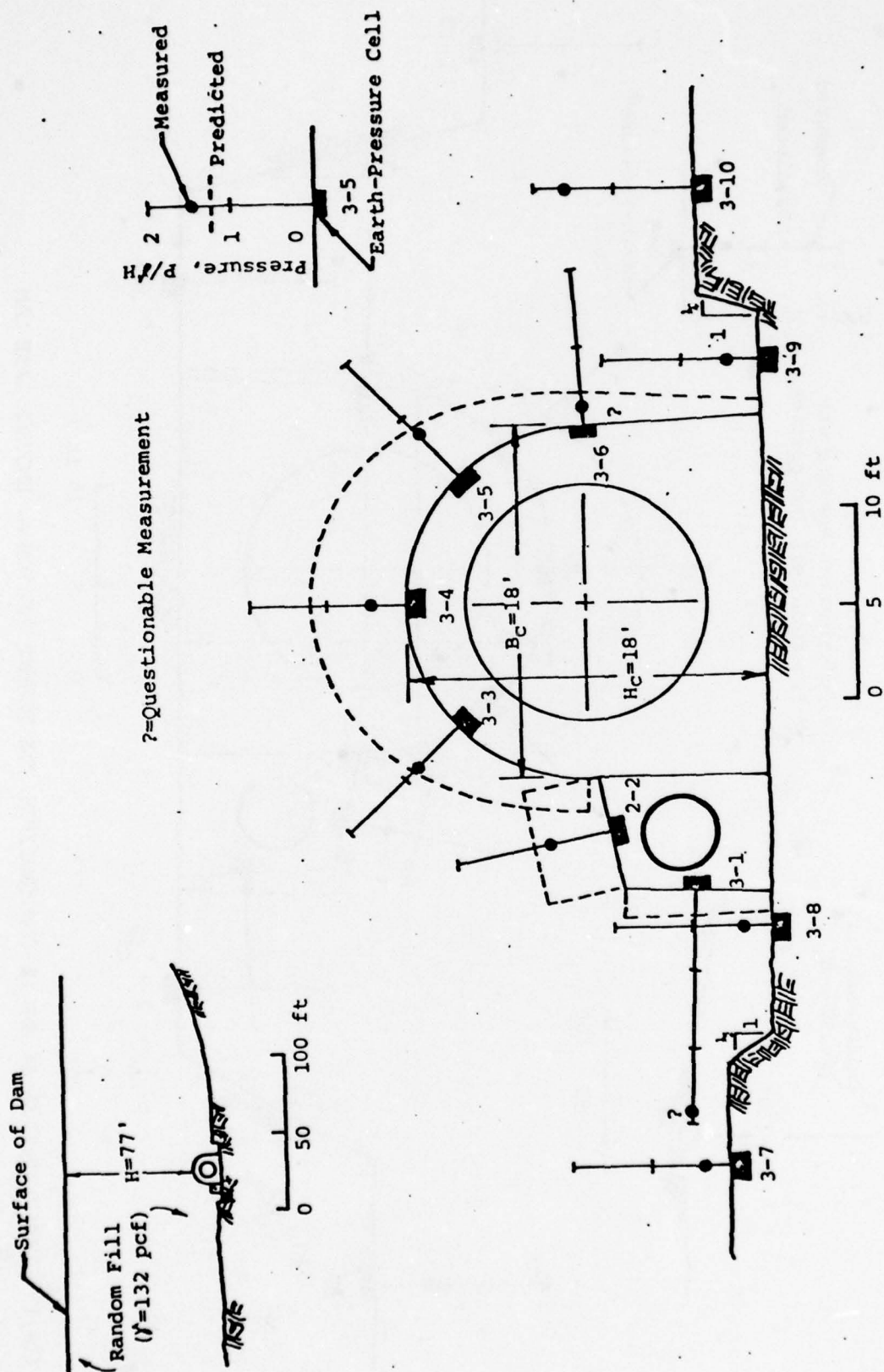


FIG. VII-12 EARTH PRESSURES AT END OF CONSTRUCTION, INSTRUMENT STATION B, DEQUEEN LAKE DAM

* Estimated on basis of last readings prior to end of construction.

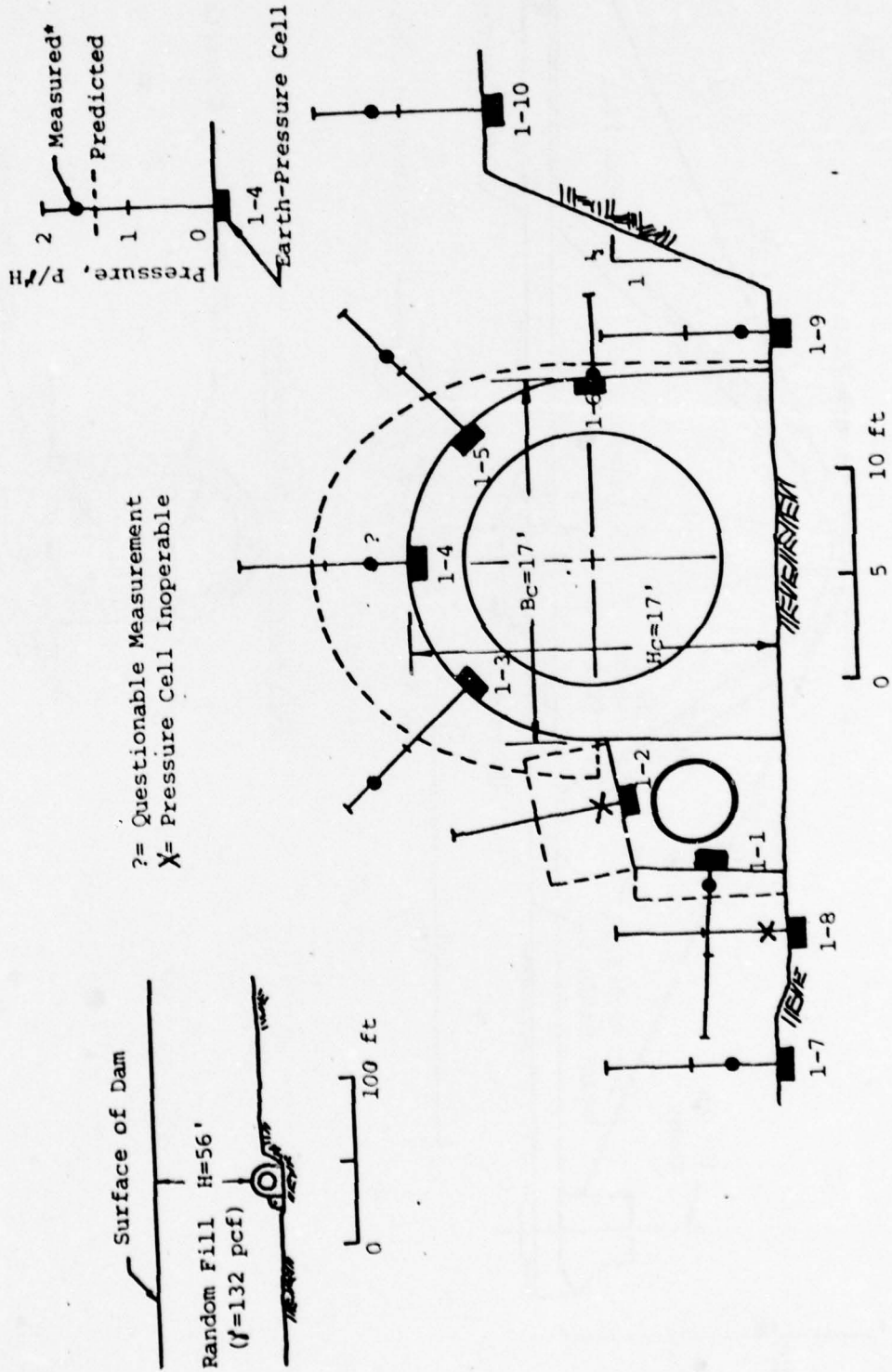
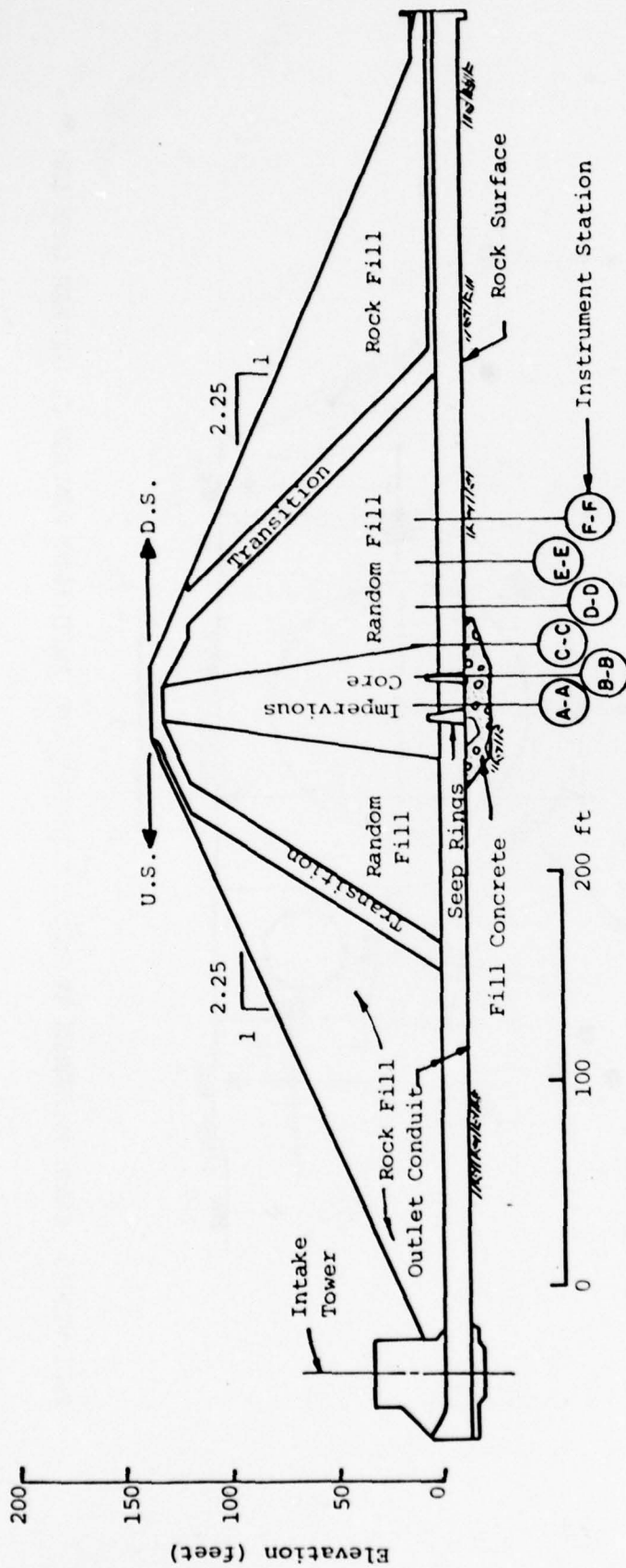
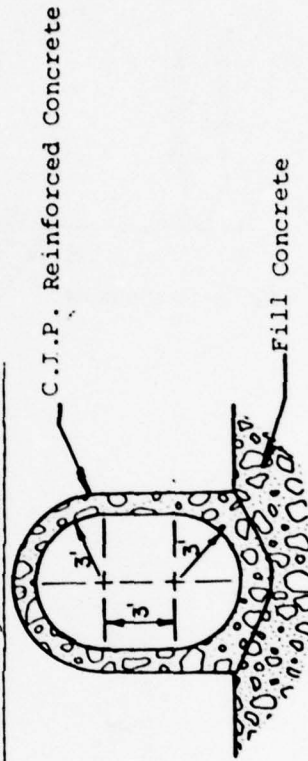


FIG. VII-13 EARTH PRESSURES AT END OF CONSTRUCTION, INSTRUMENT STATION C, DEQUEEN LAKE DAM



Profile along $\frac{1}{4}$ of Outlet Works



Typical Section - Outlet Conduit

FIG. VII-14 OUTLET WORKS, DIERKS LAKE DAM

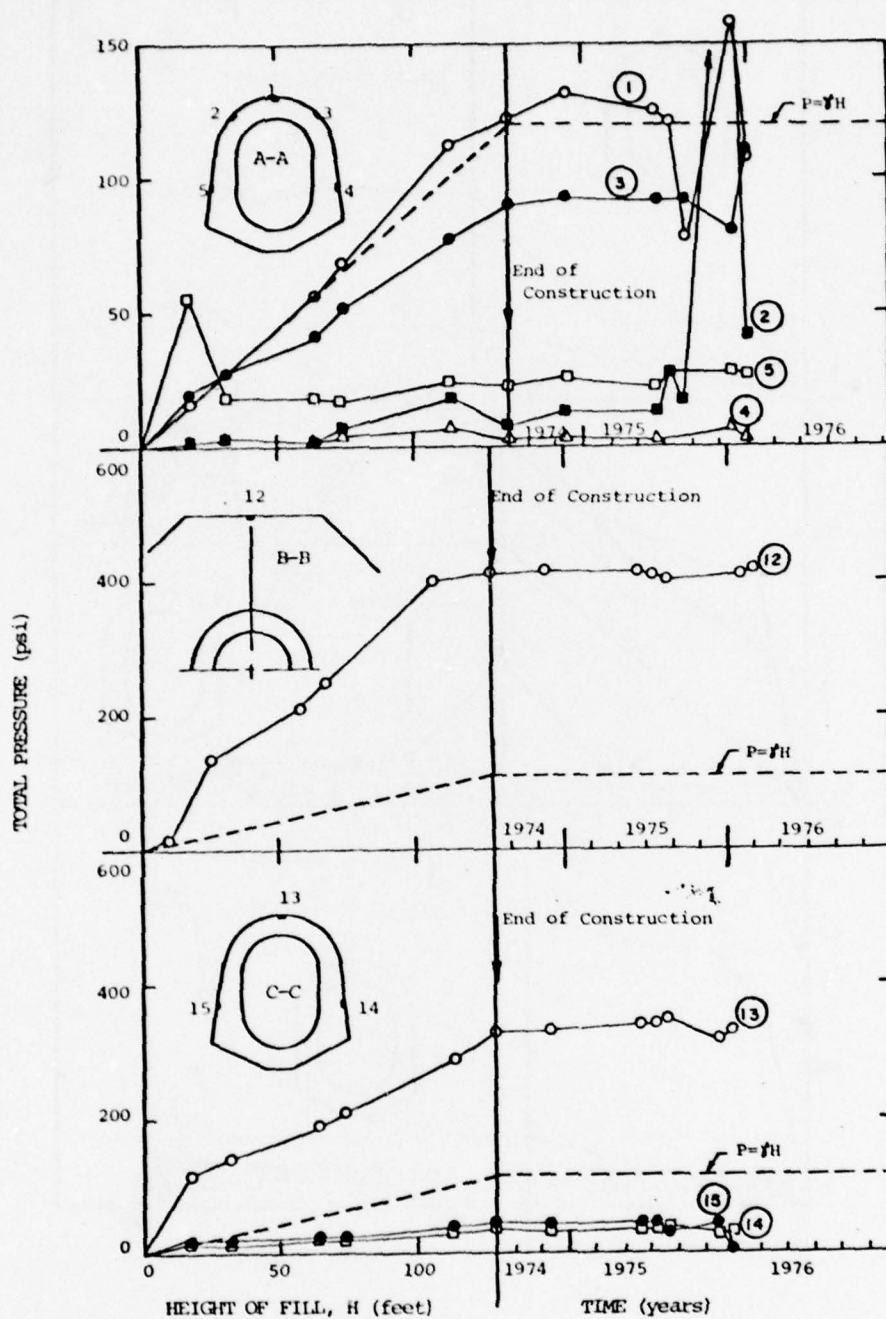


FIG. VII-15 MEASURED PRESSURES AT INSTRUMENT STATIONS A-A, B-B, AND C-C, DIERKS LAKE DAM

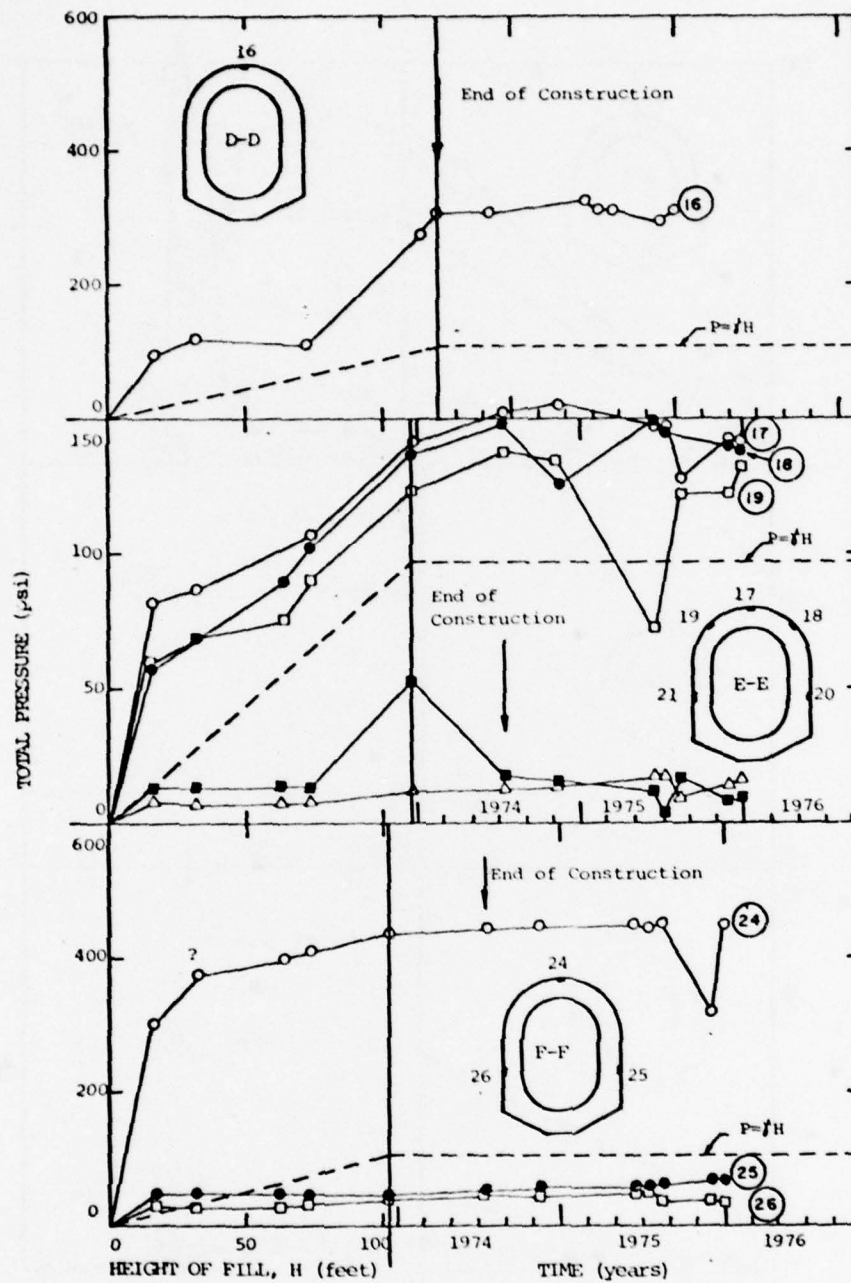


FIG. VII-16 MEASURED PRESSURES AT INSTRUMENT STATION D-D, E-E, AND F-F, DIERKS LAKE DAM

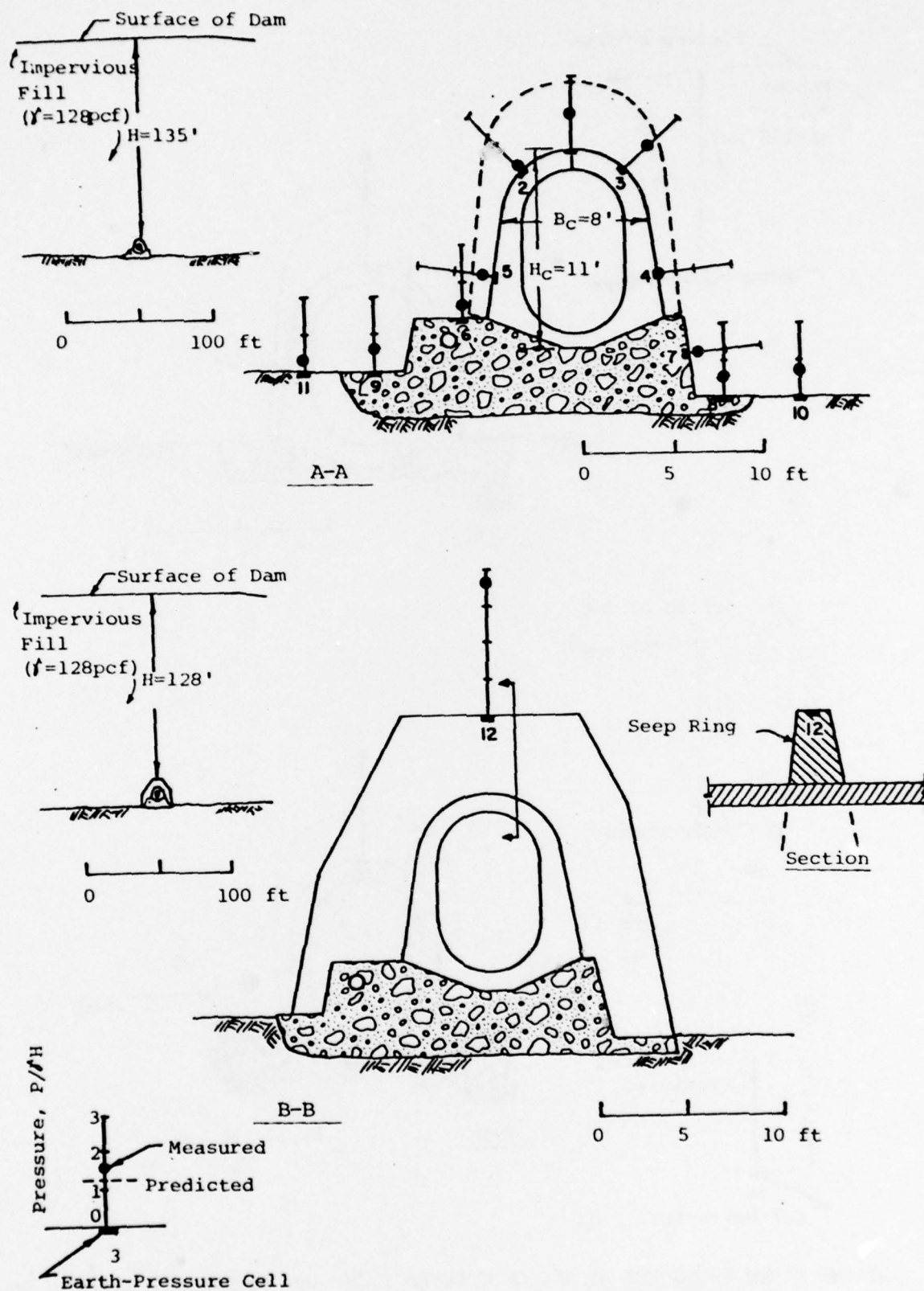


FIG. VII-17 EARTH PRESSURES AT END OF CONSTRUCTION, INSTRUMENT STATIONS A-A AND B-B, DIERKS LAKE DAM

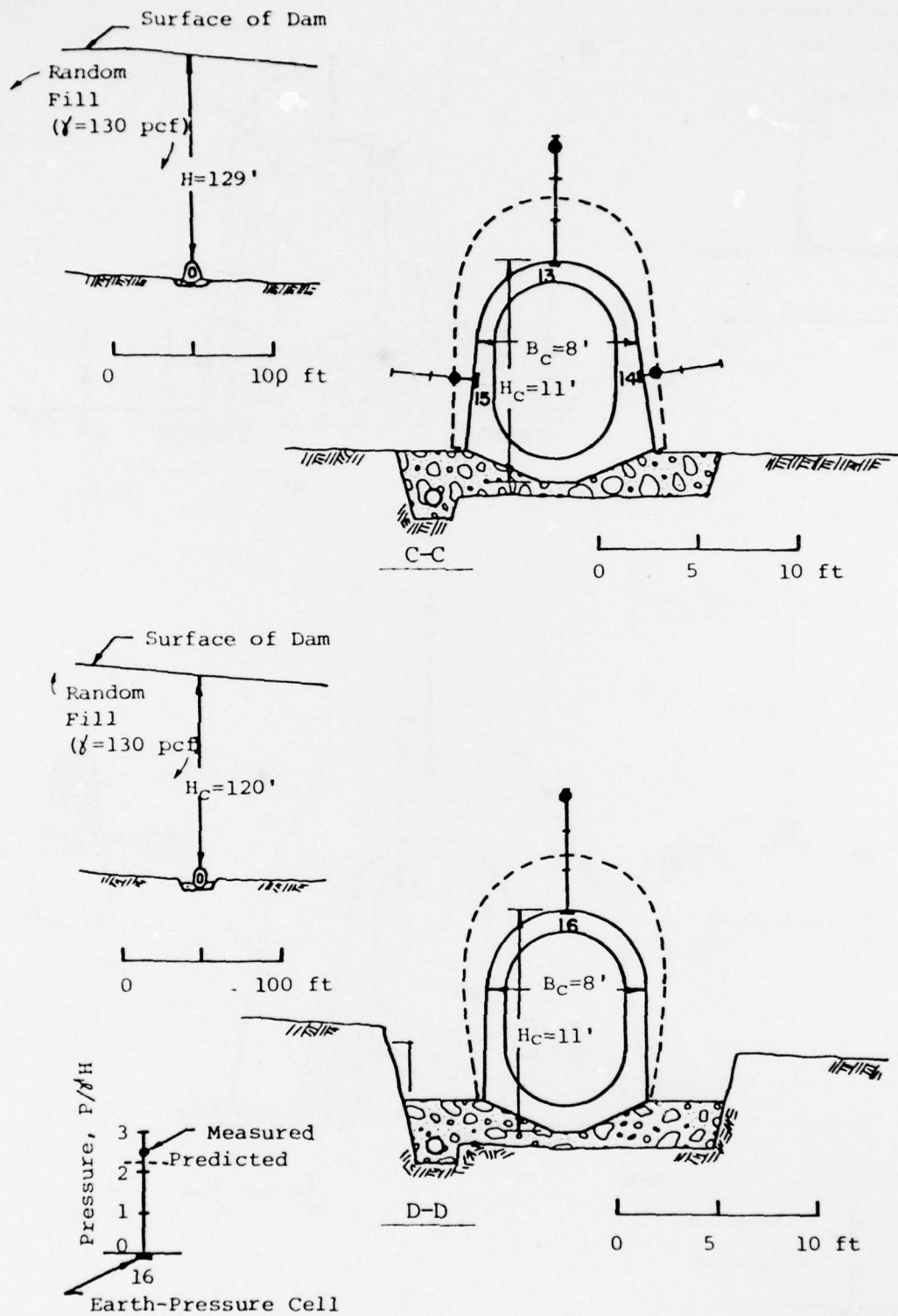


FIG. VII-18 EARTH PRESSURES AT END OF CONSTRUCTION, INSTRUMENT STATIONS C-C AND D-D, DIERKS LAKE DAM

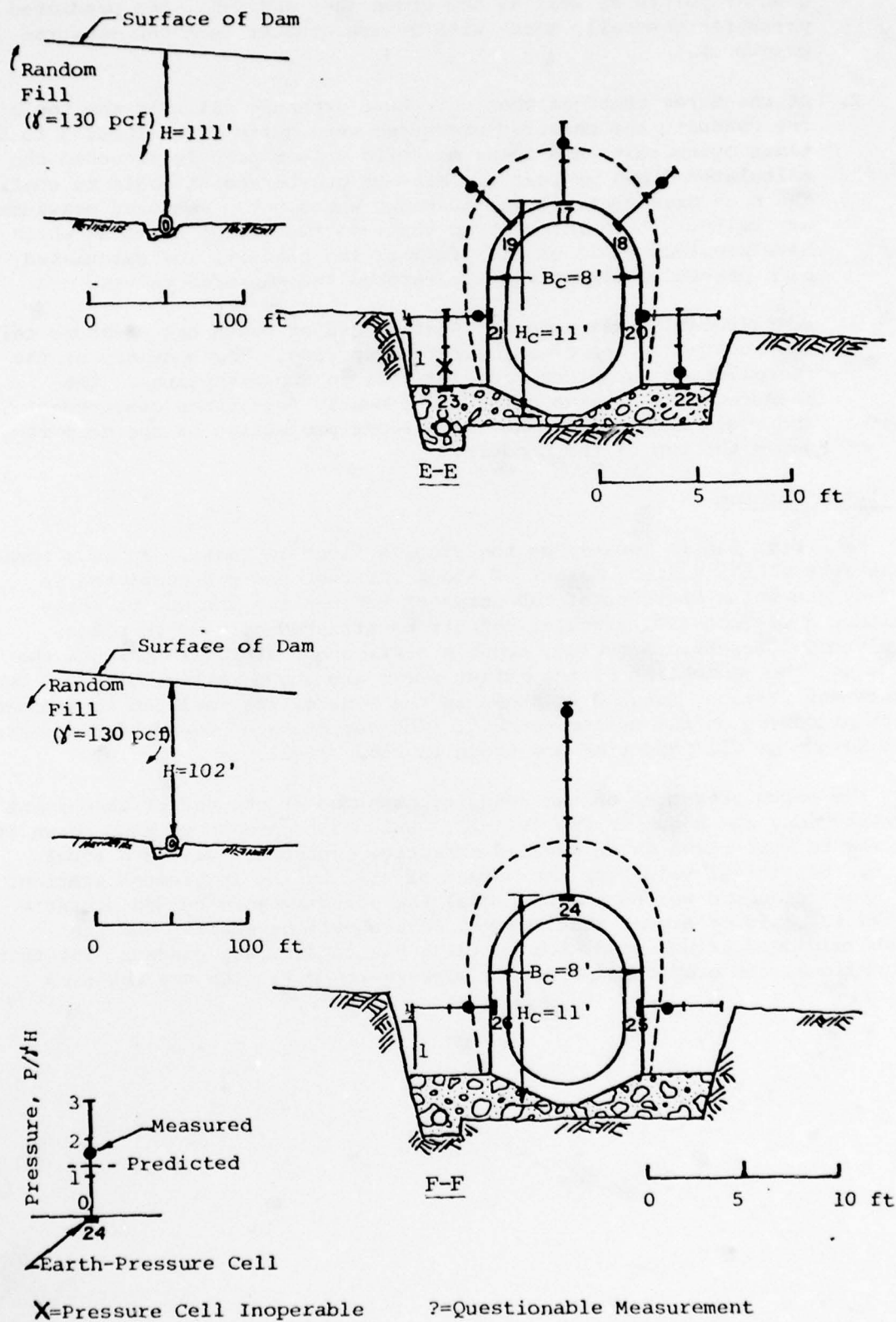


FIG. VII-19 EARTH PRESSURES AT END OF CONSTRUCTION, INSTRUMENT STATIONS E-E AND F-F, DIERKS LAKE DAM

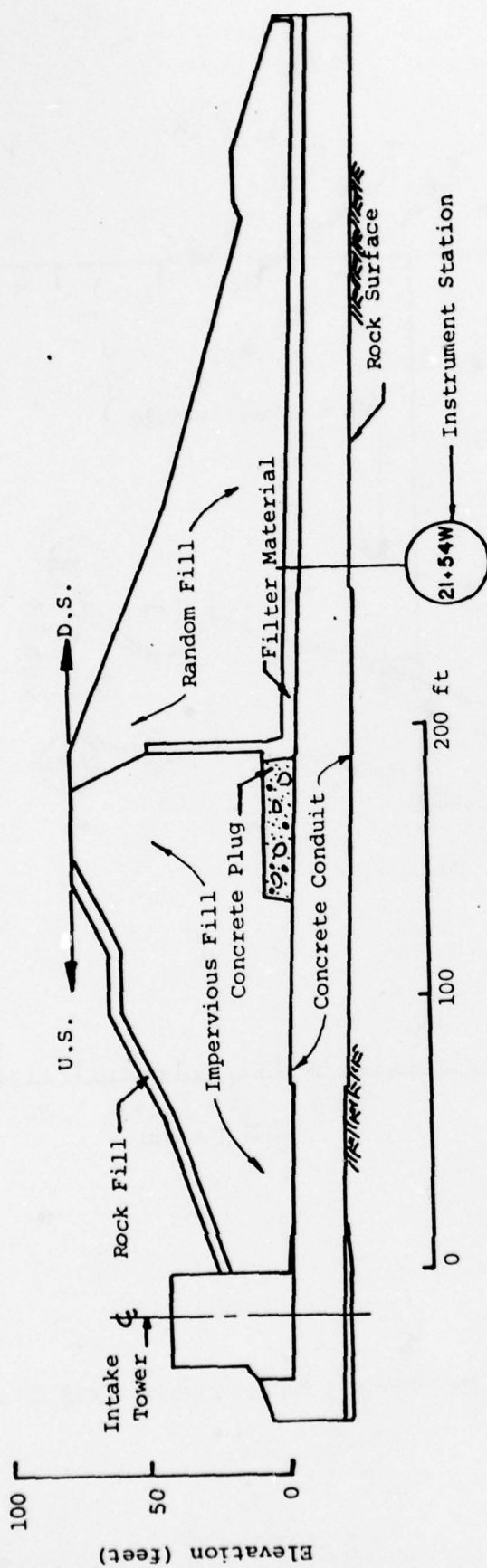
quarter points as well as the crown (A-A and E-E), the predicted pressures generally agree with or are greater than the measured pressures.

2. At the three stations that only have pressure cells at the top of the conduit, the measured pressures were quite high (about 3 to 5 times overburden) and these measured values greatly exceeded the calculated crown pressures. Without quarter-point cells to confirm the high pressures, it is not known whether the measured pressures are valid. It is interesting that, at two of the stations which have pressure cells on the sides of the conduit, the calculated side pressures almost exactly matched the measured values.
3. No calculation was made for Station B-B at which one pressure cell was located on top of a concrete seep ring. The geometry of the installation cannot be modelled well in two dimensions. The measured pressure was quite high (nearly four times overburden) and could result from the significant projection of the seep ring above the top of the conduit.

D. Lake Kemp Dam

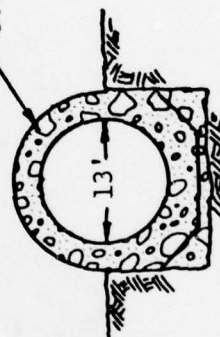
Lake Kemp Dam is located on the Wichita River in Texas. It is a zoned embankment with a maximum height of about 100 feet and was completed in 1972 by the Tulsa District of the Corps of Engineers. The outlet works includes a 13-foot-I.D. circular conduit constructed of cast-in-place, reinforced concrete. A typical conduit section and a profile through the dam along the centerline of the outlet works are shown in Fig. VII-20. One instrument station, located as shown in the figure, was included to measure earth pressures on the outlet conduit. The variation of measured pressures with height of fill and time are shown in Fig. VII-21.

The earth pressures on the conduit, measured at the end of embankment construction, are shown in Fig. VII-22. Calculated pressures also shown in the figure were based on an assumed effective overburden pressure equal to the theoretical value for the height of fill at the instrument station. The crown pressure was assumed to equal the effective overburden pressure though it could be argued that the pressure should be smaller for the relatively deep trench condition in which the conduit was placed. For these assumptions, the predicted pressures agree quite well with the measured values.



Profile along centerline of Outlet Works

C.I.P. Reinforced Concrete



Typical Section - Outlet Conduit

FIG. VII-20 OUTLET WORKS, LAKE KEMP DAM

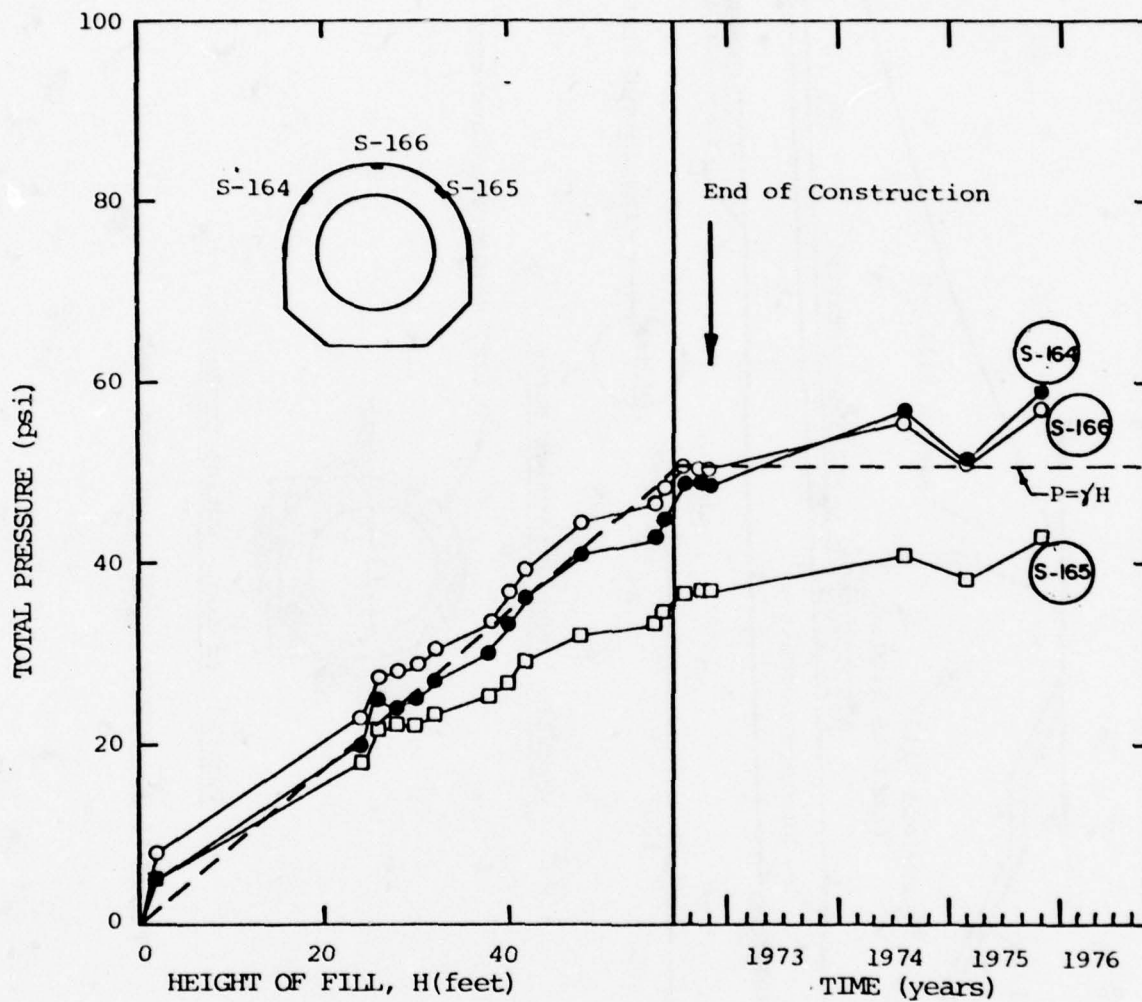


FIG. VII-21 MEASURED PRESSURES AT INSTRUMENT STATION 21+54W, LAKE KEMP DAM

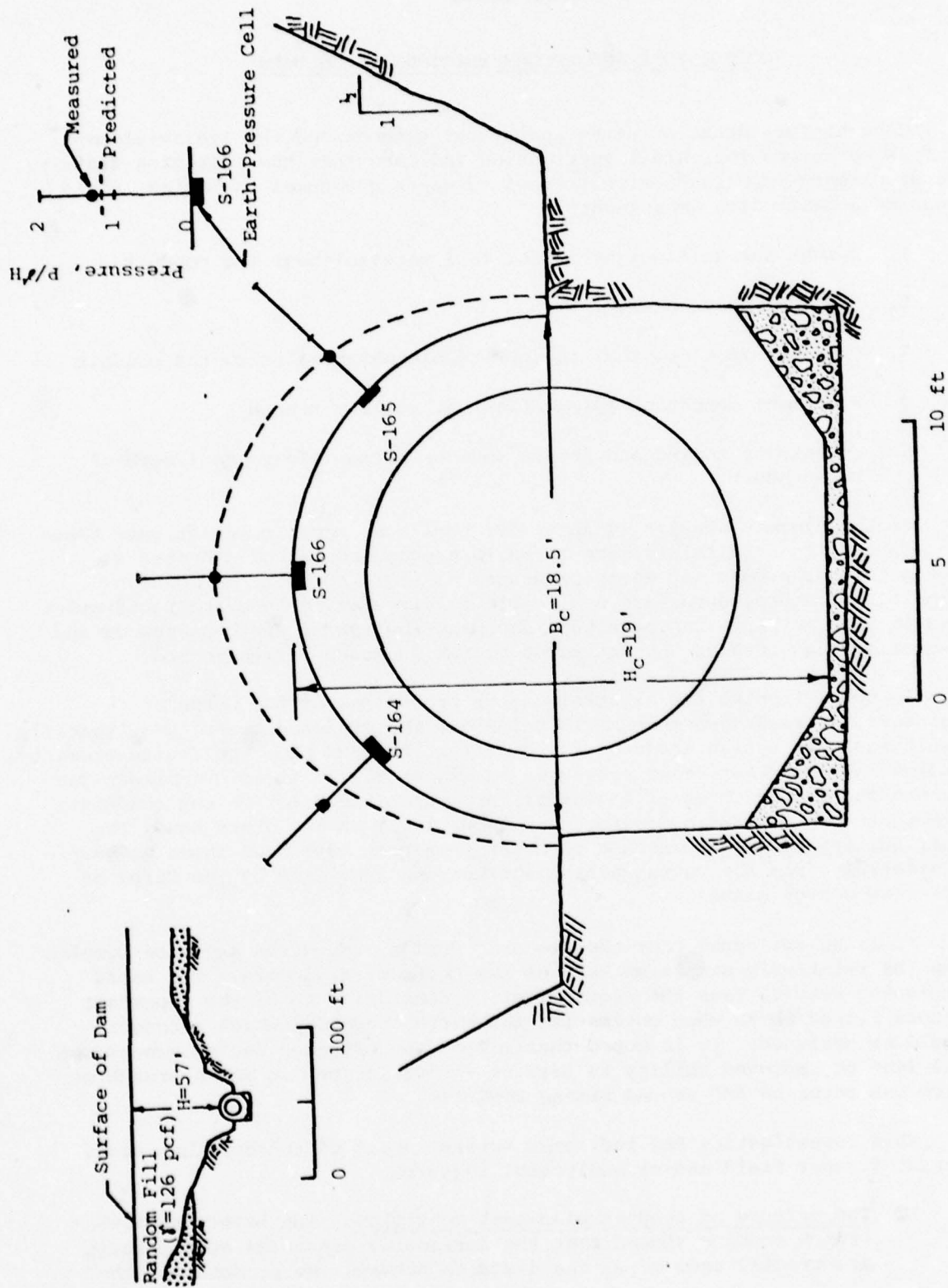


FIG. VII-22 EARTH PRESSURES AT END OF CONSTRUCTION, INSTRUMENT STATION 21+54W, LAKE KEMP DAM

CHAPTER VIIICONCLUSIONS AND RECOMMENDATIONS - CONDUITS

Case history data, existing analytical methods and the finite-element studies performed for this investigation indicate that the following factors are of primary importance with respect to earth pressures on buried, rigid conduits beneath high embankments:

1. Height and unit weight of the fill material over the conduit
2. Shape of the conduit
3. Depth to rock or other incompressible material below the conduit
4. Placement condition (projection vs. shallow trench)
5. Embankment zoning and stress redistribution along the length of the conduit.

Finite-element studies (Chapter IV) have been made to investigate these factors and the results are summarized in a proposed method (Chapter VI, Section A) for predicting earth pressures on rigid conduits for design purposes. The procedures are applicable to circular, oblong and rectangular conduit shapes. Both the magnitude and distribution of earth pressures and foundation reactions can be estimated by the proposed design method.

In comparison to the existing design procedures of the Corps of Engineers, as recommended in EM 1110-2-2902, the proposed techniques typically result in lower design loads on the conduit. For example, the finite-element studies indicate that crown pressures in excess of 1.5 times overburden (as recommended by the Corps of Engineers) are only likely for oblong conduits of height-to-width ratio greater than about 1.4. On the other hand, the distributions of embankment and reaction pressures have been shown to vary considerably from the rectangular distributions suggested by the Corps of Engineers design manual.

It is acknowledged that the proposed design procedures are more complex than the relatively simple methods of the Corps of Engineers. The extra complexity results from the requirement to consider each of the important factors listed above when estimating the earth loads for which a conduit should be designed. It is hoped that use of the proposed design procedures will lead to improved ability to predict the variations in earth pressures which can occur on and around buried conduits.

This investigation has indicated several areas of concern that could warrant further field and/or analytical research:

1. The effects of conduit placement condition. The brief shallow-trench studies showed that the horizontal pressures on a conduit are greatly reduced as the distance between the conduit and the

walls of the trench is made smaller. The importance of the low pressures is obvious for conduit design and it is also pertinent to the evaluation of the potential for hydraulic fracturing in embankment dams (see Chapter V).

2. The effects of embankment stress redistribution adjacent to a conduit. The zones of low minor principal stress which occur within an embankment near the sides of a conduit can increase the potential for hydraulic fracture and subsequent seepage and piping through an otherwise impervious core (see Chapter V).
3. The effects of stress redistribution in zoned embankment-dams. Finite-element studies have shown that vertical pressures on a horizontal plane through a zoned embankment-dam can vary considerably from the pressure corresponding to just the weight of the overlying fill (Chapter V). Improved "rules of thumb" are needed for estimating design pressures for conduits beneath such dams.

PART B - RETAINING WALLS

CHAPTER IX

CURRENT DESIGN METHODS FOR PREDICTING

EARTH PRESSURES ON RETAINING WALLS

A. Classical Earth-Pressure Theories

In marked contrast to the relatively few analytical methods for predicting earth pressures on conduits, there are many theoretical solutions for problems of earth pressures on retaining walls. The various theories are fully described in many text books and in the geotechnical engineering literature. This discussion will be limited to a general statement of the basic assumptions upon which the more widely recognized theories are based.

All classical earth-pressure theories assume that the soil mass adjacent to the retaining wall is in a state of limiting equilibrium (on the verge of failure) and that the strength of the soil can be expressed in terms of the Mohr-Coulomb failure criterion:

$$\tau = C + \sigma \tan \phi \quad (\text{IX-1})$$

where τ = shear stress on the failure plane

σ = normal stress on the failure plane

C = soil cohesion

ϕ = soil friction angle

The theoretical solutions belong to a much larger field of study; namely, the Theory of Plasticity. Pre-failure wall movements and deformations of the soil mass are not considered, and the theory of plasticity provides no means for evaluating the amount of wall movement required to mobilize the strength of the backfill. As a result, the required movements are usually estimated on the basis of laboratory model tests and field experience.

The classical earth pressure theories are addressed to the two limiting states of equilibrium:

1. The active condition in which the retaining wall moves away from the soil mass.
2. The passive condition in which the wall moves towards the soil.

The simplest of the earth pressure theories is that of Rankine (1857). Considering a cohesionless soil mass adjacent to a wall with a frictionless backface, he determined the state of stress at the soil/wall interface for the active and passive conditions. According to Rankine's theory, the

total active and passive earth pressures are:

$$P_a = \frac{1}{2} K_a \gamma H^2 \quad (\text{IX-2})$$

and $P_p = \frac{1}{2} K_p \gamma H^2 \quad (\text{IX-3})$

where, P_a = total active force on the wall which acts at one-third the wall height for the Rankine Case

P_p = total passive force

K_a = active pressure coefficient

K_p = passive pressure coefficient

γ = unit weight of soil behind the wall

H = height of the wall

Rankine's active and passive pressure coefficients are given by:

$$K_a = \frac{1 - \sin\phi}{1 + \sin\phi} \quad (\text{IX-4})$$

and $K_p = \frac{1 + \sin\phi}{1 - \sin\phi} \quad (\text{IX-5})$

Because of the simplicity of the equations, Rankine's theory is widely used even though the assumptions upon which it is based often do not agree with reality.

Most retaining walls do not have a frictionless back-face and it has been found that wall friction can significantly affect the earth pressures on the wall. Coulomb's (1776) theory and its subsequent development by others was the first to take account of wall friction as well as many other factors that were not considered by Rankine such as soil cohesion, sloping backfills and inclination of the wall. Coulomb, rather than considering the state of stress within the soil mass as had Rankine, assumed a specific shape for the sliding surface along which soil movement would occur if the wall were to fail. His assumption of a plane surface of sliding has been found to be approximately correct for the active condition but not nearly so accurate for passive cases involving wall friction angles larger than $\phi/3$. For complex retaining wall problems, it is necessary to use graphical techniques in applying Coulomb's method to design (Terzaghi and Peck, 1967). However, for certain conditions, closed-form solutions can be expressed mathematically. For the case of a horizontal backfill and no shear stresses on a vertical plane in the soil mass:

$$P_a = \frac{1}{2} K_a \gamma H^2 - 2cH\sqrt{K_a} \quad (\text{IX-6})$$

$$\text{and } P_p = \frac{1}{2} K_p \gamma H^2 + 2cH\sqrt{K_p} \quad (\text{IX-7})$$

where K_a and K_p are equal to the Rankine pressure coefficients (Eqs. IX-4 and IX-5). For a cohesionless soil, the following equations are valid for sloping backfills and inclined walls with friction:

$$P_a = \frac{1}{2} K_a \gamma H \quad (\text{IX-8})$$

$$\text{and } P_p = \frac{1}{2} K_p \gamma H \quad (\text{IX-9})$$

$$\text{where } K_a = \left[\frac{\csc\beta \sin(\beta - \phi)}{\sqrt{\sin(\beta + \delta)} + \sqrt{\frac{\sin(\phi + \delta)\sin(\phi - i)}{\sin(\beta - i)}}} \right]^2 \quad (\text{IX-10})$$

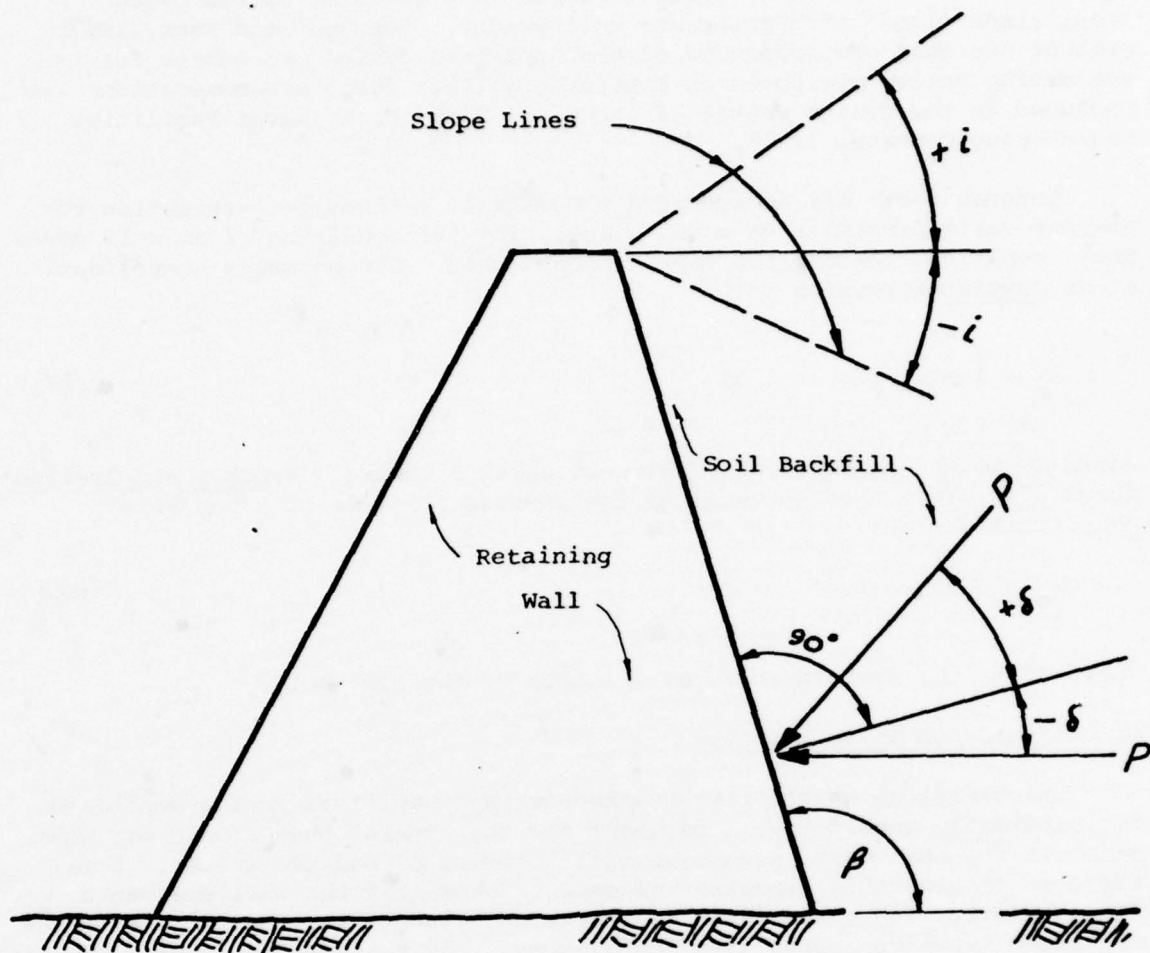
$$\text{and } K_p = \left[\frac{\csc\beta \sin(\beta + \phi)}{\sqrt{\sin(\beta + \delta)} - \sqrt{\frac{\sin(\phi - \delta)\sin(\phi + i)}{\sin(\beta - i)}}} \right]^2 \quad (\text{IX-11})$$

The terms i , β , and δ are defined in Fig. IX-1.

Other investigators have developed earth-pressure theories that improve upon Coulomb's, particularly for the passive condition, because they include curved slip surfaces that are more realistic than plane slip surfaces. Because of the greater complexity of the resulting equations, theoretical solutions are usually presented in graphical or tabular form from which values of active or passive pressure coefficients can be selected for any particular design problem. Examples of such analytical solutions are those given by Caquot and Kerisel (1948), Janbu (1957), U. S. Naval Facilities Engineering Command (1971) and Sokolovski (1965). Of all the methods, Sokolovski's is accepted as being the most rigorous. However, solutions have been developed for only a small number of conditions using Sokolovski's theory.

B. Empirical Methods

The engineering profession is generally aware of the idealized assumptions upon which the various classical earth-pressure theories are based. Thus it is common in design to temper the calculated earth pressure coefficients with judgment based on experience. For relatively low walls (less than about 20 feet high), it is common practice to design on the basis of an "equivalent fluid pressure" corresponding to the backfill soil type (see for instance Hough, 1957). The active or passive pressures on



P = Resultant of active or passive pressures

δ = Angle of wall friction

β = Inclination of back-face of wall

i = Slope of backfill surface

FIG. IX-1 DEFINITIONS OF TERMS USED IN COULOMB EQUATIONS FOR ACTIVE AND PASSIVE EARTH PRESSURES

the wall are assumed to be equal to those that would be caused by an "equivalent fluid" of appropriate unit weight. Terzaghi and Peck (1967) present the most comprehensive of the empirical design procedures for estimating active pressures on retaining walls. Their recommendations are included in the design manual of the U. S. Navy (U. S. Naval Facilities Engineering Command, 1971).

Because there are no accepted theoretical methods for estimating the at-rest earth pressures on a wall, i.e., for the condition of no wall movement, empirical formula are most commonly used. For normally-consolidated sands Jaky's expression is:

$$K_o = 1 - \sin\phi \quad (IX-12)$$

where K_o is the coefficient of at-rest earth pressure. Brooker and Ireland's formula^o is often used to estimate the at-rest pressure of a normally-consolidated clay:

$$K_o = 0.95 - \sin\phi' \quad (IX-13)$$

where ϕ' is the drained angle of friction of the clay soil.

C. Elastic-Continuum Methods

The classical earth-pressure theories and empirical design methods do not explicitly consider wall movement nor the strains that in reality must occur in the soil mass to develop full activity or passive states. Yet there is considerable experimental data to show that the wall movements significantly affect the earth pressures and vice-versa. Recently elastic-continuum techniques have been employed to study the effects of wall movement.

Besprosvannaya (1965) developed a solution which considers the wall to be a beam on an elastic foundation. The earth pressures and movements are determined by the values of compression and shear moduli of subgrade reaction assumed for the backfill, and by the flexibility of the wall.

The finite-element method appears to be a useful and powerful technique for the study of soil-structure-interaction problems, of which retaining walls are but one example. Because the finite-element technique requires considerable effort for analysis of each individual problem, it is most useful for (1) parameter studies to identify the factors of most importance to a particular class of problems and for (2) analyses of high-cost, complicated wall installations to which classical earth pressure theories or empirical procedures do not apply.

Clough and Duncan (1971) presented results of finite-element analysis of hypothetical retaining walls to study the effects of wall rotation and foundation settlement. The same authors (Duncan and Clough, 1971) reported the results of extensive studies of the behavior of a U-frame lock structure during and after construction. Soil-structure-interaction effects were

shown to be responsible for otherwise unexplainable field observations (such as the movement of the lock walls toward the centerline of the structure as it was filled with water). Moore (1971) described how the finite-element technique was used to assist in the design of a 40-foot-high bridge pier that had to retain an additional 33 feet of rockfill at a 1.5 to 1 slope. Kulhawy (1974) described the finite-element studies that were performed during design of a 104-foot-high gravity retaining wall to be built within an earth dam. The effects of soft rock layers within the foundation were studied as well as the question of whether wall movements would be sufficient to achieve an active pressure condition.

D. Corps of Engineers Design Method

The practice of the Corps of Engineers is reflected by the design recommendations given in EM 1110-2-2502 (Department of the Army, 1961). The design manual is intended primarily for concrete gravity or cantilever retaining walls. Active and passive earth pressures are determined by Coulomb's theory (Eqs. IX-10 and IX-11), neglecting soil cohesion entirely. At-rest earth pressures are estimated from empirical coefficients related to soil type. The type of wall and its foundation determine whether active or at-rest pressures are used for design, and at what point on the wall the resultant force acts. Stability criteria are given for various foundation conditions and include requirements for the location of the resultant force within the foundation, the maximum foundation pressure, and the factor of safety with respect to shear-failure in the foundation.

CHAPTER X

REVIEW OF CASE HISTORIES IN LITERATURE -

RETAINING WALLS

A. Measured Earth Pressures

Field studies of the magnitude and distribution of earth pressures on retaining walls are useful for developing an understanding of earth pressure phenomena, and the degree to which they are reflected by currently available design theories, and empirical procedures.

1. Oroville Dam, California. Kruse (1965) reported the results of earth-pressure measurements made during construction of a 405-foot-high cofferdam, which forms the upstream portion of Oroville Dam. The toe of the cofferdam was retained by a 100-foot-high vertical concrete core block as shown in Fig. X-1. To reduce the earth pressures that would occur on the core block, a 20-foot-thick zone of soft clay was placed immediately adjacent to the upstream face of the wall. The figure shows the earth pressures measured on the core block upon completion of the cofferdam. It can be seen that the pressures are low in the zone where the soft clay was placed next to the core block, and very high in the zone of stiffer backfill below the soft clay. The highest pressures on the wall are about three times the overburden pressure ($K=1$ line). It is unlikely that any method except the finite-element method could be used to predict the earth pressures on a wall having such complex backfill conditions.

2. Cow Green Dam, Great Britain. Vaughan and Kennard (1972) reported earth pressures measured during and after construction of the 25-meter-high Cow Green Dam. The dam, which was built between 1967 and 1970, consists of a concrete-gravity section and an earth embankment. The designers were concerned that low embankment stresses, at the junction between the concrete section and the clay core of the embankment could lead to cracking and subsequent piping of the core. As shown in Fig. X-2, earth pressure and pore-water pressure cells were installed in the surface of the concrete end wall to monitor the earth pressures exerted by the core. The pressures measured on the end face of the wall, at the end of construction, are given in the figure. The total lateral earth pressures increased with depth and were about 70 percent of the overburden pressure ($K=1$ line). The lateral pressure measured on the upstream face of the wall was about half as large. In terms of effective stress, the lateral pressures on the end face at the end of construction, were about 40 percent of the effective overburden pressure, a fact that the authors felt was consistent with Jaky's expression for at-rest earth pressures (Eq. IX-12). The authors also noted that the lateral earth pressures decreased slightly after construction.

3. Pleasant Valley Pumping Plant. Gould (1970), in an excellent state-of-the-art paper regarding lateral pressures on rigid permanent structures, described the earth pressures measured at the Pleasant Valley Pumping Plant. As

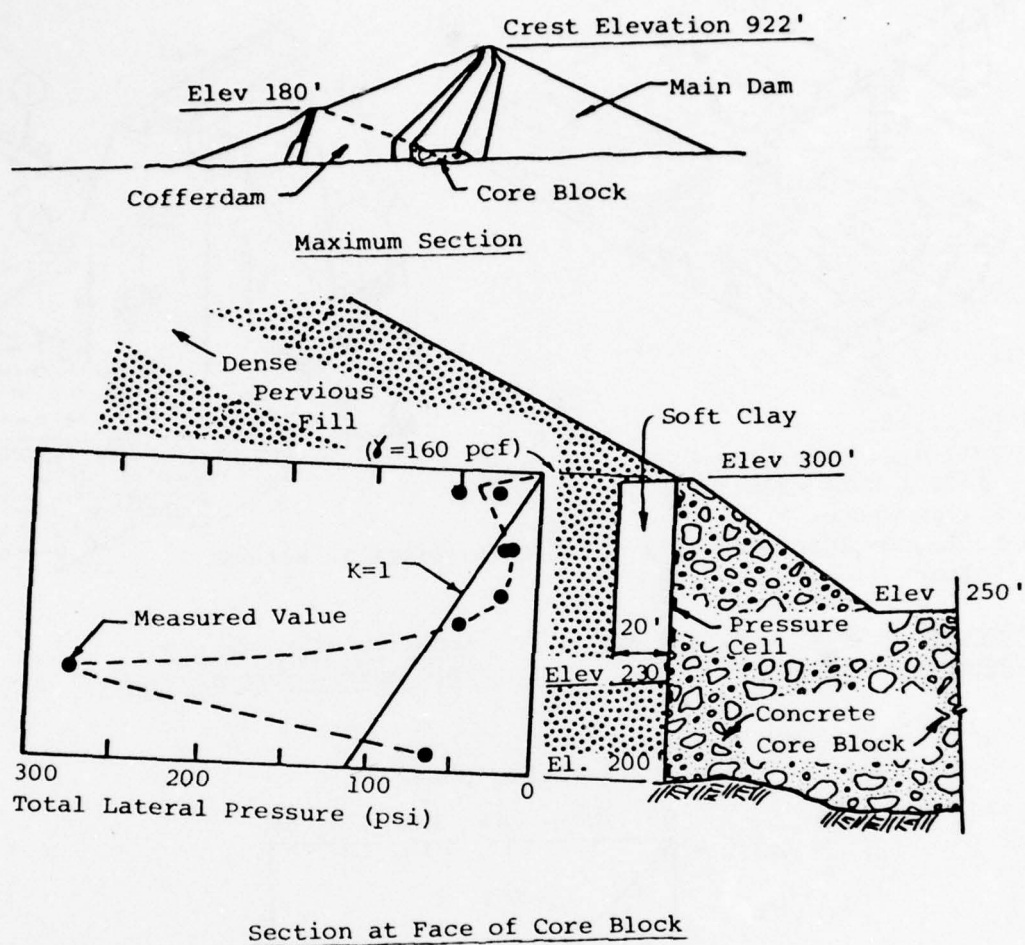
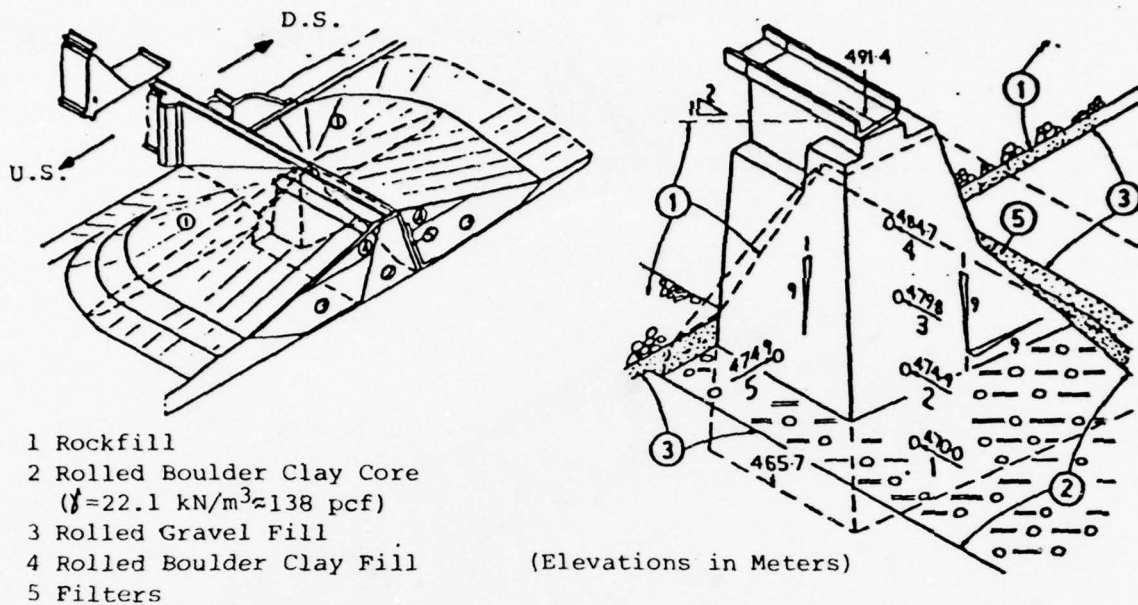


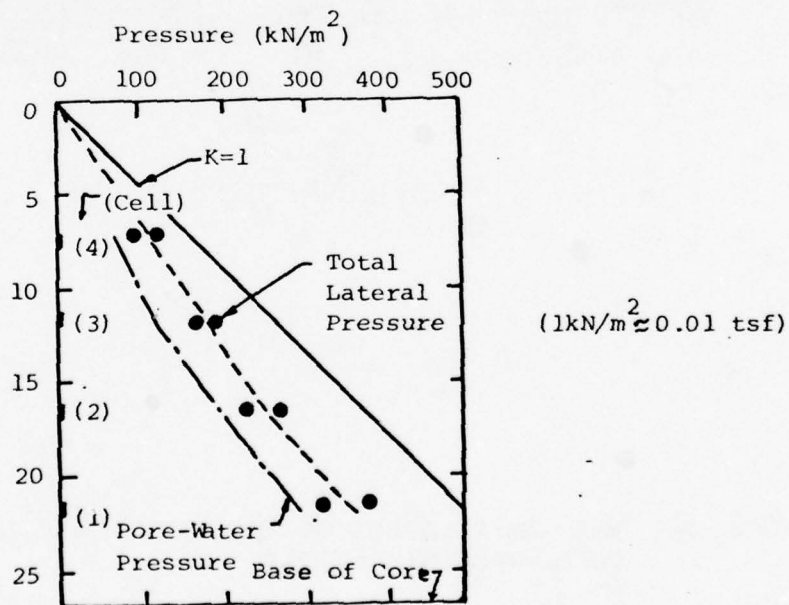
FIG. X-1 MEASURED PRESSURES ON CORE BLOCK, OROVILLE DAM, AT END OF COFFERDAM CONSTRUCTION

(Kruse, 1965)



Junction Between Concrete and Embankment Sections

Location of Earth and Pore-Water Pressure Cells



Measured Pressures on End Face of Wall at End of Construction

FIG. X-2 PRESSURE MEASUREMENTS AT COW GREEN DAM

(Vaughan and Kennard, 1972)

shown in Fig. X-3, the project included a subsurface structure located in a backfilled excavation. Earth and pore-water pressures were measured on two walls of the structure, as shown in the figure. The effective horizontal earth pressures generally agreed with experimental values ($K_0 = 0.55$) from K_0 -triaxial tests on the compacted backfill soils. The greatest differences were at the base of the walls, where low lateral pressures are likely to have been associated with reduced vertical pressures caused by stress redistribution within the narrow wedge of backfill.

4. Roenkhausen Pump Storage Plant, Germany. Kany (1972) described the earth-pressures measured on the subsurface walls of a buried powerhouse that is 30 meters in diameter and 43 meters high. As shown in Fig. X-4, the powerhouse was constructed in a deep dewatered, rock excavation, which was subsequently backfilled with rockfill boulders (maximum of 0.8 meters in diameter). Pressures exerted by the backfill on the wall were measured during and after construction at four horizons (I-IV in the figure) around the wall. Wall friction was measured at one location in Horizon II. The earth pressures measured on the north and south sides of the powerhouse, at the completion of backfilling are shown in the lower part of Fig. X-4. A reference line, for $K_0 = 0.25$, is also given in the figure. This value was determined from Jaky's expression (Eq. IX-12) using a friction angle of 48.5° , as measured by field direct-shear tests on the rockfill. The measured pressures were generally larger than those predicted.

However, after the construction dewatering was discontinued and the adjacent storage reservoir filled for the first time, the measured effective lateral pressures from the then-saturated backfill decreased by more than could be attributed to simple effects of buoyancy. It is possible that, as the rock backfill became saturated, it settled and stress relaxation occurred in a manner described by Nobari and Duncan (1972). Similar effects were observed for the wall friction measurements.

5. Underground Factory, Germany. Tschebotarioff (1973) described the earth pressures measured in 1942, on a 79-foot-deep basement wall of an underground factory building. As shown in Fig. X-5, the excavation around the building was backfilled with uncompacted clean sand. The angle of repose for the sand, when dry, was 34° . The pressures on the wall as measured about a year after completion of backfilling are shown in the figure. The at-rest pressure ($K_0 = 0.28$ line) was computed from Jaky's expression (Eq. IX-12) for a friction angle of 34° . The measured pressures are somewhat larger.

6. Highway US-59, Texas. Coyle, et. al, (1974) reported results from a research study conducted to determine lateral earth pressure for use in retaining wall design. Earth pressures on a 16-foot high, cantilever retaining wall were monitored for more than a year after the end of construction. The wall was constructed of cast-in-place concrete and supported by steel H-piles, as shown in Fig. X-6. The space between the wall and the clay embankment fill was back-filled with a slightly silty sand placed at a relatively high moisture content and lightly compacted. The friction angle of the sand, as determined by direct shear tests, was 32° . The graph in the lower part of Fig. X-6 shows that the measured horizontal pressures fluctuated with time, apparently seasonally. The lowest pressures were recorded during the winter and were about two-thirds of the

THIS PAGE IS BEST QUALITY PRACTICABLE
FROM COPY FURNISHED TO DDC

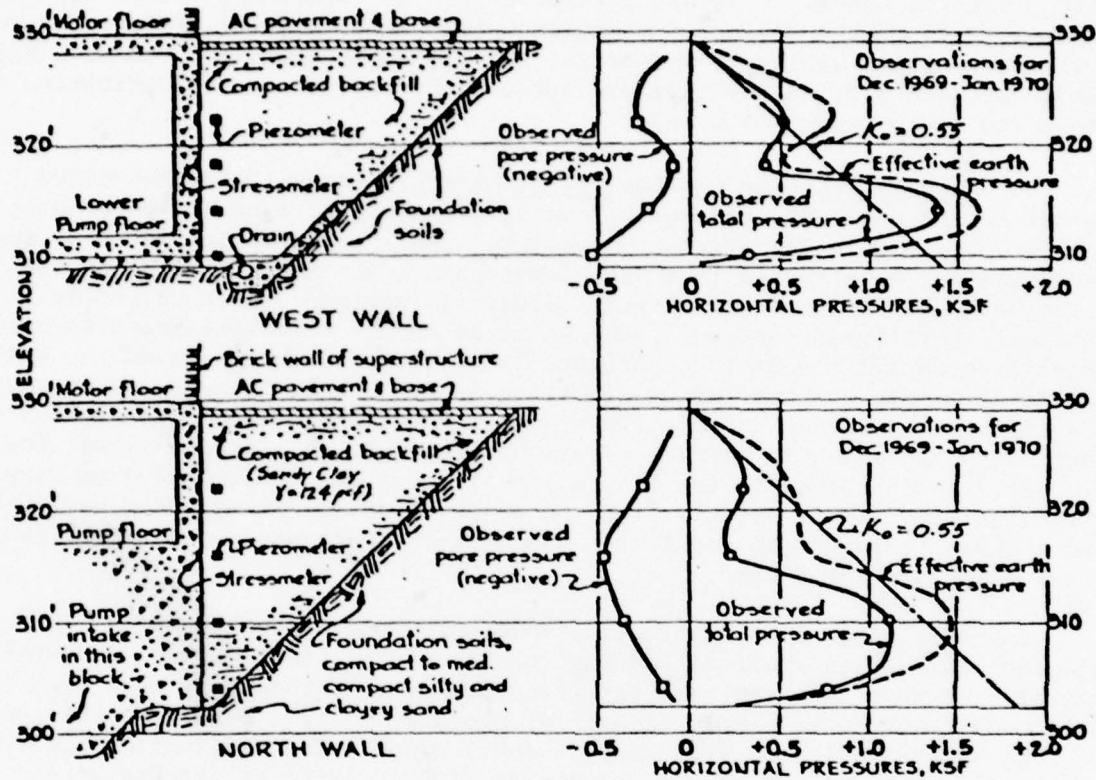
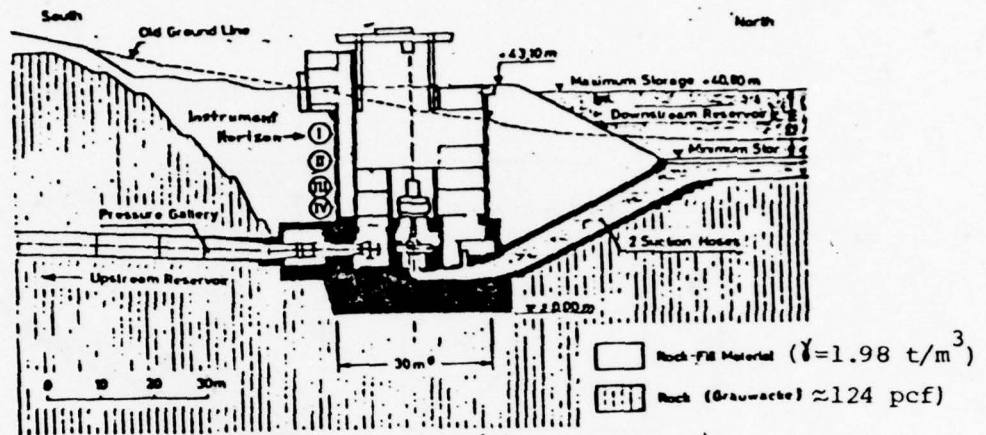


FIG. X-3 MEASURED PRESSURES ON SUBSURFACE WALLS, PLEASANT VALLEY PUMPING PLANT

(Gould, 1970)



North-South Cross-Section Through Powerhouse

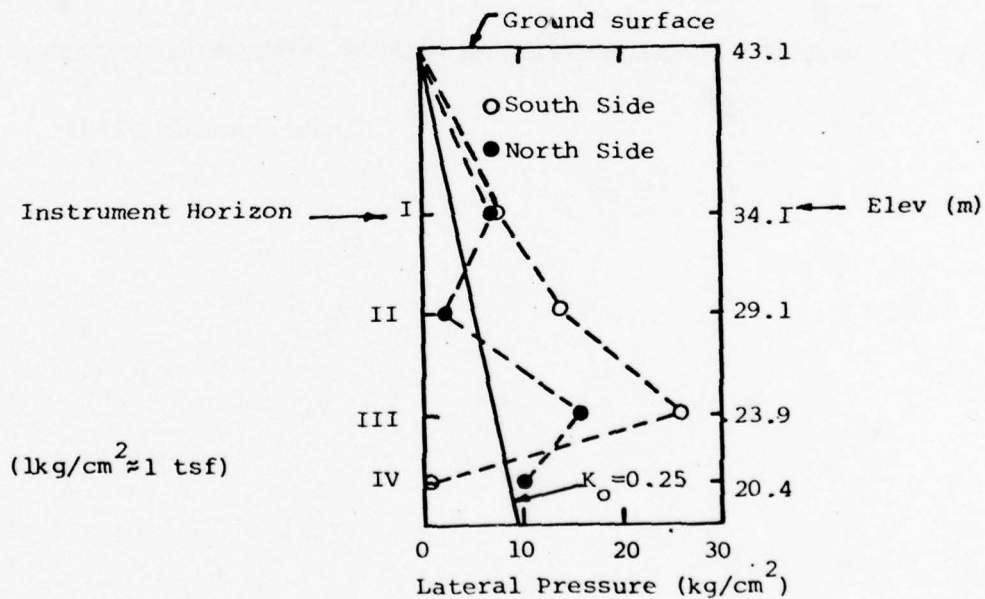


FIG. X-4 MEASURED EARTH PRESSURES ON NORTH AND SOUTH SIDES OF POWERHOUSE, ROENKHAUSEN PUMP STORAGE PLANT

(Kany, 1972)

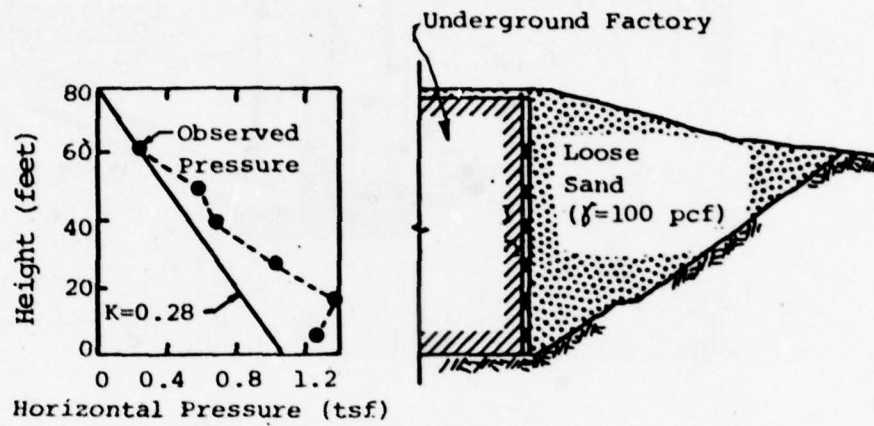
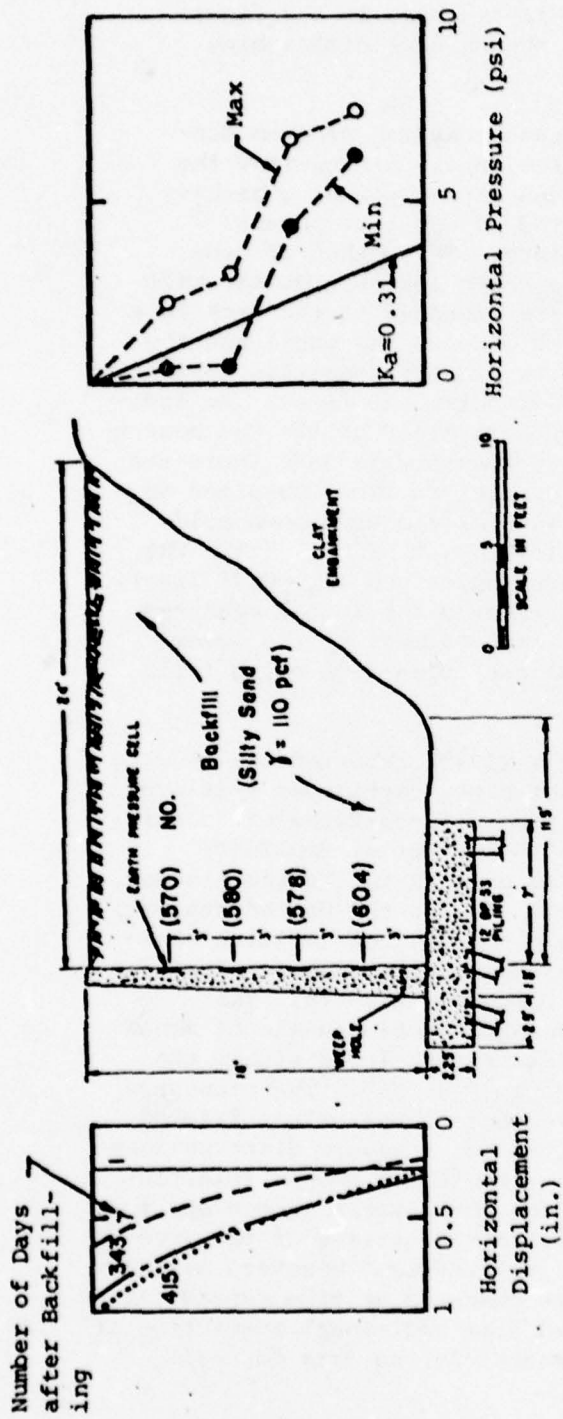


FIG. X-5 MEASURED EARTH PRESSURE ON WALL OF UNDERGROUND FACTORY

(Tschebotarioff, 1973)



Wall Displacement and Maximum/Minimum Measured Pressures

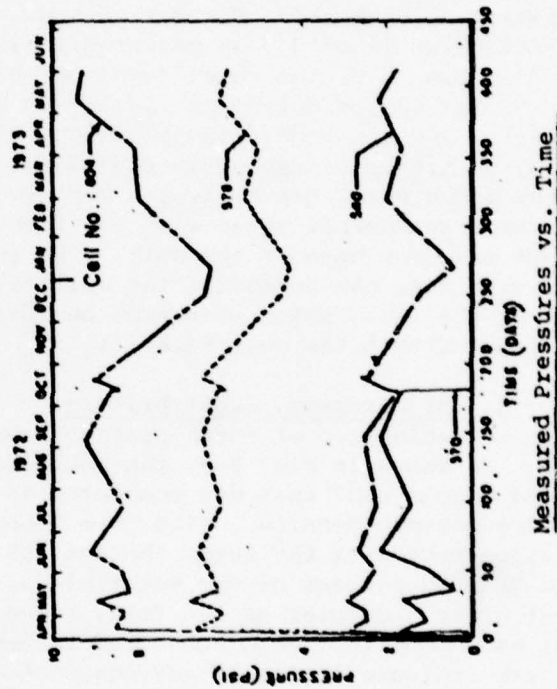


FIG. X-6 MEASURED EARTH PRESSURES AND WALL DISPLACEMENT, HIGHWAY US-59 RETAINING WALL (Coyle, et.al. 1974)

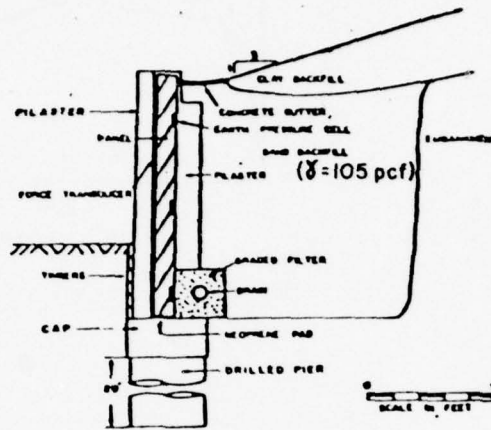
maximum summer values. The minimum and maximum pressures are compared with Rankine values ($K_a = 0.31$ line) in the upper part of the figure. The authors attributed the greater pressures near the base of the wall to the relatively small outward wall displacements that occurred there as shown in the figure. Note that the wall progressively tilted outwards, though at a diminishing rate, as time passed.

7. Highway US-290, Texas. As part of the same research program described in the preceding example, Coyle and Bartoskewitz (1976) reported the observations of a 10-foot-high retaining wall placed at the toe of a highway embankment. As shown in Fig. X-7 the wall consisted of concrete panels spanning between pilasters supported by drilled piers. The method of construction allowed the investigators to measure the earth forces upon the wall by two independent means. Earth-pressure cells were embedded in the back face of the wall panel and force transducers were placed between the panel and the pilasters at each end. The wall was backfilled with lightly compacted sand with a friction angle of 32° as measured in laboratory direct-shear tests. As indicated in Fig. X-8, the total force on the wall, as determined by the two measuring systems varied during the period in which measurements were made (more than a year). The apparent seasonal fluctuations are similar to those observed in the US-59 project, previously described. Wall pressures measured on a cold-winter and a warm summer day are compared in the lower part of Fig. X-8. The pressures reasonably agree with the theoretical Rankine values ($K_a = 0.31$ line), except near the base of the wall. The authors attributed the larger measured pressures near the bottom of the wall to insufficient movement of the lower part of the wall, which prevented an active stress condition from being fully developed within the soil backfill.

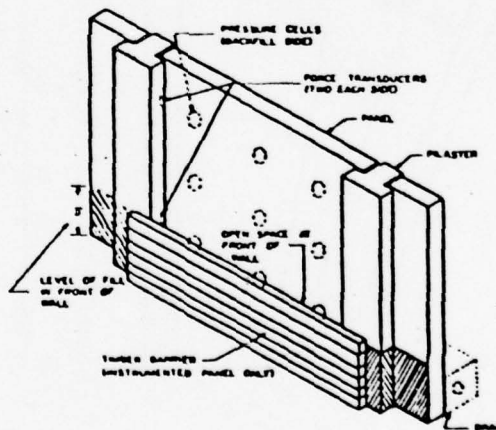
8. M1 Motorway, Great Britain. Sims, et al. (1970) reported the results of an investigation of earth pressures on a 40-foot-high, cantilever retaining wall. As shown in Fig. X-9, the backfill behind the wall consisted of "conditioned hopper ash" that was compacted to at least 95 percent of Modified-Proctor maximum density. (The term "hopper ash" as used in the United Kingdom, is synonymous with the terms "bottom ash" or "slag" used in the United States.) More than 80 percent of the material was finer than the No. 200 (British standard) sieve. Samples of the fill, taken from borings about two years after the wall was completed, were subjected to laboratory compression tests. The results indicate little if any cohesion and an average friction angle of about 26° . Horizontal earth pressures, measured by stress cells placed within the backfill about two feet behind the wall, are shown in Fig. X-9. The pressures increased dramatically with time; after four years some of the values tripled or quadrupled. Also shown in the figure are theoretical pressure distributions based on Rankine theory ($K_a = 0.22$ line) and on the results of simple (elastic) finite-element analysis (Sims and Jones, 1974). The theoretical values are in close agreement with each other and are moderately representative of the pressure measurements taken when the roadway was open to traffic. However, neither predicts the large increases in pressure that were observed as time passed. The authors believed that the large pressures resulted from additional compaction of the backfill by traffic using the roadway. Unfortunately, no data for wall deflections were reported.

9. M40 Motorway Bridge, Great Britain. Another example of a retaining wall with a compacted ash backfill was given by Symons and Wilson (1972). As

THIS PAGE IS BEST QUALITY PRACTICABLE
FROM COPY FURNISHED TO DDC



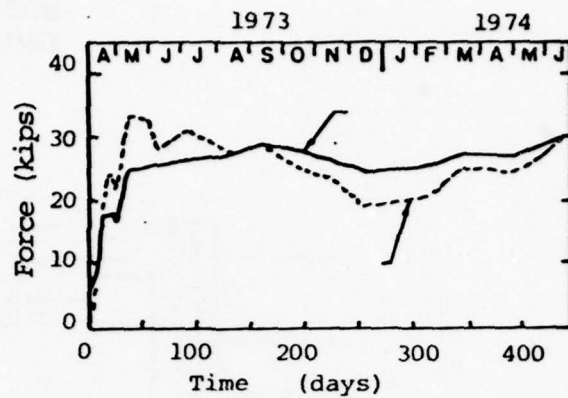
Cross Section of Test Wall



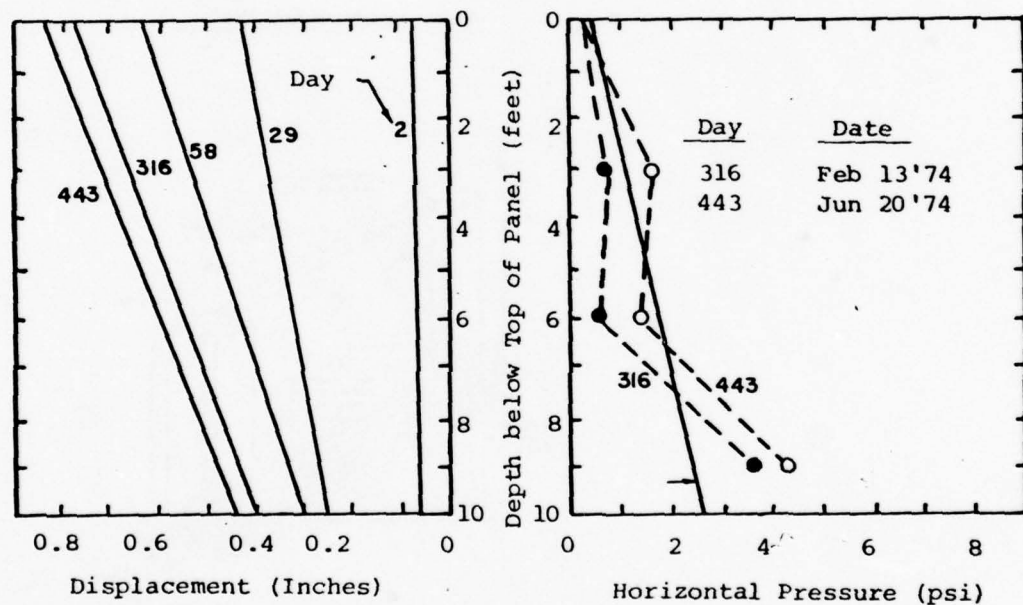
Front View of Wall Panel

FIG. X-7 TEST PANEL INSTALLATION, HIGHWAY US-290 RETAINING WALL

(Coyle and Bartoskewitz, 1976)



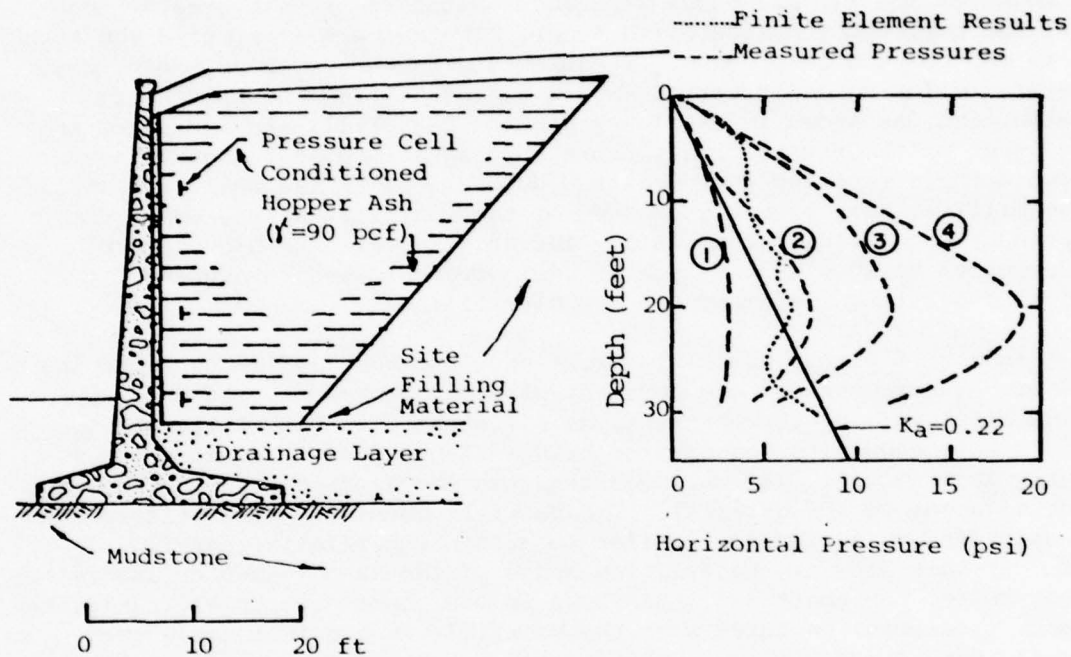
Measured Forces on Wall Panel vs. Time



Measured Wall Displacement and Earth Pressures at Various Times after Backfilling

FIG. X-8 MEASURED FORCES, DISPLACEMENTS AND EARTH PRESSURES, HIGHWAY US-290 RETAINING WALL

(Coyle & Bartoskewitz, 1976)



Measured
Pressures: 1-Feb 8 '68 (Initial Readings)
 2-Jun 12 '68 (Roadway opened
 to traffic)
 3-Jan 6 '71
 4-Aug 30 '72

(Note: Backfilling completed in April '67)

FIG. X-9 MEASURED EARTH PRESSURES, M1 MOTORWAY RETAINING WALL

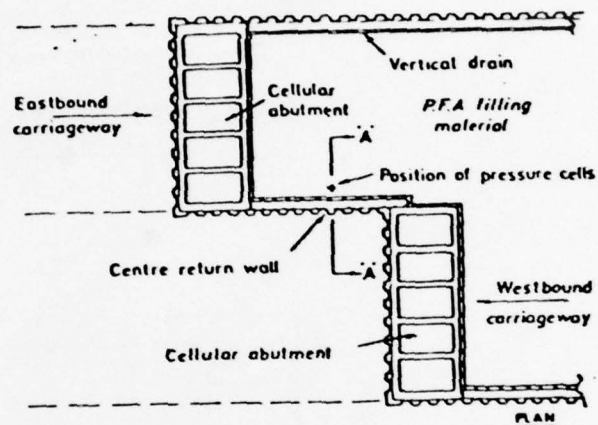
(Sims, et.al., 1970 & Sims & Jones, 1974)

shown in Fig. X-10, an 11-meter high cantilever retaining wall, which formed part of the abutment of a highway bridge, was instrumented with pressure cells to observe the earth pressures from the backfill. The backfill material was a pulverized, fuel ash compacted to 85 percent of the maximum dry density (2-1/2 kg Rammer Method of British Standards Institution, 1967). Laboratory tests on compacted samples of the fuel ash showed significant pozzolanic action. At an age of 56 days, undrained triaxial compression tests indicated an apparent cohesion of about 2000 psi and a friction angle of 35°. The results of pressure measurements made during backfilling are shown in the upper part of Fig. X-11. For the first few feet of fill placed above each cell, the measured lateral pressures were about equal to or even greater than the theoretical overburden pressure (γH line). The authors attributed the high pressures to the compaction process. Measurements taken over a period of more than two years following construction showed a general trend of increasing pressure with time, as shown in the lower part of Fig. X-11. As indicated in the figure, some of the fluctuations in pressure appear to be seasonal in nature. The authors reported that measured deflections of the wall were small (one or two millimeters), probably because of the restraint at the ends of the wall provided by the cellular abutments. The authors felt the high lateral pressures occurred because of the lack of wall movement which prevented mobilization of shearing resistance in the backfill.

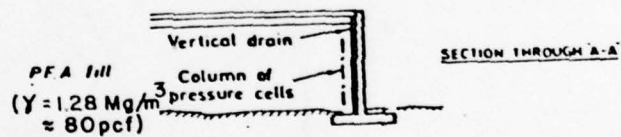
10. Highway E4 Bridge, Sweden. Broms and Ingelson (1971) described the earth pressure measurements on one abutment of a 500-foot-long, rigid-frame bridge. The front wall of the abutment, as illustrated in Fig. X-12, was designed to rotate about its base as the bridge slab expanded and contracted with changing temperature. The wall was designed for Rankine passive pressures on the face adjacent to the backfill. The backfill consisted of a uniform sand which was compacted by a vibratory roller to an average relative density of 82 percent. At this density the friction angle of the sand, based on laboratory direct shear tests, was about 33°. As shown in the upper part of Fig. X-13, the initial earth pressures, measured when the backfill was two feet above each pressure cell, were quite high and exceeded the overburden pressure. Later pressures, corresponding to additional heights of fill, did not necessarily increase. For comparison, lines corresponding to the theoretical overburden pressure and to Rankine active (K_a) and passive (K_p) values are included in the figure. After the bridge was completed, the earth pressures varied as the bridge slab expanded and contracted against the wall, as shown in the lower part of Fig. X-13. The authors found that, when the wall rotated outwards about $H/1000$ (where H is the height of the wall), the pressures approached Rankine active values. When the wall rotated inwards about $H/600$, the pressures were approximately equal to Rankine passive values.

11. Highway 922 Bridge, Sweden. Ingelson (1972) also reported the earth pressures measured on an abutment of a 110-meter-long reinforced-concrete frame bridge. As shown in Fig. X-14, the front wall of the abutment is hinged along the lower edge at the bottom slab and fixed along the upper edge at the bridge slab and longitudinal beams. The backfill material behind the wall consists of sands and gravels which were lightly compacted by a vibratory roller (relative densities of about 60%). In the lower part of Fig. X-14, the earth pressures measured at four stages of back-filling are shown to have increased with increasing height of backfill. This is in contrast to the measurements at the

THIS PAGE IS BEST QUALITY PRACTICABLE
FROM COPY FURNISHED TO DDC



0 10 20 m



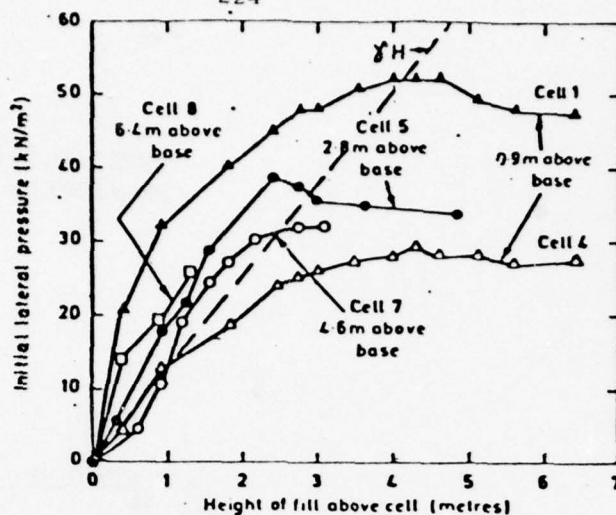
(P.F.A.=Pulverized Fuel Ash)

FIG. X-10 RETAINING WALL DETAILS, M40 MOTORWAY BRIDGE

(Symons & Wilson, 1972)

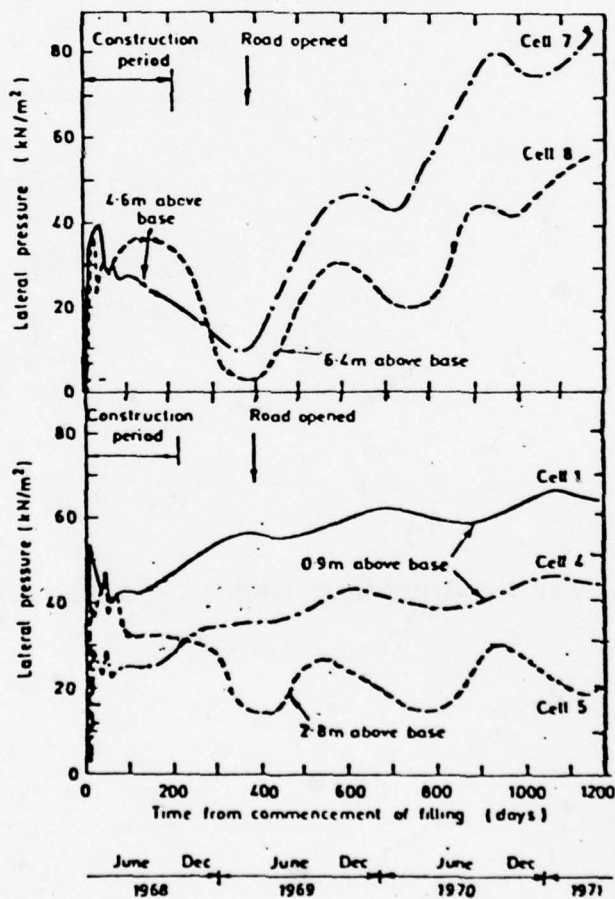
THIS PAGE IS BEST QUALITY PRACTICABLE
FROM COPY FURNISHED TO DDC

224



Average Lateral Pressures During the
First Period of Filling

(1kN/m^2
 $\approx 0.01\text{ tsf}$)



Measured Pressures vs. Time

FIG. X-11 MEASURED EARTH PRESSURES ON RETAINING WALL, M40 MOTORWAY BRIDGE
(Symons and Wilson, 1972)

THIS PAGE IS BEST QUALITY PRACTICABLE
FROM COPY FURNISHED TO DDC

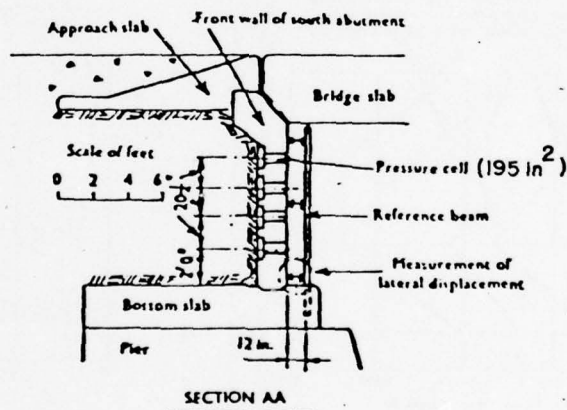
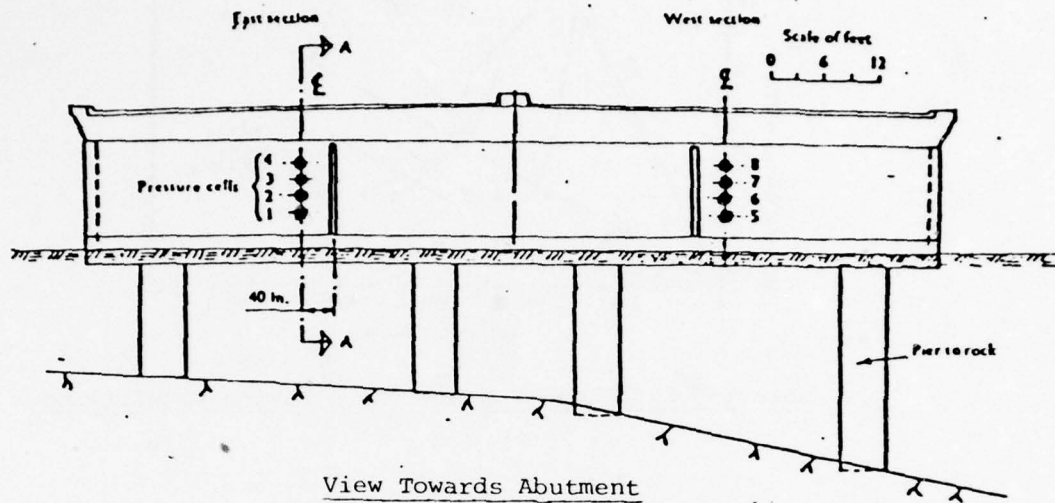
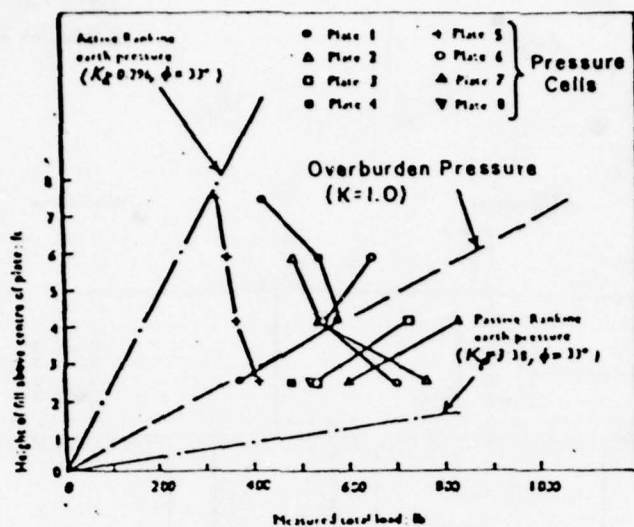
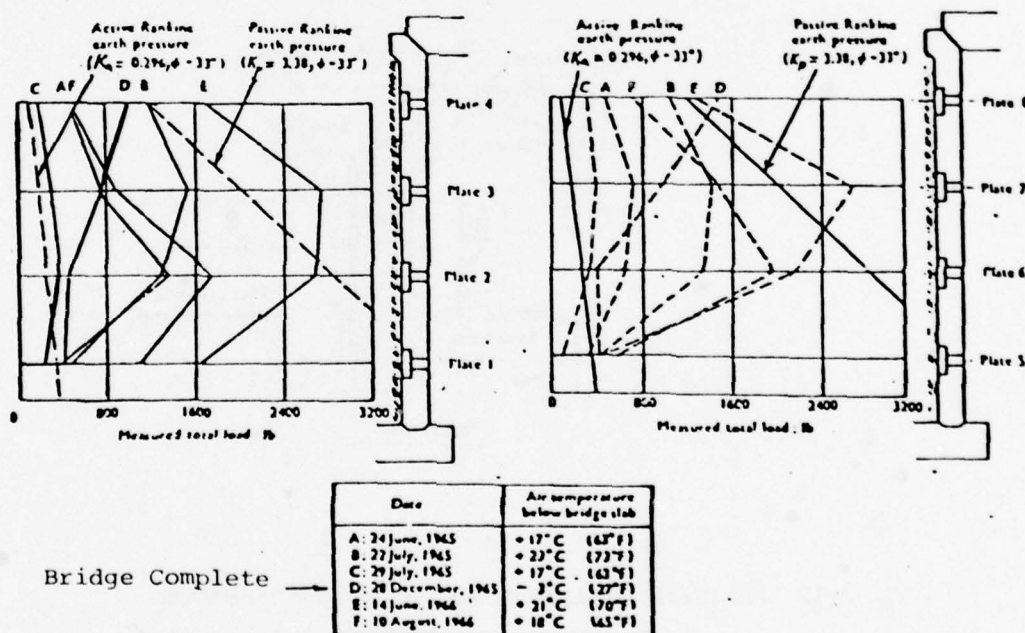


FIG. X-12 ABUTMENT WALL DETAILS, HIGHWAY E4 BRIDGE
(Brons & Ingelson, 1971)



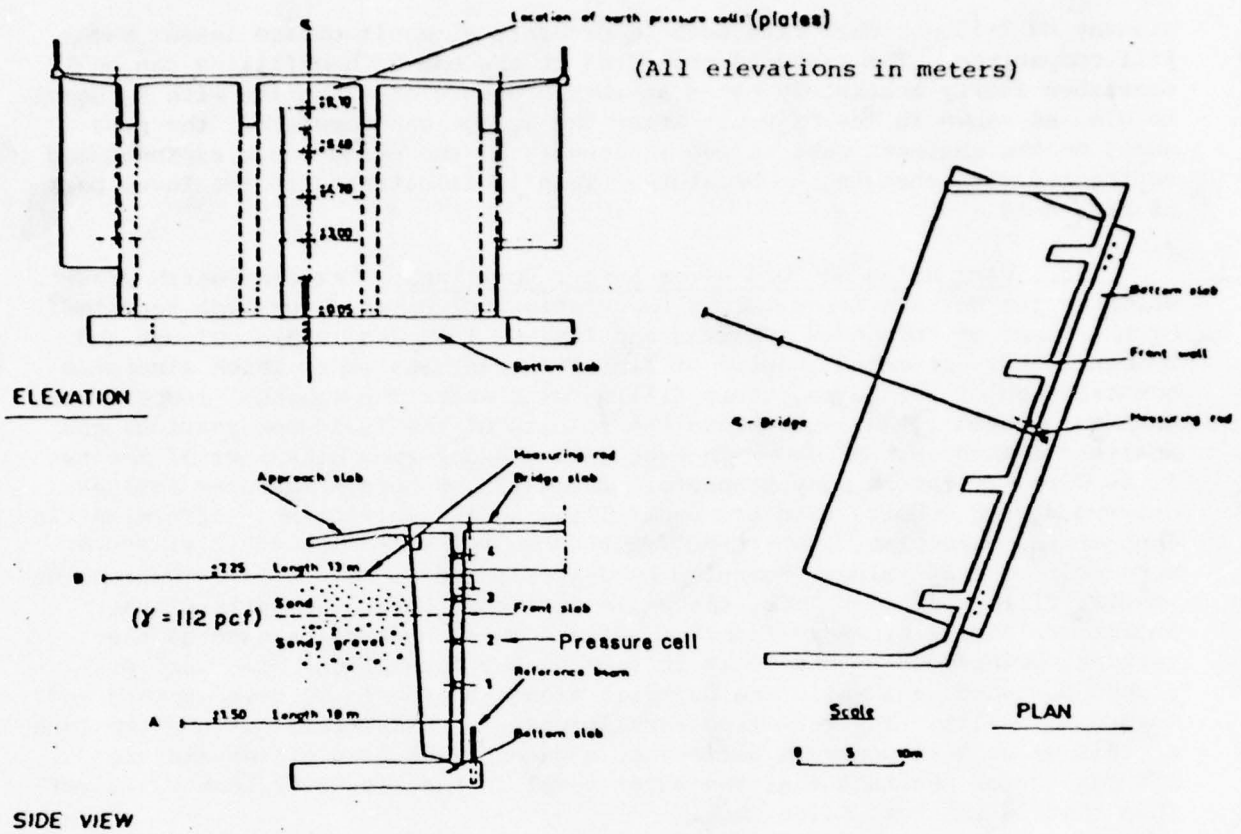
Measured Loads on Pressure Cells During Backfilling



Distribution of Measured Loads on Pressure Cells after Backfilling

FIG. X-13 PRESSURE-CELL MEASUREMENTS ON ABUTMENT WALL, HIGHWAY E4 BRIDGE

(Broms & Ingelson, 1971)



Details of Abutment Wall

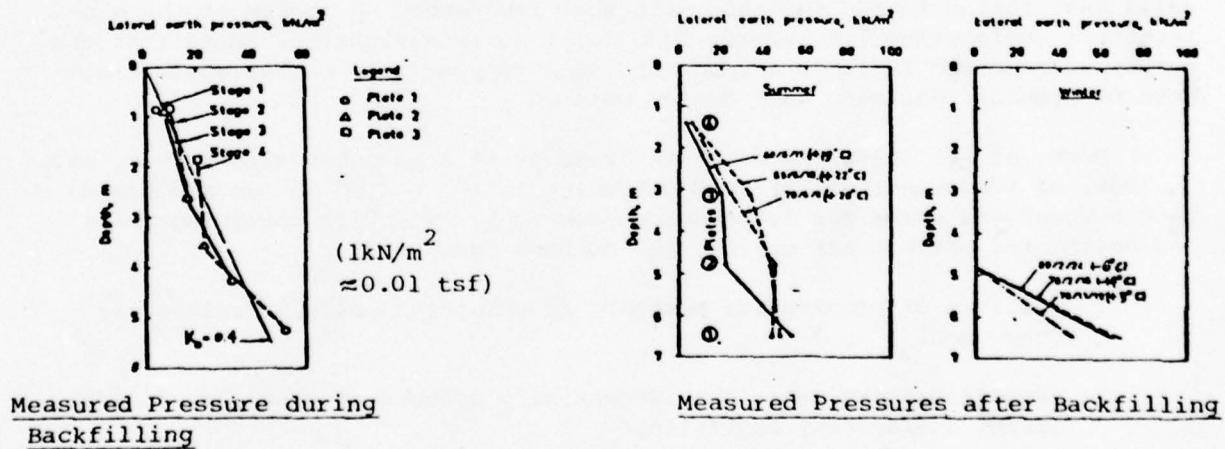


FIG. X-14 PRESSURE MEASUREMENTS ON ABUTMENT WALL, HIGHWAY 922 BRIDGE

(Broms & Ingelson, 1972)

Highway E4 Bridge. The difference is probably a result of the lesser backfill compaction. The measured pressures at the end of backfilling can be described fairly accurately by an at-rest pressure distribution with K_0 equal to 0.4, as shown in the figure. After the bridge was completed, the pressures on the abutment were varied seasonally as the bridge deck expanded and contracted with changing temperature. This is illustrated in the lower part of Fig. X-14.

12. Port Allen and Old River Locks, Louisiana. Measured earth pressures on two U-frame locks, along the Mississippi River, have been reported by the Corps of Engineers (Sherman and Trahan, 1968 and 1969). Clough and Duncan (1969) presented results of finite-element analyses, which simulated construction of the locks, their filling with water and seasonal temperature changes. Gould (1970) summarized the results of the field observations and analytical studies. As shown in Fig. X-15 the observed behaviour of the two locks were similar in many respects. The walls of both structures rotated outward during construction and backfilling as a result of non-uniform settlement of the base slab. Consequently the measured effective earth pressures were near at-rest values (computed by Jaky's formula, Eq. IX-12). During the initial filling of each lock, the walls deflected inward in spite of the increased lateral pressure from the water. This occurred because as the vertical water load on the locks increased, the foundation soils were displaced downward, and while the backfill alongside the locks moved upward and toward the walls. The resulting earth pressures on the walls of the two locks at this stage were somewhat different, apparently because of temperature effects and/or the fact that the water level in the Old River lock was lower than that in the Port Allen lock.

B. Retaining Wall Failures

To place the question of the prediction of earth pressures on retaining walls in its proper perspective, it is desirable to consider how retaining walls have failed in the past and with what frequency. A review of the geotechnical engineering literature, made for this investigation, found that the number of reported failures are few and thus support the general appropriateness of present retaining wall design methods.

Peck, et al. (1948) reported the results of a questionnaire survey, made in 1945, of the principal railroad companies in the United States and Canada. Each company was asked for information about unsatisfactory retaining walls and abutments. From their survey, the authors concluded:

1. Failure or progressive movement of retaining walls is relatively uncommon,
2. Unsatisfactory behaviour is generally associated with clay foundations and/or clay backfills,
3. It is doubtful that traffic vibrations in granular backfills are of serious importance, and
4. Unsatisfactory behaviour is caused primarily by designer's misjudgment of foundation conditions.

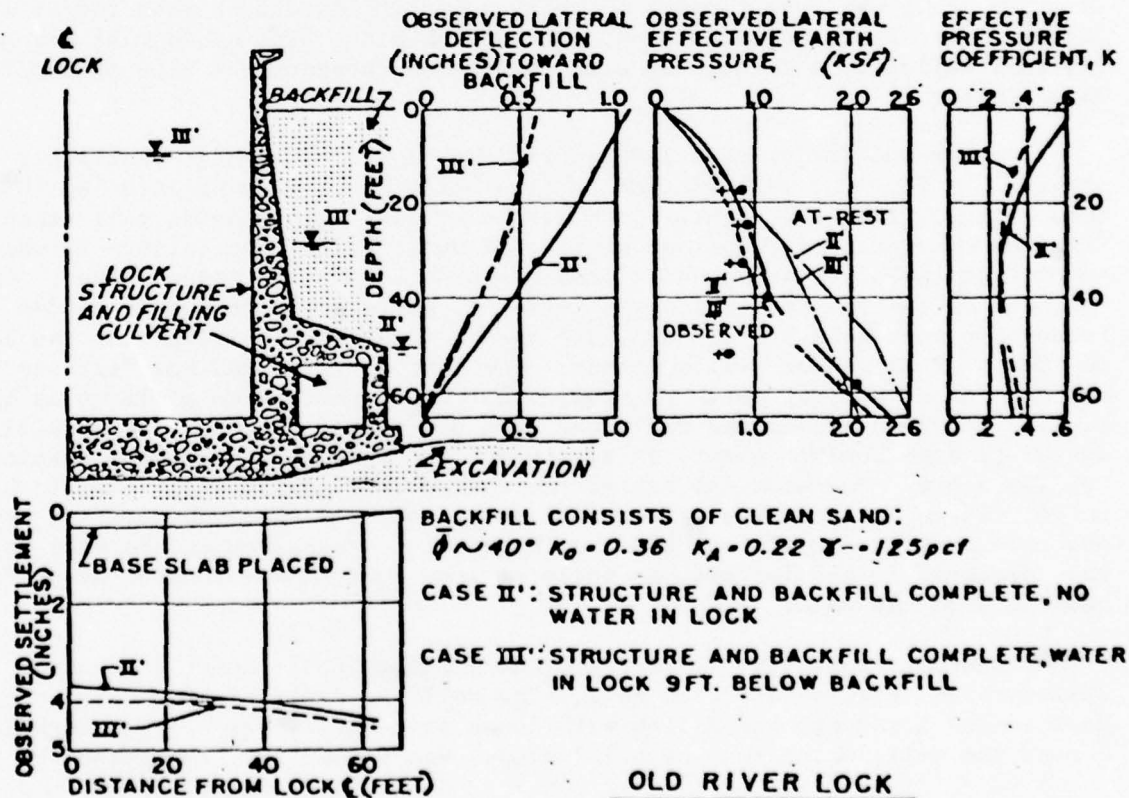
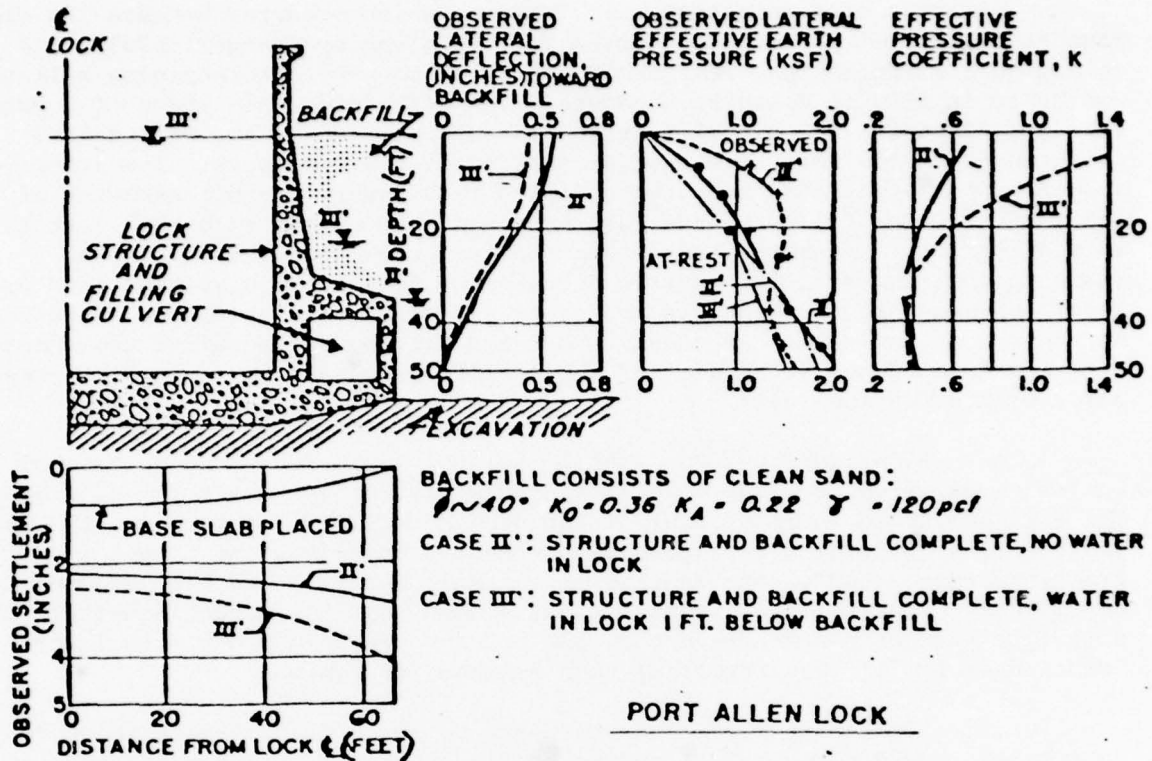


FIG. X-15 MEASURED DEFLECTIONS AND EARTH PRESSURES, PORT ALLEN AND OLD RIVER LOCKS

(Gould, 1970)

An example of a retaining wall failure, which occurred because its clay foundation was not properly accounted for, is given by Granger (1965). He described a 23-foot-high, reinforced-concrete, counterfort retaining wall that was built in 1960 in Southern Rhodesia. The wall formed the sides of a water-storage reservoir, 287 by 247 feet in plan. A portion of the wall failed about three months after the initial filling of the reservoir. Investigations showed that the wall had been founded on a thin layer (18-inches-thick) of gravel fill. The fill was underlain by a variably weathered gabbro. At the failed section, the gabbro had decomposed to a weak silty clay. It was reasoned that the failure occurred because the foundation clay, softened by water leaking through joints in the reservoir floor slab, had been overstressed at the toe of the wall. Progressive outward tilting had occurred and eventually water penetrated below the heel of the wall footing and, by its uplift pressure, overturned the wall.

James (1965) reported the 1958 failure of a 310-foot-long section of a 60-foot-high, L-shaped, concrete retaining wall, located in Portland, Oregon. The wall collapsed shortly after it had been backfilled. Apparently the wall had been designed for a Rankine active pressure corresponding to a soil friction angle of 40° . The density of the soil backfill had been assumed to be 110 pcf. Post-failure investigations showed that the actual backfill (the soil type was not reported) weighed 150 pcf and probably had a much lower friction angle (11° was reported) than assumed for design.

Brand and Kraesin (1971) reported the failure of a 2.5-meter-high concrete cantilever retaining wall that supported the flanks of a road embankment in Thailand. The wall was founded on short wooden piles driven into the stiff weathered crust of the underlying, soft Bangkok clay. The embankment and retaining wall failed by a rotational slip that passed beneath the tips of the foundation piles.

Casagrande (1973) reported the failure of a 23-foot-high cantilever retaining wall. The wall was one of five being built on a hillside up to more than 100 feet in height. Each was backfilled with glacial till taken from the excavation for another section of wall. After the failure it was noted that the other walls had tilted outwards as much as seven inches. Because the base of the failed section was perfectly horizontal, it was concluded that foundation instability could not have been a cause of the failure or the large movements of the other wall sections. The author attributed the distress to the development of at-rest earth pressures that were about twice as large as the active values for which the walls had been designed. Although the backfill contained some boulder sizes, it also had between 30 and 40 percent passing the No. 200 sieve. The backfill behind the failed wall section was found to be saturated. It appears to this writer that it is possible that the backfill might not have been free-draining, and that hydrostatic pressures on the wall could have assisted in its failure, in spite of some drainage provisions along the back-face of the wall.

Tschebotarioff (1973) described the bulging of the upper portion of a 34-foot-high, double-cell crib wall. The wall was built of precast-concrete headers and stretchers and filled with loose granular material. The backfill behind the wall, which rose on a 12° slope, was compacted. The author

reasoned that the observed distress probably resulted from an increase in active pressure on the back of the wall caused by downward settlement of the wall with respect to the backfill and a corresponding change in wall friction from a positive to a negative value. The unusual relative settlement between wall and backfill was attributed to an overload of the foundation below the heel of the wall.

CHAPTER XI

ANALYTICAL AND EXPERIMENTAL STUDIES OF EARTH PRESSURES ON RETAINING WALLS

In this chapter various theories for predicting earth pressures on retaining walls are considered in the light of analytical and experimental data. The purpose is to assess the differences between the various theories and the degree to which the theories are supported by experience. In addition, consideration is given to factors such as wall movement and backfill compaction, which influence the applicability of the theories to retaining-wall design.

A. Active Earth Pressures

1. Comparison of Theories. Because there are quite a number of earth-pressure theories that can be used for design, it is helpful to determine difference in magnitudes of active pressure, for a variety of wall and backfill conditions, which are predicted by the theories. Morgenstern and Eisenstein (1970) showed that for the theories which take wall friction into account, there is less than ten percent difference in calculated values of the horizontal component of active earth pressure for the case of a vertical wall, a horizontal (cohesionless) backfill and positive angles of wall friction between ϕ and $\phi/2$, as illustrated in Fig. XI-1. The figure also shows that for these wall and backfill conditions, Rankine's theory to which the other values have been normalized, is generally conservative by 10 to 20 percent.

For the same conditions, but with negative wall friction, the differences between theories for which solutions are published, excluding Rankine's, are significant only for large values of wall friction (Fig. XI-2). Rankine's theory, which does not take wall friction into account is unconservative but significantly so only at large negative values of wall friction.

Fig. XI-3 shows comparisons for the case of a sloping (cohesionless) backfill. The Rankine values are those computed from Eq. IX-4, which apply to a level backfill. True Rankine values--for a sloping backfill--could have been calculated, but for consistency in all the comparisons that have been made, the "level-backfill" values which are familiar to most practicing engineers have been used. The figure shows that when the slope of the backfill equals the friction angle of the backfill soil, the active pressures are quite large. However, the differences between the various theories that include wall friction are not large. Rankine's level backfill theory considerably underestimates the active pressures for a steeply sloping backfill.

The case of a wall with a sloping back is considered in Fig. XI-4. For a wall inclined into the backfill ($\beta = 75^\circ$), there is virtually no difference between the theories that consider wall friction. Rankine values are conservative, particularly at large values of ϕ . For the wall inclined away from the backfill ($\beta = 120^\circ$), Coulomb's theory gives the highest values

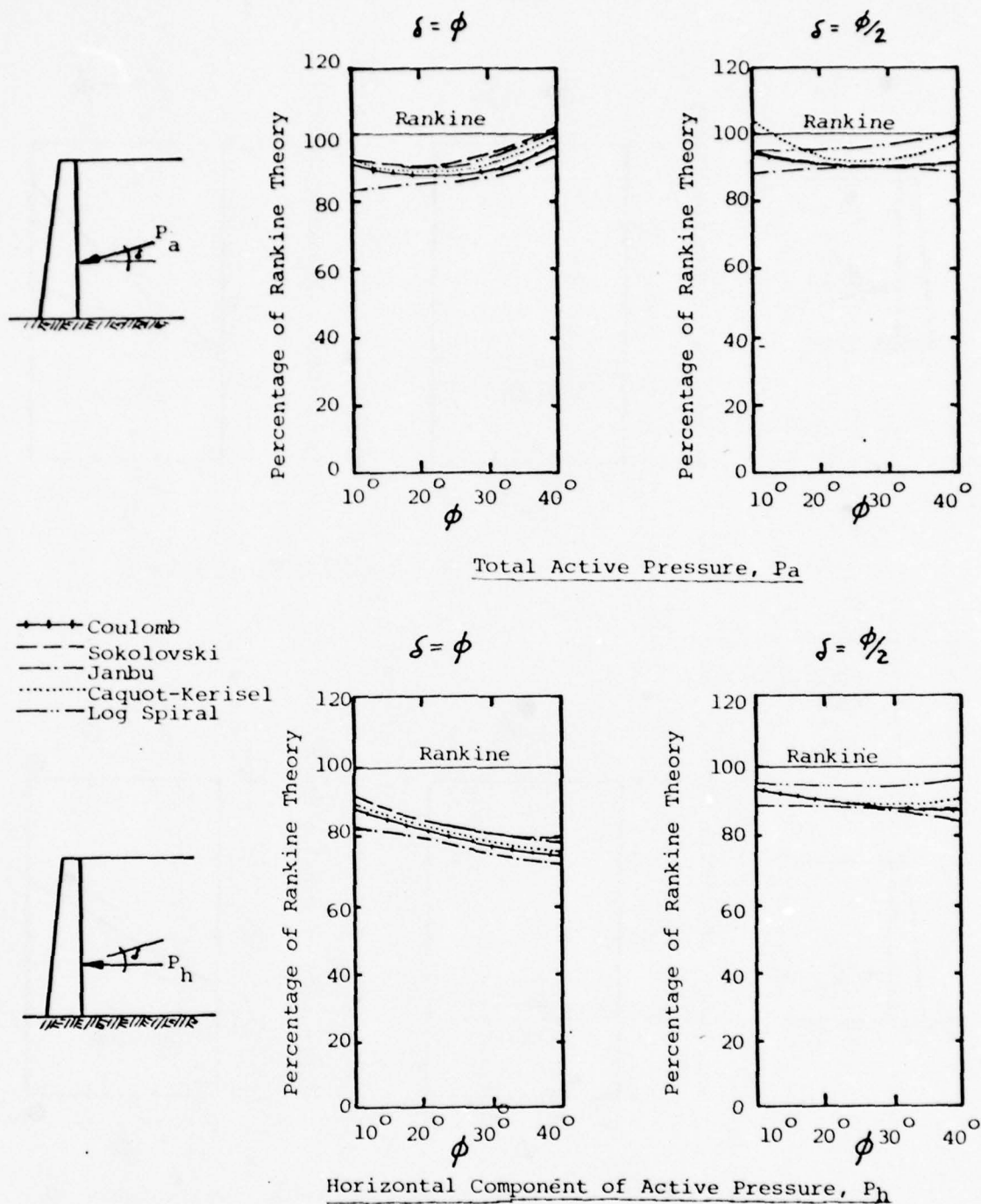


FIG. XI-1 COMPARISON OF COEFFICIENTS OF ACTIVE PRESSURE FOR VARIOUS THEORIES, POSITIVE WALL FRICTION

(Morgenstern and Eisenstein, 1970)

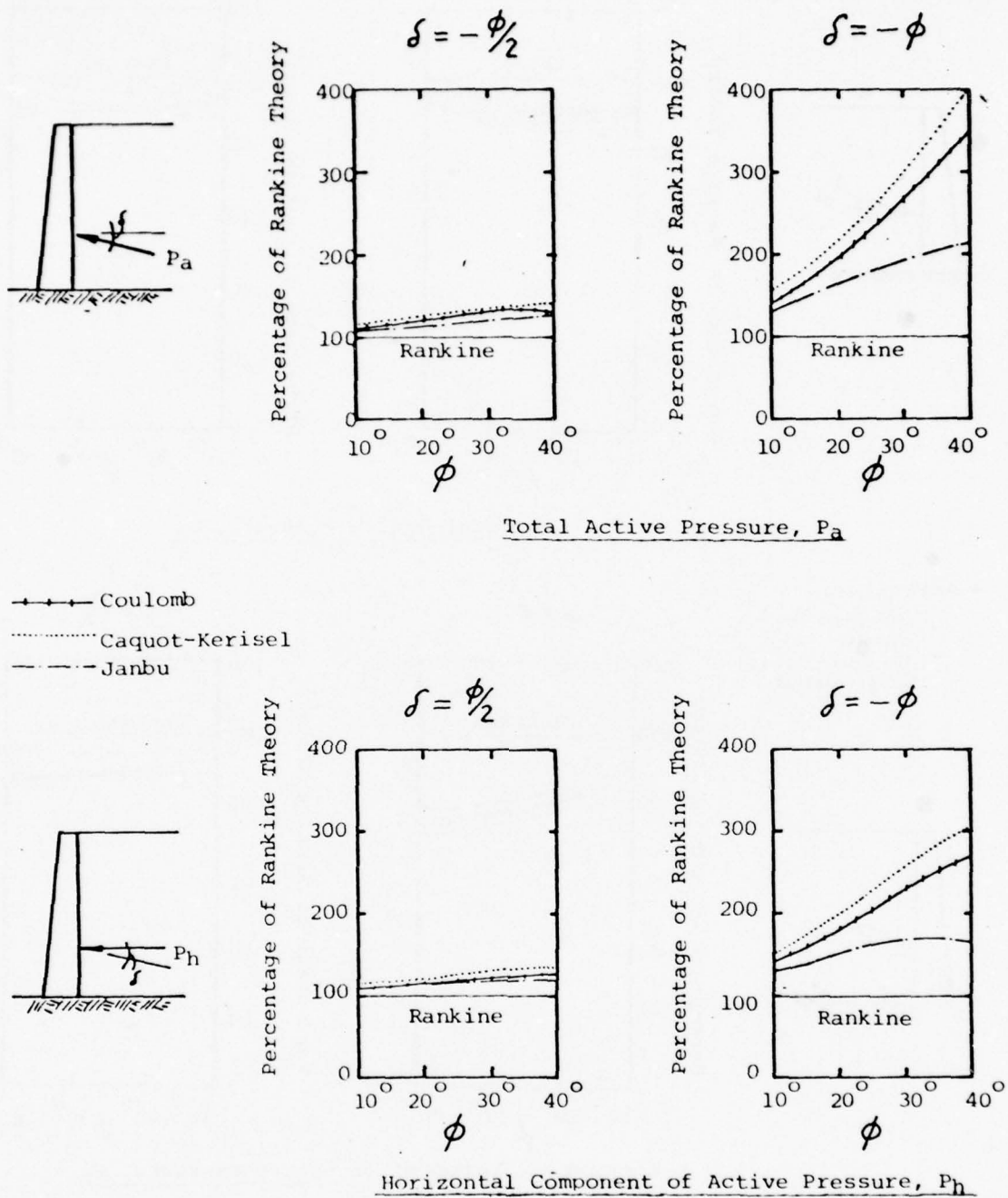
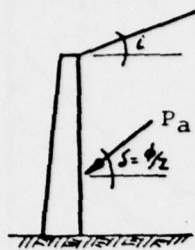
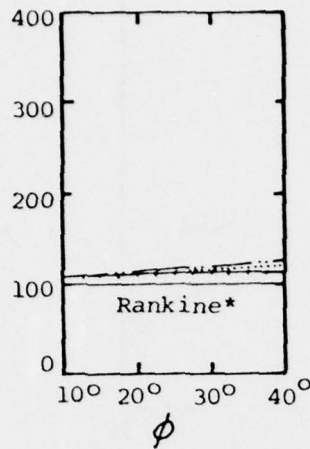


FIG. XI-2 COMPARISON OF COEFFICIENTS OF ACTIVE PRESSURE FOR VARIOUS THEORIES, NEGATIVE WALL FRICTION



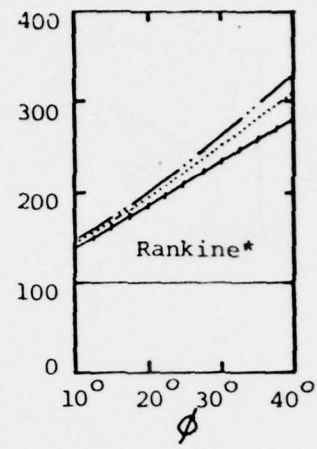
Percentage of Rankine Theory

$$i = \phi/2$$



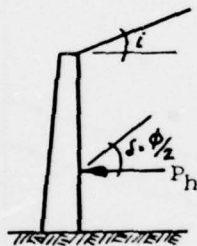
Percentage of Rankine Theory

$$i = \phi$$

Total Active Pressure, P_a

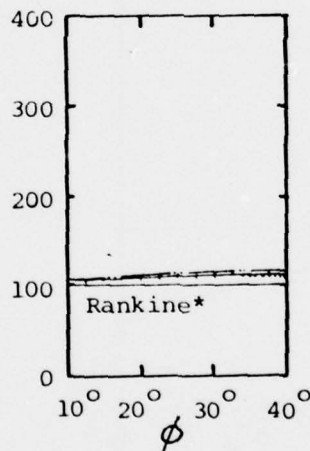
+++++ Coulomb
 --- Log Spiral
 Caquot-Kerisel

*Level Backfill



Percentage of Rankine Theory

$$i = \phi/2$$



Percentage of Rankine Theory

$$i = \phi$$

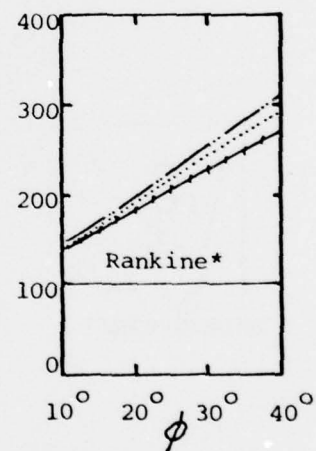
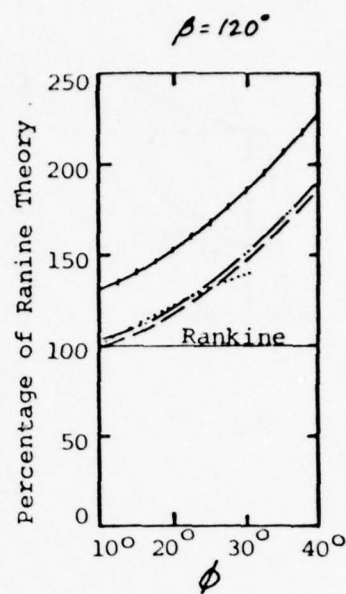
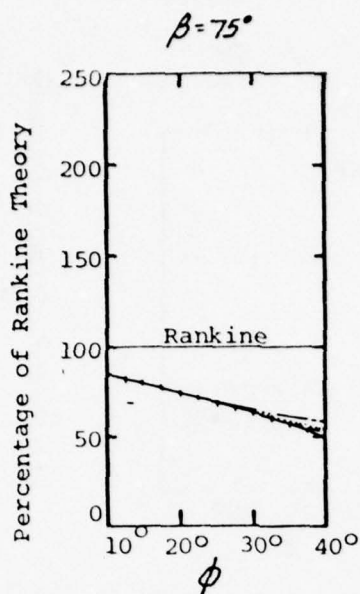
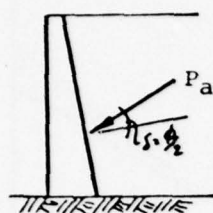
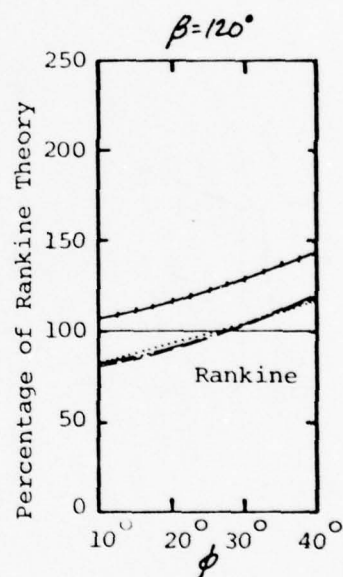
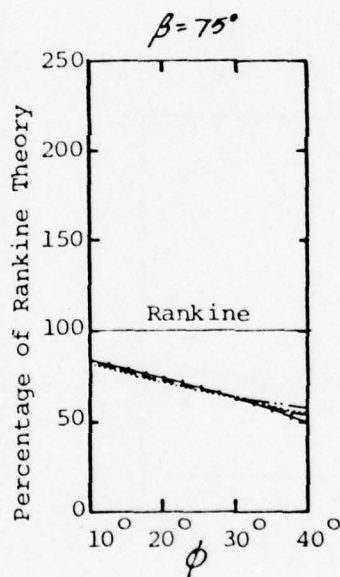
Horizontal Component of Active Pressure, P_h

FIG. XI-3 COMPARISON OF COEFFICIENTS OF ACTIVE PRESSURE FOR VARIOUS THEORIES, SLOPING BACKFILL



- +—+—+— Coulomb
- — — — — Log-Spiral
- Caquot-Kerisel
- - - - - Sokolovski

Total Active Pressure, P_a



Horizontal Component of Active Pressure, P_h

FIG. XI-4 COMPARISON OF COEFFICIENTS OF ACTIVE PRESSURE FOR VARIOUS THEORIES, WALL WITH SLOPING BACK FACE

of active earth pressure. Rankine's theory is in reasonable agreement with the values of horizontal component of active pressure calculated by the other theories, except for Coulomb's which gives earth pressures that are consistently larger than the Rankine values.

The comparisons shown in Figs. XI-1 through XI-4 did not include all possible wall and backfill conditions. However, the specific cases studied do represent a wide range of conditions which encompass most of those encountered in practice. For these conditions, the differences in theoretical active pressures, computed from theories that include wall friction are not large. Coulomb's theory is undoubtedly sufficiently accurate for design purposes. Rankine's simple theory (Eq. IX-4) gives values of the horizontal component of active pressure that are often close to or more conservative than those computed by the more correct theories. Only for conditions of negative wall friction or sloping backfills does Rankine's theory give unconservative values.

2. Comparison of Theory with Experimental Data. An interesting result of the literature review performed for this investigation was the finding that so few experimental studies of active earth pressures on retaining walls have been published. The following publications describe studies of considerable general interest.

a. Terzaghi (1940) described the results of laboratory tests on a five-foot-high wall which could be rotated or translated in a controlled manner after backfilling. Both loose and dense dry sand backfills were used. The horizontal and vertical components of the total active earth pressure and their point of application on the wall were determined for each test.

b. Jansson, et. al. (1948) presented results of their laboratory tests on a two-meter-high retaining wall that was backfilled with loose crushed stone or gravel. The flexibility of the wall which controlled the amount of rotation during backfilling was made comparable to that of field installations. Measurements were made only of the deflections of the wall and the overturning moment caused by the backfill. Earth-pressure coefficients could be estimated by assuming a triangular pressure distribution.

c. Rowe (1969a) reported the results of laboratory tests on a 1.5-meter-high wall that could be translated, after backfilling, in any prescribed direction in the plane of the model. Tests were performed for loose and dense dry sands. Active pressures and wall friction values could be determined from the measurements made for each test.

d. Matteotti (1970) described active-pressure laboratory tests performed on a one-meter-high wall. The tests were performed using submerged loose sand backfill. The wall was allowed to rotate after the backfill was placed. Active earth pressures and values of wall friction were measured in each test.

e. Rehman and Broms (1972) reported their field tests on a full-size, 2.5-meter-high, concrete retaining wall. Two backfill materials, a gravelly sand and a silty fine sand at field moisture contents were placed behind the wall in both loose and compacted conditions. For the loose soil tests, the

wall was allowed to rotate outwards after backfilling in order to reduce the earth pressures to minimize active values.

It is important to note that the experimental studies considered the simple case of a vertical wall with a horizontal cohesionless backfill. Even for these conditions most of the experimental data cannot be directly compared with existing earth pressure theories because of uncertainty as to the friction angle of the backfill material. Either the friction angle was not determined or the reported values were based on angle of repose, direct shear or triaxial compression tests. Only Rowe's data include the results of plane-strain compression tests. For the other test reports, the relationships given by Rowe (1969b), relating friction angles determined by various test methods, have been used to estimate plane-strain values of ϕ . Based on these estimates the reported value of horizontal component of active earth pressure, K_h , are compared in Fig. XI-5, with theoretical values according to Coulomb and Rankine. The experimental data generally agree with the theoretical values in that the measured values of K_h are smaller for the larger values of ϕ .

One other comparison can be made using Rowe's data for translating walls. In Fig. XI-6, results of two tests with positive and negative wall friction are compared with theoretical values according to Coulomb. Though numerical agreement is only fair, the trend of the data confirms the theoretical prediction of higher active earth pressures for negative values of wall friction.

Rowe (1969a) showed that much of the variation of experimental results from theoretical predictions could be explained in terms of progressive failure--caused by non-uniform shear strains within the backfill behind a retaining wall. Particularly for dense sands, he found that the average friction angle in the soil mass at the point of overall wall failure was less than the peak friction angle. He proposed a progressivity index, r , which could be used to determine the average value of ϕ , as follows:

$$r = \frac{\phi_{ps} - \phi_{mass}}{\phi_{ps} - \phi_{cv}} \quad (XI-1)$$

where

ϕ_{ps} = peak friction angle as determined by plane-strain compression tests

ϕ_{mass} = average value of friction angle in the soil mass to fit current failure theory

ϕ_{cv} = critical-state value of friction angle for the given normal pressure (i.e., friction angle at large shear strains)

Based on his tests he recommended values of r , for active pressure calculations equal to 1.0 for loose sands and 0.4 for medium to dense sands.

3. Wall Movements. There are no general theoretical procedures for

(rep=angle of repose;ps=plane-strain; triax=triaxial;ds=direct shear)

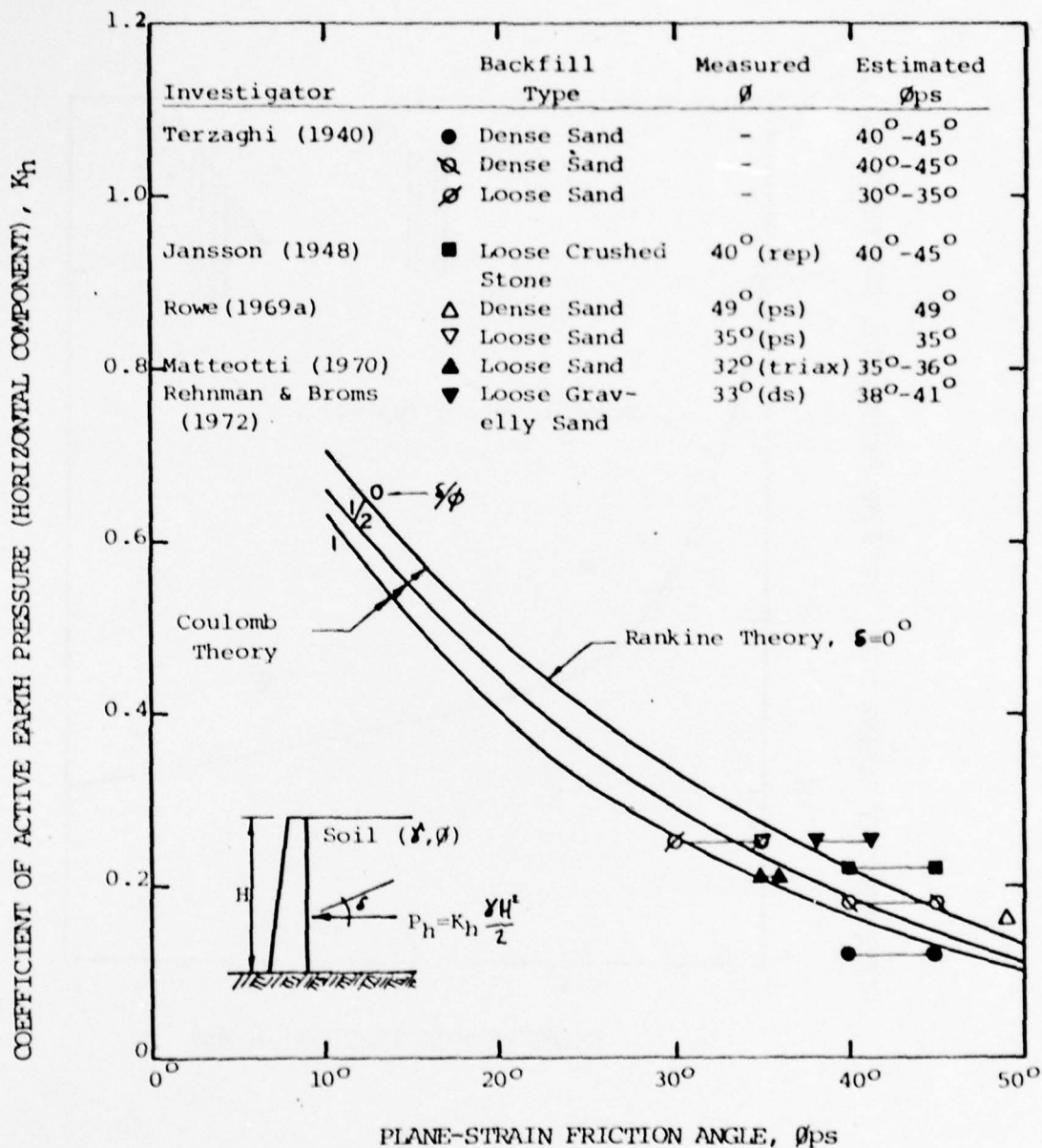


FIG. XI-5 COMPARISON OF COEFFICIENTS OF ACTIVE EARTH PRESSURE (HORIZONTAL COMPONENT) FOR VARIOUS EXPERIMENTAL INVESTIGATIONS, POSITIVE WALL FRICTION.

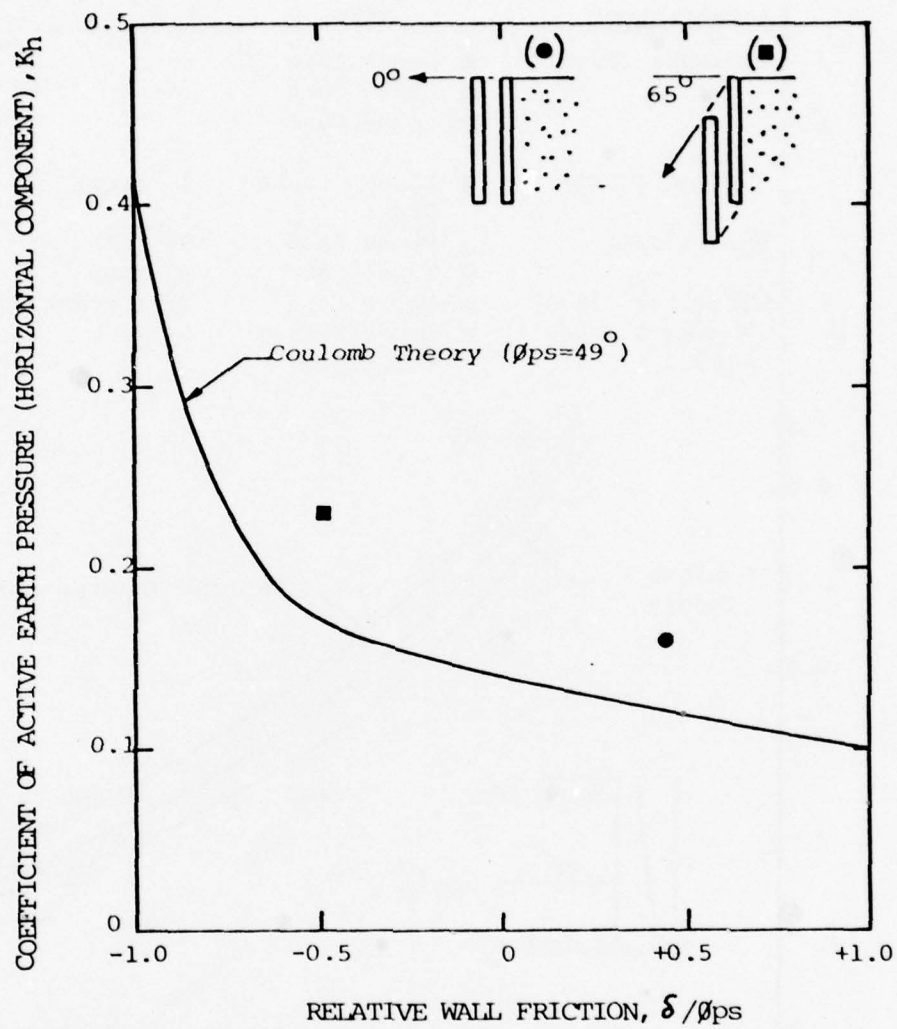


FIG. XI-6 COMPARISON OF COEFFICIENTS OF ACTIVE EARTH PRESSURE (HORIZONTAL COMPONENT) FOR ROWE'S TEST RESULTS FOR DENSE SAND, POSITIVE AND NEGATIVE WALL FRICTION

estimating the amount of wall movements that must occur for minimum active earth pressures to develop. Practical experience has been that the required movements are small and that most free-standing walls do rotate or translate sufficiently to reduce earth pressures to active values.

Wall movements, which were measured in the experimental studies discussed in the previous section, are given in Table XI-1. It can be seen that the wall movements required to develop minimum earth pressures varied from 0.001 to 0.20% of the wall height, i.e., $0.0001 H$ to $0.002 H$, where H is the height of the wall. A commonly used "rule of thumb" is that the deflection at the top of the wall must be approximately $0.005 H$, which is consistent with the deflections at failure (i.e., the development of visible failure planes) in Terzaghi's test on dense sand (see Notes 1 and 2 in Table XI-1). On the basis of the measured movements required to reach the condition of minimum active pressures, the guideline appears to be quite conservative.

Ladanyi (1958) presented a method for estimating the lateral earth pressure that would result from any amount of wall movement. The method requires that stress-strain curves be obtained from triaxial compression tests performed in such a way that the normal stress on the critical plane is kept constant throughout the test. The initial, or at-rest earth pressure must also be assumed. Gould (1970) simplified Ladanyi's procedures and obtained an approximate relationship which implies that the shear resistance mobilized by wall tilt is equal to the shear stress at an axial strain, ϵ , of four times the wall movement, Δ , divided by the wall height ($\epsilon = 4 * \Delta/H$), where the axial strain is measured in a triaxial compression test.

A more complex but potentially more accurate method of estimating the wall movement required for active pressures was suggested by Lambe and Whitman (1969). Their procedure is as follows:

- a. Perform triaxial or (preferably) plane strain compression tests on representative samples of the backfill material. The initial test conditions should be established by anisotropically consolidating the samples to the estimated at-rest pressures that will exist after backfilling. After consolidation to the K_0 condition, the specimens should be brought to failure by holding the vertical stress constant while the lateral stress is reduced.
- b. Multiply the measured horizontal strain at failure in the laboratory test by the width of the probable failure wedge in the field installation. The result will be the approximate wall movement required to achieve minimum active earth pressures in the field. It should be kept in mind that the necessary wall movements will occur only if the flexibility of the retaining wall and/or the compressibility of the foundation soils are sufficient to permit the movement.

B. Passive Earth Pressures

1. Comparison of Theories. Morgenstern and Eisenstein (1970) compared

Table XI-1

Measured Wall Movements Required to Develop Minimum
Active Earth Pressures

<u>Investigator</u>	<u>Backfill Type</u>	<u>Deflection at Top of Wall (H=wall height)</u>		
		<u>Rotation</u>	<u>Translation</u>	<u>Total</u>
Terzaghi (1940)	Dense Sand	0.0006H	0.0002H	0.0008H (1)
	Dense Sand	0	0.0006H	0.0006H (2)
	Loose Sand	0.0006H	0.0002H	0.0008H
Jansson (1948)	Loose Crushed Stones	0.0002H	0.0001H	0.0003H
Rowe (1969a)	Dense Sand	0	0.002H	0.002H
	Loose Sand	0	0.0015H	0.0015 (3)
Matteotti (1970)	Loose Sand	0.0008H	0	0.0008H
Rehman & Broms (1972)	Loose Gravelly Sand	0.0007H	0	0.0007H
	Compacted Gravelly Sand	0.001H-0.002H	0	0.001H-0.002H (3)

-
- Notes:
1. Total deflection of 0.004H at failure (development of visible failure planes in backfill).
 2. Total deflection of 0.0055H at failure.
 3. Slight additional decrease in pressure during continued wall movement.

several theories of determining passive earth pressures for the case of a vertical wall with a level (cohesionless) backfill and negative angles of wall friction equal to $\phi/2$ and ϕ . As shown in Fig. XI-7, all the theories that take wall friction into account give similar values of passive pressure, except for Coulomb's which is quite unconservative at large values of wall friction. Rankine's theory (Eq. IX-5), which neglects wall friction, predicts much lower passive pressures.

Comparisons for the less common case (for the passive condition) of positive wall friction are given in Fig. XI-8. Rankine values are unconservative, for this case, in comparison to the other theories which take wall friction into account.

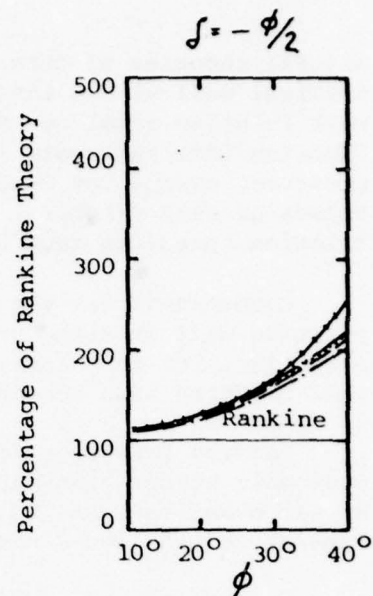
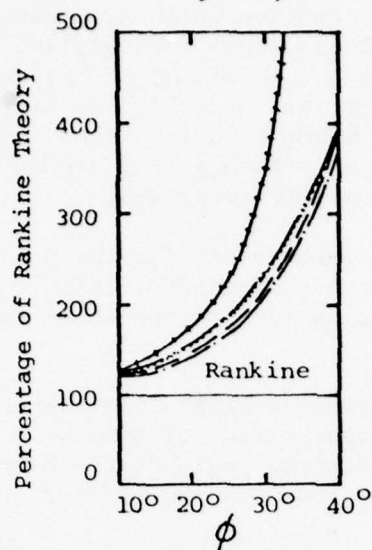
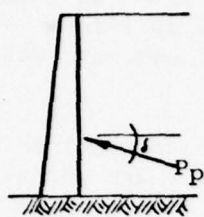
Passive pressures for sloping backfills are compared in Fig. XI-9. Coulomb's theory gives the largest values of passive pressure, particularly at slope angles equal to the friction angle of the backfill soil. The Rankine values (level backfill) are much smaller than the others.

The effects of inclined walls are shown in Fig. XI-10. For walls inclined into the backfill ($\beta = 75^\circ$), Coulomb's theory gives unconservative results, in comparison to the more exact theories which consider curved failure surfaces, while Rankine values are quite conservative. For walls inclined outward from the backfill ($\beta = 120^\circ$), all the theories give results within about 25% of the Rankine values.

Based on these limited comparisons, it can be said that, with respect to calculated values of passive earth pressure:

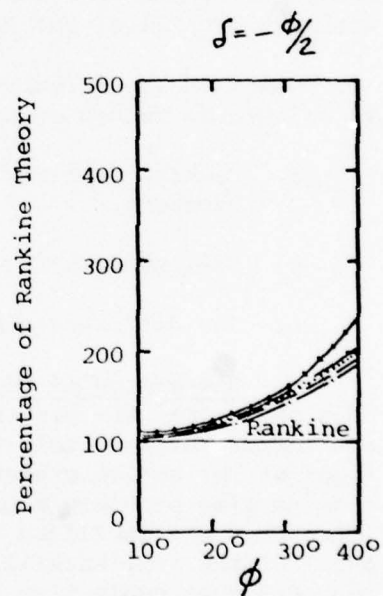
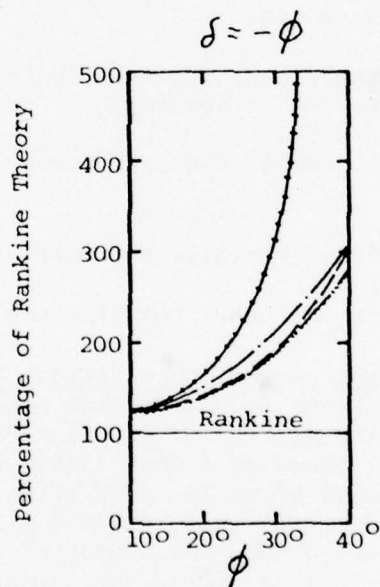
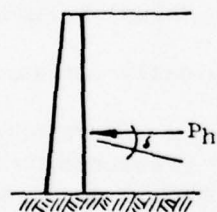
- a. Rankine's theory gives generally conservative (low) values of passive pressure.
- b. Coulomb's theory predicts generally unconservative (high) values.
- c. The differences between the other theories are typically not large.

2. Comparison of Theory with Experimental Data. Various investigators have shown that the present theories for predicting passive pressures do not compare as favorably with the results of experimental studies as do the theories for active pressures. Rowe and Peaker (1965) presented results from passive pressure measurements of walls translating into sand. They found that the mobilized wall friction angle and the mobilized friction angle of the soil backfill depended upon the amount of wall movement. They reasoned that neglecting the effect of wall deformations would lead to errors in the use of all existing theories. The amount of error involved is indicated in Table XI-2 by their proposed changes to the British Code of Practice.



+++++Coulomb
 ---Sokolovski
 ---Janbu
Caquot-Kerisel
 ---Log-Spiral

Total Passive Pressure, P_p



Horizontal Component of Passive Pressure, P_h

FIG. XI-7 COMPARISON OF COEFFICIENTS OF PASSIVE PRESSURE FOR VARIOUS THEORIES,
NEGATIVE WALL FRICTION

(Morgenstern & Eisenstein, 1970)

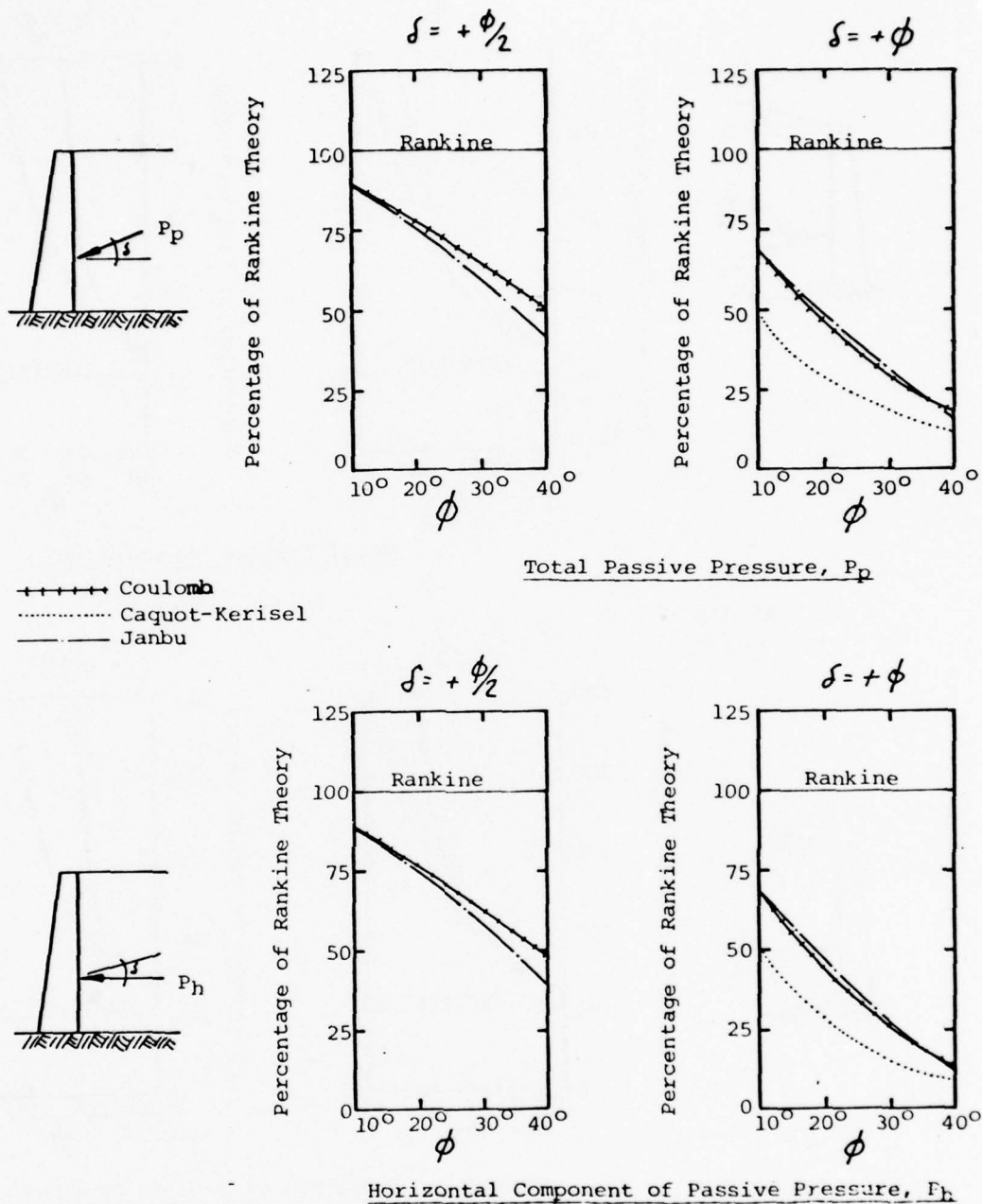
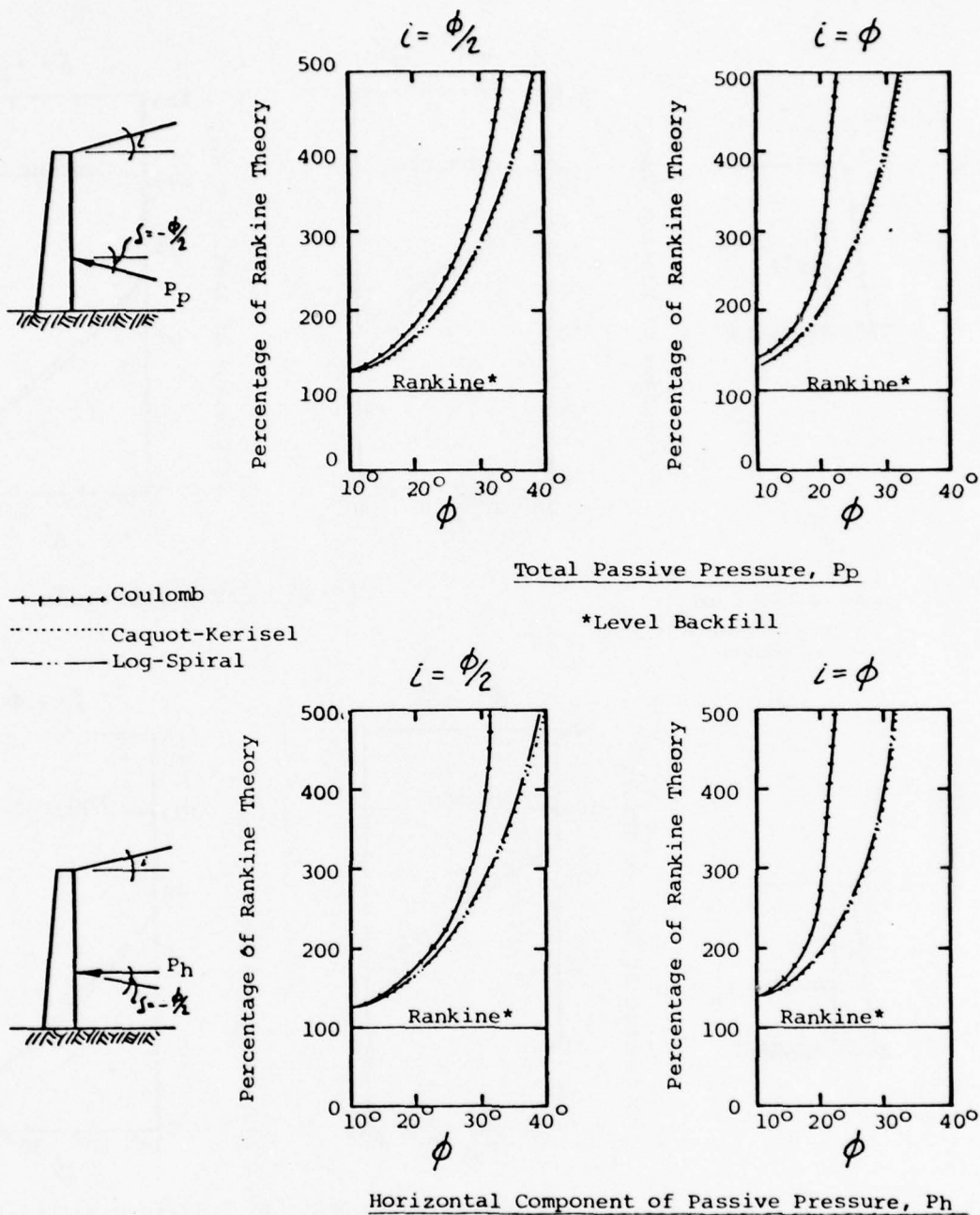
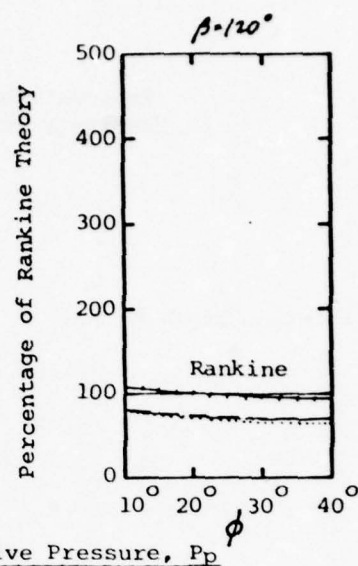
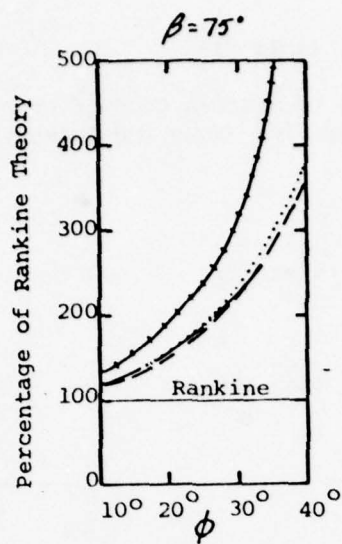
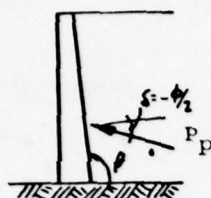


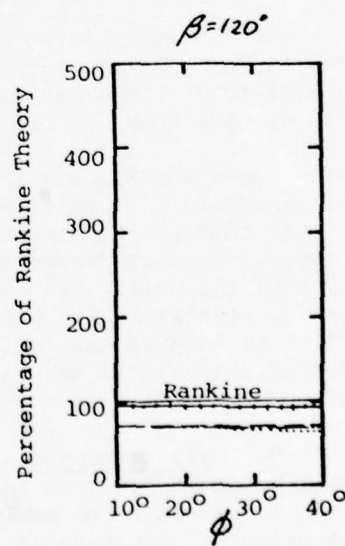
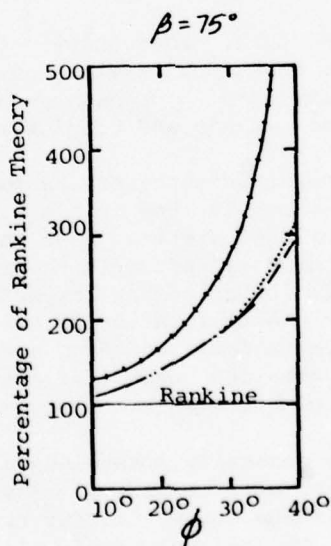
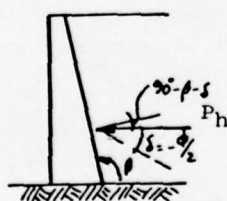
FIG. XI-8 COMPARISON OF COEFFICIENTS OF PASSIVE PRESSURE FOR VARIOUS THEORIES, POSITIVE WALL FRICTION





Total Passive Pressure, P_p

- +++++ Coulomb
- · — Log-Spiral
- Caquot-Kerisel
- — — Sokolovski



Horizontal Component of Passive Pressure, P_h

FIG. XI-10 COMPARISON OF COEFFICIENTS OF PASSIVE PRESSURE FOR VARIOUS THEORIES, INCLINED WALL

Table XI-2

Proposed Changes to British Code of Practice,
Passive Earth Pressures (Rowe and Peaker, 1965)

		<u>Code</u>		<u>Proposed**</u>	
Friction angle of soil	ϕ triaxial:	33°	40°	33°	40°
	(or)				
	ϕ plane strain:	---	---	34°	42°
	δ_m^*	K_p		K_p	
	0°	3.4	4.6	2.5	4.6
	10°	4.5	6.5	3.0	5.8
	20°	5.6	8.8	3.6	7.2
	30°	6.7	11.4	4.3	8.8

* δ_m = mobilized wall friction angle;

**Corresponds to wall movement of 0.05H

Rowe (1969a) introduced the term, progressivity index, as defined by Eq. XI-1, to relate the average developed strength of the backfill behind a wall to its peak laboratory strength. For passive pressures, he recommended values of r equal to 1.0 for loose sands and 0.8 for medium to dense sands.

James and Bransby (1970) reported test results for passive pressure measurements on a wall rotated about its toe into a sand backfill. They showed that their data agreed with predictions made using Sokolovski's theory (the most "correct" of the earth pressure theories) except near the base of the wall. Graham (1971) indicated how the data could be fit by making certain modifications in the application of Sokolovski's theory. First he assumed that wall friction decreased from a maximum value near the top of the wall to zero at the toe; and second, he assumed that the lower 30% of the wall does not reach plastic failure stresses.

3. Wall Movements. It is generally acknowledged that the amounts of wall movement required to develop maximum passive pressures is much larger than is necessary to achieve minimum active pressures. The difference is an order of magnitude or more. Typical values of wall movement are about 2 percent of the wall height for dense sands to 15 percent for loose sands (Lambe and Whitman, 1969).

C. At-Rest Earth Pressures

1. Normally-Consolidated Soils. If soils were elastic materials with

constant Poisson's ratio, ν , the lateral pressure coefficient (K_o) within a soil mass at-rest would be given by the formula:

$$K_o = \frac{\nu}{1 - \nu} \quad (\text{XI-2})$$

Unfortunately, the value of ν for a real soil is not easily determined, nor can it be considered a constant. Among other factors, Poisson's ratio has been found to be dependent upon confining pressure and stress history. Consequently, Jaky's formula for sands (Eq. IX-12) and Brooker and Ireland's expression for clays (Eq. IX-13) which are essentially empirical, are often used instead to estimate at-rest pressure coefficients. The degree to which the formula are supported by experimental data is shown in Fig. XI-11. Values of K_o are plotted against soil friction angle, ϕ , for data reported by Terzaghi (1940), Matteotti (1970), Rehman and Broms (1972), and by Brooker and Ireland (1965), which included data from Hendron (1963). For the Brooker and Ireland and the Hendron data, the reported values of ϕ , which are thought to have been determined from direct-shear tests, are included in the figure along with the estimated plane-strain values. Note that only the results of Terzaghi's tests on dense sands do not fit the general trend of the data. As discussed subsequently, the high values of K_o reported by Terzaghi have been attributed to the vibratory compaction that was used to densify the sand behind the model wall. Considering the scatter of the other data, it is quite likely that Jaky's expression for K_o is sufficiently accurate for obtaining reasonable estimates of at-rest earth pressures for both normally-consolidated sands and clays.

Janbu (1972) proposed a method for determining K_o for soils with both cohesion and internal friction. He suggests using certain empirical relationships to obtain Mohr circles of stress for at-rest conditions from the Mohr-Coulomb failure envelope for a given soil. For cohesionless soils, the following expression for K_o was obtained by Janbu:

$$\frac{1 - K_o}{K_o} \approx 1.25 \tan \phi \quad (\text{XI-3})$$

For values of ϕ greater than 25° , Eq. XI-3 gives at-rest coefficients very nearly equal to those resulting from Jaky's expression.

Alpan (1967) studied the data for clays reported by Brooker and Ireland and by Kenney (1959) and concluded that values of K_o for normally consolidated clays could be related to soil plasticity index, PI , by the following empirical expression:

$$K_o = 0.19 + 0.233 \log (PI) \quad (\text{XI-4})$$

This could be a more useful expression than Jaky's for clays because of the relative ease by which plasticity indices can be determined as opposed to the difficulty in determining drained friction angles.

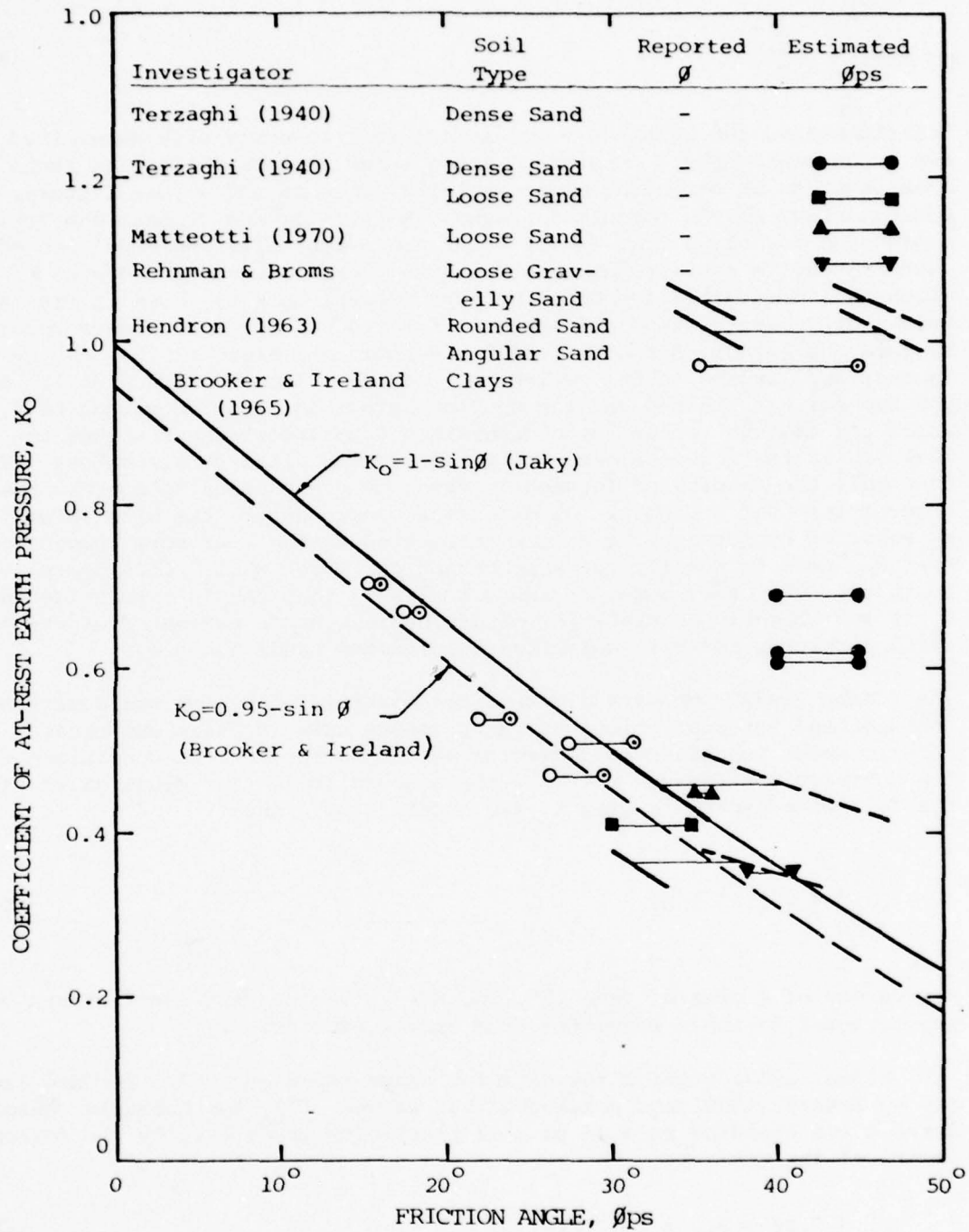


FIG. XI-11 COMPARISON OF COEFFICIENTS OF EARTH PRESSURE AT-REST FOR NORMALLY CONSOLIDATED SOILS

2. Overconsolidated Soils. Brooker and Ireland's paper summarizes the results of an extensive laboratory testing program wherein the effect of overconsolidation upon the coefficient of earth pressure at-rest, K_o , was studied for five different clays. Some of their results are shown in Fig. XI-12. In the figure, Overconsolidation Ratio, OCR, is taken as the maximum previous (effective) vertical pressure on a sample divided by the present (effective) vertical pressure.

Alpan has proposed the following empirical expression based on the experimental data of Brooker and Ireland and that of Wiseman (1962):

$$\frac{K_{or}}{K_o} = (OCR)^\lambda \quad (XI-5)$$

where

OCR = overconsolidation ratio

K_o = coefficient of at-rest pressure during primary loading

K_{or} = coefficient of at-rest pressure during unloading (rebound)

λ = empirical coefficient

He used Brooker and Ireland's data for clays to determine the following expression for λ :

$$PI = -281 \log (1.85\lambda) \quad (XI-6)$$

as shown in the upper part of Fig. XI-13. He also suggested a relationship between λ and ϕ , based on limited data as shown in the lower part of Fig. XI-13.

According to Alpan, for sands the value of λ is dependent only the soil friction angle. However, data from a report by Obrcian (1969) show that λ decreases for larger values of OCR, as demonstrated in Fig. XI-14. On the other hand, Hendron's data do show a relatively constant value of λ for a large range of OCR. Obrcian's data also cloud the picture with respect to the dependence of λ upon ϕ . There is no clear trend for smaller values of λ to be associated with sands having higher relative densities (and presumably higher values of ϕ) as predicted by Alpan. Obrcian's data also indicate that the value of λ depends on the maximum pressure to which the sand is consolidated. Results from one consolidation test on a medium-dense sand are given in Fig. XI-15. The shape of the rebound portions of the test curves, and therefore the values of λ , are seen to vary as the maximum vertical pressure is varied.

3. Compacted Soils. There is considerable controversy over the questions of whether backfills behind rigid, unyielding walls should be compacted. Terzaghi's retaining wall tests indicated larger values of K_o .

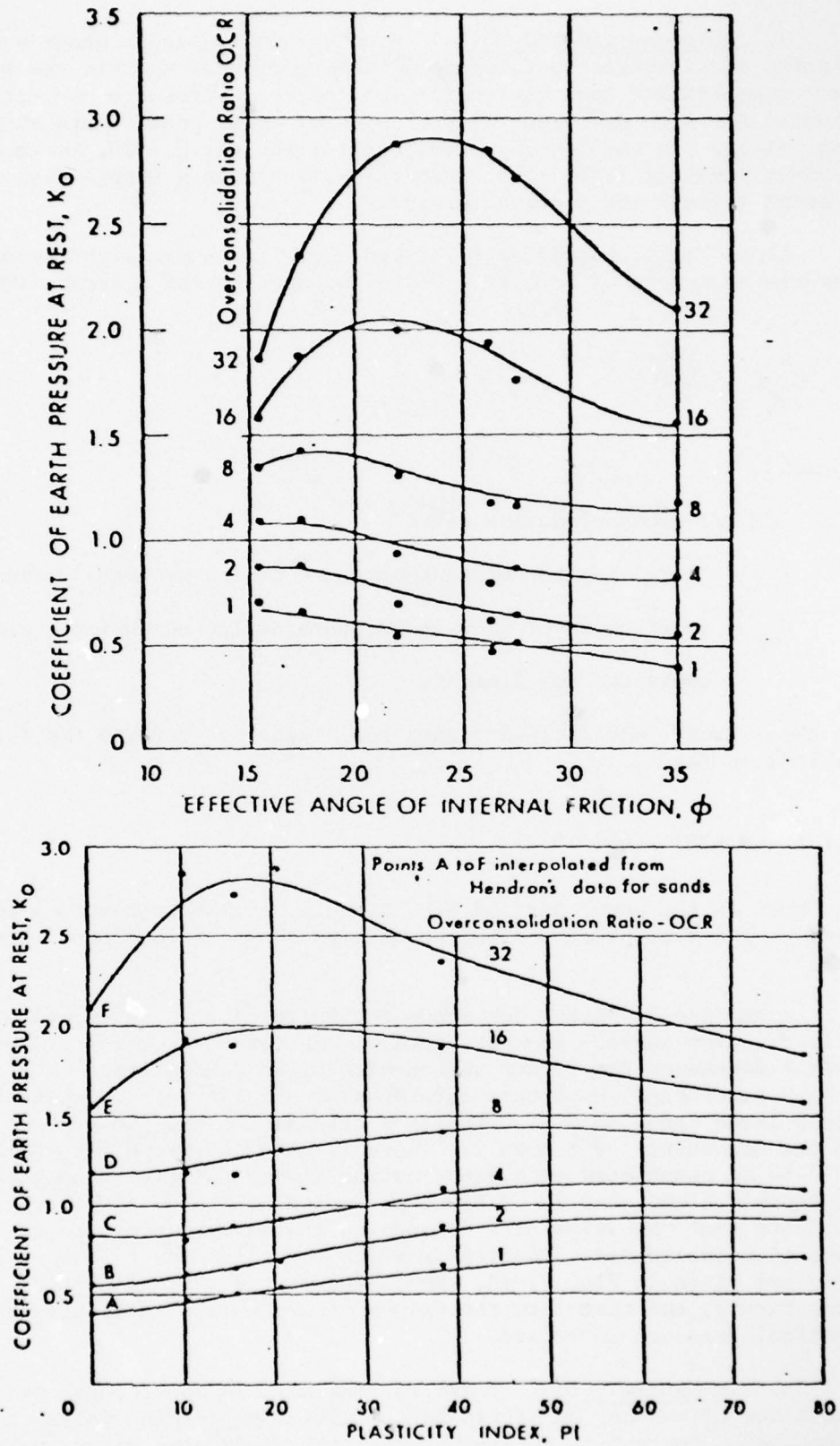


FIG. XI-12 BROOKER AND IRELAND'S (1965) DATA FOR COEFFICIENTS OF EARTH PRESSURE AT-REST FOR OVER-CONSOLIDATED SOILS

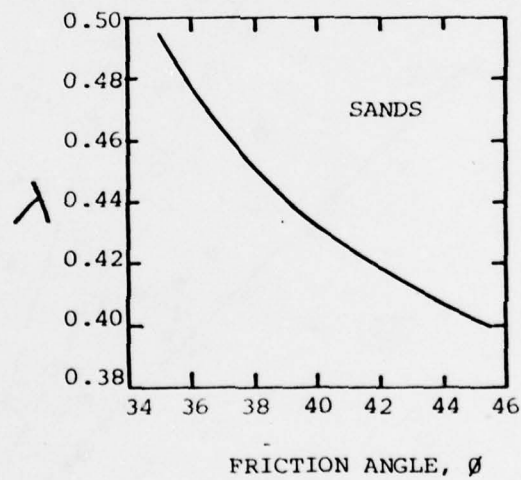
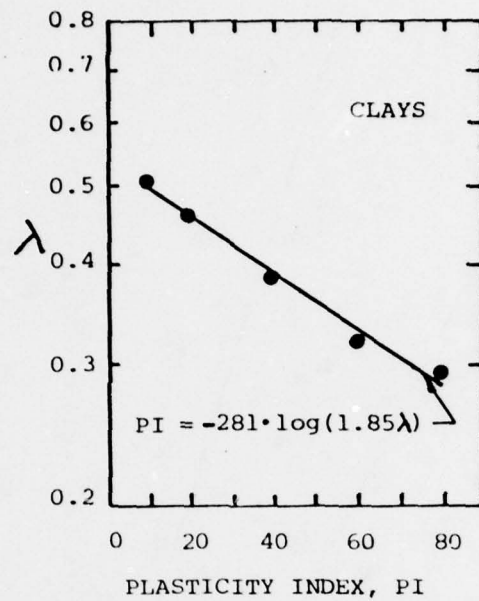


FIG. XI-13 EMPIRICAL COEFFICIENT λ FOR CLAYS AND SANDS
(Alpan, 1967)

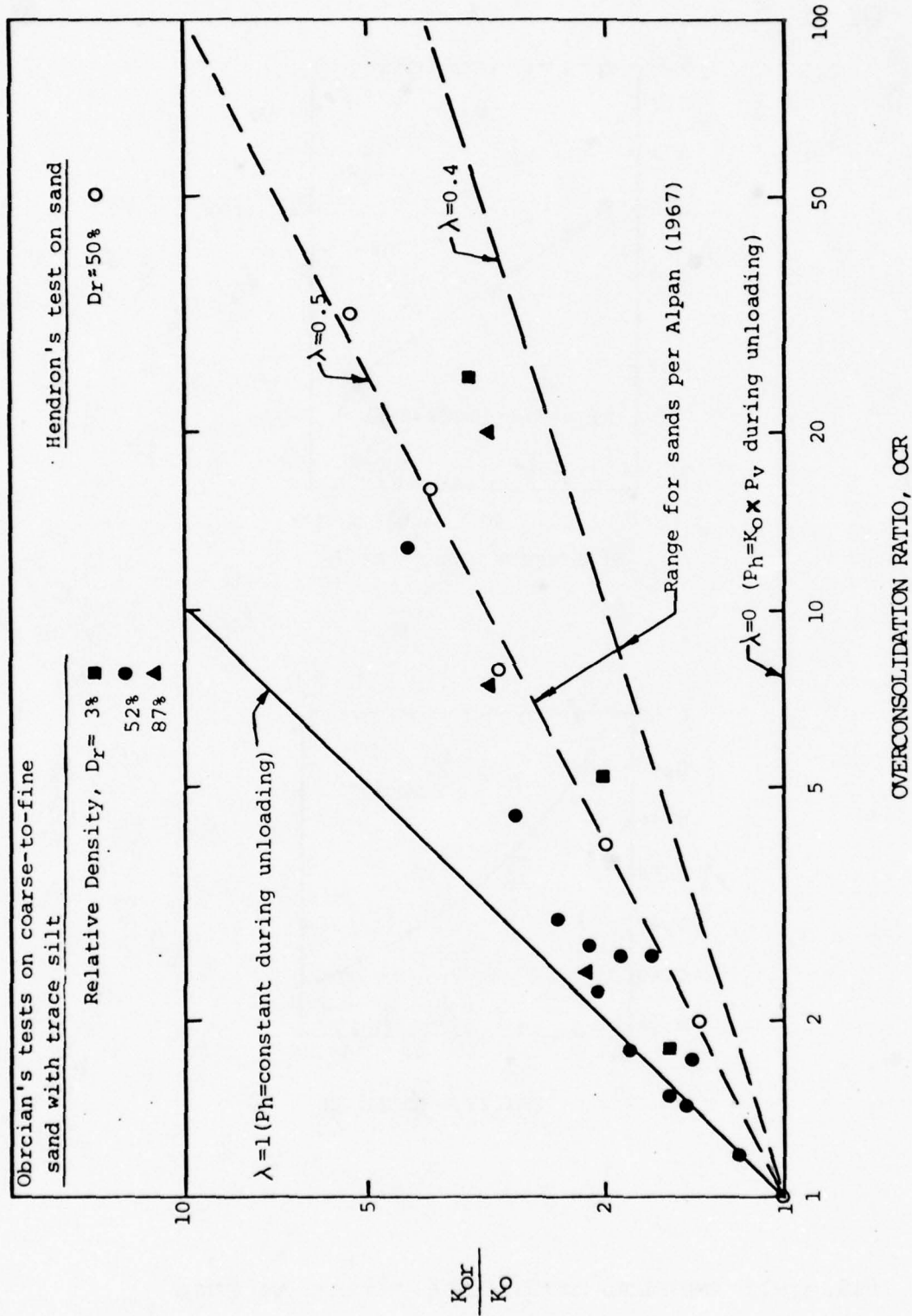


FIG. XI-14 VARIATION OF COEFFICIENTS OF AT-REST EARTH PRESSURE FOR LOADING (K_0) AND UNLOADING ($(K_{Or})_{sands}$) - SANDS

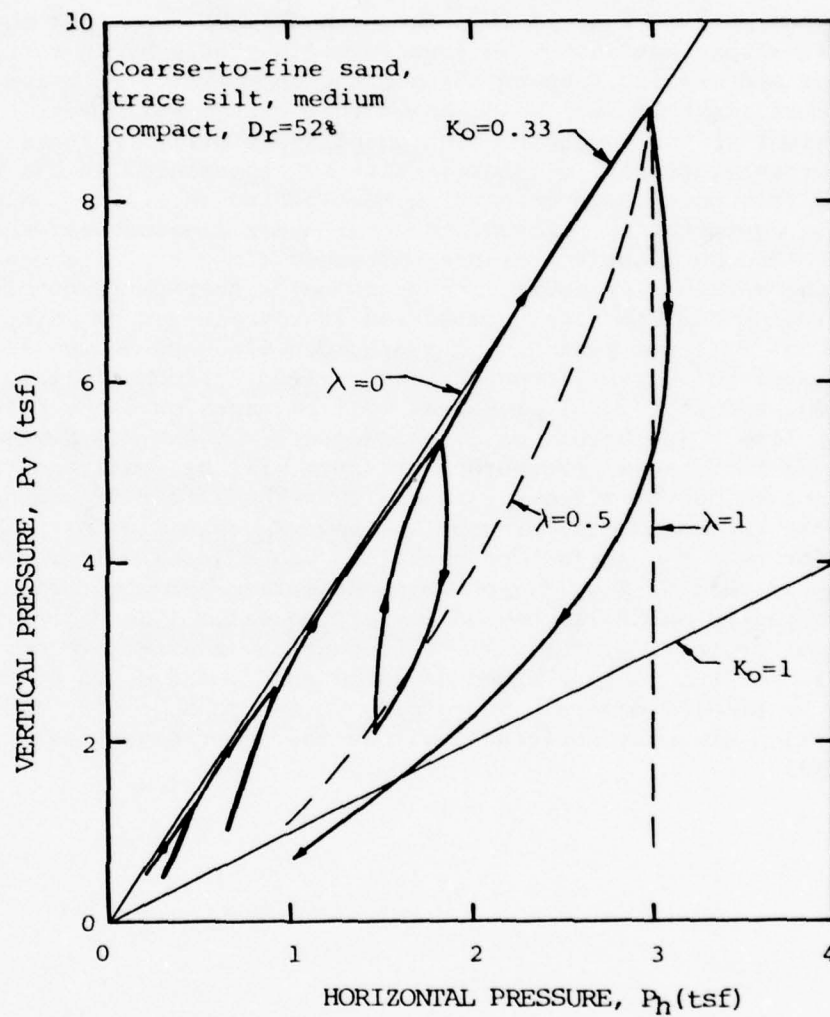
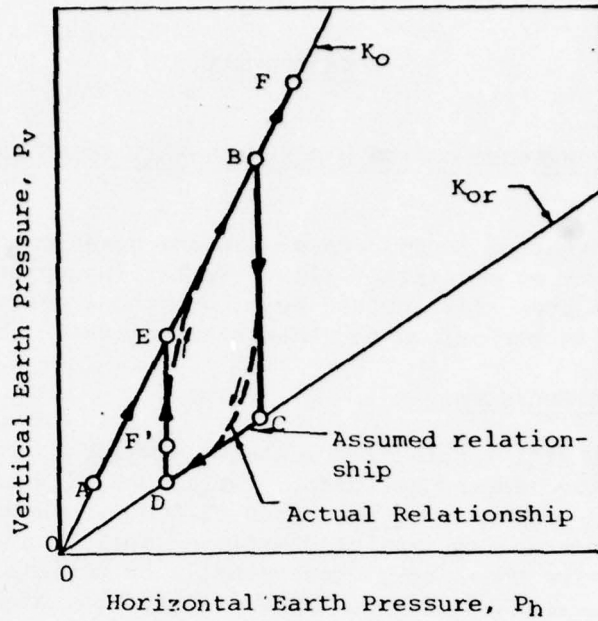


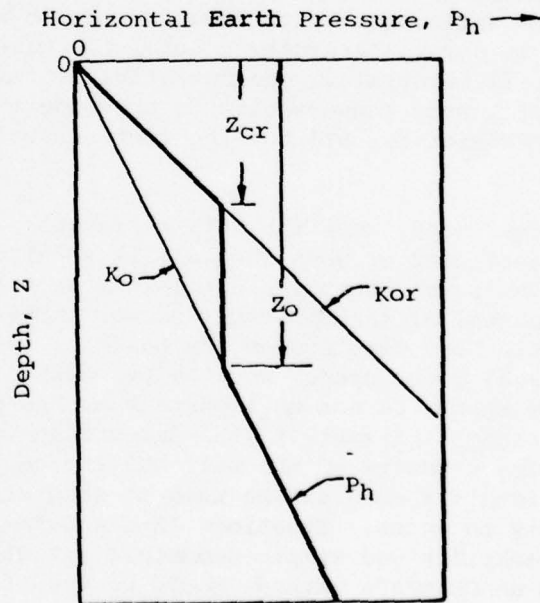
FIG. XI-15 VERTICAL AND HORIZONTAL PRESSURES IN CONSOLIDATION TEST MEASURED BY OBRICAN (1969)

for dense sands than for loose sands. This is in direct opposition to Jaky's equation and has been attributed to quasi-overconsolidation caused by compaction of the sand during backfilling. Sowers et. al. (1957) also showed by experimental studies that compacted backfills of both sand and clay gave higher wall pressures than uncompacted fills.

Broms (1971) has given a plausible explanation for the behavior of compacted backfills. To illustrate his reasoning, he used relationships between overburden pressure and lateral earth pressures which are given in the upper part of Fig. XI-16. The dashed lines represent the actual relationships that have been found experimentally by investigators such as Brooker and Ireland. Broms assumed the approximate relationships as shown by the straight lines. He reasoned that when a soil layer is compacted, the weight of the compaction equipment temporarily increases the effective overburden (vertical) pressure. This is represented in the figure by moving from point A to point B on the loading (K_o) line. When the compaction equipment is removed, the overburden pressure returns to its original value. The horizontal pressure decreases along the unloading (K_{or}) line only when the vertical pressure is reduced below that corresponding to point C. The final condition after compaction is represented by point D. As additional layers of fill are placed, the overburden pressure at the elevation of the soil layer being considered becomes greater. If the fill is deep, the final vertical and horizontal pressures will be represented by point F, which is on the K_o line. The stress path followed will be D-E-F. However, for a shallow fill the increase in overburden pressure will be small and the final point, E, will not be far from the K_{or} line. Thus the effect of compaction should be to increase the horizontal pressures, above K_o values within backfills behind low walls or near the surface of backfills behind high walls. This is shown in the lower part of Fig. XI-16, which summarizes Brom's design recommendations for compacted backfills behind unyielding walls. He determined that values of critical depth, Z_{cr} , for various compaction machines are on the order of 0.5 meters. If K_{or} is four times as large as K_o , the depth of influence, Z_o , would be about 2 meters. Therefore, it is probable that the effects of compaction are only noticeable within the upper seven feet or so of any backfill.



RELATIONSHIPS BETWEEN VERTICAL AND HORIZONTAL PRESSURES DURING LOADING AND UNLOADING



PROPOSED DESIGN HORIZONTAL PRESSURE DISTRIBUTION

FIG. XI-16 BROM'S RELATIONSHIPS FOR COMPACTED BACKFILLS, UNYIELDING WALLS

CHAPTER XIIRECOMMENDED DESIGN PROCEDURES--RETAINING WALLS

This investigation is concerned with the question of predicting earth pressures that act on retaining walls. Rather than proposing new design methods, this chapter will instead point out those existing methods which have most merit in comparison to other alternatives.

A. Active Earth Pressures

Walls which will rotate or translate outwards during backfilling can be designed for active earth pressures. The amount of wall movement that is necessary is not likely to be more than $0.005H$, where H is the wall height. In general, free-standing retaining walls on soil foundations can be designed for active pressures, whereas walls on unyielding foundations such as rock or end-bearing piles should be designed for at-rest earth pressures. However, the stem of a cantilever wall on an unyielding foundation may have sufficient flexibility to allow the required wall movement to occur.

For most walls less than 20-feet-high, it is probably most efficient to select the design value of active earth pressure from empirical charts or tables, such as those recommended by Terzaghi and Peck (1967). As they point out, it is not usually economically feasible to thoroughly investigate the strength characteristics of backfills to be placed behind relatively inexpensive low walls, nor is it feasible to provide such walls with adequate drainage systems nor to carefully control the placement and compaction of the wall backfill materials. Consequently, empirical pressure coefficients which are sufficiently conservative to preclude the possibility of unsatisfactory wall behavior for all but the most unusual of circumstances should be used.

On the other hand, when the wall represents a substantial portion of the total project cost or when the wall is so high (more than about 20 feet) that significant economics can result from appropriate design details and careful control of the construction work, then the active earth pressures should be determined on the basis of the actual strength of the backfill material to be used. For the purposes of design, the choice of earth pressure theory is not as important as the proper prediction of soil density and strength parameters, the direction and magnitude of wall friction and the geometry of the wall and its backfill. For all practical purposes, Coulomb's theory can be used to predict the active earth pressures that are likely to occur. Equations IX-10 and IX-11 are convenient for homogeneous backfills and simple geometric installations. Graphical procedures, such as Culman's method, could be used for more complicated conditions.

Special care should be taken whenever retaining walls must be built on clay foundations or with clay backfills. Experience has shown that most difficulties with retaining walls have been associated with these conditions. In particular, clay backfills should be avoided if at all possible because of the difficulty of providing adequate drainage of the backfill, the

potential for swelling pressures to occur, and the possibility of long-term creep of the backfill and progressive outward tilting of the wall.

Whenever theoretical formulae are used to determine design wall pressures, the factor of safety should be sufficient to account for seasonal variations in pressure that are known to occur. Seasonal effects are likely to be of lesser importance for higher walls; nevertheless, the possibility of seasonal pressure variations should always be considered during design.

For unusual wall conditions, the finite-element method can be a valuable tool for design. At the present time the finite-element method is the only practical means by which quantitative analyses can be made of soil-structure-interaction problems.

B. At-Rest Earth Pressures

Walls which cannot move sufficiently to develop active earth pressures should be designed for at-rest values. Because at-rest pressures can often be 50 to 100 percent greater than the corresponding active pressures for a given soil, it is probably more important to make the appropriate choice of type of pressure than it is to determine which active or which at-rest pressure coefficient to use.

The design guidance provided by Jaky's expression, by Brooker and Ireland's test data, and by Alpan's empirical relationships form a rational basis for estimating at-rest earth pressures for design purposes. The effects of backfill compaction can be taken into account by the method suggested by Broms.

For low walls, the effects of seasonal changes in earth pressures should be considered. In fact, seasonal effects could be more pronounced for unyielding walls that are not free to deflect and thereby relieve any increased pressure. At the present time, seasonal effects can only be evaluated qualitatively by referring to the pressures that have previously been measured on similar walls with comparable backfills.

C. Passive Earth Pressures

The accuracy of predictions of passive earth pressures which can be relied upon for resisting the movement of retaining walls and foundation elements is considerably less than the accuracy of predictions of active pressures. The wall movements required to achieve full passive resistance are normally so large that pressures predicted by classical theories must be substantially reduced by a factor of safety to achieve a reliable working resistance compatible with the movements that can be tolerated by the structure. Because of the non-linear relationship between passive resistance and wall movement, there remains much uncertainty as to whether the desired resistance can in fact be achieved within the wall movement allowed. Because of its uncertain nature, passive earth pressures are often disregarded when other, more positive means of resistance are available.

Because of the generally unconservative nature of Coulomb's theory for predicting passive pressures, it should not be used. On the other hand, Rankine values are usually quite conservative, particularly at larger soil

friction angles and greater values of wall friction. For conditions of sloping backfills, inclined walls and positive wall friction, other more exact theories can be used to obtain reasonable estimates of ultimate passive resistance. Of the theories considered in this investigation, Caquot and Kerisel's is the most useful because of the wide variety of conditions for which published solutions (in graphical and tabular form) are available.

It is quite likely that current research investigations using finite-element techniques and improved constitutive relationships for soil stress-strain behavior will improve the present state of knowledge with regard to passive earth pressures.

CHAPTER XIII

ANALYSIS OF CORPS OF ENGINEERS CASE HISTORIES -

RETAINING WALLS

It is instructive to compare measured earth pressures on retaining walls with values that would be predicted by the design procedures recommended in the preceding chapter. By so doing, the applicability of the design methods can, in a limited way, be evaluated in the context of actual wall installations.

The data from four Corps of Engineers projects were supplied by the District offices responsible for construction. Source documents, from which project information was obtained, are listed in the bibliography.

A. Bankhead Lock and Dam

The John Hollis Bankhead Lock and Dam, located on the Black Warrior River in Alabama, was constructed by the Mobile District of the Corps of Engineers. As shown in Fig. XIII-1, the lock is about 110 feet wide by 1000 feet long and is formed by independent gravity retaining walls along each side, and a concrete floor sill. The walls of the lock are on the order of 100-feet-high. The south (land) wall abuts against an earth and rock dam as shown in the figure. Earth and pore-water pressures were measured against the back-face of three of the concrete monoliths in the land wall (Nos. 6L, 10L and 13L), as shown in Fig. XIII-1. No measurements were made of wall movement during or after back-filling, but Mobile District personnel expressed the opinion that the movements would have been very small because the walls are supported on rock foundations.

The wall pressures recorded over a period of about two years are given in Figs. XIII-2 for the three instrumented monoliths. Both total and effective pressure data are given for Monolith 6L, which was located within the impervious core of the dam. No piezometers were installed at Monoliths 10L and 13L, but it is likely that that water level in the rockfill adjacent to these wall sections was no higher than the measured tailwater on the dam, as shown in the figure.

The measured wall pressures generally increased to maximum values at the end of construction and then decreased slightly as the reservoir was filled, which is indicated in Fig. XIII-2 by the headwater elevation data. The total pressures measured at Monolith 6L increased during reservoir filling evidently as the core became saturated.

The total earth pressures measured at the end of construction (prior to reservoir filling) are shown, for each instrumented monolith, in Figs. XIII-3 through XIII-5. The pressures are compared with theoretical values that have been determined as follows:

1. The core material adjacent to Monolith 6L consisted of sandy clay (CL-CH) compacted to at least 95 percent of its Standard Proctor maximum density. The core material was placed near optimum moisture

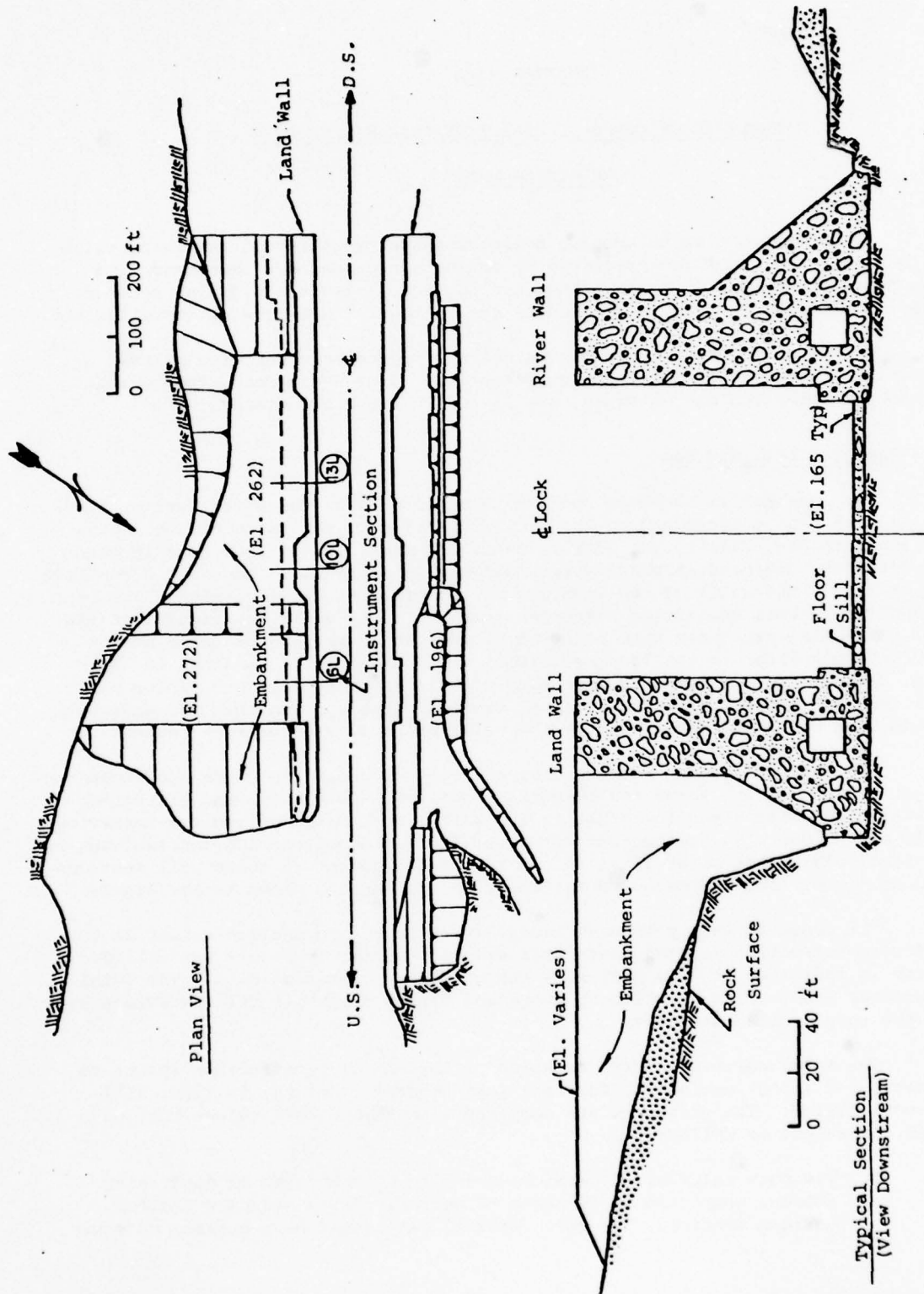


FIG. XIII-1 PLAN AND SECTION VIEWS OF BANKHEAD LOCK AND DAM

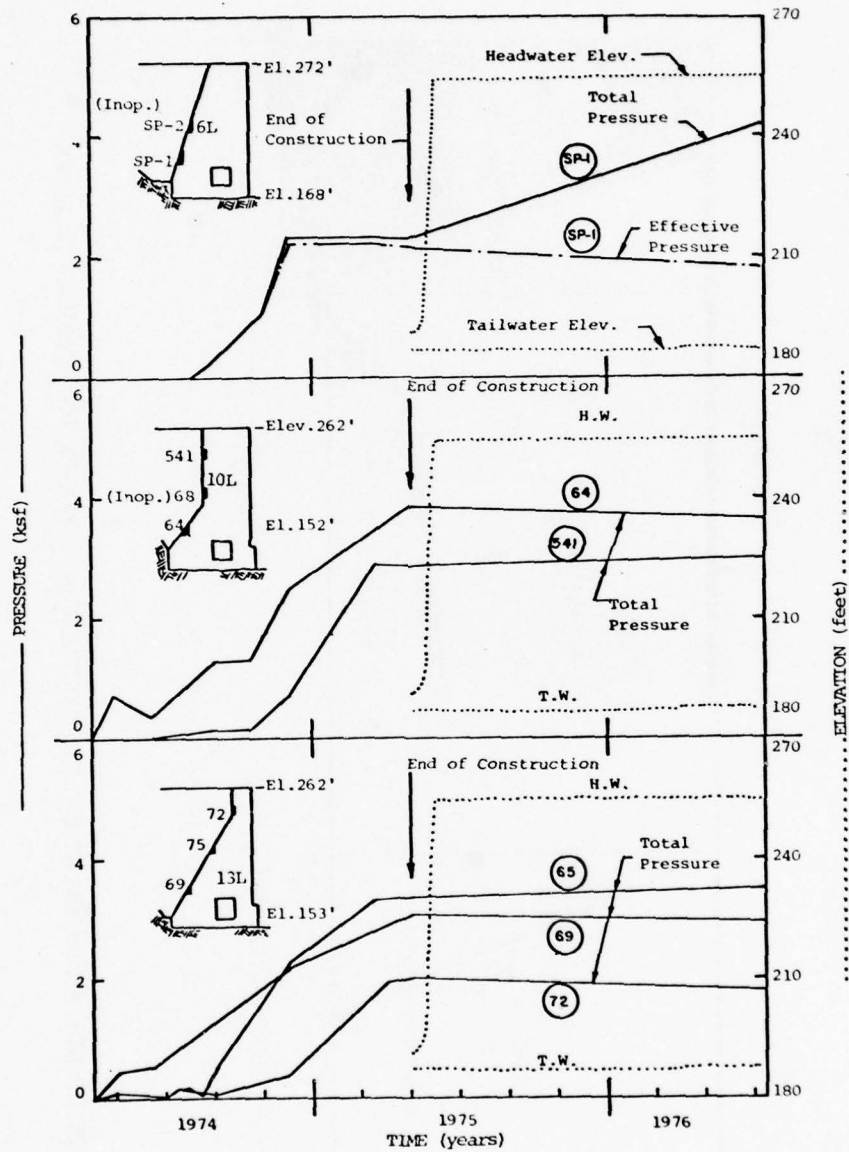


FIG. XIII-2 MEASURED PRESSURES AT WATER LEVEL ELEVATIONS AT MONOLITHS 6L, 10L AND 13L, BANKHEAD LOCK AND DAM

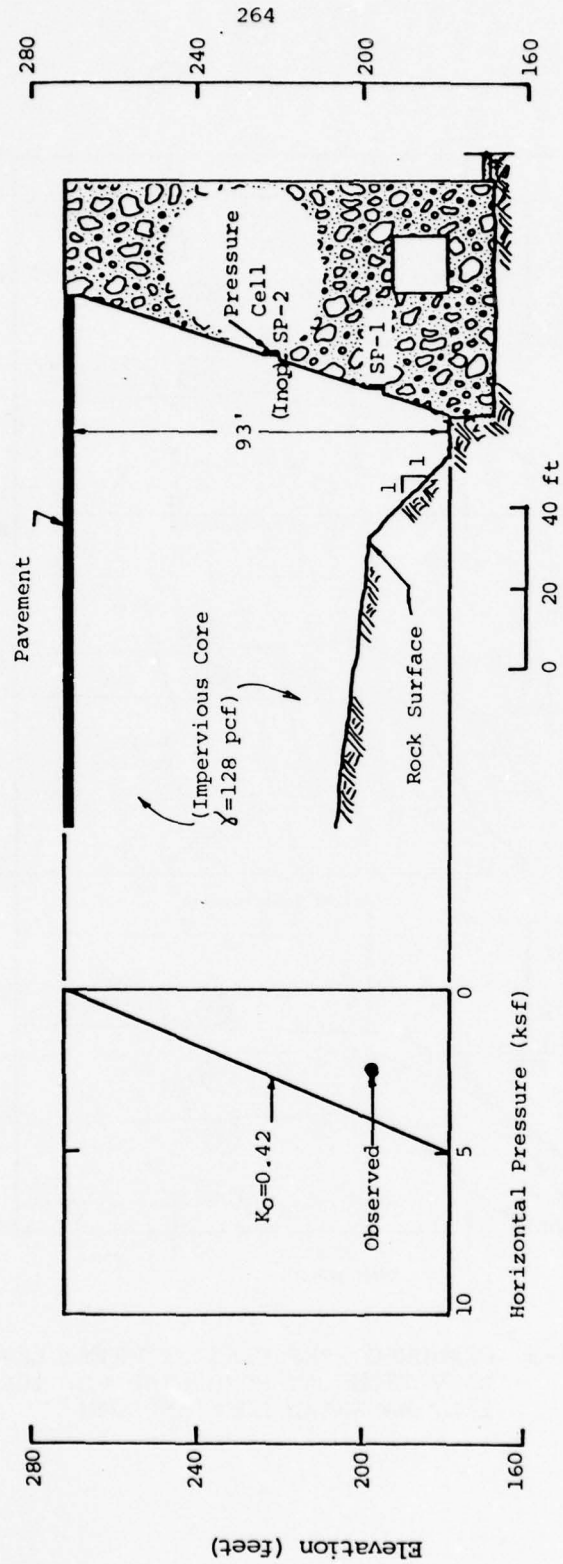


FIG. XIII-3 TOTAL EARTH PRESSURES AT END OF CONSTRUCTION, MONOLITH 6L, BANKHEAD LOCK DAM

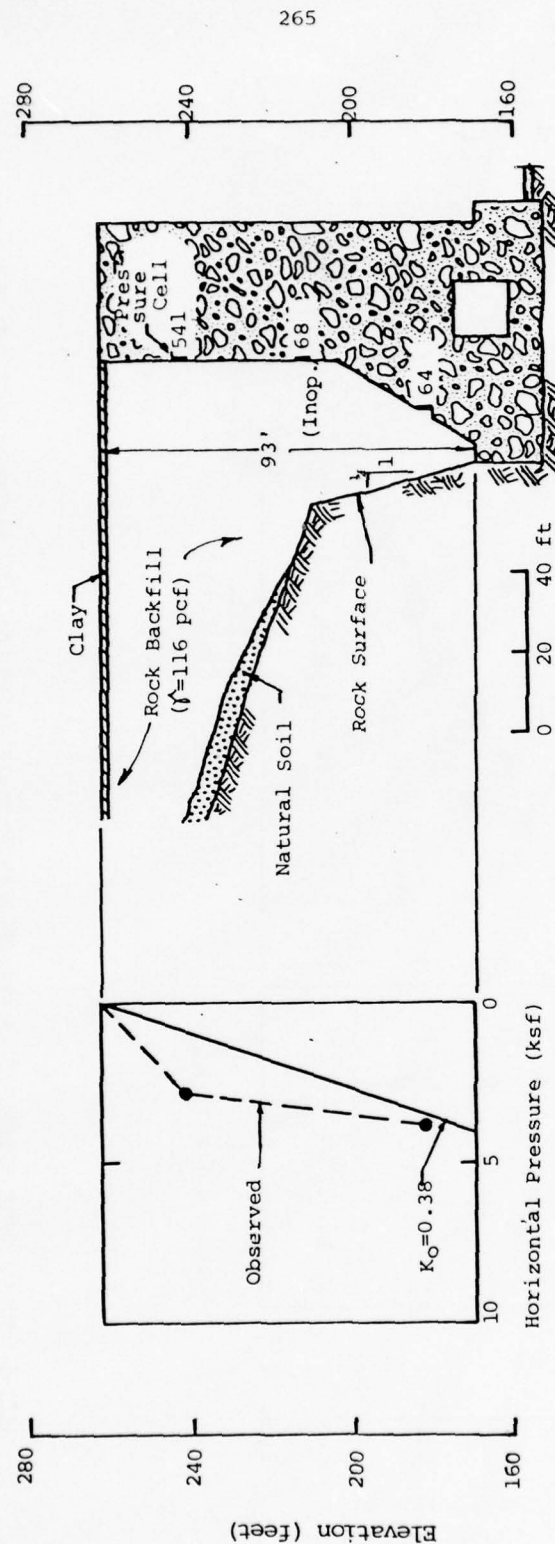


FIG. XIII-4 TOTAL EARTH PRESSURE AT END OF CONSTRUCTION, MONOLITH 10L, BANKHEAD LOCK AND DAM

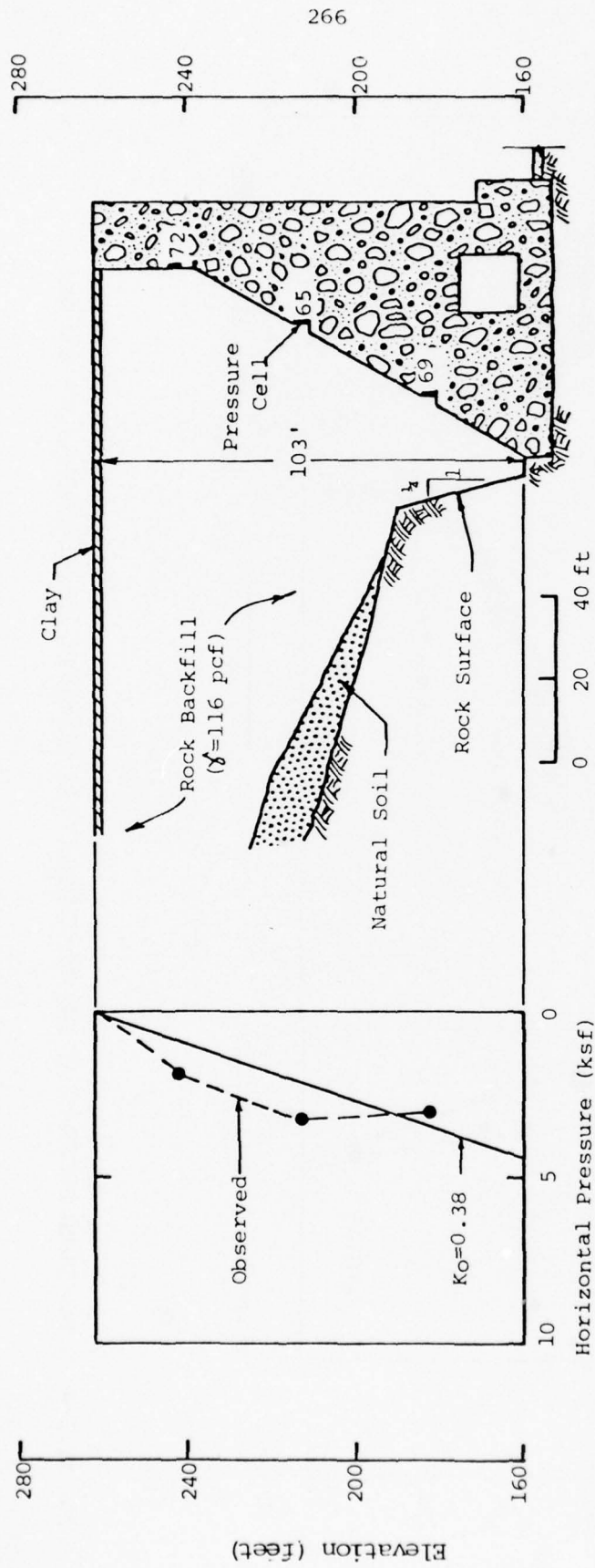


FIG. XIII-5 TOTAL EARTH PRESSURES AT END OF CONSTRUCTION, MONOLITH 13L, BANKHEAD LOCK AND DAM

content. As shown in Fig. XIII-2 the pore pressure measured in the compacted clay adjacent to the wall, at the end of construction, was very small. Consequently the material was probably close to a fully drained condition. Therefore, either Jaky's or Brooker and Ireland's expressions could be used to estimate the at-rest pressure coefficient. Jaky's equation was used with a friction angle of 35.5° (as assumed in design), to obtain a value of K_0 equal to 0.42.

2. The backfill behind Monoliths 10L and 13L consists of lightly-compacted, shaley-sandstone rockfill. Using the design friction angle of 38° in Jaky's equation results in an at-rest pressure coefficient of 0.38. Pore-water pressures are likely to have been small and were neglected in estimating the earth pressures.

The measured pressures are less than the theoretical values at Monolith 6L (clay backfill) and generally greater at Monoliths 10L and 13L (rock backfill). The pressure distributions measured on the walls backfilled with rock are approximately trapezoidal or parabolic in contrast with the theoretical triangular distribution.

B. West Point Dam

The West Point Dam is located on the Chattahoochee River in Georgia. It has a maximum height of 125 feet and was constructed by the Savannah District of the Corps of Engineers. As shown in Fig. XIII-6, the east earth embankment is retained by a concrete gravity wall in the vicinity of the concrete overflow spillway section of the dam. The retaining wall has a maximum height of about 120 feet and a total length of about 500 feet. Two of the wall sections, Blocks D and F were instrumented with earth pressure cells and piezometers. The instrument locations are shown in Fig. XIII-6.

The measured total earth pressures and water levels within the backfill are plotted for each instrument section in Fig. XIII-7. The decrease in earth pressures from late 1973 to mid-1974 resulted from removal and replacement of a portion of the east embankment. The full embankment was essentially complete by December, 1974. During construction, wall movements were monitored by slope indicators at each instrument section. Reported data for Block F indicated about 0.1 inches of relative movement between the top and bottom of the wall, or a rotation of about 0.0001 - a very small amount.

The horizontal components of the total earth pressures measured at the end of embankment construction are given, for each instrument section, in Figs. XIII-8 and XIII-9. A wall friction angle of 11° (representative of the steel face plate of the pressure cells) was used in calculating the horizontal pressures on the inclined walls. The maximum error in the calculated horizontal pressures that could result from reasonable variations in wall friction angle is probably less than 25 percent. Also shown in the figures are theoretical values of at-rest pressures calculated by using Jaky's equation with a value of ϕ equal to 30° , the design assumption for the pervious (sand) fill. The insitu-friction angle could be larger because sand was heavily compacted (100 percent of Modified Proctor). On the other hand the sand contained a substantial amount of fines (12 percent maximum) which would tend to lower the

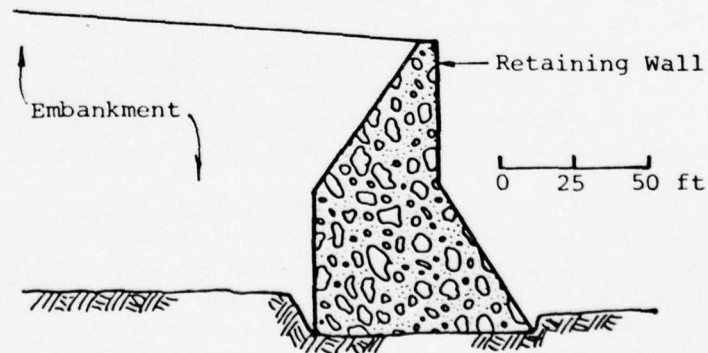
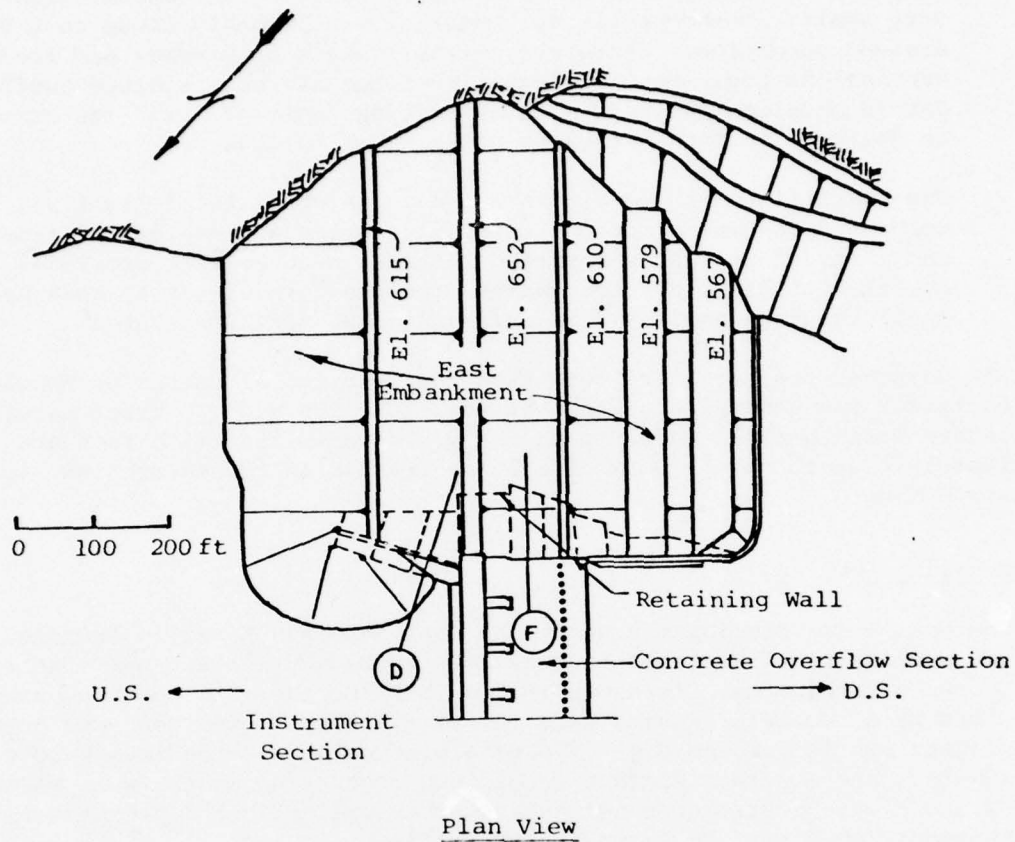


FIG. XIII-6 PLAN AND SECTION VIEWS OF RETAINING WALL AT EAST EMBANKMENT, WEST POINT DAM

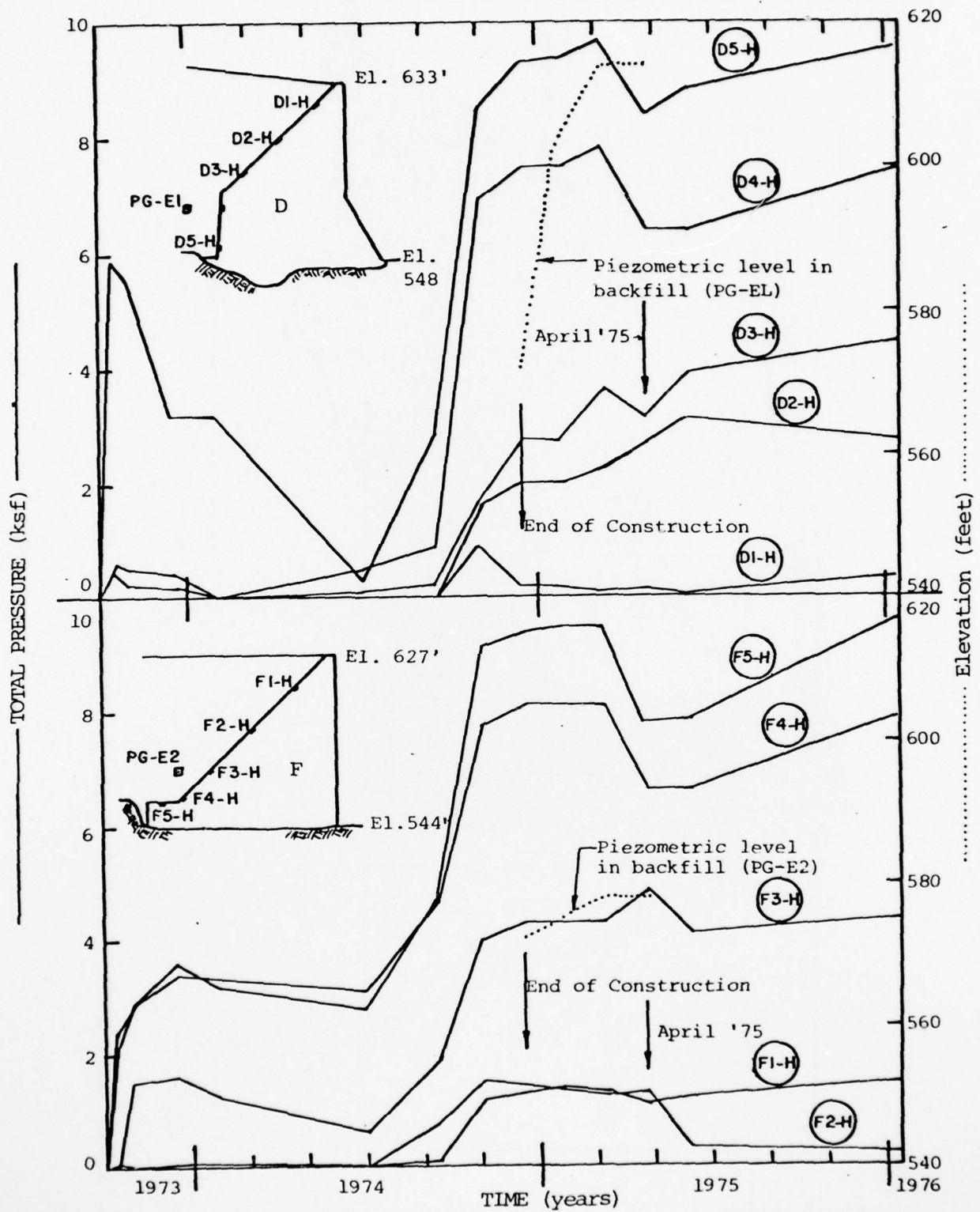


FIG. XIII-7 MEASURED PRESSURES AND PIEZOMETRIC LEVELS AT BLOCKS D AND F, WEST POINT DAM

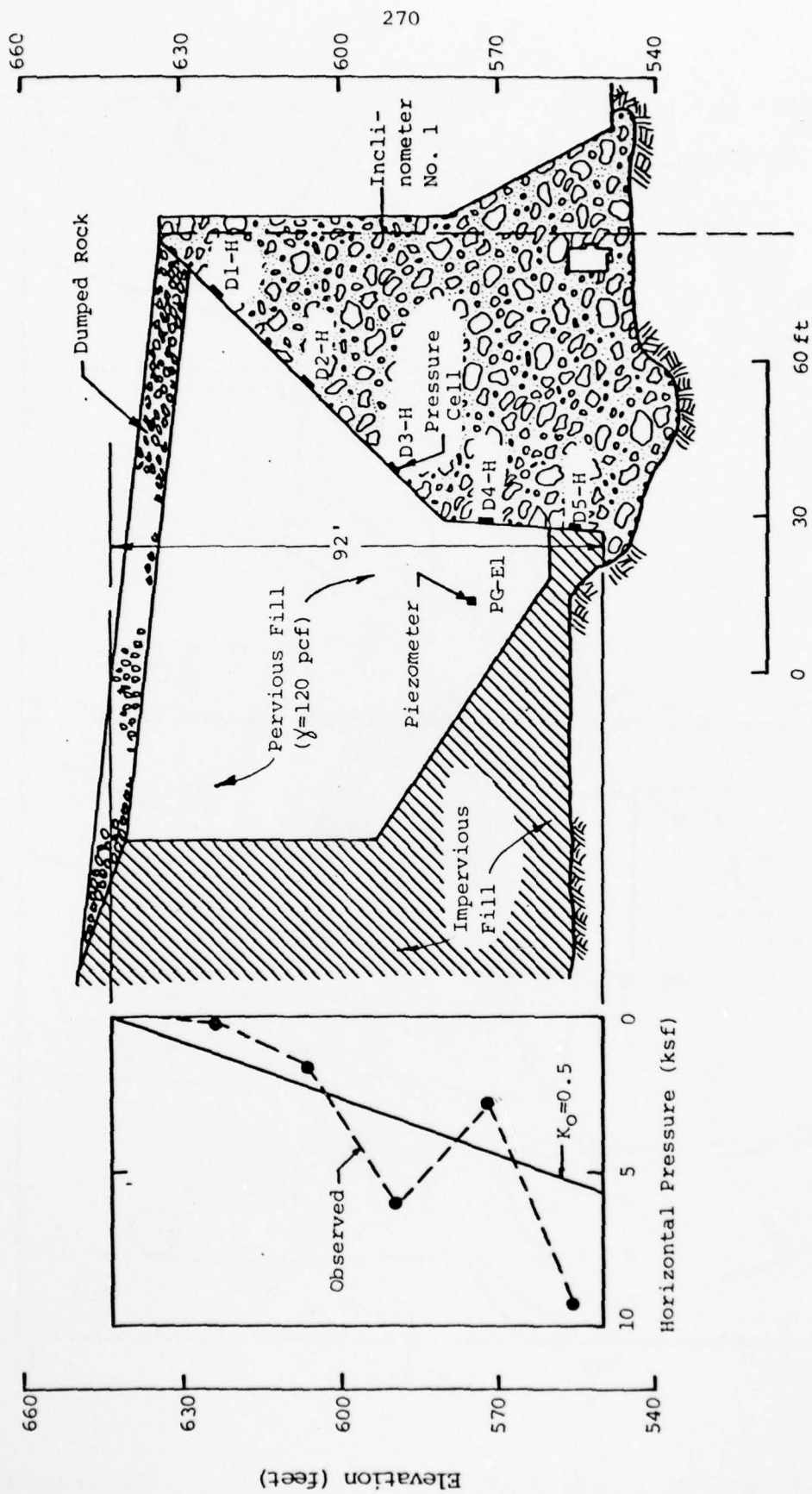


FIG. XIII-8 TOTAL EARTH PRESSURES AT END OF CONSTRUCTION, BLOCK D, WEST POINT DAM

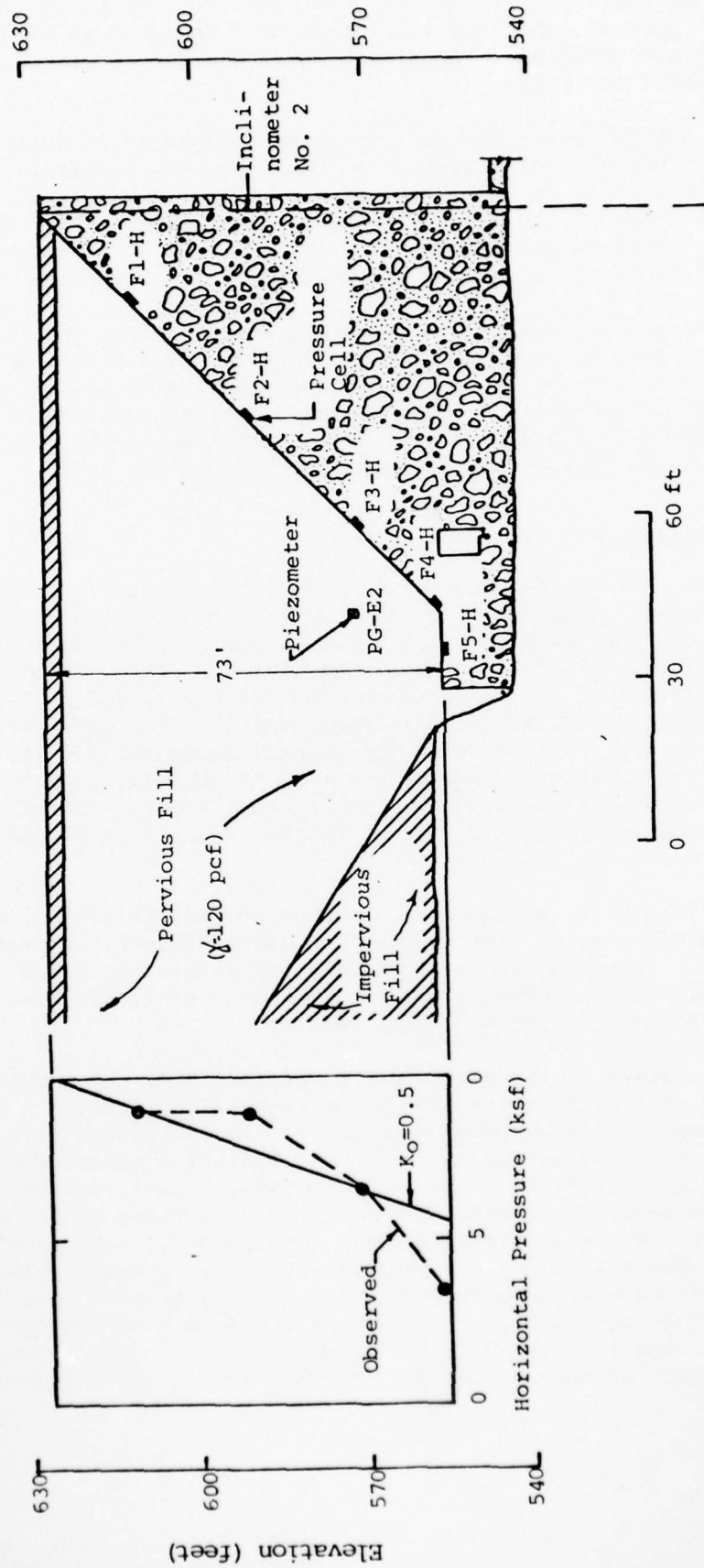


FIG. XIII-9 TOTAL EARTH PRESSURES AT END OF CONSTRUCTION, BLOCK F, WEST POINT DAM

friction angle. No pore-water pressures have been included in the theoretical predictions. However, the high total pressures measured at elevations below the piezometers could be an indication that pore pressures existed in the lower portions of the fills.

Horizontal components of the wall pressures, measured in April, 1975, are given in Figs. XIII-10 and XIII-11. By that time the backfills had become partially saturated as the reservoir was filled. Both total and effective pressures are plotted in the figures. The assumed water levels in the backfills are based on the piezometer data. Theoretical pressure distributions, based on Jaky's equation, are included in each figure.

Though there is some scatter in the measured pressures, they generally agree with the theoretical predictions shown in Figs. XIII-8 through XIII-11. The agreement is best for the later measurements when water had saturated the lower portions of the backfills. The high and low pressures measured at cells D3-H and D4-H at Block D could be an indication of stress redistribution adjacent to the change of inclination along the back of the wall.

C. Thompson Creek Channel

The Thompson Creek Channel is a flood control project of the Los Angeles District of the Corps of Engineers. A five-mile section of the channel (Mountain Avenue to White Avenue in Los Angeles County) was constructed in 1964. The channel is concrete lined and varies from 15 to 30 feet wide with 7 to 14 feet high vertical sides. The sides of the channel are formed by L-shaped, cantilever, retaining walls, as shown in Fig. XIII-12. The walls were backfilled with on-site soils removed from the channel excavations. The backfills consisted primarily of silty and gravelly sands, though clayey sands and sandy clays were used in some sections. The backfills were generally compacted to at least 95 percent of Standard Proctor maximum density at a moisture content near optimum.

Three wall panels (A, B and C), each about 50 feet in length, were instrumented to measure earth pressures on the walls, pore-water pressures in the backfills and strains in the reinforcing steel within the walls. Instrument readings were taken at three lines on each wall panel, as shown in Fig. XIII-12. Wall deflections were also measured.

Data were obtained as the walls were backfilled, but the results are scattered because of the irregular effects of backfill compaction. In general the pressures increased at any particular cell as the height of fill above the cell increased, but not in all cases. The wall pressures measured on Panels A and B, one day after backfilling, are shown in Figs. XIII-13 and XIII-14, respectively. The backfill at Panel C was placed in a loose condition and then compacted from the surface in a single lift. The data for this panel are shown in Fig. XIII-15. The data are total pressures, but are probably close to effective pressures because no pore-pressure measurements were reported and are presumed to have been negligible. The wall deflections observed during backfilling are also shown in Figs. XIII-13 through XIII-15. Wall movements are less than 0.5 percent of the wall height, as indicated in each figure.

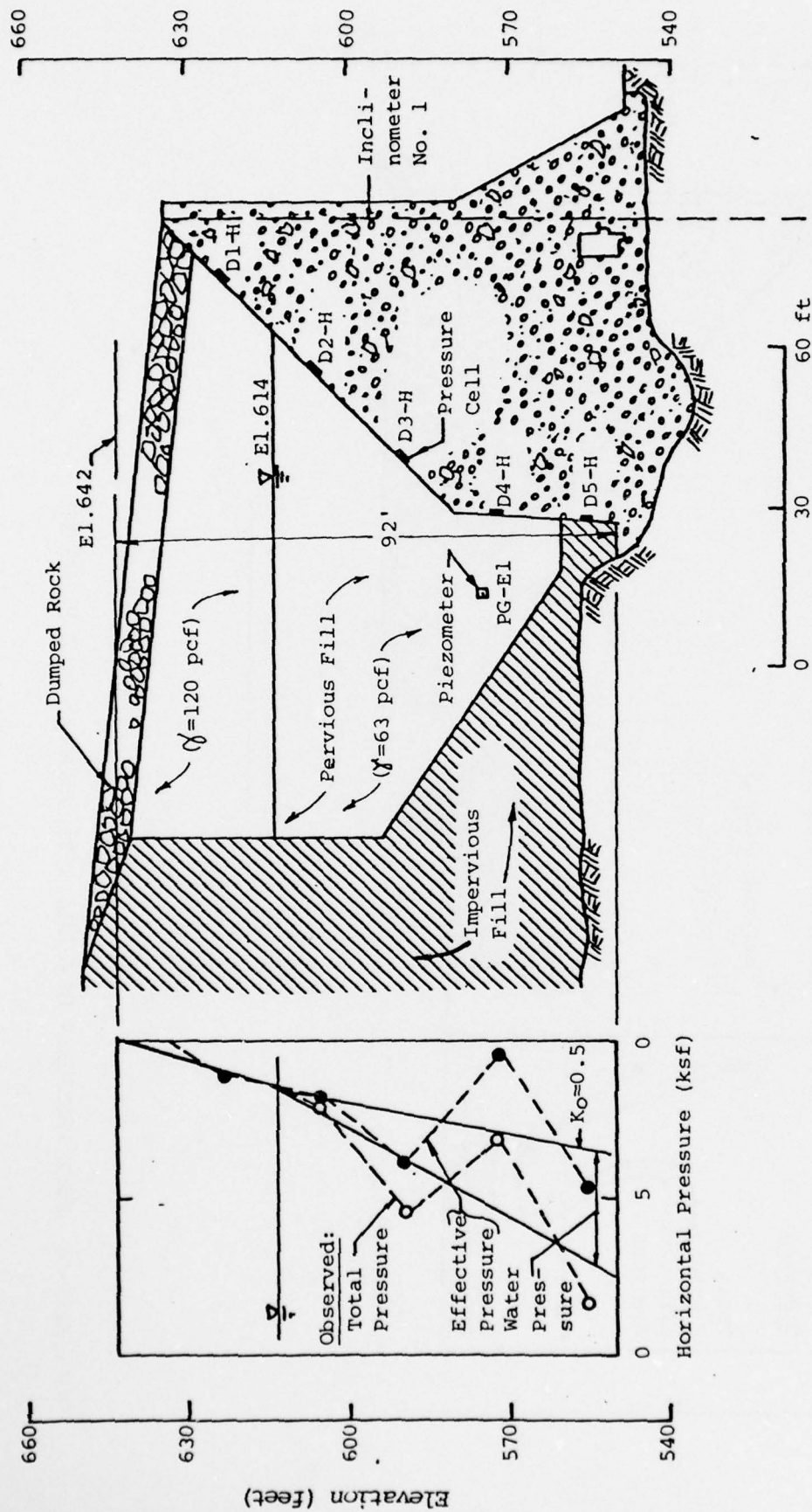


FIG. XIII-10 EARTH PRESSURES IN APRIL, 1975, BLOCK D, WEST POINT DAM

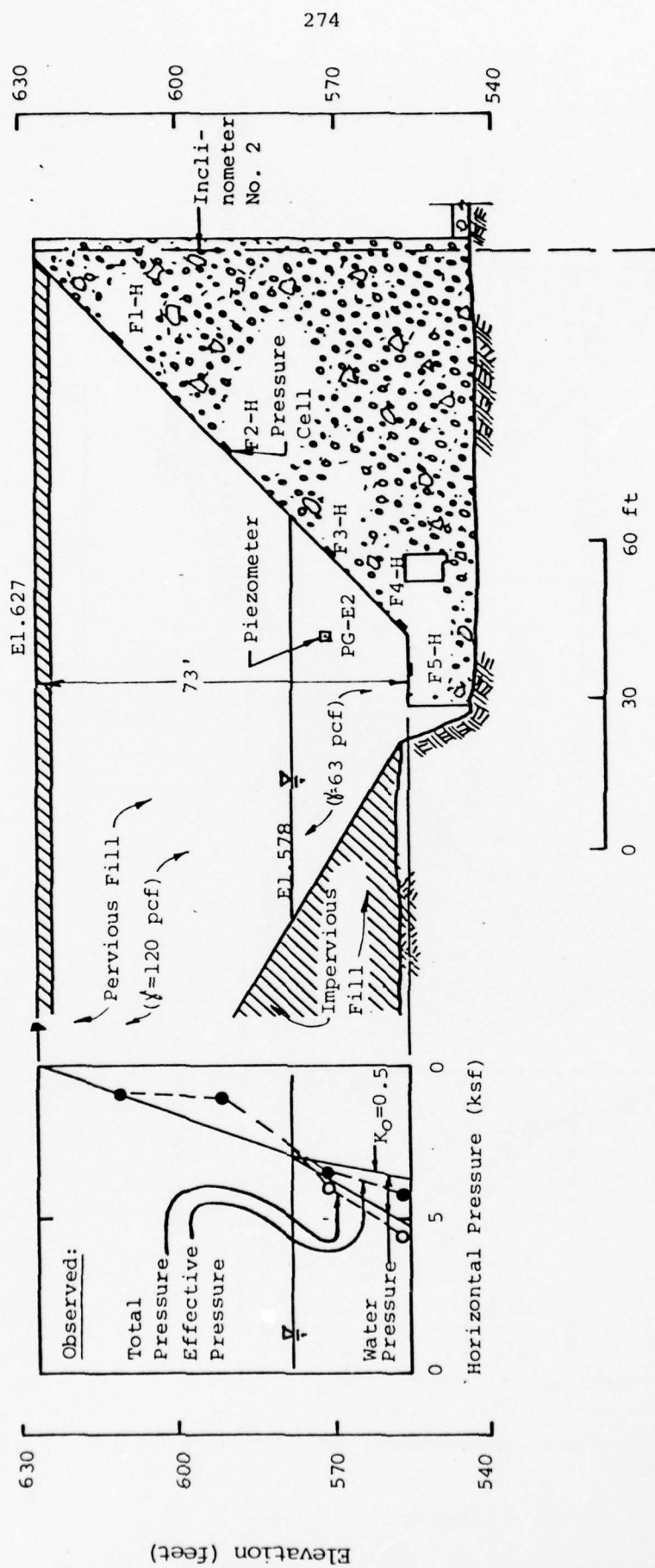


FIG. XIII-11 EARTH PRESSURES IN APRIL, 1975, BLOCK F, WEST POINT DAM

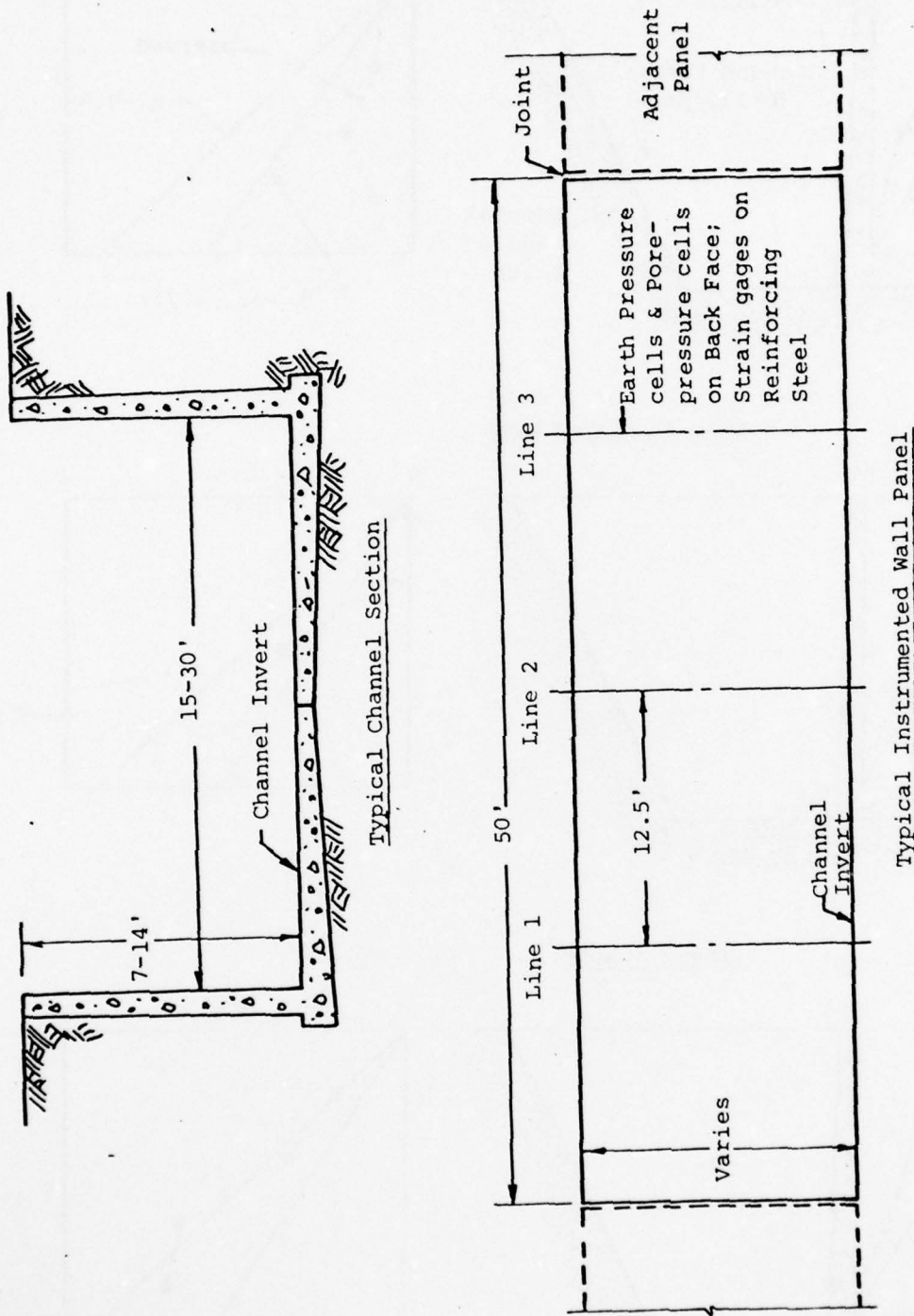
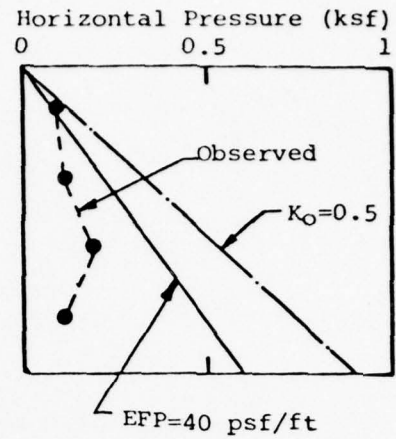
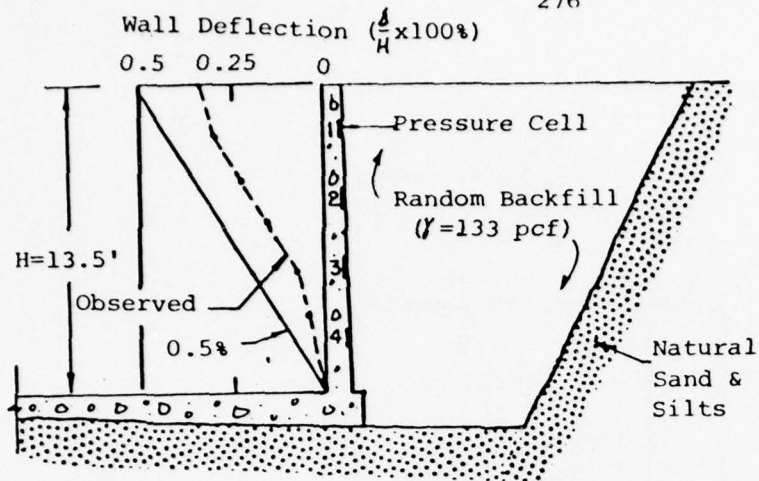
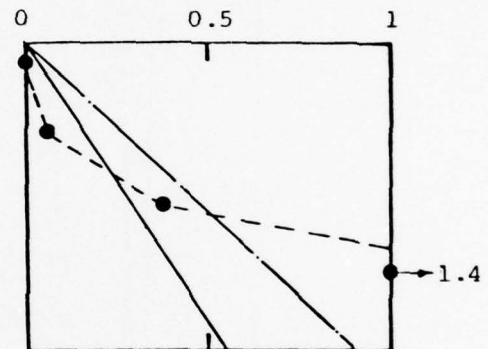
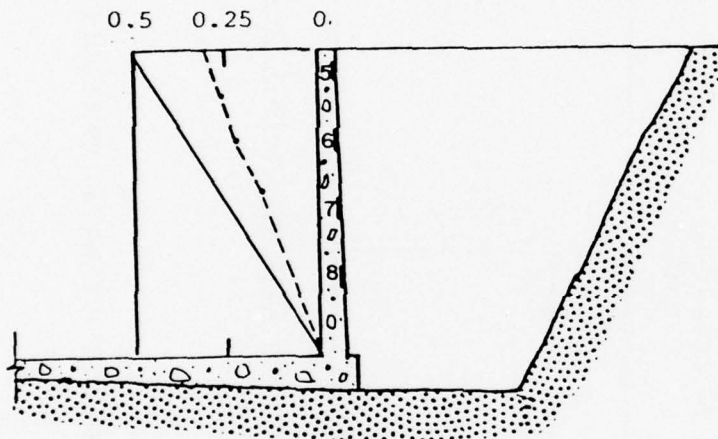


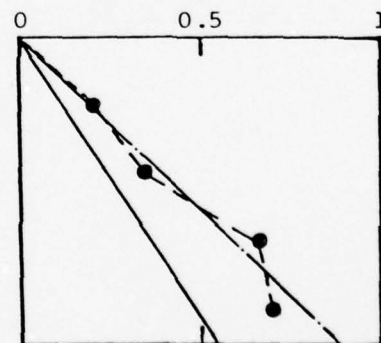
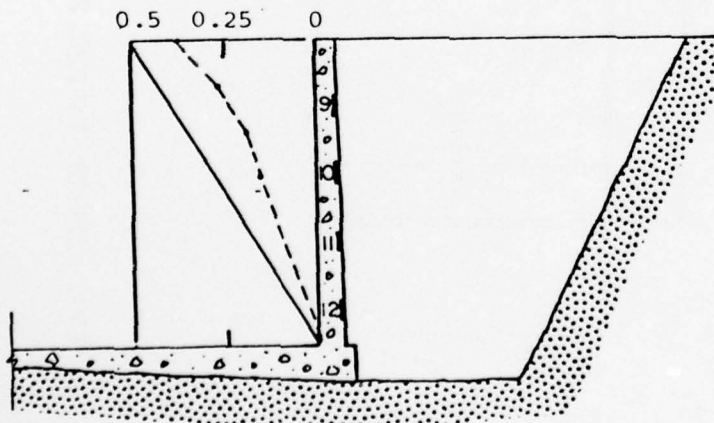
FIG. XIII-12 TYPICAL SECTIONS OF RETAINING WALLS, THOMPSON CREEK CHANNEL



Line 1 (Downstream)



Line 2 (Center)



Line 3 (Upstream)

0 5 10 ft

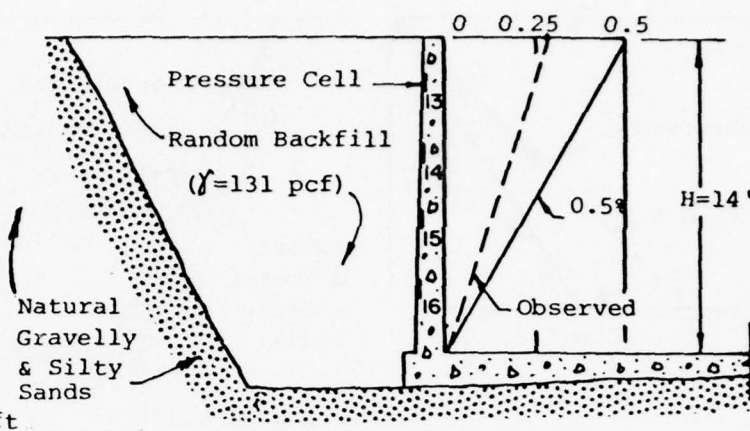
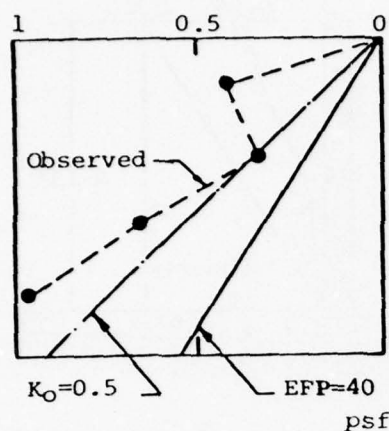
(Views Downstream)

FIG. XIII-13 EARTH PRESSURES AND WALL DEFLECTIONS AT END OF BACKFILLING, WALL PANEL A (STA. 76+00), THOMPSON CREEK CHANNEL

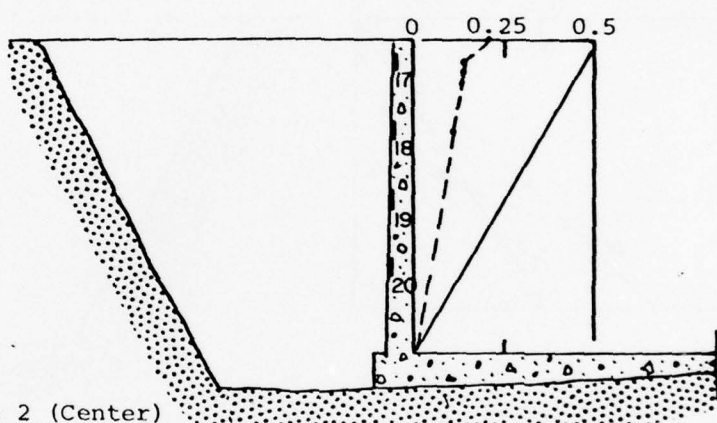
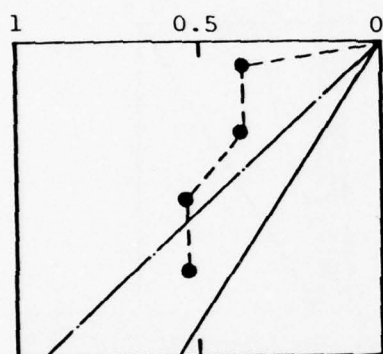
Horizontal Pressure (ksf)

277

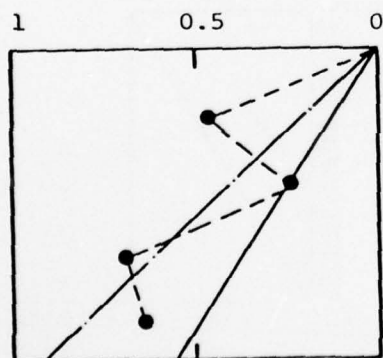
Wall Deflection ($\frac{in}{ft} \times 100\%$)



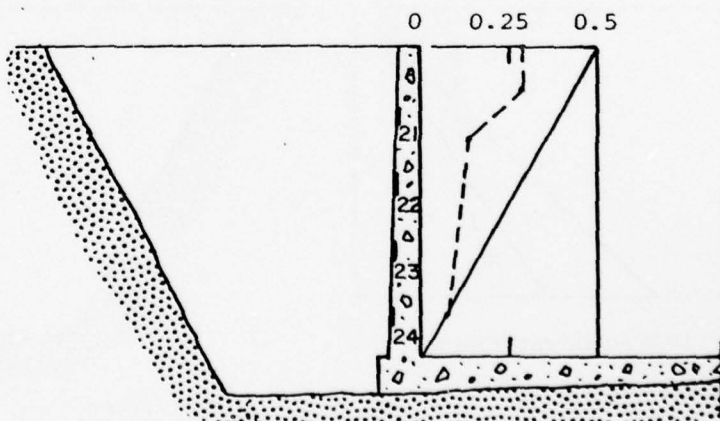
Line 3 (Downstream)



Line 2 (Center)



(Views Downstream)



Line 1 (Upstream)

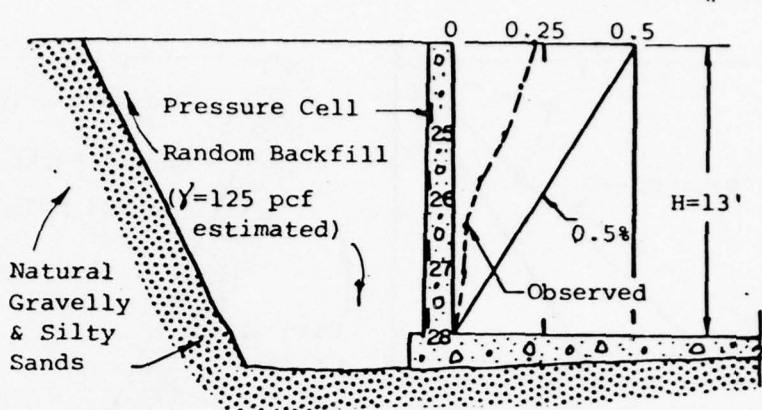
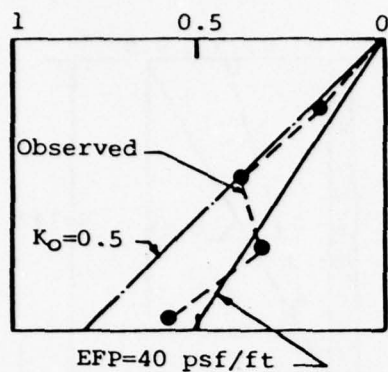
0 5 10 ft

FIG. XIII-14 EARTH PRESSURES AND WALL DEFLECTIONS AT END OF BACKFILLING, WALL PANEL B (STA. 97+00), THOMPSON CREEK CHANNEL

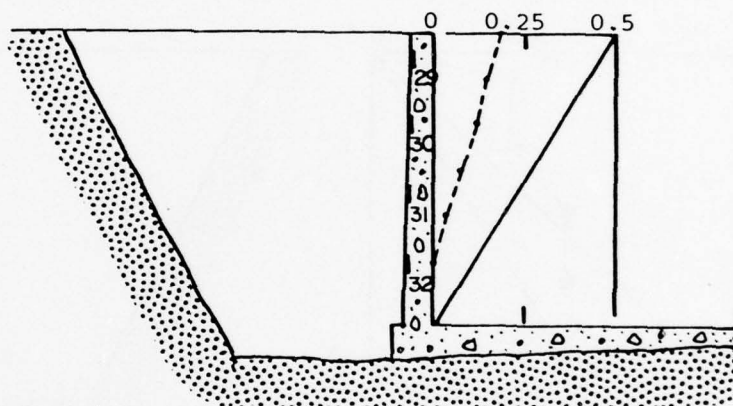
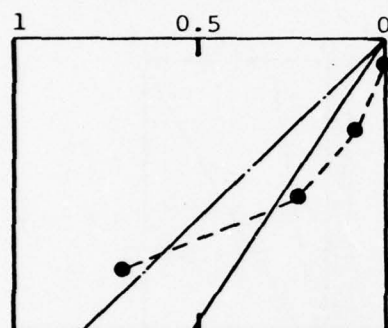
Horizontal Pressure (ksf)

278

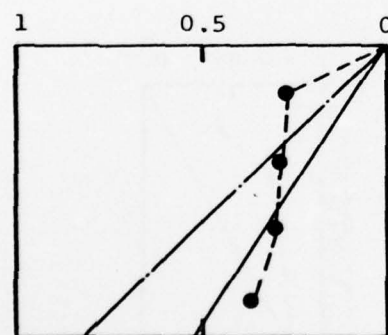
Wall Deflection ($\frac{1}{H} \times 100\%$)



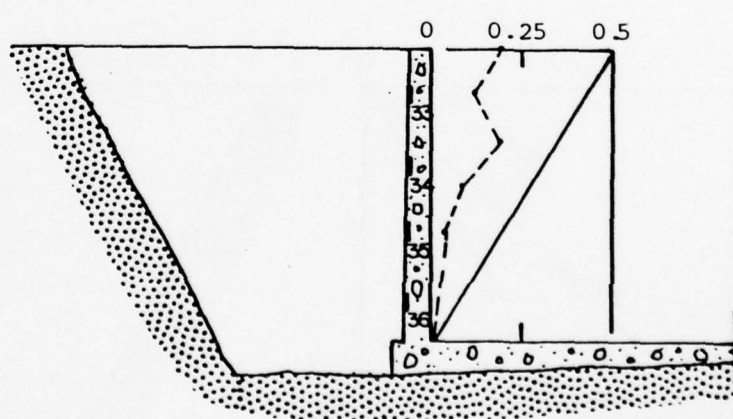
Line 3 (Downstream)



Line 2 (Center)



(Views Downstream)



Line 1 (Upstream)

0 5 10 ft

FIG. XIII-15 EARTH PRESSURES AND WALL DEFLECTIONS AT END OF BACKFILLING, WALL PANEL C (STA. 149+00), THOMPSON CREEK CHANNEL

Because of the relatively wide footings which support these walls, it is not clear whether they should be designed for active or at-rest earth pressures. It would be expected that the wall pressures would depend largely upon the flexibility of the wall stem. If active pressures are assumed, they could be estimated by Terzaghi and Peck's (1967) empirical method. The backfill type is intermediate between their Type 2 (course-grained soil of low permeability due to a mixture of particles of silt size) and Type 3 (residual soil with stones, fine silty sand, and granular materials with conspicuous clay content). Their recommended equivalent fluid pressure (EFP) would be 36 psf/ft for Type 2 soil and 46 psf/ft for Type 3 soil. A value of 40 psf/ft has been assumed to determine the earth pressures shown in Figs. XIII-13 through XIII-15. On the other hand, if at-rest pressures were assumed, a value of K_0 equal to 0.5 might be appropriate. The value is obtained from Jaky's equation for a friction angle of 30° . The at-rest pressures are also included in Figs. XIII-13 through XIII-15. Neither the at-rest nor the active pressures are in agreement with the observed pressures at all of the instrument sections. The variation in measured results could be a result of short-term effects (soil cohesion, capillary moisture, etc.) that are significant shortly after backfilling. It is not known whether measurements were taken at the test panels beyond the completion of construction. Such data would be useful for purposes of determining how the pressures changed, subsequently, as a result of long-term or seasonal effects.

The strain gage data for the test panels can also be studied to obtain an approximate understanding of the earth pressures on the wall. Measured strains in the reinforcing steel, at various depths below the top of each wall, are shown in Figs. XIII-16 through XIII-18. The calibration data are for loading tests performed on the walls prior to backfilling. A horizontal 800-plf line load was applied one foot below the top of each wall (towards the channel centerline). The other strain data were measured at the end of the backfilling and correspond to the earth pressure measurements in Figs. XIII-13 through XIII-15. Calculated strains are also shown in Figs. XIII-16 through XIII-18, and are based on the assumption that the average calibration strains would be increased in direct proportion to the total overturning moment on the wall. Calculated strains correspond to an (active) equivalent fluid pressure of 40 psf/ft and an at-rest coefficient of 0.5. Most of the measured strains fall within the bounds of the calculated values, with typically lower values near the top and higher values near the base of the wall.

D. San Jose Creek Channel

The Los Angeles District of the Corps of Engineers also constructed the San Jose Creek Channel in 1964. A one-mile-long section, from Sixth Avenue to the San Jose Diversion Channel (Los Angeles County), is similar to the Thompson Creek Channel except that it is much wider (100 to 130 feet), and it has higher sidewalls (13 to 18.5 feet). Wall construction procedures and backfill materials were similar to those at the Thompson Creek Channel. (The projects are within 15 miles of each other.) Three of the concrete wall panels were instrumented with earth pressure cells and pore pressure cells on the back-face of each wall, and with strain gages on the reinforcing steel within the walls.

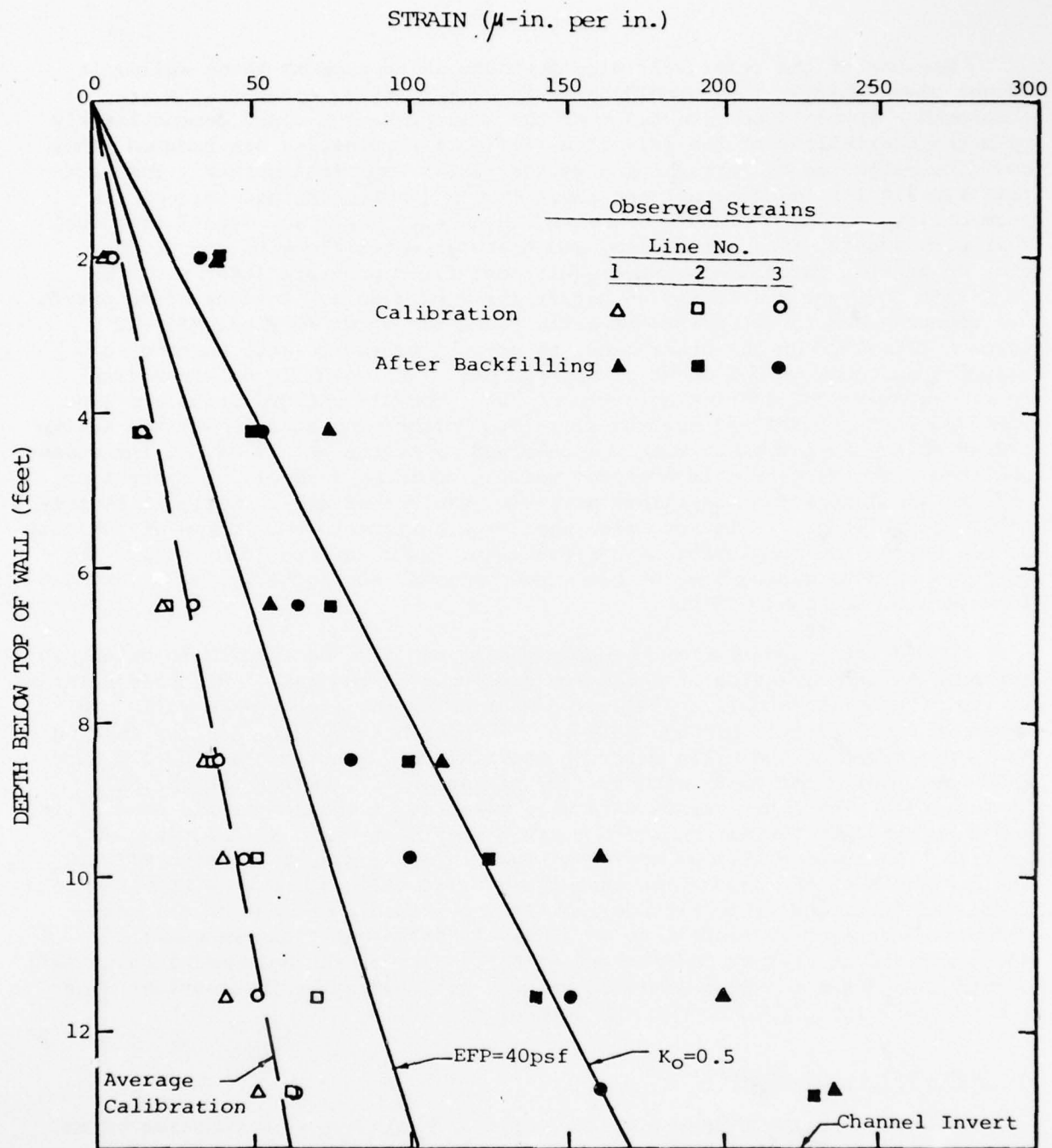


FIG. XIII-16 STRAIN GAGE DATA DURING CALIBRATION LOADING AND AFTER BACKFILLING, WALL PANEL A (STA. 76+00), THOMPSON CREEK CHANNEL

AD-A064 169

CALIFORNIA UNIV BERKELEY GEOTECHNICAL ENGINEERING
EARTH PRESSURES ON CONDUITS AND RETAINING WALLS. (U)
SEP 78 D W QUIGLEY, J M DUNCAN

F/6 13/2

DACW39-76-C-0035

NL

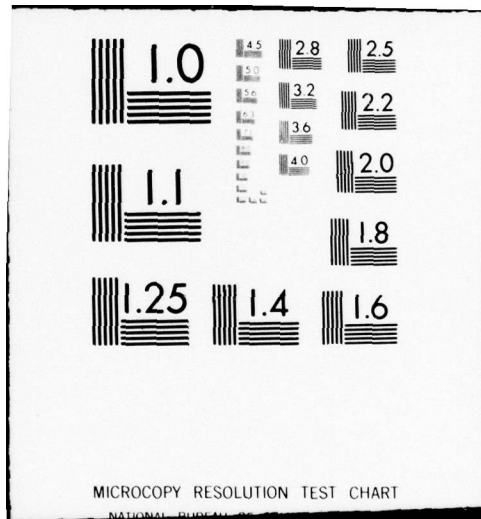
UNCLASSIFIED

UCB/GT/78-06

4 OF 4
AD
A064169



END
DATE
FILMED
3-79
DDC



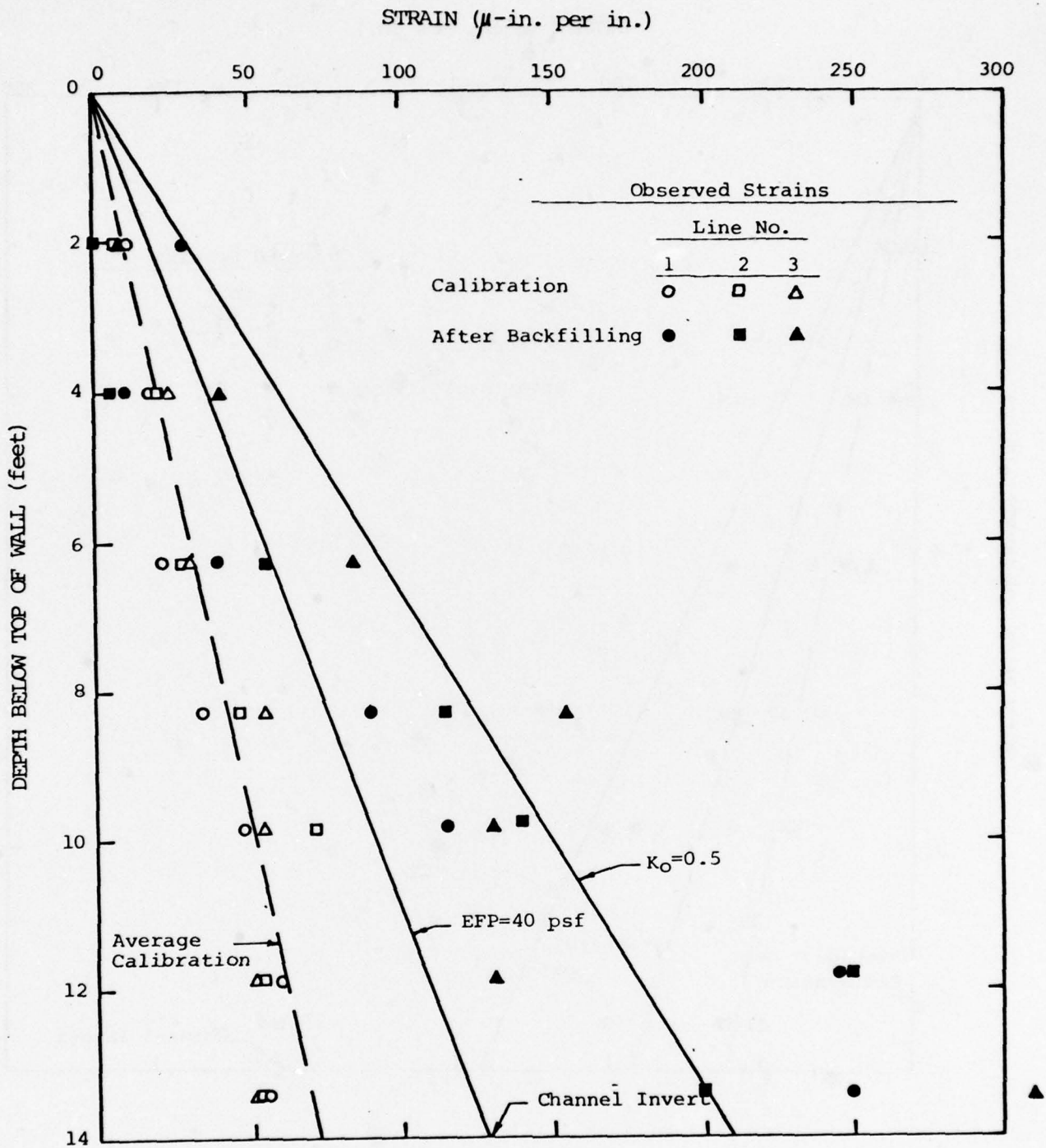


FIG. XIII-17 STRAIN GAGE DATA DURING CALIBRATION LOADING AND AFTER BACKFILLING, WALL PANEL B (STA. 97+00), THOMPSON CREEK CHANNEL

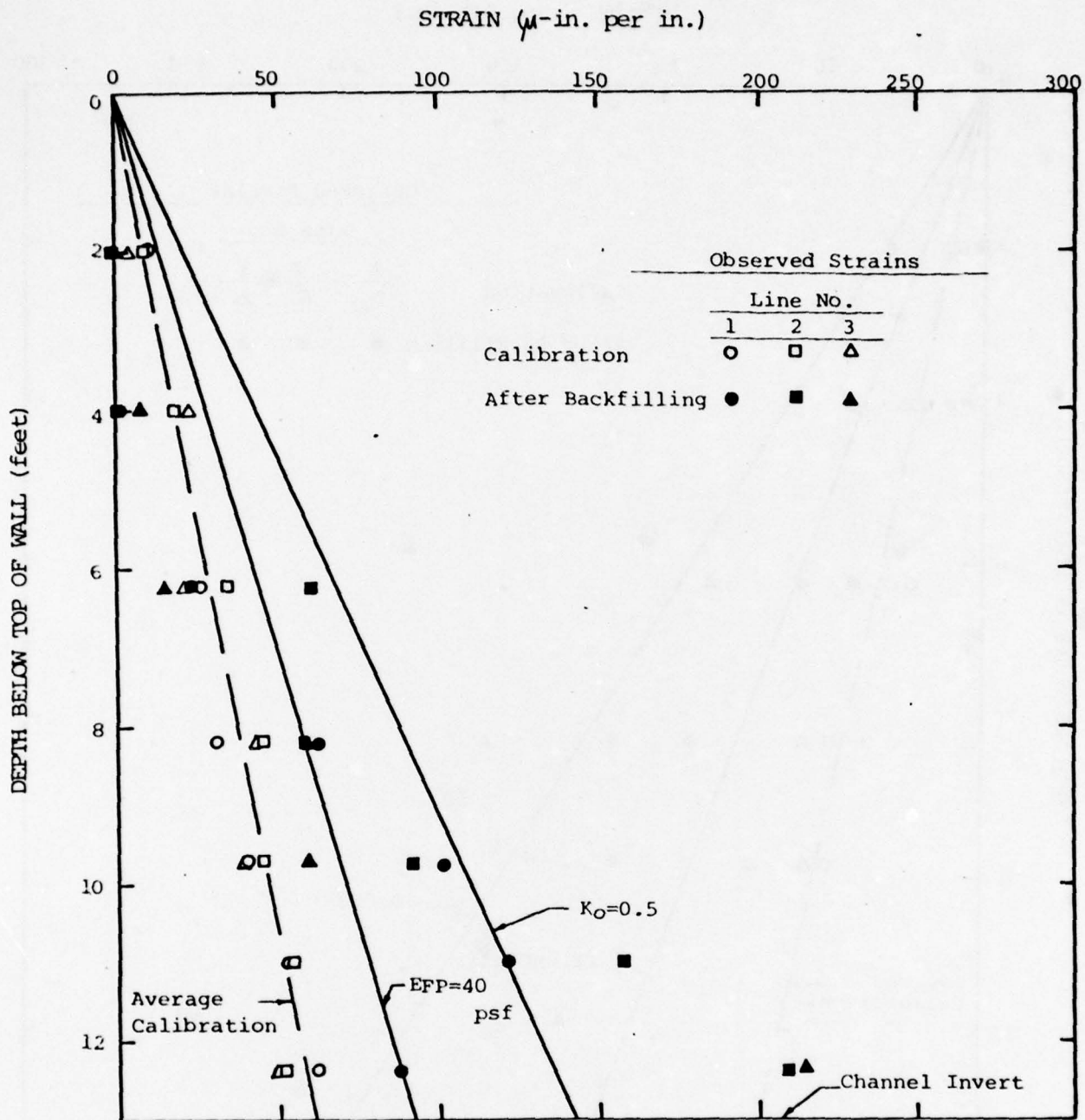


FIG. XIII-18 STRAIN GAGE DATA DURING CALIBRATION LOADING AND AFTER BACKFILLING, WALL PANEL C (STA. 149+00), THOMPSON CREEK CHANNEL

Wall pressures measured after backfilling are shown in Figs. XIII-19 through XIII-21 for the three test panels. Measurements were taken at Panels A and B upon completion of backfilling and again more than a month later. The measured pressures for Panel C were taken upon completion of backfilling. The total pressures shown in the figures are approximately equal to effective pressures because reported pore pressures were small or negligible. The reported wall movement data is also shown in the figures. The walls deflected less than 0.5 percent of the wall height, as indicated. Note also that the lower portion of the wall stem deflected very little.

Active pressures, corresponding to an equivalent fluid pressure of 40 psf (per Terzaghi and Peck, 1967), and at-rest pressures, based on a value of K_0 equal to 0.5 (per Jaky's equation with $\phi = 30^\circ$), are included in Figs. XIII-19 through XIII-21 for comparison with the measured values. The observed data are somewhat scattered and in fact negative earth pressures are indicated in some instances. This could be a result of instrumentation errors or simply an indication of the nonuniformity of pressures on relatively low walls retaining compacted backfills.

The reported strain gage data are inconsistent with the observed wall pressures and in addition do not appear to be credible (large scatter; some very high strains indicative of stresses approaching the yield-point of the steel in some locations; compressive stresses indicated at other locations). Therefore no attempt was made to compare the observed strain gage data with values predicted for the active and at-rest earth pressures.

Horizontal Pressure (ksf)

284

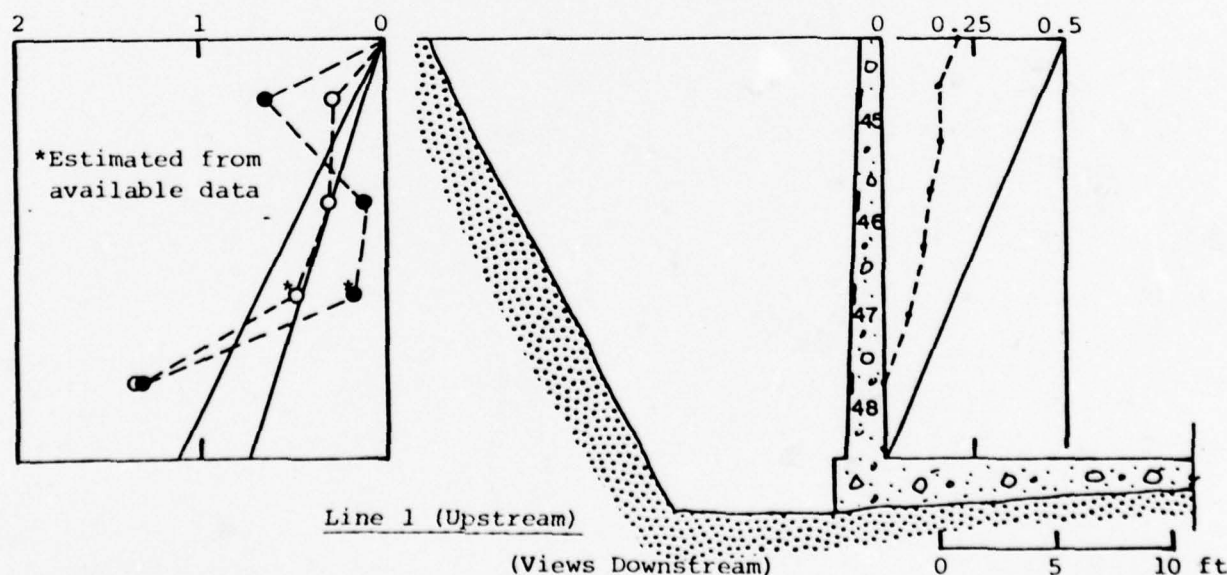
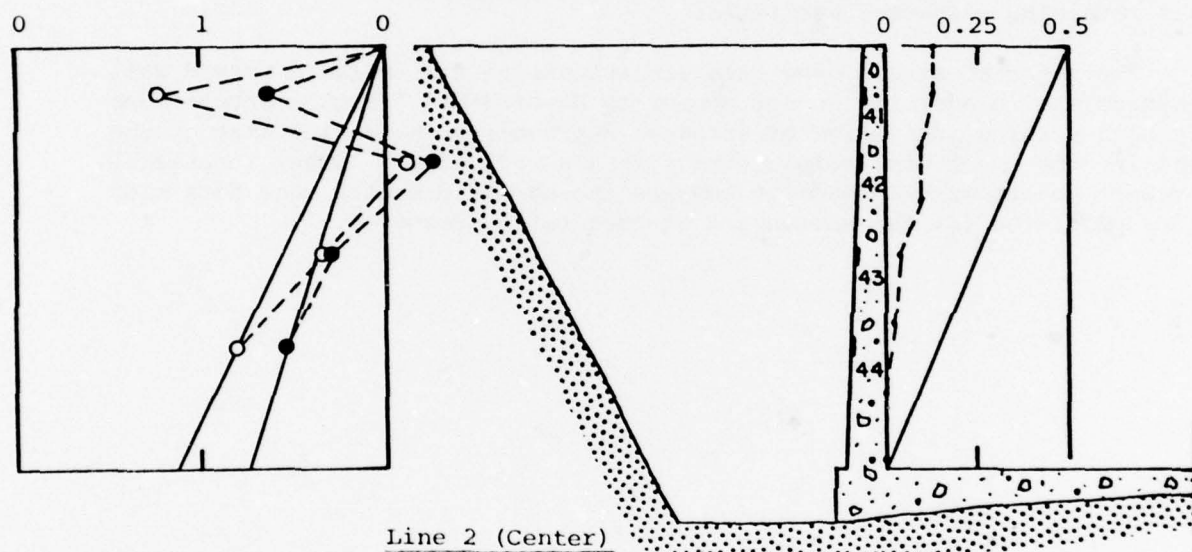
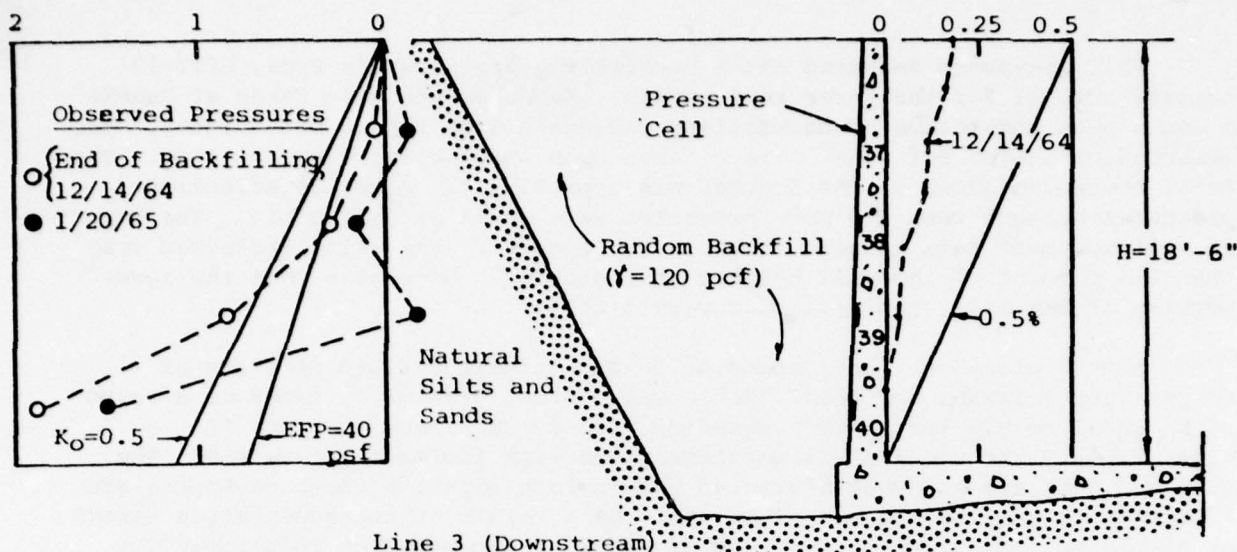
Wall Deflection ($\frac{\Delta}{H} \times 100\%$)

FIG. XIII-19 EARTH PRESSURES AND WALL DEFLECTIONS AFTER BACKFILLING, WALL PANEL A, (STA. 130+00), SAN JOSE CREEK CHANNEL

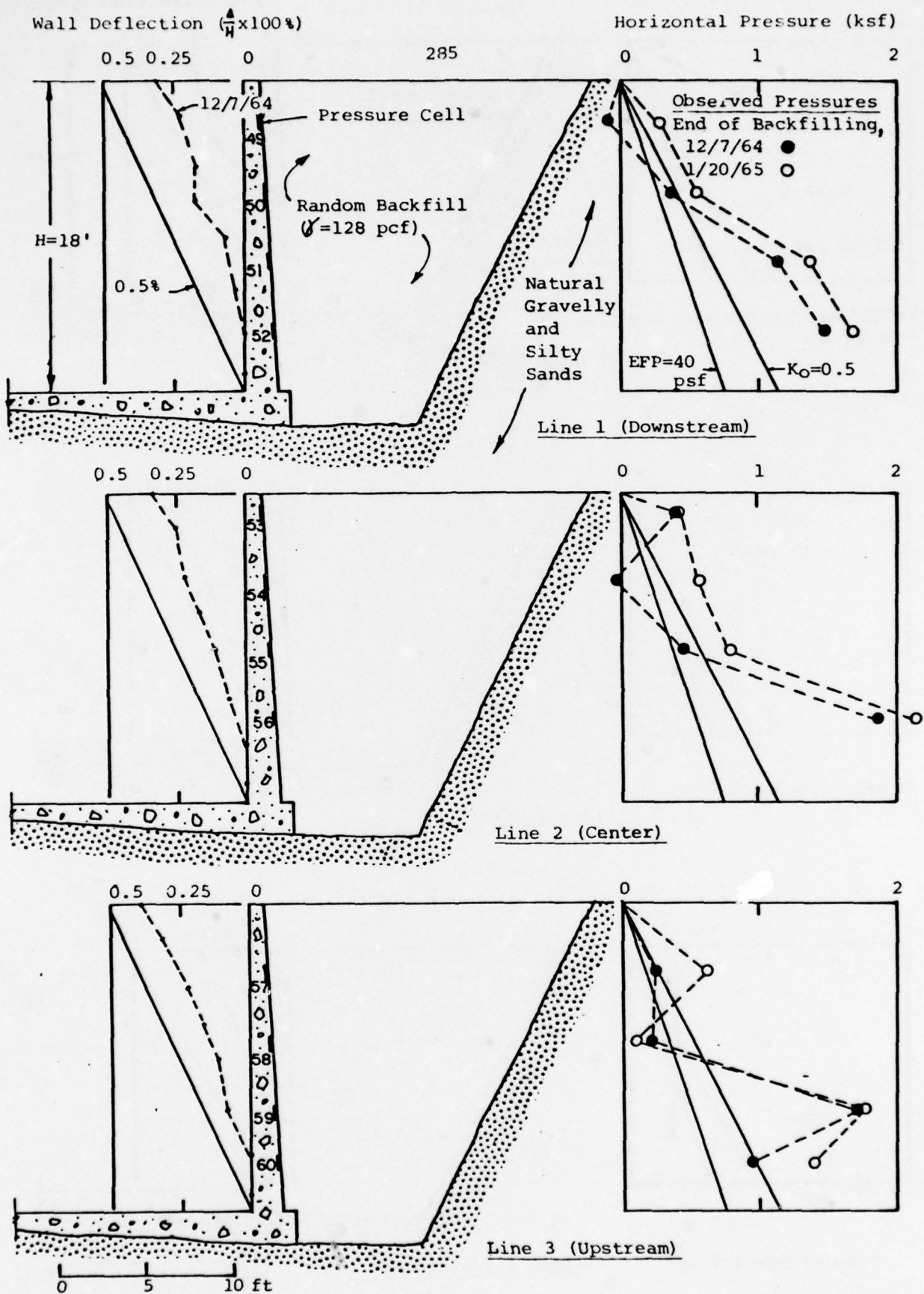


FIG. XIII-20 EARTH PRESSURES AND WALL DEFLECTIONS AFTER BACKFILLING, WALL PANEL B, (STA. 116+00), SAN JOSE CREEK CHANNEL

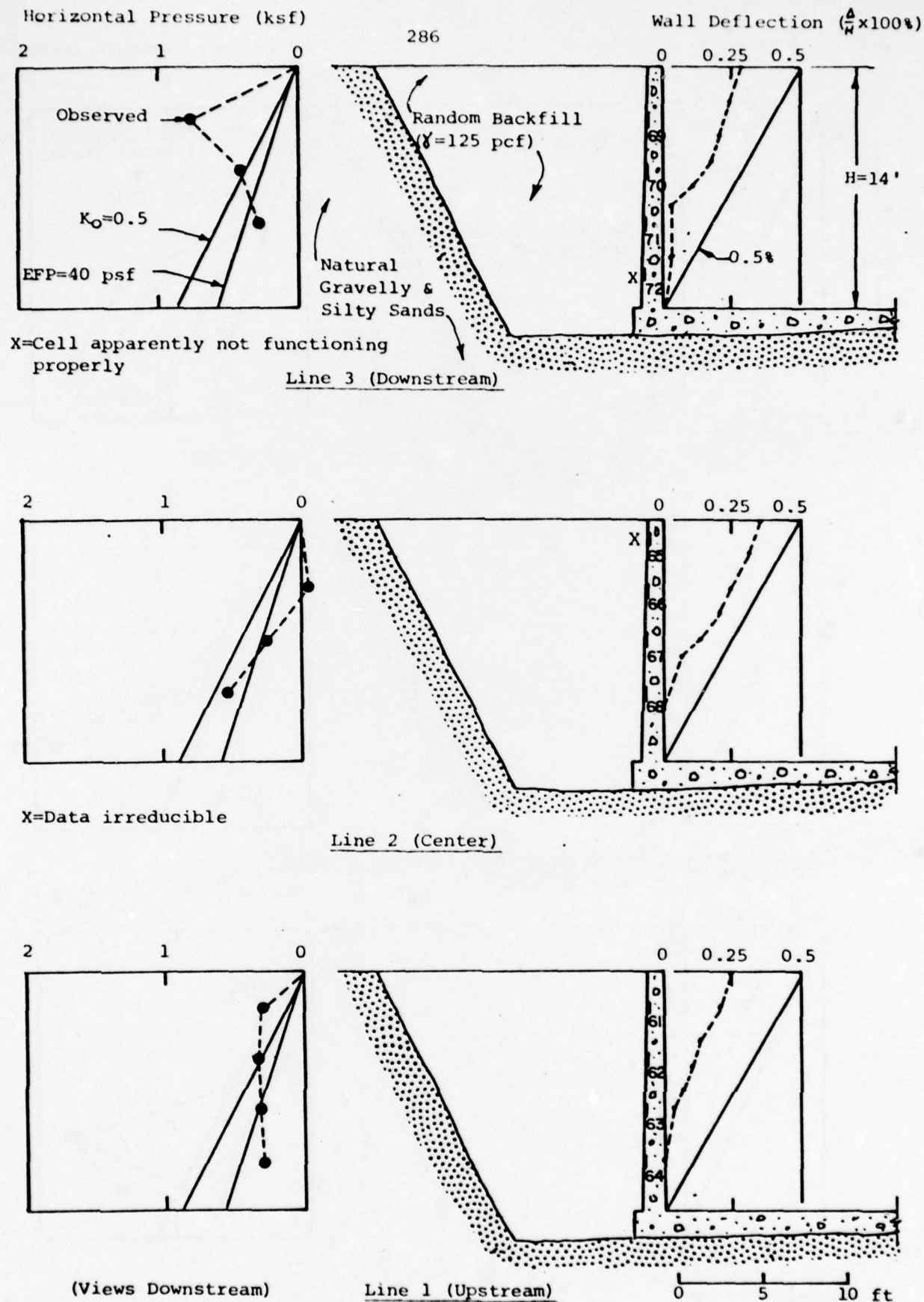


FIG. XIII-21 EARTH PRESSURES AND WALL DEFLECTIONS UPON COMPLETION OF BACKFILLING, WALL PANEL C, (STA. 91+00), SAN JOSE CREEK CHANNEL

CHAPTER XIV

CONCLUSIONS AND RECOMMENDATIONS - RETAINING WALLS

Because the number of reported retaining wall failures is small, existing methods of design to resist earth loadings are probably conservative. Safe and economical retaining walls are therefore likely to result if the present design methods are properly applied. In this regard, the most important steps the designer must take are to determine:

1. The type and unit weight of backfill to be used and the foundation conditions (cohesive or granular soils?)
2. The amount of wall movement to be expected (deflecting or unyielding?)
3. The direction of wall friction (for active or passive conditions) that will occur as a result of relative movement between the wall and backfill, and
4. The groundwater conditions that will exist within the backfill (hydrostatic pressures or not?)

If these four factors can be adequately determined, and as long as reasonable assumptions for soil strength are used in conjunction with a reasonable theory (or alternatively a reasonable empirical design value), then predicted pressures will be sufficiently accurate for design purposes.

The present Corps of Engineers procedures, as represented by the recommendations of EM 1110-2-2502, are generally consistent with current design practice. Based on literature review, analytical studies and case-history analyses performed for this investigation, the following comments and/or recommendations are suggested for changes to the present Corps of Engineers procedures:

1. Coulomb's theory should not be used for prediction of passive pressure (Eq. IX-10) because it gives unsafe results for many conditions. The design values of Caquot and Kerisel (1948) are more appropriate.
2. Jaky's formula (Eq. IX-II) or Brooker and Ireland's (Eq. IX-12) should be used for predicting effective at-rest earth pressures. Pore pressures must also be included if appropriate.
3. Low walls, of minor importance, should be designed by empirical methods such as that of Terzaghi and Peck (1967).
4. The finite-element method should be used for unusual design problems where soil-structure-interaction effects are likely to be significant.

The method is most applicable when the four factors listed above cannot be adequately determined by judgment alone.

These studies have indicated several areas that could benefit from further research:

1. The effect of seasonal variations in earth pressures. Field data are needed, for both yielding and rigid walls, regarding the magnitude of changes in wall pressures that can occur. The reasons for the changes must be better understood.
2. The effects of backfill compaction. The question of whether backfill compaction is desirable, particularly for unyielding walls, can only be decided conclusively by comparative field studies.
3. Unusual design problems. Well-instrumented field studies of unusual wall installations, coupled with analyses by finite-element methods, are desirable to reduce the number of retaining wall problems that must now be classified as "unusual" because of our inadequate knowledge and understanding of earth-pressure phenomena.

BIBLIOGRAPHY

A. REFERENCES FROM LITERATURE

Abel, J. F. & Kay, J. N. (1976) "Synthesis of Finite Element Analyses of Culverts" 2nd Int'l. Conf. on Numerical Methods in Geomechanics, Blacksburg, Va., June, 1976, p. 873-885.

Allgood, J. R. (1971), "Structures in Soil Under High Loads" Proc. ASCE, No. SM3, Proc. Paper 8006, March, 1971.

Allgood, J. R. & Takahashi, S. K. (1972) "Balanced Design and Finite-Element Analysis of Culverts", HRR No. 413, 1972 pp.45-56.

Alpan, I. (1967) "The Empirical Evaluation of the Coefficient K_O and K_{OR} " Soil and Foundations, Vol. 7, No. 1, 1967, pp. 31-40.

American Concrete Pipe Assn. (1974), "Concrete Pipe Design Manual" Arlington, Va., 1974.

ASCE/USCOLD(1975) "Lessons from Dam Incidents, USA" by The Committee on Failures and Accidents to Large Dams of the United States Committee on Large Dams, J. F. Redlinger, Chm. ASCE & USCOLD, New York, N. Y., 1975.

Besprozvannaya, I. M. (1965) "Determination of Earth Pressure on a Retaining Wall with an Inclined Back Face in Relation to its Displacements and Rigidity of the Foundation Soil" Soil Mech. & Found. Engr., July-Aug, 1965, pp. 201-207.

Bozozuk, M. & Leonards, G. A. (1972) "The Gloucester Test Fill" Procs. of the Spec. Conf. on Perf. of Earth and Earth-Supported Structures, ASCE, Purdue, Ind., June 1972, pp. 299-317.

Brand, E. W. & Krasaesin, P. (1971) "Investig. of an Embankment Failure in Soft Clay" Geot. Engrg. J., Southeast Asian Soc. Soil Energy, Bangkok, 1971, No. 1, pp. 53-66.

British Standards Institution (1967) "Methods of Testing Soil for Civil Engineering Purposes" British Standard 1377, London, 1967.

Broms, B. (1971) "Lateral Earth Pressures due to Compaction of Cohesionless Soils", Proc. 4th Budapest Conf. on Soil Mech. and Found. Engr., Oct., 1971, pp. 373-384.

Broms, B. B. & Ingelson, I. (1971), "Earth Pressure Against the Abutments of a Rigid Frame Bridge" Geotechnique, Vol. 21, No. 1, 1971, pp. 15-28.

Broms, B. B. & Ingelson, I. (1972) "Lateral Earth Pressure on a Bridge Abutment" Procs. 5th Eur. Conf. on S. M., Madrid, 1972, Vol. I, pp. 117-123.

Brooker, E. W. and Ireland, H. O. (1965), "Earth Pressures at Rest Related to Stress History," Canad. Geotech. Journ. Vol. 2, 1965, pp. 1-15.

Brown, C. B. (1967), "Forces on Rigid Culverts Under High Fills," Proc. ASCE Vol. 93 No. ST5, October, 1967; pp. 195-215.

Brown, C. B., Green, D. R., and Pawsey, S. (1968) "Flexible Culverts Under High Fills" • Struct. Div., Proc. ASCE, V. 94 No. ST 4, April 1968, pp. 905-917.

Burns, J. Q. and Richard, R. M. (1964), "Attenuation of Stresses for Buried Cylinders" Proc. Symp. for Soil Struct. Interaction, Univ. of Arizona, 1964, pp. 378-392.

Butler, B. E. (1972), "Structural Design Practice of Pipe Culverts," HRR #413, 1972, pp. 57-66.

Cappleman, H. L. Jr. (1967) "Movements in Pipe Conduits under Earth Dams" J. SM & FD, ASCE, V. 93, No. SM6, Nov. 1967, pp. 1-15.

Caquot, A. & Kerisel, J. (1948) "Tables for the Calculation of Passive Pressure, Active Pressure and Bearing Capacity of Foundations" Gauthier-Vitlars, Imprimeur-Editeur, Paris, 1948.

Casagrande, L. (1973) "Comments on Conventional Design of Retaining Structures" J. SMFD, Vol. 99, No. SM2, 1973, pp. 181-198.

Clarke, N. W. B. (1963) "The Wide Trench Condition and its Effect on the Loads Imposed on Rigid Underground Conduits," Procs. Instit. of Civil Engrs. Great Britain, Sept. 1963, pp. 105-118.

Clarke, N. W. B. (1967) "The Loads Imposed on Conduits Laid Under Embankments or Valley Fills," Proc. Inst. of Civil Engrs., London. Vol. 36, Jan., 1967, pp. 63-98.

Clough, G. W. and Duncan, J. M. (1969) "Finite Element Analyses of Port Allen and Old River Locks," USAEWES, Vicksburg, Miss. Contract Report S-69-6, Sept. 1969.

Clough, G. W. & Duncan, J. M. (1971) "Finite Element Analyses or Retaining Wall Behaviour" J. SMFD, Procs. ASCE, Vol. 97, No. SM12, December, 1971, pp. 1657-1673.

Coulomb, C. A. (1776) "Essai Sur Une Application des Regles de Maximis et Minimis a Quelques Problems de Statique Relatifs a L'architecture," Mem. Div. Savants, Acad. Sci, Paris, Vol. 7, 1776.

Coyle, H. M. & Bartoskewitz, R. E. (1976) "Earth Pressure on Precast Panel Retaining Wall" J. GED, Proc. ASCE V. 102, No. GT5, 1976, pp. 441-456.

Coyle, H. M. Bartoskewitz, R. E. Milberger, L. J., Butler, H. D. (1974) "Field Measurements of Lateral Earth Pressures on a Cantilever Retaining Wall" TRR #517, 1974, pp. 16-29.

Davis, R. E. & Bacher, A. E. (1968), "Calif.'s Culvert Research Crogram - Description, Current Status, and Observed Peripheral Pressures." HRR #249, 1968 pp. 14-23.

Davis, R. E. & Bacher, A. E. (1972)"Concrete Arch Culvert Behaviour - Phase 2" J. Struct. Div. ASCE, V. 98 No. ST11, 1972, p. 2329-2350.

Davis, R. E. & Bacher, A.E. (1974) "Concrete Pipe Culvert Behaviour - Part 2" J. SD ASCE Vol. 100 No. ST3, 1974, pp. 615-630.

Davis, R. E., Bacher, A.E. & Obermuller, J. C. (1974) "Concrete Pipe Culvert Behaviour" Part 1" Journ. Struct. Div. ASCE. Vol. 100, No. ST3 1974, pp. 599-614.

Deen, R. C. (1969) "Performance of a Reinforced Concrete Pipe Culvert Under Rock Embankment," Highway Research Record No. 262, 1969 pp. 14-26, w/discussion by M. G. Spangler, pp. 27-28.

Department of the Army (1961), EM 1110-2-2502 "Retaining Walls" May 29, 1961.

Department of the Army (1969) EM 1110-2-2902 "Conduits, Culverts & Pipes 3 Mar. 1969.

Duncan, J. M. (1975), "Finite Element Analysis of Buried Flexible Metal Culvert Structures" Prelim. Copy of a paper prepared for publication in the Laurits Bjerrum Memorial Volume March 1975.

Duncan, J. M. (1976a) "Design of Circular and Elongated Flexible Metal Culverts" A paper prepared for presentation at the 1976 Annual Meeting of the Transportation Research Board.

Duncan, J. M. (1976b) "Design Method for Flexible Metal Culverts - Pipes, Pipe Arches, and Arches," Res. Rept. prepared for Kaiser Alum. & Chemical Sales Corp. Oakland, Calif. May 24, 1976, Revised Sept. 23, 1976.

Duncan, J. M. (1977) "Behaviour and Design of Long-Span Metal Culvert Structures" a paper prep. for presentation at the Technical Session on "Soil-Struct Interact for Shallow Friction and Buried Structures" during the Oct. 77 ASCE Conv. in SF and for publ. in the JGED, ASCE.

Duncan, J. M. & Clough, G. W. (1971) "Finite Element Analyses of Port Allen Lock" J. SMFD, Proc. ASCE, vol. 97, No. SM8, August, 1971, pp. 1053-1067.

Fetzer, C. A. (1967) "Electro-osmotic Stabilization of West Branch Dam" JSMFD, Proc. ASCE, Vol. 93, No. SM 4, July, 1967, pp. 85-106.

Flathau, W. J. & Sager, R. A. (1964) "The Design of Buried Arches to Resist Blast Loads" Proc. of the Symposium on Soil-Structure Interaction," Univ. of Arizona, Tuscon, Ariz. Sept. 1964, pp. 554-573.

Gould, J. P. (1970) "Lateral Pressures on Rigid Permanent Structures" ASCE Spec. Conf. on Lateral Stresses in the Ground and Design of Earth-Retaining Structures, Ithaca, N. Y., 1970, p. 219-269.

Graham, J. (1971) "Calculation of Passive Pressure in Sand" Canad. Geotech. J., Vol. 8, No. 4, 1971, pp. 566-578.

Granger, V. L. (1965) "Failure of A Reinforced Concrete Reservoir" Proc. 6th Int'l Conf. SMFE, Montreal, 1965, Vol. II, pp. 56-60.

Hale, H. T. & Dyer, E. A. (1963) "The Subsidence at Fylde Street, Farnworth," Procs., The Instit. of Civil Engrs, Feb. 1963, pp. 207-222.

Hendron, A. J. (1963) "The Behaviour of Sand in One-Dimensional Compression" PhD Thesis, Dept. of Civil Engr. Univ. of Illinois, 1963.

Hoeg, K. (1968) "Stresses Against Underground Structural Cylinders" J. SM & FD, ASCE, V. 94, No. SM 4, July, 1968, pp. 883-858.

Hough, B. K. (1957), "Basic Soils Engineering," The Ronald Press Company, New York, N. Y. 1957.

Hughes, J. M. O. (1969) "Culvert Elongations in Fills Founded on Soft Clays" Canad. Geot. J., V.G, No. 2, May, 1969, pp. 111-117.

James, A.M. (1965) "Low Friction and High Density of Fill Toppled Wall" ENR, July 8, 1965, pp. 80-81.

James R. G. & Bransby, P. L. (1970) "Experimental and Theoretical Investigations of A Passive Earth Pressure Problem" Geotechnique, V. 20, #1, 1970, pp. 17-37.

Janbu, N. (1957) "Earth Pressure and Bearing Capacity Calculations by Generalized Procedure of Slices," Proc. 4th Int'l. Conf. on SMFE, Vol. 2, 1957, pp. 207-212.

Janbu, N. (1972) "Earth Pressure Computations in Theory and Practice" Proc. 5th Europ Conf. on Soil Mech. & Found. Engrg. Madrid, April, 1972, Vol. 1, Theme 1, pp. 47-54.

Jansson, H. Wickert, A. & Rinkert, A. (1948) "Earth pressure against retaining walls" Proc, 2nd Int'l. Conf. on Soil Mech. Rotterdam, 1948, V. 2, pp. 71-76.

Kany, M. (1972) "Measurement of Earth Pressures on A Cylinder 30 m in diameter (pump storage plant)" Procs. 5th Eur. Conf. SM, Madrid, 1972, pp. 535-542.

Karadi, G. M. (1969) "Culvert Design in Some European Countries" Highway Research Record No. 266, 1969, pp. 29-43.

Kenney, T. C. (1959) "Disc. on Proc. Paper 1732" Proc. ASCE Vol. 85, No. SM 3 1959, pp. 67-79.

Krizek, R. J., Corotis, R. B. & Farzin, M. H. (1974) "Field Performance of Reinforced Concrete Pipe" TRR #517, 1974, pp. 30-47.

Krizek, F. J. and Kay, J. M. (1972) "Material Properties Affecting Soil-Structure Interaction of Underground Conduits" HRR No. 413, 1972, pp. 13-29.

Krizek, R. J., Parmeter, R. A., Kay, J. N. & Elnaggar, H. A. (1971) "Structural Analysis and Design of Pipe Culverts" NCHRP Rept. No. 116, 1971.

Kruse, G. H. (1965) "Measurement of Embankment Stresses on A Hundred-foot-high Retaining Wall" ASTM STP 392: Instruments and Apparatus for Soil and Rock Mechanics, 1965, pp. 131-142.

Kulhawy, F. H. (1974) "Analysis of A High Gravity Retaining Wall" Proc. of the Conf. on Analysis and Design in Geotech. Engrg., Austin, Texas, 1974, Vol. 1, pp. 159-172.

Kulhawy, F. H. and Gurtowski, T. M. (1976) "Load Transfer and Hydraulic Fracturing in Zoned Davis" JGED, Proc. ASCE Vol. 102, No. GT9, Sept. 1976, pp. 963-974.

Kulhawy, F. H., Duncan, J. M. and Seed, H. B. (1969) "Finite Element Analyses of Stresses and Movements in Embankments During Construction" Report No. TE-69-4, Office of Res. Svcs, College of Engr., Univ. of Calif. Berkeley, Ca., November, 1969.

Ladanyi, B. (1958) "The Mobilization of Shear Strength in the Active Rankine Case of Earth Pressure," Proc. Brussels Conf. on Earth Pressure Problems, 1958, Vol. 1, p. 133.

Lambe, T. W. & Whitman, R. V. (1969), "Soil Mechanics" John Wiley & Sons, New York, 1969.

Lee, K. L. & Shen, C. K. (1969) "Horizontal Movements Related to Subsidence" J. SMFD, Proc. ASCE, Vol. 94, No. SM6, Jan. 1969, pp. 139-166.

Lefebvre, G., Duncan, J. M. & Wilson, E. L. (1973) "Three-dimensional Finite Element Analyses of Dams", JSMFD, Proc. ASCE, Vol. 99, No. SM7, July 1973, pp. 495-507.

Malishev, M. V. (1965) "Calculations of Soil Pressures on Pipelines in Embankments" Procs, 6th Int. Conf. on Soil Mech. & Foundation Engr., Montreal, 1965, Vol. II, pp. 401-404.

Matteotti, G. (1970) "Some Results of Quay-Wall Model Tests on Earth Pressure" Proc. Instit. Civ. Engrs., 47, Oct. 1970, pp. 185-204.

Moore, H. E. (1971) "Finite Element Analyses of the Earth Pressures Against A Bridge Pier" Proc. Engr. Geol. Soils Engr. Symp. 9th Annual Mfg, Boise & Moscow, Idaho, April, 1971, pp. 91-105.

Morgenstern, N. R. & Eisenstein, F. (1970), "Methods of Estimating Lateral Loads and Deformations" ASCE Spec. Conf. on Lateral Stresses in the Ground and Design of Earth-Retaining Structures, June 1970, pp. 51-102.

Mueser, Rutledge, Wentworth & Johnston (1968) "Report on Study of Movements of Articulated Conduits under Earth Dams on Compress. Fndtns" Soil Cons. Service, USDA, June, 1968.

Nobari, E. S. and Duncan, J. M. (1972) "Effect of Reservoir Filling on Stresses and Movements in Earth and Rockfill Dams" College of Engineering, Office of Research Services, Univ. of Calif. Berk. Ca., Rept. No. TE-72-1, January, 1972.

Obrcian, V. F. (1969) "Determination of Lateral Pressures Associated with Consolidation of Granular Soils," HRR #284, 1969.

Ortiz, I. S. (1967) "Zumpango Test Embankment" JSMFD, Proc ASCE, Vol. 93 No. SM-4, July, 1967, pp. 199-289

Pawsey, S. and Brown, C. B. (1968) "The Modification of the Pressures on Rigid Culverts with Fill Procedures," HRR #249, 1968, pp. 37-43, w/discussion by M.G. Spangler.

Pettibone, H. C. & Howard A. K. (1967) "Distribution of Soil Pressure on Concrete Pipe" J. Pipeline Div. ASCE, July, 1967, pp. 85-102.

Portland, Cement Assn" (1958) "Concrete Sewers," Chicago, Ill., 1958.

Poulos, H. G. (1972) "Difficulties in Prediction of Horizontal Deformations of Foundations" JSMFD, Proc. ASCE, Vol. 98, No. SM8, August, 1972, pp. 843-848.

Quigley, D. W. Duncan, J. M., Caronna, S., Morous, P. J. and Chang, C. S. (1976), "Three-Dimensional Finite Element Analysis of New Melones Dam" Rept. No. TE 76-3, Coll. of Engrs. off of Res. Svcs, Univ. of Ca., Berk., Ca., December, 1976.

Rankine, W. J. M. (1857) "On the Stability of Loose Earth", Trans. R. Soc. of London, Vol. 147

Rehman, S. E. & Broms, B. B. (1972) "Lateral Pressures on Basement Wall, Results from Full-Scale Tests" Proc. 5th Europ. Conf. on Soil Mech. & Found. Engr. Madrid, April 1972, Vol. 1, Theme 2, pp. 189-197.

Rowe, P. W. (1969a) "Progressive Failure and Strength of a Sand Mass" Proc. 7th Int'l Conf. SMFE, Mexico City, 1969, Vol. 1, pp. 341-349.

Rowe, P. W. (1969b) "The relation between the Shear Strength of Sands in Triaxial Compression, Plane Strain and Direct Shear" Geotechnique, V. 19, No. 1, 1969, pp. 75-86.

Rowe, P. K. and Peaker, K. (1965) "Passive Earth Pressure Measurements" Geotechnique, V. 15, 1965, pp. 57-78.

Rutledge, P. C. & Gould, J. P. (1973) "Movements of Articulated Conduits under Earth Dams on Compressible Foundations" in Embankment-Dam Engineering, Casagrande Volume, ed. by Hirschfield, R. C. and Poulos, S. J., John Wiley and Sons, New York, 1973, pp. 209-237.

Sherard, J. C. (1973) "Embankment Dam Cracking," in "Embankment-Dam Engineering, Casagrande Volume," ed. by Hirschfield, L. C. and Poulos, S. J., John Wiley, & Sons, New York, 1973, pp. 271-353.

Sherard, J. C., Woodward, R. J., Gizienski, S. F., Clevenger, W. A. (1963) "Earth and Earth-Rock Dams" John Wiley and Sons, Inc. New York, 1963.

Sherard, J. L., Decker, R. S. and Ryker, N. L. (1972) "Hydraulic Fracturing in Low Dams of Dispersive Clay "Proc. of the spec. conf. on perf. of earth and earth-supported struct's." ASCE/Purdue Univ., Lafayette, Ind. 1972, pp. 653-689.

Sherman, W. C. and Trahan, C. C. (1968) "Analysis of Data from Instrumentation Program, Port Allen Lock" USCE WES Tech. Rept. S-68-7, Vicksburg, Miss., Sept., 1968.

Sherman, W. C. and Trahan, C.C. (1969) "Analysis of Data from Instrumentation Program, Old River Lock" USCE WES Draft Rept. Vicksburg, Miss., 1969.

Sims, F. A., Forrester, G. R. & Jones, C. J. F. (1970) "Lateral Pressures on Retaining Walls" Journ. Instit. of Highway Engrs. V. 17, No. 6, 1970, pp. 19-30.

Sims, F. A. & Jones, C. J. F. (1974) "Comparison between Theoretical and Measured Earth Pressures Acting on A Large Motorway Retaining Wall" Highway Engrg. Vol. 21, No. 12, 1974, pp. 26-29.

Sokolvskii, V.V. (1965) "Statics of Granular Media," Permagon, Oxford, 1965.

Sowers, G. F., Robb, A. D., Mullis, C. H. & Glenn, A. J. (1957) "The Residual Lateral Pressures Produced by Compacting Soils" Proc. IV Int'l. Conf. SM & FE, 1957, Vol. 2, pp. 243-247.

Spangler, M. G. (1951), "Soil Engineering" International Textbook Co., Scranton, Pa., 1951.

Spangler, M. G. (1962), "Culverts and Conduits" in Foundation Engrg. ed. by G. A. Leonards McGraw-Hill Book Co., Inc., New York, 1962, pp. 965-999.

Spangler, M. G. (1974) "Discussion of "Field Performance of Reinforced Concrete Pipe" by Krizek, et. al. (1974)" TRR #517, 1974, pp. 42-46.

Symons, I. F. & Wilson, D. S. (1972) "Measurement of Earth Pressures in Pulverized Fuel Ash Behind A Retaining Wall" Proc. 5th Europ. Conf. on Soil Mech. and Found. Engr. Madrid, April, 1972, Vol. 1, Theme 4, pp. 569-575.

Terzaghi, K. (1940) "Earth Pressure of Sands on Walls" Proc., Purdue Conf. on Soil Mech. and its Applications, 1940, p. 240.

Terzaghi, K. & Peck, R. B. (1967) "Soil Mechanics in Engrg. Practice (2nd Ed.) John Wiley & Sons, New York, 1967.

Townsend, M. (1963), "Reinforced Concrete Pipe Culverts: Criteria for Structural Design and Installation," US BPR, 1963.

Trollope, D. H., Speedie, M. G. & Lee, I. K., (1963) "Pressure Measurements on Tullaroop Dam Culvert," Proc. of the Fourth Australia-New Zealand Conf. on Soil Mechanics and Foundation Engrg. 1963, pp. 81-92.

Tsdrebotarioff, G. P. (1973) "Foundations, Retaining and Earth Structures" (2nd Ed.) McGraw-Hill Book Co., New York, 1973.

U. S. Bureau of Reclamation (1960), "Design of Small Dams," US Dept. of Interior, 1960.

U. S. Army Engineer Waterways Experiment Station, Corps of Engrs. (1962), "Design and Analysis of Underground Reinforced-Concrete Arches," Tech. Rept. No. 2-590, Vicksburg, Miss., Jan., 1962.

U. S. Navy Facilities Engineering Command (1971) "DM-7, Soil Mechanics, Foundations and Earth Structures," March, 1971.

Valera, J. E. & Chen, J. C. (1974) "Stresses in An Earth Dam Due to Construction and Reservoir Filling" Procs. of the Conf. on analysis and design in geotechnical engineering, ASCE/Univ. of Texas, Austin, Texas, June 9-12, 1974, pp. 33-50.

Vaughan, P. R. & Kennard, M. F. (1972) "Earth Pressure at A Junction Between An Embankment and A Concrete Dam" Proc. 5th Em. Conf. SM Madrid, 1972, pp. 215-221.

Watkins, R. K. (1975), Buried Structures" Chap. 23 in Foundation Engrg. Handbook, ed. by Winterkorn, H. F. and Fang, H. Y., Van Nostrand Reinhold Co., New York, N. Y., 1975.

Wiseman, G. (1962) "Laboratory Soil Engineering Studies on Dune Sand" Publ. No. 20, Faculty of Civil Engrg. Israel Instit. Geotechnology, 1962.

Wong, K. S. (1977) "SSTIPN - Soil Structure Interaction Program with Interface Elements," University of California, Berkeley.

Wong, K. S. and Duncan, J. M. (1974) "Hyperbolic Stress-Strain Parameters for Nonlinear Finite Element Analyses of Stresses and Movements in Soil Masses" Rept. No. TE-74-3, College of Engineering, Office of Research Services, Univ. of Calif. Berkeley, Ca., July, 1974.

B. CORPS OF ENGINEERS PROJECT DATA

1. Cochiti Dam (Albuquerque District, Corps of Engineers, Albuquerque, New Mexico).

"Cochiti Dam and Reservoir, Rio Grande, New Mexico, Design Memorandum No. 8, Outlet Works," 1965.

"Conduit Instrumentation, Supplement No. 1 to Design Memorandum No. 8, Outlet Works," December, 1966.

"Conchiti Dam and Reservoir, Rio Grande, New Mexico, Design Memorandum No. 9, Embankment and Conveyance Channel, Vols. I-VI," July, 1967.

"Cochiti Lake, New Mexico, Rio Grande Basin, Periodic Inspection and Continuing Evaluation of Completed Civil Works Structures," ER-1110-2-100, May, 1975.

"Cochiti Lake, Rio Grande, New Mexico, Interim Report, Conduit Strain Gage Instrumentation," September, 1975.

"Specifications: Embankment, Cochiti Dam and Reservoir, Section 2E, Embankment, undated.

"Letter from Jasper H. Coombes, P. E., Chief, Engrg. Division, July 8, 1977.

Letter from Jasper H. Coombes, P. E., Chief, Engrg. Division, July 26, 1977.

Catanach, R. B. and McDaniel, T. N. (1971) "Cement Stabilized Fill for Conduit Support" Journ. S. M. & FD, Procs. ASCE, Vol. 97, No. SM 6, June, 1971, pp. 959-963.

2. DeQueen Lake Dam (Tulsa District, Corps of Engineers, Tulsa, Oklahoma)

Various drawings, "DeQueen Lake, Embankment Dikes and Spillway," March, 1971.

"Specifications, DeQueen Lake and Dam, Section 7," undated.

"DeQueen Lake, Outlet Works Conduit, Carlson Stress Cell Data," various dates.

"Open System Prizometer Data, DeQueen Lake," various dates.

3. Dierks Lake Dam (Tulsa District, Corps of Engineers, Tulsa, Oklahoma)

Various drawings "Dierks Dam, Embankment, Outlet Works, Spillway and Access Roads," December, 1968.

"Specifications, Dierks Dam, Section 6," undated.

Various reports, "Results of Tests of Soil Construction Samples, Embankment, Dierks Dam - Tulsa District" SWD Laboratory, Dallas, Texas, various dates.

"Dierks Lake, Carlson Stress Cell Data," various dates.

4. Lake Kemp Dam (Tulsa District, Corps of Engineers, Tulsa, Oklahoma)

Various drawings, "Lake Kemp Dam, Embankment, Outlet Works, and Spillway," March, 1970.

Specifications, Lake Kemp Dam, Sections V and VI, undated.

Various Reports, "Construction Control and Records Testing - Lake Kemp Dam," SWD Laboratory, Dallas, Texas, various dates.

"Kemp Lake, Instrumentation, Carlson Stress Cell Data, various dates.

5. Bankhead Lock and Dam (Mobile District, Corps of Engineers, Mobile, Alabama).

Various drawings, "Construction Plans, John Hollis Bankhead Lock and Dam, Replacement Lock," March, 1972.

"Specifications, Bankhead Lock and Dam," Section 2 undated.

"Construction Control Reports, Bankhead Replacement Lock," various dates.

"Record Tests, Bankhead Lock and Dam," SAD Laboratory, Marietta, Georgia, various dates.

Letter from H. L. Lawson, Chief, E. & M. Branch, June 23, 1977.

6. West Point Dam (Savannah District, Corps of Engineers, Savannah, Georgia)

Various drawings, "West Point Project," 1970-1974.

"Design Approach and Criteria for Left Embankment Retaining Wall at the West Point Project," undated.

"West Point Project, Supplement to Periodic Inspection Brochure No. 1," undated.

7. Thompson Creek Channel (Los Angeles District, Corps. of Engineers, Los Angeles, California)

Various drawings, "Thompson Creek Channel, Mountain Ave. to White Ave.," undated.

"Instrumentation Test Report No. 6439, Thompson Creek Channel, Mountain Ave. to White Ave.," Specialized Testing Service, North Hollywood, California, December 21, 1964.

Various reports "Construction Control Data, Thompson Creek Channel," various dates.

"Soil Test Results, Foundation Investigation, Thompson Creek," undated.

"Specifications, Thompson Creek Channel," Section 5, undated.

"Test Panel Compaction Data, Thompson Creek," undated.

8. San Jose Creek Channel (Los Angeles District, Corps of Engineers, Los Angeles, California)

Various drawings, "San Jose Creek Channel, Sixth Ave. to San Jose Division Channel," undated.

"San Jose Creek Flood Control Channel, Wall Instrumentation and Test," BLA Electronics, Pasadena, California, undated.

"Soil Test Results, Foundation Investigation, San Jose Creek," undated.

Various reports, "Construction Control Data, San Jose Creek," undated.

"Specifications, San Jose Creek Channel," Section 5, undated.

"Test Panel Compaction Data, San Jose Creek," undated.

APPENDIX AFINITE-ELEMENT ANALYSES1. Finite-Element Method

The analytical studies of earth pressures on conduits were made using methods for static finite-element analyses of soil-structure interaction problems developed at the University of California, Berkeley. The procedures have been developed largely under the sponsorship of the Corps of Engineers and are characterized by the following:

- a. The analyses are performed in a series of steps, each simulating the placement of all or a portion of the structure or a layer of backfill.
- b. The values of Young's Modulus and Poisson's ratio assigned to each soil element during successive steps of the analysis can be adjusted in accordance with the calculated values of stress in the element.
- c. The parameters used to relate the values of modulus and Poisson's ratio to the stresses are determined using data from laboratory triaxial, direct shear and consolidation tests on backfill materials.
- d. The analyses calculate stresses within the backfill, moments, thrusts and shears within the structure and displacements of the structure and the backfill.

The computer program SSTIPN, (Wong, (1977)), was used to analyze the response of buried conduits to backfill loads. The analyses represented two-dimensional, plane-strain conditions. Soil elements were either triangular or rectangular, whereas the conduit was represented by one-dimensional beam elements. One-dimensional interface elements were used along the perimeter of the conduit to allow for slippage between the conduit and the backfill. The calculated normal and shear stresses in the interface element was also an indication of the normal pressure and shear (traction) on the conduit caused by the backfill.

The program TWODEF-B, developed at the University of California, Berkeley, was used for simple structural analyses of conduits acted upon by idealized pressure distributions. These analyses were made to calculate the moments, thrusts and shears within a conduit that are caused by assumed pressure distributions, representative of the results of the more-complex SSTIPN analyses. The TWODEF-B studies served as a check on the validity of the assumed pressures. The program was also used to determine moment, thrust and shear coefficients for the simplified design procedures developed during this investigation.

The program ISBILD (Ozawa and Duncan, (1973)) was used to analyze the earth pressures occurring during the construction of Cochiti Dam. The program

is similar to SSTIPN but is specifically designed for the analysis of earth masses, such as embankment.

2. Soil Stress-Strain Parameters

Hyperbolic, stress-dependent, stress-strain relationships were used to represent the non-linear behavior of the backfill and foundation soils in the finite element analyses. Initially the relationships developed by Kulhawy, Duncan and Seed (1969) were used:

$$\text{Tangent Modulus, } E_t = K \cdot P_a \left[1 - \frac{R_f (1 - \sin \phi) (\sigma_1 - \sigma_3)}{2C \cdot \cos \phi + 2\sigma_3 \cdot \sin \phi} \right]^2 \left(\frac{\sigma_3}{P_a} \right)^2 \quad (A-1)$$

$$\begin{aligned} \text{Tangent Poisson's Ratio, } v_t = & \frac{G - F \log(\sigma_3 / P_a)}{\left[1 - \frac{d \cdot (\sigma_1 - \sigma_3)}{K \cdot P_a (\sigma_3 / P_a)^n \cdot \left[1 - \frac{R_f (1 - \sin \phi) (\sigma_1 - \sigma_3)}{2C \cdot \cos \phi + 2\sigma_3 \cdot \sin \phi} \right]} \right]^2} \quad (A-2) \end{aligned}$$

where

K = Modulus Number for primary loading (for unloading-reloading, the symbol K_{ur} is used); value of initial tangent modulus at confining pressure, σ_3 , equal to atmospheric pressure, P_a .

N = Modulus Exponent; equals change in tangent modulus for a ten-fold increase in σ_3 .

C = Cohesion Intercept.

ϕ = Friction Angle.

(C and ϕ relate the deviator stress at failure $(\sigma_1 - \sigma_3)_f$ to σ_3)

R_f = Failure Ratio; relates hyperbolic asymptote to $(\sigma_1 - \sigma_3)_f$.

G = Poisson's Ratio Parameter; equals the initial tangent Poisson's ratio at σ_3 equal to atmospheric pressure, P_a .

F = Poisson's Ratio Parameter; equals the decrease in initial tangent Poisson's ratio for a ten-fold increase in σ_3 .

d = Poisson's Ratio Parameter; equals the rate of increase of v_t with strain.

In the majority of the analyses, however, volume change parameters based on the concept of constant bulk modulus (at a given confining pressure) were

used. This relationship, which will be described in a future research report by Professor J. M. Duncan and his colleagues at the University of California, Berkeley, is as follows:

Tangent Poisson's Ratio:

$$\nu_t = \frac{3K_b \cdot P_a (\sigma_3/P_a)^m - \left[1 - \frac{R_f(1 - \sin\phi)(\sigma_1 - \sigma_3)}{2C \cdot \cos\phi + 2\sigma_3 \cdot \sin\phi} \right]^2 \cdot KP_a (\sigma_3/P_a)}{6K_b \cdot P_a (\sigma_3/P_a)^m}$$

where

K_b = Bulk Modulus Parameter; value of initial bulk modulus at σ_3 equal to P_a

m = Bulk Modulus Parameter; equals the change in bulk modulus for a tenfold increase in σ_3

Conservative hyperbolic parameters were selected to represent the various soil types considered in the analyses. The parameters were determined by Professor Duncan after reviewing the data for a variety of soil types and laboratory test conditions (Wong and Duncan, 1974). The soil parameters are presented in Table A-1. Values used to represent concrete and rock materials are also given in the table.

Interface element behaviour was also represented by hyperbolic relationships in the finite-element analyses. The relationships for equivalent normal and shear springs developed by Wong (1977) were used:

$$\text{Tangent Shear Modulus, } K_{st} = \left[1 - \frac{R_f \cdot \sigma_s}{C + \sigma_n \tan\phi} \right]^2 K_s \gamma_w (\sigma_n/P_a)^n \quad (\text{A-4})$$

where

K_s = Shear Spring Coefficient of primary loading (for unloading - reloading, the symbol K_{sur} is used); value of initial tangent shear modulus (divided $_{sur}$ by unit weight of water, γ_w) at a normal pressure, σ_n , of one atmosphere, P_a

n = Modulus Exponent; equals change in tangent shear modulus for a tenfold increase in σ_n

C = Adhesion Intercept of interface

ϕ = Wall Friction Angle of interface

TABLE A-1
HYPERBOLIC STRESS-STRAIN PARAMETERS

Material Type	Relative Density, D_r or Relative Compaction, RC	Unit Weight, γ (pcf)	C (ksf)	(2) ϕ (o)	(3) ϕ (o)	R_f	K	n	G	F	d	Kb	m
GW	$D_r = 100\%$	147.5	0	42	9	.70	600	.40	-	-	-	350	.10
	$D_r = 50\%$	135	0	36	5	.70	300	.40	-	-	-	150	.10
SM	RC = 100%	142.5	0	36	8	.70	600	.25	-	-	-	450	0
	RC = 90%	130	0	32	4	.70	300	.25	-	-	-	250	0
SM - SC	RC = 100%	137.5	0.5	33	0	.70	400	.70	-	-	-	200	.50
	RC = 90% (1)	125	0.5	34	0	.65	100	.180	.22	.045	6.0	-	-
	RC = 90%	125	0.3	33	0	.70	150	.60	-	-	-	75	.50
CL	RC = 100%	132.5	0.4	30	0	.70	150	.45	-	-	-	140	.20
	RC = 90%	120	0.2	30	0	.70	90	.45	-	-	-	80	.20
Concrete Rock	-	150	400	0	0	0	2.7×10^5	0	-	-	-	0.9×10^5	0
	-	150	400	0	0	0	2.7×10^5	0	-	-	-	1.5×10^5	0

Notes: (1) Initial Studies
(2) Friction angle at σ_3 equal to one atmosphere
(3) Decrease in friction angle for a ten-fold increase in σ_3

(C and ϕ relate the shear stress at failure, $(\sigma_d)_f$, to σ_n)

R_f = Failure Ratio; relates hyperbolic asymptote to $(\sigma_s)_f$.

For each analysis the adhesion and wall friction angle were made equal to the soil strength values and the shear spring coefficient was arbitrarily selected at a high value. Thus the interface element allowed slip to occur only when the shear strength of the soil adjacent to the wall was exceeded.

The normal spring modulus was arbitrarily made very large to effectively prevent relative movement between the conduit and adjacent soil in a direction normal to the conduit wall.

3. Details of Finite-Element Analyses

a. Circular Conduit Studies. The finite-element mesh shown in Fig. A-1 was used for the studies of circular conduits. The mesh is composed of 257 nodal points, 212 soil elements, 12 beam elements, which represent the conduit, and 12 interface elements between the conduit and the surrounding soil. Because of symmetry, only a half-section of the conduit was analyzed. The majority of the analyses were begun with the conduit in place with soil adjacent to the lower half of the conduit ($p=0.5$), as shown in Fig. A-1. Nine construction layers were used to simulate the placement of soil to a thickness of three conduit diameters above the crown of the conduit. Greater fill thicknesses were simulated by the addition of distributed loads across the top of the mesh. Five load increments were used to achieve final fill thicknesses on the order of 600 feet. The thickness of foundation soil below the conduit was varied by fixing all nodal points below any specified elevation.

The circular conduit studies are summarized in Table A-2. The purpose of each analysis is indicated in the table, as well as the geometry of the conduit installation, the conduit properties, the foundation and backfill soil types, and the characteristics of the interface elements along the outside of the conduit.

The finite-element mesh used to determine moments, thrusts and shears in circular conduits for assumed pressure distributions, by the program TWODEF-B, is shown in Fig. A-2. The mesh consists of 25 nodal points and 24 beam elements, assumed pressures were converted to horizontal and vertical loads at each nodal point.

b. Modified Circular Conduit Studies. The mesh shown in Fig. A-3 was used for the finite-element analyses of the modified circular section. The mesh is composed of 215 nodal points, 175 soil elements, 12 beam elements and 12 interface elements. The conduit is represented by the beam elements and by certain "soil" elements, beneath its springline, that were given properties of concrete. Eight construction layers were used to simulate the placement of backfill from the springline of the conduit to a thickness of two conduit diameters above the crown of the conduit. Additional fill placement was simulated by six distributed load movements along the top of the mesh to achieve a maximum fill thickness of 600 feet. The various cases analyzed, for the modified circular conduit are summarized in Table A-3.

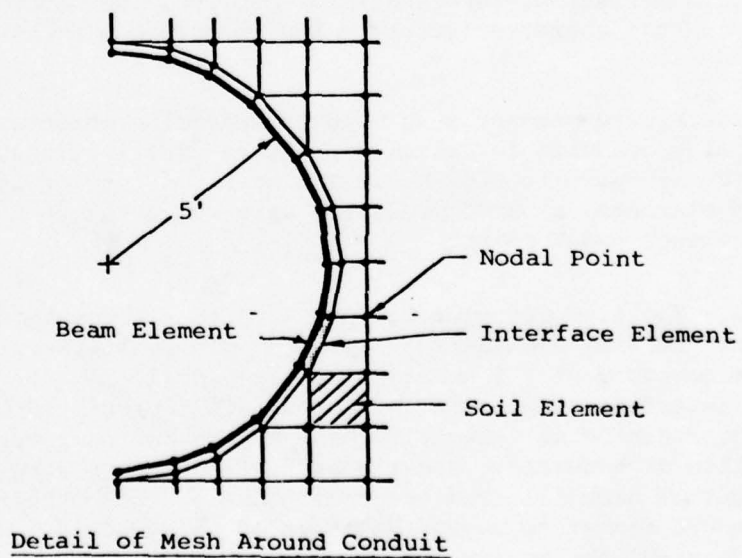
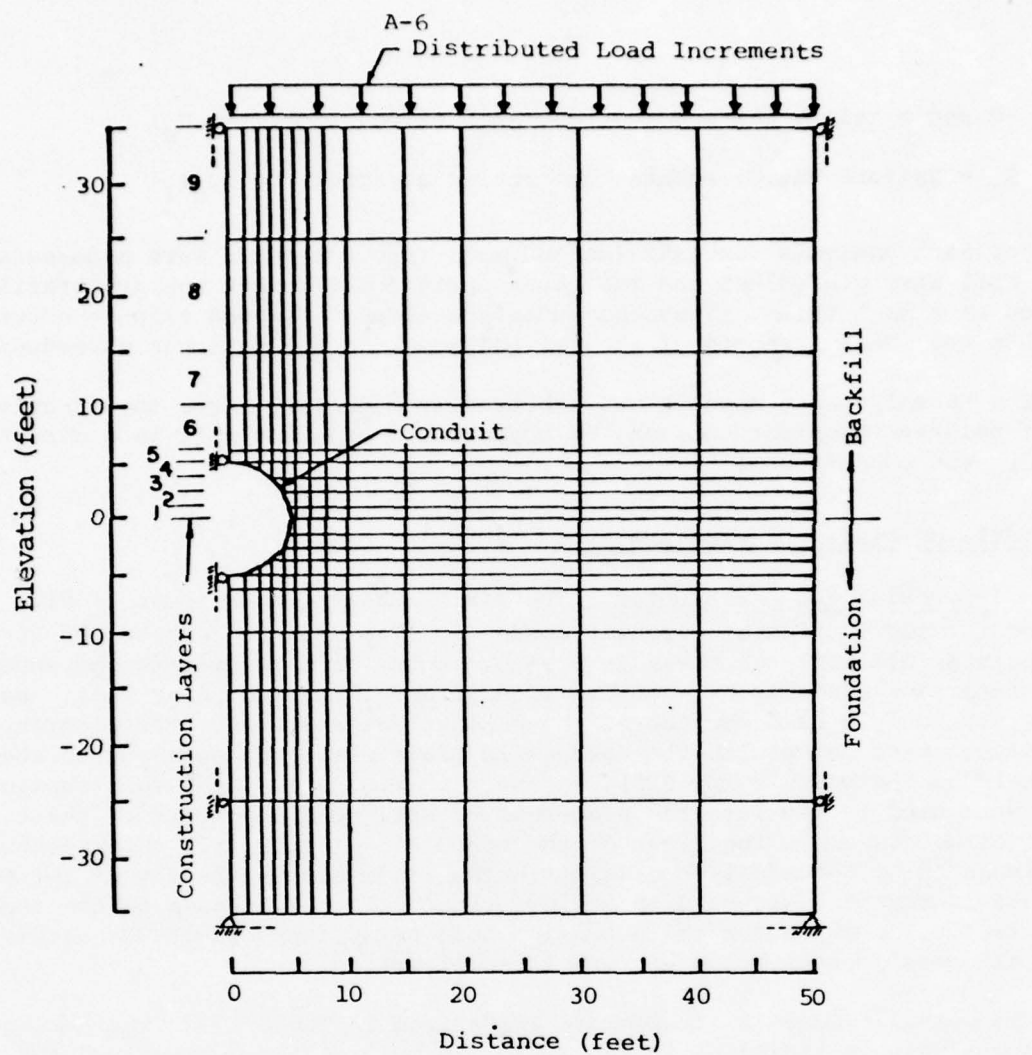


FIG. A-1 FINITE-ELEMENT MESH, CIRCULAR CONDUIT STUDIES

TABLE A-2
SUMMARY OF CIRCULAR CONDUIT STUDIES

Study Objective	Case No.	Conduit			Backfill		Foundation	
		D (ft)	P	E (ksf)	b (ft/ft)	Type	Type	H _f (ft)
Conduit Flexibility*	1	10	0.5	8.6×10^5	0.558	SM-SC(RC=90%)*	SM-SC(RC=90%)*	30
	2	10	0.5	5.7×10^5	0.203	SM-SC(RC=90%)	SM-SC(RC=90%)	30
	3	10	0.5	5.7×10^5	1.30	SM-SC(RC=90%)	SM-SC(RC=90%)	30
	4	30	0.5	5.7×10^5	1.30	SM-SC(RC=90%)	SM-SC(RC=90%)	30
	5	30	0.5	5.7×10^5	35.2	SM-SC(RC=90%)	SM-SC(RC=90%)	30
	6	3.33	0.5	5.7×10^5	.0013	SM-SC(RC=90%)	SM-SC(RC=90%)	10
	7	3.33	0.5	5.7×10^5	.1000	SM-SC(RC=90%)	SM-SC(RC=90%)	10
Soil Type	14	10	0.5	5.7×10^5	3.51	GW(D _r =100%)	GW(D _r =100%)	1
	15	10	0.5	5.7×10^5	3.51	GW(D _r =50%)	GW(D _r =50%)	1
	16	10	0.5	5.7×10^5	3.51	SM(RC=100%)	SM(RC=100%)	1
	17	10	0.5	5.7×10^5	3.51	SM(RC=90%)	SM(RC=90%)	1
	18	10	0.5	5.7×10^5	3.51	SM-SC(RC=100%)	SM-SC(RC=100%)	1
	19	10	0.5	5.7×10^5	3.51	SM-SC(RC=90%)	SM-SC(RC=90%)	1
	20	10	0.5	5.7×10^5	3.51	CL(RC=100%)	CL(RC=100%)	1
	21	10	0.5	5.7×10^5	3.51	CL(RC=90%)	CL(RC=90%)	1
	22	10	0.5	5.7×10^5	3.51	SM-SC(RC=100%)	SM-SC(RC=100%)	30
	23	10	0.5	5.7×10^5	3.51	CL(RC=90%)	CL(RC=90%)	30
	27	10	0.5	5.7×10^5	3.51	SM-SC(RC=100%)	SM-SC(RC=100%)	5
Depth of Soil Foundation	28	10	0.5	5.7×10^5	3.51	SM-SC(RC=100%)	SM-SC(RC=100%)	10
	24	3	0.5	5.7×10^5	3.51	SM-SC(RC=100%)	SM-SC(RC=100%)	0.3
Conduit Diameter	25	30	0.5	5.7×10^5	3.51	SM-SC(RC=100%)	SM-SC(RC=100%)	3
	44	10	0.75	5.7×10^5	3.51	SM-SC(RC=100%)	Rock	0
Effect of Rock Foundation	45	10	0.5	5.7×10^5	3.51	SM-SC(RC=100%)	Rock	0
	49	10	0.5	5.7×10^5	3.51	SM-SC(RC=100%)	Rock (no shear at interface)	0
	50	10	0.75	5.7×10^5	3.51	SM-SC(RC=100%)	Rock (no shear at interface)	0

*Initial Studies; G, F and d volume change parameters used to represent soil behavior.

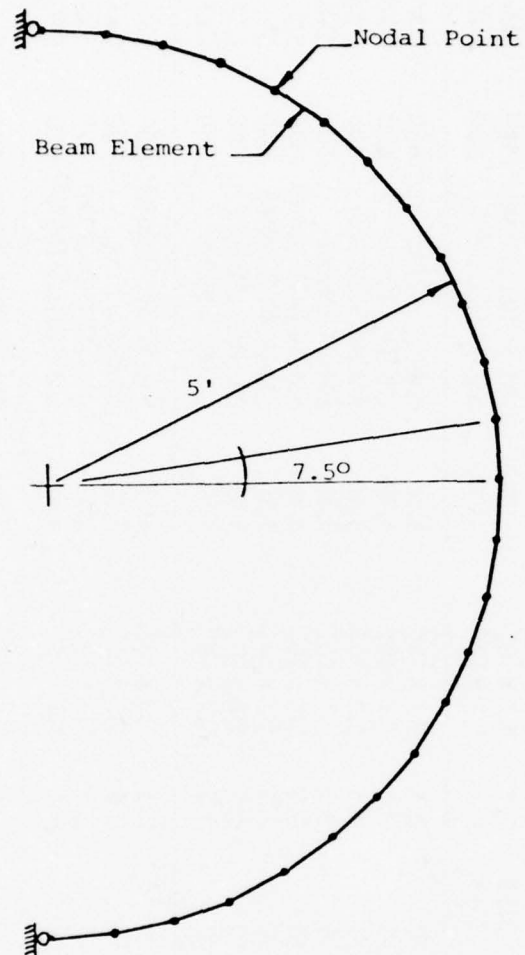


FIG. A-2 TWODEF-B MESH, CIRCULAR CONDUIT STUDIES

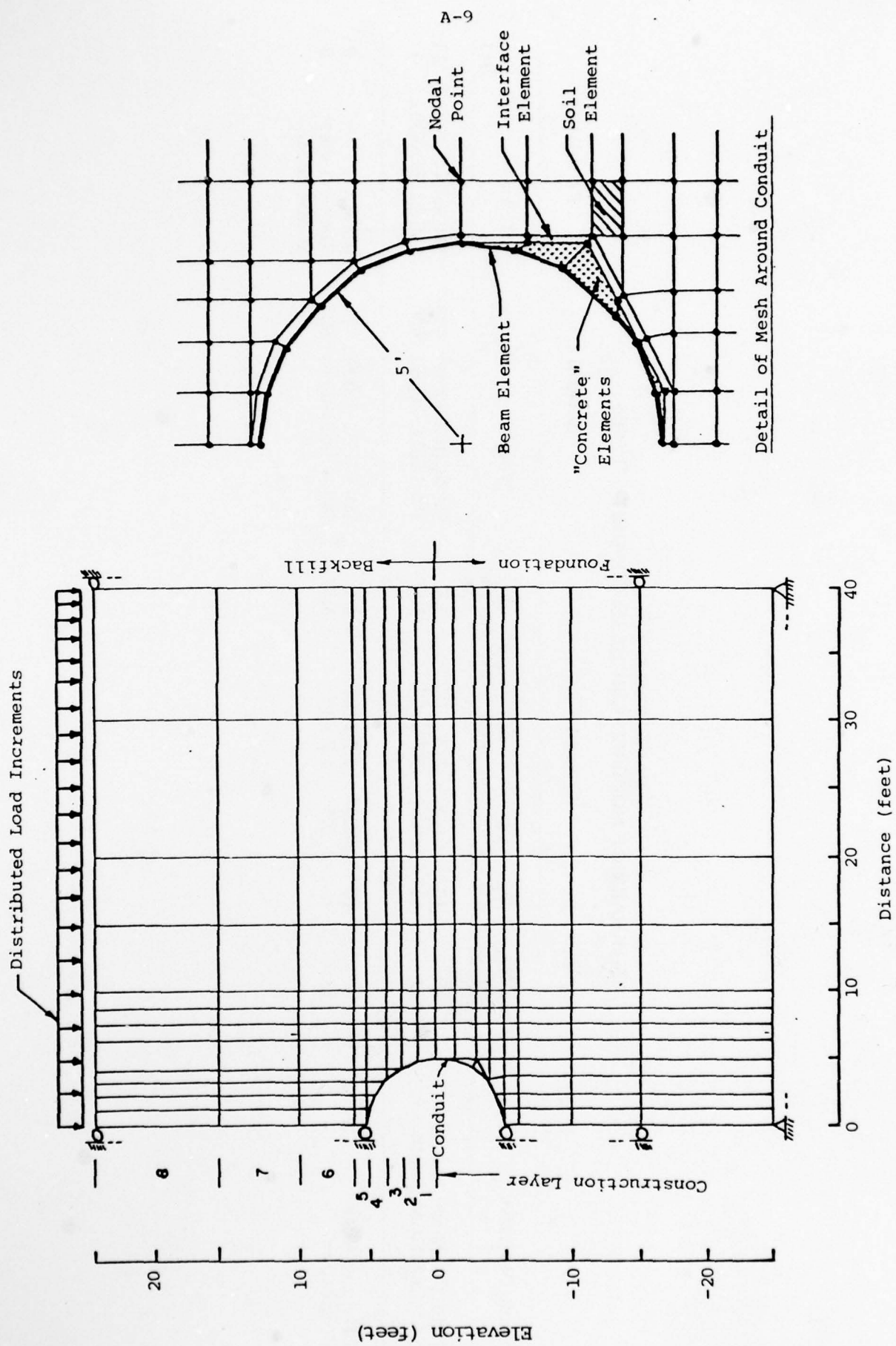


FIG. A-3 FINITE-ELEMENT MESH, MODIFIED CIRCULAR CONDUIT STUDIES

TABLE A-3
SUMMARY OF MODIFIED CIRCULAR CONDUIT STUDIES

Study Objective	Case No.	Conduit				Backfill		Foundation	
		D (ft)	P	E (ksf)	$d^*/(ft)$	Type	Max H (ft)	Type	H _f (ft)
Effect of Shape and Soil Foundation Depth	26	10	0.5	5.7×10^5	3.51	SM-SC(RC=100%)	600	SM-SC(RC=100%)	20
	29	10	0.5	5.7×10^5	3.51	SM-SC(RC=100%)	600	SM-SC(RC=100%)	1
Effect of Rock Foundation	51	10	0.5	5.7×10^5	3.51	SM-SC(RC=100%)	420	Rock	0
	52	10	0.5	5.7×10^5	3.51	SM-SC(RC=100%)	600	Rock (no shear at interface)	0

A-10

c. Oblong Conduit Studies. Fig. A-4 shows the finite-element mesh used for the studies of oblong conduits with a height-to-width ratio (H_c/B_c) equal to 1.25. The mesh contains 229 nodal points, 184 soil elements, 14 beam elements, to represent the conduit, and 14 interface elements. The placement of backfill above the conduit was simulated by nine construction layers and six distributed load cases. The maximum height of fill over the crown of the conduit was 600 feet. The cases analyzed are summarized in Table A-4.

The finite-element mesh used for the study of oblong conduits, with $H_c/B_c = 1.5$, is shown in Fig. A-5. The mesh contains 247 nodal points, 198 soil elements, 16 beam elements, representing the conduit, and 16 interface elements. A maximum height of 600 feet of fill was simulated by the placement of ten construction layers and six distributed load increments. The cases analyzed are summarized in Table A-4.

The meshes used to represent the TWODEF-B structural analyses of the oblong conduits, for various assumed earth pressure loadings, are shown in Figs. A-6 and A-7. The mesh for the conduit with $H_c/B_c = 1.25$ has 29 nodal points and 28 beam elements. The mesh for the conduit with $H_c/B_c = 1.5$ has 33 nodal points and 32 beam elements.

d. Rectangular Conduit Studies. The finite-element mesh used for the analyses of rectangular conduits with $H_c/B_c = 0.25$ is shown in Fig. A-8. The mesh consists of 169 nodal points, 132 soil elements and 12 interface elements. The conduit was represented by the shaded "soil" elements in Fig. A-8, which were given the properties of concrete. In other words, the conduit was represented by a solid mass of concrete. As discussed below, this form of representation is satisfactory for the very stiff conduit sections that were analyzed. The analytical results of interest were the normal pressures and shear stresses (traction) on the "conduit" as measured in the interface elements. Six construction layers and six distributed load cases were used in the analyses to represent the placement of a maximum of 600 feet of fill over the conduit. Details of the cases studied are given in Table A-5.

The mesh used for the analyses of a rectangular conduit, with $H_c/B_c = 1.0$ (square), is shown in Fig. A-9. The mesh consisted of 221 nodal points, 176 soil elements, 16 beam elements and 16 interface elements. The various cases studied are described in Table A-4. In cases 34, 35, 40, 41 and 42 the conduit was represented by a solid mass of concrete composed of the shaded "soil" elements in Fig. A-9. The beam elements were not used. In cases 43, 46, 47 and 48 the beam elements were used to represent the conduit while shaded "soil" elements were given the properties of air (essentially zero stiffness). Comparisons between Cases 35 and 43 indicated that the two methods for representing the conduits in the analyses resulted in essentially the same earth pressures on the conduit. In all the analyses eight construction layers and six distributed load cases to achieve maximum fill thicknesses above the conduit on the order of 600 feet. The mesh used to perform structural analyses (TWODEF-B) of square conduits is shown in Fig. A-10. The mesh included 33 nodal points and 32 beam elements.

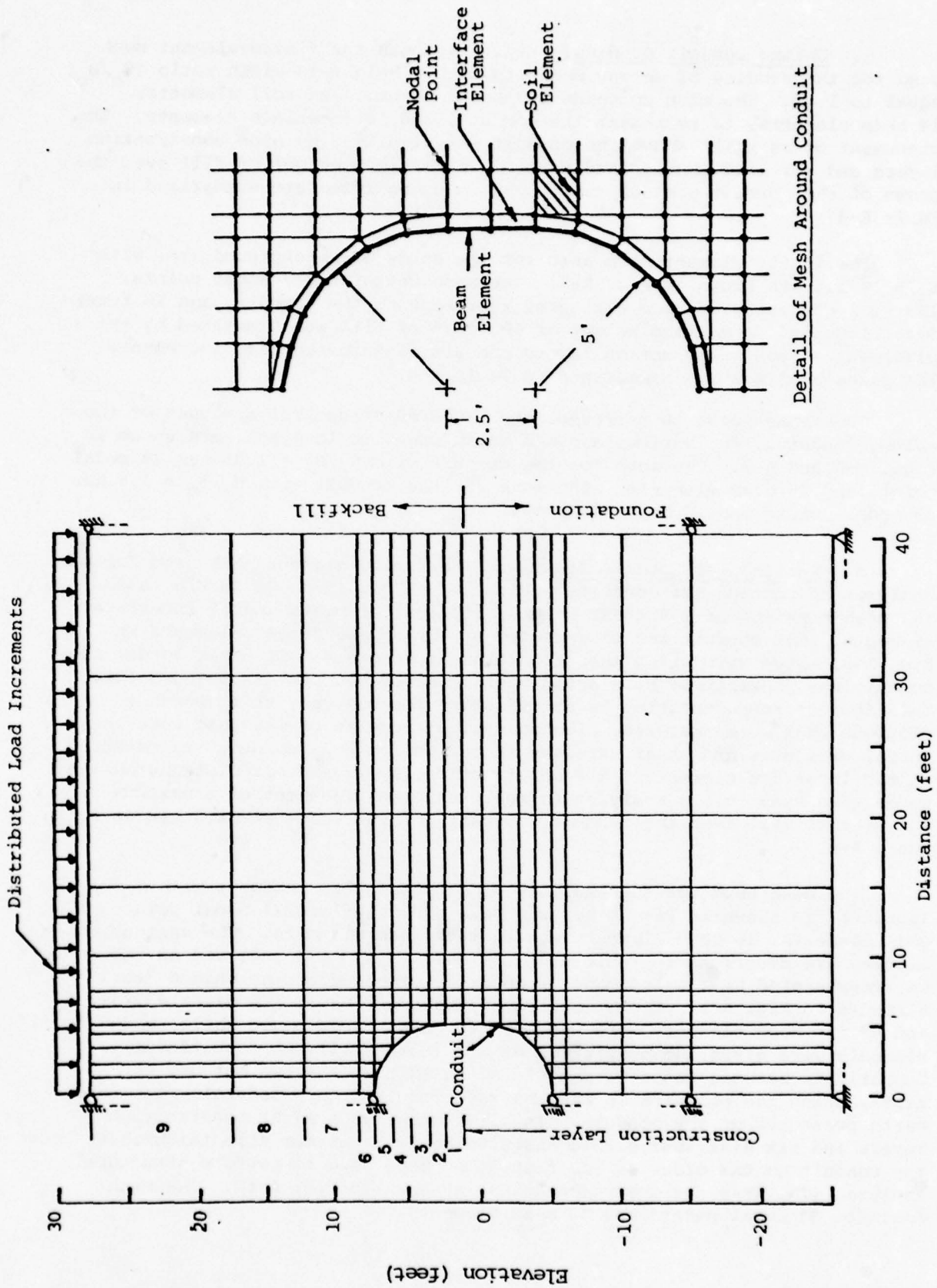
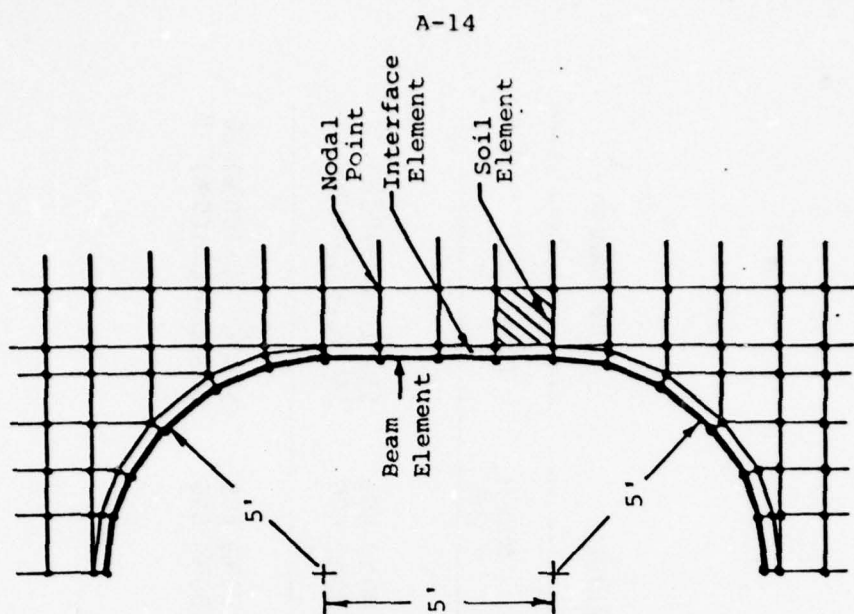
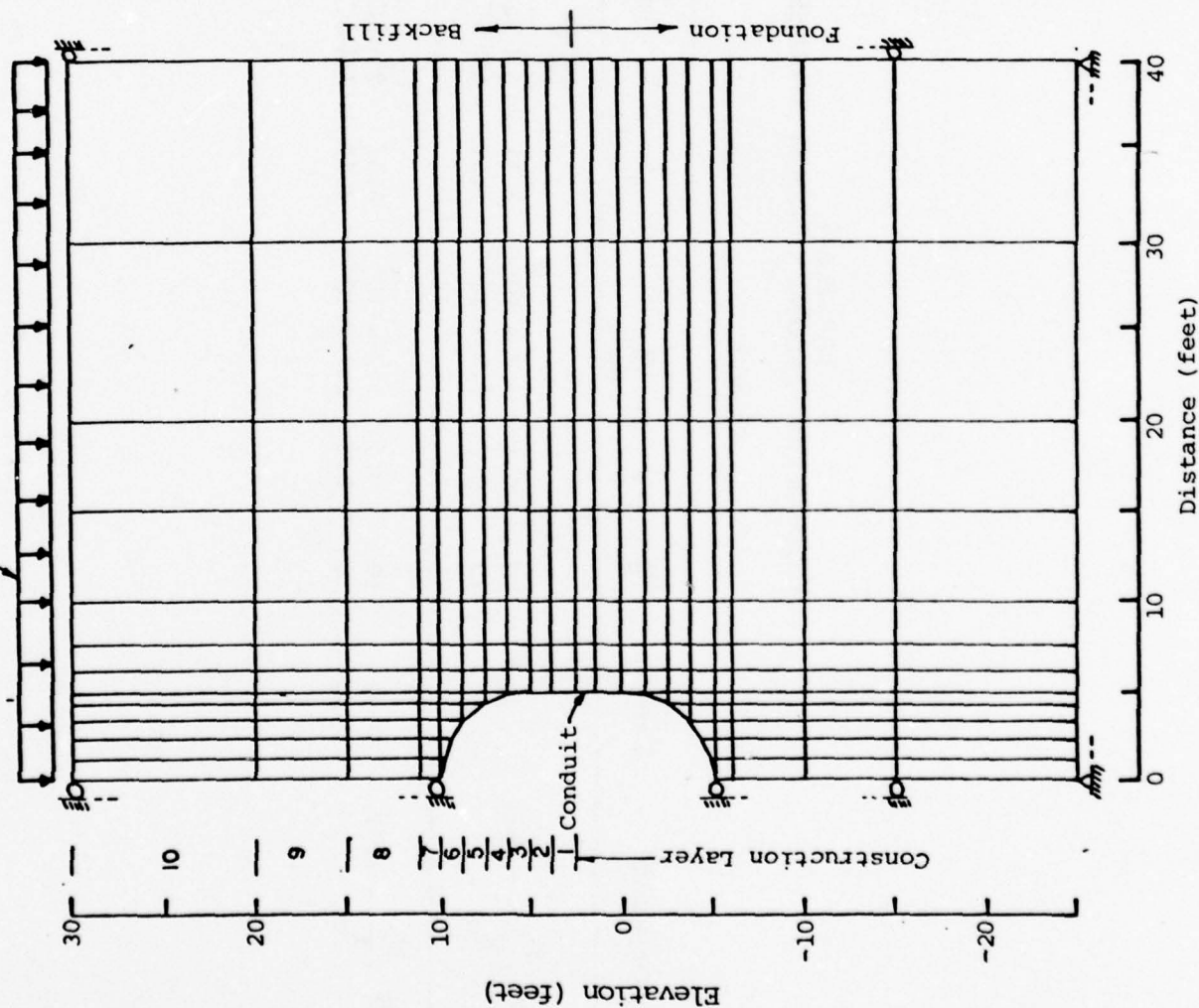
FIG. A-4 FINITE-ELEMENT MESH, OBLONG CONDUIT STUDIES ($H_C/B_C=1.25$)

TABLE A-4
SUMMARY OF OBLONG CONDUIT STUDIES

Study Objective	Case No.	Conduit			Backfill		Foundation	
		D_c (ft)	P	E (ksf)	I (ft^4/ft)	Type	Max H (ft)	Type
Shape $(\frac{H_c}{B_c} = 1.25)$	30	10	0.5	5.7×10^5	3.51	SM-SC(RC=100%)	600	SM-SC(RC=100%)
	31	10	0.5	5.7×10^5	3.51	SM-SC(RC=100%)	600	SM-SC(RC=100%)
Shape $(\frac{H_c}{B_c} = 1.5)$	32	10	0.5	5.7×10^5	3.51	SM-SC(RC=100%)	600	SM-SC(RC=100%)
	33	10	0.5	5.7×10^5	3.51	SM-SC(RC=100%)	600	SM-SC(RC=100%)

Distributed Load Increments



Detail of Mesh Around Conduit

FIG. A-5 FINITE-ELEMENT MESH, OBLONG CONDUIT STUDIES ($H_c/B_c = 1.5$)

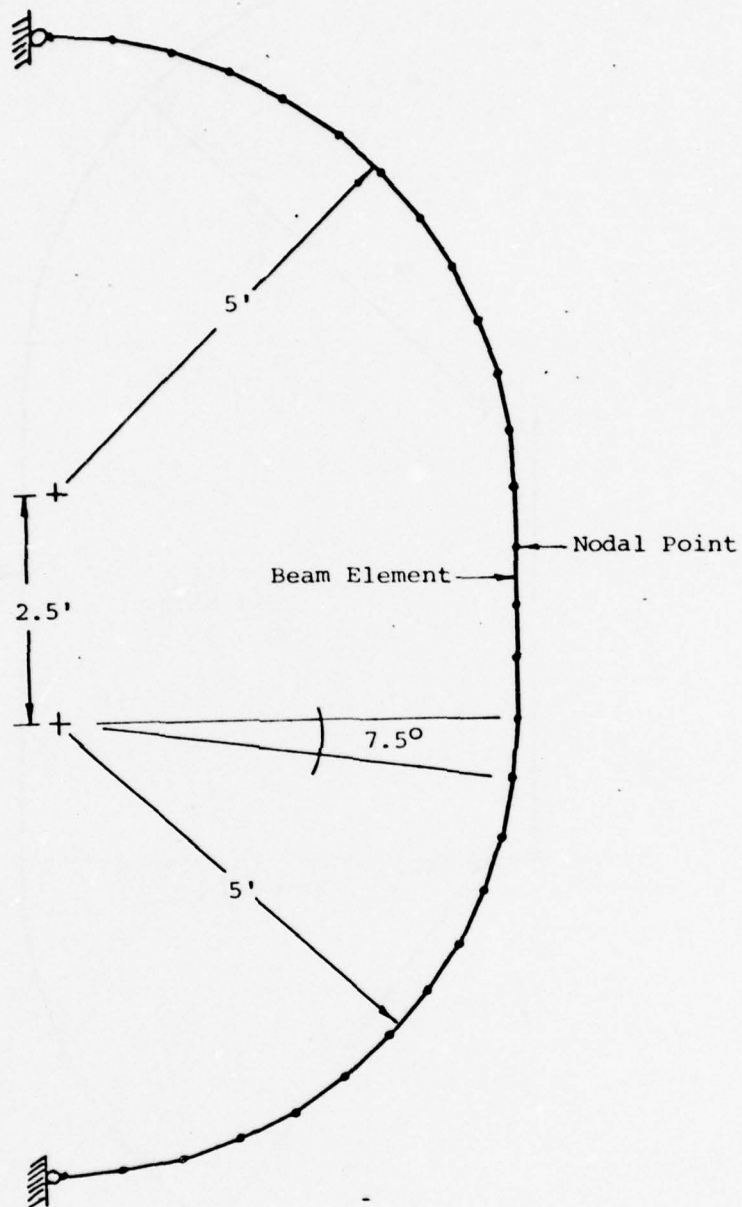


FIG. A-6 TWODEF-B MESH, OBLONG CONDUIT STUDIES ($H_C/B_C=1.25$)

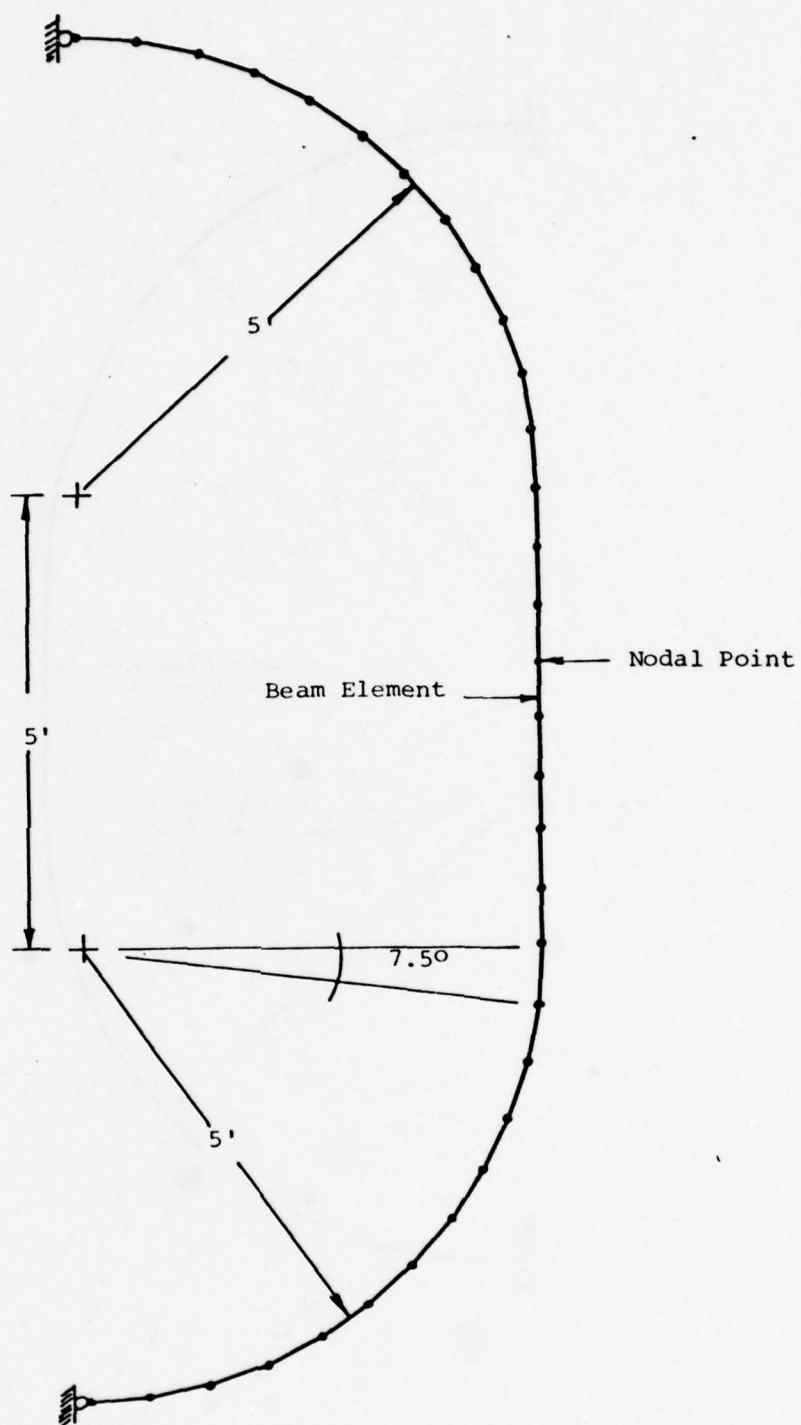


FIG. A-7 TWODEF-B MESH, OBLONG CONDUIT STUDIES ($H_C/B_C=1.5$)

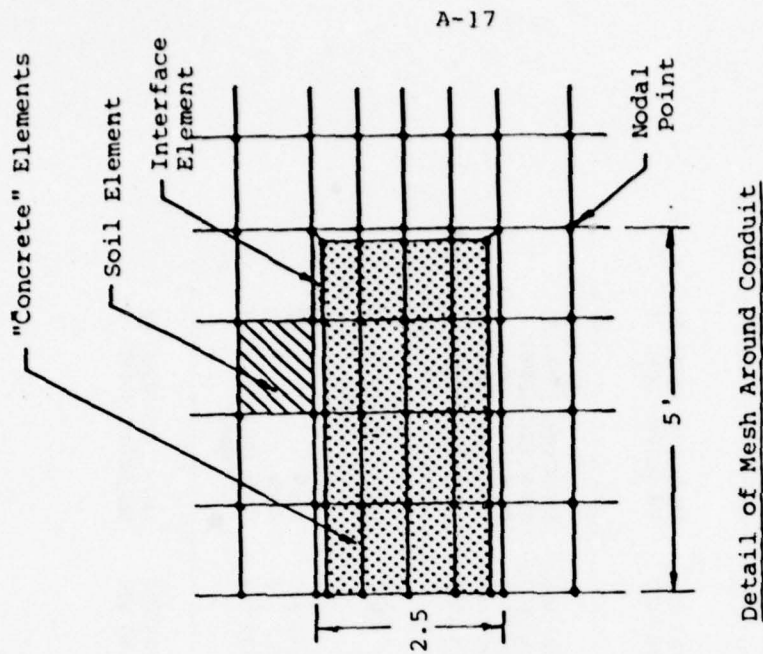
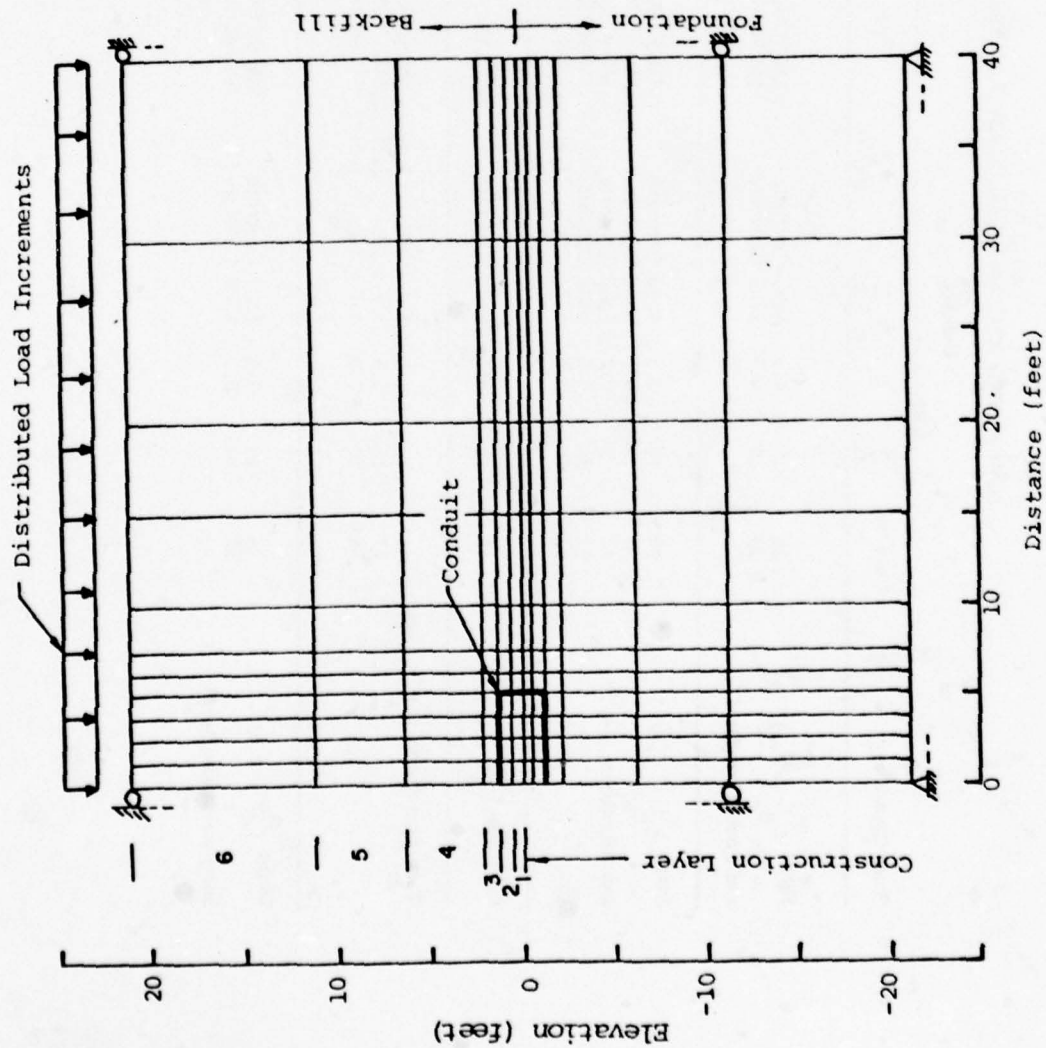
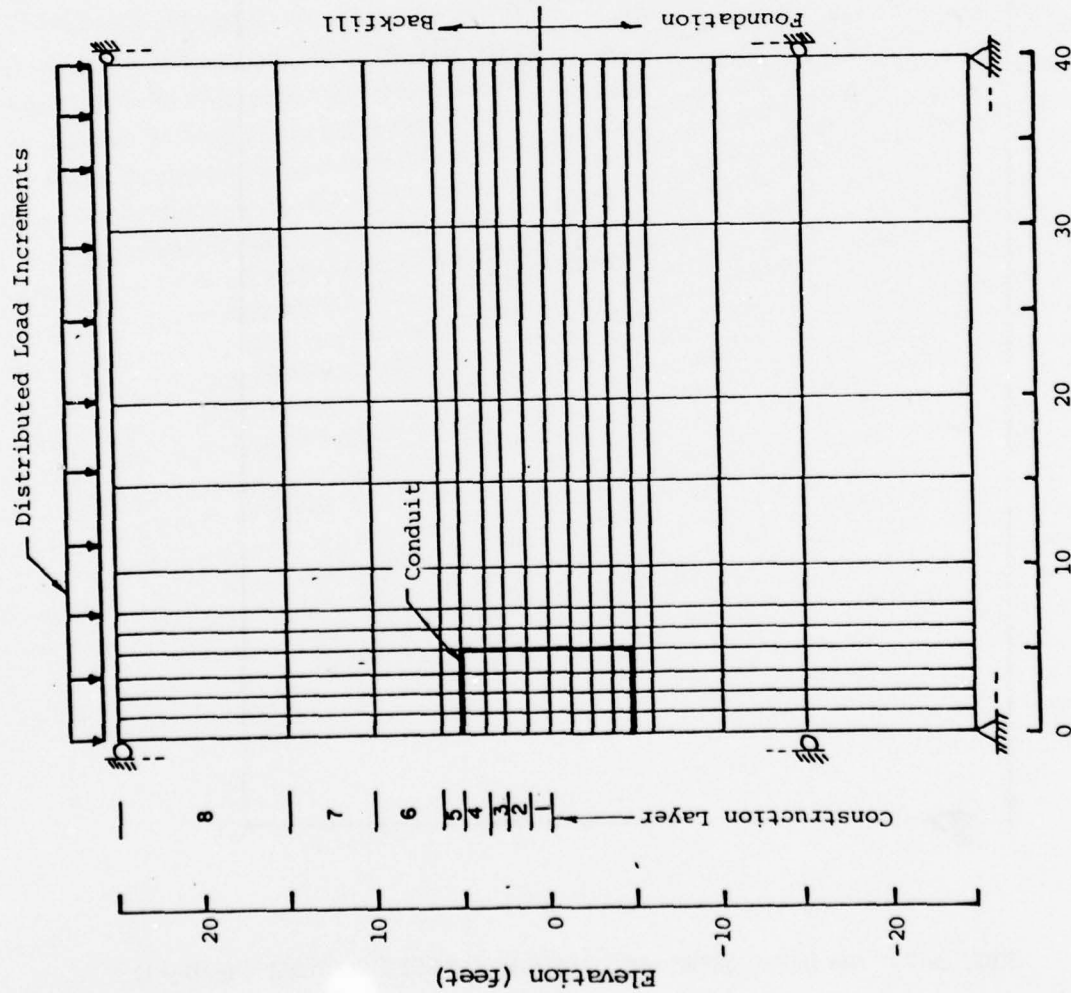
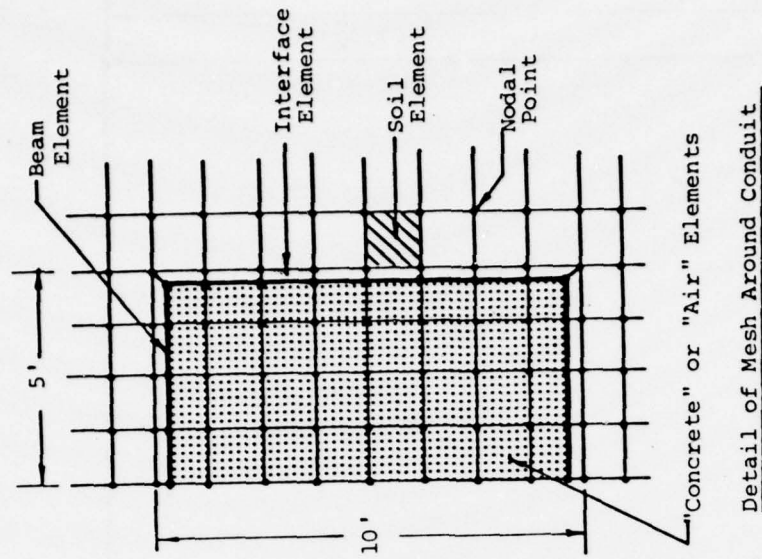


FIG. A-8 FINITE-ELEMENT MESH, RECTANGULAR CONDUIT STUDIES ($H_C/B_C=0.25$)

TABLE A-5
SUMMARY OF RECTANGULAR CONDUIT STUDIES

Study Objective	Case No.	Conduit			Backfill		Foundation	
		B (ft)	P	E (ksf)	d _f (ft)	Type	Max H (ft)	Type
Shape ($\frac{H_c}{B_c} = 0.25$) and Foundation Depth	38	10	0.5	Solid Concrete		SM-SC (RC=100%)	600	SM-SC (RC=100%) 20
	39	10	0.5	Solid Concrete		SM-SC (RC=100%)	600	SM-SC (RC=100%) 1
Shape ($\frac{H_c}{B_c} = 1.0$) and Foundation Depth	34	10	0.5	Solid Concrete		SM-SC (RC=100%)	600	SM-SC (RC=100%) 20
	35	10	0.5	Solid Concrete		SM-SC (RC=100%)	600	SM-SC (RC=100%) 1
	40	3	0.5	Solid Concrete		SM-SC (RC=100%)	586	SM-SC (RC=100%) 0.3
	41	30	0.5	Solid Concrete		SM-SC (RC=100%)	640	SM-SC (RC=100%) 3
	43	10	0.5	5.7×10^5	3.51	SM-SC (RC=100%)	600	SM-SC (RC=100%) 1
Soil Type ($\frac{H_c}{B_c} = 1.0$)	42	10	0.5	Solid Concrete		CL (RC=90%)	600	CL (RC=90%) 1
Rock Foundation ($\frac{H_c}{B_c} = 1.0$)	46	10	1.0	5.7×10^5	3.51	SM-SC (RC=100%)	600	Rock 0
	47	10	0.5	5.7×10^5	3.51	SM-SC (RC=100%)	600	Rock 0
	48	10	0.5	5.7×10^5	3.51	SM-SC (RC=100%)	420	Rock (no side shear) 0
Shape ($\frac{H_c}{B_c} = 1.5$) and Foundation Depth	36	10	0.5	Solid Concrete		SM-SC (RC=100%)	600	SM-SC (RC=100%) 20
	37	10	0.5	Solid Concrete		SM-SC (RC=100%)	600	SM-SC (RC=100%) 1

FIG. A-9 FINITE-ELEMENT MESH, RECTANGULAR CONDUIT STUDIES ($H_C/B_C=1$)

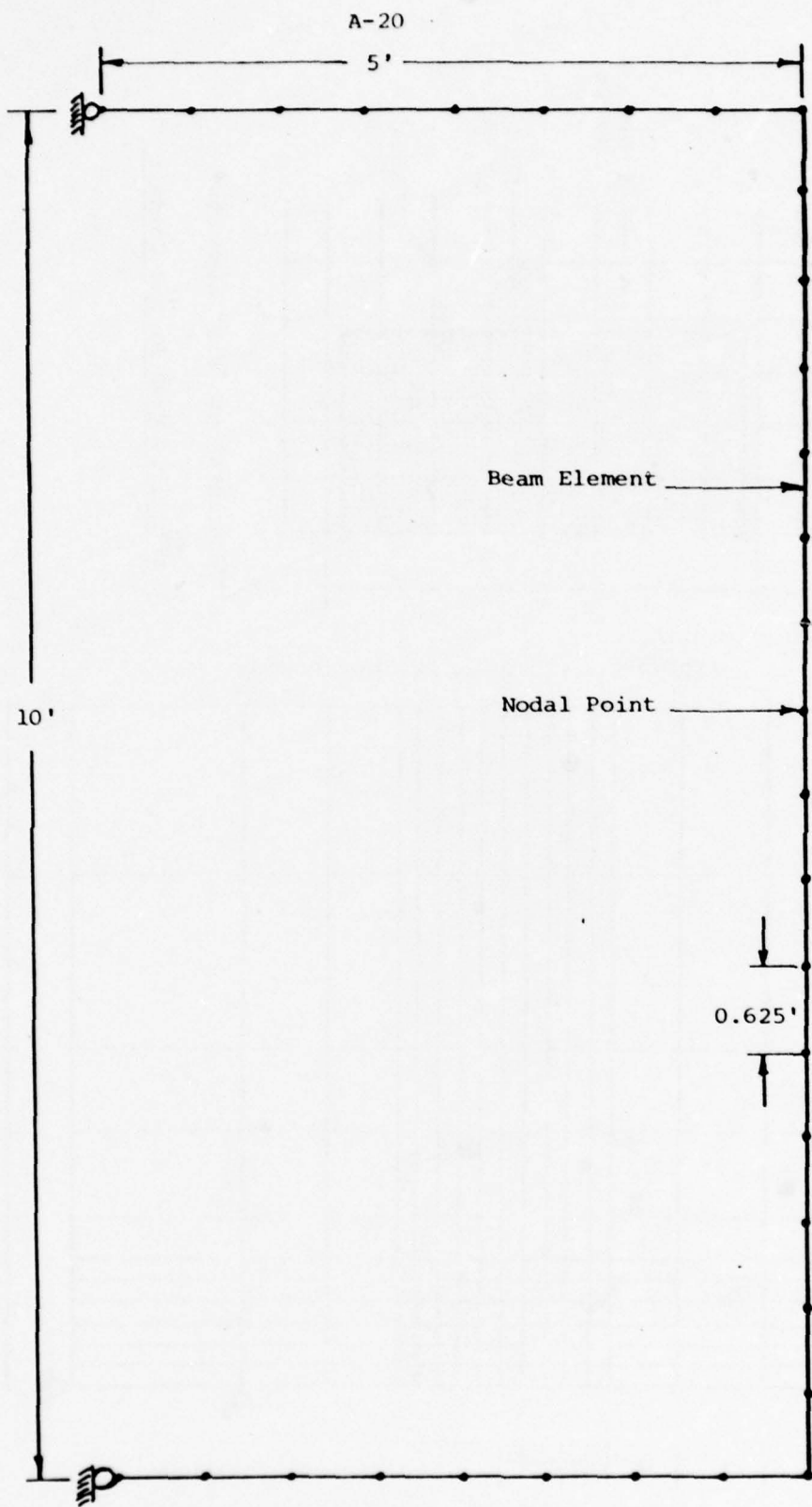


FIG. A-10 TWODEF-B MESH, RECTANGULAR CONDUIT STUDIES ($H_C/B_C=1$)

The mesh used for the analyses of a rectangular conduit with $H_c/B_c = 1.5$ is shown in Fig. A-11. The mesh is composed of 273 nodal points, 220 soil elements and 20 interface elements. The conduit was represented by a solid mass of concrete, which consisted of the shaded "soil" elements in Fig. A-11. A maximum of 600 feet of backfill was placed over the conduit in ten construction layers and six distributed load increments. Details of the analyses are summarized in Table A-5.

e. Shallow Trench Placement Analyses. The finite-element mesh shown in Fig. A-12 was used for the studies of the effects of conduit placement in shallow trenches. The mesh consists of 201 nodal points, 152 soil elements and 14 interface elements. As shown in the figure, a half-section of a rectangular conduit resting on rock (or other stiff foundation) was represented by fixed nodal points along its top and side surfaces. The opposite side of the trench adjacent to the conduit was also represented by fixed nodal points. Different trench geometries were attained by fixing selected nodes within the trench, which effectively varied the trench width-to-depth ratio. For the sloping trench analyses, some alterations in nodal point locations were made to achieve the desired geometries. Five construction layers, as shown in Fig. A-12, and a variable number of distributed load increments were used to simulate the placement of fill over the conduit and trench to maximum heights on the order of 600 feet. The shallow trench placement analyses are summarized in Table A-6.

f. Construction Analysis of Cochiti Dam. The finite-element mesh used in the analysis of the construction of the Cochiti Dam at the outlet works section is shown in Fig. A-13. The mesh has 221 nodal points and 204 elements. Three material types were used (core, shell and cement-stabilized soil) and the hyperbolic parameters for each are given in Table A-7. The parameters were selected on the basis of available laboratory test data for the embankment materials and correlations with data for similar soils. A total of eleven construction layers, as shown in Fig. A-13, were used to simulate the embankment construction.

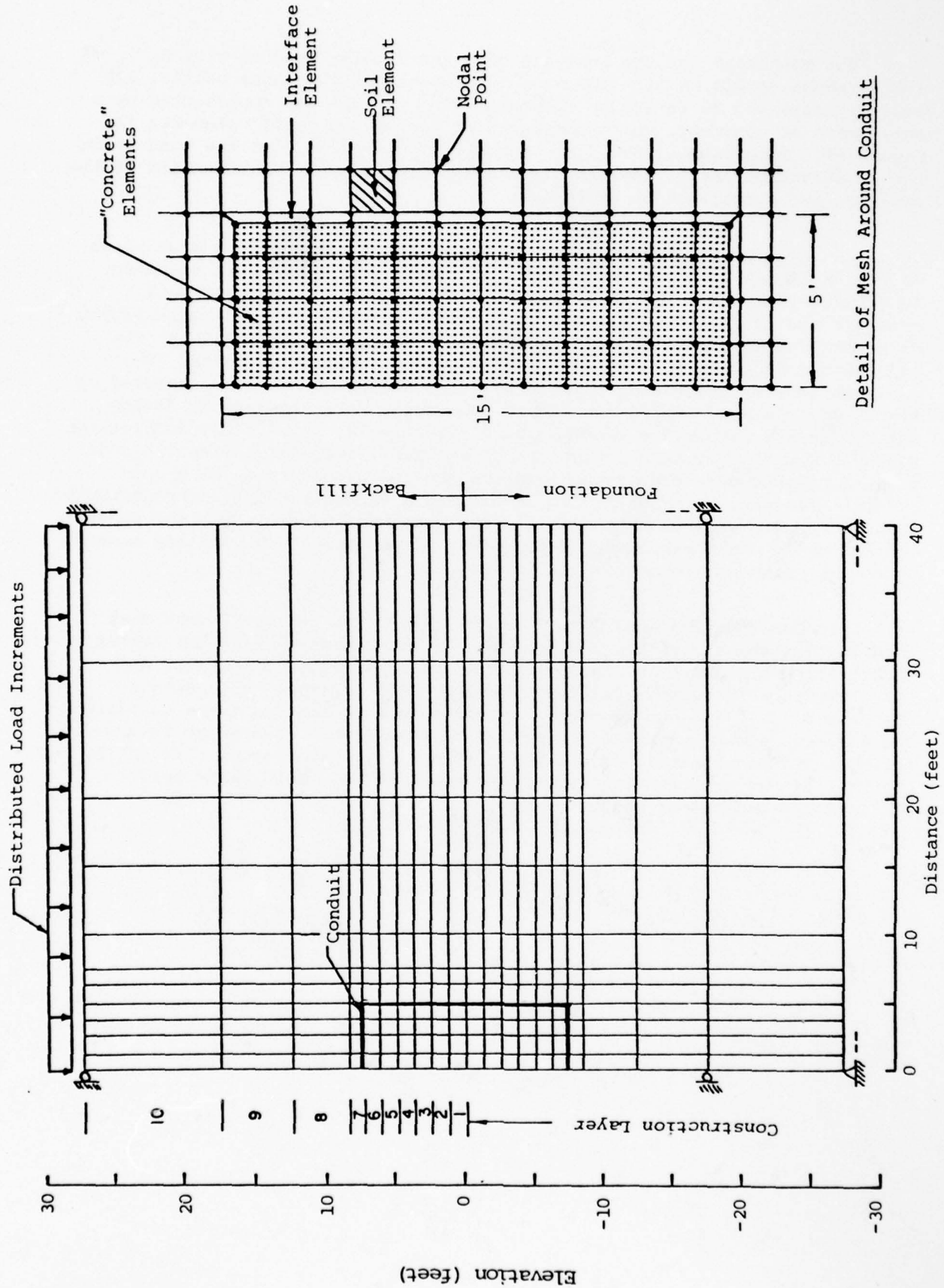


FIG. A-11 FINITE-ELEMENT MESH, RECTANGULAR CONDUIT STUDIES ($H_C/B_C = 1.5$)

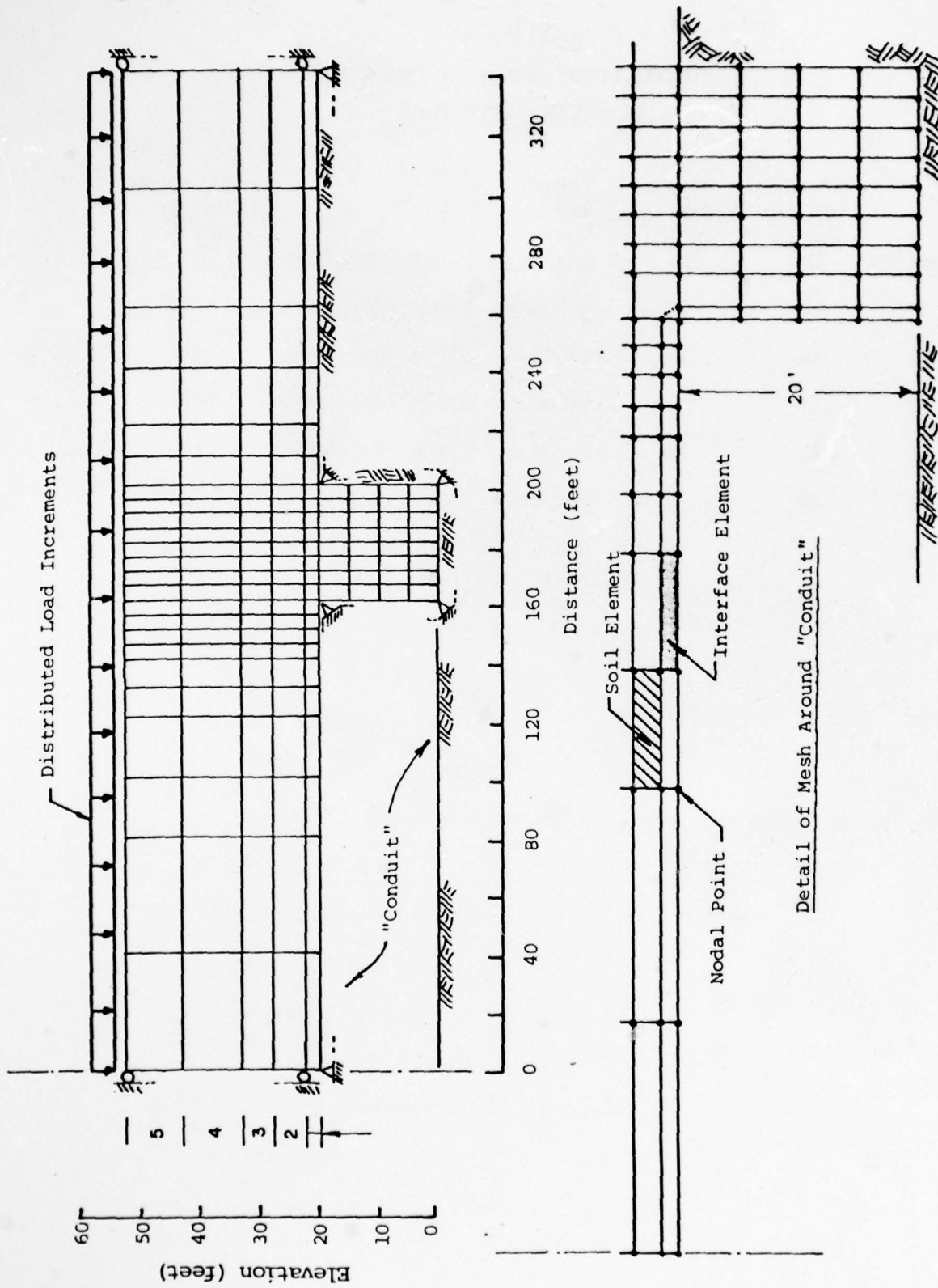


FIG. A-12 FINITE-ELEMENT MESH, SHALLOW TRENCH PLACEMENT STUDIES

TABLE A-6
SUMMARY OF SHALLOW TRENCH
PLACEMENT STUDIES

Case No.	Conduit/ Trench Depth (ft)	Trench Base Width (ft)	Trench Side Slope (h:v)	Backfill Soil Type	Maximum Height of Fill (ft)
1	20	20	vertical	SM-SC (RC=100%)	600
2	10	10	vertical	SM-SC (RC=100%)	584
3	10	5	vertical	SM-SC (RC=100%)	584
4	10	20	vertical	SM-SC (RC=100%)	600
5	10	2.5	vertical	SM-SC (RC=100%)	584
6	10	5	0.5:1	SM-SC (RC=100%)	584
7	10	5	1:1	SM-SC (RC=100%)	584

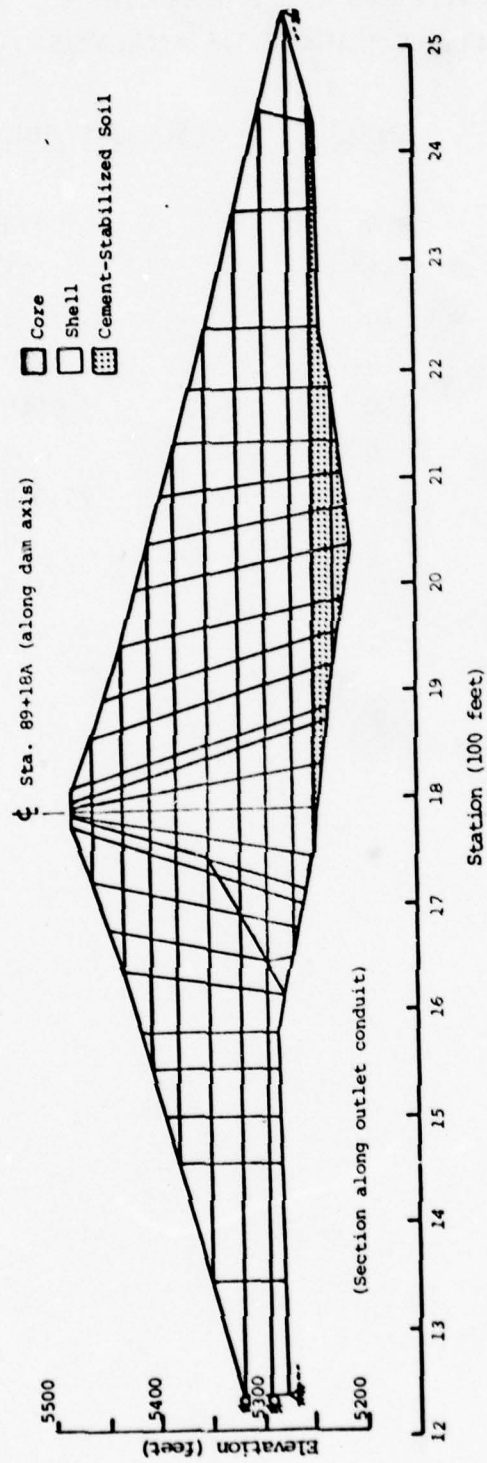


FIG. A-13 FINITE-ELEMENT MESH, COCHITI DAM ANALYSIS

TABLE A-7
HYPERBOLIC PARAMETERS
FOR COCHITI DAM ANALYSIS

	<u>CORE</u>	<u>SHELL</u>	<u>CEMENT-STABILIZED SOIL</u>
C(ksf)	0.4	0	125
ϕ_o	30°	42°	42°
$\Delta\phi$	0°	10°	0°
R_f	0.7	0.7	0.7
K	150	600	50,000
n	0.45	0.4	0.1
K_b	140	175	25,000
m	0.2	0.2	0.1
γ (pcf)	124.4	125.3	143.0

APPENDIX B

CALCULATIONS OF PRESSURES ON CONDUITS1. Cochiti Dam

a. Instrument Station A. The conduit and its installation geometry are shown in Figs. VII-1 and VII-6. Earth pressures are predicted on the basis of a rectangular conduit in a shallow rock trench.

Given:

Width of conduit, $B_c = 32'$

Height of conduit, $H_c = 18'$

Top width of trench adjacent to conduit, $W = 10.5'$

Bottom width of trench, $\overline{W} = 6'$

Trench wall slope, $\beta = 76^\circ$

Height of fill over conduit, $H = 111'$

Unit weight of fill over conduit, $\gamma = 125$ pcf

Solution:

Effective overburden pressure, $p = \frac{13.9 \text{ ksf}}{(0.125)(111)} \gamma H = 1.0 \gamma H$ (Fig. VII-2)

Rise-to-span ratio, $R/S = 18'/32' = 0.56$

For embankment condition and large $H (> 10 B_c)$:

Crown Pressure Factor, $N = 1.10$ (Fig. VI-3)

For actual $H/B_c = 111'/32' = 3.5$:

$N = 1.05$ (Fig. VI-5)

For trench condition and $W/B_c = 10'/32' = 0.33$:

$N = 1.0$ (Fig. VI-9)

Therefore, Crown Pressure, $\Delta \sigma_c = 1.0 (p) = 1.0 \gamma H$ (Fig. VI-2)

For $W/H_c = 11'/18' = 0.61$:

Edge-pressure (top), $\Delta \sigma_v = 1.6 (\Delta \sigma_c) = 1.6 (1.0 \gamma H) = 1.6 \gamma H$ (Fig. IV-87)

The increased edge-pressure acts over a distance of $W/2 = 11'2'' =$

$5.5'$ from the edge of the conduit (Fig. IV-86), or $5.5'/32' = 1/6$

of B_c . The edge-pressure factor, $m = 1.6 - 1.0 = 0.6$

The Foundation Pressure is therefore:

$$\Delta\sigma_v(\text{Foundation}) = (1+m/8) \Delta\sigma_c + [0.2(R/S)] \Delta\sigma_c \quad (\text{Fig. VI-2})$$

$$= (1+0.6/8)(\gamma H) + [0.2(0.56)](\gamma H)$$

$$\Delta\sigma_v(\text{Foundation}) = 1.21 \gamma H$$

For embankment condition:

$$\text{Horizontal Pressure (midheight), } \Delta\sigma_h = 0.4 \Delta\sigma_c = 0.4 \gamma H \quad (\text{Fig. VI-2})$$

$$\text{Horizontal Pressure (top and bottom), } \Delta\sigma_h = 0.2 \Delta\sigma_c = 0.2 \gamma H \quad (\text{Fig. VI-2})$$

For the actual trench condition and $\bar{W}/H_c = 6/8$ and $\beta = 76^\circ$:

$$\Delta\sigma_h(\text{midheight}) = 0.36(0.4 \gamma H) = 0.14 \gamma H \quad (\text{Fig. VI-10})$$

$$\Delta\sigma_h(\text{top and bottom}) = 0.36(0.2 \gamma H) = 0.07 \gamma H \quad (\text{Fig. VI-10})$$

b. Instrument Station C. The conduit and its installation geometry are shown in Figs. VII-1 and VII-7. Earth pressures are predicted on the basis of a rectangular conduit in an embankment condition.

Given:

Width of conduit, $B_c = 34'$

Height of conduit above its base, $H_c = 21'$

Height of conduit above base of cement-stabilized fill, $H'_c = 40'$

Height of fill over conduit, $H = 211'$

Unit weight of fill over conduit, $\gamma = 125 \text{ pcf}$

Solution:

$$\text{Effective overburden pressure, } p = \frac{19.0 \text{ ksf}}{(0.125)(211)} \gamma H = 0.72 \gamma H \quad (\text{Fig. VII-2})$$

If foundation was horizontal at base of conduit:

$$R/S = 21'/34' = 0.62$$

If conduit extended to base of cement-stabilized fill:

$$R/S = 40'/34' = 1.18$$

$$\text{Effective } R/S = (0.62 + 1.18) \div 2 = 0.90$$

For embankment condition and large $H (> 10 B_c)$:

$$N = 1.17 \quad (\text{Fig. VI-3})$$

For actual $H/B_c = 211/34 = 6.2$:

$$N = 1.13 \quad (\text{Fig. VI-5})$$

$$\begin{aligned} \text{Therefore, Crown Pressure, } \Delta\sigma_c &= 1.13 (p) \quad (\text{Fig. VI-2}) \\ &= 1.13 (0.72 \gamma H) \end{aligned}$$

$$\text{Crown Pressure, } \Delta\sigma_c = 0.81 \gamma H$$

For $R/S = 0.90$, $m = 0.8$ (Fig. VI-6)

$$\begin{aligned} \text{Edge Pressure (top), } \Delta\sigma_v &= (1 + 0.8) \Delta\sigma_c \quad (\text{Fig. VI-2}) \\ &= (1.8)(0.81 \gamma H) \end{aligned}$$

$$\text{Edge Pressure (top), } \Delta\sigma_v = 1.46 \gamma H$$

The increased edge pressure acts over a distance of $B_c/8 = 34'/8 = 4.25'$ from the edge of the conduit (Fig. IV-2)

The Foundation Pressure is therefore:

$$\Delta\sigma_v (\text{Foundation}) = (1 + 0.8/8)(0.81 \gamma H) + [0.2(0.90)] (0.81 \gamma H) \quad (\text{Fig. VI-2})$$

$$\Delta\sigma_v (\text{Foundation}) = 0.99 \gamma H$$

$$\text{Horizontal Pressure (midheight), } \Delta\sigma_h = 0.4 (0.81 \gamma H) = 0.32 \gamma H \quad (\text{Fig. VI-2})$$

$$\text{Horizontal Pressure (top and bottom), } \Delta\sigma_h = 0.2 (0.81 \gamma H) = 0.16 \gamma H \quad (\text{Fig. VI-2})$$

c. Instrument Station E. The conduit and its installation geometry are shown in Figs. VII-1 and VII-8. Earth pressures are predicted on the basis of a rectangular conduit in an embankment condition.

Given:

Width of conduit, $B_c = 32'$

Height of conduit above its base, $H_c = 18'$

Height of conduit above base of cement-stabilized fill, $H'_c = 50'$

Height of fill over conduit, $H = 138'$

Unit weight of fill over conduit, $\gamma = 125 \text{ pcf}$

Solution:

$$\text{Effective overburden pressure, } p = \frac{17.3 \text{ ksf}}{(0.125)(138)} \gamma H = 1.0 \gamma H \quad (\text{Fig. VII-2})$$

If foundation was horizontal at base of conduit:

$$R/S = 18'/32' = 0.56$$

If conduit extended to base of cement-stabilized fill:

$$R/S = 50'/32' = 1.56$$

$$\text{Effective } R/S = (0.56 + 1.56) \div 2 = 1.06$$

For embankment condition and large $H (> 10 B_c)$:

$$N = 1.20 \quad (\text{Fig. VI-3})$$

For actual $H/B_c = 138'/32' = 4.3$:

$$N = 1.13 \quad (\text{Fig. VI-5})$$

Therefore, Crown Pressure, $\Delta \sigma_c = 1.13 (p)$ (Fig. VI-2)

$$= 1.13 (1.0 \gamma H)$$

$$\text{Crown Pressure, } \Delta \sigma_c = 1.13 \gamma H$$

For $R/S = 1.06$, $m = 0.9$ (Fig. VI-6)

Edge Pressure (top), $\Delta \sigma_v = (1 + 0.9) \Delta \sigma_c$ (Fig. VI-2)

$$= (1.9)(1.13 \gamma H)$$

$$\text{Edge Pressure (top), } \Delta \sigma_v = 2.15 \gamma H$$

The increased edge pressure acts over a distance of $B_c/8 = 32'/8 = 4'$ from the edge of the conduit (Fig. VI-2)

The Foundation Pressure is therefore:

$$\Delta \sigma_v (\text{Foundation}) = (1 + 0.9/8)(1.13 \gamma H) + [0.2(0.56)](1.13 \gamma H) \quad (\text{Fig. VI-2})$$

$$\Delta \sigma_v (\text{Foundation}) = 1.38 \gamma H$$

$$\text{Horizontal Pressure (midheight), } \Delta \sigma_h = 0.4 (1.13 \gamma H) = 0.45 \gamma H \quad (\text{Fig. VI-2})$$

$$\text{Horizontal Pressure (top and bottom), } \Delta \sigma_h = 0.2 (1.13 \gamma H) = 0.23 \gamma H \quad (\text{Fig. VI-2})$$

2. DeQueen Lake Dam

a. Instrument Station A. The conduit and its installation geometry are shown in Figs. VII-9 and VII-11. Earth pressures are predicted on the basis of a conduit in a shallow rock trench. Consider the conduit to be oblong with a fully-supported base on rock.

Given:

Width of conduit, $B_c = 19'$

Height of conduit, $H_c = 19'$

Top width of trench on right side of conduit, $W=14'$

Bottom width of trench on right side of conduit, $\bar{W}=10'$

Trench wall slope on right side of conduit, $\beta=76^\circ$

Bottom width of trench on left side of conduit, $\bar{W}=9'$

Trench wall slope on left side of conduit, $\beta=63^\circ$

Height of fill over conduit, $H=130'$

Unit weight of fill over conduit, $\gamma=125$ pcf

Solution:

Assume effective overburden pressure, p , equals that below crest of dam ($H=137'$), per Fig. V-7:

$$p = \frac{137'}{130'} (\gamma H) = 1.05 \gamma H$$

Above base of conduit, $R/S=19'/19'=1.0$

For embankment condition and large $H (> 10 B_c)$:

$$N=1.34 \quad (\text{Fig. VI-3})$$

For actual $H/B_c=130'/19'=6.8$:

$$N=1.29 \quad (\text{Fig. VI-5})$$

Above 42-inch-diameter pipe below springline of conduit on left side, $R/S=9.5/19=0.5$.

For embankment condition and large $H (> 10 B_c)$:

$$N=1.28 \quad (\text{Fig. VI-3})$$

For actual $H/B_c=6.8$:

$$N=1.23 \quad (\text{Fig. VI-5})$$

For the trench condition at the right of the conduit and $W/B_c=$

$$14'/19'=0.74:$$

$$N=1.0 \quad (\text{Fig. VI-9})$$

Actual value of N would be between 1.23 and 1.0. As an approximation, say:

$$N = (1.23 + 1.0) / 2 = 1.12$$

$$\begin{aligned} \text{Therefore, Crown Pressure, } \Delta\sigma_c &= 1.12 p \quad (\text{Fig. VI-1}) \\ &= 1.12 (1.05 \gamma' H) \end{aligned}$$

$$\text{Crown Pressure, } \Delta\sigma_c = 1.18 \gamma' H$$

For embankment condition:

$$\text{Horizontal Pressure (top), } \Delta\sigma_h = 0.4(1.18 \gamma' H) = 0.47 \gamma' H \quad (\text{Fig. VI-1})$$

$$\text{Horizontal Pressure (back), } \Delta\sigma_h = 0.25(1.18 \gamma' H) = 0.30 \gamma' H \quad (\text{Fig. VI-1})$$

$$\text{Horizontal Pressure (springline), } \Delta\sigma_h = (0.47 + 0.30) \gamma' H / 2 = 0.38 \gamma' H \quad (\text{Fig. VI-1})$$

For actual trench condition on right side, it is conservative to reduce horizontal pressures as if the conduit were rectangular.

$$\text{For } \bar{W}/H_c = 10'/19' = 0.53 \text{ and } \beta = 76^\circ:$$

$$\Delta\sigma_h(\text{top}) = 0.47(0.47 \gamma' H) = 0.22 \gamma' H \quad (\text{Fig. VI-10})$$

$$\Delta\sigma_h(\text{base}) = 0.47(0.30 \gamma' H) = 0.14 \gamma' H \quad (\text{Fig. VI-10})$$

$$\Delta\sigma_h(\text{springline}) = 0.47(0.38 \gamma' H) = 0.18 \gamma' H \quad (\text{Fig. VI-10})$$

$$\Delta\sigma_h(\text{quarter-point}) = 0.18 \gamma' H + (0.22 \gamma' H - 0.18 \gamma' H)(0.707) = 0.21 \gamma' H \quad (\text{Fig. VI-1})$$

Normal Pressure at quarter-point:

$$\Delta\sigma_n(\text{quarter-point}) = (0.707)^2(1.18 \gamma' H) + (0.707)^2(0.21 \gamma' H)$$

$$\Delta\sigma_n(\text{quarter-point}) = 0.70 \gamma' H$$

For actual trench condition on left side, the horizontal pressures should only be reduced below the springline of the conduit, which is at the level of the top of the trench. Therefore:

$$\Delta\sigma_h(\text{top}) = 1.0(0.22 \gamma' H) = 0.47 \gamma' H$$

$$\Delta\sigma_h(\text{springline}) = 1.0(0.18 \gamma' H) = 0.38 \gamma' H$$

$$\Delta\sigma_h(\text{quarter-point}) = 0.38 \gamma' H + (0.47 \gamma' H - 0.38 \gamma' H)(0.707) = 0.44 \gamma' H \quad (\text{Fig. VI-10})$$

Normal Pressure at quarter-point:

$$\Delta\sigma_n(\text{quarter-point}) = (0.707)^2(1.18 \gamma' H) + (0.707)^2(0.44 \gamma' H) = 0.81 \gamma' H$$

For $W/H_C = 9'/9.5' = 0.95$ and $\beta = 63^\circ$:

$$\Delta\sigma_h (\text{base}) = 0.72(0.30 \gamma H) = 0.22 \gamma H \quad (\text{Fig. VI-10})$$

$$\Delta\sigma_h (\text{springline}) = 0.72(0.38 \gamma H) = 0.27 \gamma H \quad (\text{Fig. VI-10})$$

Assume the normal pressure on top of the 42-inch-diameter pipe =

γH (conservative).

b. Instrument Station B. The conduit and its installation geometry are shown in Figs. VII-9 and VII-12. Earth pressures are predicted on the basis of a conduit in a shallow rock trench. Consider the conduit to be oblong with a fully-supported base on rock.

Given:

Width of conduit, $B_C = 18'$

Height of conduit, $H_C = 18'$

Bottom width of trench on right side of conduit, $\bar{W} = 5'$

Depth of trench on right side of conduit, $H'_C = 3'$

Trench slope on right side of conduit, $\beta = 76^\circ$

Bottom width of trench on left side of conduit, $\bar{W} = 7'$

Depth of trench on left side of conduit, $H'_C = 2'$

Trench slope on left side of conduit, $\beta = 63^\circ$

Height of fill over conduit = 77'

Unit weight of fill over conduit, $\gamma = 132 \text{ pcf}$

Solution:

Assume effective overburden pressure, $p = 1.0 \gamma H$ (Fig. V-7)

Above base of conduit, $R/S = 18'/18' = 1.0$

Above 42-inch-diameter pipe, $R/S = 9'/18' = 0.5$

Average $R/S = (1.0 + 0.5) / 2 = 0.75$

For embankment condition and large $H (> 10 B_C)$:

$$N = 1.29 \quad (\text{Fig. VI-3})$$

For actual $H/B_C = 77'/18' = 4.3$:

$$N = 1.22 \quad (\text{Fig. VI-5})$$

Therefore, Crown Pressure, $\Delta\sigma_c = 1.22 p$ (Fig. VI-1)

$$= 1.22 (1.0 \gamma H)$$

$$\text{Crown Pressure, } \Delta\sigma_c = 1.22 \gamma H$$

For embankment condition:

$$\text{Horizontal Pressure (top), } \Delta\sigma_h = 0.4(1.22 \gamma H) = 0.49 \gamma H \quad (\text{Fig. VI-1})$$

$$\text{Horizontal Pressure (base), } \Delta\sigma_h = 0.25(1.22 \gamma H) = 0.31 \gamma H \quad (\text{Fig. VI-1})$$

$$\text{Horizontal Pressure (springline), } \Delta\sigma_h = (0.49 + 0.31) \gamma H \div 2 = 0.40 \gamma H \quad (\text{Fig. VI-1})$$

The shallow trenches would not be expected to affect horizontal pressure above the springline. Therefore:

$$\Delta\sigma_h (\text{top}) = 0.49 \gamma H$$

$$\Delta\sigma_h (\text{springline}) = 0.40 \gamma H$$

$$\Delta\sigma_h (\text{quarter-point}) = 0.40 \gamma H + (0.49 \gamma H - 0.40 \gamma H)(0.707) = 0.46 \gamma H \quad (\text{Fig. VI-1})$$

Normal pressure at quarter-point:

$$\Delta\sigma_n (\text{quarter-point}) = (0.707)^2 (1.22 \gamma H) + (0.707)^2 (0.46 \gamma H)$$

$$\Delta\sigma_n (\text{quarter-point}) = 0.84 \gamma H$$

For the trench condition on the right side,

$$\overline{W}/H'_c = 5'/3' = 1.67 \text{ and } \beta = 76^\circ$$

$$\text{Therefore, } \Delta\sigma_h (\text{base}) = 0.74 (0.31 \gamma H) = 0.23 \gamma H \quad (\text{Fig. VI-10})$$

For the trench condition on the left side,

$$\overline{W}/H'_c = 7'/2' = 3.5 \text{ and } \beta = 63^\circ$$

$$\text{Therefore, } \Delta\sigma_h (\text{base}) = 0.92 (0.31 \gamma H) = 0.29 \gamma H \quad (\text{Fig. VI-10})$$

Assume the horizontal pressure varies linearly from the springline to the base of the conduit. Assume the normal pressure on top of the 42-inch-diameter pipe = γH (conservative)

c. Instrument Station C. The conduit and its installation geometry are shown in Figs. VII-9 and VII-13. Earth pressures are predicted on the basis of a conduit in an embankment condition (left side) and a shallow rock trench (right side). Consider the conduit to be oblong with a fully-supported base.

Given:

Width of conduit, $B_c = 17'$

Height of conduit, $H_c = 17'$

Top width of trench on right side of conduit, $W = 9'$

Bottom width of trench on right side of conduit, $\overline{W} = 4'$

Depth of trench on right side of conduit, $H'_c = 14'$

Trench slope on right side of conduit, $\beta = 63^\circ$

Height of fill over conduit, $H = 56'$

Unit weight of fill over conduit, $\gamma = 132 \text{ pcf}$

Solution:

Assume effective overburden pressure, $p = 1.0 \gamma H$ (Fig. V-7)

Above base of conduit, $R/S = 17'/17' = 1.0$

For embankment condition and large $H (> 10 B_c)$

$$N = 1.34 \quad (\text{Fig. VI-3})$$

For actual $H/B_c = 56'/17' = 3.3$:

$$N = 1.22 \quad (\text{Fig. VI-5})$$

Above 42-inch-diameter pipe below springline on left side,

$$R/S = 8.5'/17' = 0.5$$

For embankment condition and large $H (> 10 B_c)$

$$N = 1.28 \quad (\text{Fig. VI-3})$$

For actual $H/B_c = 3.3$:

$$N = 1.18 \quad (\text{Fig. VI-5})$$

For the trench condition at the right side of the conduit and

$$W/B_c = 9'/17' = 0.53:$$

$$N = 1.0 \quad (\text{Fig. VI-9})$$

Actual value of N would be between 1.18 and 1.0. As an approximation, say:

$$N = (1.18 + 1.0) / 2 = 1.09$$

Therefore, Crown Pressure, $\Delta\sigma_c = 1.09 (p)$ (Fig. VI-1)

$$= 1.09 (1.0 H)$$

$$\text{Crown Pressure, } \Delta\sigma_c = 1.09 \gamma H$$

For embankment condition:

$$\text{Horizontal pressure (top), } \Delta\sigma_h = 0.4 (1.09 \gamma H) = 0.44 \gamma H \quad (\text{Fig. VI-1})$$

$$\text{Horizontal pressure (base), } \Delta\sigma_h = 0.25 (1.09 \gamma H) = 0.27 \gamma H \quad (\text{Fig. VI-1})$$

$$\text{Horizontal pressure (springline), } \Delta\sigma_h = (0.44 + 0.27) \gamma H \div 2 = 0.36 \gamma H \quad (\text{Fig. VI-1})$$

For the left side of the conduit, an embankment condition exists.

Therefore:

$$\Delta\sigma_h (\text{top}) = 0.44 \gamma H$$

$$\Delta\sigma_h (\text{springline}) = 0.36 \gamma H$$

$$\Delta\sigma_h (\text{quarter-point}) = 0.36 \gamma H + 0.707 (0.44 \gamma H - 0.36 \gamma H)$$

$$\Delta\sigma_h (\text{quarter-point}) = 0.42 \gamma H$$

Normal pressure at quarter-point:

$$\Delta\sigma_n (\text{quarter-point}) = (0.707)^2 (1.09 \gamma H) + (0.707)^2 (0.42 \gamma H)$$

$$\Delta\sigma_n (\text{quarter-point}) = 0.75 \gamma H$$

$$\Delta\sigma_n (\text{base}) = 0.27 \gamma H$$

For the right side of the conduit, a shallow trench condition exists.

For $\bar{W}/H'_c = 4'/14' = 0.29$ and $\beta = 63^\circ$:

$$\Delta\sigma_h (\text{top}) = 0.50 (0.44 \gamma H) = 0.22 \gamma H \quad (\text{Fig. VII-10})$$

$$\Delta\sigma_h (\text{springline}) = 0.50 (0.36 \gamma H) = 0.18 \gamma H \quad (\text{Fig. VI-10})$$

$$\Delta\sigma_h (\text{quarter-point}) = 0.18 \gamma H + 0.707 (0.22 \gamma H - 0.18 \gamma H) \quad (\text{Fig. VI-1})$$

$$\Delta\sigma_h (\text{quarter-point}) = 0.21 \gamma H$$

Normal pressure at quarter-point:

$$\Delta\sigma_h(\text{quarter-point}) = (0.707)^2(1.09\gamma H) + (0.707)^2(0.21\gamma H)$$

$$\Delta\sigma_h(\text{quarter-point}) = 0.65\gamma H$$

$$\Delta\sigma_h(\text{base}) = 0.50(0.27)\gamma H = 0.14\gamma H \quad (\text{Fig. VI-10})$$

3. Dierks Lake Dam

a. Instrument Station A-A. The conduit and its installation geometry are shown in Figs. VII-14 and VII-17. Earth pressures are predicted on the basis of an oblong conduit in an embankment condition and fully-supported on a rock foundation.

Given:

Width of conduit, $B_c = 8'$

Height of conduit, $H_c = 11'$

Rise of conduit above rock foundation, $R = 13'$

Height of fill over conduit, $H = 135'$

Unit weight of fill over conduit, $\gamma = 128 \text{ pcf}$

Solution:

Assume effective overburden pressure, $p = 1.0\gamma H$ (Fig. V-7)

Effective $R/S = 13'/8' = 1.63$

For embankment condition and large $H (> 10 B_c)$:

$N = 1.8$ (Fig. VI-3)

For actual $H/B_c = 135'/8' = 16.9$:

$N = 1.8$ (Fig. VI-5)

Therefore, Crown Pressure, $\Delta\sigma_c = 1.8 p = 1.8\gamma H$ (Fig. VI-1)

Horizontal Pressure (top), $\Delta\sigma_h = 0.4(1.8\gamma H) = 0.72\gamma H$ (Fig. VI-1)

Horizontal Pressure (base), $\Delta\sigma_h = 0.25(1.8\gamma H) = 0.45\gamma H$ (Fig. VI-1)

Horizontal Pressure (springline):

$$\Delta\sigma_h(\text{springline}) = [0.45 + (9/12)(0.72 - 0.45)]\gamma H \quad (\text{Fig. VI-1})$$

$$\Delta\sigma_h(\text{springline}) = 0.64\gamma H$$

Horizontal Pressure at quarter-point:

$$\Delta\sigma_h(\text{quarter-point}) = 0.64 = 0.707(0.72-0.64)\gamma H \quad (\text{Fig. VI-1})$$

$$\Delta\sigma_h(\text{quarter-point}) = 0.70\gamma H$$

Normal pressure at quarter-point:

$$\Delta\sigma_n(\text{quarter-point}) = 0.707^2 (1.8+0.70)\gamma H$$

$$\Delta\sigma_n(\text{quarter-point}) = 1.25\gamma H$$

b. Instrument Station B-B. The conduit and its installation geometry are shown in Figs. VII-14 and VII-17. No earth pressures are predicted for the top of the Seep Ring, but it would be expected that the pressures would be significantly greater than the overburden pressure because of the extreme projection condition.

c. Instrument Station C-C. The conduit and its installation geometry are shown in Figs. VII-14 and VII-18. Earth pressures are predicted on the basis of an oblong conduit in an embankment condition and fully-supported on a rock foundation.

Given:

Width of conduit, $B_c = 8'$

Height of conduit, $H_c = 11'$

Rise of conduit above foundation, $R = 10'$

Height of fill over conduit, $H = 129'$

Unit weight of fill over conduit, $\gamma = 130\text{pcf}$

Solution

Assume effective overburden pressure, $p = \frac{135}{129}\gamma H$ (Fig. V-7)

$$p = 1.05\gamma H$$

$$R/S = 10'/8' = 1.25$$

For embankment condition and large $H (> 10B_c)$:

$$N = 1.48 \quad (\text{Fig. VI-3})$$

For actual $H/B_c = 129'/8' = 16.1$:

$$N = 1.48 \quad (\text{Fig. VI-3})$$

Therefore, Crown Pressure, $\Delta\sigma_c = 1.48p = 1.48(1.05\gamma H)$ (Fig. VI-1)

$$\Delta\sigma_c = 1.55\gamma H$$

Horizontal Pressure (top), $\Delta\sigma_h = 0.4(1.55\gamma H) = 0.62\gamma H$ (Fig. VI-1)

Horizontal Pressure (base), $\Delta\sigma_h = 0.25(1.55\gamma H) = 0.39\gamma H$ (Fig. VI-1)

Horizontal Pressure at Springline:

$$\Delta\sigma_h \text{ (Springline)} = [0.39 + (6/10)(0.62 - 0.39)]\gamma H = 0.53\gamma H \text{ (Fig. VI-1)}$$

Horizontal Pressure at quarter-point:

$$\Delta\sigma_h \text{ (quarter-point)} = [0.53 + 0.707(0.62 - 0.53)]\gamma H \text{ (Fig. VI-1)}$$

$$\Delta\sigma_h \text{ (quarter-point)} = 0.59\gamma H$$

Normal Pressure at quarter-point:

$$\Delta\sigma_n \text{ (quarter-point)} = [0.707^2(1.55 + 0.59)]\gamma H$$

$$\Delta\sigma_n \text{ (quarter-point)} = 1.07\gamma H$$

e. Instrument Station D-D. The conduit and its installation geometry are shown in Figs. VII-14 and VII-18, Earth pressures are predicted on the basis of an oblong conduit in a shallow trench and fully-supported on a rock foundation.

Given:

Width of conduit, $B_c = 8'$

Height of conduit, $H_c = 11'$

Rise of conduit above foundation, $R = 10'$

Depth of trench, $H' = 2.5'$

Bottom width of trench, $\bar{W} = 4'$

Trench wall slope, $\beta = 76^\circ$

Height of fill over conduit, $H = 120'$

Unit weight of fill over conduit, $\gamma = 130 \text{ pcf}$

Solution:

Assume effective overburden pressure, $p = 1.0\gamma H$ (Fig. V-7)

Above foundation, $R/S = 10'/8' = 1.25$

For large $H (> 10B_c)$, $N=1.48$ (Fig. VI-3)

Above top of trench $R/S=6.5/8=0.81$

For large H , $N=1.30$ (Fig. VI-3)

Therefore, for large H , say $N=1.4$.

For actual $H/B_c = 120/8 = 15$: $N=1.4$

Therefore, Crown Pressure, $\Delta\sigma_c = 1.4p = 1.4\gamma H$ (Fig. VI-1)

For embankment condition:

Horizontal Pressure (top), $\Delta\sigma_h = 0.4(1.4\gamma H) = 0.56\gamma H$ (Fig. VI-1)

Horizontal Pressure (base), $\Delta\sigma_h = 0.25(1.4\gamma H) = 0.35\gamma H$ (Fig. VI-1)

For trench condition and $\bar{W}/H' = 4'/2.5' = 1.60$, $\beta = 76^\circ$

$\Delta\sigma_h$ (base) $= 0.43 (0.35\gamma H) = 0.15\gamma H$ (Fig. VI-9)

Horizontal Pressure at Springline:

$\Delta\sigma_h$ (Springline) $= [0.35 + (6/10)(0.56 - 0.35)] \gamma H$ (Fig. VI-1)

$\Delta\sigma_h$ (Springline) $= 0.48\gamma H$

Horizontal Pressure at quarter-point:

$\Delta\sigma_h$ (quarter-point) $= [0.707(0.56 - 0.48) + 0.48] \gamma H$ (Fig. VI-1)

Normal Pressure at quarter-point:

$\Delta\sigma_h$ (quarter-point) $= 0.707^2(1.4 + 0.54)\gamma H = 0.97\gamma H$

e. Instrument Station E-E. The conduit and its installation geometry are shown in Figs. VII-14 and VII-19. Earth pressures are predicted on the basis of an oblong conduit in a shallow trench and fully-supported on a rock foundation.

Given:

Same as Instrument Station D-D except that:

Height of fill over conduit, $H = 111'$

Solution:

Effective overburden pressure, $p = 1.0\gamma H$ (Fig. V-7)

Since $H/B_c = 13.9$ is greater than 10, earth pressures are the same as for Instrument Station D-D.

f. Instrument Station F-F. The conduit and its installation geometry are shown in Figs. VII-14 and VII-19. Earth pressures are predicted on the basis of an oblong conduit in a shallow trench and fully supported on a rock foundation.

Given:

Same as Instrument Station D-D except that:

Height of fill over conduit, $H = 102'$

Solution:

Effective overburden pressure, $p = 1.0\gamma H$ (Fig. V-7)

Since $H/B_c = 102'/8' = 12.8$ is greater than 10, earth pressures are the same as for Instrument Station D-D.

4. Lake Kemp Dam

At Instrument Station 21+54W, the conduit and its installation geometry are shown in Figs. VII-20 and VII-22. Earth pressures are predicted on the basis of a circular conduit in a shallow trench and fully supported on a rock foundation.

Given:

Width of conduit, $B_c = 18.5'$

Height of conduit, $H_c = 19'$

Projection of conduit above foundation, $R = 9.3'$

Width of trench at top of conduit, $W = 10'$

Bottom width of trench, $\overline{W} = 5.5'$

Trench Slope angle, $\beta = 63^\circ$

Height of fill above conduit, $H = 57'$

Unit weight of fill above conduit, $\gamma = 126 \text{ pcf}$

Solution:

Assume effective overburden pressure, $p = 1.0\gamma H$ (Fig. V-7)

The geometry of the trench installation is such that the

crown pressure on the conduit could be less than the overburden pressure. To be conservative assume $\Delta\sigma(\text{crown}) = 1.0p = \gamma H$

Horizontal pressures for embankment condition:

$$\Delta\sigma_h(\text{top}) = 0.4(1.0\gamma H) = 0.4\gamma H \quad (\text{Fig. VI-1})$$

$$\Delta\sigma_h(\text{springline}) = 0.25(1.0\gamma H) = 0.25\gamma H \quad (\text{Fig. VI-1})$$

$$\Delta\sigma_h(\text{quarter-point}) = [0.25 + 0.707(0.40 - 0.25)] \gamma H \quad (\text{Fig. VI-1})$$

$$\Delta\sigma_h(\text{quarter-point}) = 0.36\gamma H$$

For a trench condition and $\bar{W}/R = 5.5'/9' = 0.61$ and $\beta = 63^\circ$

$$\Delta\sigma_h(\text{springline}) = 0.65(0.25\gamma H) = 0.16\gamma H \quad (\text{Fig. VI-9})$$

$$\Delta\sigma_h(\text{quarter-point}) = 0.65(0.36\gamma H) = 0.23\gamma H \quad (\text{Fig. VI-9})$$

Therefore, normal pressure at quarter-point:

$$\Delta\sigma_n(\text{quarter-point}) = 0.707^2(1.0 + 0.23)\gamma H$$

$$\Delta\sigma_n(\text{quarter-point}) = 0.62\gamma H$$